School of Applied Chemistry

Urolithiasis:
Occurrence and Function of Intracrystalline Proteins in Calcium Oxalate Monohydrate Crystals

David Elliot Fleming

This thesis is presented for the Degree of
Doctor of Philosophy
of
Curtin University of Technology

May 2004

Declaration

This thesis contains no material which has been accepted for the award of any other degree or diploma in any university.

To the best of my knowledge and belief this thesis contains no material previously published by any other person except where due acknowledgment has been made.

Signature: ....

Date: .....28/4/04.....

ACKNOWLEDGEMENTS

My sincere thanks to supervisors, Associate Professor Wihelm van Bronswijk and Professor Rosemary Ryall for their advice, guidance and dedication during the course of my Ph.D. candidature.

There are also a large number of people and institutions I wish to express my gratitude to, for without their input, this undertaking would have not been completed. For the sake of brevity, I will only mention a few:

A special thanks to my wife, Betty for her understanding and immense support throughout this endeavour.

To Curtin University (WA) and Flinders Medical Centre (SA) for their support and generous allowances given for overseas conferences.

To my son, Sean for his help in computer modelling.

To Professor Gordon Parkinson, Dr Anthony Taylor (Urologist, WA) and Associate Professor Arie van Riessen for their significant contributions to the early part of this study.

To Dr P. Grover and Ms M. Chauvet, scientific staff of the Flinders Medical Centre, for supplying Tamm-Horsfall Glycoprotein and for preparing urinary calcium oxalate crystals respectively.

To Dr Brett Hunter, ANSTO, for his advice on Rietveld analysis.

To the staff of the Microscopy Centres, both at Curtin University and the University of Western Australia for their advice on FESEM and TEM analysis.

To Dr John Hosking, Chemistry Centre (WA) for his encouragement throughout my academic career.

ABSTRACT

The broad aim of the work presented in this thesis was to examine the relationship between the mineral and organic phases of calcium oxalate monohydrate (COM) crystals, which are the principal components of human kidney stones. The results presented, clearly demonstrate the presence of some amino acids and urinary proteins in the crystals and suggest a role for intracrystalline proteins in urolithiasis.

The adsorptive affinities of twenty amino acids to COM, calcium hydrogen phosphate, tricalcium phosphate and hydroxyapatite were assessed over the physiological urinary pH range (pH 5-8) in aqueous solutions. In all cases adsorption was strongest at pH 5 and decreased as the pH increased as a result of the increasing negative charge of both substrate and adsorbate. Binding was higher to COM than to the phosphate minerals, owing to differences in the surface charge or coordination-site availability. Aspartic acid (Asp), glutamic acid (Glu) and γ-carboxyglutamic acid (Gla), which each have at least two carboxyl groups, exhibited the highest binding affinities, suggesting that binding occurs by chelation. Further, binding affinity was reasoned to result from the ability of the zwitterions of Asp, Glu and Gla to adopt favourable conformations in which two carboxyl groups, and possibly the amino group, can interact with the mineral surface without further rotation. Although free amino acids are unlikely to fulfil a prominent inhibitory role in stone pathophysiology, they could, nonetheless, fulfil an important function as terminal residues or as exposed components of calcium-binding domains of proteins involved in stone formation.

The existence of intracrystalline proteins and amino acids in COM crystals was demonstrated by Synchrotron X-ray Diffraction (SXRD) analysis. Non-uniform strains and crystallite sizes were derived from SXRD whole pattern line widths using Rietveld analysis, which showed an increase in average non-uniform strain and a decrease in average crystallite size. These were attributed to intracrystalline molecules. Occluded molecules were Glu, Gla, human prothrombin (PT) and to a lesser extent, human serum albumin (HSA), as well as crystal matrix extract (CME), which comprises a complex mixture of soluble organic molecules remaining after

demineralization of COM crystals grown in centrifuged and filtered (CF) urine. COM grown in CF urine possessed greater non-uniform strain and smaller crystallite size than COM grown in ultrafiltered (UF) urine, indicating that the majority of intracrystalline macromolecules in crystals derived from CF urine were >10kDa in molecular mass. Asp, AspAsp, GluGlu and Tamm Horsfall glycoprotein (THG) were non-occluded molecules. Proteinase treatment of COM crystals grown in CF urine produced a marked decrease in non-uniform strain and an increase in crystallite size, suggesting that smaller crystallite material, more intimately associated with proteins than the bulk COM, was liberated during the treatment.

A reciprocal relationship was found between non-uniform strain and crystallite size, which was dependent upon the type of molecule(s) in which the COM crystals were grown. For a given increment in non-uniform strain, the corresponding decrease in crystallite size was found to be considerably greater for occluded macromolecules, than for amino acids. This difference was attributed to the capacity of macromolecules, once incorporated into the crystal, to disrupt a larger volume of the mineral bulk than amino acids. Alternatively, unlike amino acids, macromolecules might possibly stabilise an amorphous phase. Amorphous contributions resulting from the occlusion of PT and molecules from CF urine and UF urine in COM were found to range between 5-9%.

The SXRD data derived from the COM crystals were further analysed for anisotropy using Williamson-Hall plots and individual peak analysis (SHADOW). Crystals grown in distilled water COM (distilled water) and COM (Asp, AspAsp, GluGlu, Gla, HSA, THG and PT) were isotropic with respect to both non-uniform strain and crystallite size. Although COM (Glu) and COM (UF) were isotropic with respect to non-uniform strain, the crystallite sizes were smaller along the (100) and (001) principal axes, respectively. COM (CF urine) and COM (CME) were also anisotropic, but with respect to crystallite size, with the shortest lengths occurring along the (100) and (001) axes. The absence of anisotropy in non-uniform strain was ascribed to experimental error. The data also showed that stacking faults contributed significantly to crystal disorder. Largest stacking faults, highest non-uniform strain and lowest crystallite sizes were generally found along the $(13\bar{1})$ plane. Computer-generated models showed that molecules as large as proteins could not effectively be

incorporated along the $(13\bar{1})$ plane in COM. It was concluded therefore, that they transmit disorder from the principal (100, 010, 001) planes in the crystal to the $(13\bar{1})$ plane by diagonal sliding of one or more rows of oxalate ions, calcium ions and water molecules.

SXRD single peak and whole pattern analysis of COM crystals grown in aqueous solutions of increasing concentrations of PT, HSA, CME and Gla showed that non-uniform strain increased, crystallite size decreased and stacking faults increased, to limiting values. This was also found for crystals grown in UF urine containing CME and HSA. When crystals with occluded proteins were treated with proteinase K, their stacking faults and non-uniform strain decreased, and crystallite size increased, indicating that the non-crystalline material is more intimately associated with the protein and is physically removed or solubilised when the protein is destroyed.

FESEM observations of the internal architecture of fractured CaOx crystals grown in human urine and synthetic solutions containing PT, revealed an inhomogeneous microstructure containing low density zones not observed in COM crystals grown in water or UF urine. Proteolytic treatment of the fractured crystals, created an internal honey combed structure that replaced the "low-density" zones. A timed growth study showed the internal ultrastructure of urinary COM crystals depended to a significant extent, upon the ratio of crystal-binding proteins to the available quantities of solute ions during growth.

Dissolution studies of COM crystals showed that the process obeyed the Shrinking Core model and was therefore surface area-dependent. Pure COM dissolved more rapidly than crystals derived from UF urine, which dissolved at a faster rate than crystals precipitated from CF urine. This was attributed to shielding of the exposed COM surface by occluded molecules, which would reduce the effective surface area and slow dissolution. There is also the possibility that the macromolecules would have bound to the ions and retard their release into solution. The use of proteinase inhibitors verified the presence of proteinases in fresh urine and showed that they were capable of attacking proteins occluded in COM, in particular, proteins with Mr > 10kDa. Although COM (CF) crystals were more difficult to dissolve than COM (UF) crystals in aqueous solutions, they were far more susceptible to endogenous proteolytic degradation in urine.

Collectively, these findings have formed the basis of a novel hypothesis, which proposes that the type and concentration of urinary proteins incorporated inside CaOx crystals are fundamental to the disposal of CaOx crystals precipitated and retained within the renal system, and may therefore play an important role in the prevention of urolithiasis.

ABBREVIATIONS

Ala	Alanine
Asp	Aspartic acid
Arg	Arginine
AspAsp	Aspartic acid dimer
CaOx	Calcium oxalate
CaP	Calcium Phosphate
CF	Centrifuged and filtered
CME	Crystal Matrix Extract
COD	Calcium oxalate dihydrate
COM	Calcium oxalate monohydrate
COT	Calcium oxalate trihydrate
Cys	Cysteine
EDTA	Ethylene diamine tetraacetic acid
FESEM	Field emission scanning electron microscopy
FWHM	Full Width at Half Maximum Height
Gla	γ-carboxyglutamic acid
Glu	Glutamic acid
GluGlu	Glutamic acid dimer
Gly	Glycine
His	Histidine
HSA	Human Serum Albumin
I-Leu	Isoleucine
Leu	Leucine
Lys	Lysine
Met	Methionine
Met-S	Methionine sulphate
n-Leu	Norleucine
NC	Nephrocalcin
OPN	Osteopontin
Phe	Phenylalanine
Pro	Proline

PT	Prothrombin
RS	Relative saturation
Ser	Serine
SXRD	Synchrotron X-ray diffraction
THG	Tamm Horsfall glycoprotein
Thr	Threonine
Tyr	Tyrosine
UF	Ultrafiltered
UPTF1	Urinary prothrombin fragment 1
Val	Valine

TABLE OF CONTENTS

II.7 Fleming D.E, Dean C.J, Chauvet M.C, Parkinson G.M, Marshall V.R, Ryall R.L. 'A timed study of the relationship between mineral and protein during calcium oxalate crystal growth in human urine', In *Urolithiasis 2000*, pp 174-177. Eds. Rodgers AL, Hibbert BE, Hess B, Khan SR, Preminger GM. University of Cape Town, South Africa.

1 INTRODUCTION

The invariable presence of proteins in urine and in renal calculi suggests they may have some function in urolithiasis. However, although many studies have demonstrated that proteins can influence the nucleation, aggregation and growth of calcium oxalate (CaOx) crystals in synthetic solutions and urine, whether they directly or indirectly cause or inhibit the formation of stones in the urinary tract remains open to debate.

The formation of crystals is intrinsic to the genesis of CaOx calculi. Such crystals occur routinely in the urines of stone formers and healthy people, yet only approximately ten percent of the world population is afflicted with renal stone disease. Although having been the focus of much research for many years, this conundrum remains largely unexplained. As a result, it is now universally accepted that stone formation is too complex to be adequately described simply in terms of classical crystallization phenomena. Urolithiasis occurs in living people, not inanimate systems, so the processes and factors initiating and underlying the formation of stones are probably more akin to those controlling the construction of biominerals in nature than to those dictating the precipitation of minerals in experiments performed on the laboratory bench. This principle guided the studies reported in this thesis, which were based on the assumption that any influences urinary proteins may have in stone formation are likely to resemble those wrought by their healthy counterparts in healthy biomineralization systems.

The broad aim of the work reported in this thesis was to investigate the relationship between the mineral phase of CaOx crystals precipitated from human urine and the intracrystalline proteins contained within them, as well as the implications of that relationship for the formation of kidney stones. The work had four specific objectives:

- To quantify, over the physiological urinary pH range, the binding of amino acids to crystals of calcium salts commonly found in human renal calculi, in order to identify those likely to influence the ability of their protein hosts to be incorporated into the crystalline interior.

- To confirm, using X-ray crystallography, the presence of proteins and amino acids within COM crystals generated from human urine and inorganic solutions of selected proteins and amino acids.

- To demonstrate visually, by proteolytic digestion and field emission scanning electron microscopy, the presence of proteins in CaOx crystals generated from human urine and synthetic solutions containing protein.

- To compare the dissolution rates of CaOx crystals grown in distilled water, centrifuged and filtered human urine and ultrafiltered urine.

Results of these studies provided experimental support for the hypothesis that intracrystalline urinary proteins protect against stone formation by enabling intracellular proteinases to penetrate into the interior of crystals trapped within the kidney, and thereby, facilitating their degradation and dissolution.

2 FROM BIOMINERALIZATION TO UROLITHIASIS: AN OVERVIEW

2.1 BIOMINERALIZATION

Biomineralization is the process by which living organisms produce inanimate, ceramic-like materials. Collectively, organisms from all five kingdoms are capable of manufacturing more than sixty different minerals that serve a variety of functions (Lowenstam and Weiner, 1989). Calcium salts, however, constitute about 50% of all known biogenic minerals (Lowenstam and Weiner, 1989). Despite the wide range of biominerals occurring in nature, the formation of all of them can be classified as either biologically controlled or biologically induced (Lowenstam, 1981), although the distinction is not sharp and depends upon the extent of biological regulation (Zaremba et al., 1996). As the processes of biomineralization span both the organic and the inorganic worlds, a multidisciplinary approach is necessary to understand some of the principles involved (Nancollas and Wu, 2000). These principles are drawn from diverse scientific fields such as biochemistry, chemistry, physics, mineralogy, crystallography, geochemistry, endocrinology, molecular biology and cell biology (Lowenstam and Weiner, 1989).

Controlled biomineralization

Materials produced by controlled biomineralization have been classified into three general groups based on the organisation of mineral components (Weiner and Addadi, 1997).

- The first group is composed of multicrystalline arrays. Examples include bone and shells (Wilbur and Saleuddin, 1983, Boskey, 1996).
- The second group comprises of single crystals or a small array of large crystals grouped into an individual structure. An example of a single crystal is the sea urchin spine (Aizenberg et al., 1997).

- The third group, which contains non-crystalline minerals such as amorphous silica and phosphates, are exemplified by diatoms and chitons respectively (Reimann, 1964, Lowenstam and Weiner, 1985).

The constructional stages of controlled biomineralisation are supramolecular organisation, interfacial molecular recognition (templating) and cellular processing (Heywood and Mann, 1994, Mann, 1993). Control occurs from the sub-nanometre to the millimetre level, involving molecules in solution and/or attached to cellular compartments and interaction with cells. Crystal nucleation, phase, morphology, microarchitecure and growth dynamics are directed on a space-time basis by macromolecules and/or biomolecular processes (Zaremba et al., 1996). Crystals that form in cellular compartments stop growing when they contact the preformed inner encasing membrane surface (Lowenstam and Weiner, 1989).

Macromolecules are involved in all constructional stages, exercising exquisite control over the formation and overall shape of the biomineral. There are three main types of macromolecules.

Framework macromolecules

When present in biomineralized tissue, these provide structural support and suitable surfaces for crystal nucleation and growth. They also tend to be hydrophobic, as well as being highly cross-linked, and are best exemplified by α-chitin in crustaceans (Addadi and Weiner, 1986).

Control (acidic) macromolecules

These macromolecules are intimately involved with the crystals at all hierarchial levels, from the nanometre to the centimetre scale (Weiner and Addadi, 1997). They are rich in aspartic acid and/or glutamic acids, and, in addition, some may have phosphorylated serine and threonine residues. The proteins are also frequently covalently bonded to acidic polysaccharides possessing carboxylic and/or sulphate groups (Lowenstam and Weiner, 1989).

Cellular processing macromolecules

Of the three types, these are least understood and are thought to form part of the transport system that ensures delivery of mineral ions to the cellular compartments

for sustained crystal growth. Transport is achieved by ion delivery vehicles or pumps, which may include enzymes, matrix vesicles, polyelectrolytes, phosphoproteins or other calcium ion binding proteins and phospholipids (Heuer et al., 1992, Ryall et al., 2000).

Biologically induced biomineralization

Biologically induced mineralization is, in essence, "uncontrolled" mineralisation. Generally, much less information has been documented about this type of biomineralization, but the main features that distinguish it from its controlled counterpart are (Lowenstam and Weiner, 1989):

- Occurrence in an open environment and not in space specifically created for the purpose.
- Paucity of cellular processes and macromolecules to facilitate or control crystallization.
- Wide range of crystal sizes, often as the result of aggregation.
- External environmental influence over biomineral formation.
- Formation of similar crystal habits to those produced spontaneously under inorganic conditions.

Like other organisms in Nature, humans also manufacture biominerals, the most obvious being bone, teeth and cartilage. Information from other biomineralization systems should thus provide further insight into the formation of human biominerals, particularly kidney stones, whose pathogenesis, except for the last point above, possesses all the hallmarks of biologically induced biomineralization.

2.2 UROLITHIASIS

Urolithiasis is defined as the formation of urinary calculi or the pathological conditions associated with their presence. The disease affects approximately 10% of the human population. Literature prior to the 1980's, showed that males have at least twice the incidence of females (Sierakowski et al., 1978, Ahlstrand and Tiselius,

1981, Wisniewski et al., 1981, Power et al., 1984). However, the trend is now changing, and has even reversed in the United Kingdom (UK), particularly before the ages of 20 to 30. In the UK, the risk has been found to diminish from 20 to 30 in both sexes until after the age of 70 when they both have the same biochemical risk of stone values (P_{sf}) for calcium-containing stones (Robertson, 2001).

Among the factors involved in the genesis of calculi are age, sex, occupation, affluence, obesity, hypertension, physical activity, diet, geographical location and race (Robinson, 1990, Curhan and Curhan, 1994). Interestingly, Afro-South Africans are practically immune to this disorder (Durrbaum et al., 2001), although a definite reason for their protection has not yet been identified. Urinary calculi may develop in the kidneys, ureters, bladder or urethra (Lonsdale, 1968). However, except for a few areas of the world where bladder calculi are still prolific in young children, urinary stones are found almost exclusively, in the upper urinary tract (Ryall, 1989).

2.3 RENAL STONE COMPOSITION

The components that make up calculi may be mineral, organic, or both, with more than 65 different entities having been found in urinary stones (Daudon et al., 1993). Renal stones have been classified chemically as below (Prien and Prien, 1968):

- Calcium oxalate (CaOx), including CaOx monohydrate (COM), known as whewellite, and CaOx dihydrate (COD), known as weddellite.
- Calcium phosphates, for example, hydroxyapatite.
- Magnesium ammonium phosphate, for example, struvite.
- Uric acid and urates.
- Cystine
- Xanthine

In a 23 year kidney stone survey study, about 70% of renal stones were found to have CaOx as the main component. Approximately 33% were regarded as pure CaOx

while the remainder consisted of CaOx in combination with various forms of calcium phosphate (Prien, 1963, Prien and Prien, 1968). Similar results were found in a Japanese study on 69,949 stones (Yoshida and Okada, 1990).

This thesis focuses only on CaOx and in particular, COM. CaOx stones, like other urinary calculi, are composed principally of an insoluble salt and an organic matrix which is interlaced throughout the entire structure (Stapleton and Ryall, 1995).

2.3.1 The mineral component of CaOx stones

The principal mineral component of CaOx stones is usually a mixture of two of the three known CaOx hydrates, COM and COD (Nancollas, 1983). COD can transform, under urinary conditions, to the most thermodynamically stable and least soluble hydrate, COM (Nakai et al., 1996). It is probably for this reason that COM is almost invariably found at the centre of 'dihydrate' stones (Nakai et al., 1996). The third hydrate, CaOx trihydrate (COT), is relatively unstable in the normal urinary environment in which it transforms to COM (Gardner and Doremus, 1978, Tomazic and Nancollas, 1979, Sheehan and Nancollas, 1984). Hence, COT is rarely seen in renal stones (Heijnen, 1982).

Calcium phosphate (CaP) is often found in CaOx stones, occurring in calculi as hydroxyapatite, brushite, whitlockite, carbonated apatite and octacalcium phosphate phases (Prien and Prien, 1968, Blomen and Bijvoet, 1983). This has led to the proposal that the formation of CaP salts in the nephron induces subsequent nucleation of CaOx (Khan, 1997a). Supporting evidence (Koutsoukos et al., 1981) has shown that under inorganic conditions epitaxial growth does occur between these two minerals as their lattices are well matched (Ebrahimpour et al., 1991). It has also been reported that CaP phases are frequently found in the centre of CaOx stones (Ebrahimpour et al., 1991). These findings suggest that the presence of CaP in urine may be of some importance in the formation of CaOx stones. However, Grover et al., (2002), have shown conclusively that seed crystals of hydroxyapatite and brushite do not promote CaOx deposition in urine in vitro and are therefore unlikely to influence CaOx crystal formation under physiological conditions. Further, they stated that as CaP crystals found in urine must be coated with organic material, an epitaxial fit between this mineral and CaOx is irrelevant.

2.3.2 The organic matrix of CaOx stones

The organic matrix constitutes about 2.5% of the stone's dry weight (Boyce, 1968, Warpehoski et al., 1981) and is approximately 64% protein (King and Boyce, 1959). Other components include glycosaminoglycans (Nishio et al., 1985, Roberts and Resnick, 1986), red blood cells (Kim, 1983), bacteria (Finlayson et al., 1984b), lipids (Khan et al., 1988b) and cellular degradation products such as membranous vesicles, mitochondria, endoplasmic reticulum and cell nuclei (Khan et al., 1988a). Most matrix components are thought to originate from two sources:

- Normal urinary macromolecules which can be incorporated in crystals and thereby, into renal stones (Doyle et al., 1991).
- Macromolecules not normally present in urine but which are released from physical and/or chemical endothelial damage (Khan et al., 1989, Peterson et al., 1989, Doyle et al., 1991, Scheid et al., 1996).

The role of macromolecules in urolithiasis is still not completely understood and excellent reviews have been published on their anomalous ability to act as inhibitors and/or promoters (Ryall and Stapleton, 1995, Ryall, 1996).

Sectioned CaOx stones clearly show concentric laminations (similar to an onion) which are always intimately related to the structure of the organic matrix. The matrix is organised in compact parallel fibrils between successive concentric laminations, as well as occurring as fibrous radial striations (Boyce, 1968). One study found that the matrix concentration increased with distance from the stone core (Warpehoski et al., 1981). The authors of that study suggested that this resulted from the migration of organic material from the older interior to the outer areas of the stone. However, a more plausible explanation is that the increased matrix concentration observed in the outer regions of the stone more likely results from macromolecular products of tissue damage consequent upon increasing injury or irritation caused by the growing stone (Ryall and Stapleton, 1995). Several electron microscopic studies have shown that the matrix material coats individual crystals, which suggests that the matrix may influence their orientation, nucleation and/or agglomeration (Boyce and King, 1968, Wickham, 1976, Khan and Hackett, 1993).

However, those studies did not conclusively demonstrate the suggested physico-chemical effects expected to be produced by the matrix.

2.4 PHYSICO-CHEMICAL ASPECTS OF URINARY STONE FORMATION

Urinary stone formation can be broadly separated into two processes (Ryall, 1993): (1) crystallization events.

(2) retention of crystals within the renal system.

The three critical crystallization events are crystal nucleation, growth and aggregation, and though interdependent on each other in some degree, they are discussed separately in this chapter.

2.4.1 Nucleation

Nucleation is the first essential step in crystal formation. It commences with the transformation from a liquid to a solid phase and occurs when a solution is supersaturated with respect to the solid phase (Finlayson et al., 1984a). The creation of a new solid surface is energy-dependent and the driving force can be expressed in terms of the free energy difference between the solid phase (G_S) and the liquid phase (G_L) shown in equation (1) (Finlayson, 1977a, van Leeuwen, 1979, van Leeuwen and Blomen, 1979, Blomen and Bijvoet, 1983).

$$\Delta G = G_L - G_S \qquad (1)$$

For undersaturated solutions, those at equilibrium, and supersaturated solutions, $\Delta G < 0$, $\Delta G = 0$ and $\Delta G > 0$, respectively.

The free energy of crystal formation can also be expressed in terms of solute concentration:

$$\Delta G = RT \ln (A_1/A_0) \qquad (2)$$

Where R is the gas constant, T is the temperature in degrees Kelvin, A_1 is the activity of the salt species and A_0 is the activity of the salt species at equilibrium (Finlayson, 1977a, van Leeuwen, 1979, van Leeuwen and Blomen, 1979, Blomen and Bijvoet,

1983). The ratio of A_1/A_0 is known as the relative supersaturation ratio (S) and provides an estimate of the measure of urinary saturation (Pak et al., 1977).

Nucleation can be broadly classified as primary and secondary (induced by crystals). Primary nucleation is further divisible into homogeneous (spontaneous) and heterogeneous (induced by foreign particles) (Mullin, 1993b). For homogeneous nucleation to take place, there must exist at supersaturation a number of minute solid bodies, embryos, nuclei or seeds that act as centres of crystallization (Mullin, 1993b). These centres are referred to as critical nuclei. The number of ions or molecules in the critical nuclei, which are thought to have a similar structure to the eventual mature crystal (Perl-Treves and Addadi, 1988), can vary from approximately ten to several thousand (Nancollas and Gaur, 1984, Nancollas, 1990, Mullin, 1993b). As supersaturation approaches, ion or molecular clusters begin to form until a critical size is reached, which represents the minimum size of a stable nucleus. This is expressed by the following equation:

$$r_c = -2\gamma / \Delta G_v \qquad (3)$$

where r_c is the critical size of the nucleus, γ is the interfacial tension and ΔG_v is the free energy change of the transformation per unit volume (Mullin, 1993b). Particles smaller than the critical size will dissolve and particles greater than the critical size will grow (Nancollas, 1990). For homogeneous nucleation of CaOx, the critical nucleus size has been estimated to be 1.3 nm (Finlayson, 1978). The critical size (r_c), which is described as the metastable limit or the formation product (Nancollas, 1983, Nancollas, 1990), is defined by equation (4) in terms of the relative supersaturation ratio (S).

$$r_c = 2\gamma v / kT \ln S \qquad (4)$$

where v is the molecular volume and k is the Boltzmann constant (Mullin, 1993b). The metastable limit represents an ill-defined boundary that must be exceeded to allow nucleation of embryonic crystals (Kavanagh, 2000). In practice, the metastable limit is usually estimated as the minimum value of S required to bring about detectable changes in a fixed time period. In terms of the rate of homogeneous nucleation (J), the following expression shows the relationship between the three main variables, T, γ and S:

$$J = A\, e^{-(b\gamma^3/T(\ln S)^2)} \qquad (5)$$

where A and b are constants (Mullin, 1993b).

Levels of supersaturation required for homogeneous nucleation in urine are almost non-existent, despite the high concentrations of solute that may occur in the collecting tubules and at the renal papillae (Finlayson, 1978, Blomen and Bijvoet, 1983, Nancollas, 1983, Finlayson et al., 1984a, Nancollas et al., 1991). The degree of saturation of urine with CaOx is usually described in terms of relative saturation (RS), which is defined as the ratio of the product of calcium and oxalate activity at equilibrium in urine, over the thermodynamic solubility product. Because homogeneous nucleation of COM does not occur until the RS reaches 70, and COM RS in mammalian urine rarely exceeds 30 (Finlayson, 1977a, Finlayson, 1978, Cifuentes-Delatte, 1982), it is generally accepted that CaOx nucleation in urine is likely to be heterogeneous rather than homogeneous (Nancollas, 1981).

Heterogeneous nucleation requires lower supersaturation levels than those for homogeneous nucleation because a suitable solid substrate can decrease the energy of activation for nucleation (Finlayson, 1978, Nancollas, 1983, Nancollas, 1990). It follows that the overall free energy change associated with the formation of a critical nucleus under heterogeneous conditions must be less than the corresponding free energy change required for homogeneous nucleation. The interfacial tension term, γ, related to the contact angle (θ) formed between the crystalline deposit and foreign solid surface, is one of the important factors controlling the nucleation process (Mullin, 1993b). This relationship is shown in equation 6 and figure 2.1.

$$\gamma_{sl} = \gamma_{cs} + \gamma_{cl}\cos\theta \qquad (6)$$

where γ_{sl} , γ_{cs} and γ_{cl} are the interfacial tensions between the foreign solid surface (s) and the liquid (l), between the solid crystalline phase (c) and the foreign solid surface (s) and between the solid crystalline phase (c) and the liquid (l), respectively.

A wetting angle equal to 180° corresponds to complete non-wetting in liquid-solid systems. For such cases, there is complete non-affinity between the crystalline solid and the foreign solid surface. This means that the factor φ (equation 7) is equal to 1

and the overall free energy of nucleation is identical to the free energy needed for homogeneous nucleation (equation 8).

$$\varphi = (2 + \cos\theta)(1 - \cos\theta)^2 / 4 \qquad (7)$$

$$\Delta G'_{crit} = \varphi \Delta G_{crit} \qquad (8)$$

Where $\Delta G'_{crit}$ is the free energy associated with the critical nucleus under heterogeneous conditions, ΔG_{crit} is the free energy associated with the critical nucleus under homogeneous nucleation and φ is a factor that can be 0, 1 or <1.

In contrast, a wetting angle equal to 0^o corresponds to complete wetting in liquid-solid systems with a free energy of nucleation of zero. When there is partial wetting of a solid with a liquid ($0 < \theta < 180^o$), it can be expected that heterogeneous nucleation is easier to achieve because the overall excess free energy required is less than that for homogeneous nucleation (Mullin, 1993b).

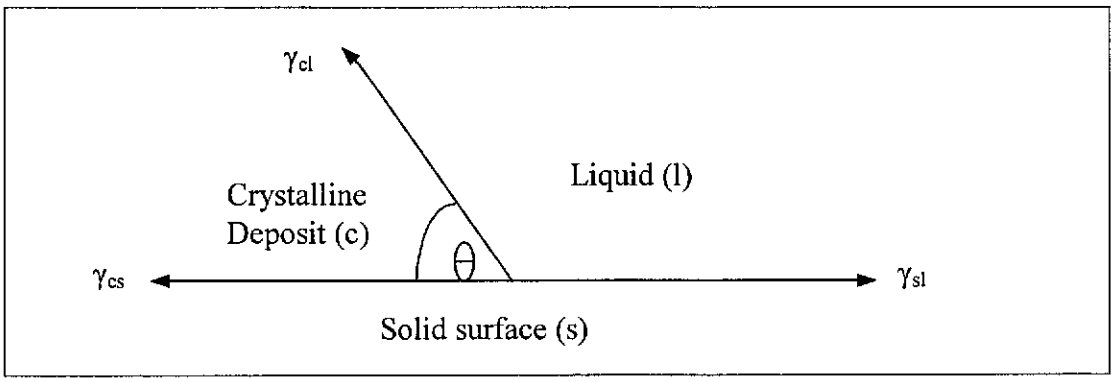

Figure 2.1 Interfacial tensions at the boundaries between three phases. Adapted from (Mullin, 1993b)

Factors influencing interfacial tension, and therefore heterogeneous nucleation, include electrostatic, chemical, stereochemical and geometric interactions at the interface (Davis and Walker, 1972, Heywood and Mann, 1994, Mandel and Mandel, 1996). These factors are primarily based on matching of charge and/or polarity, complementarity in size and molecular shape, spatial charge distributions and lattice geometry of the interacting surfaces. The heterogeneous nucleation mechanisms incorporating these factors are complex, but whatever the details, the main role of the substrate is primarily to lower the activation energy of nucleation (Mann et al., 1991).

A number of substrates have been implicated as being suitable for the heterogeneous nucleation of CaOx in urine. These include CaP (Khan, 1997a), silicate (Thomas, 1994), sodium urate (Pak and Arnold, 1975, Grases et al., 1988), cellular products (Khan, 1997b), living renal epithelial cells (Lieske et al., 1998) and proteins (Resnick et al., 1980, Thorne and Resnick, 1983, Lanzalaco et al., 1988, Morse and Resnick, 1988). There has been, however, some controversy about sodium urate being a likely heterogeneous nucleating agent *in vivo* (Burns and Finlayson, 1980, Meyer, 1981, Grover et al., 1990b). While these substrates have been recognised as potential heterogeneous nucleators, currently there is no absolute evidence that any one of them is actually responsible for the formation of crystal nuclei in the kidney.

2.4.2 Crystal growth

Stable nuclei (that is, particles > critical size), once formed, may grow into crystals of detectable dimensions in a supersaturated solution. Above a supersaturation ratio of S = 1, increasing values of S offer an increasing thermodynamic potential for crystals and calculi to grow (Kavanagh, 2000). There are a considerable number of proposed mechanisms attempting to describe crystal growth. These include surface energy theories (Gibbs, 1948), adsorption layer theories (Read, 1953, Verma, 1953, Bennema, 1969, Chernov, 1989), kinematic theories (Frank, 1958), Burton-Cabrera-Frank (BCF) theory (Nancollas, 1979), diffusion-reaction theories (Bennema, 1967, Sobczak, 1990) and birth and spread models (Van der Eerden et al., 1978, Nielson, 1984). While all these mechanisms are different in approach, they have a considerable degree of compatibility, a fact that has led to a general proposal (Mullin, 1993a) of the growth process, which incorporates most of the above in terms of the following steps, all of which may occur simultaneously:

- Bulk diffusion of hydrated ions through the diffusion boundary layer.
- Bulk diffusion of hydrated or dehydrated ions through the adsorption layer.
- Surface diffusion of hydrated or dehydrated ions.
- Partial or total dehydration of ions.
- Integration of ions into the lattice.
- Counter-diffusion of released water through the adsorption layer.

- Counter- diffusion of water through the boundary layer.

CaOx growth rate is now accepted to be a bimolecular surface-controlled reaction that follows second order kinetics (Dent and Sutor, 1971, Robertson and Peacock, 1972, Meyer and Smith, 1975a, Finlayson, 1977a, Miller et al., 1977, Finlayson, 1978, Ryall et al., 1981a, Ryall et al., 1981c). According to Nancollas, the rate of crystallization is controlled by the integration of crystal ions, rather than by adsorption at growth sites (Nancollas, 1983, Nancollas, 1984). The CaOx growth equation frequently quoted in publications is given below:

$$dc/dt = sk(C-C_o)^2 \qquad (9)$$

where C is the concentration of the solution, C_o is the concentration saturation, s is surface area and k is the rate constant (Finlayson, 1977a, Finlayson et al., 1984a).

Crystal growth can be highly affected by the presence of impurities in a system. Impurities have been known to completely suppress or enhance growth and to exert a highly selective effect, adsorbing only on specific crystallographic faces, and thereby modifying the crystal morphology (Mullin, 1993a). Growth inhibition is thought to involve the adsorption of an inhibitor onto the crystal surface, which disrupts the surface symmetry and blocks growth sites (Thorne and Resnick, 1983). If there is some degree of lattice similarity with a foreign entity, it may be incorporated into the crystal (Mullin, 1993a) or grow on a crystal face in one or more particular orientations (epitaxy) (Modlin, 1967, Lonsdale, 1968). Growth promotion may arise from the incorporation of such an impurity, creating crystal defects and phenomena such as screw dislocations at the growing crystal face, and favouring more rapid integration of growth units (Nancollas, 1983, Nancollas, 1984, Nancollas, 1990). It is likely that such crystal growth proceeds in a spiral fashion (Nancollas, 1983, Nancollas, 1984, Nancollas, 1990, Mullin, 1993a).

2.4.3 Crystal aggregation

In addition to growth, the size of crystalline particles may be increased by aggregation, the process occurring when multiple crystals group together to form large clumps. Aggregation is considered to be a critical event in renal calculi formation (Kok et al., 1990) since it allows the formation of crystals likely to be retained within the collecting duct within the time taken for urine to pass from the

glomerulus to the collecting ducts (Kok, 1996). Growth alone is too slow to allow this to occur. In addition, ultrastructural studies of kidney stones have shown that calculi consist of highly aggregated crystals (Meyer et al., 1971).

Normal human urine is considered to be a colloidal system (Cao et al., 1996) and like all colloidal systems is susceptible to the forces of destabilisation, resulting in aggregation. In general, important forces for aggregation in urine are van der Waals forces, electrostatic forces between crystals, viscous binding forces, and solid bridges between crystals, formed as a consequence of recrystallization (Finlayson, 1978). Van der Waals forces are attractive forces that are proportional to the size of the particle and inversely proportional to the square of the intercolloid distance at first approximation (Masterton, 1977, Stumm, 1990). Viscous binding forces can arise from the presence of hydrophilic molecules attached to the crystal surface, while electrostatic forces arise from repulsive forces between particles of like charge (Scurr and Robertson, 1986). A model for colloid stability is presented in Figure 2.2. Curves of the interaction energies describe electrostatic repulsion (V_R), van der Waals attractions (V_A), and total (net) interaction (V_T) as a function of the interparticle distance. The electrostatic repulsion curves (V_R) for two electrolytes of different ionic strength are shown as (C_S^a) and (C_S^b), the electrolyte concentration of the former being less than that of the latter. Born repulsion (repulsion between electronic clouds) becomes important at very small distances, and at closest approach, the potential energy is minimal. This is the point where aggregation occurs.

The stability of a colloid may be increased by two partially understood phenomena. The first is by steric stabilisation (adsorption stabilisation) where entities (e.g. macromolecules) attached to colloidal particles can impart stability through increased particle-solvent affinity and by an entropic mechanism (Shaw, 1980). The second, known as depletion stabilisation, results from the presence of macromolecules that are free in solution (Napper, 1983). These mechanisms may help to explain the significant inhibition of CaOx aggregation that occurs in urine when macromolecules such as proteins are present (Koide et al., 1981, Edyvane et al., 1987, Hess et al., 1989).

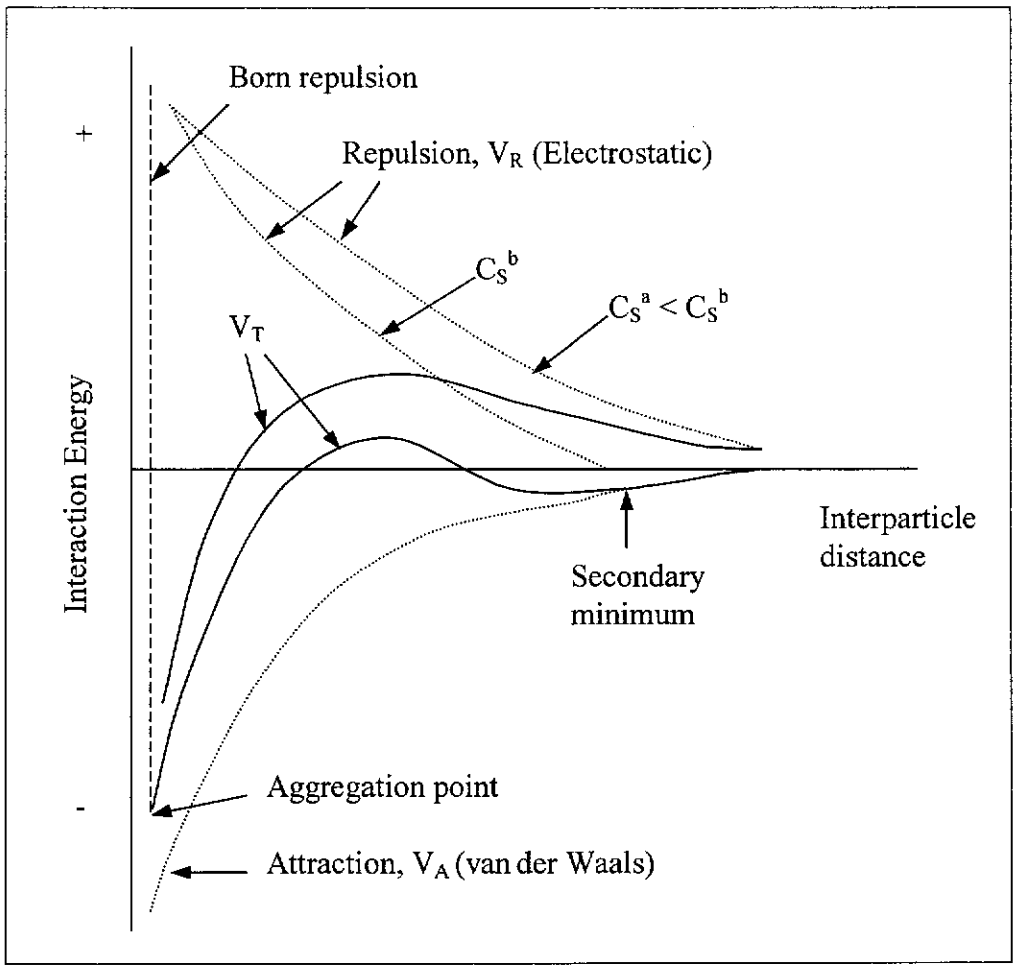

Figure 2.2 A Model for colloid stability. (Adapted from (Stumm, 1990)

2.5 THEORIES OF KIDNEY STONE FORMATION

There is no single theory that can completely account for the formation of calcific uroliths within the human urinary tract, despite its being one of the oldest known diseases. The main reason is that kidney stone formation appears to arise from multifactorial causes (Koul et al., 2000), involving a higher degree of interactive complexity between renal and urinary components than was previously thought. Superficially, stone formation should be a simple example of classical solubility product equilibria, but is complicated by biological factors. Causes include a combination of physico-chemical, genetic, environmental, dietary, hormonal and metabolic factors (Pak et al., 1985, Robertson and Peacock, 1985, Butz, 1986, Liebmann and Chai, 1997). A considerable number of risk factors, mechanisms,

models and theories have been advanced to explain renal calculus formation. These, along with references that discuss the various theories, are shown in table 2.1.

Table 2.1 Models and theories of stone formation

Models and Theories	**Authors**
CaOx saturation	(Robertson et al., 1968, Robertson et al., 1976b, Hallison and Rose, 1978)
Hyperoxaluria	(Williams and Wandzilak, 1989, Robertson and Hughes, 1993)
Hypercalciuria	(Curhan et al., 1993)
Hypocitraturia	(Hodgkinson, 1962, Rudman et al., 1982, Menon and Mahle, 1983, Nicar et al., 1983)
Hyperuricosuria	(Coe, 1973, Grover et al., 1993)
Gastrointestinal bacteria	(Sidhu et al., 1999)
Nanobacteria	(Kajander and Ciftcioglu, 1998)
Renal tubular cell injury	(Khan, 1995a, Muthukumar and Selvam, 1997)
Hypertension	(Madore et al., 1998)
Solute transfer system defects	(Chabra and Manocha, 1991)
Crystal adhesion and endocytosis	(Lieske et al., 1997b)
Protein induced crystallization	(Boyce and Garvey, 1956, Pak, 1978, Nicar et al., 1980)
Epitaxy	(Nancollas and Gardner, 1974, Meyer et al., 1975, Meyer et al., 1976, Meyer et al., 1977, Ebrahimpour et al., 1991)
Glycosaminoglycans-depletion theory	(Robertson et al., 1976a)
Randall plaque theory	(Randall, 1936, Randall, 1937, Mandel and Riese, 1991)
Anderson Carr theory	(Patriquin and Robitaille, 1986)
Free and fixed particle theory	(Finlayson and Reid, 1978)
Inhibitor theory	(Ryall, 1993)
Matrix theory	(Ryall, 1989)

As mentioned above, despite the many factors likely to be involved in stone formation, and the number and complexity of the theories advanced, there are still only two critical parameters required for stone formation: (1) crystal formation and (2) retention of those crystals within the urinary tract (Ryall, 1993), and every theory and model of urolithiasis must account for them. To discuss their relevance and connection to all models and theories mentioned above is beyond the scope of this thesis. However, four theories have particular bearing on the content of this thesis and are discussed in more detail.

2.5.1 Free Particle theory

The Free Particle theory is based on the premise that crystals will nucleate and grow by deposition of solute, or more likely, by aggregation, to a size likely to be trapped in the renal collecting ducts, thereby providing a nidus for stone formation. Finlayson and Reid questioned this concept by demonstrating, theoretically, that a crystal could not grow to the critical size during normal urinary transit time though the renal tubules (Finlayson and Reid, 1978). Their reasoning was based on a crystal growth rate of 1.6 nm/minute, glomerulous to pelvis transit time of 8-12 minutes and a transit time of 3 minutes across the duct of Bellini (Finlayson, 1977a, Finlayson, 1977b, Finlayson, 1978, Finlayson and Reid, 1978). However, their estimates were modelled on a "plug flow" configuration (Finlayson, 1972) which does not satisfactorily account for crystal aggregation. This is an important consideration as findings have shown that stone formers' urines contain crystals that are more aggregated than those found in normal urine (Robertson et al., 1969, Doremus et al., 1978, Fleisch, 1978). More recent theoretical computations (Kok and Khan, 1994) have shown that by the mechanism of agglomeration, free particles are capable of blocking a tubule during normal urinary transit times. Thus the free particle concept cannot be disregarded, as it could still provide a valid mechanism for stone formation, as was first put forward by Vermeulen and Lyon, (1968).

2.5.2 Fixed Particle theory

This theory assumes that stone formation must begin with the fixation of newly formed crystals to cell membranes. Such a mechanism was first proposed by Finlayson and Reid, (1978) and its wide acceptance has been mainly based on experimental studies of nephrolithiasis induced in laboratory animals (Khan et al.,

1979, Khan et al., 1982, Khan and Hackett, 1991, Kumar et al., 1991, Khan, 1995b). Supporting evidence drawn from *in vitro* experiments has included the following:

- *In vitro* crystal nucleation on epithelium cell fragments (Khan et al., 1990).
- *In vitro* CaOx nucleation on kidney membranes (Khan et al., 1990).

Additional evidence has come from pathological calcification associated with cellular membranes, which includes Randall's plaque (Finlayson and Reid, 1978), lipids and phospholipids (Bosky, 1981, Bosky et al., 1983, Boyan et al., 1989), atherosclerotic and dental plaque (Anderson, 1983), large arteries and aortic valve (Kim and Huang, 1971, Kim, 1976, Kim et al., 1986) and tumors (Slavin et al., 1993). Cell culture experiments demonstrating CaOx crystal adhesion to cultured animal renal epithelial cells have also supported the theory (Riese et al., 1988, Mandel, 1994, Verkoelen et al., 1995, Lieske et al., 1996a, Lieske et al., 1996b, Lieske et al., 1999). In summary, experimental evidence for crystal attachment in stone formation is very strong and the theory certainly cannot be readily dismissed.

2.5.3 Inhibitor theory

This theory recognises the existence in urine of various substances that are capable of preventing or retarding crystal nucleation, growth or aggregation and postulates that their presence in the urine of healthy subjects prevents stone development. It follows that stone formers are susceptible to urolithiasis because their urines lack or are deficient in these inhibitors. Urolithiasis is thus regarded as the net result of an imbalance between the opposing promotory influences of urinary supersaturation and the inhibition of crystal nucleation, aggregation and growth (Robertson et al., 1976b).

A number of low and high molecular weight urinary compounds have been shown to inhibit growth and aggregation of CaOx crystallization in model experimental systems. The mechanism is presumed to involve poisoning the surface of the crystals and thus preventing deposition of new solute or aggregation with other crystals, or the binding of calcium or oxalate ions, which reduces the level of supersaturation (Ryall, 1993). In addition, urinary substances may be capable of preventing crystal adhesion to cells in the urinary tract (Lieske et al., 1996).

Low molecular weight inhibitors

Low molecular weight species include magnesium, citrate and pyrophosphate ions (Robertson and Peacock, 1972, Ryall et al., 1981b, Ryall et al., 1989). Because magnesium, citrate and phosphate ions are capable of binding with various components of CaOx crystals, they are considered to be both thermodynamic and kinetic inhibitors, affecting both crystal solubility and rate of formation (Meyer and Smith, 1975b, Felix et al., 1977, Robertson et al., 1981, Ryall et al., 1981b, Robertson and Scurr, 1986). Magnesium is known to form ion complexes with oxalate and it is in this capacity that it is considered to act as an inhibitor of CaOx crystallization. Although magnesium has been reported to inhibit CaOx crystal nucleation (Li et al., 1985), growth (Doremus et al., 1978) and aggregation (Ryall et al., 1981b) in inorganic solutions, other researchers have been unable to confirm these findings (Robertson et al., 1973, Meyer and Smith, 1975a, Meyer and Smith, 1975b, Doremus et al., 1978). Contradictory results have also been reported on the effects of magnesium on CaOx crystallization in urine (Hallson et al., 1982, Ryall et al., 1989). A number of studies have shown that citrate inhibits CaOx crystal nucleation (Doremus et al., 1978), growth (Meyer and Smith, 1975b) and aggregation (Ryall et al., 1981b) in aqueous media and CaOx crystallization in undiluted (Ryall et al., 1985) and concentrated urine (Hallson et al., 1983). The ability of citrate to form strong complexes with calcium is associated with its notable effect on crystal nucleation and growth (Robertson and Scurr, 1986). Citrate is also known to bind to CaOx crystal surfaces, an attribute that may explain its influence on crystal growth and aggregation (Ryall, 1997). Pyrophosphate has been reported to inhibit crystal nucleation (Doremus et al., 1978), growth (Welshman and McGeown, 1972) and aggregation (Ryall et al., 1981b) in inorganic solutions. The capacity of pyrophosphate to inhibit CaOx crystallization events is almost certainly due to its strong affinity for the crystal surface. In undiluted urine, pyrophosphate does reduce the deposition of CaOx but has little or no effect on the inhibition of nucleation and aggregation (Ryall et al., 1985). The contradictory findings reported in the studies cited above exemplify the problem of comparing known inhibitory effects of substances on crystallization events in inorganic solutions with those in urine. Hence it is difficult to comment about the effects of pyrophosphate under physiological conditions.

Macromolecular inhibitors

High molecular weight inhibitors such as proteins (Robertson et al., 1984, Grover et al., 1990a, Sorensen et al., 1990, Ryall et al., 1995), nucleic acids (Ito and Coe, 1977) and glycosaminoglycans (Bowyer et al., 1979, Ryall et al., 1981b, Sallis, 1987) are generally considered to exert a greater influence than low molecular weight compounds in urolithiasis. This is mainly due to their inhibitory effects on crystal aggregation, which is the critical step in stone formation (Kok et al., 1990). In keeping with this, a number of researchers have found that CaOx crystals in stone former's urine are larger and more aggregated than those in the urine of normal subjects (Robertson et al., 1969, Robertson and Peacock, 1972, Hallson and Rose, 1976). Similarly, precipitated CaOx crystals from whole human urine were found to be smaller and less aggregated than those precipitated from ultrafiltered urine (Edyvane et al., 1987). As ultrafiltration in those studies removed macromolecules greater than 10kDa and the concentrations of low molecular weight compounds remained constant, it is tempting to postulate that a lack of macromolecules greater than 10 kDa contributes to stone formation. The same authors cited above also found that macromolecules greater than 10 kDa had no discernible effect on the detection of nucleation of CaOx crystals from undiluted human urine (Edyvane et al., 1987).

One of the serious drawbacks to the inhibitor theory is the lack of published literature demonstrating consistent differences between the inhibitory activity of urine of stone formers and healthy subjects (Dent and Sutor, 1971, Robertson et al., 1973, Coe et al., 1980, Kitamura et al., 1982, Ryall and Marshall, 1984, Ryall et al., 1988). Such inconsistencies have been attributed to the use of various techniques for measuring inhibitory activity (Ryall, 1997) and have resulted in calls for a standard reference crystallization system (Rodgers and Jappie, 1996). For example, researchers examining the inhibitory/promotory effects of urinary macromolecules on crystallization have used inorganic solutions (Koide et al., 1981, Lanzalaco et al., 1988), synthetic urines (Randolph and Drach, 1981, Kohri et al., 1989) and undiluted urine (Ryall et al., 1991). Although experiments conducted in inorganic solutions and synthetic urine have yielded valuable information, caution should be applied whenever a comparison is made with the real situation, as naturally occurring urine has a complex composition that cannot be reproduced artificially. Innumerable

interactions between dissolved species occur in urine and erroneous conclusions can be drawn as a consequence of the impossibility of taking them all into account.

Another consideration is the anomalous behaviour of some macromolecules to behave as crystallization inhibitors and promoters. Tamm Horsfall glycoprotein, for example, has been shown to act as an inhibitor (Kitamura and Pak, 1982, Scurr and Robertson, 1986) as well as a promoter (Rose and Sulaiman, 1982) of CaOx crystallization. Although this almost certainly results from differences in experimental methodology, it is also possible that an inhibitor's activity can be influenced by other urinary components. Thus, while the inhibitor theory provides some strong evidence leading to a plausible mechanism for stone formation, it has yet to be proved.

2.5.4 Matrix theory

The organic matrix has been widely accepted as an integral component of urinary stones and its ubiquitous presence in urinary calculi has led to the development of the matrix theory of stone formation. The matrix theory regards the organic matrix as undesirable, since it views components of the matrix as promoters of crystallization. The theory, largely developed by Boyce and co-workers (Boyce et al., 1954a, Boyce et al., 1954b, Boyce and Garvey, 1956, Boyce and King, 1959, Boyce and King, 1963, Boyce, 1968), runs parallel with the broader aspects of biomineralized tissue formation, such as in bone, teeth and cartilage. However, while the formation of healthy biomineralized tissue is recognized as being tightly directed by macromolecules (Ryall et al., 2000), their role in kidney stone development is still largely unknown. A further important distinction between healthy biomineralization systems and stone pathogenesis is that the former is a highly controlled process whereas the latter is not. Nonetheless, the matrix theory proposes that at least some urinary macromolecules are capable of inducing CaOx crystal nucleation and promoting their continued deposition, by acting as heterogeneous nucleators of the mineral phase of the stone (Khan, 1995b). Adsorption characteristics of several proteins on CaOx have been shown to be consistent with the Langmuir adsorption model, which is based on the assumption that there is a monolayer coverage and constant energy of desorption (Leal and Finlayson, 1977). Growth takes place by further addition of solute and macromolecules to the nucleated particles. Once

attached, however, macromolecules may then adhere to similar particles to form large clusters, thus providing a base for further growth.

From the assumptions of the matrix theory, there are at least two separate or combined possibilities that could exist (Ryall, 1993):

(1) urine from stone formers contains more of the crystal-inducing macromolecules than does urine from healthy people.

(2) macromolecules in both urine types are generically the same, but structurally different.

However, it has not been demonstrated thus far that the proteins of stone former's urine is materially and consistently different from those of non stone former's urine, either in molecular structure or amount.

One of the major problems facing researchers attempting to verify the matrix theory is the complete analysis of the matrix itself (Ryall, 1993). Full matrix analysis should show the types of macromolecules present in renal calculi and whether they are different from those occurring in normal urine. This formidable task has not been achieved for several reasons:

- Approximately 75% of the matrix is considerably resistant to dissolution (Ryall, 1993). As a consequence, most knowledge of the chemical constituents of matrix (Boyce et al., 1962) relates only to the 25% soluble fraction.

- The matrix can undergo changes such as dehydration, oxidation, chemical cross-linking and polymerisation, altering the structure of the original components (Finlayson et al., 1961).

- It is possible that the matrix composition could alter through bacterial action. The existence of nanobacteria has been shown in a number of kidney stones (Sharma et al., 2000). These bacteria are extremely small in size (0.05 – 0.5 μm diameter) and belong to the probacteria family. Once in the kidney, they are difficult to destroy, being resistant to antibiotics such as penicillins and aminoglycosides.

- Matrix constituents could be degraded by urinary proteases (Peterson et al., 1989).

- Stones contain additional macromolecules resulting from tissue damage, which becomes incorporated into the final structure. Thus, although a number of macromolecules may be involved with CaOx crystal formation, those in stones may, in addition, be there as a result of irritation or damage to the urothelial wall (Stapleton and Ryall, 1994). Consequently, it is impossible to distinguish between macromolecules that may have induced or inhibited crystal formation from those caused by the presence of the stone itself.

In summary, there is insufficient evidence either to prove or invalidate the matrix theory. Despite this, an increasing understanding of calculi formation has been achieved in recent years through the study of some of the more important components of the matrix, namely glycosaminoglycans and proteins.

2.6 MACROMOLECULES

2.6.1 Glycosaminoglycans

Glycosaminoglycans (GAGs) are polyanionic compounds possessing unbranched polysaccharide chains of variable length. GAGs have been estimated to account for between 0.19 and 0.58% of a stone's weight, depending upon the composition of the stone (Anderson, 1983, Nishio et al., 1985). The presence of GAGs in the organic matrix of urinary stones and their ability to affect crystallization of CaOx have raised speculation about their possible involvement in kidney stone formation (Suzuki et al., 1994a). Of the naturally occurring GAGs known, five have been found in urine (see table 2.2) and of these, only two have been detected in CaOx stones, namely hyaluronic acid (HA) and heparan sulphate (HS) (Nishio et al., 1985, Roberts and Resnick, 1986, Hesse et al., 1991), although Yamaguchi et al. (1993) could not detect HA.

Table 2.2 Glycosaminoglycans detected in human urine (Ryall, 1996).

Glycosaminoglycans
Chondroitin sulphate (ChS)
Dermatan sulphate (DS)
Heparan sulphate (HS)
Hyaluronic acid (HA)
Keratan sulphate (KS)

With the exception of keratan sulphate (KS), GAGs consist of hexuronic and hexosamine residues connected with alternating B 1-3 and B 1-4 linkages. In KS, hexuronic acid units are replaced by galactose units (Roberts and Resnick, 1986, Hesse et al., 1991). The selectivity of specific GAGs for CaOx stones was verified by Suzuki et al., (1995a), who showed that only HS was found in CaOx crystals precipitated from whole human urine. The same group also showed that chondroitin sulphate (ChS) could be found associated with the crystals, but only in the absence of HS. This selectivity was reasoned to be the result of competitive adsorption for the possible binding sites on CaOx.

A number of studies have indicated that some GAGs inhibit crystal growth and aggregation (Bowyer et al., 1979, Ryall et al., 1981b, Fellstrom et al., 1986, Robertson and Scurr, 1986, Scurr and Robertson, 1986). Those studies, however, were carried out in aqueous inorganic media, which cannot accurately reflect the physiological urinary environment. Further, Ryall, (1996) reported that a number of studies designed to test the inhibitory effects of ChS and HS on CaOx crystallization in urine, or in animal models *in vivo*, were at variance with the results obtained from the inorganic media studies. Results from aqueous inorganic solutions can be expected to be vastly different from those obtained in urine because the binding capacity of GAGs to CaOx crystals is related to their charge and the ionic strength of the solution (Fellstrom et al., 1989). Thus, although studies have demonstrated that individual GAGs can affect CaOx crystallization in inorganic media, as yet, there is no evidence showing unambiguously that any specific GAG plays a definite role in stone formation.

2.6.2 Proteins

Approximately twenty proteins have been found in the organic matrix of kidney stones (Table 2.3). As noted previously, matrix proteins can originate from several sources (Stapleton et al., 1993a, Ryall, 1996, Ryall et al., 2000):

(1) Proteins synthesised and excreted into the urine by healthy cells located at different regions of the renal tubules. These locations are discussed in 2.6.3-8.

(2) Low molecular weight protein fragments such as the F1 fragment of prothrombin, passing through healthy glomeruli into the urine.

(3) Glomerular damage, leading to greater permeability and allowing leakage of blood proteins into the urine.

(4) The result of nephron cell damage caused by attached crystals and urinary constituents such as high oxalate concentration.

The potential importance of proteins in CaOx stone formation lies in their capacity to interact with the mineral in a number of ways and thereby, to affect subsequent crystallization processes. These depend on the crystal polymorph, conditions in the surrounding urinary medium such as pH (Leal and Finlayson, 1977) and ionic strength (Utsunomiya et al., 1993), as well as structural features of the proteins themselves and their own concentrations. Depending upon prevailing conditions, proteins can:

- alter CaOx crystal morphology (Wesson et al., 1998).
- alter the surface properties (i.e. charge) of CaOx crystals (Lieske and Toback, 1996).
- affect aggregation, nucleation, growth of CaOx (Ryall, 1996).
- affect the binding of CaOx to renal cells (Lieske et al., 1995, Lieske et al., 1997a).

Table 2.3 Proteins detected in kidney stones (Ryall, 2003)

Proteins	**Reference**
human serum albumin	(Boyce et al., 1962)
α and γ-globulins	(Boyce et al., 1962)
Tamm-Horsfall glycoprotein	(Melick et al., 1980)
nephrocalcin	(Nakagawa et al., 1987)
α-1- microglobulin	(Morse and Resnick, 1988)
haemoglobin	(Peterson et al., 1989)
neutrophil elastase	(Peterson et al., 1989)
transferrin	(Fraij, 1989)
osteopontin (uropontin)	(Shiraga et al., 1992)
α-1-antitrypsin	(Umekawa et al., 1993)
CD59 protein (protectin)	(Binette and Binette, 1993)
superoxide dismutase	(Binette and Binette, 1994)
β-2-microglobulin	(Dussol et al., 1995)
α-1-acid glycoprotein	(Dussol et al., 1995)
apolipoprotein A1	(Dussol et al., 1995)
retinol-binding protein	(Dussol et al., 1995)
renal lithostathine	(Dussol et al., 1995)
urinary prothrombin fragment 1	(Stapleton et al., 1996)
inter-α-trypsin inhibitor chains	(Dawson et al., 1998a)
calprotectin	(Umekawa and Kurita, 1994)
fibronectin	(Masao et al., 2000)
calgranulin	(Pillay et al., 1998)

However, some urinary proteins also possess a further property, which has previously unrecognised implications for the routine prevention of urolithiasis. They can bind to and become incorporated into the mineral bulk, which may then facilitate

intracellular crystal deconstruction and removal following attachment to renal cells and phagocytosis (Ryall et al., 2001). Much of the work upon which this concept is based is described in this thesis.

The specific functions of urinary proteins are poorly understood and their roles, if indeed they have any, are still open to speculation. Some urinary proteins have been shown to behave as crystallization inhibitors (Ryall et al., 1995), crystallization promoters (Campbell et al., 1989) and modifiers of the attachment of crystals to epithelial cells of the renal collecting system (Lieske et al., 1997a). They have also been proposed, on the basis of the work presented in this thesis, to facilitate the deconstruction and dissolution of crystals phagocytosed by those cells (Fleming et al., 2000, Ryall et al., 2000, Ryall et al., 2001). Those activities, however, do not necessarily define their role(s) in urolithiasis. Of the stone matrix proteins given in Table 2.3, the presence of proteins in renal stones, although suggestive of an active role in urolithiasis may result from accumulation of inflammatory products caused by the stone itself and/or passive inclusion (Ryall et al., 2000). Some researchers have also proposed that molecular abnormalities of urinary proteins may cause stone formation (Hess et al., 1991, Cao et al., 1993) by reducing their ability to inhibit crystal growth or aggregation. A list of stone matrix proteins found to date is given in table 2.3. Of those listed, Tamm-Horsfall glycoprotein (THG), nephrocalcin (NC), osteopontin (OPN), inter-α-inhibitor (IαI), urinary prothrombin fragment 1 (UPTF1) and Human Serum albumin (HSA) are discussed below in more detail, as their possible roles in urolithiasis have been studied in greater depth.

2.6.3 Tamm-Horsfall glycoprotein (THG)

THG, an acidic glycoprotein with a molecular mass of about 80 kDa (Hoyer and Seiler, 1979), was isolated from urine by Tamm and Horsfall, (1950) and its presence in stones confirmed by Melick et al., (1980). THG has a carbohydrate content of 30% by weight (Muchmore and Decker, 1985) and can undergo self-association, which increases in the presence of calcium ions (Stevenson et al., 1971) and albumin (Pesce et al., 1977), and decreases with rising urea concentration (Curtain, 1953) and alkalinity (Stevenson et al., 1971). The macromolecule is excreted from the renal epithelial cells of the ascending loop of Henlé and the distal convoluted tubules at the rate of 20-200 mg each day, making it the most abundant protein in human urine

(Hunt et al., 1994). Although small quantities are found in the matrix of CaOx stones, THG is absent from CaOx crystals precipitated from whole human urine (Doyle et al., 1991).

Despite the considerable research carried out over the last 3 decades on THG, its role is still poorly understood and its reported functions contradictory (Ryall and Stapleton, 1995). For example, THG has been reported to be a crystallization inhibitor (Kitamura and Pak, 1982, Scurr and Robertson, 1986, Hess et al., 1989, Grover et al., 1990a, Ryall et al., 1991, Grover et al., 1994), a promoter (Hallson and Rose, 1979, Rose and Sulaiman, 1982, Yoshioka et al., 1989, Grover et al., 1990a) and to have no effect on crystallization (Sophasan et al., 1980). Ryall and Stapleton, (1995) attributed these conflicting findings to differences in methodology and the ability for THG to polymerize under certain experimental conditions. Variation in molecular structure of the protein was considered to be a possible contributing factor to stone formation (Hess, 1991) but subsequent studies (Grover and Resnick, 1995, Trewick and Rumsby, 2000) have shown that THG in the urine of stone formers and healthy subjects does not differ significantly. It is clear that further research is required to elucidate the precise nature of this protein's physiological functions in stone pathogenesis, particularly in the presence and absence of other urinary proteins.

2.6.4 Nephrocalcin (NC)

NC was first isolated from human urine and described by Nakagawa and his colleagues as a glycoprotein containing 10.3% carbohydrate (Nakagawa et al., 1978). Subsequent work showed that the protein could be separated as a monomer, dimer, trimer and tetramer with molecular weights of approximately 14-15, 23-30, 45-48 and 60-68 kDa respectively (Nakagawa et al., 1981, Nakagawa et al., 1985, Nakagawa et al., 1987, Netzer et al., 1990).

The protein has been shown to be located in the epithelium of the proximal tubules and thick ascending limb of the loops of Henlé (Nakagawa et al., 1994), with urinary concentrations ranging from 5 mg/L (Nakagawa et al., 1983) to 16 mg/L (Kaiser and Bock, 1989). Its primary structure has been reported to contain 2-3 residues of γ-carboxyglutamic acid (Gla), a powerful calcium binding amino acid, assumed to be associated with the protein's ability to inhibit crystal growth (Nakagawa et al., 1983). Several studies (Nakagawa et al., 1985, Nakagawa et al., 1987, Nakagawa et al.,

1995) reported that stone patients have NC deficient in Gla, which has been assumed to reduce the protein's inhibitory effect on CaOx crystallization. Supporting research showed that three different Gla-containing proteins, namely blood coagulation factor X, osteocalcin and urinary Gla-protein, lose their crystallization inhibitory activity after thermal decarboxylation of their Gla-residues (van de Loo et al., 1987). However, another study (Colette et al., 1991) showed there was no difference in the Gla content of stone formers urinary protein compared with healthy individuals.

Ninety percent of the total inhibitory activity of urine was initially attributed to NC (Nakagawa et al., 1983, Nakagawa et al., 1984) but was later changed to 16% (Worchester et al., 1993). These estimates, however, were based on inorganic solutions and not urine. However, nephrocalcin has never been fully sequenced and evidence indicates that it may be related to bikunin, a fragment of inter-α-tripsin inhibitor (Tang et al., 1995). It is probable therefore, that nephrocalcin is not a substantive protein, which raises serious doubt about the possibility that it fulfils any function at all in urolithiasis.

2.6.5 Osteopontin (OPN)

OPN is a phosphorylated, aspartic acid-rich, 50 kDa glycoprotein, which was isolated from urine using monoclonal antibody immunoaffinity chomatography (Shiraga et al., 1992). The urinary macromolecule, initially believed to be a new protein, was named uropontin, but since its N-terminal sequence is identical to the bone mineralization protein, osteopontin, the names have become interchangeable. It was also isolated from mouse kidney cortical cells (Worcester et al., 1992) and its DNA sequenced (Kohri et al., 1992). OPN is present in renal calculi (Hoyer, 1995, McKee et al., 1995, Tawada et al., 1999) and its structure is rich in serine, aspartic acid and glutamic acid, which are the same amino acids generally abundant in proteins involved in biomineralization (Franzen and Heinegard, 1985, Prince et al., 1987). Therefore it is hardly surprising that it is one of the main proteins associated with CaOx crystals precipitated from normal human urine (Atmani et al., 1996).

OPN is localized to the cytoplasm of many epithelial cells of the distal tubules and collecting ducts of the human kidney (Brown et al., 1992) and its mean urinary level has been estimated to be approximately 3mg/L (Hoyer, 1995). Although its effects on CaOx crystallization in urine have not yet been reported, OPN has been found to

inhibit CaOx nucleation (Asplin et al., 1998), aggregation (Asplin et al., 1998) and crystal growth (Shiraga et al., 1992) in inorganic solutions. Using cultured kidney cells, Lieske et al., (1995) showed that OPN inhibits the attachment of CaOx and hydroxyapatite (Lieske and Deganello, 1999) crystals to renal cell membranes. Further work by Lieske et al., (1997a) demonstrated that the production of OPN by cultured monkey renal cells is increased by the presence of COM crystals, thus indicating a possible defence mechanism against crystal-cell attachment and possibly, an inflammatory response. Other researchers (Yamate et al., 1996, Yamate et al., 1999), however, have found that deposition of CaOx on the surface of cultured canine cells is increased in the presence of OPN. It must therefore be concluded that although there is much evidence linking OPN to stone formation, its true role remains obscure.

2.6.6 Inter-α-inhibitor

Inter-α-inhibitor, which is a three chain macromolecule complex of Mr 220 kDa, is a member of the Kunitz-type protease inhibitor superfamily (Salier, 1990, Michalski et al., 1994). Its structure consists of two heavy peptide chains (H1 and H2) and a light chain known as bikunin. Bikunin is covalently linked to the two heavy chains by a chondroitin sulphate moiety (Salier, 1990). The active part of bikunin is thought to be the carboxy-terminal domain of the molecule (Kobayashi et al., 1998).

Inter-α-inhibitor and dimers of its two heavy peptide chains with bikunin are found in healthy human urine, but more frequently in urine of male stone formers (Marengo et al., 1998). Although fragmented portions of inter-α-inhibitor have been found in renal calculi, intact bikunin has not been detected (Dawson et al., 1998a), which may result from bacterial degradation or chemical alteration of the molecule. However, bikunin is present in CaOx crystals precipitated from human urine (Atmani et al., 1996, Dawson et al., 1998b).

Some researchers have reported that only the bikunin portion of inter-α-inhibitor has the capacity to significantly inhibit CaOx crystallization in an inorganic medium (Kobayashi et al., 1998, Dean et al., 2000). Atmani and his group also demonstrated the inhibitory activity of bikunin on CaOx crystallization in inorganic solutions (Atmani et al., 1993a, Atmani et al., 1993b, Atmani et al., 1994). However, the role

of bikunin still remains unclear as its effects on crystallization in urine have yet to be tested.

2.6.7 Urinary prothrombin fragment 1 (UPTF1)

UPTF1, formerly called crystal matrix protein (CMP), is a glycoprotein of approximate Mr 31 kDa (Ryall, 1996). The protein's name was changed when immunological and amino acid sequencing studies showed that it was related to human prothrombin (Stapleton et al., 1993b, Suzuki et al., 1994b). A further study identified the protein as the F1 activation peptide of prothrombin (Stapleton and Ryall, 1995). UPTF1, like a number of blood clotting proteins, has a high capacity to complex calcium ions, a property that has been attributed to the γ carboxyglutamic acid (Gla) domain located at the N-terminal region of the molecule (Grover and Ryall, 1999, Soriano-Garcia et al., 1992). That region of UPFT1 contains 10 residues of Gla, the amino acid found only in vitamin K dependent proteins (Soriano-Garcia et al., 1992). Gla is formed by vitamin-K-dependent post-translational γ-carboxylation of glutamic acid residues, and imparts an extraordinary Ca^{++}-binding capacity to proteins in which it occurs (Burnier et al., 1981).

Interest in UPTF1 began when it was shown to be the principal protein associated with CaOx crystals precipitated from human urine (Doyle et al., 1991). Further, it was found strongly to inhibit CaOx crystal growth and aggregation in undiluted, ultrafiltered urine (Ryall et al., 1995). UPTF1 is located in the thick ascending loops of Henlé and the distal convoluted tubules (Stapleton et al., 1993a, Stapleton et al., 1998, Suzuki et al., 1999).

The protein has been reported to bind to the surface of urinary CaOx crystals (Suzuki et al., 1995b) as well as to be located within the crystal bulk (Ryall et al., 2000). These properties of the protein may have significant implications for crystal attachment to renal cells (Wesson et al., 1998, Ebisuno et al., 1999) as well as crystal comminution and dissolution following phagocytosis (Fleming et al., 2000, Ryall et al., 2000, Ryall et al., 2001). Like other urinary proteins discussed, the role of UPTF1 is not fully understood but it does possess attributes strongly linking it to stone formation.

2.6.8 Human Serum albumin (HSA)

HSA has long been associated with urolithiasis, having been shown to be present in the matrix of kidney stones (Fraij, 1989, Dussol et al., 1995) and because stone formers excrete higher levels of serum proteins than non-stone formers (Boyce et al., 1954b). HSA, which is one of the most abundant proteins found in urine, has been shown to be a powerful nucleator of CaOx, inducing the formation of COD crystals in preference to COM (Cerini et al., 1999). This has important implications for CaOx crystal-cell interactions, as COM has been reported to have a greater affinity for renal tubule cell membranes than COD (Wesson et al., 1998). HSA has also been demonstrated to have an antioxidant effect in urine, by virtue of its ability to reduce the concentration of free radicals (Chen et al., 2001). Free radicals are mainly produced by oxalate, which can damage renal tubular cells and promote the retention of CaOx crystals (Scheid et al., 1996, Thamilselvan et al., 1997). On that basis, HSA may play a protective role against stone formation.

The protein has been shown to have an affinity for COM crystals in inorganic solutions (Dussol et al., 1995), but is only a minor component of CaOx crystals precipitated from human urine (Doyle et al., 1991). It has also been reported to inhibit CaOx crystal aggregation, but not growth, in inorganic solutions (Edyvane et al., 1986), and to have no significant effect on either process in undiluted ultrafiltered human urine (Ryall et al., 1991). Like other urinary proteins, the role of HSA in urolithiasis is still open to speculation.

2.7 THE UNIQUE ROLE OF INTRACRYSTALLINE PROTEINS IN UROLITHIASIS

Although the role of proteins in urolithiasis is still poorly defined, their influence on calcium minerals is well recognised as being fundamental to the understanding of stone formation. Now emerging is a recognition that the identification of protein function must extend to the study of interaction between protein and mineral at the molecular level. Individual proteins are constructed from sequentially, but uniquely linked amino acids, which may interact in a specific manner with the array of atoms and molecules that make up the ordered architecture of crystals, provided that there

is complementarity and molecular recognition of the chemical groups of each (Addadi et al., 2001). Molecular recognition requires a match between the regularly repeating components of the crystal lattice with a compatible molecular sequence along the protein backbone. The amino acid groups of proteins are of prime importance in the interaction of protein with crystals (Addadi et al., 2001), since their sequence and cross-linking through disulphide bridges dictate the conformation that the molecules will adopt in solution, and thus, the stereospecific way the molecule docks on to the crystal surface. The most likely parts of the amino acids that bind to calcium mineral surfaces are the free carboxyl groups of terminal amino acids (Addadi and Weiner, 1986). Thus aspartic acid, glutamic acid and Gla, having at least two carboxyl groups capable of binding to the surfaces simultaneously, are expected to bind more avidly to calcium minerals than amino acids possessing only one carboxyl group.

The ultimate goal of the work described in this thesis was to obtain detailed information about the physical relationship between the organic and inorganic phases of human kidney stones – particularly between intracrystalline proteins and their mineral hosts. In view of the importance of the type and structure of amino acids in determining whether a protein will interact with a calcium mineral, a study of the adsorption affinity of amino acids with calcium salts comprising human kidney stones was considered to be the first step. Chapter 4 of this thesis is therefore devoted to a study of the binding of amino acids to various calcium salts. Chapter 3 describes the materials and methods used for this and subsequent chapters.

3. MATERIALS AND METHODS

3.1 MATERIALS

3.1.1 Chemicals and biochemicals

$CaCl_2$ (Sigma Chemicals, 99.5%,)

$(COONa)_2$ (Ajax Chemicals, 99.0-100%)

$CaHPO_4$ $2H_2O$. (Ajax Chemicals, 98%)

$Ca_3(PO_4)_2$ (Prolabo, Rectapur, 98%)

$Ca_5(PO_4)_3OH$ (Aldrich Chemicals, 98.5%)

$(COO)_2Ca.H_2O$ (Unilab, 98%)

NaOH (Ajax Chemicals, 97%)

NaOH 0.1M and 1.0M (Convol standard reagents BDH Lab Supplies)

HCl 0.1M and 1.0M (Convol standard reagents BDH Lab Supplies)

Ethylene diamine tetraacetic acid (Ajax Chemicals, 99.0-101%)

Tris[hydroxymethyl]-aminomethane (Sigma Chemicals, 99.8-100.1%)

Proteinase K (Boehringer Mannheim)

Phenylmethylsulfonyl fluoride (PMSF) (Sigma Chemicals, 99%)

N-α-p-tosyl-L-lysine chloromethyl ketone hydrochloride (TLCK) (Sigma Chemicals, 97%)

N-tosyl-L-phenylalanine chloromethyl ketone (TPCK) (Sigma Chemicals, 97%)

Prothrombin (Prepared by Flinders Medical Centre) (Stapleton et al., 1995)

Tamm-Horsfall glycoprotein (Prepared by Dr Phulwinder Grover and Ms Magali Chauvet, Flinders Medical Centre) (Grover et al., 1990a)

Crystal Matrix Extract (CME) (Prepared by Ms Magali Chauvet, Flinders Medical Centre). CME is the organic portion (mainly macromolecules) remaining after demineralization of CaOx crystals precipitated in CF urine (Doyle et al., 1995, Ryall et al., 1995).

Gelatin (BDH Chemicals)

Human Serum albumin (Sigma Chemicals, 96-99%)

L-forms of aspartic acid, threonine, serine, glutamic acid, proline, glycine, alanine, cysteine, valine, methionine, methionine sulphate, isoleucine, leucine, norleucine, tyrosine, phenylalanine, lysine, histidine and arginine. (BDH Chemicals, not less than 98.5%)

γ-carboxyglutamic acid (Sigma Chemicals)

Aspartic-aspartic acid (BDH Chemicals)

Glutamic-glutamic acid (BDH Chemicals)

Double-distilled water was used in all experiments.

3.1.2 Standard solutions for Atomic Absorption Spectrophotometry

Primary calcium standard solution (10.00 ±0.03 mg/L, High Purity Standards, Charleston, USA)

3.2 METHODS

3.2.1 Amino acid adsorption

A saturated aqueous solution of CaOx at pH 5 was prepared by stirring 2 g of COM in 50 mL of distilled water at 37°C for 1 day, adjusting the pH to 5, then leaving it to stand for a further two days to equilibrate. The residual crystals were separated by vacuum filtration through a 0.5 μm polyvinyl chloride membrane filter (Millipore) and discarded. A 10 mL aliquot of the filtrate was added to a glass vessel containing crystals of COM (500 mg), and a single amino acid at a final concentration of 4 mg/L, which is in the range reported for amino acids in urine (Kohri et al., 1989).

The pH was checked and adjusted to the original value, and the crystal suspension incubated for 15 hours at 37°C with gentle stirring. The pH values of the aqueous solutions were adjusted with either 0.1M HCl or 0.1M NaOH. After filtration (Acrodisc Millipore 0.45 μm), 10 mL of each solution was mixed with 0.4 mL 1M HCl and the amino acid concentration determined by High Performance Liquid Chromatography, (HPLC: Waters, Model 510, Australia) using a Waters cation ion exchange column and post column derivatisation with ninhydrin to achieve the required sensitivity (Spackman et al., 1958, Blackburn, 1968). The difference between the concentration of amino acids before and after contact with the CaOx monohydrate was used as a measure of adsorption on to the crystals. Measurements for each amino acid were performed in triplicate. To assess the possibility of removal of amino acids by bacterial contamination, parallel experiments were carried out from which the calcium mineral salts were omitted. In every case, the concentration of amino acid at the end of the incubation period was identical to that at the beginning. Furthermore, bacteria were never evident in FESEM micrographs of crystals incubated with amino acids. This procedure was repeated for the other amino acids and COM at other pH values encompassing those occurring in healthy human urine (pH 5-8).

3.2.2 Effect of free calcium ions on amino acid adsorption

To determine whether the presence of free calcium ions in solution affected the binding of amino acids to CaOx monohydrate and calcium phosphate, the amino acids were dissolved in solutions of $CaCl_2$ (1000 mg/L) at a final concentration of 4mg/L then added to each of the substrates as described in the adsorption experiments.

3.2.3 Molecular dimensions and surface coverage

Van der Waals dimensions of the Zwitterion forms of aspartic acid, glutamic acid and γ-carboxyglutamic acid were calculated using PC Spartan Plus (Wavefunction Inc., Irvine, CA, U.S.A.) molecular modelling software. The molecular area projections were used along with measured adsorption densities and substrate surface areas to calculate the fraction of the surface area covered by the adsorbed molecules.

3.2.4 Preparation of CaOx crystals grown in synthetic solutions

Crystals of CaOx were generated by mixing 5mL of aqueous solutions of 0.15 M calcium chloride and 0.15 M NaOx at a rate of 0.4 mL per hour from glass syringes using an infusion pump (Sage Instruments, USA), into distilled water (30 mL) at 37°C. The mixture was gently agitated with an overhead stirrer fitted with a glass stirring rod at 37°C. After chosen growing periods, a small portion of the mixture was removed and crystals separated by vacuum filtration and dried under nitrogen. These crystals served as controls for comparison with the other crystals.

In Chapters 5, 6 and 7 CaOx crystals were prepared identically to the control but grown for fifteen hours in solutions of prothrombin (10.0 mg/L), Tamm-Horsfall glycoprotein (20.0 mg/L), Human Serum albumin (20.0 mg/L), Crystal Matrix Extract (2.0 mg/L), (γ-carboxyglutamic acid 220.0 mg/L) and other amino acids (1000.0 mg/L).

In Chapter 8, CaOx crystals were prepared identically to the control grown at fifteen hours, but in aqueous solutions of prothrombin (0.66, 4.3, 10.3, & 21.4 mg/L), Human Serum Albumin (12.2, 31.6, 61.4, 123.9, 160.4 & 312.5 mg/L), Crystal Matrix Extract (0.7, 2.3, 3.1, 4.2 & 11.0 mg/L) and γ-carboxyglutamic acid (2.5, 10.0, 50.6, 71.8, 98.0, 162.0 & 250 mg/L).

In Chapter 9, calcium oxalate crystals were grown in an aqueous solution of prothrombin (20 mg/L), as previously described in Section 3.2.4. The crystals were harvested after 1 and 13 hours, separated by vacuum filtration, washed with a saturated solution of CaOx and dried under nitrogen.

Bulk samples of pure CaOx crystals were prepared by mixing together 200 mL of aqueous 0.1 mol/L $CaCl_2$ and 0.1 mol/L NaOx solutions dropwise, into 600 mL distilled water at 37°C. The mixture was gently agitated for 13 hours with an overhead stirrer fitted with a glass stirring rod. Precipitated crystals were separated by vacuum filtration, washed with a saturated solution of CaOx and dried under nitrogen. These crystals were used as controls.

3.2.5 CaOx crystals grown in gelatin

CaOx monohydrate crystals were grown in gelatin at room temperature in accordance with the method outlined by Henisch, (1970). Solutions of $CaCl_2$ (0.15M) and NaOx (0.15M) were introduced into each side of a glass U tube containing a plug of gelatin gel at the U bend. After a growth period of twelve weeks, COM crystals were removed from the gelatin layer with tweezers, washed with saturated CaOx solution, separated by vacuum filtration, dried under nitrogen and stored in a desiccator.

3.2.6 Collection and treatment of urines

Approval for urine collection was obtained from the Flinders Clinical Research Ethics Committee of the Flinders Medical Centre. Urine samples were collected over a 24 hour period from healthy individuals who had no history of kidney stone disease. The samples were refrigerated during the collection period and during storage before use. Absence of blood from the specimens was confirmed using Multistix test strips (Miles Laboratories Mulgrave, Victoria, Australia). The samples were pooled and centrifuged at 10,000 x g for 15 min at 20°C in a Beckman J2-21 M/E centrifuge (Beckman Instruments, Palo Alto, CA, USA.). The supernatant was filtered through 0.22 μm Millipore filters (# GVWP 14250, Millipore Corporation, Bedford, MA, USA.). A portion of the centrifuged and filtered (CF) urine was ultrafiltered (UF) using Millipore hollow fibres to exclude macromolecules >10 kDa.

3.2.7 CaOx crystals grown from human urine

The metastable limits of the centrifuged and filtered (CF) urine and ultrafiltered (UF) urine were initially determined as described by Ryall et al., (1985). Briefly, the metastable limit of urine with respect to CaOx is the minimum amount of oxalate required to elicit spontaneous detectable CaOx crystallization using a Coulter Counter.

In Chapter 9, urine samples were collected under refrigeration from five healthy subjects. They were pooled, confirmed to be free of blood by dipstick analysis (Miles Diagnostics, Vic, Australia), centrifuged (10,000 x g) in a Beckman J2-21 M/E centrifuge, Millipore filtered (0.22 μm) and divided into four 50 mL portions. A standard load of oxalate in excess of the metastable limit was then added drop-

wise to each portion to induce CaOx crystallization, and the four urine samples incubated with shaking at 37°C. After one hour, crystals were isolated by vacuum filtration from the urine in flask 1, while a second oxalate load was added drop-wise to the flasks 2 and 3. After two hours, crystals were harvested from flask 2, and a further load added drop-wise to flask 3, from which the crystals were removed after a further two hours incubation. Crystals in flask 4 were allowed to grow in the urine sample for four hours having received only one standard oxalate load. The same procedure was repeated for a UF urine sample (Section 3.2.6). After separation from the CF and UF urine samples, the crystals were washed with distilled water, dried under nitrogen and fractured using a diamond cell (High Pressure Diamond Optics).

In chapter 10, CaOx crystals were precipitated from the urine of a healthy individual by the addition of oxalate. Prior to the addition of oxalate, one half of the CF urine sample was centrifuged at 10,000 x g and filtered (0.22 μm), and the other half (UF) ultrafiltered to remove proteins > 10kDa. The resulting crystals, were washed with distilled water, separated by vacuum filtration and dried (Doyle et al., 1991).

3.2.8 COM crystals grown from ultrafiltered human urine

UF urine contains only small peptides and proteins <10kDa whereas CF urine contains most of its protein complement. A description of the preparation of COM crystals grown in UF urine is given in Section 3.2.6.

In Chapter 8, the concentrations of CME added to the UF urine were 0.05, 0.50, 1.0 and 5.0 mg/L. The concentrations of HSA added to the UF urine were 10.0, 30.0 and 60.0 mg/L.

In Chapter 9, the same procedure was adopted, as in Section 3.2.7 for CF urine, but only one load of oxalate load was added in this instance.

3.2.9 Proteolytic digestion of CaOx crystals

A sample of CaOx crystals (5 mg) grown in distilled water was incubated at 37°C for 12 hours in a 2 mL CaOx saturated aqueous solution containing 0.25 mg/mL Proteinase K and 12.5 mM Tris-HCl buffer, pH 7.0. The crystals were separated by vacuum filtration, washed with CaOx saturated distilled water and dried under

nitrogen. The same procedure was carried out for all other whole and fractured CaOx crystals.

3.2.10 Crystal phase confirmation

The composition of the CaOx phases was determined by powder X-ray diffraction analysis using a Philips PW 1830 (Almelo, The Netherlands) X-ray diffractometer. For confirmation of the crystal phases, the spectra were compared with the Inorganic Crystal Structure Database, collection code 30782 (Inorganic Crystal Structure Database, 1999).

3.2.11 Crystal surface area

The average surface area of each batch of substrate was determined by nitrogen adsorption using a Quantachrome Autosorb instrument (New York, USA) and the Brunauer-Emmett-Teller (BET) method with adsorption being measured at five different pressures.

3.2.12 Field emission scanning electron microscopy

CaOx crystals were mounted on double sided carbon tape fixed on aluminium stubs. The samples were coated with carbon (25 nm, speedivac model 12E6) and examined using a JEOL 6300F field emission scanning electron microscope (FESEM; JEOL, Tokyo, Japan). Imaging was performed with secondary electrons generated by a 3 keV primary electron beam. Images were recorded digitally.

3.2.13 Collection of data for Synchrotron X-ray diffraction

SXRD patterns were collected on BIGDIFF, a synchrotron diffractometer installed on Beamline 20B, Australian National Beamline Facility (ANBF) at the Photon Factory Synchrotron-Radiation Facility within the National Laboratory for High Energy Physics (KEK), Tsukuba, Japan. The radius of the camera is 573 mm, which gives a scaling factor of 1°/cm along the circumference. The monochromator was set at a wavelength close to the CuKα radiation doublet and the incident beam dimensions were fixed at a height of 0.8 mm and width of 10 mm. Sample run times were 900 seconds for both COM and a lanthanum hexaboride (LaB_6) line profile standard, and 300 seconds for silicon wavelength standard. Four imaging plates (400mm x 200mm; Fuji Photo Film Co., Tokyo, Japan) were used to record the

diffraction patterns. The diffraction pattern image on the plate was digitised to produce an eight bit image which gave an angular resolution of 0.01° 2θ. This is less than the ultimate resolution determined by the footprint of the capillary (0.05° for a capillary diameter of 0.5 mm). BIGDIFF is fitted with 8 radioactive fiducial markers which were used to determine the 2θ offset for each imaging plate by using the known 2θ values for the markers, as determined by tests with the silicon standard of known Bragg angle (θ) values. Crystals were packed into glass capillaries made of low-absorption lithium borate with a 0.5 mm internal diameter and a wall thickness of 0.01 mm.

3.2.14 Rietveld whole pattern-fitting of X-ray diffractograms

The X-ray data were subjected to Rietveld refinement (Hill et al., 1995) using Rietica for Windows 95/98/NT Version 1.72 (Hunter, 1998). Gaussian and Lorentzian contributions to X-ray peak profiles were obtained using a Voigt function (Langford, 1978, Langford et al., 1991). These contributions, expressed as whole pattern refined values, were used in equations 2 and 3 to calculate lattice strain and crystallite size. Parameters refined were phase scale, overall thermal parameter, unit cell parameters (a,b,c,β), atomic coordinates for Ca_1, Ca_2, background (Cheby 1), zero offset, Gaussian peak broadening coefficient (U), crystallite size, preferred orientation and Gaussian peak anisotropy (U_{anis}). These refinement conditions are shown in Appendix I 3. The model was set up for COM using as initial parameters the space group (P 1 21/c 1) and cell parameters (a,b,c & β) obtained from the Inorganic Crystal Structure Database, collection code 30782 (Inorganic Crystal Structure Database, 1999). A silicon NBS powder standard (NIST SRM 640) (Certificate of Analysis, 1974) was used to determine accurately the wavelength of the X-ray radiation used and to establish the 2θ offset for each image plate according to the fiducial marker images. SXRD data obtained from the LaB_6 powder standard was used to construct a plot of full width of the peak at half maximum height (FWHM) - *versus* - 2θ in order to determine the instrument profile. Coefficients U, V and W of Equation 1 (Cagliotti et al., 1958, Klug and Alexander, 1974) were obtained for use in the Rietveld refinements of all X-ray crystal data. The U value was used as an initial value which was open to refinement, but the V and W values were kept constant throughout each refinement, being functions of the instrumental conditions.

$$FWHM = [U (\tan^2\theta) + V(\tan\theta) + W]^{1/2} \quad (1)$$

where

U is the strain peak broadening coefficient, and V and W are instrument contributions to the broadening

Non-uniform strain information was obtained by subtracting the instrumental broadening contribution and then separating crystallite size effects from strain effects. For Rietveld analysis, the instrumental contribution was determined using a LaB_6 standard (NIST SRM 660) (Certificate of Analysis, 1989), which has little broadening caused by particle size or non-uniform strain.

The non-uniform lattice strain (root mean square; rms) strain, $\langle \varepsilon^2 \rangle^{1/2}$, was calculated using equation (2) (Cagliotti et al., 1958, Klug and Alexander, 1974), where U and U_r were determined from the Gaussian contribution to the peak shape profile of the sample and a strain free reference respectively, by Rietica.

$$\langle \varepsilon^2 \rangle^{1/2} = \pi (U-U_r)^{1/2} / [(720) (2\ln 2)^{1/2}] \quad (2)$$

The error in $\langle \varepsilon^2 \rangle^{1/2}$ was calculated using the total derivative:

$$\delta \text{ (total error)} = C (\delta U - \delta U_r) / 2(U-U_r)^{1/2} \quad \text{where } C = \pi / [(720) (2\ln 2)^{1/2}]$$

δU and δU_r were determined by Rietica.

Average crystallite size (D) was computed by Rietica and was derived from the Lorentzian contribution to the peak shape profile according to Equation 3 (Hunter, 1998), where the sec θ dependent term describes particle-size effects and λ is the wavelength of x-rays used (0.149576 nm). This was reasonable as the Lorentzian value (γ) for the strain free reference was very close to zero.

$$FWHM_L = [180\lambda \sec\theta] / [\pi D] \quad (3)$$

The errors in non-uniform strain and crystallite size are estimated from the statistical variation of the diffraction data and do not include systematic errors.

3.2.15 Statistical analyses

Assessment of the significance of differences in non-uniform strain, crystallite size and linear relationships was based on the null hypothesis, i.e. there being no difference in the two quantities being compared. Both the z value (Equation 4) and probability (p) of the null hypothesis being true are presented.

$$Z = [(O_1 - O_2) - (E_1 - E_2)]/[\sigma_1^2/n_1 + \sigma_2^2/n_2]^{1/2} \quad (4)$$

Where O_1, O_2 are the observed values

E_1, E_2, are the expected values (null hypothesis, $E_1 - E_2 = 0$)

σ_1, σ_2 are the root mean standard errors of the observed values

n_1, n_2 are the population sizes of the observations

3.2.16 Discrete peak analysis

Shadow (SHADOW, 1998) computations were conducted to determine Gaussian and Lorentzian contributions to individual x-ray peak shape profiles arising from specific lattice planes. Lattice strain along individual planes (S) was calculated using the Gaussian contribution to the line shape function using equation 5 (Klug and Alexander, 1974, Langford et al., 1991), where $FWHM_G$ and $FWHM_{GC}$ are derived from the Gaussian contributions to the peak shape profile of the sample and the "strain free" control.

$$S = \pi [FWHM_G^2 - FWHM_{GC}^2]^{1/2} / [(360)(8\ln 2)^{1/2}(\tan\theta)] \quad (5)$$

Crystallite size (D_p) was calculated from the Lorentzian contribution to the peak line shape function using equation 6 (Langford et al., 1991), where $FWHM_L$ and $FWHM_{LC}$ are the Lorentzian contributions to the peak line shape of the sample and the "strain free" control. Peak profiles are shown in Appendix I.4 and I.5.

$$D_p = 180\lambda\sec\theta / [\pi(FWHM_L - FWHM_{LC})] \quad (6)$$

The errors for Gaussian and Lorentzian contributions were determined by SHADOW and are derived from the statistical variation of the diffraction data, and do not include systematic errors. The error for the lattice strain and crystallite size was calculated using the total derivative of equations 5 and 6.

3.2.17 Williamson-Hall plots

The Williamson-Hall plot was introduced in 1953 to study dislocation broadening. Previous to this, Stokes and Wilson, (1944a, 1944b) had shown that broadening of X-ray diffraction peaks (reflections) was due to small particle size and lattice strain and had the angular dependencies,

$$\beta_p = \lambda / D \cos\theta$$

$$\beta_s = 2\varepsilon \tan\theta$$

where

β (integral breadth) = peak area / peak intensity

β_p is the size contribution to the integral breadth

β_s is the non-uniform strain contribution to integral breadth

ε is the strain

D is the average crystallite size

λ = wavelength of x-ray radiation used

Williamson and Hall, (1953) used these dependencies to graphically analyse the broadening, i.e.

$$\beta = \lambda / D \cos\theta + 2\varepsilon \tan\theta$$

hence $\beta \cos\theta / \lambda = 1/D + 2 \varepsilon \sin\theta / \lambda$

and $\beta^* = 1/D + d^* \varepsilon$

where

$$\beta^* = \beta \cos\theta / \lambda$$

$$d^* = 2 \sin\theta / \lambda = 1/d$$

d = crystal lattice plane d spacing

When it is difficult to obtain an accurate measure of the peak area because of low signal to noise ratios (as was the case for many COM peaks), the FWHM (Γ) is preferred to integral breadth, as it will have the lower error. It is generally accepted that $\Gamma^* = 0.9\ \beta^*$ (Ungar et al., 1988) and calculated integral breadths and measured FWHM for well-defined diffraction peaks in COM were found to correlate well with this ratio.

Therefore the expression

$$\Gamma^* = 0.9/D + d^* \varepsilon \qquad \text{where } \Gamma^* = \text{FWHM} \cos\theta / \lambda$$

was used to analyse the data, i.e. strain is proportional to the slope of the plot whilst crystallite size is inversely proportional to the intercept.

3.2.18 X-ray diffraction profiles

In addition to the broad "humps" in X-ray diffractograms resulting from amorphous COM material, there is also contribution from the glass of capillary tube sample holders. To define the contribution of the glass capillary tube, the diffractograms of a pure silicon standard (NIST SRM 640) (Certificate of Analysis, 1974) was compared with that of highly crystalline COM grown slowly in gelatin (Section 3.2.5). The silicon standard is a well characterised highly crystalline substance which has negligible amorphous content. Therefore it can be used to quantify any contribution to peak broadening contributed by the glass capillary alone.

3.2.19 Optical crystallography

Crystals were examined under crossed polarisers using an Olympus BH-2 microscope and X1000 magnification.

3.2.20 Computer Modelling: COM crystal structure

The modelling program used was acquired from http://gdis.seul.org and the COM crystallographic data used was that published by Tazzoli and Domeneghetti, (1980), (Inorganic Crystal Structure Database, 1999).

3.2.21 Maximum concentration of PT in COM crystals

For Chapter 7, the mass of total COM produced (Section 3.2.4) = 0.096 g

Mass of PT used in 40 mL solution = 10μg/mL(mg/L) X 40 mL = 400 μg
Estimated maximum incorporated % PT in COM = (400 μg X 100)/ 0.096 g = 0.42%

For Chapter 9, the mass of COM produced = 0.096 g.
The mass of PT used in 40 mL solution = 20 mg/L X 40 mL = 800 μg.
Therefore the % PT with respect to COM = 0.84% (mass/mass) or 0.0017% (mole/mole).
Note: MW of COM = 146.12 and MW of PT = 72,000.

3.2.22 Crystal dissolution

A quantity of CaOx crystals (approximately 20mg) prepared from CF urine was accurately weighed using a five decimal place Mettler balance (Model AE 163) into a 100 mL glass beaker positioned in a water bath set at 37°C. The dissolution solution (60 mL, 37°C) was added to the glass beaker and the mixture stirred with an overhead stirrer (~200 rpm). After the addition of the dissolution solution, one mL aliquots were removed from the reaction mixture with pre-weighed 10mL plastic syringes fitted with Acrodisc (0.2 μm) filters at different times over 60 minutes. The weights of the filtered liquid samples were accurately determined by reweighing the plastic syringes. Approximately 0.5mL of the filtered aliquots were dispensed into 25 mL glass scintillation vials and reweighed. Approximately 10 mL of 0.1M HCl was added to each vial, and the vials were weighed again to obtain the final solution weights. The concentration of calcium in the solutions was determined by atomic absorption spectrophotometry (Section 3.2.24). This procedure was repeated for CaOx crystals grown in distilled water and UF urine. The dissolution experiment was carried out in quadruplicate for each crystal type and these values are documented in Appendix I.13.

3.2.23 CaOx dissolution solution

A stock dissolution solution was prepared by dissolving 5.094g of disodium EDTA in 800 mL of 10 mM sodium acetate adjusted to pH 7.5 with 1.0 M and 0.10 M NaOH and HCl. The solution was made to volume in a one litre calibrated volumetric flask with distilled water. By diluting the stock solution (30mL to 100mL) with distilled water, the final dissolution solution consisted of an aqueous

solution of 4.5 mM EDTA buffered with 3.3 mM sodium acetate at pH 7.5. The solution was prepared daily and kept at 37°C prior to each experiment.

3.2.24 Atomic absorption spectrophometry (AAS)

The instrument used in the determination of aqueous levels of calcium was an atomic absorption spectrophotometer, Varian Techtron model AA-875 (Varian Techtron, Springvale, Victoria, Australia). The AAS instrumental parameters used were as follows:

- Wavelength: 422.6 nm
- Slitwidth: 200 μm
- Flame conditions: N_2O / Acetylene
- Lamp current: 7 mA

The primary calcium standard solution (10.00 ± 0.03 mg/mL) was diluted with distilled water and HCl added to give working standard solutions of 2.0, 6.0 and 10.0mg/L calcium in 0.1M HCl. A blank solution was included to provide a zero concentration point on the calibration curve generated from the working standard solutions. The blank solution was identical in composition to the standard solutions but without the addition of calcium.

3.2.25 Incubation of CaOx crystals in fresh urine: effect of proteinase inhibitors

A quantity of fresh human urine (~ 4L) was divided into two portions: one was left unaltered, while to the other was added a mixture of proteinase inhibitors containing PMSF in 100% ethanol, TLCK dissolved in 1 mM HCl, and TPCK dissolved in 100% ethanol. The final concentrations of PMSF, TLCK and TPCK in the incubations were 1mM, 135 μM, and 248 μM, respectively. CaOx crystals derived from the same urine (UF and CF urine) were each incubated for four hours at 37°C in an aliquot of the urine without proteinase inhibitors and an aliquot of the urine with proteinase inhibitors.

At the end of the incubation period (4 hrs), the crystals were harvested, washed with distilled water and dried. Finally, the crystals were coated with carbon (speedivac model 12E6) and examined by FESEM.

3.2.26 COM produced *in vivo* in human urine

Approximately 200 mL of healthy male's fresh urine was immediately filtered (0.22μm Millipore). The filtrate was dried under nitrogen and examined by FESEM.

4 AMINO ACID ADSORPTION ON CALCIUM MINERALS

The effects of individual amino acids on CaOx crystallization are difficult to study in a complex medium such as urine where their properties may be altered, or their actions frustrated by other components in solution, or when they also comprise part of the primary structure of proteins. In fact, determining whether specific amino acid residues within a protein are essential for a function would require production of mutant molecules using site-directed mutagenesis. This would be an immense and unprofitable undertaking when little is currently known about the mechanisms by which urinary proteins influence CaOx crystallization in inorganic media, and even less is understood about their true role in stone pathogenesis. An alternative approach to assessing the possible role of specific amino acids in the inhibition of CaOx crystallization is to determine their relative binding affinities for calcium stone minerals under controlled conditions, free of contamination and possible interference by other agents. Hence the binding of twenty individual amino acids to the principal calcium minerals found in kidney stones was assessed over the physiological urinary pH range. The amino acids selected were alanine (Ala), arginine (Arg), aspartic acid (Asp), γ-carboxyglutamic acid (Gla), cysteine (Cys), glutamic acid (Glu), glycine (Gly), histidine (His), leucine (Leu), isoleucine (l-Leu), norleucine (n-Leu), lysine (Lys), methionine (Met), methionine sulphate (Met-S), phenylalanine (Phe), proline (Pro), serine (Ser), threonine (Thr), tyrosine (Tyr) and valine (Val). In addition to calcium oxalate monohydrate (COM), three forms of calcium phosphate [$CaHPO_4.2H_2O$, $Ca_3(PO_4)_2$ and $Ca_5(PO_4)_3OH$; collectively referred to as CaP] were included. Although pure calcium phosphate stones are exceedingly rare, the salts are commonly associated with stones composed principally of CaOx (Prien and Prien, 1968, Yoshida and Okada, 1990).

4.1 Amino acid adsorption densities

The amount of substrate used in the adsorption experiments was based on masses that gave equal surface areas for the four minerals (Table 4.1) (Section 3.2.11). The adsorption of amino acids on the calcium minerals was monitored over an 18 hour period and little or no increase in adsorption density was observed after 6 hours contact. A typical example of the adsorption profile for the amino acids is shown in

Figure 4.1. To ensure that equilibrium had been reached, and for convenience, a contact time of 15 hours was employed for all amino acid adsorption studies (Section 3.2.1).

Table 4.1 Mass of calcium minerals used for amino acid adsorption.

Mineral	**BET Surface Area (m^2/g)**	**Mass Used (g)**
COM	2.6 (5%)	0.500 (0.0001)
$Ca_3(PO_4)_2$	24 (5%)	0.054 (0.0001)
$CaHPO_4.2H_2O$	2.1 (5%)	0.619 (0.0001)
$Ca_5(PO_4)_3OH$	76 (5%)	0.017 (0.0001)

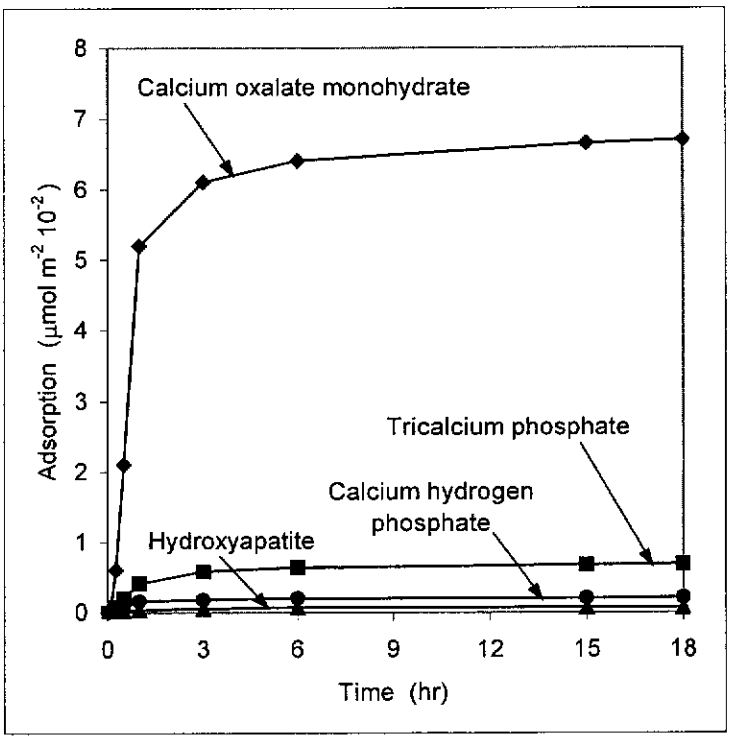

Figure 4.1 Adsorption of glutamic acid onto calcium minerals as a function of time

The presence of free calcium ions in solution did not affect the ability of the amino acids to bind to the calcium minerals, since pre-incubation with $CaCl_2$ had no measurable effect on their equilibrium concentrations in solution following contact

with the substrates (Appendix I.1) (Section 3.2.2). Adsorption of the amino acids on to the minerals over the pH range 5 to 8 showed the degree of adsorption to be greatest at pH 5 and decreasing to pH 8, with the trend of adsorption of each amino acid being similar over the pH range (Figures 4.2-4.5). The numeric results of the individual assays are listed in Appendix I.2.

The amino acids which adsorbed most strongly were Asp, Glu, Gla, with the last displaying a noticeably stronger affinity for all the minerals than the remaining amino acids. Adsorption on to $CaHPO_4.2H_2O$ was generally higher than for $Ca_3(PO_4)_2$ and $Ca_5(PO_4)_3OH$, for which all amino acids, with the exception Gla, had only a weak affinity. All amino acids demonstrated a stronger binding affinity for COM than for any of the CaP minerals.

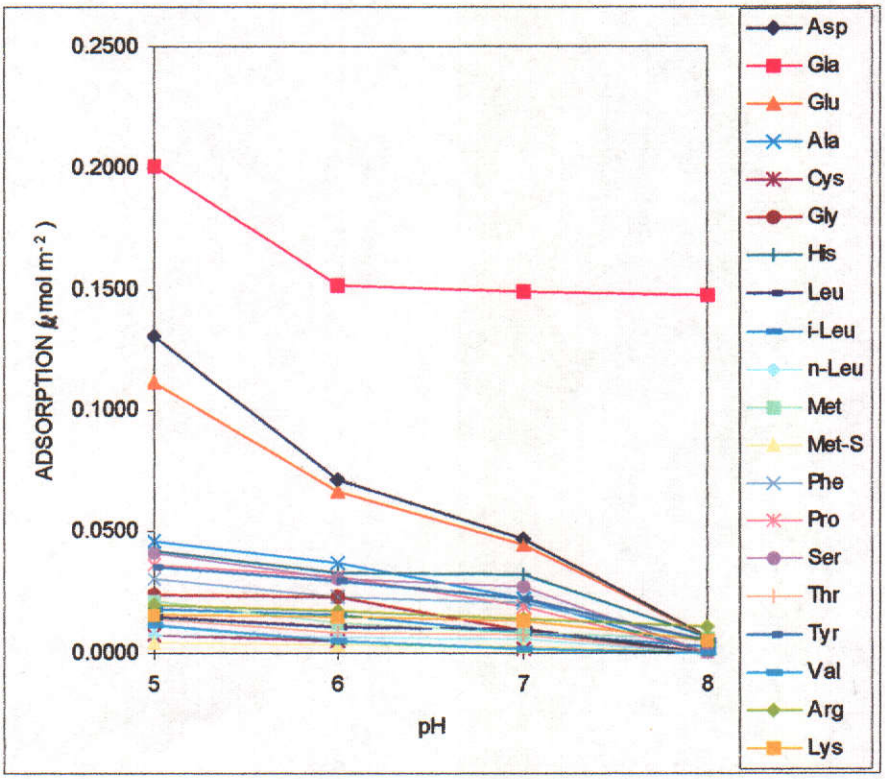

Figure 4.2 Amino acid adsorption onto COM

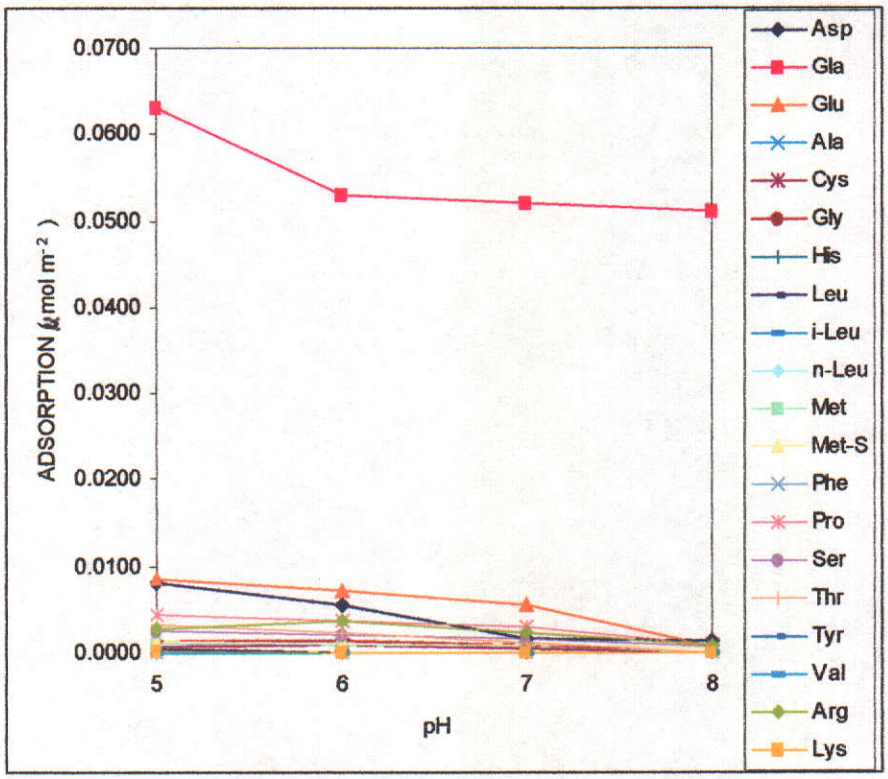

Figure 4.3 Amino acid adsorption onto $Ca_3(PO_4)_2$

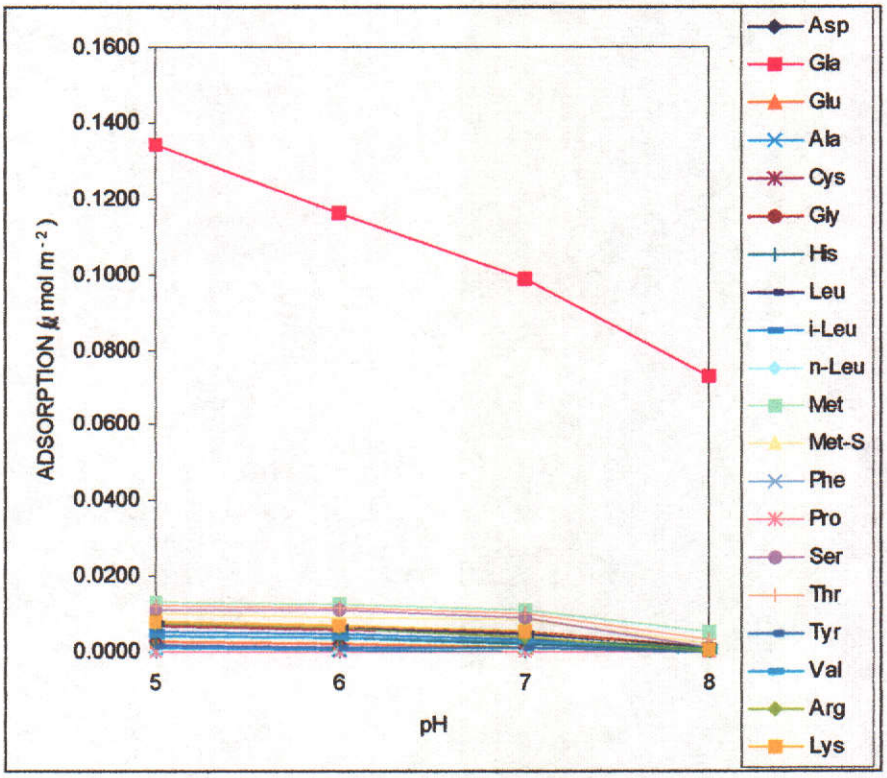

Figure 4.4 Amino acid adsorption onto $CaHPO_4.2H_2O$

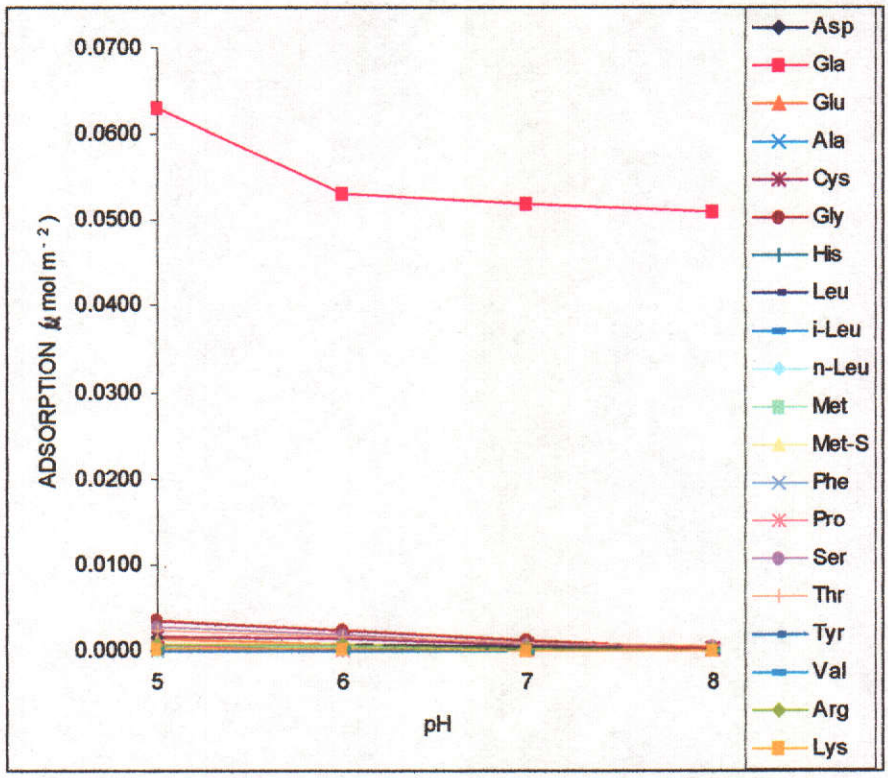

Figure 4.5 Amino acid adsorption onto $Ca_5(PO_4)_3OH$

None of the amino acids, other than Gla, showed significant adsorption at pH 8. Gla, which has two γ-carboxyl groups, adsorbed most strongly and showed little decrease in adsorption above pH 6. Asp and Glu, which have one β- or γ-carboxyl group, were slightly less adsorbed than Gla, and showed a similar decrease in adsorption between pH 5 and pH 6, but their adsorption continued to lessen significantly as the pH decreased from pH 6 to pH 8. The remaining amino acids, which have only α-carboxyl groups, were less adsorbed and their adsorption decreased most rapidly over the pH 6 to pH 8 range.

4.2 Relative adsorption strengths of Asp, Glu and Gla

The equilibrium between a molecule or ion in solution and adsorbed on a surface is described by

$$K_{ads} = [\text{adsorbed species}] / [\text{solution species}]$$

However, as amino acids in solution are an equilibrium mixture of differently ionised species, equilibrium constants based on total solution concentrations are pseudo constants (K'). They would be expected to vary with pH as either a dissociated or undissociated species could adsorb preferentially. Hence adsorption and dissociation must be treated simultaneously, ie.

$$[HAA]_{ads} \leftrightarrow [HAA]_{soln}$$

$$K_{ads} = [HAA]_{ads} / [HAA]_{soln}$$

$$[HAA]_{soln} \leftrightarrow [H^+] + [AA^-]_{soln}$$

$$K_a = [H^+] \times [AA^-]_{soln} / [HAA]_{soln}$$

$$\text{Thus} \quad K' = K_{ads} - K' \times K_a / [H^+]$$

$$K' = [HAA]_{ads} / ([HAA]_{soln} + [AA^-]_{soln})$$

$$\text{and} \quad 1 / K' = 1 / K_{ads} + (K_a / K_{ads}) / [H^+]$$

This enables both K_{ads} (the true adsorption equilibrium constant) and K_a (the amino acid dissociation constant) to be determined from the variation of K' with pH.

It should be noted that the surface charge of the substrate may also change as a function of pH, and hence the K_a values obtained may be a reflection of amino acid or surface protonation, or both.

The difference in the adsorption of the most strongly adsorbing amino acids, Asp, Glu, and Gla, is clearly illustrated by the pseudo equilibrium constants (K') obtained for their adsorption on to COM and the three CaP minerals (Table 4.2). Their typical adsorption trend as a function of pH is illustrated, for COM, in Figure 4.6. Asp and Glu adsorb identically, within experimental error, but Gla behaved differently above pH 6 on COM and the CaP minerals (Figure 4.6). All three adsorbed differently from the monocarboxy amino acids, and alanine has been included in Figure 4.6 to illustrate this. The data suggest that at least two factors are involved in the adsorption process, even though the three acids are highly ionised at the β- or γ-carboxyl groups in pH 5 and above solutions (pKa_2= 3.71, 4.15 and 3.20 respectively) (Lide, 1999).

Table 4.2 Adsorption of Asp, Glu and Gla onto calcium minerals.

		Asp		Glu		Gla	
	pH	μmol m^{-2}	10^6 K' * (m)	μmol m^{-2}	10^6 K' * (m)	μmol m^{-2}	10^6 K' * (m)
CaOx	5	0.131	10.0	0.112	8.8	0.201	12.8
monohydrate	6	0.071	3.43	0.067	3.60	0.151	6.81
	7	0.047	1.94	0.045	2.10	0.149	6.59
	8	0.0067	0.23	0.0062	0.23	0.147	6.56
$Ca_3(PO_4)_2$	5	0.0081	0.28	0.0085	0.32	0.063	1.81
	6	0.0055	0.19	0.0071	0.27	0.053	1.48
	7	0.0017	0.058	0.0055	0.21	0.052	1.44
	8	0.0013	0.043	0.0007	0.026	0.051	1.41
$CaHPO_4.2H_2O$	5	0.0028	0.094	0.0026	0.097	0.134	5.30
	6	0.0023	0.077	0.0021	0.078	0.116	4.23
	7	0.0012	0.040	0.0010	0.037	0.099	3.34
	8	0.0001	0.003	0.0001	0.003	0.073	2.21
$Ca_5(PO_4)_3OH$	5	0.0014	0.045	0.0013	0.048	0.063	1.93
	6	0.0008	0.027	0.0007	0.025	0.053	1.56
	7	0.0005	0.015	0.0003	0.010	0.052	1.52
	8	0.0003	0.010	0.0002	0.007	0.051	1.48

* K' = $[\text{amino acid}]_{abs}$ / $[\text{total amino acid}]_{solution}$, in units of 10^{-6}.

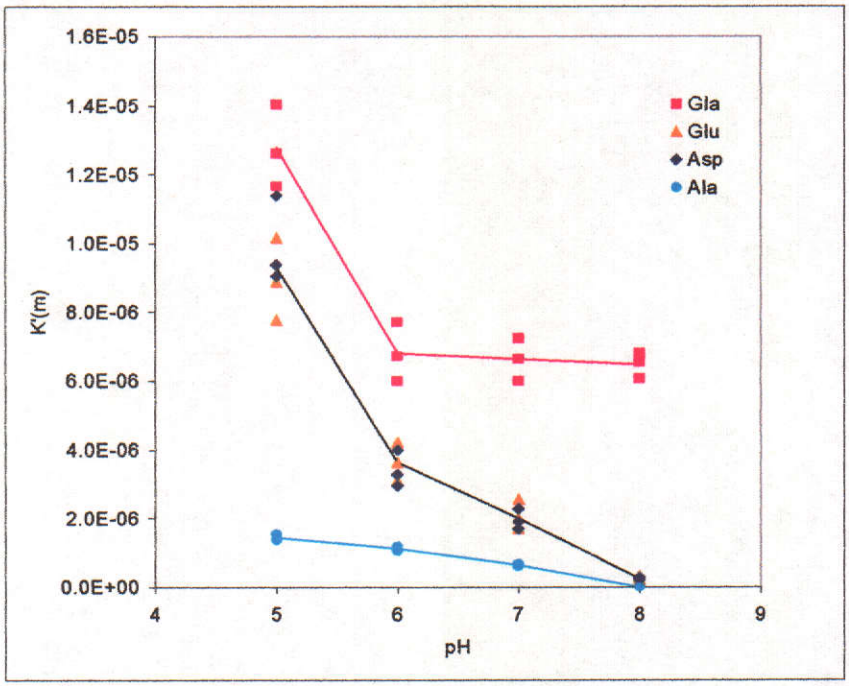

Figure 4.6 Adsorption trend of Gla, Glu, Asp and Ala onto COM as a function of pH.

Equilibrium constants for amino acid adsorption (K_{ads}) and dissociation (K_a) were obtained on the basis that Henry's Law (K = [adsorbed species]/[solution species]) can be applied. It is reasonable to do so in this instance as the adsorption densities are low, and hence adsorbed particle-adsorbed particle interaction is minimal.

The maximum area projections of Asp, Glu and Gla were calculated to be 5.0×10^{-19}, 6.0×10^{-19} and 6.5×10^{-19} m^2 respectively. The molecular area projections were used along with measured adsorption densities and substrate surface areas to calculate the fraction of the surface area covered by the adsorbed molecules (Section 3.2.3). Maximum surface coverage of Asp, Glu and Gla on COM was 4%, 4% and 8% respectively. The pK_{ads} values show the adsorption affinity of Asp, Glu and Gla for COM and the CaP minerals to have only a modest pH and substrate dependence. The major factor influencing adsorption is clearly amino acid (and/or substrate) ionisation, as indicated by the significant differences in the pK_a values obtained for Gla and for Asp and Glu, and their variation with pH (Table 4.3).

Table 4.3 Adsorption and acid dissociation equilibrium constants for Asp, Glu and Gla adsorption onto calcium minerals.

Adsorbent - Substrate	$pK_{ads}(\pm 0.2)$		$pK_a(\pm 0.2)$	
	5<pH<6	6<pH<8	5<pH<6	6<pH<8
Asp - COM	4.9	5.3	2.6	3.7
Glu - COM	5.0	5.2	2.7	3.6
Gla - COM	4.8	5.2	3.0	6.4
Gla - Ca_3P	5.7	5.8	3.6	6.4
Gla - CaHP	5.3	5.5	3.5	5.2
Gla - HOAp	5.7	5.8	3.6	6.4

4.3 DISCUSSION

The amino acids studied cover the full classification range, namely acidic, neutral and basic types. Asp, Glu and Gla bound most strongly to all of the calcium minerals tested, especially at low pH values. These three amino acids have in common at least two carboxyl groups, and as residues in certain proteins, display a high affinity for calcium (Binette et al., 1996). The strong correlation of adsorption with the number of carboxyl groups suggests that multiple binding (chelation) of the amino acid to the COM surface is a major factor, and that entropy plays a significant role, in the adsorption process. This concurs with what has been observed for citric acid, which has three carboxyl groups and is a natural component of healthy urine. It has long been known that citrate binds efficiently to CaOx crystals and inhibits deposition of further lattice ions (Meyer and Smith, 1975); consequently, it is now widely used as a therapeutic agent for preventing stone recurrences.

The other major factor contributing to adsorption strength is pH, as in most instances adsorption decreased markedly as pH was increased. For the monocarboxylic amino acids, adsorption generally decreased most rapidly between pH 6 and 8, suggesting that the zwitterion was the adsorbing species (pI ~ 6 for these acids). A decrease in adsorption with increasing pH above the isoelectic point was also observed for the dicarboxylic amino acids (aspartic acid pI = 2.77, glutamic acid pI = 3.22: (Lide,

1999) and the tricarboxylic amino acid Gla, whose pI would be expected to be less than that of Asp and Glu, reinforcing the zwitterion hypothesis. This is intriguing, as COM would be positively charged under the conditions used in this study, as a result of Ca^{2+} adsorption (Callejas Fernandez et al., 1990), and the fact that adsorption decreases as the charge on the adsorbing species becomes more negative with increasing pH.

Adsorption of Asp and Glu was significantly affected by pH, and fitted to pK_a ~3.7 in the pH range 6 to 8, suggesting that protonation of the β or γ-carboxyl group (pK_3 = 3.71 for Asp and 4.15 for Glu: Lide, 1999) was responsible. Below pH 6 the adsorption fitted to pK_a ~2.7, suggesting that protonation of the α-carboxyl group (pK_1 = 1.95 for Asp and 2.16 for Glu: Lide, 1999) also contributed to the increased adsorption. Not unexpectedly, the observed pK_a values were between those of the α and β or γ-carboxyl groups, as both would be increasingly protonated between pH 6 and 5. In contrast, the adsorption of Gla at pH 6-8 fitted to pK_a ~ 6.4, indicating that virtually no change in its protonation, which affected adsorption, occurred over this range. Below pH 6 adsorption increased markedly and protonation did occur, presumably at one of the two γ-carboxyl groups, as pK_a below pH 6 is ~3.4 ($pK_{3,4}$ = 4.75, 3.2: Lide, 1999). Thus, the results indicated that the carboxyl groups were not fully ionised over the entire pH 5 to 8 range and that the adsorbing species are significantly protonated.

This is in agreement with Noszál and Sándor (Noszal and Sandor, 1989) who showed that at pH 7.2 both carboxyl groups of Asp were deprotonated and that when the pH was decreased to the isoelectric point protonation of the β-carboxyl was not exclusive, with up to 5% of the protonation occurring at the α-carboxyl group. Furthermore, protonation was found to alter the distribution of the Asp rotation isomers (rotamers), and the gauche-$\beta COO^-/\alpha COO^-$: gauche-$\beta COO^-/\alpha NH_3^+$ (g2) rotamer populations increased as pH decreased. This rotamer has all three functional groups positioned for adsorption to a surface without further rotation (Figure 4.7). Theoretical studies of the Asp zwitterion support this view and show that the gauche-$\beta COOH/\alpha COO^-$: gauche-$\beta COOH/\alpha NH_3^+$ (g2) rotamer is the second most abundant species (Nagy and Noszal, 2000). The most abundant species, trans-βCOO^- /αCOOH:gauche-$\beta COO^-/\alpha NH_3^+$ (g1), would need to rotate about the CH-CH_2 bond

to bring all three functional groups into contact with a surface. The different rates of change of adsorption observed for Asp and Glu at pH 5-6 and pH 6-8 could thus be due to relative changes in the protonation of the α and β-carboxyl groups and consequent rotamer distributions.

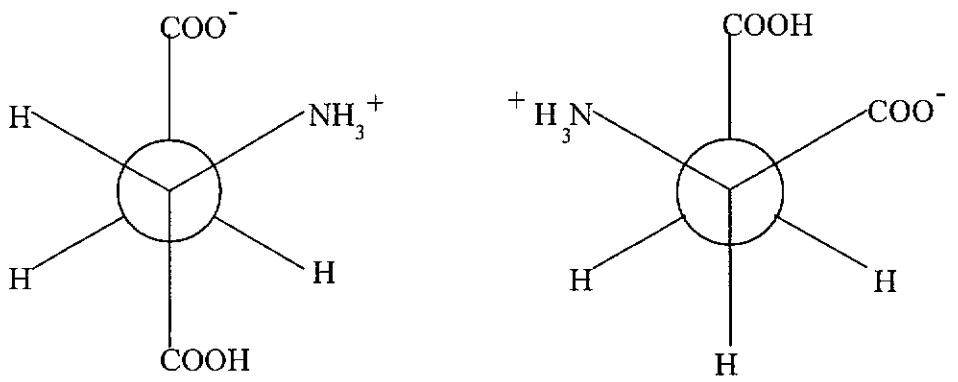

beta gauche 1 alpha gauche 2

Figure 4.7 The two most stable of six aspartic acid zwitterion rotamers.

The greater adsorption observed for Gla at pH 6 to 8 can be attributed to two of its three rotameric conformations having the required gauche-gauche arrangement, as opposed to one of three for Asp. The almost negligible change in adsorption at pH 6-8 is therefore likely to be caused by the greater capacity of the two γ-carboxyl groups to accept protons, since protonation effects on the rotamer distribution do not become apparent until pH <6. This is conceivable as the gauche-βCOOH/αCOO⁻:gauche-βCOOH/αNH_3^+ rotamer is stabilised by βCOOH/αNH_3^+ hydrogen bonding (Nagy and Noszal, 2000).

The data are thus consistent with the adsorbing species being a protonated gauche-βCOO⁻/αCOO⁻:gauche-βCOO⁻/αNH_3^+ (g2) rotamer, with protonation most probably occurring at the β carboxyl group. The initial interaction could thus be an approach of the zero-charged amino acid to the positively charged COM surface. Subsequently this could lead to the more exposed αCOO⁻ ion binding to Ca^{2+}, followed by the loss of a proton from the βCOOH and its binding to another Ca^{2+}, and possibly a further loss of a proton from the αNH_3^+ group to allow it to bind. This

tridentate binding is similar to the hexadentate binding of EDTA to calcium ions and would account for the greater adsorption of the di and tricarboxy amino acids, as the monoacids would bind as bidentates at best.

The difference in affinity of the four calcium minerals for amino acids may be a result of differences in surface charge, ion adsorption or coordination-site availability at the crystal surfaces. The pK_{ads} (5.8) obtained for both $Ca_3(PO_4)_2$ and $Ca_5(PO_4)_3OH$ suggests that these two phosphates behave similarly and with little change as a function of pH. The hydrogen phosphate ($CaHP.2H_2O$, pK_{ads} 5.4) is a slightly stronger adsorbent for amino acids and the oxalate (COM, pK_{ads} 4.8 - 5.3) is the strongest adsorbent. This sequence may be a reflection of the acid/base properties of the anions, and consequent surface charge and cation adsorption. The differences in pK_a values for Asp, Glu acid and Gla on COM at pH 5-6 compared to pH 6-8 are just sufficient to suggest that surface changes may have occurred, e.g. displacement of calcium ions by protons.

The chelation, amino acid protonation and stereochemical factors of Asp, Glu and Gla identified are significant in attempting to account for the adsorption behaviour of urinary proteins on the same mineral surfaces. For example, the principal protein associated with CaOx crystals precipitated from human urine is urinary prothrombin fragment 1 (UPTF1), an acidic degradation peptide of prothrombin (Ryall et al., 1995). The N-terminal region of this peptide contains 10 Gla residues, which almost certainly determines the extraordinary affinity of UPTF1 for CaOx crystals. Osteopontin, another urinary protein known to be present in CaOx crystals and stones and which, like UPTF1, possesses properties consistent with a role in stone formation, is rich in Asp residues (Shiraga et al., 1992). In contrast, Tamm-Horsfall glycoprotein (THG) strongly inhibits CaOx crystal aggregation in urine (Grover et al., 1990), but does not bind irreversibly to CaOx, and in consequence, is not present in alkali-washed urinary CaOx crystals (Doyle et al., 1991). An important difference between these proteins, which may explain their relative affinities for the various crystal types is the presence of acidic amino acid groups in UPTF1 and osteopontin, but their absence from THG. This is supported by observation that on removing the Gla residues from osteocalcin and urinary Gla protein by thermal decarboxylation, the inhibitory activity of these proteins on CaP and CaOx precipitation was lost (van de Loo et al., 1987). On the basis that UPTF1 has been shown to be incorporated in

CaOx crystals precipitated from human urine (Ryall et al., 1995), Asp, Glu and Gla, as well as urinary proteins possessing an abundance of these terminal acidic amino acids, such as prothrombin, were considered likely candidates for studying amino acid and protein occlusion into COM. Hence these were investigated further to help clarify the contested phenomenon of protein intracrystallinity.

5 X-RAY DIFFRACTION OF CALCIUM OXALATE MONOHYDRATE GROWN IN URINE AND AQUEOUS SOLUTIONS OF AMINO ACIDS AND PROTEINS

Evidence demonstrating the existence of intracrystalline proteins in urinary CaOx crystals has consisted of sodium dodecyl sulphate polyacrylamide gel electrophoretic (SDS-PAGE) and Western blot analysis (Doyle et al., 1991, Suzuki et al., 1994, Doyle et al., 1995, Dawson et al., 1998, Atmani and Khan, 2002). However, those studies provide no direct information about the physical basis of the relationship between the organic and inorganic crystal phases and the nature of the mineral itself. Consequently, the possibility cannot be discounted that the CaOx materials examined were not single crystals infiltrated with protein, but rather, crystallites or amorphous mineral stabilised by organic material and assembled into structures having the appearance of single crystals. Further, despite clear evidence that proteins can be incorporated into calcite crystals (see below), the possibility that urinary proteins can intercalate into calcium oxalate crystals has been disputed (Mandel, 1997).

Addadi and her colleagues used synchrotron X-ray diffraction (SXRD) to demonstrate that the spicule of the sea urchin consists of a single crystal impregnated throughout with intercalated proteins (Addadi et al., 1999). Located at the boundaries of the crystal domains, the proteins adsorb on to preferred crystallographic faces where they induce crystal defects that alter crystallite size and hence increase crystal disorder, as well as change morphology and cleavage fracture characteristics (Aizenberg et al., 1997). The inclusion of amino acids and proteins into COM would therefore also be expected to increase crystal disorder. Disorder mainly arises from imperfections and structural defects, including stacking faults, dislocations and crystallite misorientation, which may generate strain in a crystal (Cullity, 1956). This strain gives rise to diffraction peak broadening, which contributes to the Gaussian component of the width of the peak at half the maximum height (FWHM). Average crystal strain and average crystallite size contributions to peak broadening can be resolved by deconvolution of the Gaussian and Lorentzian components of a peak profile using Reitveld analysis (Langford, 1978, Langford et al., 1991). The strain contribution to line broadening is described as non-uniform

strain arising from misorientated crystallite grains. Stacking faults caused by misalignment of the crystallites also contribute to the line width (Figure 5.1). As Rietveld analysis cannot differentiate between non-uniform strain and stacking fault contributions, the former term will be used generically in this chapter. Another contribution to the strain component is uniform strain (macrostrain) which causes shifts in the Bragg peak positions (Cullity, 1956) and is hence easily distinguished from non-uniform strain.

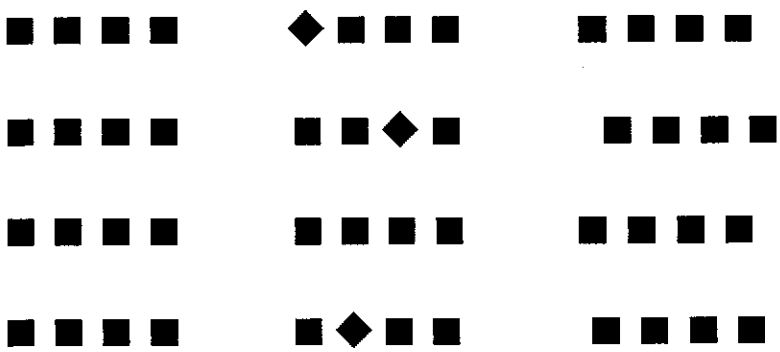

Figure 5.1 Schematic diagrams of three crystallite arrangements of a crystal with (a) no strain, (b) non-uniform strain and (c) stacking faults.

The aim of the work presented in this chapter was to clarify the relationship between the organic and mineral phases of CaOx crystals precipitated from ultrafiltered urine (UF), centrifuged and filtered (CF) urine and aqueous solutions containing selected amino acids and urinary proteins, using SXRD. The amino acids chosen were those that were shown in Chapter 4 to possess the strongest adsorption affinities for COM, namely Asp, Glu and Gla. Dimers of aspartic acid (AspAsp) and glutamic acid (GluGlu) were also used to evaluate the effect of doubling the amino chain length. Because the binding of proteins to mineral crystals will depend significantly upon their primary amino acid composition and sequence, prothrombin (PT), a Gla-containing urinary protein was selected. In contrast, urinary proteins Tamm Horsfall glycoprotein (THG) and Human serum albumin (HSA) were used because they do not contain Gla. Although lacking Gla, THG is the most abundant urinary protein and has been reported to function in urine both as an inhibitor and promoter of CaOx crystallization (Grover et al., 1990), and also as a regulator of COM adhesion to urothelial cells (Lieske et al., 1996). A further reason for studying PT and THG is

that PT is present in demineralised extracts of alkali-washed crystals precipitated from healthy male urine (Buchholz et al., 1999), whilst THG is not (Doyle et al., 1991). Crystal matrix extract (CME) was also included in the study because it has been reported to be a potent macromolecular inhibitor of crystal growth and aggregation in undiluted human urine in vitro (Doyle et al., 1995). CME is the organic portion (mainly macromolecules) remaining after demineralization of CaOx crystals precipitated in CF urine (Ryall et al., 1995). Crystals grown in CF urine and UF urine enabled the generation of crystals from urine samples with an identical complement of low molecular weight components, but markedly different macromolecular compositions. COM grown in distilled water was used as the control to allow effects resulting specifically from the influence of proteins and amino acids to be identified.

Although CaOx exists as COM, COD and COT, COM was selected for the study because it is regarded as the critical polymorph in urolithiasis (Prien, 1963, Wesson et al., 2000). It is thermodynamically stable and is the dominant phase found in CaOx renal calculi (Mandel and Mandel, 1989). Polycrystalline, rather than single crystal analysis was carried out because the amount of protein associated with individual crystals in a given preparation is variable (Ryall et al., 2001b) and an average response was required to enable comparisons to be made. XRD analysis techniques have advanced sufficiently to enable this to be carried out.

5.1 CaOx crystallography

Field emission scanning electron microscope (FESEM) (Section 3.2.12) and SXRD studies (Section 3.2.13) using Rietveld analysis (Section 3.2.14) were carried out on CaOx crystals grown in gelatin (Reference), distilled water, UF urine, CF urine and aqueous solutions of Asp, AspAsp, Gla, Glu, GluGlu, CME, HSA, THG and PT (Sections 3.2.4-8). The crystals were also examined by optical microscopy using crossed polarisers (Section 3.2.19).

COM was the only polymorph of CaOx generated from aqueous solutions and the major polymorph precipitated from UF and CF urine, which also produced a small proportion of COD. COT was not observed in any of the samples. COM crystals grown in distilled water and aqueous solutions of amino acids exhibited the classic COM hexagonal plate morphology (Figure 5.2a). A schematic diagram of COM

morphology showing commonly observed faces is presented in Figure 5.2b. COM grown in UF urine, CF urine and in PT solution had a similar morphology, but the crystals were more plate-like and had rounder edges (Figure 5.3). X-ray diffraction lines of the minor phase, CaOx dihydrate (COD), did not interfere significantly with COM diffraction lines in the urinary crystals and allowed Rietveld refinement of the crystallographic parameters to be carried out successfully. An electron micrograph of COD grown in CF urine is shown in Figure 5.4. Peak shifts in the SXRD patterns were negligible and the crystallographic parameters of all samples fell in a very narrow range (0.6294 nm < a <0.6303 nm, 1.4585 nm < b < 1.4600 nm, 1.0120 nm < c < 1.0123 nm, 109.41° < β < 109.49°) (Appendix I 3). These are in excellent agreement with published data for COM (a = 0.6290 nm, b = 1.4583 nm, c = 1.0116 nm and β = 109.50°) (Inorganic Crystal Structure Database, 1999).

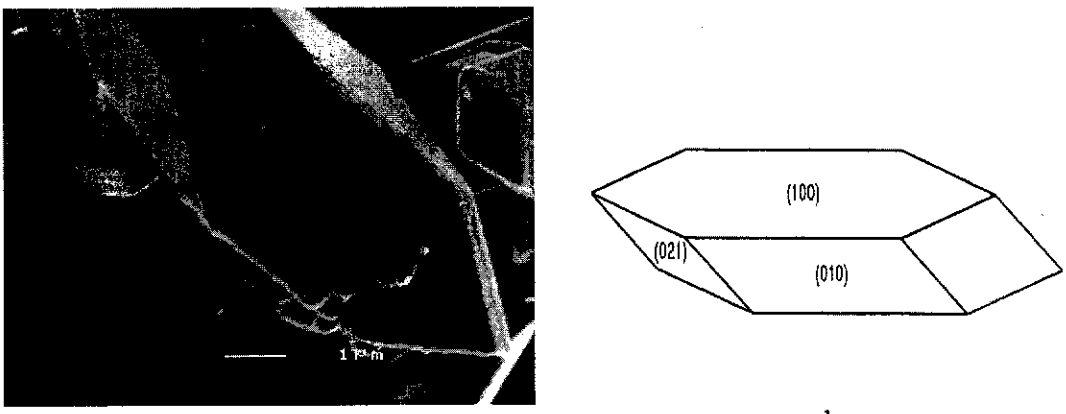

a b

Figure 5.2 COM morphology.
(a) An electron micrograph of COM crystals grown in distilled water.
(b) A schematic diagram of COM morphology showing commonly observed faces. The index settings are presented in accordance with published literature (Guo et al., 2002).

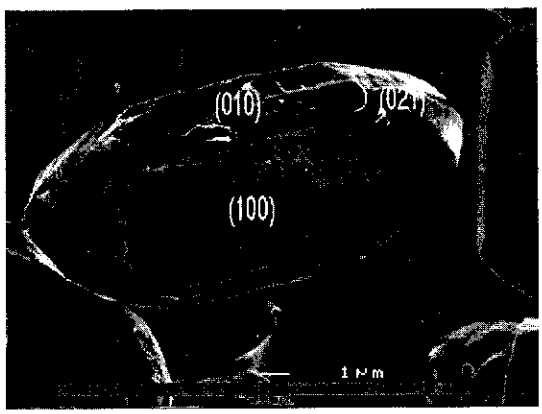

Figure 5.3 Electron micrograph of COM crystals grown in CF urine.

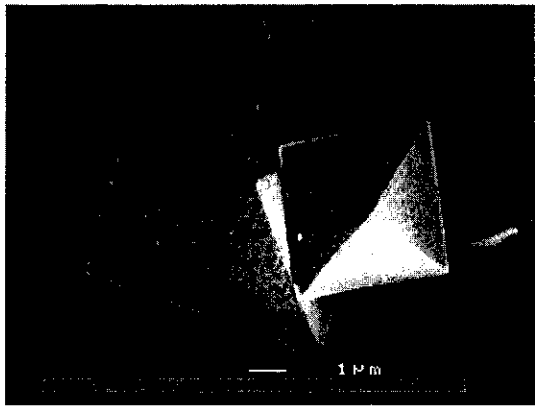

Figure 5.4 Electron micrographs of COD grown in CF urine.

The FWHM trends of SXRD peaks for each type of crystal, as defined by equation 1 (Section 3.2.14) and determined by Rietveld refinement, showed a marked variation in the rate of peak broadening as a function of 2θ (Figure 5.5).

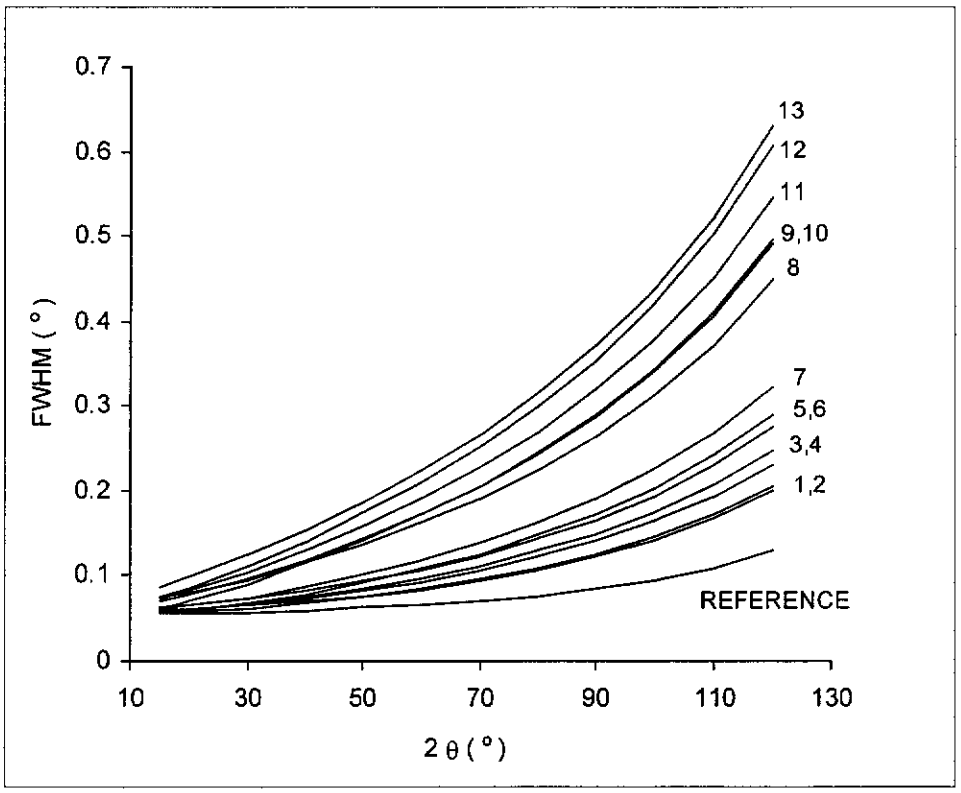

Figure 5.5 FWHM trends of SXRD peaks as a function of 2θ for COM crystals grown in gelatin gel (Reference), distilled water (1), UF urine (8), CF urine (12); solutions of THG (2), GluGlu (3), Asp (4), AspAsp (5), HSA (6), Glu (7), CME (10), Gla (11), and PT (13); and crystals grown in CF urine and subsequently treated with proteinase (9). Individual data points have been omitted for clarity.

COM grown in gelatin showed the smallest broadening rate, which confirmed it to be the least disordered sample. A greater rate of broadening, and hence greater disorder, was observed for COM grown in distilled water (control) and in the THG solution. Solutions of GluGlu, Asp, AspAsp, HSA and Glu produced COM with progressively greater broadening rates, whereas the most marked increases in broadening rates were found for UF and CF urine, and CME, Gla, and PT. Proteinase treatment of COM grown in CF urine reduced its broadening rate markedly.

Average non-uniform strain (ε) and crystallite sizes (D) calculated from the fitted peak width trends using equations 2 and 3 (Section 3.2.14) are shown in Table 5.1

Table 5.1 Average non-uniform strain and average crystallite size.

Growing Medium	Strain (ε) (%)	Crystallite Size (D) (μm)
Gelatin gel (reference)	0	> 2.60
1 Distilled water (control)	0.040 ± 0.003	2.59 ± 0.19
2 THG	0.041 ± 0.004	2.45 ± 0.17
3 GluGlu	0.043 ± 0.004	2.54 ± 0.23
4 Asp	0.045 ± 0.008	2.54 ± 0.23
5 AspAsp	0.049 ± 0.004	2.54 ± 0.23
6. HSA	0.067 ± 0.007	0.86 ± 0.08
7 Glu	0.064 ± 0.003	2.01 ± 0.26
8 UF urine	0.088 ± 0.005	0.50 ± 0.04
9 CF urine and protease	0.092 ± 0.003	0.51 ± 0.13
10 CME	0.095 ± 0.006	0.65 ± 0.07
11 Gla	0.112 ± 0.008	1.19 ± 0.09
12 CF urine	0.128 ± 0.009	0.31 ± 0.03
13 PT	0.128 ± 0.008	0.31 ± 0.03

COM grown in distilled water and in THG solution was found to have the least non-uniform strain and among the largest crystallite sizes, relative to crystals grown in gelatin. The presence of GluGlu, Asp or AspAsp in solution gave rise to a slight

increase in non-uniform strain but had little or no effect on crystallite size, whilst HSA led to a more significant increase in non-uniform strain and decrease in crystallite size ($z = 3.5$, $p \sim 0$) ($z = 8.4$, $p = \sim 0$). Similar effects were observed for Glu ($z = 5.6$, $p \sim 0$) ($z = 1.8$, $p < 0.04$), UF urine ($z = 8.2$, $p \sim 0$) ($z = 10.8$, $p \sim 0$) and CME ($z = 8.2$, $p \sim 0$) ($z = 9.6$, $p \sim 0$) (Section 3.2.15). COM grown in Gla solution was even more strained than CME ($z = 1.7$, $p = 0.04$) but had a much greater crystallite size ($z = 4.7$, $p \sim 0$). The highest non-uniform strains and smallest crystallite sizes were found for COM grown in the PT solution (0.128 ± 0.008 and 0.31 ± 0.03, respectively) and in CF urine (0.128 ± 0.009 and 0.31 ± 0.03, respectively). Proteinase treatment of the crystals grown in CF urine reduced non-uniform strain and increased crystallite size to the levels observed for crystals grown in CF urine ($z = 3.8$, $p \sim 0$, $z = 1.5$, $p < 0.07$).

Figure 5.6 shows the plotted data from Table 5.1 and reveals the existence of two reciprocal relationships between non-uniform strain and crystallite size, with proteins other than THG generating a smaller crystallite size than the amino acids for the same degree of non-uniform strain.

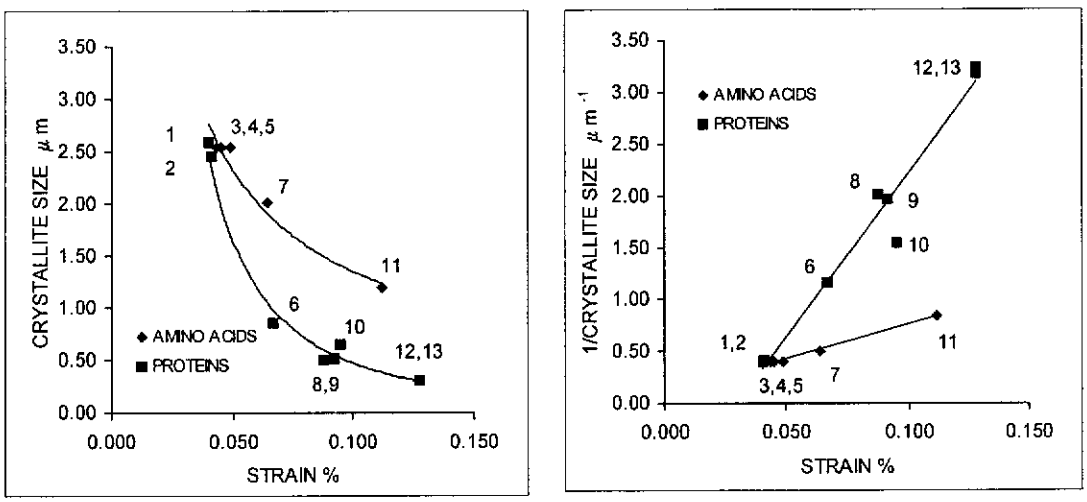

a b

Figure 5.6 Crystallite size (a) and the reciprocal of crystallite size (b) as a function of non-uniform strain, for COM grown in distilled water (1), UF urine (8), CF urine (12) and CF urine, followed by treatment with proteinase (9); solutions of THG (2), GluGlu (3), Asp (4), AspAsp (5), HSA (6), Glu (7), CME (10), Gla (11) and PT (13).

The slopes of the transformed relationships in Figure 5.6b demonstrate that the two populations, proteins (slope = 32.3 ± 0.6) and amino acids (slope = 6.6 ± 0.3), are significantly different ($z = 85$, $p \sim 0$). Figure 5.6 thus clearly shows that the degree of crystal disorder, that is, increased non-uniform strain and decreased crystallite size, is influenced by molecular size and properties, such as charge and orientation of functional groups. The non-uniform strain and crystallite size values for CME fit between those of amino acids and proteins, suggesting that it contained a mixture both of small molecules and macromolecules. Urinary prothrombin activation peptide fragment 1 (UPTF1), a 31kDa glycoprotein, has been found to be the main component of CME along with a few other proteins (Stapleton, 1995).

5.2 Optical microscopy

Microscopic examination under crossed polarisers of a random selection of crystals (6-50 micron) grown in each of the various aqueous and urine media showed the classic four distinct extinctions per 360° rotation of birefringent single crystals in every instance (Section 3.2.19). The extinctions were uniform and demonstrated that optically, all behaved as single crystals rather than individual structures comprising of aggregates of randomly oriented microcrystals.

5.3 DISCUSSION

The broad objective of the study was to obtain quantitative data describing the relationship between the organic and mineral components of COM crystals grown in UF urine, CF urine and aqueous solutions containing selected amino acids and proteins. A perfect single crystal would not consist of smaller crystallites, and therefore have an "infinite" crystallite size and zero non-uniform lattice strain. However, all crystals, even if single, can have a mosaic structure caused by dislocations and/or foreign molecules that create defects and zones of disorder, thereby reducing crystallite domain size and increasing non-uniform lattice strain (Rosenberg, 1988). Consequently, a decrease in crystallite domain size and associated increase in non-uniform crystal strain, relative to a control, would support the hypothesis that extraneous molecules are present in the crystal bulk and constitute proof that they are intracrystalline (Addadi and Weiner, 1992).

COM was the only CaOx polymorph formed in distilled water and in the presence of aqueous amino acid and protein solutions, whilst both COM and minor quantities of COD were precipitated in UF urine and in CF urine. This is in agreement with the view that the urinary matrix stabilises the less thermodynamically stable COD phase (Wesson et al., 1998). The thinning of the hexagonal shaped plates and rounding of edges observed for COM crystals grown in the aqueous PT solution, UF urine and CF urine indicated a reduction in the growth rates of the (001) and (100) faces. Slowing the growth of the (001) face resulted in blunted ends of the crystals, and rounding at the junction of the (021) and (010) faces. Slowing the growth of the (100) faces led to the thinning of the crystals. Thus the alteration in morphology was caused by adsorbed species and produced the familiar "coffin" shaped COM crystals commonly found in urine.

All refined Rietveld crystallographic values were close to those in published data (Inorganic Crystal Structure Database, 1999), indicating that the unit cell dimensions were not altered significantly by the presence of amino acids and proteins. Thus, the organic molecules, where present, were either surface-adsorbed or dispersed about the crystallites, or both, and not intercalated within the COM crystallite lattice itself.

COM grown in Asp, AspAsp, GluGlu and THG solutions exhibited non-uniform strains and crystallite sizes comparable to those of the control COM grown in distilled water. It is therefore reasonable to conclude that those molecules were not occluded into the mineral. Crystals grown in solutions of CME, Gla, Glu, HSA and PT, as well as those generated from UF and CF urine, however, had notably higher non-uniform stains and lower crystallite sizes than the control. Because increased non-uniform strain and decreased crystallite size result from incorporated molecules or ions that increase the number of stacking faults and zones of disorder within crystals (Addadi and Weiner, 1992), it can be concluded that CME, Gla, Glu, HSA, PT and endogenous urinary proteins and molecules were occluded into the COM crystals during crystal growth. The increase in crystallite size and decrease in non-uniform strain observed after proteinase treatment of the crystals grown in CF urine indicated that the smaller crystallite material, more intimately associated with proteins than with the bulk mineral, was probably liberated during the proteinase treatment.

A dominant factor that influences the occlusion of amino acids into COM is their ability to bind to calcium. Gla, which is well known for its strong affinity for calcium, is likely to attach to the COM surface and be enveloped by a growing crystal front, while amino acids with lower binding affinity are less likely to become interred within the mineral bulk. This appeared to be the case for Asp and Glu. Why Glu should create more crystal disorder than Asp, AspAsp and GluGlu is not clear, but may be associated with the stereochemistry of their binding to calcium ions on the crystal face, as discussed in Chapter 4. Stereochemistry and intramolecular hydrogen bonding may also be determining factors in reducing the binding capacity of Asp and Glu dimers for COM, producing lower non-uniform strains and higher crystallite sizes than occurred with their corresponding monomers.

The type and sequence of amino acids comprising the primary structure of proteins are of great importance in determining the nature of protein-crystal interactions (Wesson et al., 2000, Addadi et al., 2001). The presence of PT within COM crystals can almost certainly be attributed to the strong calcium-binding properties of its Gla residues. However, affinity for calcium ions is insufficient to guarantee that a protein will be incarcerated within growing COM. THG has no Gla, but still has considerable affinity for calcium (Grover et al., 1990), and therefore might be expected to be incorporated into CaOx crystals. However, the protein is not occluded into the mineral (Doyle et al., 1991, Chauvet et al., 2001), probably because of its size. THG, which has a monomeric molecular mass of approximately 94 kDa, condenses in urine and at high concentrations in aqueous solutions into polymers with molecular masses in the millions. In contrast, Osteopontin (OPN), another urinary protein thought to play a major role in stone formation, and which also lacks Gla residues, is, nonetheless, an intracrystalline component of urinary CaOx crystals (Ryall et al., 2001a). It has been generally assumed that the inhibitory effects of OPN on CaOx crystallization (Shiraga et al., 1992) as well as its association with CaOx crystals can be attributed to its unusually high content of serine, glutamate and aspartate residues (Denhardt et al., 1993), which mediate its binding to the CaOx crystal surface. OPN also contains an acidic poly-Asp domain (Hunter et al., 1996) which has been shown to have a high affinity for hydroxyapatite (and presumably CaOx) (Denhardt, 1993, Giachelli et al., 2000). However, since the work reported in this chapter has shown that Asp is not an intracrystalline component of CaOx

crystals, it would appear that OPN's properties, as well as its presence in stones and CaOx crystals, are dictated by factors other than its individual component Asp moieties. Collectively, these facts demonstrate that the inclusion of an individual protein into the COM mineral bulk is not solely determined by its calcium-binding ability, or by the presence of Gla within its primary chain.

The reciprocal relationship between non-uniform strain and crystallite size that was found for polycrystalline COM has been noted in other systems. For example, Fievet et al., (1979) showed that non-uniform strain and the reciprocal of crystallite size both varied linearly in the NiO system, and Addadi et al. (1999) made similar, qualitative observations of calcite crystals in sponges and sea urchins. In those cases it was clear that a reduction in crystallite size increased misalignment and hence non-uniform strain. The observation in this chapter that the relationship differs greatly between amino acids and proteins is the first demonstration that, for a given increment in non-uniform strain, the corresponding decrease in crystallite size is markedly greater for macromolecules than for small molecules. The difference can probably be attributed to the large disparity between the sizes and shapes of proteins and amino acids. Because of their small size, amino acids would be expected to inhibit growth only at, or very near to, the sites at which they bind to the crystal surface and therefore to cause only small local imperfections. On the other hand, a macromolecule such as a protein has the potential to interfere with the deposition of solute ions over a much larger region of the crystal surface. Delivery and attachment of solute ions to a crystal will be prevented at any point on the surface covered by the specific binding domain of any protein. However, such domains account for only a small proportion of a protein's structure, whose remaining molecular bulk also has the potential to hinder physically the transport of solute ions to the crystal surface. Crystals formed in the presence of macromolecules would therefore be more likely to incur larger disruptions to their structures than they would from the inclusion of smaller guests such as amino acids. Consequently, they would exhibit more pronounced non-uniform strain, as greater crystallite disorientation would occur with decreased crystallite size. Because of their large size, proteins are unlikely to intercalate into the COM lattice, but once adsorbed onto preferred crystal faces they could be occluded as a consequence of engulfment by the advancing growth front.

It is also possible that instead of proteins being adsorbed on to COM surfaces, the proteins themselves act as nucleating sites for COM crystallites. This would lead to disordered crystallites in regions of the crystal that are more associated with proteins than those that have no protein. It is thus expected that when batch methods are used for growing COM crystals in solutions containing protein, the outer regions of the crystal would be more ordered than their respective cores, owing to the depletion of protein concentration during crystal growth.

In summary, the work reported in this chapter has shown that selected amino acids and urinary proteins can be incorporated into COM, producing crystal disorder accompanied by an increase in non-uniform strain and a decrease in crystallite size as computed by Rietveld analysis. However, in addition to non-uniform strain and crystallite size, Rietveld also computes an anisotropy value, which was observed to vary over a considerable range for these samples (Appendix I.3). This indicates that for COM crystals, non-uniform strain and crystallite size vary with crystallographic direction (i.e. non-uniform strain and crystallite size are anisotropic) and their magnitude is sample dependent. Hence a detailed study of anisotropy in COM was carried out, the results of which are presented in Chapter 6. Moreover, the X-ray diffractograms also displayed clear evidence of a broad peak that underlay the sharp crystalline COM peaks and varied between samples, which, according to Addadi et al., (1999) may be indicative of the presence of amorphous material. As this could also shed light on the relationship between mineral and proteins, and would have implications for the development of CaOx urolithiasis, a study on the amorphous content of COM crystals was conducted. Those results are presented in Chapter 7.

6 ANISOTROPY IN CALCIUM OXALATE MONOHYDRATE

COM, like most crystals, are anisotropic in that their mechanical, electrical, magnetic and optical properties can vary according to the direction in which they are measured (Mullin, 1993). COM is classified as belonging to the monoclinic crystal system in which the lengths of principal axes are unequal i.e. $a \neq b \neq c$ and the angles between the principal axes are $\alpha = \beta = 90^{o} \neq \gamma$ (Mullin 1993). If the fault rate and the average distance between faults are the same along the a, b and c axes then the crystal is isotropic in both non-uniform strain and crystallite size (rhomboid, spherical or cubic in shape). Should foreign molecules, such as proteins become occluded into COM crystals then the fault rate could differentially change along particular axes producing anisotropy. If there are greater fault rates along other axes that would be expected from the principal axes fault rates, then there are other defects, such as stacking faults. It is expected that any anisotropic fault rate change will also affect crystal morphology.

The Rietveld refinement used to determine non-uniform strain and crystallite size in Chapter 5, calculates those values on the basis that they are invariant with respect to crystallographic direction, i.e. isotropic. It does however, give a general indication of the degree of anisotropy in these values by way of it's anisotropic parameter, ($U_{anisotropy}$) (Hunter, 1998). This is only an average value and does not indicate the magnitudes of non-uniform strain and crystallite size along the crystallographic axes, nor if other types of disorder are a contributing factor. It is also used as a factor in the fit to prevent it being dominated by the broadening of non-principal plane reflections due to defects such as stacking faults. A more detailed analysis of the anisotropy in COM crystals was therefore undertaken by calculating their non-uniform strain and crystallite size from individual peak profiles of principal plane reflections using SHADOW software (Shadow, 1998) (Section 3.2.16) and their FWHM dependence on lattice spacing using Williamson Hall plots.

Williamson and Hall (1953) showed that the broadening contribution due to non-uniform strain was linearly dependent on the reciprocal lattice spacing ($d^* = 1/d$) but that broadening resulting from small crystallite size was independent of it (Section 3.2.17). In the absence of other factors, the integral breadth (an adjusted line width

parameter $\beta = 0.9 * FWHM * \cos\theta / \lambda$) of reflections of isotropic crystals shows a single linear dependence on d* of which the non-uniform strain is determined by the slope, and the crystallite size by the intercept (Ungar et al., 1988, Langford, 1999). If the crystals were anisotropic (i.e. different non-uniform strain and/or crystallite size along the principal axes) then different linear relationships would be observed for those axes. As stacking faults only contribute to broadening of non-principal plane reflections, an estimate of their magnitude can be made from the extent to which they deviate from the principal plane trends. Furthermore, computer generated views of COM along the three principal planes and a selected non-principal plane were constructed to help visualise the adsorption surfaces as well as their potential for interaction with amino acids and proteins (Section 3.2.20).

6.1 Peak broadening

The anisotropy values obtained by Rietveld analysis indicate that there is a degree of anisotropy (and/or stacking faults), even in COM grown in gelatin or distilled water, and that it increases dramatically for COM grown in the presence of Glu, Gla, HSA, PT and CME, and in urine (Table 6.1). This parallels the non-uniform strain and crystallite size trends (Chapter 5), and shows that amino acids and proteins also increase line width anisotropy, which could result from non-uniform strain/size anisotropy and/or stacking faults.

Table 6.1 The Rietveld anisotropy parameter for COM grown in various media.

Growing Medium	$U_{anisotropy}$	Growing Medium	$U_{anisotropy}$
Gelatin gel (reference)	0.003	THG	0.003
Distilled water (control)	0.002	HSA	0.012
Asp	0.002	PT	0.015
AspAsp	0.002	CME	0.019
GluGlu	0.004	UF urine	0.016
Glu	0.011	CF urine	0.023
Gla	0.013	CF urine (after proteinase)	0.011

Because the reflections are better resolved and have higher intensities at low values of θ, only the profiles of individual peaks in the 10-50° (2θ) region were analysed. Above 50° (2θ) they are too overlapped and weak (Figure 6.1). Even in the lower region some significant peaks, for example, at 18.02° degrees (2θ), are difficult to

analyse with a high degree of certainty because of their low signal to noise ratio (3:1) (Figure 6.2).

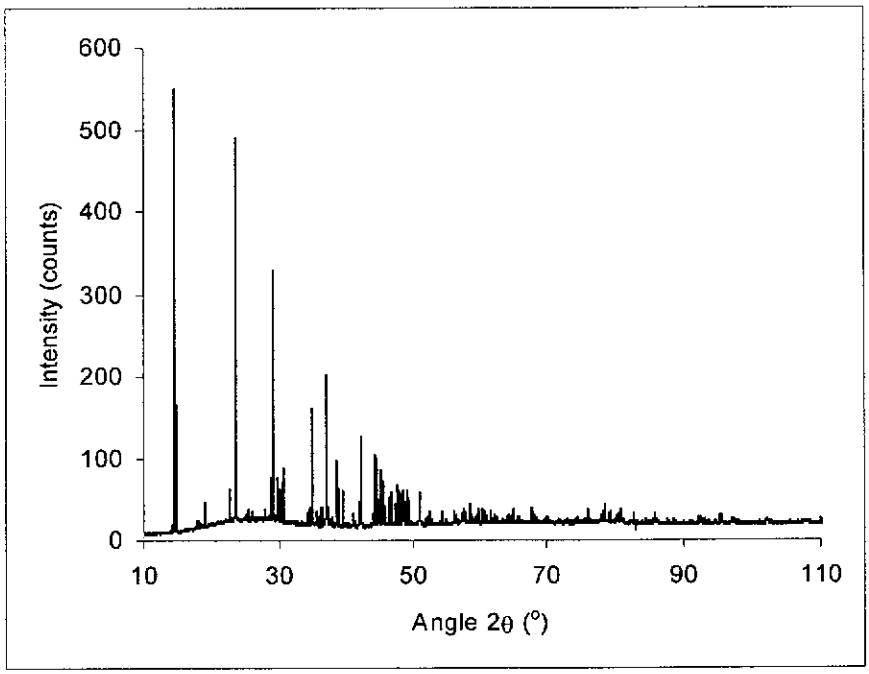

Figure 6.1 Full XRD profile of COM grown in distilled water

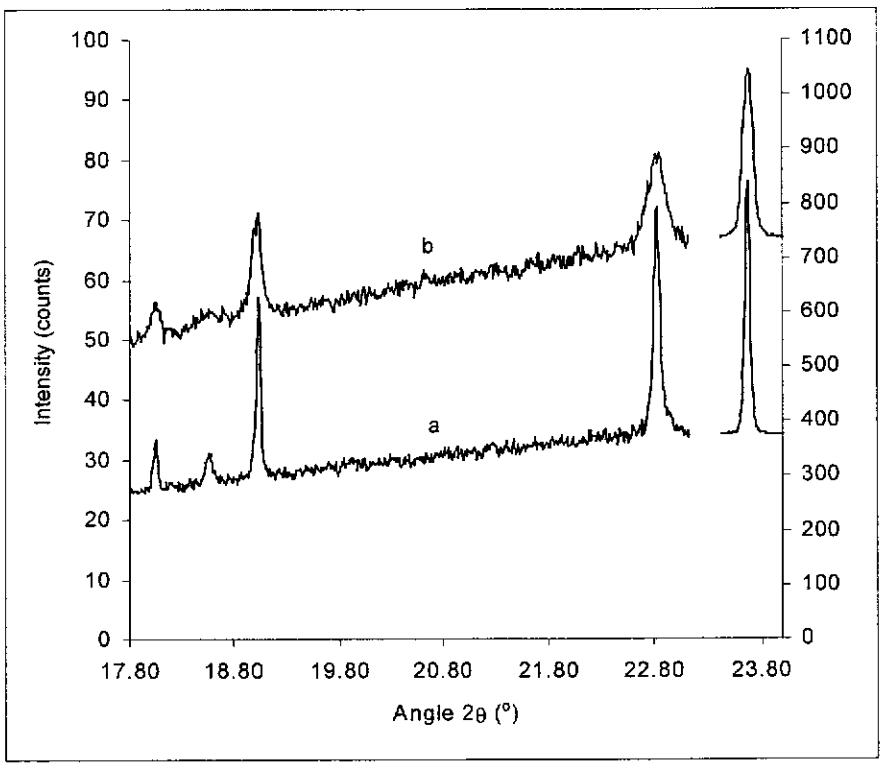

Figure 6.2 Selected XRD peak profiles of COM grown in distilled water (a) and an aqueous solution of PT (b).

Figure 6.2 shows the anisotropy of the line widths for a selected region (18-24° 2θ) for COM grown in distilled water and in an aqueous solution of PT, with the 22.82° (2θ) peak being clearly broader than the 23.67°(2θ) peak by a factor of approximately two i.e.(FWHM = 0.04822, 0.08036 and 0.10848, 0.20088 ° 2θ respectively). The patterns of the anisotropy in COM grown in distilled water and in the presence of PT is shown in Figure 6.3, where FWHM values determined by SHADOW are displayed against the Rietveld calculated trends show anisotropy to be significant for PT. The Rietveld fit to COM (distilled water) shows a relatively small and uniform distribution of the reflections' FWHM about the fit line, indicating that anisotropy is low in these crystals and leads to low $U_{anisotropy}$ (0.00230) (Appendix I.3). However, COM (PT) shows a much larger range of FWHM, indicating much greater anisotropy. Rietveld deals with this phenomenon by weighing the fit in favour of the principal component reflections and accounting for deviations of the non-principal reflections from that fit by a much larger $U_{anisotropy}$ (0.01468).

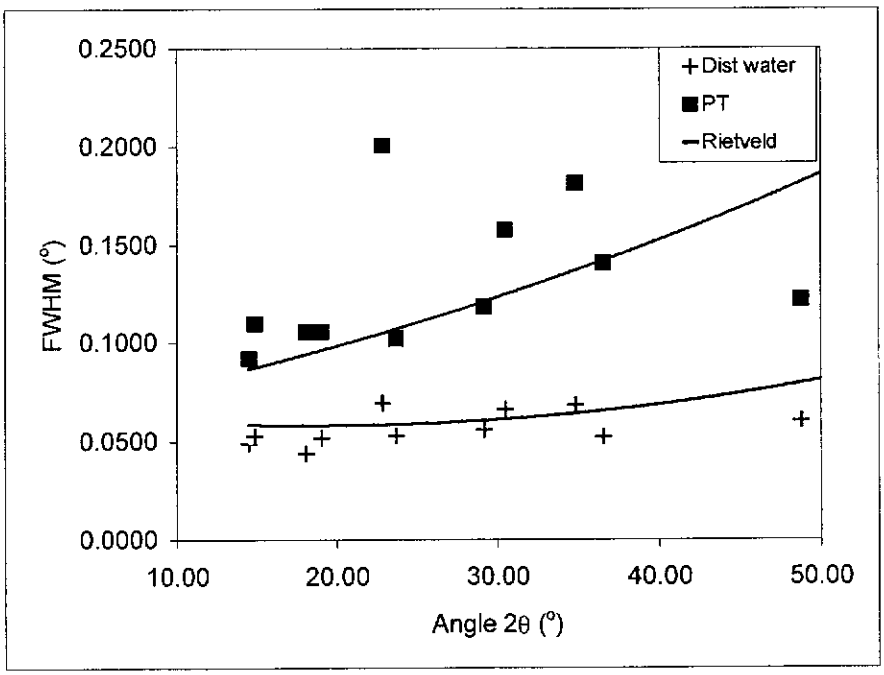

Figure 6.3 SXRD discrete peak and Rietveld calculated FWHM of COM grown in distilled water and in an aqueous solution of PT.

The hkl assignments, d spacings and COM (gelatin) relative intensities of the six principal planes and the five most intense non-principal (diagonal) plane reflections

in the 10-50°(2θ) region are given in Table 6.2. Their peak widths are plotted in Figure 6.4 and listed in Appendix I.4.

Table 6.2 COM crystal planes (hkl), angle (2θ), d spacing and intensity.

Crystal Plane	Angle (2θ)	d spacing (nm)	Relative peak intensities of COM (gel)
(100)	14.49	0.5928	100
$(02\bar{1})$	14.85	0.5785	37
(002)	18.04	0.4768	2
$(10\bar{2})$	19.04	0.4520	6
$(13\bar{1})$	22.82	0.3789	8
(040)	23.67	0.3645	73
(200)	29.19	0.2964	63
$(14\bar{2})$	30.52	0.2840	19
$(22\bar{3})$	34.88	0.2494	30
(004)	36.54	0.2384	6
(080)	48.77	0.1822	7

The errors associated with the FWHM points in Figures 6.4a and 6.4b, were computed by SHADOW and were generally less than 10%. However, some of the FWHM measurements at higher angle crystallographic planes such as (004) and (080), had errors up to 26%. These large errors were caused by peak overlap and low peak intensities.

In general, the samples followed a similar trend, the greatest widths occurring for the 22.82° $(13\bar{1})$, 30.52° $(14\bar{2})$ and 34.88° $(22\bar{3})$ body diagonal reflections, with the principal axis reflections at 14.49° (100), 18.04° (002), 23.67° (040), 29.19° (200), 36.56° (004) and 48.77° (080) broadening least. This indicated that stacking faults contributed to broadening of diagonal plane reflections in addition to the non-uniform strain and crystallite size broadening that were shown by principal plane reflections.

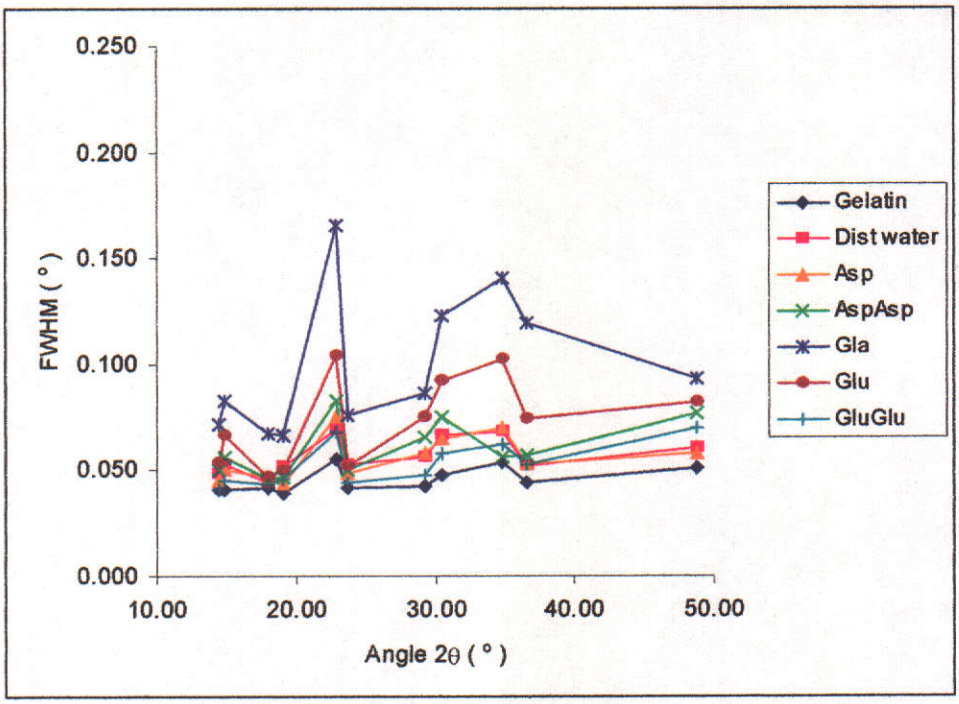

Figure 6.4a Variation of FWHM with angle 2θ (°) for COM grown in gelatin, distilled water and different aqueous amino acid media as indicated by the legend.

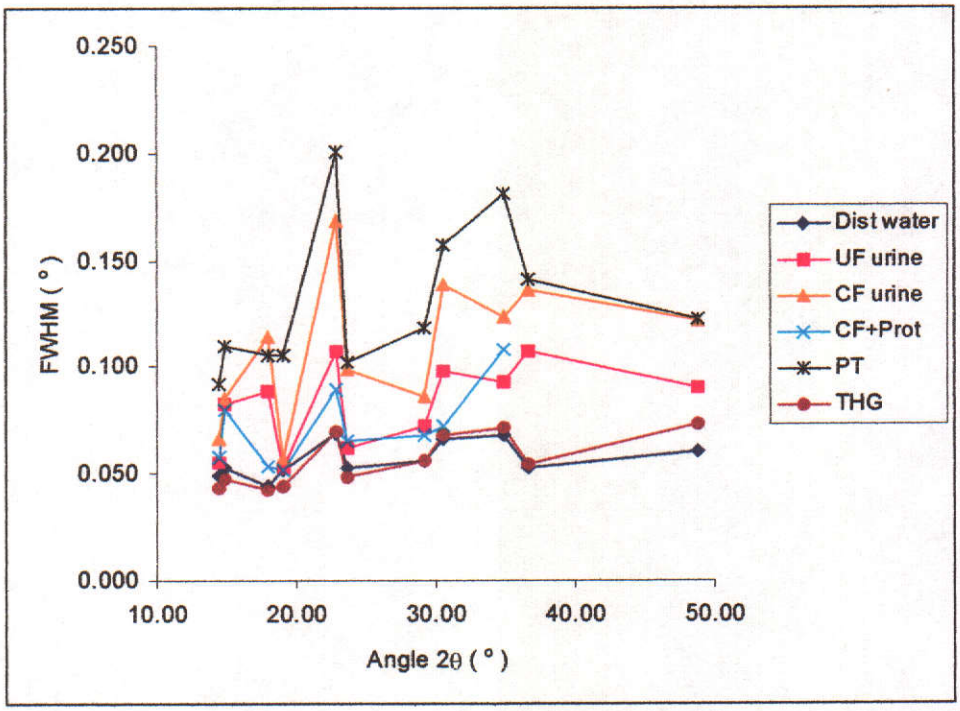

Figure 6.4b Variation of FWHM with angle 2θ (°) for COM grown in distilled water, urinary media and different aqueous protein media as indicated by the legend.

6.2 Williamson-Hall plots

Williamson-Hall plots for the COM crystal types along six principal crystallographic planes and the $(13\bar{1})$ plane are shown in Figures 6.5-6.18. They have been plotted on the same abscissa and ordinate scales to allow direct visual comparison of the data's scatter. Only the two lowest index planes observed could be used for each principal axis because of the poor resolution and low signal to noise ratios of higher plane reflections. The diagonal plane with the greatest deviation from the Rietveld trends $(13\bar{1})$ was used to assess stacking faults (Snyder et al., 1999).

As described in Section 3.2.17, the plots of Γ^* (integral breadth) as a function of d^* (reciprocal of crystal lattice plane d spacing) enabled crystallite size to be obtained from the intercept and non-uniform crystal strain from the slope. A solid line has been used in the Williamson-Hall plots to represent the trend line for a group of at least two pairs of reflections, whereas a broken line draws attention to one pair of reflections. The broken lines, arising from only two points, are thus an indication of anisotropy and any quantitative or semi-quantitative information derived from them must be treated with due caution.

The FWHMs used for the Williamson-Hall plots have not been corrected for instrument contributions to the line broadening, as subtraction of a reference (COM grown in gelatin) significantly increases the error and hence could mask trends. The calculated non-uniform strain and crystallite sizes are thus not absolute and not directly comparable to Reitveld derived data. Because the experimental FWHM are greater than the true line widths, Williamson-Hall derived data will have higher non-uniform strain and smaller crystallite size than Reitveld data. However, both methods could be expected to give the same or similar trends.

The plot of COM grown in gelatin (Figure 6.5) shows that all points, with the exception of $(13\bar{1})$ fit within experimental error on a single, nearly horizontal trend line of the principal axes. This result is indicative of little or no non-uniform crystal strain and suggests that the crystallite shapes are isotropic (i.e. spherical or rhombohedral). It confirms that COM (gelatin) was an appropriate strain free sample for use as a standard in the Rietveld analysis. The only disorder apparent in the sample is caused by stacking faults, as shown by the deviation of the $(13\bar{1})$ reflection from the trend line.

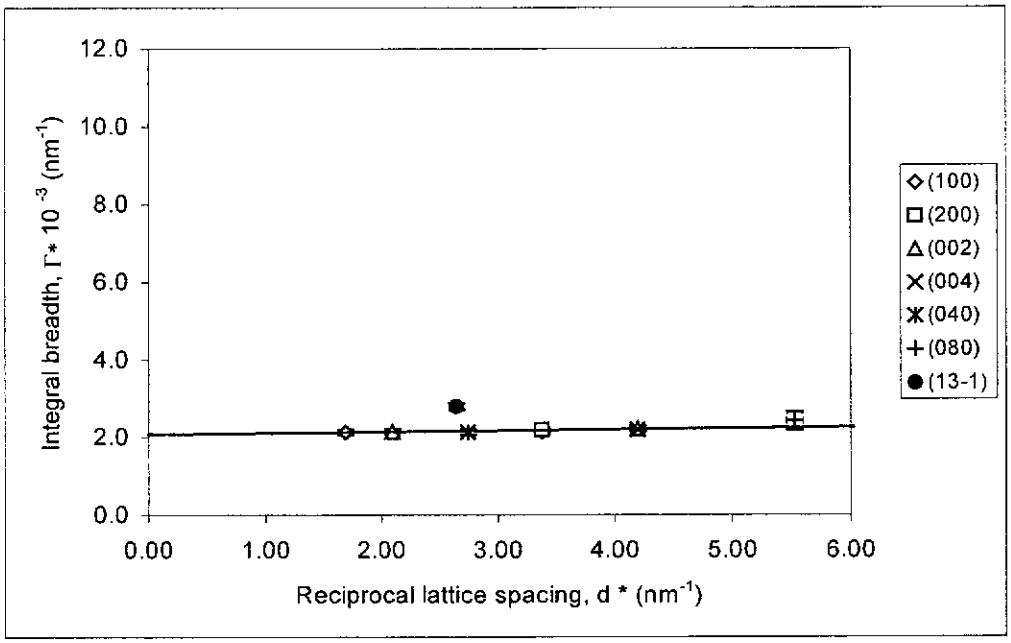

Figure 6.5 Williamson-Hall plot of COM grown in gelatin

The trendlines of the principal axes reflection integral breadths for COM grown in distilled water and aqueous solutions of Asp, AspAsp, GluGlu, THG, Gla, HSA, and PT (Figures 6.6-6.13) indicate that the crystals have greater non-uniform strain and smaller crystallite size than COM (gel) and COM (distilled water). The largest non-uniform strain and smallest crystallite size observed was COM (PT). With the possible exception of COM (AspAsp) and COM (GluGlu), the principal axes reflections fit to a single trend line within experimental error (± 5%). This indicates that both disorientation of the crystallites (non-uniform strain) and their lateral displacement (stacking faults) contribute to disorder of the crystals.

Whilst the (200) reflection is strong (relative intensity = 63) and hence its integral breadth has a high degree of accuracy (± 5%), the trendline includes very weak reflections, such as (002), (004) and (080) with relative intensities of 2-7, which make it less certain. Thus the apparent deviation may well be due to experimental error. The possibility that the deviation of the (200) reflections of COM (AspAsp) (Figure 6.8) and COM (GluGlu) (Figure 6.9) from the other principal plane reflections results from non-uniform stain and crystallite size can be discounted, since that this would imply that the (100) axis has greater non-uniform strain than the (010) and (001) axes but larger crystallite size. This is contrary to the generally

accepted view that larger non-uniform strain is associated with smaller crystallite size.

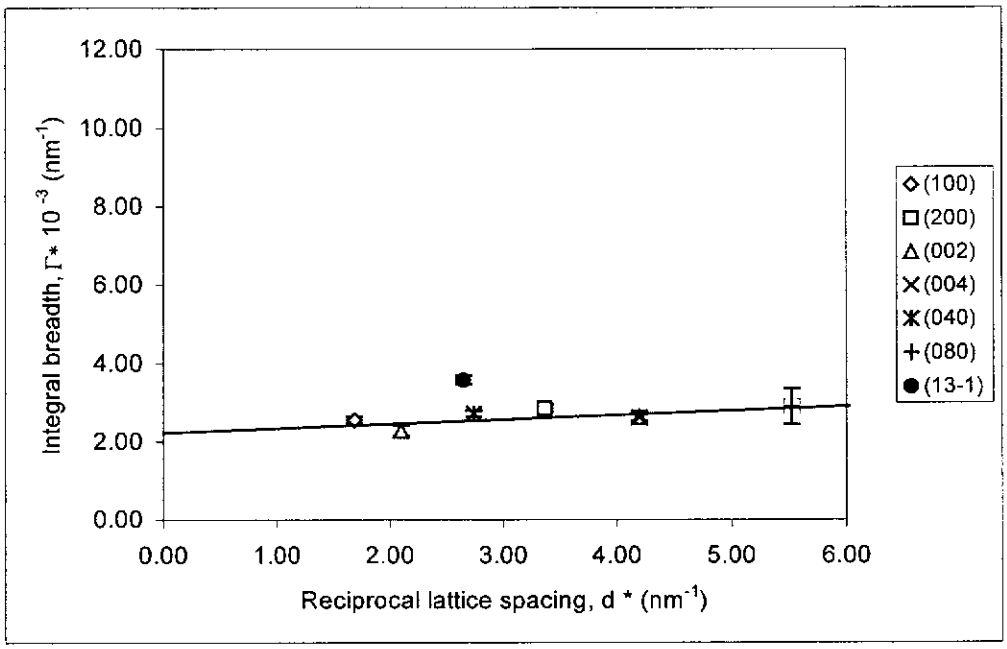

Figure 6.6 Williamson-Hall plot of COM grown in distilled water

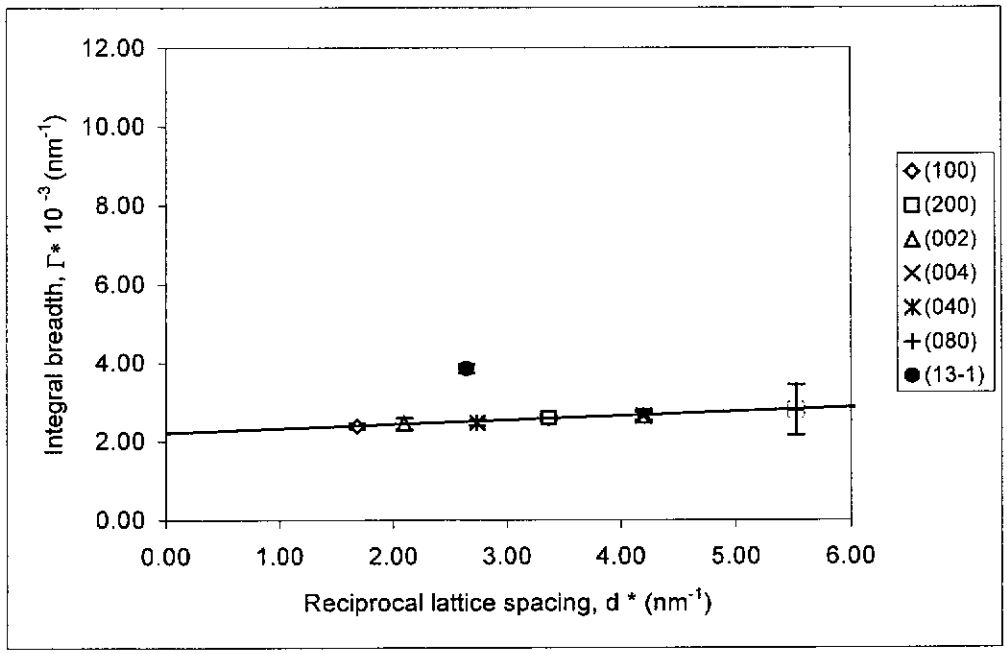

Figure 6.7 Williamson-Hall plot of COM grown in an aqueous solution of Asp

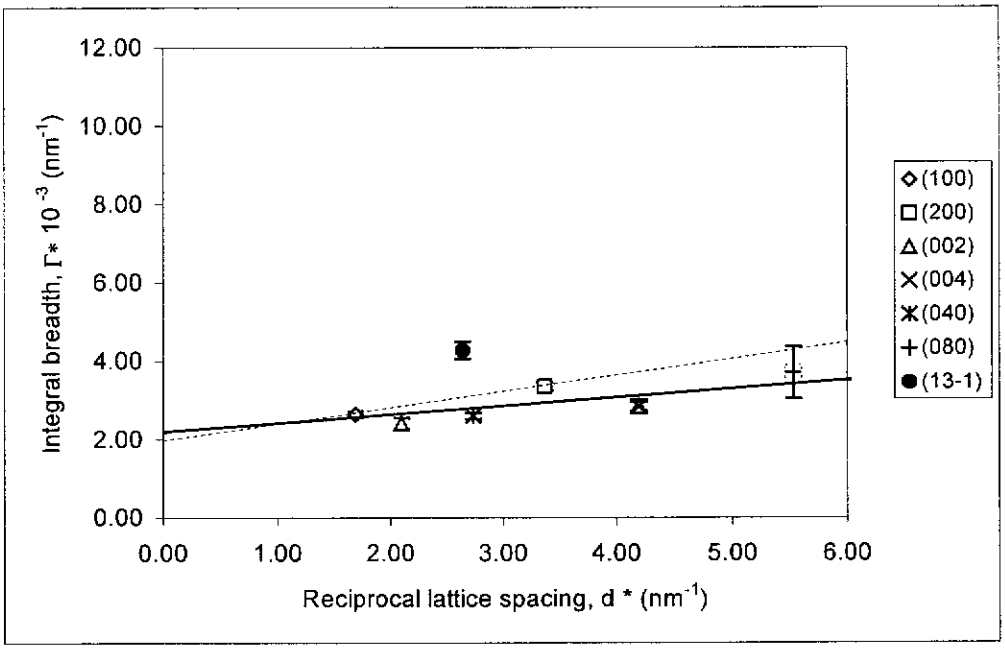

Figure 6.8 Williamson-Hall plot of COM grown in an aqueous solution of AspAsp. The broken line represents one pair of principal axis reflections that deviate significantly from the trend line of the other two pairs of principal axis reflections, shown as a solid line.

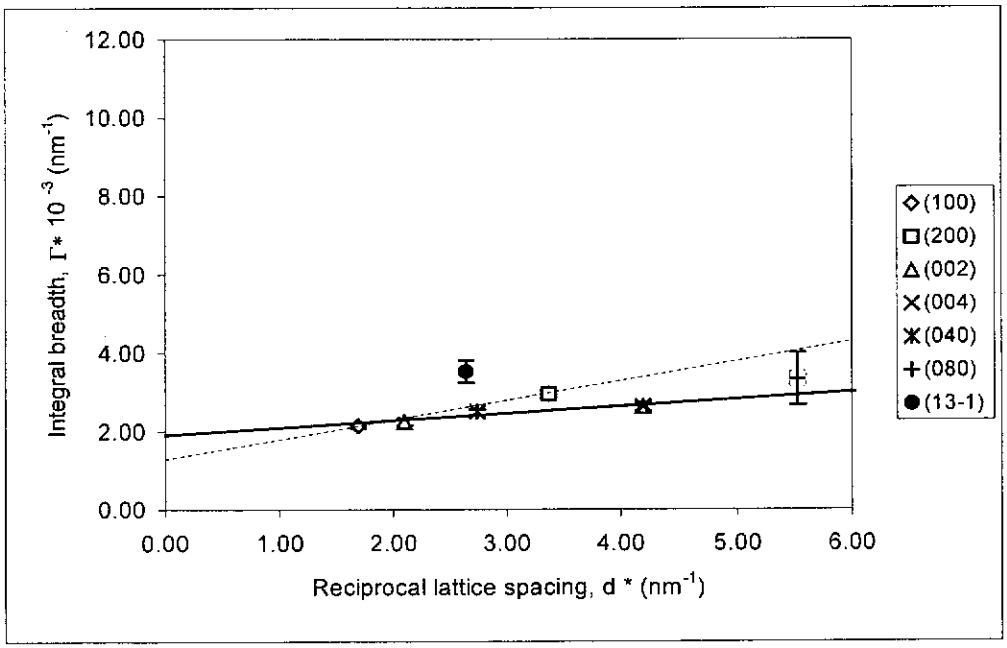

Figure 6.9 Williamson-Hall plot of COM grown in an aqueous solution of GluGlu

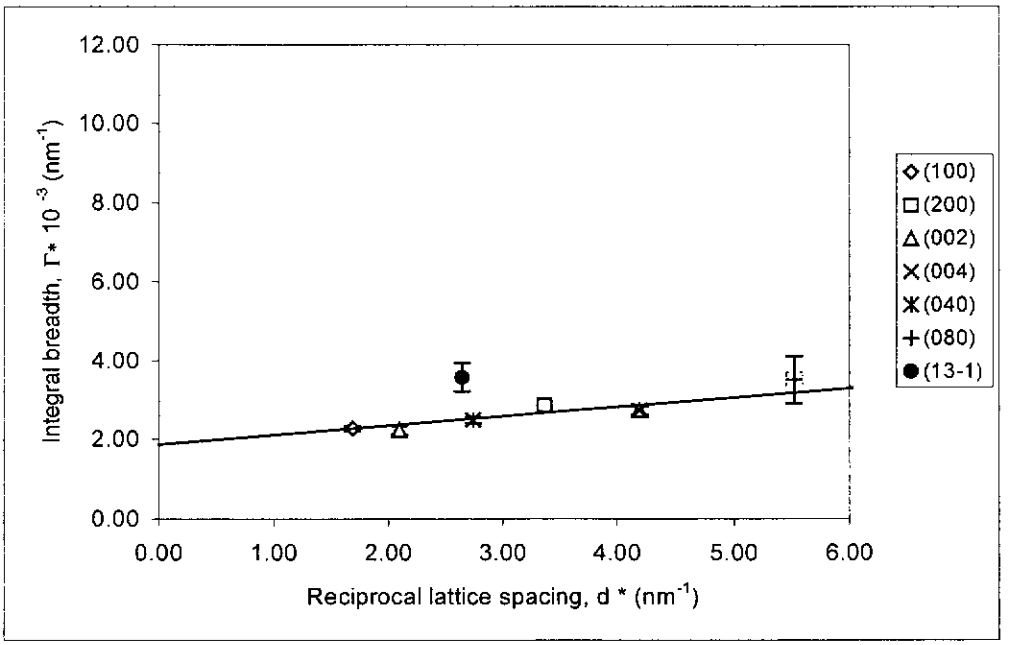

Figure 6.10 Williamson-Hall plot of COM grown in an aqueous solution of THG

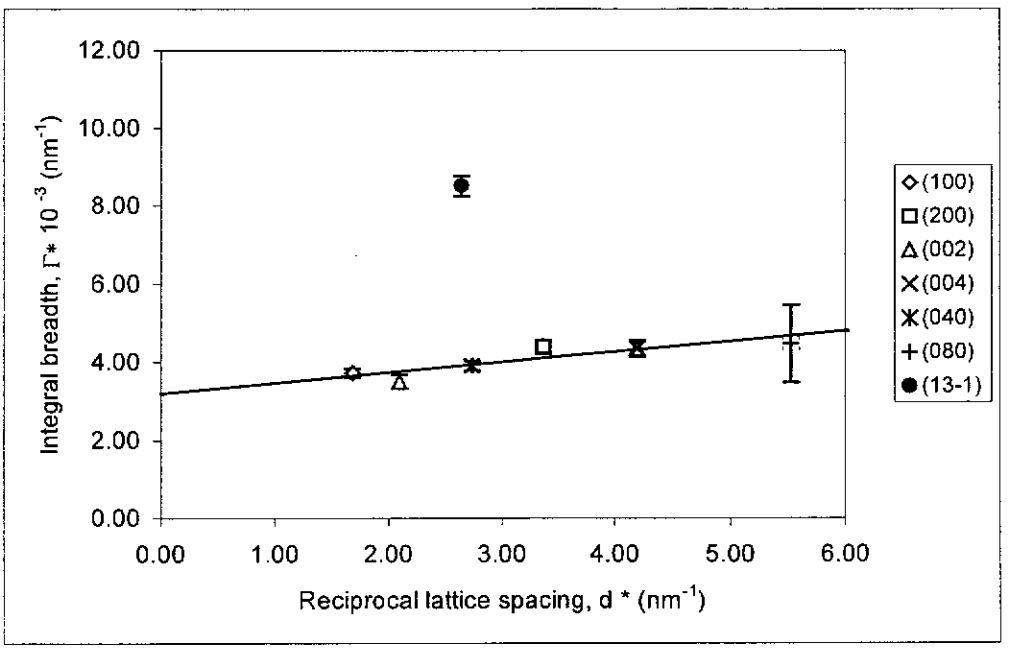

Figure 6.11 Williamson-Hall plot of COM grown in an aqueous solution of Gla

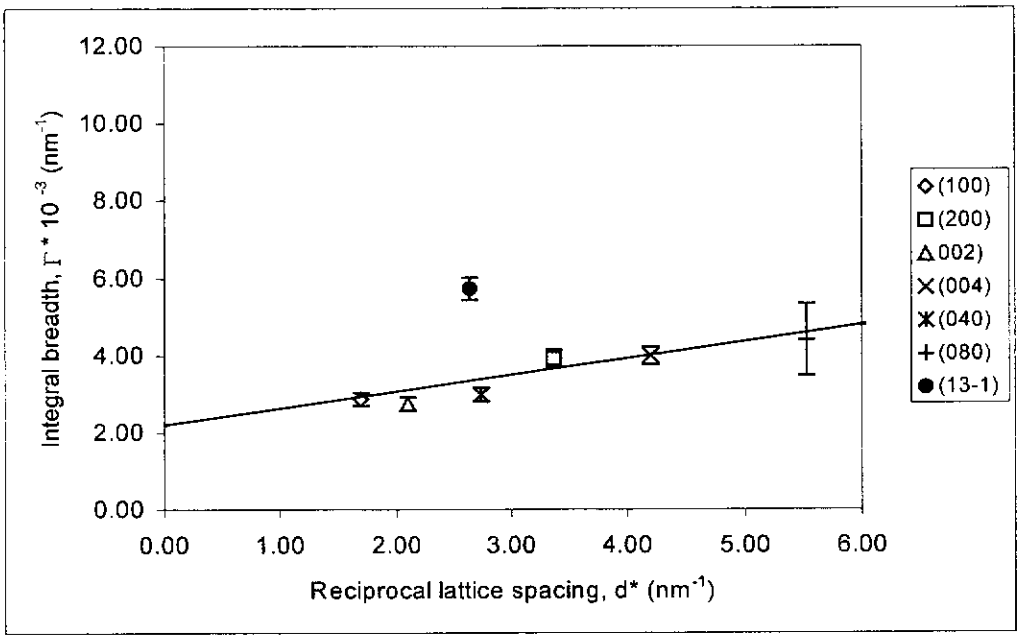

Figure 6.12 Williamson-Hall plot of COM grown in an aqueous solution of HSA

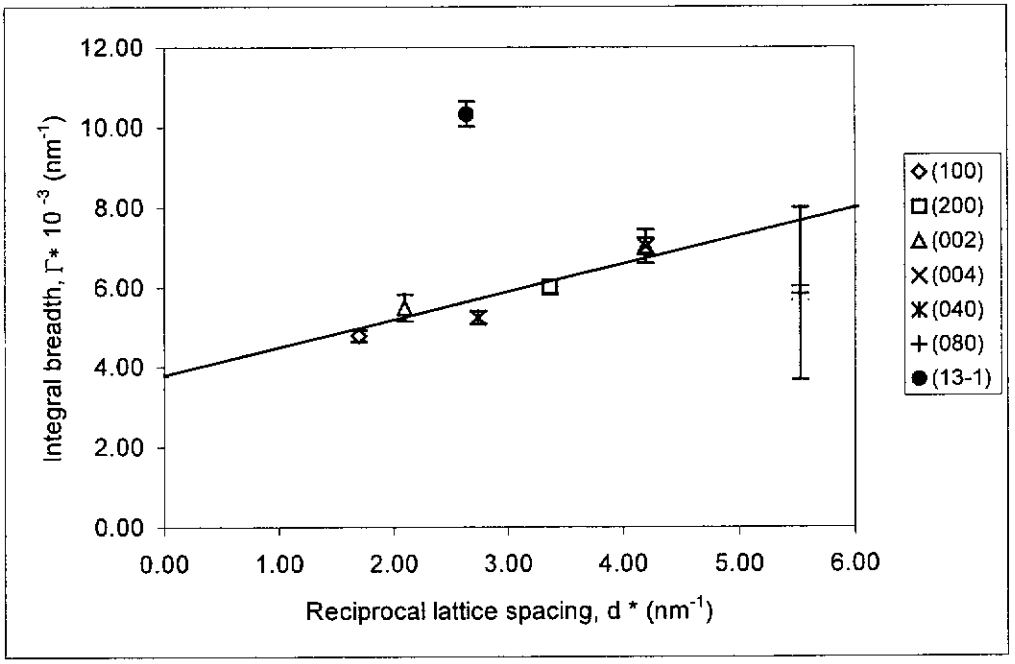

Figure 6.13 Williamson-Hall plot of COM grown in an aqueous solution of PT.

COM (Glu), COM (UF), COM (CME) and COM (CF) (Figures 6.14-6.17) also have isotropic moderate to high non-uniform strain but exhibit anisotropic crystallite size in the Williamson-Hall plots. Anisotropy in crystallite size is indicated by more than one line in the Williamson-Hall plots. The broken line in both COM (Glu) (Figure 6.14) and COM (UF) (Figure 6.15) represent one pair of principal axis reflections that deviate significantly from the trend line of the other two pairs of principal axis

reflections, shown as a solid line. The three broken lines in COM (CME) (Figure 6.16) and COM (CF) (Figure 6.17) represent pairs of principal axis reflections that differ significantly from each other. Within experimental error, the slopes of the trendlines, which are a measure of non-uniform strain, are the same for any one of these samples, indicates that non-uniform strain is probably isotropic in each case. However, their intercepts, from which crystallite size is derived, are markedly different and strongly suggest that the crystallites are anisotropic. COM (Glu) (100) = 0.59, (010) = 0.91, (001) = 0.91) and COM (UF) (100) = 0.43, (010) = 0.43, (001) = 0.25) crystallites appear to be oblate relative to the (001) axis, whilst COM (CF) and COM (CME) appear to be prolate relative to the (100) axis or even lower symmetry (100) = 0.39, (010) = 0.23, (001) = 0.20 and (100) = 0.38, (010) = 0.33, (001) = 0.20) respectively.

Treating COM (CF urine) with proteinase (Figure 6.18) to remove macromolecules reduces non-uniform strain and increases crystallite size (ε = 0.42 to 0.28, D = 0.27μm to 0.41μm), as would be expected from concurrent removal of smaller more strained material that might be more closely associated with the macromolecules.

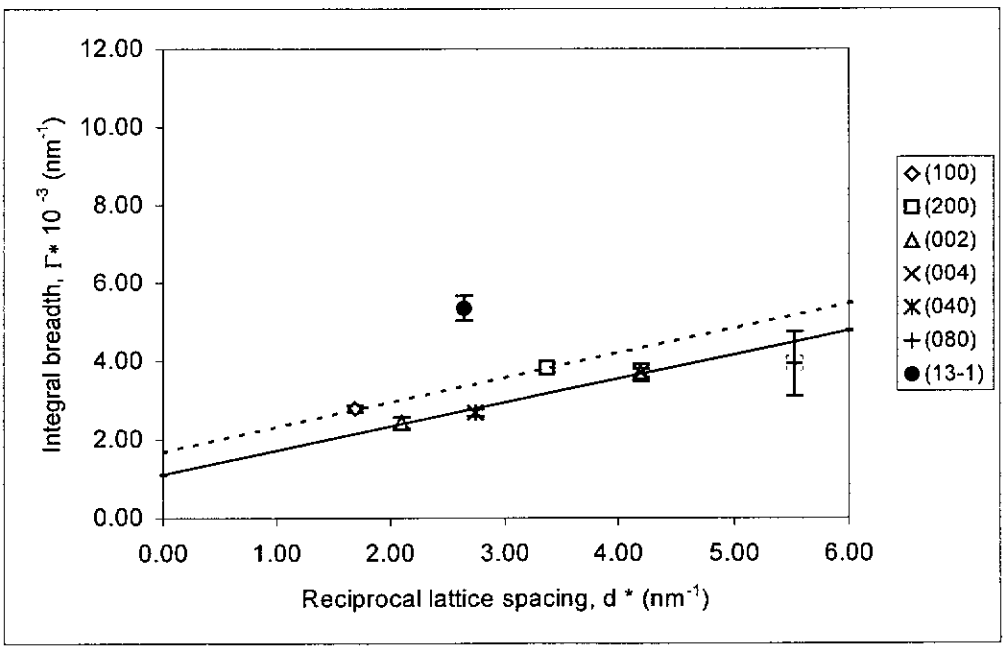

Figure 6.14 Williamson-Hall plot of COM grown in an aqueous solution of Glu. The broken line represents one pair of principal axis reflections that deviate significantly from the trend line of the other two pairs of principal axis reflections, shown as a solid line.

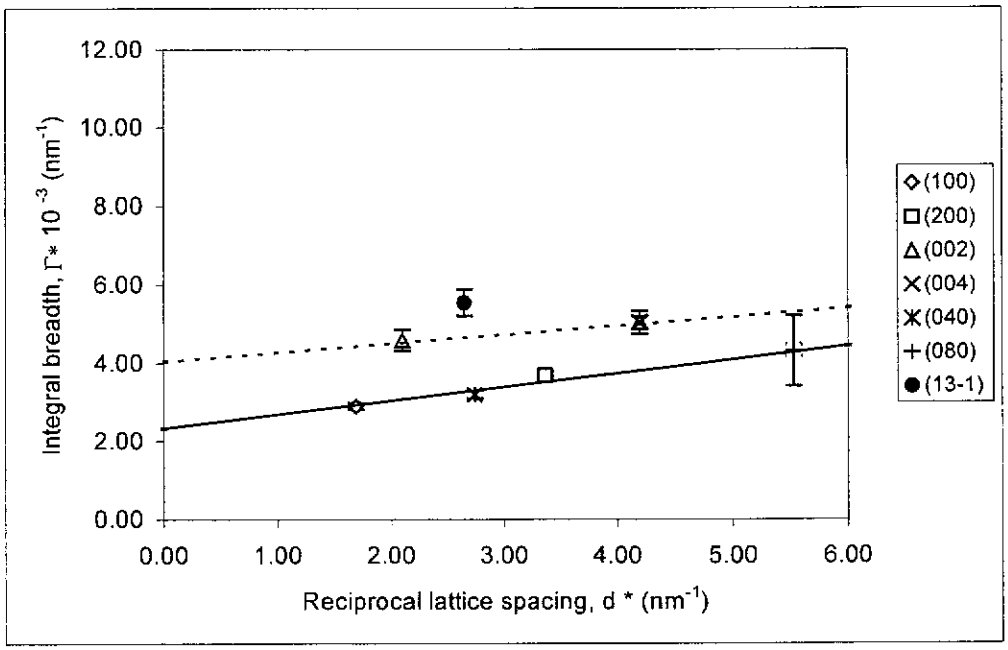

Figure 6.15 Williamson-Hall plot of COM grown in UF urine.

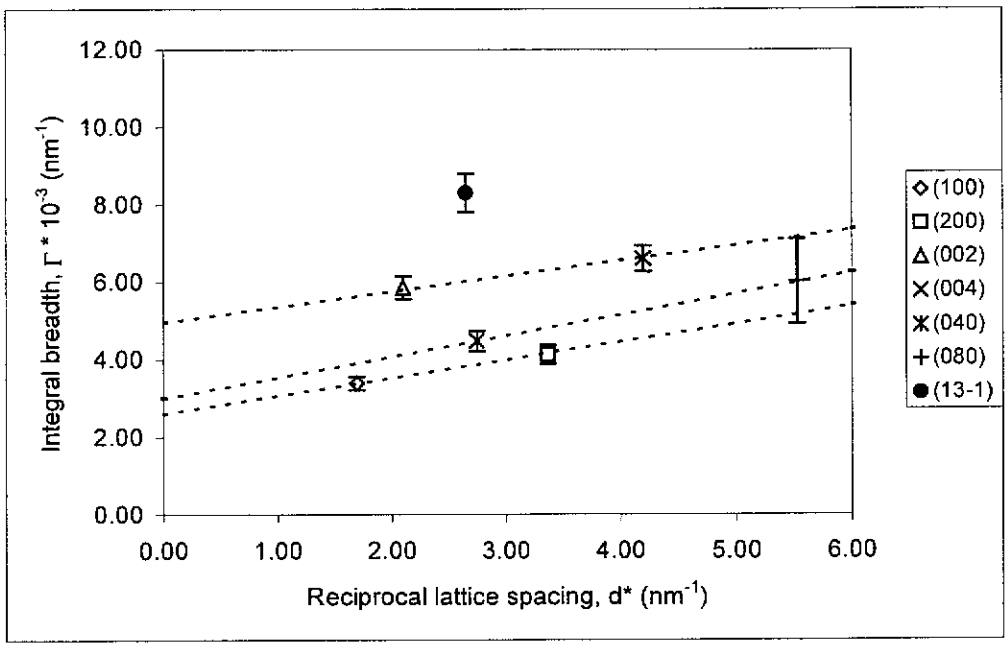

Figure 6.16 Williamson-Hall plot of COM grown in an aqueous solution of CME. Each broken line represents one pair of principal axis reflections that deviate from the others.

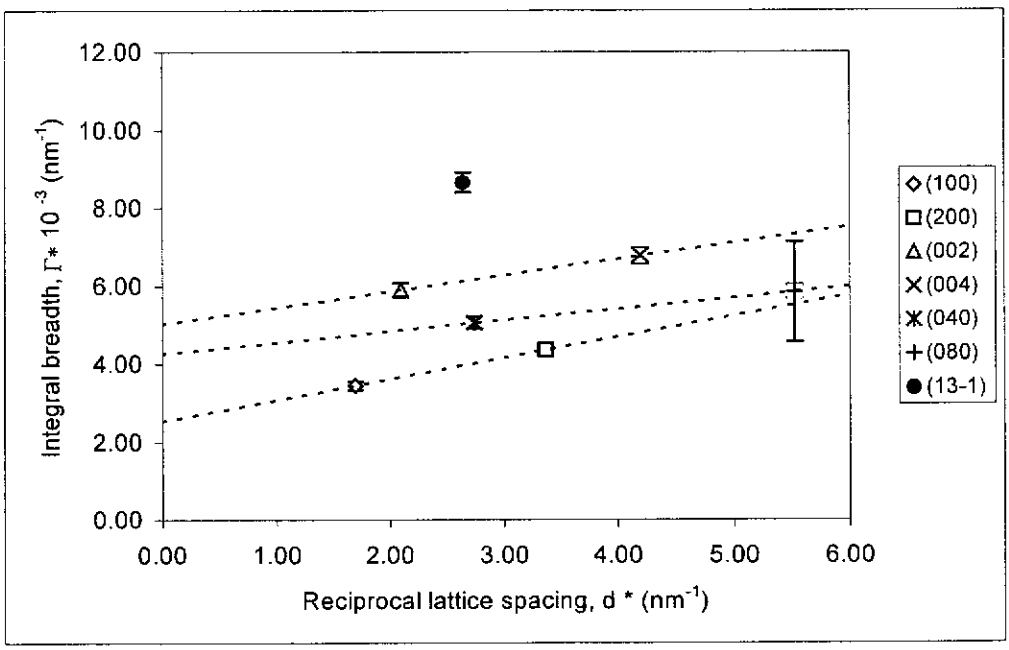

Figure 6.17 Williamson-Hall plot of COM grown in CF urine. Each broken line represents one pair of principal axis reflections that deviate from the others.

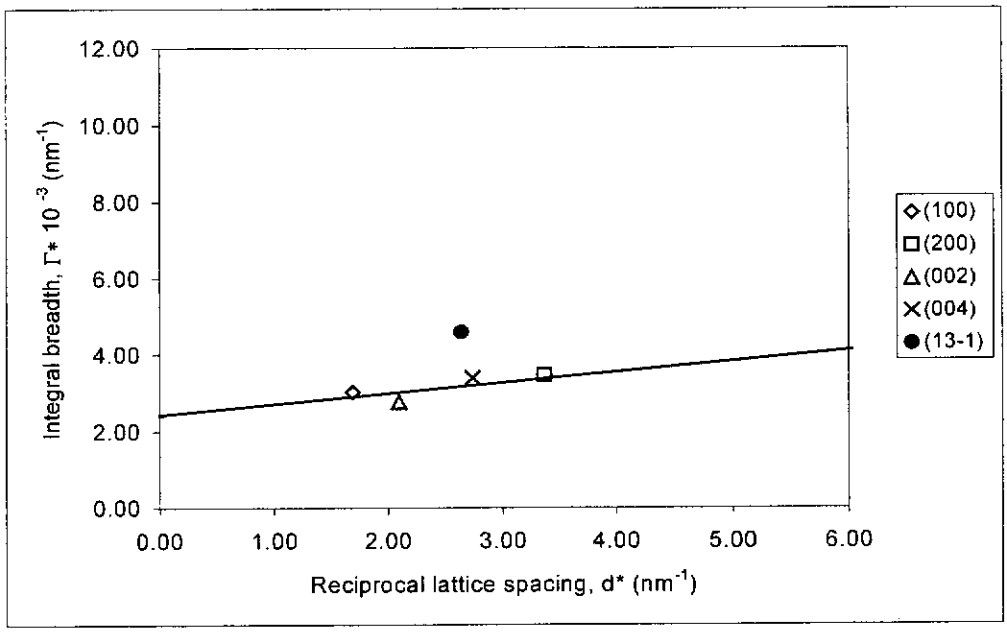

Figure 6.18 Williamson-Hall plot of COM grown in CF urine then treated with Proteinase K

The Williamson-Hall data are summarised in Table 6.3 in which the Reitveld data from Table 5.1 have been included. For a more direct comparison of the two sets of

results, non-uniform strain and crystallite size values were also determined from Williamson-Hall plots, where the FWHMs of COM grown in gelatin had been subtracted from the FWHM of the other crystal types to correct for the effects of instrument broadening (Appendix I-4). It was reasoned that as the non-uniform strain of COM (gelatin) is very small and the crystallite size very large, the corresponding FWHM values would reflect instrumental contributions to line broadening.

The corrected FWHM values for the crystal types give non-uniform strain and crystallite size that are similar to those obtained from Rietica, indicating that intrinsically, the two methods are capable of generating directly comparable results. Unfortunately, in the present study, the corrected Williamson-Hall results have greater scatter, making the trends less certain. Therefore, non-uniform strain and crystallite size values obtained from uncorrected FWHM in the Williamson-Hall plots were preferentially used in trend comparisons with other data.

There were insufficient related non-principal axes reflections to distinguish between different types of dislocations, e.g. stacking faults, screw dislocations and twin faults. Hence, the deviation of the $(13\bar{1})$ plane from the principal axes trend-lines was taken as an indication of the degree of stacking faults in general: the larger the deviation the greater the degree of stacking faults. The order of magnitude of stacking faults was found to be COM grown in gelatin < distilled water, THG < GluGlu < CF urine/proteinase, Asp < UF urine < AspAsp < HSA < Glu < CF urine < CME < Gla < PT (Table 6.4). As would be expected, samples which had a small crystallite size, that is, COM (PT), COM (Gla) and COM (CF), generally also had the greatest number of stacking faults.

Table 6.3 Initial and corrected non-uniform strain and crystallite sizes of COM grown in different media obtained from Williamson-Hall plots and by Rietveld analysis.

Growing Medium	Strain (ε)	Crystallite size (D) μm	Strain (ε)	Crystallite size (D) μm	Strain (ε)	Crystallite size (D) μm
	Williamson-Hall uncorrected		Williamson-Hall corrected		Rietveld	
Gelatin gel (reference)	0.03	0.48			0.000	>2.60
Distilled water (control)	0.11	0.45	0.05	3.33	0.040	2.59
Asp (aqueous)	0.11	0.45	0.02	3.33	0.045	2.54
AspAsp (aqueous)	0.22	0.45	0.10	2.50	0.049	2.54
GluGlu (aqueous)	0.18	0.53	0.05	3.33	0.043	2.54
THG (aqueous)	0.28	0.53	0.05	3.33	0.041	2.45
Gla (aqueous)	0.27	0.31	0.15	0.77	0.112	1.19
Glu (aqueous)	0.62	(100) = 0.59 (010) = 0.91 (001) = 0.91	0.37	(100) = 2.00 (010) =2.00 (001) = 2.00	0.064	2.01
HSA (aqueous)	0.43	0.45	0.05	1.00	0.067	0.86
PT(aqueous)	0.71	0.26	0.62	0.56	0.128	0.31
CME (aqueous)	0.47	(100) = 0.38 (010) = 0.33 (001) = 0.20	0.40	(100) = 1.72 (010) = 0.91 (001) = 0.33	0.095	0.65
UF (urine)	0.29	(100) = 0.43 (010) = 0.43 (001) = 0.25	0.15	(100) = 1.25 (010) = 1.25 (001) = 0.49	0.088	0.50
CF (urine)	0.42	(100) = 0.39 (010) = 0.23 (001) = 0.20	0.37	(100) = 2.45 (010) = 0.42 (001) = 0.34	0.128	0.31
CF (urine) and protease	0.28	0.41	0.28	3.33	0.092	0.51

Table 6.4 Deviation of $(13\bar{1})$ relative to the main crystallographic axes for COM grown in different media.

Growing Medium	**Deviation of $(13\bar{1})$ relative to the main crystallographic axes $\Gamma^* 10^{-3}$ (nm^{-1})**
Gelatin gel (reference)	0.6
Distilled water (control)	0.9
Asp (aqueous)	1.2
AspAsp (aqueous)	1.6
GluGlu (aqueous)	1.0
THG (aqueous)	0.9
Gla (aqueous)	4.1
Glu (aqueous)	2.5
HSA (aqueous)	2.4
PT(aqueous)	4.3
CME (aqueous)	3.8
UF (urine)	1.5
CF (urine)	3.6
CF (urine) and protease	1.2

6.3 Non-uniform crystal strain and crystallite size from individual peak profiles

An alternative to Williamson-Hall plots for obtaining non-uniform strain and crystallite size along crystal planes is to determine them from the contribution they make to the shape and width of individual XRD reflections. Accordingly, Gaussian and Lorentzian contributions to peak profiles were determined using SHADOW software (Appendix I 5), which were in turn used to calculate non-uniform strain and crystallite size (Appendices I 6 and 7) using equations 5 and 6 (Section 3.2.16).

In both Rietveld and SHADOW, the standard's (COM gelatin) peak were subtracted from the samples's peak widths before calculations of non-uniform strain and

crystallite size were made. Hence, as the same peaks were used in a similar manner, the average results obtained by Rietveld, was expected to possess similar magnitudes to those obtained from single reflections by SHADOW. Each pair of principal axes reflections should give the same result for non-uniform strain and crystallite size, but this is not always the case as the error in the Gaussian/Lorentzian apportionment introduces further uncertainty, in addition to that caused by subtraction of the reference. The error in Gaussian/Lorentzian separation, reported by SHADOW, gives only a statistical error of separated Gaussian and Lorentzian components, and hence the stated errors are an underestimate (Section 3.2.16). This is particularly true for the weaker (080), (004) and (002) reflections. There is thus some subjectivity in deciding between isotropy and anisotropy based solely on SHADOW data and the Williamson-Hall data were therefore taken into consideration. In general, the non-uniform strain and crystallite size obtained from single peak analysis, were similar to those obtained from whole pattern analysis but anisotropy was less clear than with the Williamson-Hall plots.

Considering the variation in strain obtained from pairs of principal axes reflections and the average non-uniform strains, Table 6.5 shows that all crystals other than COM (Glu) and COM (HSA), had isotropic non-uniform strain. For these two crystal types, the non-uniform strain might be highest along the (100) principal axis, as both reflections gave a similar 'above average' value. However, that judgement is subjective. In view of the large uncertainties and the inconsistency with the Williamson-Hall plots, non-uniform strain anisotropy for any of the samples was discounted.

COM grown in CF urine showed a decrease in non-uniform strain after treatment with proteinase K indicating that removal of protein from within the crystal matrix relaxes internal stress, or aids the removal of the most stressed material.

Table 6.5 Principal axes non-uniform strain for COM grown in different media.

Medium	Non-uniform strain %						
	(100)	(200)	(040)	(080)	(002)	(004)	Average
Distilled water	0.047 ±0.003	0.051 ±0.003	0.050 ±0.003	0.022 ±0.016	0.059 ±0.009	0.040 ±0.009	0.040
Asp (aqueous)	0.039 ±0.003	0.051 ±0.005	0.048 ±0.004	0.016 ±0.032	0.068 ±0.013	0.017 ±0.008	0.040
AspAsp (aqueous)	0.046 ±0.003	0.049 ±0.005	0.048 ±0.005	0.040 ±0.022	0.070 ±0.007	0.049 ±0.009	0.050
GluGlu (aqueous)	0.047 ±0.005	0.052 ±0.006	0.049 ±0.004	0.037 ±0.030	0.062 ±0.008	0.023 ±0.008	0.045
THG (aqueous)	0.029 ±0.002	0.060 ±0.004	0.054 ±0.003	0.021 ±0.013	0.060 ±0.010	0.039 ±0.007	0.044
Gla (aqueous)	0.175 ±0.009	0.106 ±0.006	0.109 ±0.020	0.055 ±0.045	0.069 ±0.008	0.094 ±0.006	0.101
Glu (aqueous)	0.100 ±0.008	0.088 ±0.004	0.047 ±0.003	0.055 ±0.024	0.068 ±0.009	0.051 ±0.008	0.068
HSA (aqueous)	0.098 ±0.006	0.089 ±0.009	0.050 ±0.008	0.056 ±0.019	0.069 ±0.007	0.073 ±0.009	0.072
PT (aqueous)	0.227 ±0.007	0.155 ±0.006	0.167 ±0.004	0.074 ±0.029	0.147 ±0.010	0.155 ±0.012	0.154
CME (aqueous)	0.121 ±0.015	0.092 ±0.009	0.157 ±0.018	0.083 ±0.009	0.149 ±0.019	0.088 ±0.008	0.115
UF (urine)	0.061 ±0.008	0.060 ±0.012	0.050 ±0.004	0.059 ±0.018	0.094 ±0.011	0.079 ±0.009	0.067
CF (urine)	0.126 ±0.011	0.098 ±0.004	0.160 ±0.005	0.088 ±0.017	0.154 ±0.012	0.093 ±0.008	0.120
CF (urine + PK)	0.064 ±0.007	0.066 ±0.006	0.070 ±0.004	no peak	0.051 ±0.012	no peak	0.063

Crystallite sizes obtained from single peak analysis (Table 6.6), like non-uniform strains, had the same order of magnitude as Rietveld data ($0.17 < D < 1.84$ μm, $0.31 < D < 2.59$ μm respectively). When data along the principal axes were averaged and compared to single reflection data, COM (water), COM (Asp), COM (AspAsp), COM (GluGlu), COM (THG), COM (Gla) and COM (PT) appeared to be isotropic. Values for COM (Glu) and COM (HSA) were consistent with the presence of anisotropy, with the crystallites possessing a shorter length along the (100) plane. Of

these however, only COM (Glu) also showed anisotropy in the Williamson-Hall plots.

Table 6.6 Principal axes crystallite for COM grown in different media.

Medium	Crystallite size μm						
	(100)	(200)	(040)	(080)	(002)	(004)	Average
Distilled water	1.44 ±0.07	1.36 ±0.05	1.46 ±0.06	1.59 ±0.29	1.14 ±0.09	1.37 ±0.08	1.39
Asp (aqueous)	1.48 ±0.10	0.90 ±0.04	1.42 ±0.06	1.45 ±0.32	1.17 ±0.11	1.43 ±0.12	1.31
AspAsp (aqueous)	1.42 ±0.05	1.29 ±0.06	1.39 ±0.07	1.47 ±0.28	1.11 ±0.08	1.41 ±0.14	1.35
GluGlu (aqueous)	1.52 ±0.08	1.33 ±0.10	1.41 ±0.07	1.52 ±0.28	1.09 ±0.09	1.46 ±0.07	1.39
THG (aqueous)	1.84 ±0.08	1.12 ±0.04	1.25 ±0.04	1.42 ±0.31	1.31 ±0.11	1.39 ±0.11	1.39
Gla (aqueous)	0.48 ±0.03	0.60 ±0.02	0.38 ±0.02	1.15 ±0.31	0.69 ±0.08	0.61 ±0.03	0.65
Glu (aqueous)	0.54 ±0.08	0.47 ±0.03	0.96 ±0.05	1.15 ±0.25	0.89 ±0.11	1.16 ±0.09	0.86
HSA (aqueous)	0.51 ±0.07	0.45 ±0.08	0.93 ±0.08	1.02 ±0.22	0.87 ±0.10	1.03 ±0.13	0.80
PT (aqueous)	0.17 ±0.03	0.19 ±0.03	0.33 ±0.03	0.78 ±0.32	0.23 ±0.07	0.28 ±0.03	0.33
CME (aqueous)	0.49 ±0.06	0.44 ±0.09	0.41 ±0.05	0.69 ±0.08	0.28 ±0.07	0.68 ±0.09	0.50
UF (urine)	1.04 ±0.05	0.82 ±0.03	1.25 ±0.04	1.06 ±0.27	0.56 ±0.13	0.56 ±0.07	0.88
CF (urine)	0.47 ±0.03	0.40 ±0.04	0.38 ±0.03	0.66 ±0.19	0.21 ±0.11	0.60 ±0.06	0.45
CF (urine + PK)	0.91 ±0.04	0.68 ±0.04	0.90 ±0.09	no peak	0.80 ±0.11	no peak	0.82

Data for COM (CF) and COM (CME) also indicated the presence of anisotropy, but the crystallites with the shortest lengths were along the (100) and (001) planes. The crystallites of COM (UF) possessed shortest lengths along the (001) plane. These results were generally consistent with the Williamson-Hall plots. COM grown in CF urine, showed an increase in crystallite size after treatment with proteinase K,

indicating that removal of protein probably also removed smaller crystallites associated with macromolecules.

The largest "apparent" non-uniform strain and smallest crystallite sizes occurred along the $(13\bar{1})$ plane (Table 6.7), confirming that stacking faults were the major contribution to the average values obtained from Rietveld trends.

Table 6.7 Non-uniform strain and crystallite size along the $(13\bar{1})$ plane for COM grown in different media

Medium	Non-uniform strain (%)	Size (μm)
Distilled water	0.080	1.18
Asp (aqueous)	0.063	1.28
AspAsp (aqueous)	0.078	1.13
GluGlu (aqueous)	0.081	1.21
THG (aqueous)	0.079	0.93
Gla (aqueous)	0.257	0.10
Glu (aqueous)	0.085	0.39
HSA (aqueous)	0.120	0.42
PT (aqueous)	0.331	0.08
CME (aqueous)	0.221	0.18
UF (urine)	0.080	0.73
CF (urine)	0.278	0.12
CF (urine + PK)	0.086	0.84

6.4 COM Crystal Structure

A schematic diagram of COM morphology showing commonly observed faces is displayed again in Figure 6.19 for convenience. Computer-generated structural views (Section 3.2.20) of COM along the three principal axes and the plane most indicative of stacking faults $(13\bar{1})$ are presented in Figures 6.20-6.23.

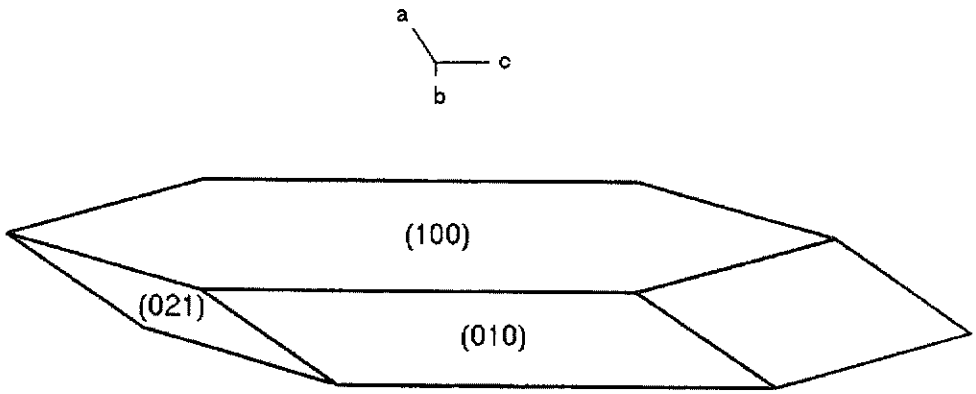

Figure 6.19 A schematic diagram of CaOx monohydrate morphology showing commonly observed faces.

In the (100) plane (Figure 6.20), calcium and oxalate ions are interplanar and alternately layered between a band of oxalate and water molecules. The (010) plane (Figure 6.21) consists of repeating layers of calcium ions, in and out of plane oxalate ions and water molecules. The (001) plane (Figure 6.22) comprises repeating out of plane calcium ions, oxalate ions and water molecules. The presence of foreign molecules between some of the layers of the principal planes could cause expansion of those layers and compression in the adjoining ones, and also slow the growth of those surfaces. The wider distribution of lattice spacings is probably the origin of both the increased non-uniform strain and reduced crystallite size observed.

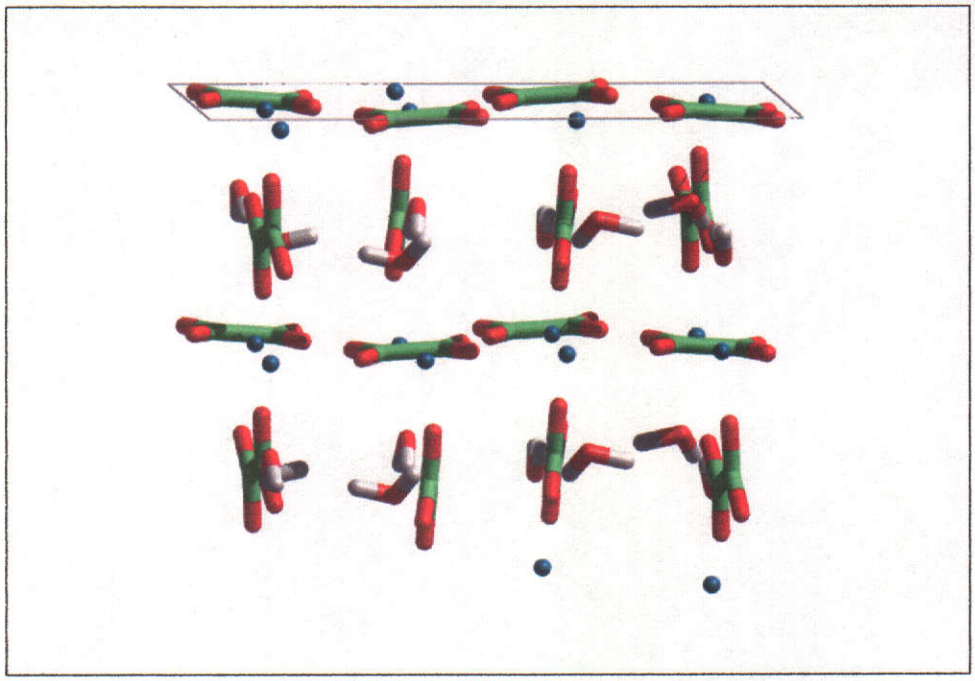

Figure 6.20 Sectional cut viewed through the plane of the white rectangle representing the (100) plane of COM. Calcium ions are blue; oxalate ions are green/red, and water molecules are red/white.

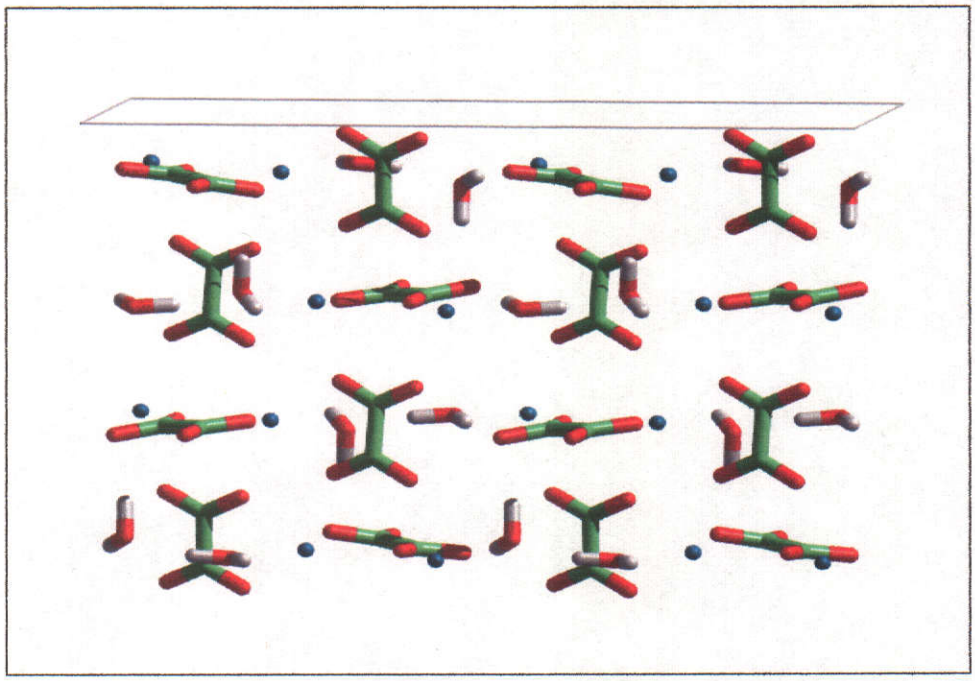

Figure 6.21 Sectional cut representing the (010) plane of COM. Calcium ions are blue; oxalate ions are green/red, and water molecules are red/white.

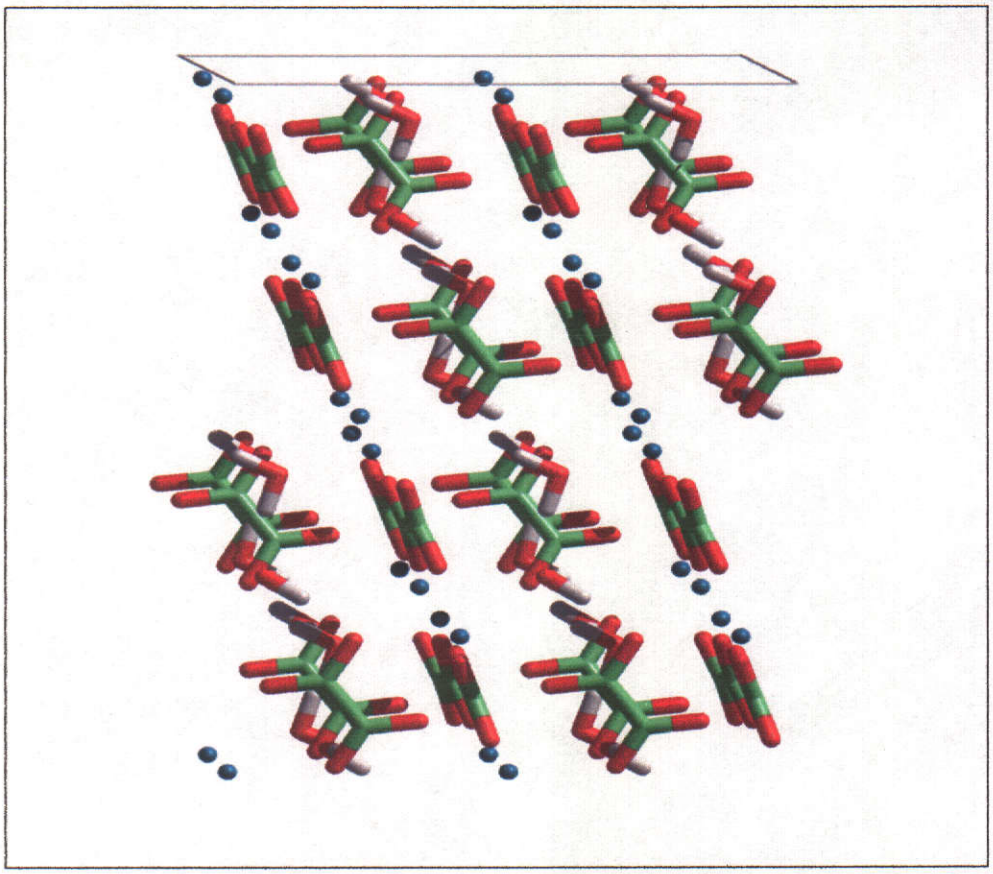

Figure 6.22 Sectional cut representing the (001) plane of COM. Calcium ions are blue; oxalate ions are green/red, and water molecules are red/white.

The diagonal planes such as the $(13\bar{1})$ (Figure 6.23), are not clearly defined layers of oxalate, water and calcium, as the (100), (010) and (001) are, where the planes do not cut through water nor oxalate molecules. The $(13\bar{1})$ plane cuts some water molecules at an oxygen atom or the middle of the carbon-carbon double bond. It is thus not a growth plane and adsorption or occlusion is not likely to occur along it. Further, the $(13\bar{1})$ plane is unlikely to incorporate large molecules, but their presence in the principal planes would nonetheless cause a significant change in this plane. For example, if a (010) layer was displaced by 50% of its d spacing, the $(13\bar{1})$ spacing would be almost zero on the compressed side and double on the expanded side. Thus it would be expected that stacking faults caused by macromolecules adsorbed onto growing crystal faces would create the largest rises in disorder, and thus peak broadening, in zones such as along the $(13\bar{1})$ plane.

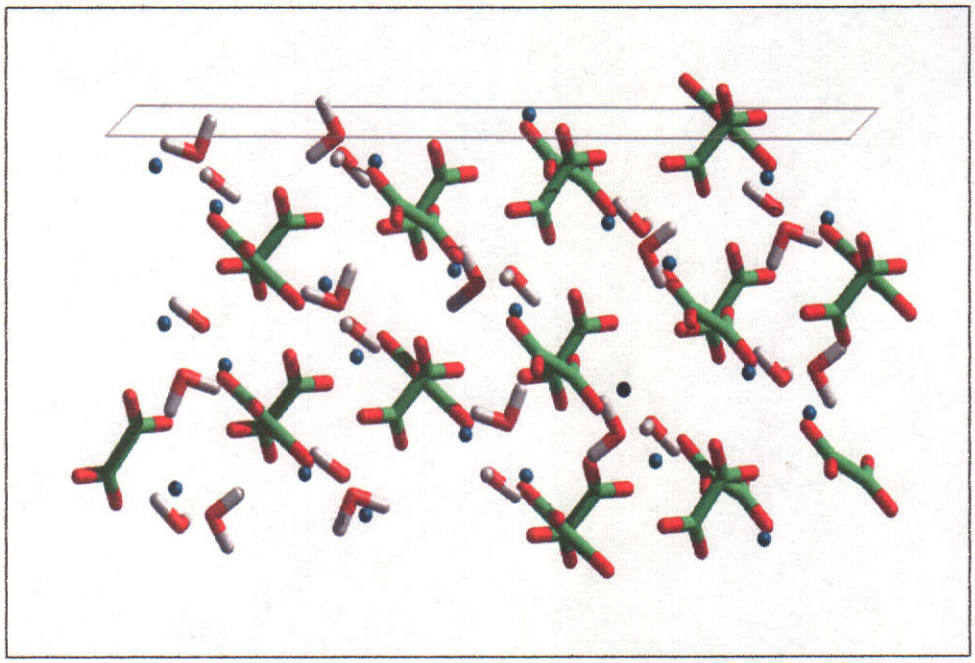

Figure 6.23 Sectional cut representing the $(13\bar{1})$ plane of COM. Calcium ions are blue; oxalate ions are green/red, and water molecules are red/white.

6.5 DISCUSSION

Isotropic/anisotropic behaviour was determined by comparing derived values of non-uniform strain and crystallite size along the major crystallographic axes, using discrete peak analysis (SHADOW) and Williamson-Hall plots. Results from both methods were found to be generally consistent, showing similar isotropic and anisotropic behaviour in COM grown in the same aqueous and urinary media. However, although useful information can be obtained from the Williamson-Hall plots, the technique is only semi-qualitative at best, and caution should be applied when using a low number of reflections (as in this study) because it can lead to erroneous conclusions (Snyder et al., 1999). Yet, despite this limitation, there was some agreement with Rietveld results, particularly when allowances were made for instrumental line broadening. In addition, the Williamson-Hall plots were able to show the degree of stacking faults, which could not be obtained from discrete peak analysis (SHADOW). Conclusions regarding each of the crystal types are discussed below, arranged in six groups, on the basis of their computed values of non-uniform strain, crystallite size, stacking faults and anisotropy.

1. COM (gelatin)

For COM grown in gelatin, the crystallites were isotropic (a = b = c), with little or no strain and few stacking faults, as the deviation of the $(13\bar{1})$ reflection from the principal axes trend line was slight. This result was expected, as crystal growth in gelatin is very slow (12 weeks), which minimises minimising growth faults, dislocations and non-uniform strain.

2. COM (distilled water, Asp, AspAsp, GluGlu, THG, CF/PK)

The crystallites comprising these crystals, were isotropic, but smaller in size than those of COM grown in gelatin. The decrease in crystallite size was probably the result of more rapid crystallizing conditions (15 hours) than were used for gelatin, which would have produced more stacking faults, and consequently, increased non-uniform strain. This was observed when COM was grown in distilled water. Addition of aspartic acid had very little effect on non-uniform strain and crystallite size, despite its moderately high adsorption affinity for COM compared with other amino acids (Chapter 4). This was supported by the work in Chapter 5, which confirmed that aspartic acid was not intracrystalline. This also held for COM grown in AspAsp, GluGlu and THG. The increase in crystallite size and decrease in non-uniform strain observed when COM (CF) was treated with Proteinase K may have resulted from the removal of smaller crystallite material packed with a higher concentration of intracrystalline protein, which would have caused a relaxation of non-uniform strain.

3. COM (UF)

COM (UF) possessed isotropic strain but anisotropic crystallite size. The smaller size indicated by the (002/004) line widths meant that the "c" axis (001) of the crystallites was shorter ($a \sim b > c$). This suggested that the molecules (probably small peptides) interred within the crystals had preferentially adsorbed onto the (001) face of the crystal, and had thus slowed growth rate relative to the other faces. Consequently, it is reasonable to expect that there would be some effect on the morphology of COM, a prediction that was confirmed in Chapter 9.

4. COM (Gla, HSA)

Data for COM (Gla, HSA) were similar to those computed for COM (distilled water, Asp, AspAsp, GluGlu, THG, CF/PK) but with still larger non-uniform strain, smaller

crystallite strain and more stacking faults. The result for Gla was not unexpected, as it already been found to have a higher affinity for COM crystals than all the amino acids tested (Chapter 4) and was therefore most likely to effect the stacking order of the growing crystal by competing with the oxalate ions for calcium. Further, both Gla and HSA were found to be intracrystalline components of COM (Chapter 5) and their presence in the mineral bulk would cause more stacking faults than would be found in COM (gelatin) and COM (distilled water, Asp, AspAsp, GluGlu, THG, CF/PK). However, the adsorption of neither molecules appeared to be face selective.

5. COM (Glu, CF, CME)

In contrast to those discussed above, the crystallites in COM (Glu, CF, CME) crystals exhibited some anisotropy. COM (Glu) had a smaller crystallite size along the (100) axis than the other two axes, indicating preferential adsorption on that face ($a < b \sim c$). The selectivity of Glu, compared to that of Gla, may be attributed to the lower adsorption affinity of the former (Chapter 4). However, the large number of stacking faults found in COM (Glu) substantiates the demonstration that Glu is incorporated into COM (Chapter 5). COM (CF) and COM (CME), were difficult to evaluate in terms of anisotropic behaviour because the results from Williamson-Hall plots and discrete peak analysis (SHADOW) differed. SHADOW showed that the (100) and (001) axes were shorter than the (010) axis ($a \sim c < b$), which indicated that the molecules in both CF urine and CME (aqueous) had adsorbed preferentially onto the (100) and (001) faces. However, their smaller face selectivity relative to Glu probably resulted from a higher affinity of CME and the components of CF urine for a greater number of COM faces. The large stacking faults found in COM (CME) and COM (CF) can almost certainly be attributable to the presence of incorporated macromolecules (Chapter 5).

6. COM (PT)

COM (PT) differed from the other crystals in that it possessed the largest strain and greatest stacking faults, as well as the smallest crystallite size. The crystallites were isotropic with respect to size. The non face-specific adsorption of PT was probably the result of its very high affinity for COM (Chapter 5).

The models of COM showed that the surface of the (001) plane (Figure 6.22) contains a higher concentration of calcium ions and water molecules relative to

oxalate ions compared to the other two principal axes planes, (100) and (010) (Figures 6.20-21). This means that there would be a greater affinity for calcium-binding amino acids and proteins at the crystal surface of this plane. The adsorption of those molecules to a preferred face, especially the larger proteins, would be expected to slow down the growth of that face relative to the other faces, thereby altering the crystal morphology. Because calcium ions are more accessible on the (100) plane than on the (010) plane, the surface adsorption of calcium-binding organic molecules would be expected to be greater on the former, producing a crystal with a relatively small (010) face, which I have commonly observed in urinary COM crystals (see, for example, Figure 5.3).

The $(13\bar{1})$ plane (Figure 6.23) differs from the planes of the principal axes in that there are fewer available calcium ions for binding with amino acids and proteins, yet the largest line broadening occurred there. However, as was shown in the Williamson-Hall plots, much of the line broadening contribution was from stacking faults. As the non-uniform strain and crystallite size contribution to line broadening is valid only for the principal axes or an overall average value, stacking faults in one principal axis direction will not significantly affect the other two principal axes, only the diagonal planes, such as the $(13\bar{1})$.

This chapter has reported the non-uniform strain, crystallite size and stacking fault contribution of occluded amino acids and proteins to XRD line broadening along eleven crystallographic planes of COM. The resulting increased internal crystal disorder and altered internal crystalline structure would be expected to have a significant effect on a crystal's biophysical properties, for example, its dissolution rate. Its biochemical properties could also be affected, as evidenced by the observation that the disorder of COM (CF urine) crystals altered after treatment with Proteinase K. These observations have important implications for urolithiasis, as they suggest that the stability of COM crystals formed in the renal system will be influenced by the macromolecular content of the surrounding urine. This possibility is addressed in Chapter 10.

7 AMORPHOUS CONTENT OF CALCIUM OXALATE MONOHYDRATE

Inherent in the definition of a crystal is the assumption that the distribution of matter within it is homogeneous and infinite. This may well apply to the vast number of known organic and inorganic crystals, but within the domain of biomineralization, many accepted concepts of crystallography cannot be too rigorously applied (Addadi et al., 1999).

In Chapters 5 and 6, it was shown that intracrystalline molecules in COM caused broadening of X-ray diffraction peaks, resulting from an increase in non-uniform strain and stacking faults, and a decrease in crystallite size. Although not presented in those chapters, the X-ray diffraction profiles also revealed the presence of a very broad underlying band, which was centred around 25° (2θ). The presence of the broad band does not influence Rietveld, SHADOW or Williamson-Hall calculations, as these are based purely on line shape and width of relatively sharp peaks originating from crystalline material. In contrast to the sharp diffraction peaks of crystalline materials, it is found that amorphous or non-crystalline substances, such as glasses, resins and unorientated polymers can generate one or more very broad peaks or "humps" (Klugg, 1974). Other researchers such as have also noted similar humps in single crystal X-ray diffraction patterns from crystalline substances, which have been attributed to the presence of amorphous material (Wang et al. 1997, Keller and Dollase 2000, Aizenberg et al., 2003). In one study, Addadi et al., (1999), concluded that up to 80% of the intensity in SXRD diffractograms of sea urchin laval spicules resulted from amorphous material, and that its presence and stability were influenced by intracrystalline proteins.

The presence of amorphous material is important, since it may influence crystal nucleation, growth and dissolution. Although a broad band in the X-ray diffractograms could represent amorphous material, there may be significant contribution from the glass capillary sample holder or material on the crystal surfaces. Therefore the aim was to quantify the amorphous content in the COM

crystals described in Chapters 5 and 6, free of any effects caused by glass or external material.

7.1 X-ray diffractogram profiles

Since both silicon and COM (gelatin) are highly crystalline it is reasonable to assume that their spectral backgrounds result solely from the glass sample capillary. On that basis, the diffractogram of a pure silicon standard was compared with that of highly crystalline COM grown slowly in gelatin (Figure 7.1). The difference in broad background between the two samples can be attributed to the relative quantities of glass (capillary tube), silicon and COM (gelatin). A glass background profile was obtained by deleting the silicon and COM peaks from the diffractograms, applying a 101 point 'smooth' to each residual background and then averaging them (Figure 7.2). The 'smooth' represents a simple moving average and that 101 points (1°, 2θ) gives a 10 fold reduction in noise, and is a small enough interval to prevent distortion of the shape of the broad peak. This is relatively simple to apply for glass, where there are no peaks due to crystalline material, and silicon where only one crystalline peak in the 2θ range selected (10° - 40° 2θ) needs to be manually removed before applying the smoothing. However, it is not practical to do this for the COM samples, where over 20 crystalline peaks would have to be deleted.

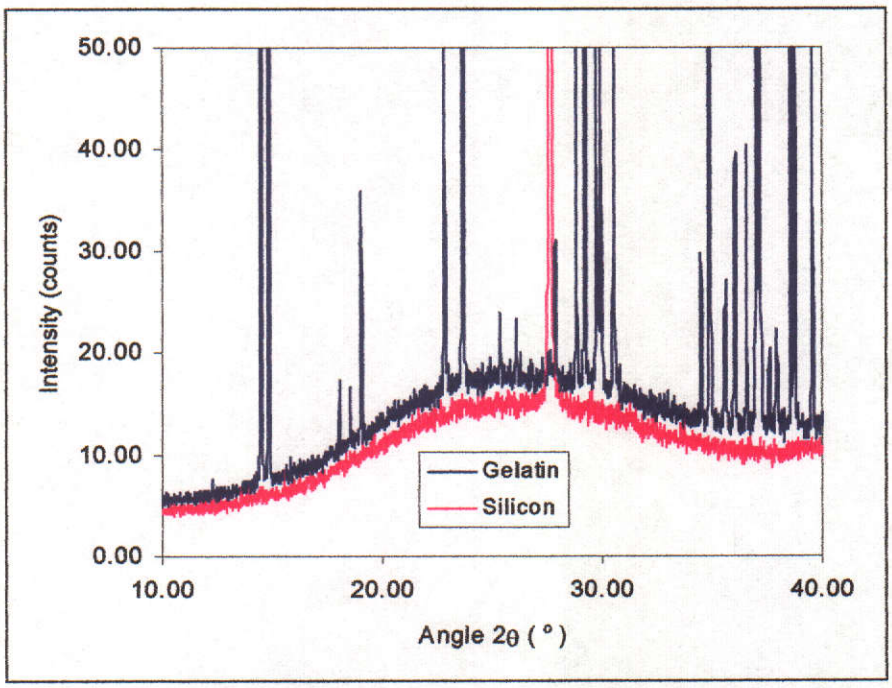

Figure 7.1 SXRD Diffractograms of (a) Silicon and (b) COM grown in gelatin.

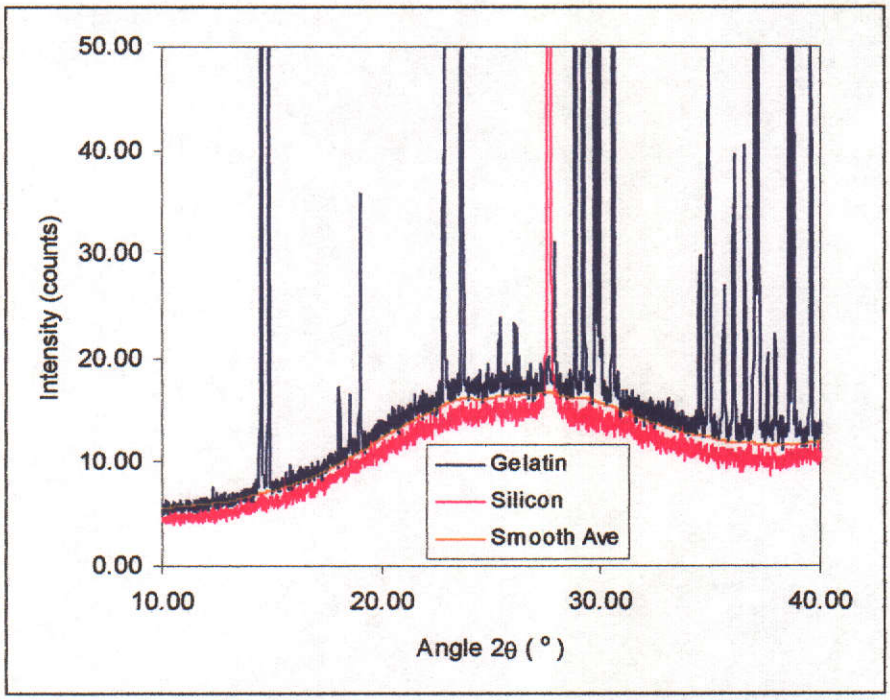

Figure 7.2 Intensity profiles versus angle 2θ (°) of COM grown in gelatin, and silicon and a smoothed averaged background.

The diffraction patterns cannot be directly compared as the differences in peak broadening and the packing density of the samples influence the observed intensities, and the latter also influences the sample/glass ratio. Scaling the spectra to the same total integrated intensity (arbitrary 100,000) and the glass background to the best visual fit to the plateau regions on each side ($10^\circ < 2\theta < 12^\circ$ and $35^\circ < 2\theta < 40^\circ$) addresses these problems. The SXRD baseline profiles of the COM samples, discussed previously in Chapters 5 and 6 are shown in Figure 7.3.

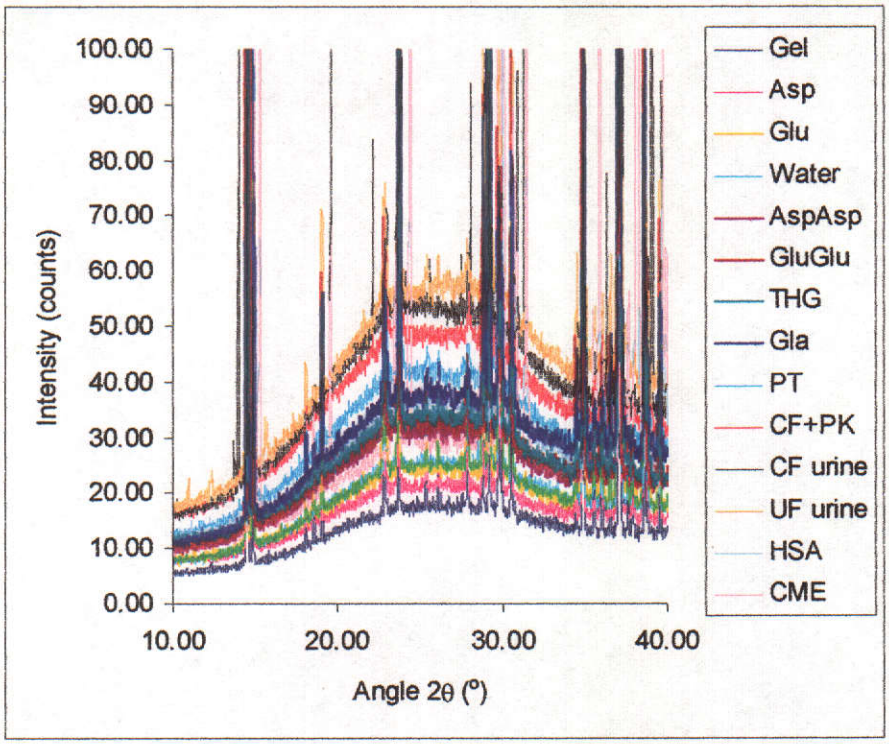

Fig 7.3 Intensity profiles versus angle 2θ (°) of COM grown in gelatin (aq), Asp (aq), Glu (aq), distilled water, AspAsp (aq), GluGlu (aq), THG (aq), Gla and (aq), PT (aq), CF urine + PK, CF urine and UF urine in ascending magnitude of the broad hump at approximately 25° 2θ.

Except for COM (UF), COM (CF) and COM (PT), the glass background fitted well to the background of all samples, indicating that the glass sample capillary is the only detectable contributor to the background signal. An example is given in Figure 7.4, which shows COM (Glu). Thus the presence of Asp, AspAsp, Glu, GluGlu, Gla, CME, HSA and THG in the growing media does not generate detectable quantities of amorphous COM. However, this is not the case with COM (UF), COM (CF) and COM (PT) where there is a clear difference between the glass and sample backgrounds, as shown in Figures 7.5-7.7. After subtraction of the glass background a broad residual peak (25°, 2θ) remains, which is shifted from the position of the glass peak (27°, 2θ), and most likely results from the presence of amorphous material and/or possibly occluded proteins. Whilst the noise level is high, it cancels out to a very large degree when integrating to obtain the area of the broad peak.

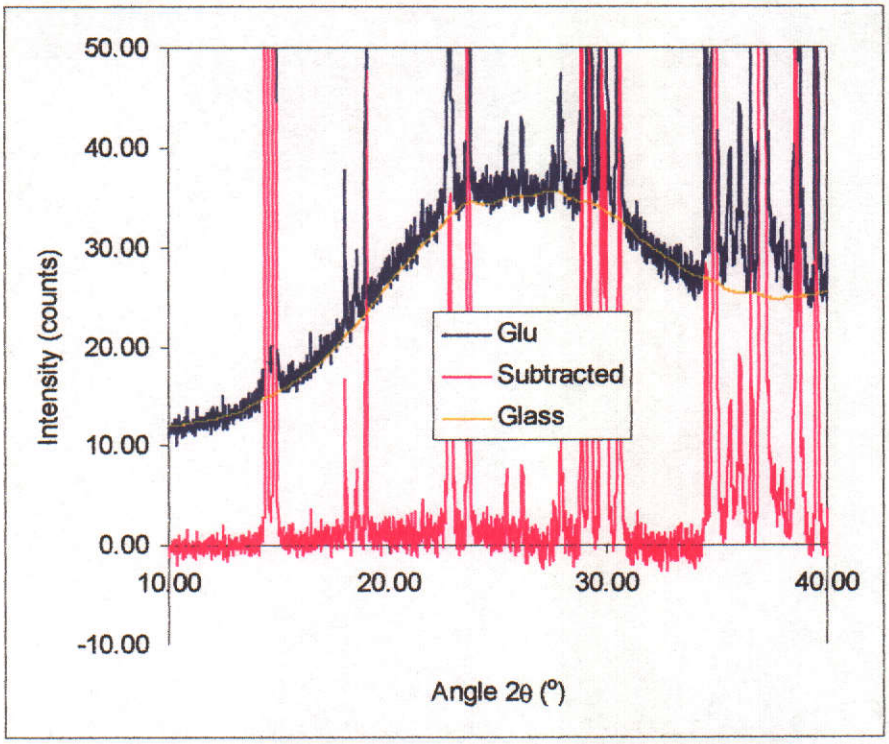

Figure 7.4 Intensity profiles versus angle 2θ (°) of a smoothed glass background and COM grown with Glu.

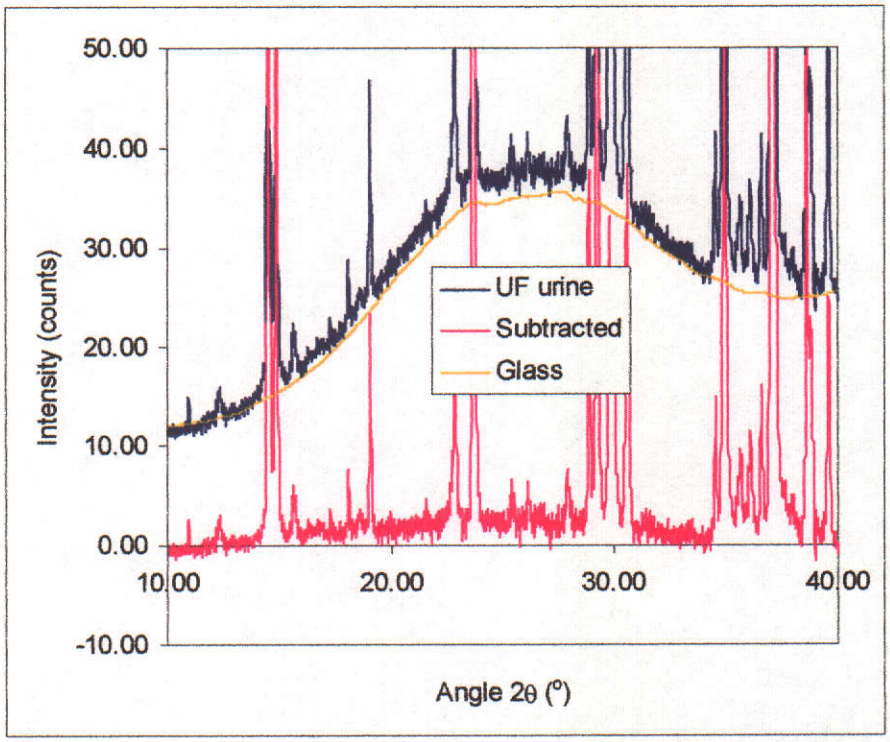

Figure 7.5 Intensity profiles versus angle 2θ (°) of a smoothed glass background and COM grown in UF urine.

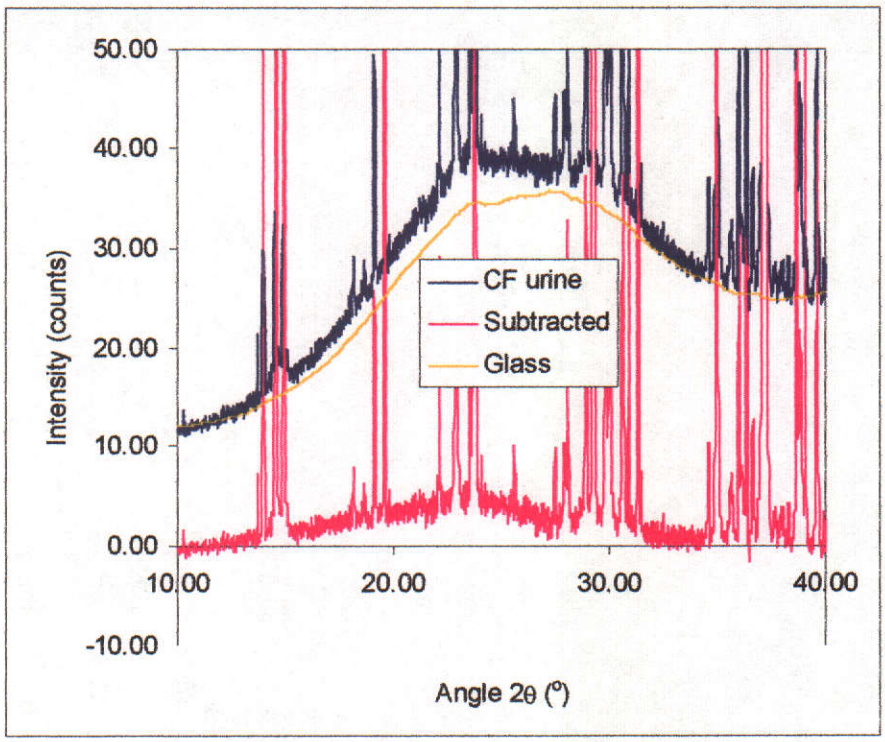

Figure 7.6 Intensity profiles versus angle 2θ (°) of a smoothed glass background and COM grown in CF urine.

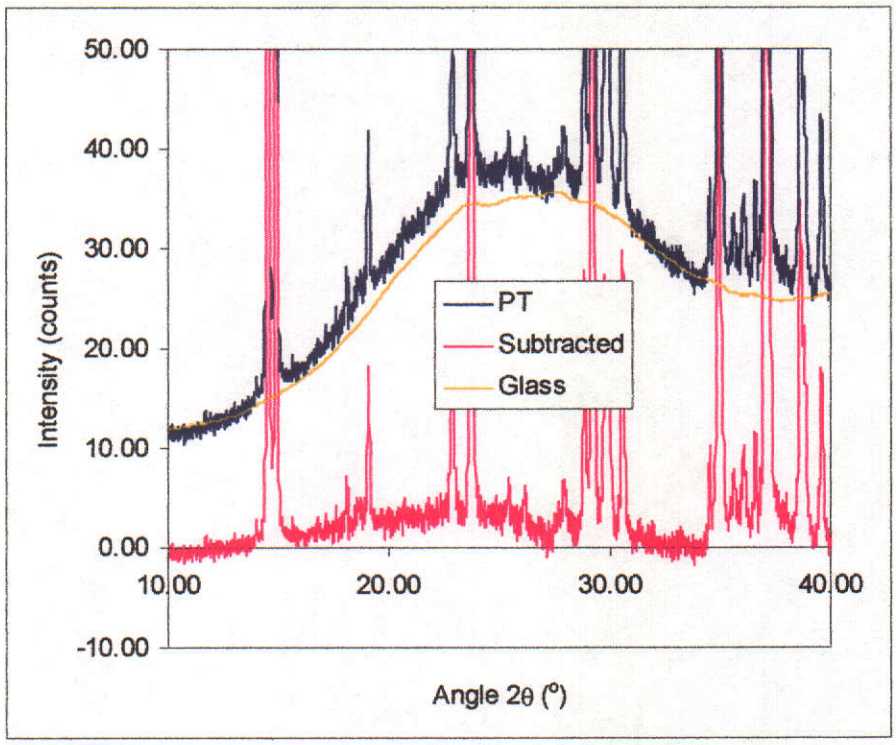

Figure 7.7 Intensity profiles versus angle 2θ (°) of a smoothed glass background and COM grown in PT.

If it is assumed that the residual broad peak is a consequence of amorphous COM and that the SXRD response of both crystalline and amorphous COM are the same,

then the amorphous/crystalline content is dependent on their relative areas (Addadi et al., 1999). These were obtained by integrating the broad smoothed residual peak and the whole SXRD pattern after background subtraction.

Based on the foregoing arguments, the amorphous contribution resulting from the presence of PT was estimated to be 9 ± 3% (Section 3.2.21), a value that is likely to be a maximum as small peaks at higher diffraction angles (>80°, 2θ) may be buried in the background noise. Though the signal to noise ratio is poor in the amorphous diffractogram (~3:1) its area is an integration of approximately 2000, which improves its accuracy by a factor of ~ 45. Hence the error quoted (3%) is a reflection of the subjectivity of visually scaling the glass background to plateau regions to the sample diffractogram rather than signal quality. The amorphous peak areas of COM (CF) and COM (UF) were estimated to be COM (CF) 8 ± 3% and COM (UF) 5 ± 3% respectively. Proteinase treatment of COM (CF) crystals reduced the amorphous content to 4 ± 3% (Figure 7.8).

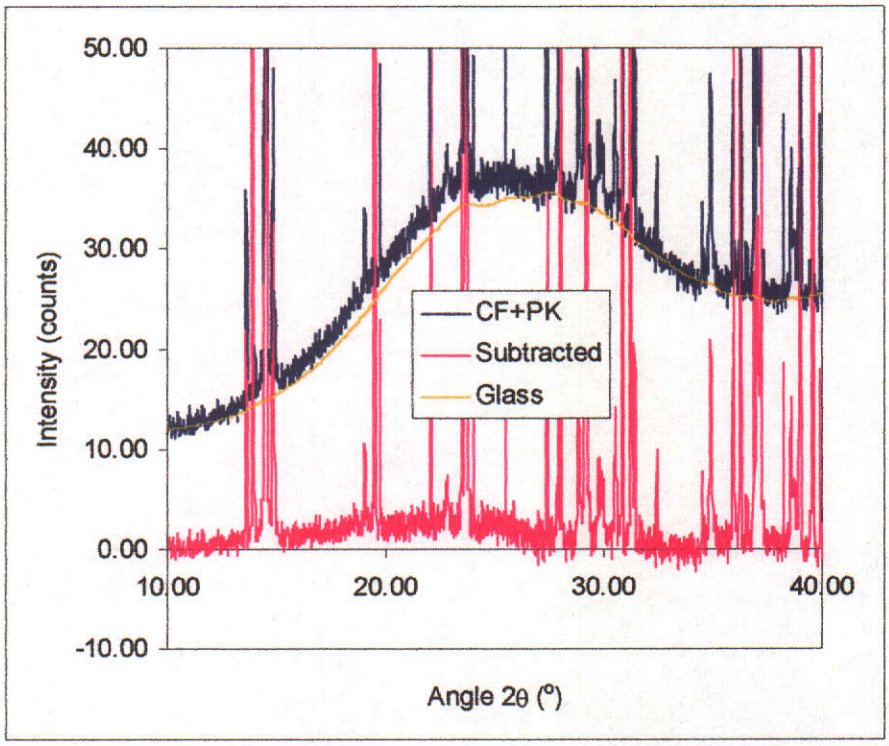

Figure 7.8 Intensity profiles versus angle 2θ (°) of a smoothed glass background and COM grown in CF urine after treatment with proteinase.

7.2 DISCUSSION

The SXRD patterns of COM grown in aqueous solutions of PT as well as in UF urine and CF urine showed that amorphous material were consistent with the presence of amorphous materials within the crystal structure at low percent concentrations (approximately 9%, 5% and 8% respectively). The same three samples were shown in Chapters 5 and 6 to have the highest non-uniform strain, greatest number of stacking faults and the smallest crystallite sizes, confirming that they contained the greatest quantities of incorporated organic molecules. It is highly likely that occluded organic molecules stabilize an amorphous CaOx phase, as was found for calcium carbonate (Addadi, 1999). It is much less likely that the broad band was due to the organic molecules themselves as they comprised of only ~0.4% of the crystal mass in COM (PT) (Section 3.2.21). Further their XRD intensity would have to be at least ten fold greater than COM's, which would seem improbable. Therefore the major contribution to the broad band must have been due to an amorphous COM phase, stabilised by PT. This may also hold for crystals of COM (UF) and COM (CF), particularly the latter, as CF urine contains PT and many other proteins that have been detected in demineralised crystal extracts (Doyle et al., 1991). Furthermore, crystals from UF urine are likely to contain organic molecules with Mr values <10kDa. For example, low molecular weight fragments (Mr 2564, 2677, 2680, 2733, 2921 and 2992) of osteocalcin, a bone protein with a strong affinity for calcium, is present in human urine (Ivaska et al., 2003). The reduction in average peak height found in COM (CF) by proteinase treatment, is a further indication that the amorphous phase is closely associated with occluded proteins. However, these conclusions are made with caution, as the data are not sufficiently rigorous to determine occluded and/or adsorbed proteins and crystalline COM with confidence.

The absence of detectable amorphous material in COM grown in aqueous solutions of Asp, AspAsp, Glu, GluGlu, Gla, THG, HSA and CME demonstrated that those molecules had little or no effect on the production of an amorphous phase. This result for the first four amino acids, as well as for THG and HSA was expected as their effect on non-uniform strain and crystallite size was small compared to PT, UF urine and CF urine, and they are not occluded (Chapter 5). Although Gla has been shown to be an intracrystalline molecule(Chapter 5), it does not appear to stabilize amorphous COM. The reason could well be an entropic one. The multiple binding

from a protein would be associated with a far greater entropy than Gla, and hence is more likely to favour the stabilisation of an amorphous COM phase. The low level of amorphous material found in COM (CME) was unexpected as the components of CME are present in CF urine.

Despite the large errors involved, the results showed that some urinary proteins with a strong affinity for COM (i.e. PT) can stabilise an amorphous phase in the crystal structure. The presence of such a phase is likely to affect the biophysical properties of the crystal, for example, its dissolution rate (Mullin 1993a). In addition to the type of intracrystalline molecules, their concentration could also influence the amorphous content in COM crystals. As the concentration of intracrystalline molecules is also likely to affect stacking faults, non-uniform strain and crystallite size in COM crystals, a study of concentration dependence was undertaken in Chapter 8.

8 THE EFFECT OF CONCENTRATION OF SELECTED AMINO ACIDS AND PROTEINS INCORPORATED IN CALCIUM OXALATE MONOHYDRATE ON NON-UNIFORM CRYSTAL STRAIN AND CRYSTALLITE SIZE

The X-ray diffraction studies described in Chapters 5, 6 and 7 showed that the inclusion of some amino acids and proteins into COM created disorder in the crystals, as evidenced by decreased crystallite size and increased non-uniform lattice strain, stacking faults and an amorphous fraction. Intuitively, raising the ambient concentrations of amino acids and proteins would be expected to increase their concentration within the mineral bulk, thus causing an increase in the degree of crystal disorder.

The aim of this chapter was to quantify the lattice strains and crystallite sizes of COM crystals grown in the presence of varying concentrations of Gla, PT, HSA, and CME in water. These compounds were selected because they were shown to be intracrystalline molecules in COM and created the greatest crystal disorder. The solution concentrations used were chosen so as to bracket the single concentrations of the samples discussed in Chapters 5-7. The crystals were prepared by the same methods, as described in Sections 3.2.4-8. For comparative purposes, COM was also grown in UF urine containing increasing concentrations of HSA and CME. The solution concentrations of the additives are expressed as mass/volume values rather than molar concentrations because the composition of CME is still not completely known.

The crystals were analysed by SXRD and their non-uniform strain and crystallite size obtained from Rietveld whole pattern peak fitting analysis, as previously described in Sections 3.2.13-14. The Rietveld refinement values are detailed in Appendix I.8. Stacking faults, as manifested by non-uniform lattice strain and crystallite size, were determined along the $(13\bar{1})$ plane, using discrete peak analysis (Section 3.2.16), as this plane showed the largest effect in Chapter 6 (Appendices I.4, I.6, I.7).

8.1 Rietveld whole pattern-fitting of X-ray diffractograms

In general, there is an increase in non-uniform strain and a decrease in crystallite size to plateau values with increasing solution concentration of the additives, i.e. the degree of crystal disorder induced is limited. However, COM grown in the presence of Gla is an exception, as it appears to incur further disorder at high solution concentrations. COM (Gla) shows an increase in non-uniform strain and decrease in crystallite size at low concentrations of Gla, showing that the greater the occlusion of Gla the greater the crystal disorder. This disorder reaches a plateau ($\varepsilon \sim 0.08$, $D \sim 0.9$ μm) at ~ 15 mg/L of Gla (Figure 8.1), suggesting that the capacity of COM to accommodate Gla is limited or that at least the disorder caused by the uptake is limited. At concentrations of Gla > 100 mg/L more disorder occurs, as there are further increases in non-uniform strain and decreases in crystallite size. The reasons for this are not clear, but it must be remembered that the results are an average over the whole SXRD pattern and include other forms of disorder. There is thus the possibility that more Gla was being occluded in the observed plateau region but not reflected in the average non-uniform strain and crystallite size, until it reaches much higher levels.

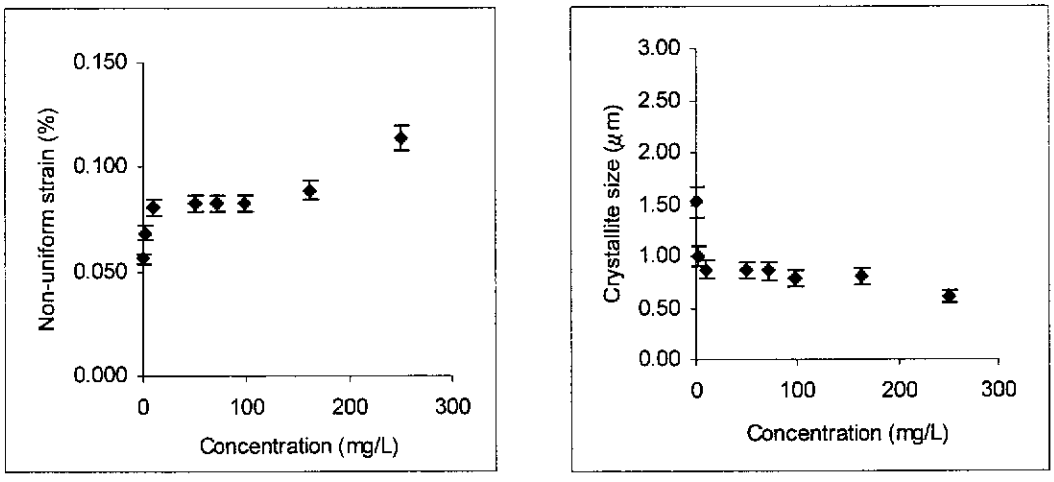

a b

Figure 8.1 Average non-uniform strain (a) and average crystallite size (b) for COM grown in aqueous solutions of Gla.

COM (PT) shows a similar increase in non-uniform strain and decrease in crystallite size as was observed for COM (Gla), with a plateau ($\varepsilon \sim 0.12$, $D \sim 0.3$ μm) probably

occurring at 20 mg/L PT or a little higher (Figure 8.2). As was observed in Chapter 5, for the similar non-uniform strain, PT generates a smaller crystallite size than Gla.

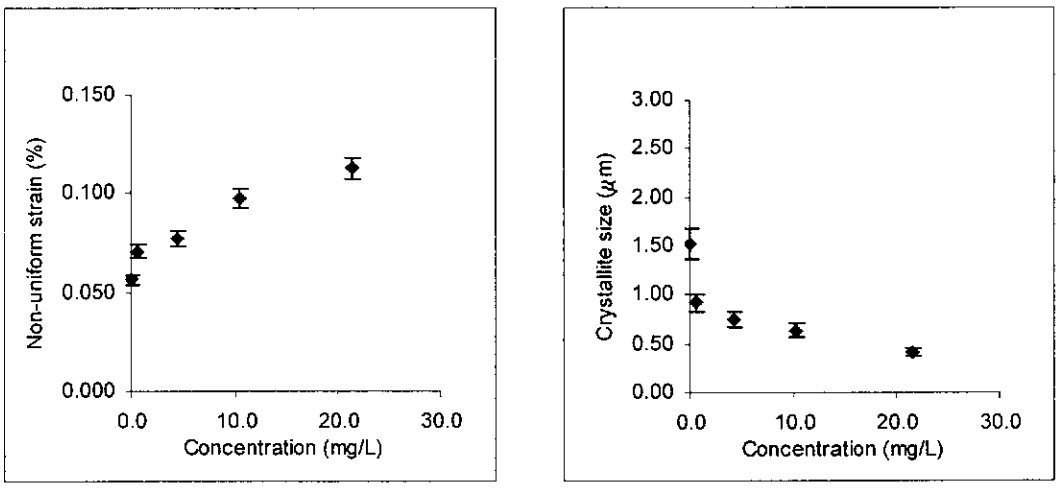

a b

Figure 8.2 Average non-uniform strain (a) and average crystallite size (b) for COM grown in aqueous solutions of PT.

COM (HSA), like COM (PT) also shows an increase in non-uniform strain and decrease in crystallite size with increasing solution concentration, but with a plateau ($\varepsilon \sim 0.08$, $D \sim 0.7$ μm) occurring at approximately 60 mg/L (Figure 8.3). This shows that the non-uniform strain limit it generates is less than COM (PT), and occurs at higher concentration. The crystallite size for COM (HSA) is also much larger than for COM (PT) at their respective limiting solution concentrations.

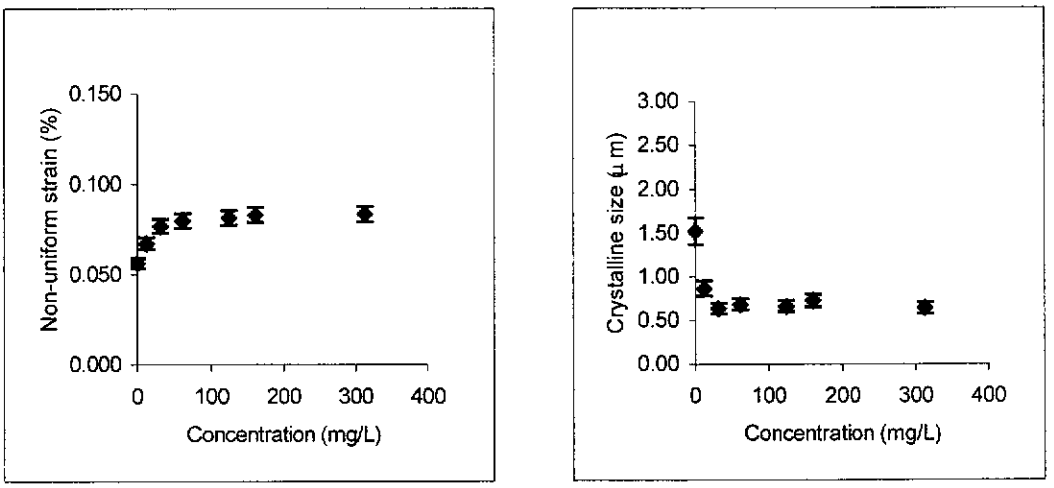

a b

Figure 8.3 Average non-uniform strain (a) and average crystallite size (b) for COM grown in aqueous solutions of HSA.

COM (CME) shows a similar increase in non-uniform strain and decrease in crystallite size as was observed for COM (PT), but with a plateau ($\varepsilon \sim 0.12$, D~0.5μm) occurring at a much lower solution concentration (~ 4 mg/L) (Figure 8.4).

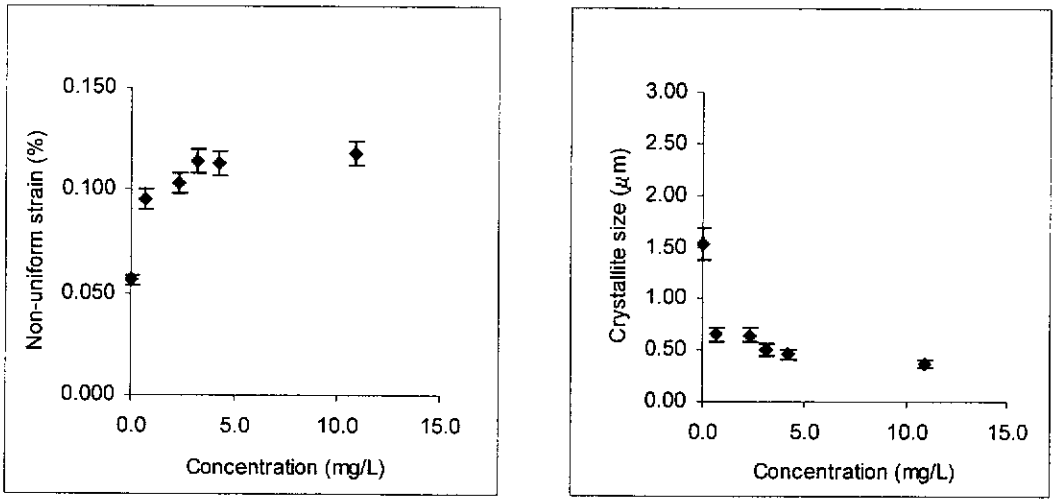

a b

Figure 8.4 Average non-uniform strain (a) and average crystallite size (b) for COM grown in aqueous solutions of CME.

The changes in non-uniform strain and crystallite size were comparatively small for COM grown with HSA in UF urine (Figure 8.5), showing a much lower effect than with aqueous COM (HSA), and having virtually no concentration dependence. However, there is a hint of a plateau ($\varepsilon \sim 0.08$, D~0.8μm) commencing at 10 mg/L.

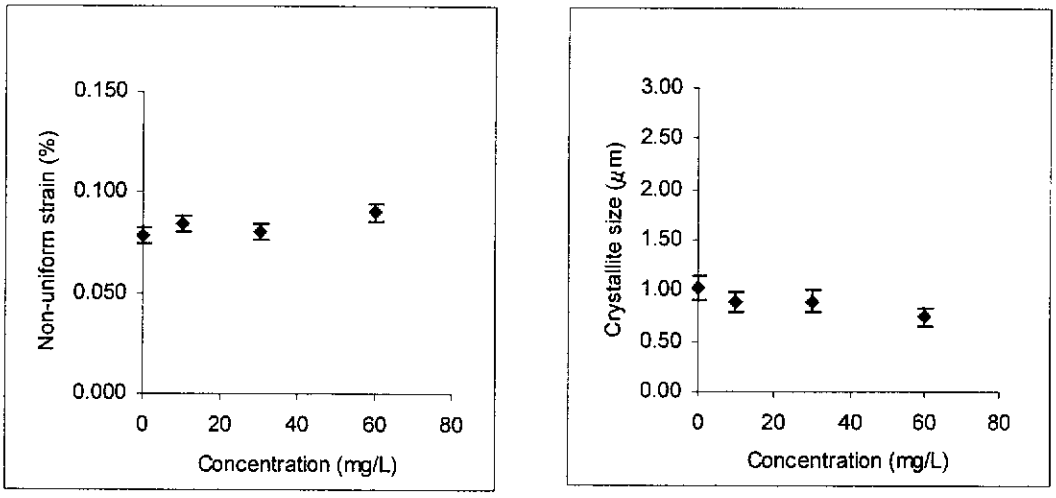

a b

Figure 8.5 Average non-uniform strain (a) and average crystallite size (b) for COM grown with HSA in UF urine.

COM (CME/UF urine) shows a similar increase in non-uniform strain and a decrease in crystallite size as was observed for aqueous COM (CME), with a plateau ($\varepsilon \sim 0.12$, D~0.5μm) occurring at ~ 3 mg/L (Figure 8.6).

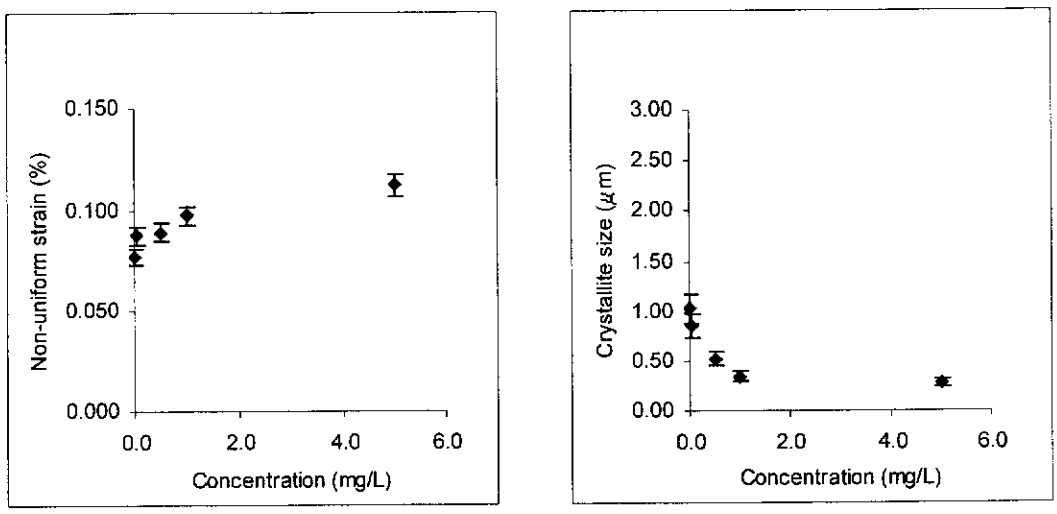

a b

Figure 8.6 Average non-uniform strain (a) and average crystallite size (b) for COM grown with CME in UF urine.

Figure 8.7 shows that a reciprocal relationship exists between average non-uniform strain and average crystallite size for COM grown with increasing concentrations of Gla (aqueous), PT (aqueous), HSA (aqueous), CME (aqueous), HSA (UF urine) and CME (UF urine). The slopes of the relationships are 16 ±1, 28 ± 4, 30 ± 5, 31 ± 4, 25 ± 5 and 82 ± 16 respectively. COM grown with CME in UF urine gave the greatest slope, indicating that the change in the crystallite size is highest for a given increase of non-uniform strain value. Conversely, COM grown with Gla gave the smallest slope. The gradients obtained for other COM crystals were similar. Statistical analysis of these plots (Appendix I 10, Section 3.2.15, equation 4) shows that the non-uniform strain and crystallite size relationship for Gla is different from PT (aq), HSA (aq), CME (aq) and HSA (UF urine), as was found in Chapter 5, and that CME (UF urine) is different again. However, HSA (UF urine) is open to question as it is displaced from the other three trend lines, covers a comparatively short range and straddles the CME/UF data. Additionally, HSA produces a far smaller additive effect in UF urine than CME in UF urine.

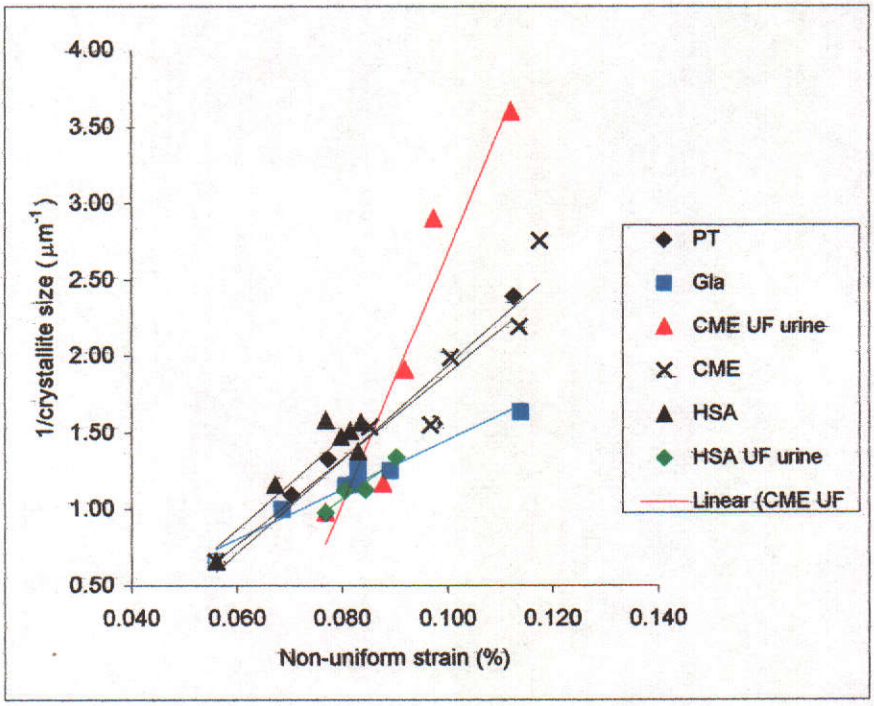

Figure 8.7 Average non-uniform strain and reciprocal of average crystallite size for COM grown in various media.

8.2 Discrete synchrotron X-ray peak analysis

Discrete peak analysis allows non-uniform strain, crystallite size and stacking faults to be obtained along a particular crystallographic direction, rather than the Rietveld global average values, which are independent of direction. The $(13\bar{1})$ axis was chosen because line broadening was generally greater along this crystallographic direction than others determined in Chapter 6. Gaussian and Lorentzian contributions to the $(13\bar{1})$ X-ray peak shape profiles were determined with SHADOW (1998) and from these contributions, lattice strains and crystallite sizes, attributable to stacking faults were calculated (Sections 3.2.16 and 6.3). Individual values with corresponding errors are given in Appendix I.9.

As in Rietveld analysis, discrete peak analysis shows that there is a general increase in non-uniform lattice strain and a decrease in crystallite size to plateau values with increasing solution concentrations of the additives. As expected, the non-uniform strain is generally higher and the crystallite size lower along the $(13\bar{1})$ axis for each corresponding solution concentration of additive than in Rietveld analysis.

COM (Gla) shows a regular increase in non-uniform strain and decrease in crystallite size, with one plateau ($\varepsilon \sim 0.26$, D ~ 0.1 μm) occurring at ~ 200 mg/L (Figure 8.8), differing in profile from the Rietveld analysis. This reflects a steady increase in crystal disorder in COM, mainly as stacking faults along the $(13\bar{1})$ axis with increasing solution concentration of Gla, to a limiting value.

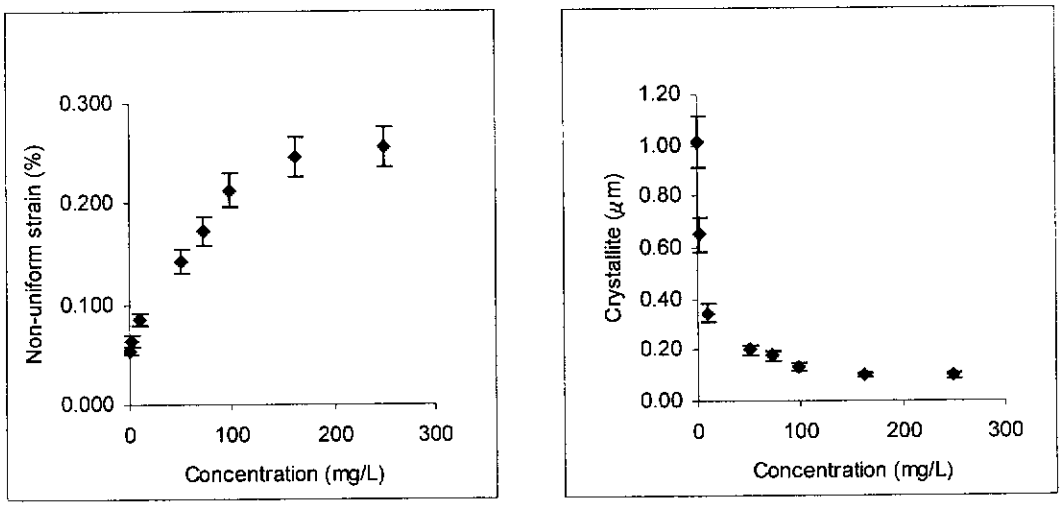

a b

Figure 8.8 Non-uniform strain (a) and crystallite size (b) along the $(13\bar{1})$ crystal plane for COM grown in aqueous solutions of Gla.

COM (PT) shows a similar increase in non-uniform strain and decrease in crystallite size as was observed for COM (Gla), but with a plateau ($\varepsilon \sim 0.24$, D ~ 0.1 μm) occurring at a much lower solution concentration (~12 mg/L PT), (Figure 8.9).

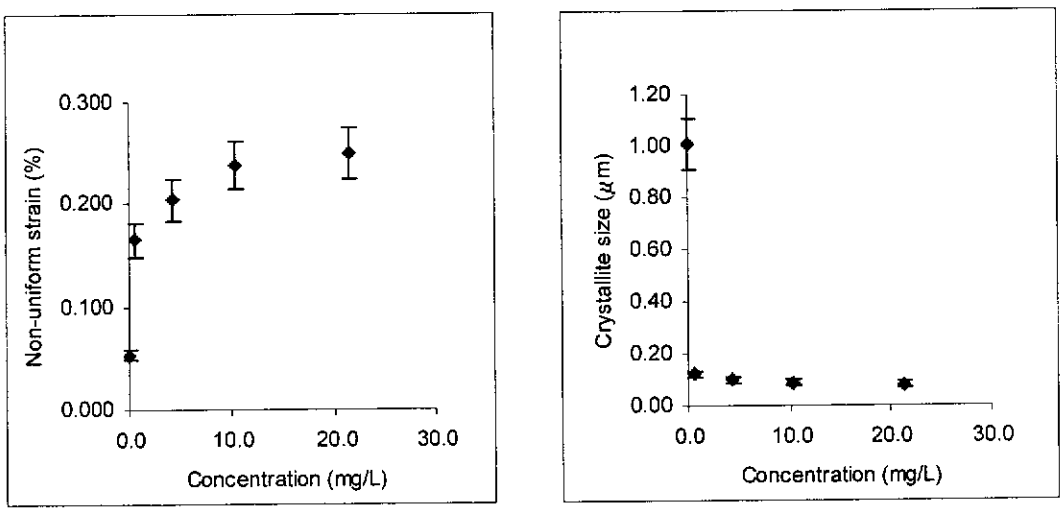

a b

Figure 8.9 Non-uniform strain (a) and crystallite size (b) along the $(13\bar{1})$ crystal plane for COM grown in aqueous solutions of PT.

COM (HSA) shows a similar increase in non-uniform strain and a decrease in crystallite size, as was observed for aqueous COM (PT), but with a plateau ($\varepsilon \sim 0.14$, D~0.1μm) occurring at a much higher concentration ~ 60 mg/L (Figure 8.10).

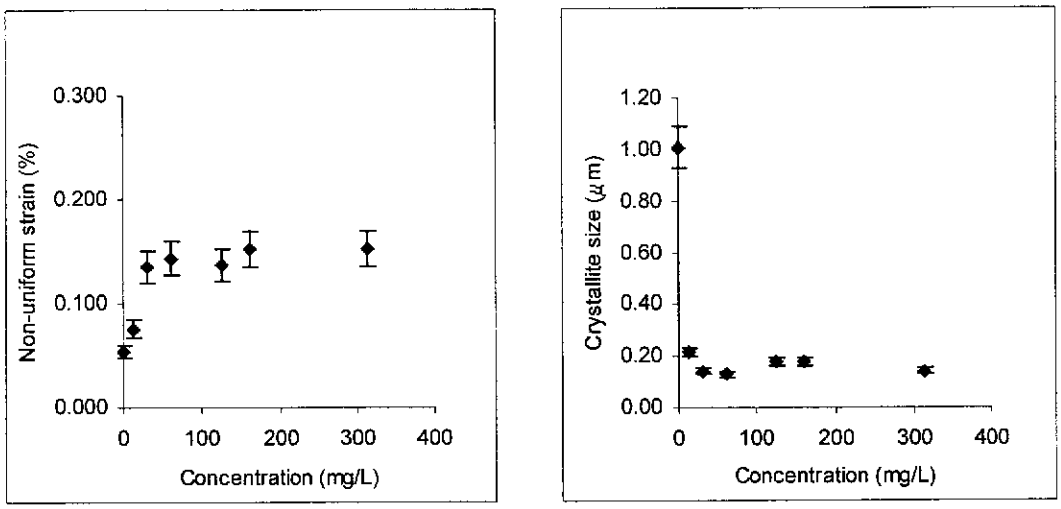

a b

Figure 8.10 Non-uniform strain (a) and crystallite size (b) along the $(13\bar{1})$ crystal plane for COM grown in aqueous solutions of HSA.

COM (CME) shows a similar increase in non-uniform strain and decrease in crystallite size as was observed for aqueous COM (PT), with a plateau ($\varepsilon \sim 0.23$, D~0.1μm) occurring at a solution concentration of ~ 4 mg/L (Figure 8.11).

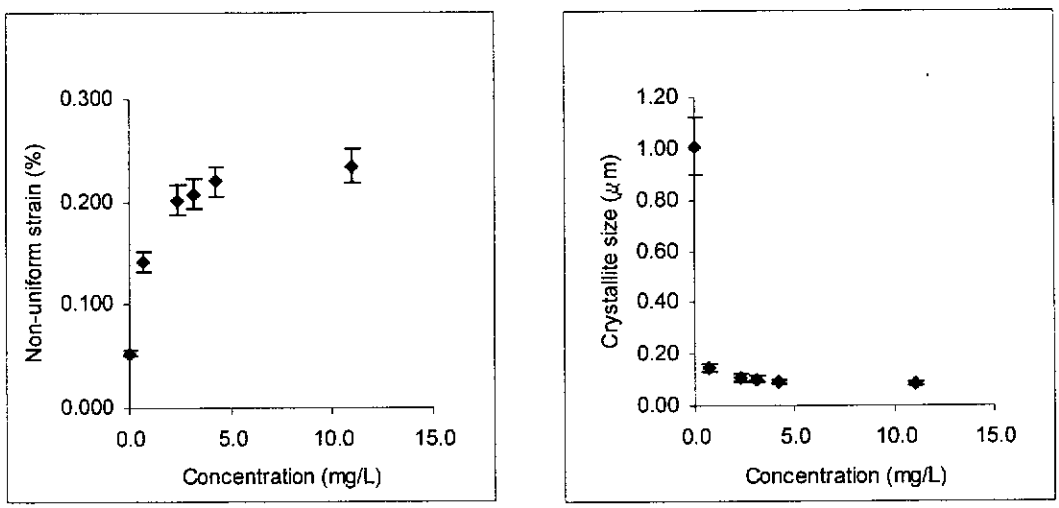

a b

Figure 8.11 Non-uniform strain (a) and crystallite size (b) along the $(13\bar{1})$ crystal plane for COM grown in aqueous solutions of CME.

COM (HSA/UF urine) shows a similar increase in non-uniform strain and decrease in crystallite size as was observed for COM (PT), with a plateau ($\varepsilon \sim 0.15$, D~0.1μm) occurring at a solution concentration of ~ 10 mg/L (Figure 8.12). In comparison to Rietveld analysis, the crystal disorder along the $(13\bar{1})$ axis in COM (HSA/UF urine) is far more concentration dependent for the same additive solution concentrations.

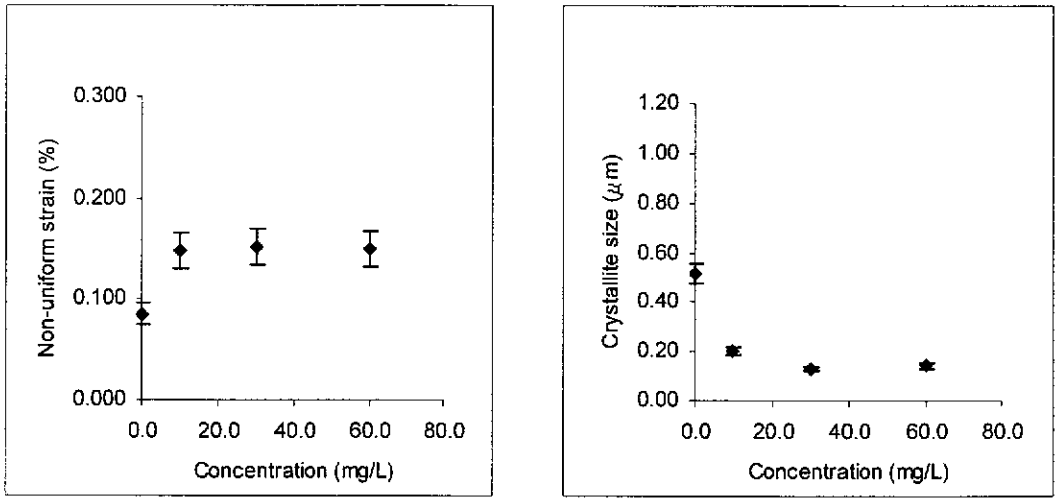

a b

Figure 8.12 Non-uniform strain (a) and crystallite size (b) along the $(13\bar{1})$ crystal plane for COM grown in UF urine containing HSA.

COM (CME/UF urine) shows a similar increase in non-uniform strain and a decrease in crystallite size as was observed for aqueous COM (CME), with a plateau ($\varepsilon \sim 0.21$, D~0.1μm) occurring at ~ 3 mg/L (Figure 8.13).

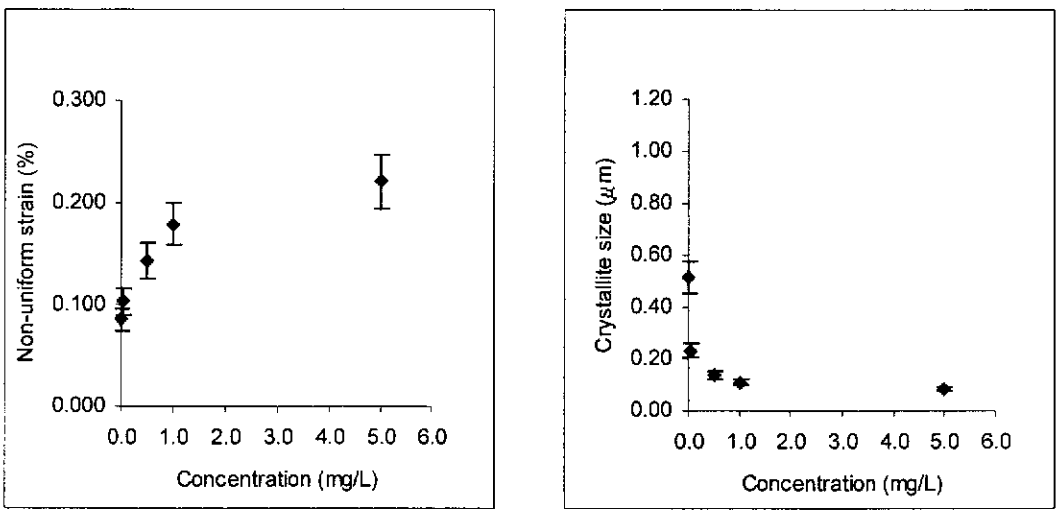

a b

Figure 8.13 Non-uniform strain (a) and crystallite size (b) along the $(13\bar{1})$ crystal plane for COM grown in UF urine containing CME.

The data in Figure 8.14 shows that a reciprocal relationship exists between lattice strain and crystallite size along the $(13\bar{1})$ crystal plane for COM grown in aqueous solutions with increasing concentrations of Gla, PT, HSA and CME. The slopes were calculated to be 43 ± 2, 57 ± 3, 50 ± 13 and 57 ± 2 respectively. A reciprocal relationship also holds for COM grown with increasing concentrations of HSA and CME grown in UF urine. The corresponding slopes were found to be 73 ± 23 and 71 ± 5 respectively.

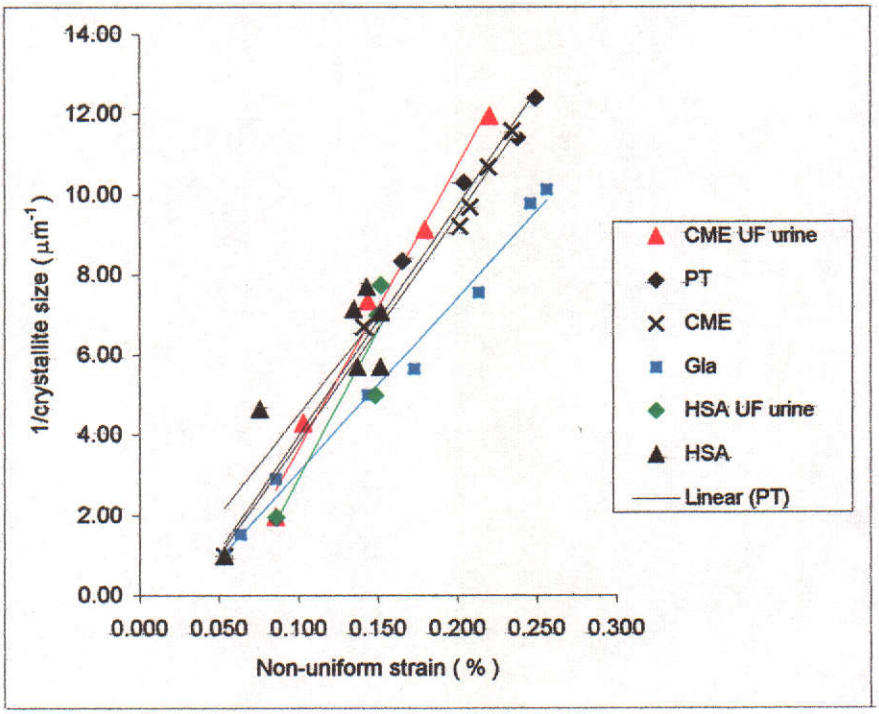

Figure 8.14 Non-uniform strain and the reciprocal of crystallite size along the $(13\bar{1})$ crystal plane for COM grown in various media.

Statistical analysis of these plots (Appendix I 11, Section 3.2.15, equation 4) shows that the non-uniform strain and crystallite size relationship for Gla is different from PT, HSA, and CME, and that HSA (UF urine) and CME (UF urine) are different again. The placement of HSA (UF urine), however, is less certain due to the substantially greater error associated with its slope. The slopes derived from discrete peak analysis are approximately double those derived from whole pattern fitting, suggesting that the broadening of the $(13\bar{1})$ peak is due to both size/non-uniform strain and stacking fault factors. The only exception to this was COM grown in CME (UF urine) solutions, which had similar slopes. The reason for this disparity is

not obvious, but it may be due to different crystallizing conditions producing different growth rates. If the crystallization with CME in UF urine is significantly slower, then the size/non-uniform strain broadening may be less than under faster crystallizing conditions, whilst the stacking faults remains unaffected. Equally well, the stacking fault rate could be decreased and the size/non-uniform strain factor could be unaffected, or it could be a combination of both.

The results of both Rietveld (average) and Shadow ($13\bar{1}$) analysis are summarised in Table 8.1.

Table 8.1 Summary of whole pattern and single peak ($13\bar{1}$) SXRD analysis

Sample	Approximate concentration to achieve plateau (mg/L)		Approximate plateau non-uniform strain (%)		Approximate plateau crystallite size (μm)		Slope (1/size v strain)	
	Rietveld	**Shadow**	**Rietveld**	**Shadow**	**Rietveld**	**Shadow**	**Rietveld**	**Shadow**
Gla	10 -20	200 -220	0.08	0.26	0.9	0.1	16 ±1	43 ±2
PT	15 - 25	10 - 15	0.12	0.24	0.3	0.1	28 ±4	57 ±3
HSA	60 - 80	50 - 70	0.08	0.14	0.7	0.1	30 ±5	50 ±13
CME	3 - 5	4 - 6	0.12	0.23	0.5	0.1	31 ±4	57 ±2
HSA /UF	7 - 15	8 - 12	0.08	0.15	0.8	0.1	25 ±5	73 ±23
CME /UF	2 - 3	3 - 4	0.12	0.21	0.5	0.1	82 ±16	71 ±5
UF			0.080 ±0.003	0.086 ±0.009				

8.3 DISCUSSION

Although an intimate association between urinary proteins and CaOx crystals precipitated from urine has now been largely accepted, no work to date has attempted to assess the effect of protein concentration on crystal disorder, i.e. crystal lattice strain and crystallite size. Both average whole pattern fitting (Rietveld) and single peak analysis ($13\bar{1}$) (SHADOW) showed a similar trend in terms of non-uniform strain and crystallite size for COM grown in aqueous solutions at increasing

concentrations of Gla, PT, HSA and CME. Generally an increase in non-uniform strain and a decrease in crystallite size to a plateau value was observed as the concentration of dopants increased. This trend was also found for COM grown with increasing concentrations of CME in UF urine, although this was only evident along the $(13\bar{1})$ plane for HSA in UF urine. The increase in crystal disorder suggests an increase in uptake of these molecules by the growing crystal from the surrounding solution. Both methods showed that a plateau region was reached, indicating that saturation occurs in the uptake of these dopants into the crystal matrix (Table 8.1). This supports the view that the organic molecules are occluded and there are limits to the non-uniform strain and crystallite size. If the agglomeration of smaller crystals with adsorbed organic molecules was occurring, then the increase in non-uniform strain and decrease in crystallite size with concentration, and their limiting values would not be seen. However, it is difficult to determine whether there is a limit on the uptake of the additives into the crystal matrix or whether there is a limit to the non-uniform strain and crystallite size that the crystal can tolerate.

Single peak analysis gave higher lattice strains and smaller crystallite sizes than whole pattern fitting for the same additive concentrations and consequently, higher slopes for the reciprocal size v non-uniform strain relationships. From the anisotropy work in chapter 6, this difference in response was expected, as whole pattern fitting gives only averaged values, whereas single peak analysis gives values along a specific plane in a crystal. In this case, the $(13\bar{1})$ plane being a body diagonal, includes a major contribution to its disorder from stacking faults in addition to crystallite misorientation and size. The latter do not contribute to principal plane disorder, and to a lesser extent to face diagonal plane disorder. Thus non-uniform strain calculated for body diagonal planes will be greater and crystallite size smaller than average values, if stacking faults are a significant contributor to the disorder.

With the exception of Gla, the solution concentrations of the additives at which the plateau region was reached using whole pattern analysis were similar to corresponding single peak analysis. For Gla, the average disorder (Rietveld non-uniform strain and crystallite size) was constant for solution concentrations from ~ 10-100 mg/L with further disorder occurring beyond this range, whilst the specific disorder along the $(13\bar{1})$ plane (SHADOW) did not plateau until 200 mg/L. The

anomaly between the two methods is probably due to the small size of Gla relative to proteins, and the effect of measuring along a specific plane as opposed to the crystal bulk average. The two plateaus observed for COM (Gla) using Rieveld analysis, may be due to average changes in types of disorder (eg screw dislocations) and growth modes, as the concentration of Gla increased. This may well differ from the type(s) of disorder occurring along only one plane. Additionally, small molecules like Gla, blocking a single or few growth sites might change the growth modes from spiral to edge or kink, or any permutation there of, depending on their surface density. Proteins, by comparison, could block a large number of adjacent sites and once engulfed by the growing crystal front could leave the growth pattern of the remaining sites alone. Proteins in solution can also act as nucleating templates for crystal growth (Addadi and Weiner, 1992), whereas it is more likely that Gla will be initially adsorbed onto formed COM surfaces. This difference in COM nucleation and growth may account for significant differences in non-uniform strain, crystallite size and stacking faults within the crystal.

Of the proteins, the concentration required to achieve plateaus in the relationship between non-uniform strain and crystallite size, showed that HSA needed the highest value, followed by PT and CME. Taking into account the molar concentrations of HSA and PT and limiting non-uniform strain values, the above order suggests that the affinity of the macromolecules for COM is PT > HSA. As CME contains a mixture of proteins, its placement in the affinity order for COM is uncertain. However, if its average Mr is similar to PT or HSA, then CME > PT > HSA. The observation that CME had a significantly greater effect on crystallite size than proteins PT and HSA was expected as it's most abundant component is UPTF1, the most powerful inhibitor of calcium oxalate crystallization in undiluted urine yet found, and is a known intracrystalline entity (Stapleton and Ryall, 1995). The high affinity of UPTF1 for calcium containing surfaces is almost certainly due to the 10 Gla residues situated in the N-terminal region of the molecule (Ryall, 1996). As was observed, PT would therefore be expected to have a greater effect on non-uniform strain and crystallite size than HSA, which does not have any Gla residues. In comparison with Gla, the affinity order would then be CME > PT > HSA > Gla, which is not surprising as Gla is able to bind to COM with 2 or 3 functional groups,

whereas HSA, PT and proteins in CME would have far more calcium binding groups.

The plateau average (Rietveld) non-uniform strain values for UF urine, HSA (aqueous) and HSA (urine) were comparable (~ 0.08%), suggesting that the contribution to non-uniform strain from HSA was similar to that from UF urine, which contains other low molecular mass species (<10 kDa) that are not present in water. Interestingly, the effect of concentration is much greater when only the $(13\bar{1})$ plane is considered for HSA (UF urine). This shows that there is a further increase in stacking faults without extra increases in non-uniform strain and decreases in crystallite size or other changes in disorder, which differs from PT (aqueous), HSA (aqueous) CME (aqueous) and CME (UF urine). The anomalous behaviour of HSA (UF urine) is difficult to account for because changes in non-uniform strain, crystallite size and stacking faults are usually linked together. The contribution of UF urine to both plateau non-uniform strain and plateau concentration for CME was smaller, indicating that CME had a much larger effect than UF urine. It can thus be concluded that the non-uniform strain and crystallite sizes and stacking faults produced are dependent on the functionality and size of the chemical species present in COM.

This is the first time that non-uniform strain and crystallite size changes in COM have been shown to be concentration dependent with respect to Gla, HSA, PT and CME. In addition, the disorder produced by their occlusion is limited. Thus the quantity of these urinary components that have the potential to become occluded in COM crystals in the urinary tract is dependent on their urinary concentration, but only up to a limit. Hence the urinary concentrations of those organic species are expected to influence the internal microstructure and biophysical properties of COM crystals, and therefore their stability in the urinary tract. These aspects are investigated in the next chapter.

9 FIELD EMISSION SCANNING ELECTRON MICROSCOPY STUDIES OF CALCIUM OXALATE CRYSTALS

Although the X-ray diffraction analysis described in Chapters 5-8 demonstrated that selected proteins and amino acids are occluded into COM crystals, the evidence was not visual. Prior to the publication of these FESEM results (Ryall et al., 2000, Ryall et al., 2001), a number of ultrastructural studies had demonstrated the existence of a close association between the organic and crystalline components of CaOx calculi (Khan and Hackett, 1984, Iwata et al., 1985, Khan and Hackett, 1987, Khan and Hackett, 1993, Khan, 1995). Those studies did not provide direct evidence that some sections of an organic coating are intracrystalline. Although Khan et al. (Khan et al., 1986, Khan and Hackett, 1987, Khan and Hackett, 1993) showed the presence of organic material within demineralised crystal "ghosts" of renal stones, the crystals from the ghosts were polycrystalline dumbbells, not single crystals. As a consequence, their micrographs depict transverse sections of organic coating adsorbed to the surfaces of the individual crystals comprising the aggregate. Further, the crystal ghosts were in some instances described as largely "empty spaces" (Khan et al., 1983), while others showed no any evidence of intracrystalline organic matter (Khan and Hackett, 1993, Khan, 1995). In summary, specific information on the relationship between the organic and mineral phases of urinary crystals was lacking in those earlier studies.

The aim of the work described in this chapter was to determine the relationship between amino acid/protein and mineral within the crystalline architecture of CaOx crystals using a combination of FESEM and proteolytic digestion. The study of COD crystals was included as they commonly precipitate from human urine because they are stabilised by urinary components such as citrate. Results are presented in three sections, primarily determined by the origin of the crystals, which were derived from the following sources:

- Aqueous solutions of Asp, Gla, Glu, and PT (Section 3.2.4). Gla, Glu and PT were selected because results presented in Chapter 5 show that they are intracrystalline, whereas Asp is not.

- CF human urine and UF human urine (Sections 3.2.6-8). As CF urine contains most of its protein complement and UF urine contains only small peptides and proteins <10kDa, it allows the effect of molecular weight to be assessed.

- CF human urine and UF human urine in a timed growth study (Section 3.2.7). By comparing COM derived from these two media, the relationship between mineral and protein could be assessed as a function of protein depletion from the induction of crystallization.

9.1 COM grown in inorganic aqueous solutions

FESEM images were obtained for CaOx crystals grown in distilled water and aqueous solutions of Asp, Gla, Glu, and PT at 37°C for 13 hours (Section 3.2.4). Both whole and fractured crystals were studied before and after treatment with Proteinase K (Section 3.2.9).

9.1.1 CaOx grown in distilled water

CaOx crystals grown in distilled water were all COM (Figure 9.1a.), and when fractured, their cleaved surfaces appeared solid and non-porous (Figure 9.1b). After treatment with Proteinase K, the outer surfaces (Figure 9.2a) and the fractured surfaces (Figure 9.2b) of the crystals were smooth and did not show any evidence of etching.

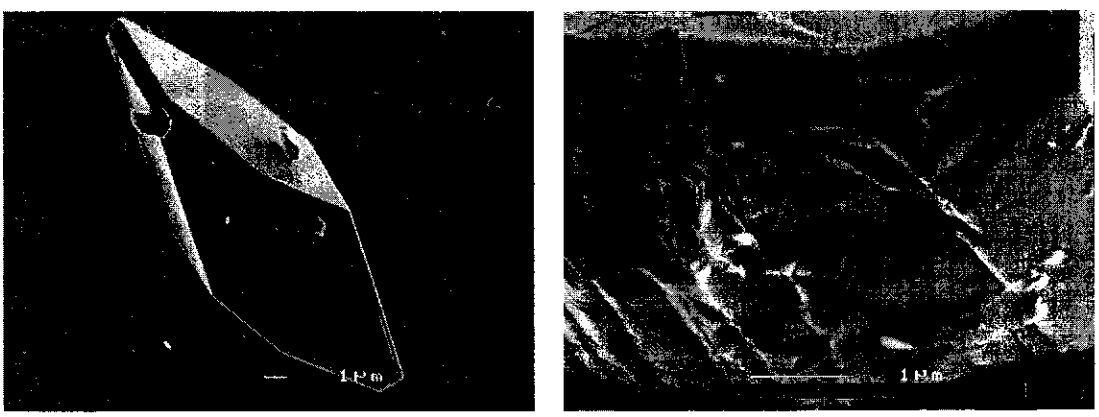

a b

Figure 9.1 FESEM images of COM crystals grown in distilled water for 13 hours: (a) whole crystal, (b) fractured crystal.

a b

Figure 9.2 FESEM images of COM crystals grown in distilled water for thirteen hours then treated with Proteinase K: (a) whole crystals, (b) exposed internal surface of fractured crystal.

9.1.2 COM crystals grown in aqueous solutions of Gla, Glu and Asp.

Crystals grown in aqueous solutions of Asp and Glu were COM (Sections 3.2.4 and 3.2.10). These crystals possessed identical exterior morphology and internal structure to the distilled water control, both before and after proteinase treatment and accordingly, are not shown. Crystals grown in the presence of Gla (Figure 9.3a), were also COM with an appearance similar to those precipitated from distilled water. Although the external surfaces of the crystals generated in the Gla solution were smooth and the edges angular (Figure 9.3a), the internal surfaces of fractured crystals had an irregular and rounded texture (Figure 9.3b) suggesting that fracture had occurred along crystallite boundaries rather than along crystal planes.

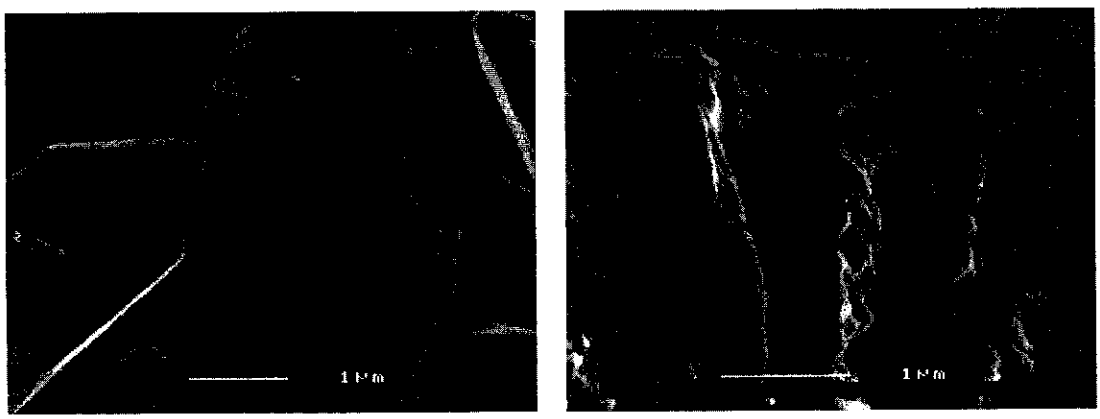

a b

Figure 9.3 FESEM images of COM crystals grown for thirteen hours in an aqueous solution of Gla: (a) whole crystals, (b) fractured crystal.

Treatment with Proteinase K (Section 3.2.9) had very little effect on internal crystal texture (Figures 9.4a and 9.4b), as would be expected since it does not attack amino acids.

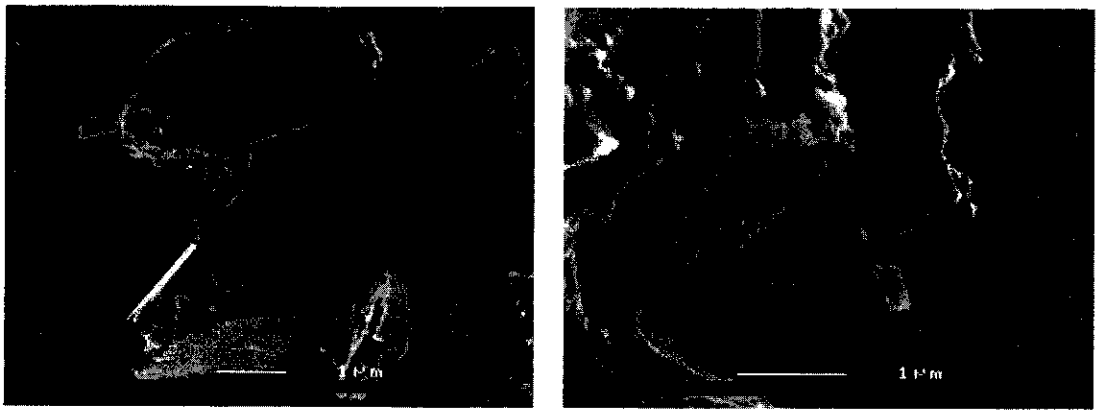

a b

Figure 9.4 FESEM images of COM crystals grown for thirteen hours in an aqueous solution of Gla then treated with Proteinase K: (a) whole crystal, (b) fractured crystal.

9.1.3 COM crystals grown in an aqueous solution of PT

CaOx crystals harvested from the PT growing medium after 1 and 13 hours (Section 3.2.4) were mainly COM with a small amount of COD (<5 %). After 1 hour's growth, the crystals consisted of sheets (~ 4 x 0.2μm) with a 'grapevine leaf' appearance (Figure 9.5a) that seemed to comprise small coffin-shaped COM crystals aggregated into closely packed sheets, more evident at higher magnification (Figure 9.5b). After 13 hours growth (Figure 9.6a), the crystals were approximately 3-4 times larger than those crystals formed after 1 hour, but similar in overall shape. In addition, the surfaces of the fractured crystals shown in Figure 9.6b, were smoother than the crystals grown for only one hour. A cross sectional view of the fractured crystal in Figure 9.6b reveals the cleaved face to have a number of dark circular patches (~ 0.1 μm diameter) arrayed across it, which were not observed in the fractured control COM crystals. After treatment with Proteinase K (Section 3.2.9), both the whole and fractured COM crystals (Figures 9.7a and 9.7b) were considerably disordered, with many small fragments being evident.

a b

Figure 9.5 FESEM images of COM crystals grown for one hour in an aqueous solution of PT: (a) whole crystals, (b) fractured crystals at higher magnification.

a b

Figure 9.6 FESEM images of COM crystals grown for thirteen hours in an aqueous solution of PT: (a) whole and fractured crystals, (b) exposed edge of a fractured crystal.

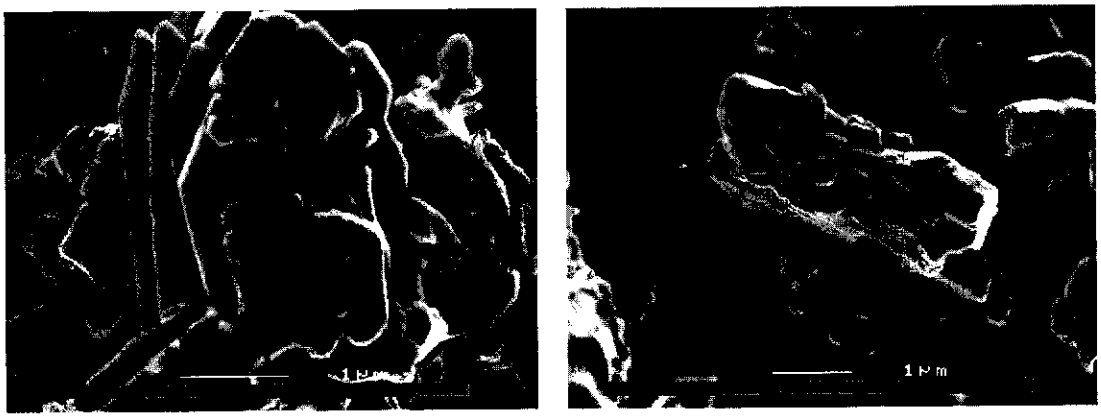

a b

Figure 9.7 FESEM images of COM grown for thirteen hours in an aqueous solution of PT then treated with Proteinase K: (a) whole crystals, (b) fractured crystals.

9.2 CaOx crystals grown in UF and CF human urine

FESEM images of COM and COD precipitated from UF urine and CF urine were obtained for whole and fractured crystals before and after Proteinase treatment (Sections 3.2.6-9).

9.2.1 COM

COM crystals precipitated from CF urine (Figure 9.8a) were hexagonally shaped with rounded edges, which differed from those grown in distilled water. Many of the crystals were coated by what appeared to be precipitated organic material. When the crystals were fractured (Figure 9.8b), the exposed edges revealed a spongy, honey combed interior. Proteolytic digestion of intact crystals (Figure 9.9a) removed much of the associated organic material and enabled more distinctive images to be seen, which revealed a network of numerous internal lacunae, as well as layering as shown in Figure 9.9b. Although the COM crystals precipitated from UF urine had a similar shape to those grown in CF urine, they were not visibly coated with organic material (Figure 9.10a) and had a homogeneous interior (Figure 9.10b). After Proteinase K treatment, the surfaces and interiors of these crystals showed them to be unaffected by proteolysis (Figure 9.11), indicating the absence of occluded protein.

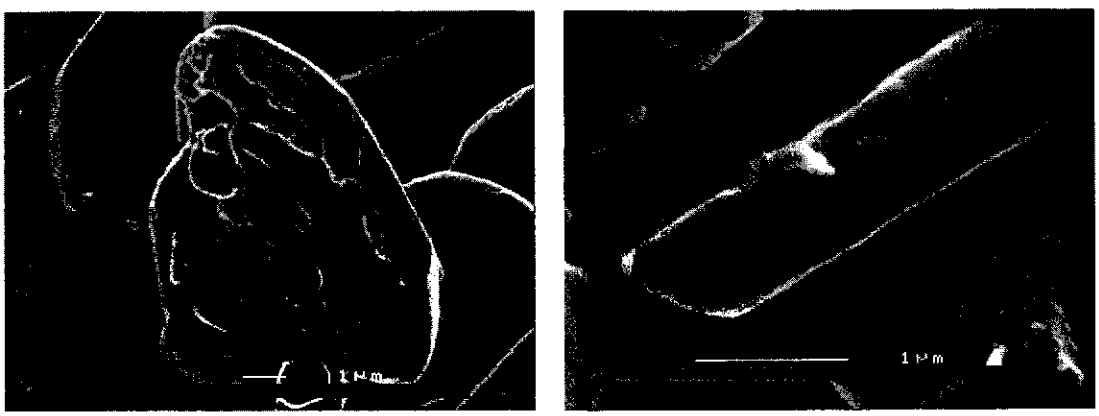

a b

Figure 9.8 FESEM images of COM crystals grown CF urine: (a) whole crystals, (b) exposed edge of a fractured crystal.

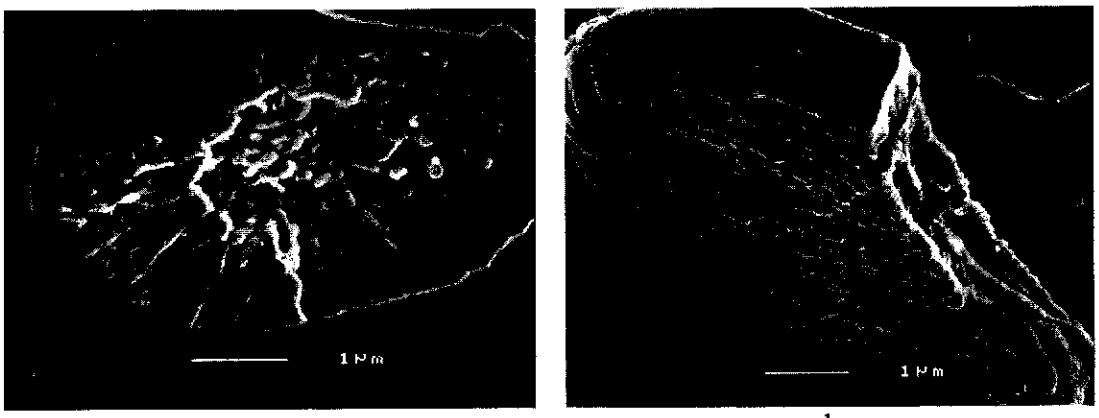

a b

Figure 9.9 FESEM images of COM crystals grown in CF urine after treatment with Proteinase K: (a) whole crystals, (b) exposed edge of a fractured crystal.

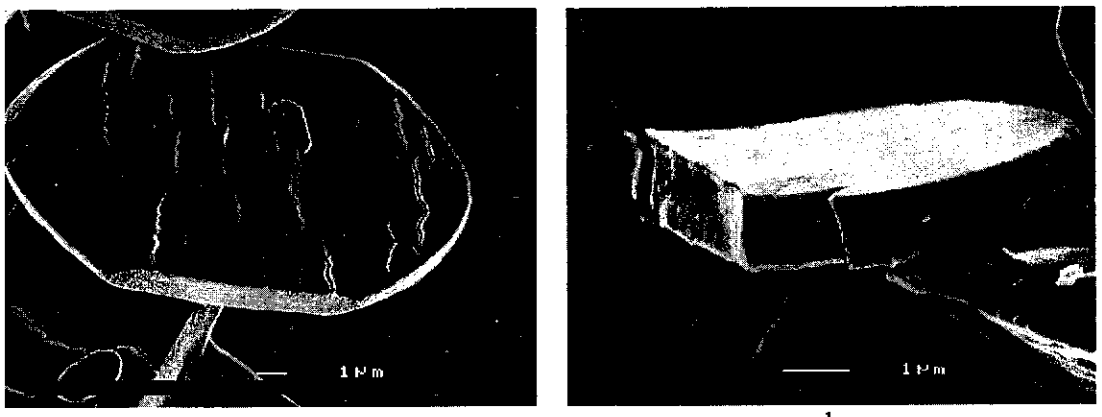

a b

Figure 9.10 FESEM images of COM crystals grown in UF urine: (a) whole crystals, (b) exposed edge of a fractured crystal.

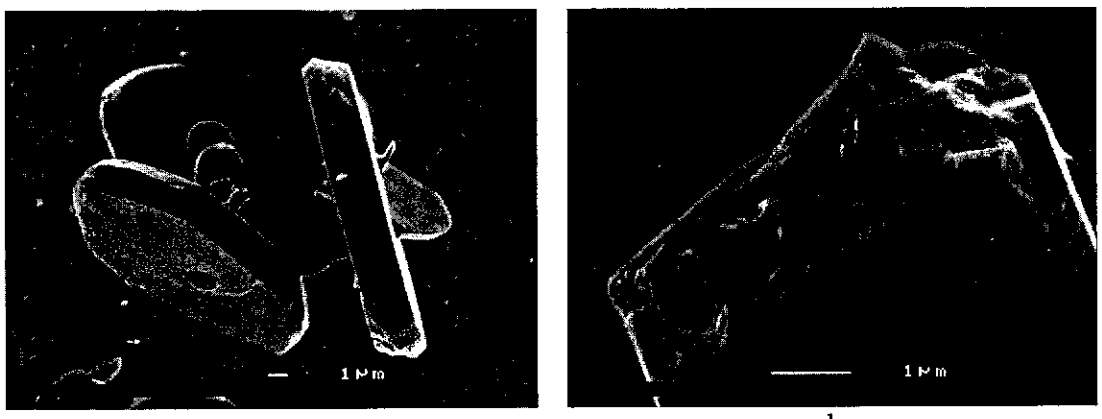

a b

Figure 9.11 FESEM images of COM crystals grown in UF urine after treatment with Proteinase K: (a) whole crystals, (b) exposed edge of a fractured crystal.

9.2.2 COD

COD crystals precipitated from CF urine (Figure 9.12a) were bipyramidal in shape, with relatively smooth faces. When the crystals were fractured (Figure 9.12b), the exposed edges revealed a coarse, grainy interior. After the intact and fractured crystals were treated with Proteinase K, the outer surfaces were pitted and etched (Figure 9.13a) and the interior surfaces of the fractured crystals appeared to be composed of rod-like structures arranged in a parallel alignment (Figure 9.13b).

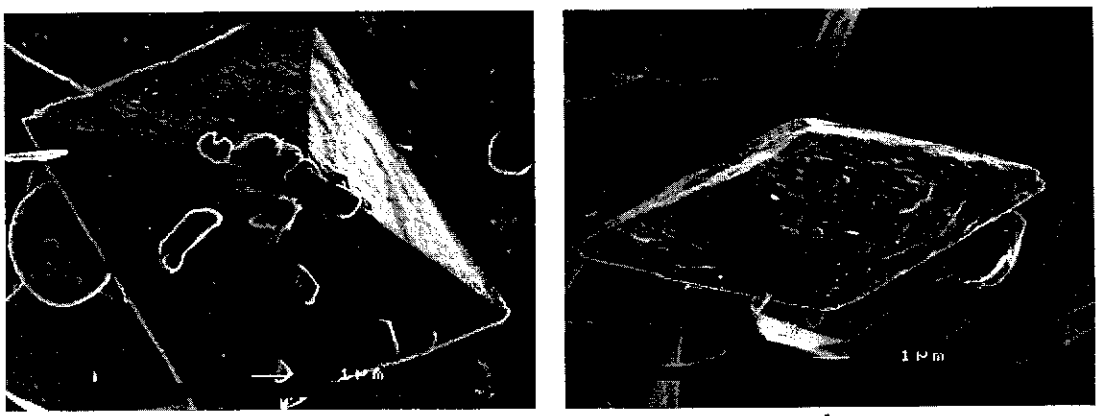

a b

Figure 9.12 FESEM images of COD crystals grown in CF urine: (a) whole crystals, (b) exposed edge of a fractured crystal.

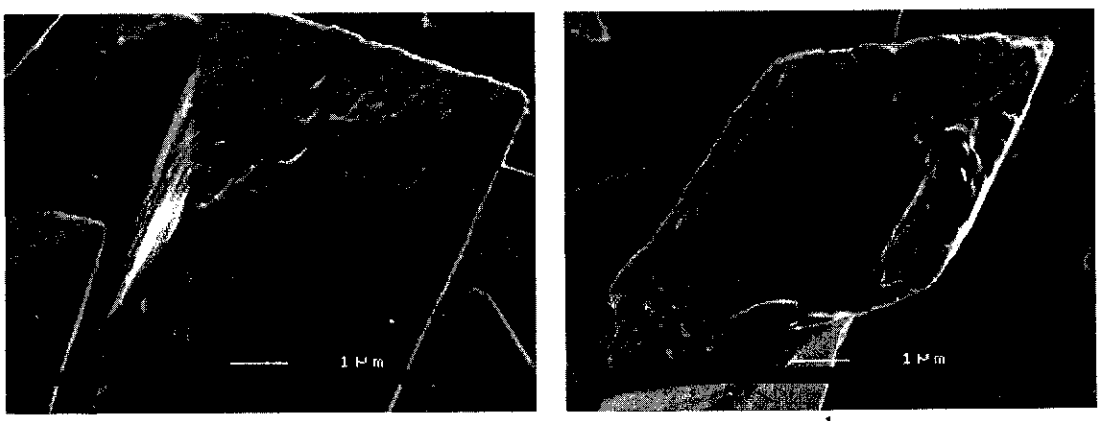

a b

Figure 9.13 FESEM images of COD crystals grown in CF urine then treated with Proteinase K: (a) whole crystals, (b) exposed edge of a fractured crystal.

COD crystals precipitated from UF urine had the same shape to those grown in CF urine (Figure 9.14a). However, unlike the internal appearance of the latter, the

fractured faces of COM (UF) crystals were smooth and occurred along crystallographic planes (Figure 9.14b). Intact COD crystals produced in UF urine and treated with Proteinase K generally possessed smooth, angular edges and surfaces as shown in Figure 9.15a, and when fractured, the exposed interior surfaces again showed fracture along crystallographic planes (Figure 9.15b).

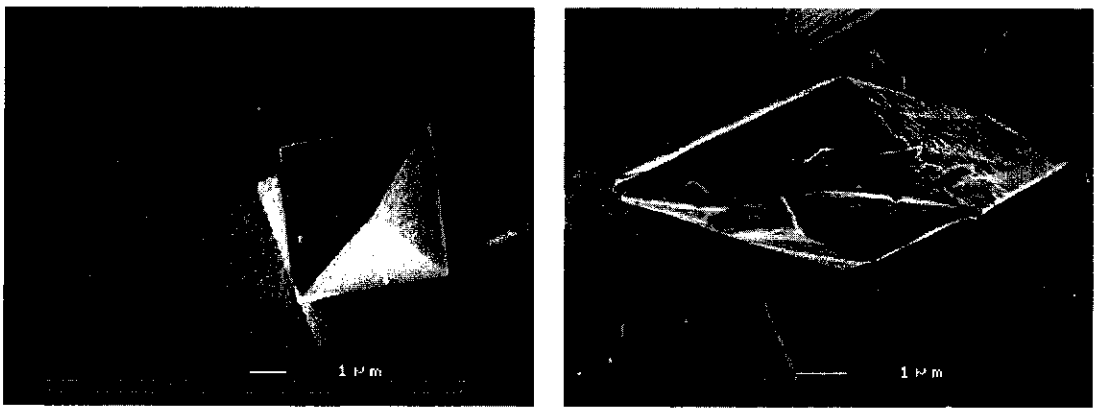

a b

Figure 9.14 FESEM images of COD crystals grown in UF urine: (a) whole crystals, (b) exposed edge of a fractured crystal.

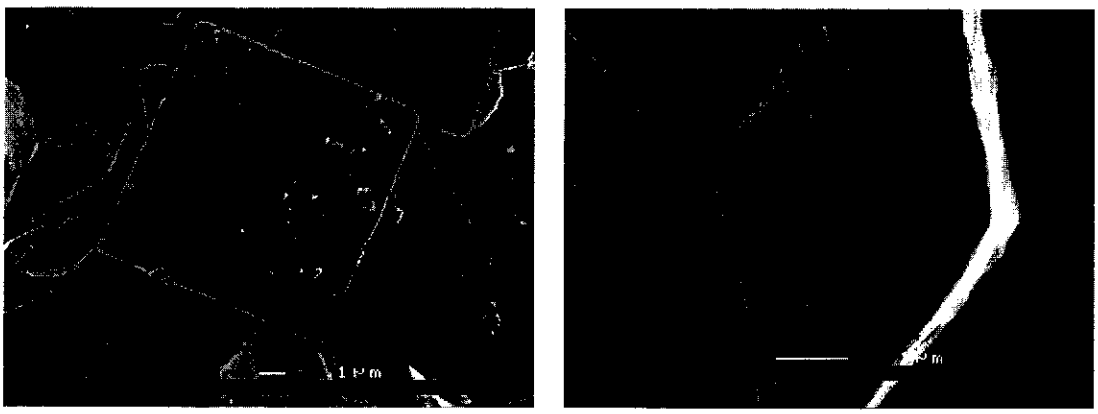

a b

Figure 9.15 FESEM images of COD crystals grown in UF urine after treatment with Proteinase K: (a) whole crystals, (b) exposed edge of a fractured crystal.

9.3 Timed experiments

FESEM images were obtained of CaOx grown in CF urine at 37°C for selected periods of time after the addition of standard loads of oxalate in excess of the metastable limit (Section 3.2.7). The urine was divided into three aliquots.

- Crystals were harvested one hour after the addition of a standard oxalate load from the first CF urine aliquot (Section 3.2.7). A second standard oxalate load was then added to the other aliquots.
- Crystals were harvested after two hours incubation from the second urine aliquot, while a further standard oxalate load was added to the third aliquot.
- Crystals were harvested after four hours incubation from the third urine aliquot.

The same procedure was repeated for a UF urine sample (Section 3.2.8).

Crystals were also deposited from CF urine and from the same urine following ultrafiltration after incubation for 4 hours, but following the addition of only a single standard oxalate load. This reduced the amount of mineral that could be deposited after protein depletion.

At one hour

Both COM and COD crystals were observed (Figure 9.11). The COM crystals consisted of compact thin hexagonal plates assembled into larger, apparently single coffin-like structures (Figure 9.12a). The small individual hexagonal plates bore a strong resemblance to the overall shape of the larger, apparently single parent crystal. At higher magnification, the plates appeared to have a porous texture (Figure 9.12b).

Figure 9.11 FESEM images of COM and COD crystals obtained from CF urine after one hour with one standard oxalate load.

a b

Figure 9.12 FESEM images of COM crystals obtained from CF urine after one hour with one standard oxalate load: (a) whole crystals, (b) centre section of a similar crystal shown in 9.12a, but at higher magnification.

At two hours

Only COM crystals were found after 2 hours. Some crystals retained the plate-like structure of those from one hour but with less superficial detail, while others appeared to have a smooth, solid coffin-shape. However, when the latter were fractured and treated with Proteinase K, most of the internal region of the crystals was markedly porous (Figure 9.13b). An impervious mineral shell was also noted to surround the interior of the fractured crystal.

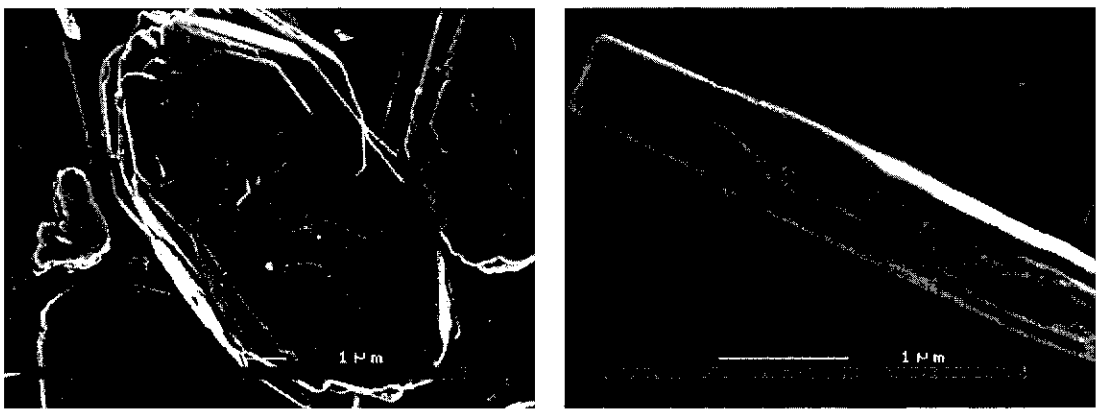

a b

Figure 9.13 FESEM images of COM crystals obtained from CF urine after two hours with two standard oxalate loads: (a) whole crystals. (b) fractured crystals after Proteinase K treatment.

At four hours

At 4 hours, the crystals that had been generated from urine after addition of 3 standard oxalate loads were larger than those precipitated at 2 hours, which had received only 2 standard oxalate loads. Furthermore, the crystals harvested at 4 hours, in contrast to those removed at 2 hours, exhibited little surface detail (Figure 9.14a). After fracturing and treatment with Proteinase K, some crystals had porous centres, indicating removal of proteinaceous material, while others appeared more solid and crystalline (Figure 9.14b). In most of the 4-hr crystals, however, the central porous region was generally smaller in size relative to the surrounding solid crystalline areas compared to those in the 2-hr crystals. This shows that with increasing mineral formation, there is a decreasing availability of endogenous protein owing to the depletion of urinary protein. It was noted that within a given crystal batch, there was considerable heterogeneity i.e. the internal structure of some crystals were "honey combed" while others appeared to be relatively solid.

Figure 9.15a shows a cross-sectional view of an untreated fractured COM crystal, grown in CF urine, which reveals dark patches distributed across the exposed face. This was not evident in crystals grown from the same urine specimen, but which had also been ultrafiltered (Figure 9.15b) or in the COM grown in distilled water (Figure 9.1b). Furthermore, proteolytic etching of whole COM crystals grown in CF urine (Figure 9.16a) created porous regions, particularly on the (100) and (021) faces. A transverse view of a fractured COM crystal grown in CF urine and treated with Proteinase K (Figure 9.16b) shows the inner portion of the crystal to have a honeycomb-like structure. In contrast there was little or no evidence of surface erosion upon the COM crystals grown in the corresponding UF urine (Figure 9.17a) or of internal erosion following fracture and proteolytic digestion (Figure 9.17b).

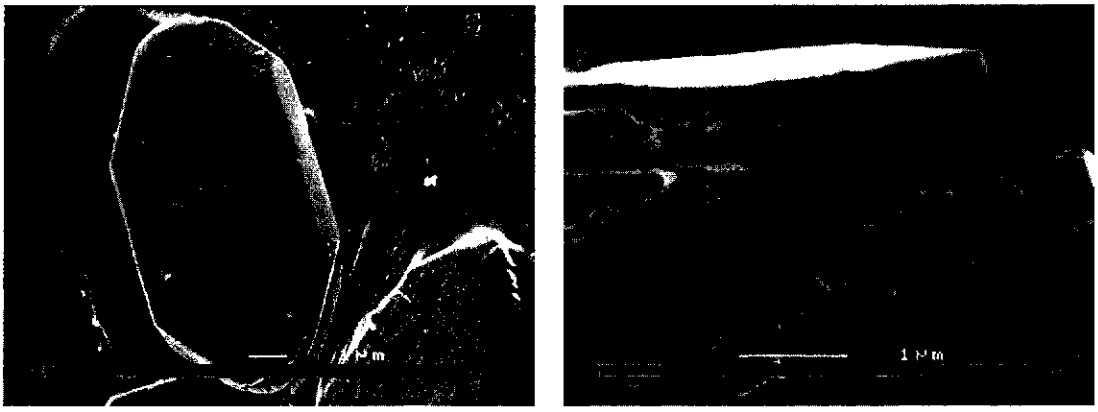

a b

Figure 9.14 FESEM images of COM crystals obtained from CF urine after four hours with three standard oxalate loads: (a) whole crystals, (b) fractured crystals after treatment with Proteinase K.

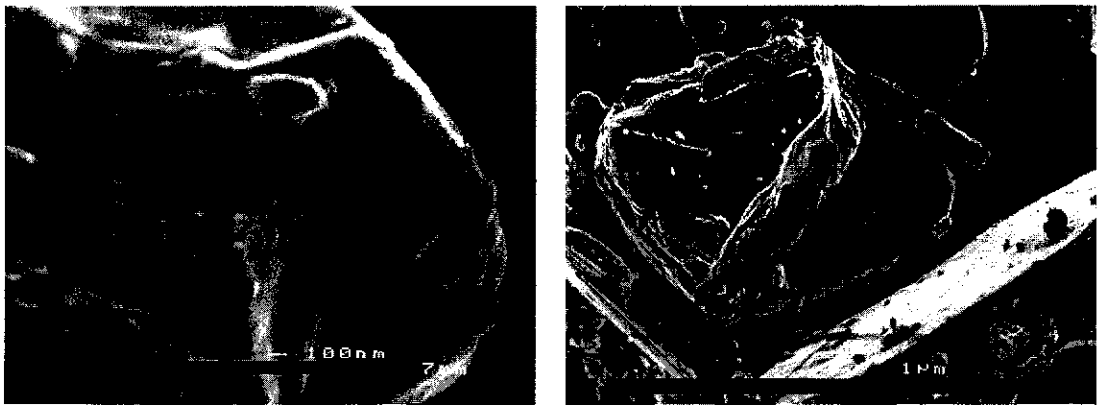

a b

Figure 9.15 FESEM images of fractured COM crystals grown in (a) CF urine, (b) UF urine after four hours of growth with one standard oxalate load.

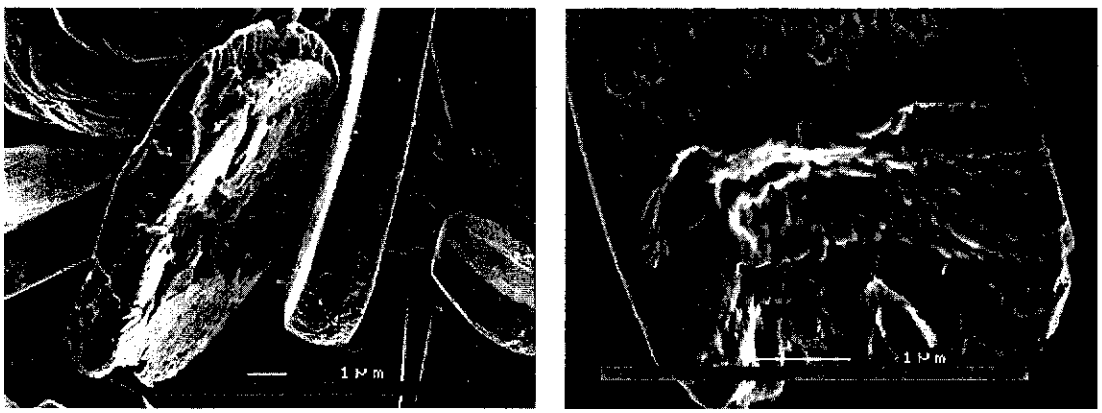

a b

Figure 9.16 FESEM images of COM crystals grown in CF urine for four hours with one standard oxalate load and then treated with Proteinase K: (a) whole crystals, (b) fractured crystal.

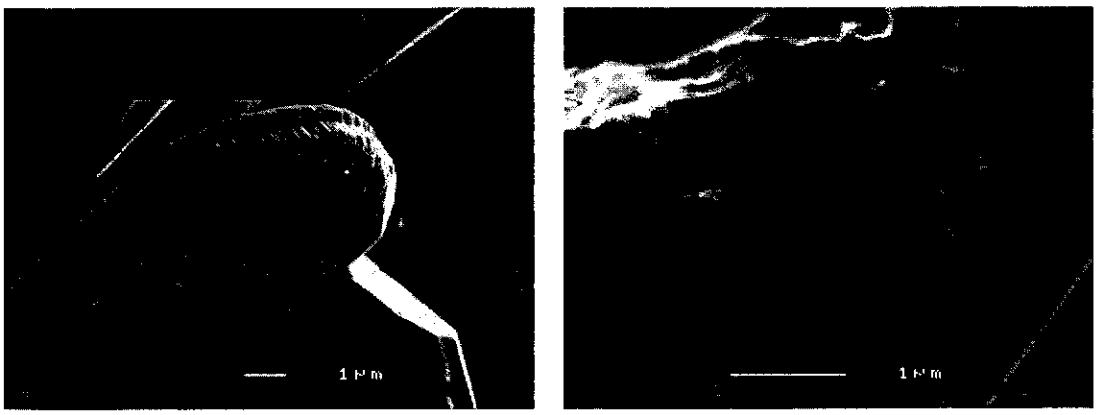

a b

Figure 9.17 FESEM images of COM crystals grown in UF urine for four hours with one standard oxalate load, then treated with Proteinase K: (a) whole crystals, (b) fractured crystal.

9.4 DISCUSSION

The FESEM observations presented in this chapter provided visual evidence of disruptions to the integrity of crystal interiors, which could only have been caused by incorporation of proteins and amino acids into the mineral bulk. The disturbances to the crystalline structure were enhanced visually by treatment of the crystals with Proteinase K, revealing a detailed microstructure that was absent from crystals grown in distilled water and UF urine.

The external and fractured surfaces of COM grown in an aqueous solution of Gla were similar to the distilled water control. Although it was shown in Chapters 5 and 6 that Gla is incorporated into the COM crystal, it would not be affected by Proteinase K. The lack of any significant effect of proteolytic digestion on the external or internal crystal surfaces was not, therefore, unexpected. Nonetheless, Gla did cause some internal texture, providing evidence of disorder and occlusion within the crystal, as was concluded from the SXRD peak broadening data presented in Chapters 5 and 6. The external and internal surfaces of COM crystals grown in aqueous solutions of Glu and Asp were similar to those grown in distilled water, before and after treatment with Proteinase K, indicating that their influence on the internal crystal structure is much less than that of Gla. These observations were again consistent with the SRXD evidence from Chapters 5 and 6, which indicated that Asp is not occluded and Glu is occluded to a lesser degree than Gla.

The external morphology and internal structure of COM crystals grown in PT solution differed markedly from the distilled water control. The plate-like structures of the COM crystals generated in the presence of PT after growth for one hour and four hours suggested that the protein was adsorbed onto selected crystal faces. This is at variance with the results in Chapter 6, which suggested that binding of PT was not face-specific. It is probable that the early vine leaf shaped crystals observed at one hour's growth developed into more block-like structures, similar to the distilled water control, as a result of the diminishing solution concentration of protein as mineral deposition proceeded. With batch methods like this, the depletion of low concentration protagonists, including proteins or smaller molecules that co-precipitate with the mineral is inevitable. As PT has a very high affinity for COM, and the mass of PT to COM can be calculated to be 0.84% (or 0.0017% mole/mole) at the maximum amount of crystal produced (Section 3.2.21), it is probable that the protein was rapidly depleted in the early stages of crystal growth. Hence the overall SXRD results for the fully developed COM (PT) crystals, reported in Chapter 6, would not have indicated the early face selectivity of PT for COM. Therefore the absence of crystallite size anisotropy possibly resulted from the fact that only small amounts of PT would have been occluded into the outer sections of the crystal, the SXRD measurement being dominated by the more crystalline shell. The dark circular areas on the exposed faces of the fractured crystals may be regions of mineral associated with occluded protein, or may represent vacuoles in the mineral caused by condensation of protein and subsequent prevention of mineral deposition. The solid portions are probably individual crystallites. Proteins have been reported to be responsible for the production and stabilisation of amorphous calcium carbonate within the antler spicules from *Pyura pachydermatina* (Addadi et al., 1999), so it is possible that the dark, contrasting regions are amorphous material, indicated in Chapter 7. This possibility is supported by the absence of similar areas from the fractured COM distilled water control crystals. Treatment of the crystals with Proteinase K caused marked erosion and pitting, unlike the COM crystals grown in distilled water, which were impervious to proteinase treatment. As Proteinase K selectively attacks proteins, but not mineral, it follows that the regions of the crystals that were vulnerable to enzymatic etching must have contained protein. Thus it can be concluded that the labyrinth of channels and/or tunnels in the mineral matrix was caused by occlusion of PT into the mineral bulk.

In the timed study, the porous appearance of the plates of COM (CF urine) observed at high magnification after one hour was consistent with the presence of organic material throughout the mineral fabric. The individual plates were assembled into a larger hexagonal and apparently single crystal with rounded edges on the (001) faces, suggesting that preferential adsorption on the (100) face had slowed the growth of that face relative to the others. This led to thinner plates compared to the distilled water control. Additionally, twinning along the (100) faces gave rise to the hexagonal (010) face observed in Figure 9.9, rather than the parallelogram shape of a single crystal. The rounding of the (001)/(021) and (021)/(010) edges compared to the control, would have been caused by the slowing of growth on the (001) face. With the exception of the (100)/(010) edge, rounding of these edges is also illustrated by COM (CF) in Figure 9.14 and COM (UF) in Figure 9.17. The crystallites of COM (CF), in particular (Chapter 6), were found to have shorter "a" and "c" axes than the "b" axis, indicating preferential adsorption on the (100) and (001) faces. This effectively slowed the growth in the "a" and "c" directions, leading to an ovoid, plate-like shape, similar to the morphology of fully developed crystals.

After two and three sequential oxalate loads, the exterior shale-like texture of the crystals disappeared, to be replaced by a smooth coating, presumably consisting of solid material. This accompanying textural change was consistent with diminishing concentration of available protein in the solution. Since proteolytic digestion caused erosion only at the core of the crystals, it can be reasoned that, as the concentration of proteins diminished, crystal porosity also decreased and the structure became enveloped in a solid mantle of mineral. In contrast, after four hours' growth, enzymatic digestion of fractured crystals generated from CF urine by the addition of only a single oxalate load showed that the resulting crystals were porous throughout. This suggests that sufficient endogenous proteins were present in the urine to ensure that no solid mineral shell was formed. Thus it is evident that the internal ultrastructure of urinary COM crystals depends to a significant extent, upon the ratio of crystal-binding proteins to the available quantities of solute ions during growth. These observations, therefore, have important ramifications for the formation of CaOx crystals in urine *in vivo*, since crystals formed in urine containing low concentrations of CaOx-binding proteins, or in the face of overwhelming levels of supersaturation, will possess different biophysical properties. This is likely to affect

the stability of formed crystals in the urinary tract and influence stone formation, discussed in Chapter 10.

Despite the fact that COD is thermodynamically unstable (Nakai et al., 1996), COD crystals are commonly observed in human urine (Kim, 1996). This has been ascribed to the presence of urinary macromolecules, citrate and pyrophosphate and their ability to stabilise the phase (Drach et al., 1982, Deganello, 1993, Wesson et al., 2000). This also could explain the presence of COD in the early stages of growth when more protein was available, relative to precipitating mineral. The absence of COD at later incubation times almost certainly resulted from a combination of depletion of protein from the growing solution and phase transition to the more thermodynamically stable COM as well as a reduction in the concentration of calcium. At the beginning, the concentration of calcium is higher, which favours COD. Once the concentration of calcium declines, COM is more likely to be deposited, especially when more oxalate has been added - COM tends to form at low calcium concentrations and COD at high calcium concentrations. Secondary nucleation of COMs can also not be discounted. When fractured and treated with Proteinase K, the internal surfaces of the COD crystals grown in CF urine consisted of ordered stacks of what appeared to be rods of mineral interspersed with organic material that had not been completely removed by enzymatic digestion. The absence of such structures from the crystals grown in the corresponding UF urine confirms that intracrystalline proteins are responsible for the internal features of the CF crystals.

The studies described in this chapter have provided visual evidence of the data presented in chapters 5 and 8, since they demonstrate graphically that COM crystals grown in CF urine, or in an aqueous solution of Gla or PT, had a heterogeneous internal structure. Similarly, COD crystals precipitated from human urine (CF) exhibited internal heterogeneity. The fact that Proteinase K digestion removed much of the internal organic material confirmed that it must consist of endogenous urinary proteins.

The relationship between proteins and calcium minerals is complex, and their coexistence in the form of a singular crystalline entity depends on a number of considerations including electrostatic, geometric and stereochemical factors (Mann et

al., 1991). The resulting biomineral may possess properties and morphologies different from the parent mineral which may be advantageous (Addadi and Weiner, 1992), but may also, as in the case of kidney stones, be deleterious to the organism in which it is produced. As shown in chapter 5, intracrystalline proteins affect non-uniform strain and crystallite size, as well as create or stabilize an amorphous phase in the crystals. Such physical alterations to the mineral structure are likely to influence the stability of crystals in urine where urinary proteases are present Petersen et al., (1989). These changes are also likely to influence the susceptibility of crystals trapped within the urinary tract and phagocytosed by epithelial cells, to intracellular degradation by lysosomal proteases. The endogenous proteases could open channels throughout the mineral architecture, allowing deeper penetration of enzyme into the crystalline core for further proteolytic digestion. This would facilitate the intracellular degradation and dissolution of crystals, aspects that are investigated in Chapter 10.

10 DISSOLUTION AND DEGRADATION OF CALCIUM OXALATE CRYSTALS

Retention of COM crystals in the urinary tract is recognised as a fundamental step in urolithiasis (Koul et al., 2000). This may occur by aggregation of crystal particles (Kok et al., 1990) or by attachment to the epithelium (Lieske et al., 1997).

The fate of retained crystals will depend partly on their susceptibility or resistance to dissolution. Common factors affecting the dissolution of COM crystals include solution composition, pH, temperature and solid-surface characteristics (Asplin et al., 1997, Nancollas and Wu, 2000). Pure COM crystals have been shown to dissolve at a rate that is proportional to the solution undersaturation and crystal surface area; that is, dissolution is a diffusion-controlled mechanism (Tomazic and Nancollas, 1979). Dissolution, like growth, can also be affected by impurities within the crystals (Nancollas, 1983, Nancollas, 1984, Nancollas, 1990). In one kinetic study, Tomažič et al., (1882) demonstrated that the dissolution rate of COM stones was slower than the corresponding pure mineral phases. This observation has important ramifications for the stability of crystals retained in the urinary tract, as urine contains a number of dissolved substances capable of being occluded into CaOx crystals, including proteins as was reported in Chapter 5. The resulting crystals can have different physical characteristics to the parent mineral, as was shown by Weiner and Addadi (1997) for calcium carbonate. Thus the presence of proteins and an amorphous phase (Chapter 7) within COM is likely to affect such properties as solubility. Further, as the distribution of proteins and associated amorphous phase is unevenly distributed throughout the crystal structure (Chapters 7 and 9), the dissolution rate is expected to change as dissolution progresses.

Attachment of COM to the epithelium can be affected by urinary components, including proteins, as well as by proteins present on the tubular cells (Lieske et al., 1999). Once attached, COM crystals may remain at the site and enlarge or migrate to the basolateral region of the epithelial cells (Khan, 1997), in either case, forming a nucleus for subsequent stone formation. However, attachment may, paradoxically, also represent a form of defence, because cells can phagocytose the crystals and then

dispose of them intracellularly (Lieske et al., 1999, Ryall et al., 2001). As was shown in Chapters 7 and 9, COM crystals precipitated in CF urine are not homogeneous but contain urinary proteins and are more disordered than pure COM crystals. Consequently, their stability in a urinary or cellular environment is likely to be affected by the occluded proteins. In Chapter 9, it was shown that COM crystals containing endogenous urinary proteins are more significantly degraded in the presence of proteinases than crystals that have little or no protein. A similar outcome should thus be expected in the intracellular (Walker, et al., 1994, Xu, et al., 1995) and urinary environments (Bautista, et al., 1996, Canduri, et al., 1998) which also contains proteinases. Thus the capacity of both environments to destroy CaOx crystals may ultimately depend on the structure of the crystal itself.

The aim of the work presented in this chapter was threefold.

1. To compare dissolution rates of COM (distilled water), COM (UF) and COM (CF) crystals in order to assess the influence of low molecular mass (<10,000 kDa) and high molecular mass (>10,000 kDa) intracrystalline proteins.

2. To determine if proteolysis begins in urine – not just after crystal attachment and phagocytosis have occurred.

3. To determine whether COM crystals produced naturally in urine, have similar structures to crystals produced artificially by addition of oxalate to urine, and behaves in the same way in the presence of urinary proteinases.

10.1 Crystal dissolution

Crystals were precipitated from CF urine and the same urine following ultrafiltration as outlined in Sections (3.2.6-8). Light microscopic examination showed them to consist of > 98% COM (Section 3.2.19). Therefore, they will be referred to in this chapter as COM. Inorganic COM crystals were prepared as described in Section (3.2.4). They consisted exclusively of COM.

Twenty milligrams of COM were added to 60 mL of 4.5 mM EDTA and 3.3 mM sodium acetate at pH 7.5 and incubated with stirring in a water bath at 37°C for 60 minutes as detailed in Sections 3.2.22-23). Dissolution was monitored by measuring

the amount of calcium released with atomic absorption spectrophotometry (Sections 3.1.2, 3.2.24). The procedure was repeated for CaOx crystals grown in distilled water and UF urine. The dissolutions were carried out in quadruplicate for each crystal type and individual results are given in Appendix I 13.

As dissolution was expected to be surface area dependent, the Shrinking Core Model was applied and used to determine the rates of dissolution. That model assumes that dissolution is irreversible and that the products are rapidly removed from the crystal surface (Wadsworth, 1979). This condition was met by ensuring that the crystals were constantly agitated and using an excess of EDTA (4.5 mM) relative to the calculated maximum concentration of calcium ions (2.3 mM). EDTA was chosen because it is still regarded as one of the most effective calcium complexing agents (Wolsey et al., 2000). Since the geometry of the dissolving crystals is an important consideration, a spherical shape was assumed, as is conventional for crystals that are neither very thin plates nor long needles (Atanassova et al., 1996). The dissolution is described by the following equations.

$$[Ca^{2+}] + [EDTA^{4-}] \leftrightarrow [Ca\ EDTA^{2-}]$$

$$K_c = [Ca\ EDTA^{2-}] / [Ca^{2+}]\ [EDTA^{4-}] = 10^{+10.7} \qquad \text{(Vogel, 1961a)}$$

As the minimum excess of $EDTA^{4-}$ (2.2mM) is approximately the same as the maximum possible $CaEDTA^{2-}$ concentration (2.3 mM), the very high value of K_c ensures that $[Ca^{2+}] \approx 1/K_c \approx 0$. Hence the solubility product of COM is virtually never exceeded and dissolution proceeds to completion.

$$COM \leftrightarrow Ca^{2+} + Ox^{2-}$$

$$K_{sp} = [Ca^{2+}]\ [Ox^{2-}] = 10^{-8.32} \qquad \text{(Vogel, 1961b)}$$

Therefore the dissolution is irreversible and the Shrinking Core Model can be applied, i.e.

$$1-(1-\alpha)^{1/3} = kt$$

where α is the extent of the dissolution, t is the time and k is the dissolution rate constant.

Raw data for the dissolution of COM crystals grown in distilled water, UF urine and CF urine for the four replicate experiments runs are shown in Figures 10.1a, 10.1b and 10.1c respectively. Results are expressed as the increase in calcium ions in solution, and give an indication of the reproducibility of the data (Appendix I 13). The averaged dissolution profiles are also shown in the same diagrams, as smooth curves.

The curve for COM (distilled water) suggests that the dissolution is a single step, that is, the rate decreases monotonically to zero with 100% dissolution occurring after approximately 15 minutes (Figure 10.1a). In contrast, the dissolution profiles of COM (UF) Figure 10.1b) and COM (CF) (Figures 10.1 c) suggest that three steps are involved. These were an initial lag phase lasting 3-4 minutes followed by a more rapid stage for approximately 10-15 minutes, and finally a much slower phase, which did not reach total dissolution, even at 60 minutes.

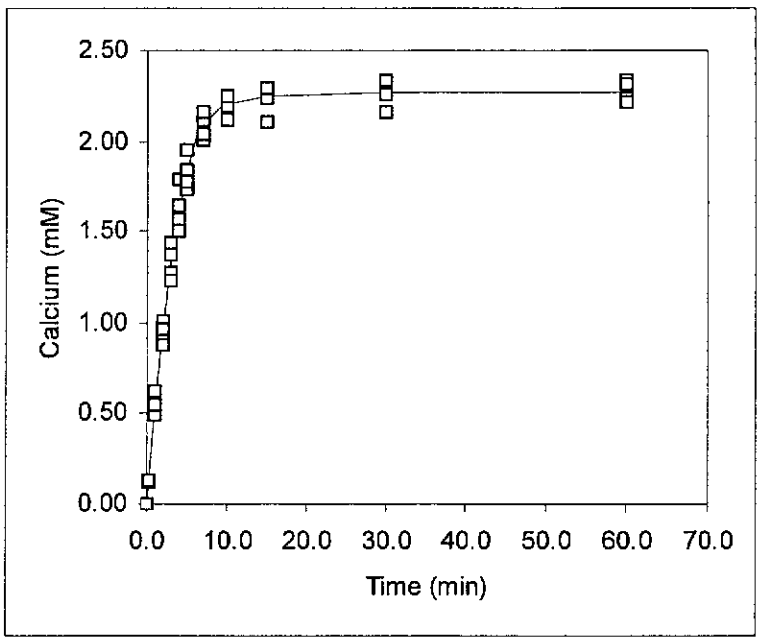

Figure 10.1a Dissolution curve of COM grown in distilled water

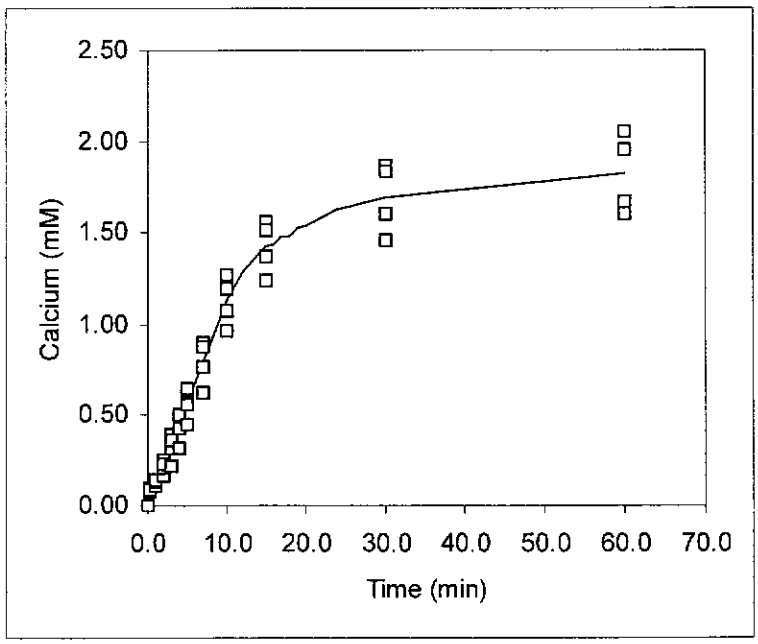

Figure 10.1b Dissolution curve of COM grown in UF urine

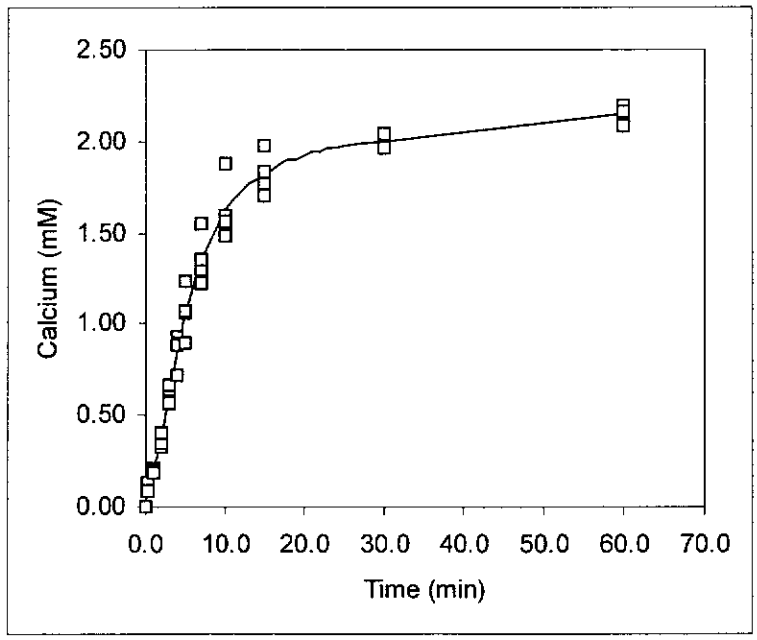

Figure 10.1c Dissolution curve of COM grown in CF urine

The plot of $1-(1-\alpha)^{1/3}$ with respect to time for COM (distilled water) (Figure 10.2a) shows that one rate constant adequately describes the dissolution to approximately $(1-(1-\alpha)^{1/3}) = 0.60$, that is, the first 90% of COM (distilled water) is accounted for by one single surface area controlled dissolution step. The remaining 10% dissolution can be attributed to the experimental error involved in measuring the solution

calcium ion concentration and/or the relative particle size distribution at near complete dissolution, being significantly different from the initial one. On that basis, it is safe to conclude that the dissolution is surface area controlled, the solute homogeneous and well described by the shrinking core model.

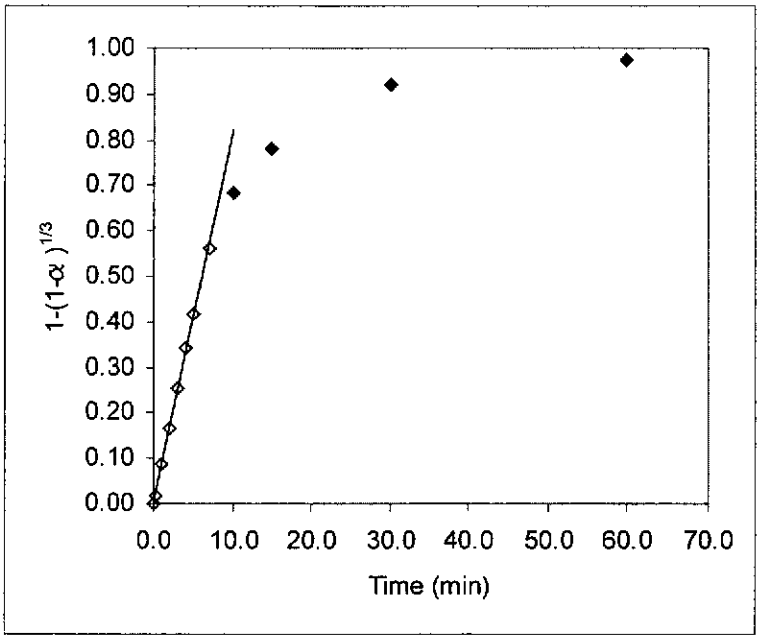

Figure 10.2a Dissolution curve of control COM grown in distilled water, fitted to the Shrinking Core model.

The dissolution curves of COM (UF) (Figure 10.2b) and COM (CF) (Figures 10.2c) also fit well to the shrinking core model, but only if three steps are assumed to occur, as was expected from the concentration versus time curves. Therefore three rate constants are required to account for the dissolution. The first three or four points to approximately $1-(1-\alpha)^{1/3}) = 0.04$, show that a slower dissolution rate occurs for the first 10% than for the major part of the dissolution, approximately $0.04 < 1-(1-\alpha)^{1/3} < 0.25$ (10% -60%). The remaining ~ 40% of the dissolution is the slowest of all, but its rate constant can only be approximated as 100% dissolution was not obtained during the timeframe of the experiment and only two data points are available for that part of the process.

The data for all three samples fit well to the Shrinking Core Model, and the dissolution process is clearly surface area controlled. Thus a valid comparison of

dissolution rates (the slope of the $1-(1-\alpha)^{1/3}$ versus time plots) can only be made on the basis of surface area, that is, the rate of calcium ion released per unit surface area.

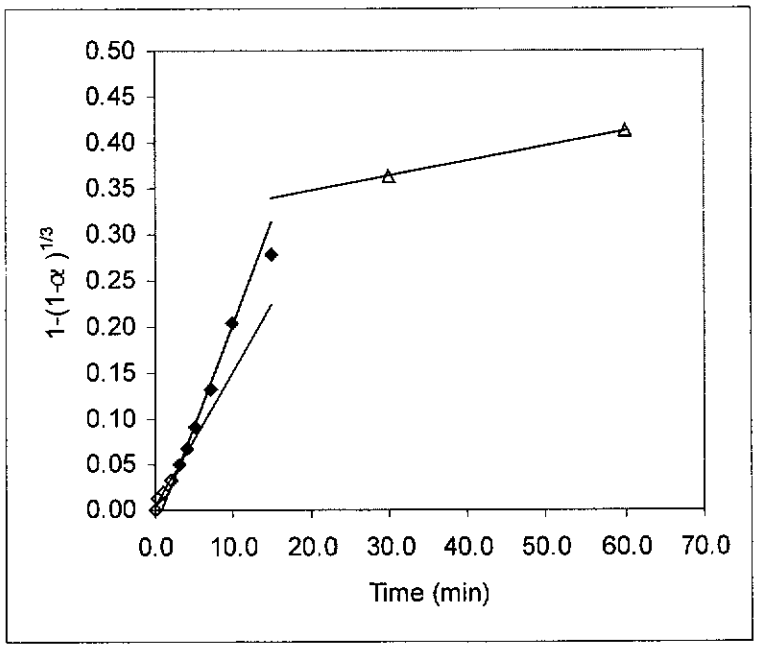

Figure 10.2b Dissolution curve of COM grown in UF urine, fitted to the Shrinking Core model

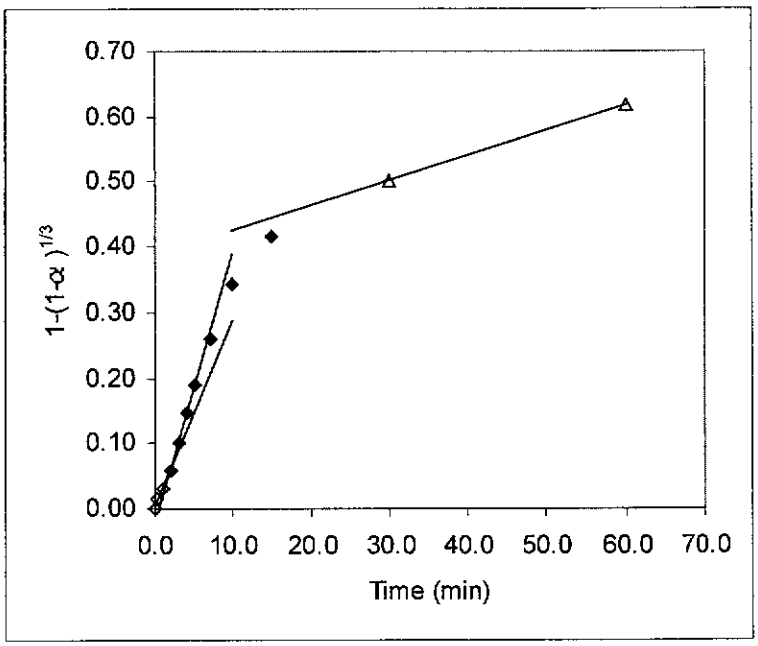

Figure 10.2c Dissolution curve of COM grown in CF urine, fitted to the Shrinking Core model

As a consequence, the mass based rate constants (k) derived from the shrinking core model fits must be corrected for differences in surface areas of the samples for valid comparison. The dissolution rate constants (k) were derived from the slope(s) of the dissolution curves of COM (distilled water), COM (UF) and COM (CF). These, as well as the crystal surface area adjusted rate constants (k*) are presented in Table 10.1. The crystal surface area adjusted rate constants, for the major parts of the dissolution of COM (UF) and COM (CF) were found to be ~50% and 40% respectively, of that found for COM (distilled water). The final dissolution stages of COM (UF) and COM (CF) were much slower, being ~4% of that calculated for COM (distilled water), whilst their initial dissolution rates were ~30% of the control rate. Electron micrographs (FESEM: Section 3.2.7) of the UF and CF urine crystals, presented in Figure 10.3, show the presence of adsorbed material, which may account for their lower initial dissolution rates, as evidenced by the lag phase in the dissolution curves shown in Figures 10.1b and 10.1 c.

Table 10.1 Mass based rate constants (k), crystal surface area adjusted rate constants (k*) and linearity range of the Shrinking Core Model for COM dissolution. Errors are shown in parenthesis.

COM Source	**Surface Area**	**Rate Constant k**	**Rate Constant k*=k/area**	**Dissolution Fraction α**
	m^2g^{-1}	min^{-1}	$min^{-1}m^{-2}$	
Distilled Water	3.00 (5%)	0.082 (0.001)	0.027 (002)	0.94
UF Urine	1.69 (5%)	0.015 (0.002) 0.022 (0.001) 0.0016	0.009 (0.001) 0.013 (0.001) 0.0010	0.00-0.09 0.14-0.50 "0.74"
CF Urine	3.69 (5%)	0.028 (0.007) 0.041 (0.001) 0.00038	0.008 (0.002) 0.011 (0.001) 0.0010	0.00-0.09 0.16-0.60 "0.88"

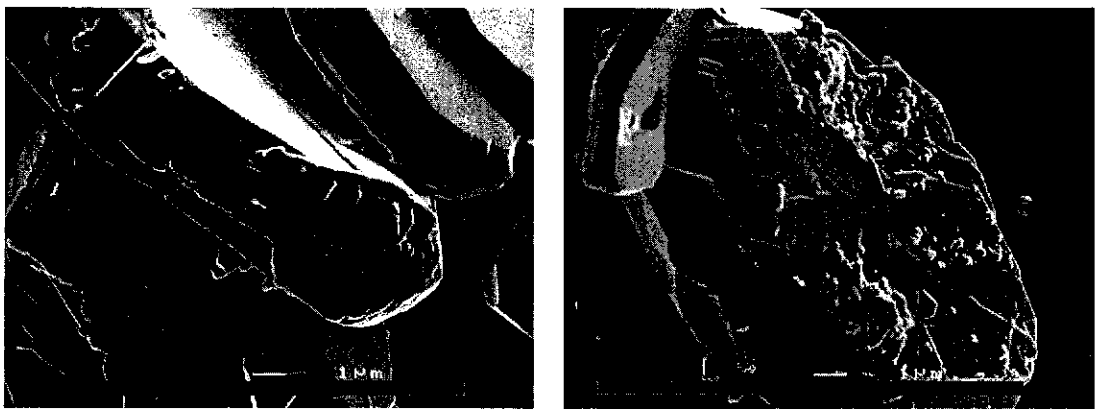

a b

Figure 10.3 FESEM images of COM crystals grown in UF urine (a) and CF urine (b) showing absorbed organic material on the crystal surfaces.

10.2 Crystal degradation

Enzymatic digestion of COM (UF) and COM (CF) crystals by natural proteases in fresh human urine was carried out in the presence and absence of proteinase inhibitors at 37°C for a four hour incubation period (Section 3.2.25). The final concentrations of proteinase inhibitors PMSF, TLCK and TPCK in the incubations were 1mM, 135 μM, and 248 μM, respectively. FESEM images were obtained for each crystal type and the degree of degradation assessed visually.

Figures 10.4 to 10.7 show electron micrographs of COM crystals precipitated from CF and UF urine after they had been incubated in urine for four hours. The faces and edges of the crystals grown in CF urine show the presence of surface fissures and erosion (Figure 10.4a), and when fractured, the crystal interior appeared have a porous structure (Figure 10.4b), an indication that material had been removed from the crystal bulk. In contrast, the crystals derived from the same urine specimen, following ultra-filtration, exhibited no obvious signs of erosion on the crystal surface (Figure 10.5a) or in the interior (Figure 10.5b). Crystals precipitated from the same CF urine and incubated in fresh urine to which protease inhibitors had been added also showed smooth exterior surfaces (Figure 10.6a), similar to the crystals shown in Figure 10.5, but have a more granular internal structure (Figure 10.6b). Crystals obtained from the ultrafiltered urine and incubated in fresh urine with added protease inhibitors possessed smooth surfaces (Figure 10.7a) and a solid interior (Figure 10.7b).

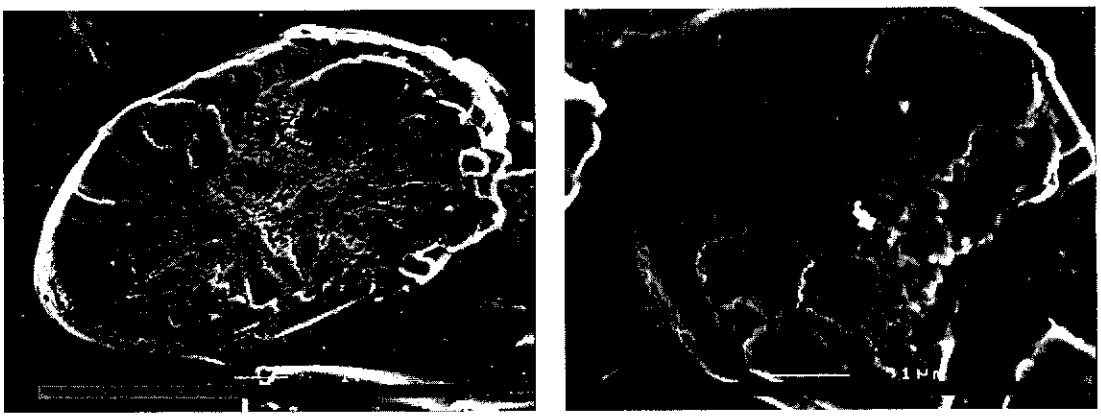

a b

Figure 10.4 Electron micrographs whole (a) and fractured (b) COM crystals derived from CF urine, after four hours incubation in fresh urine in the absence of added protease inhibitors

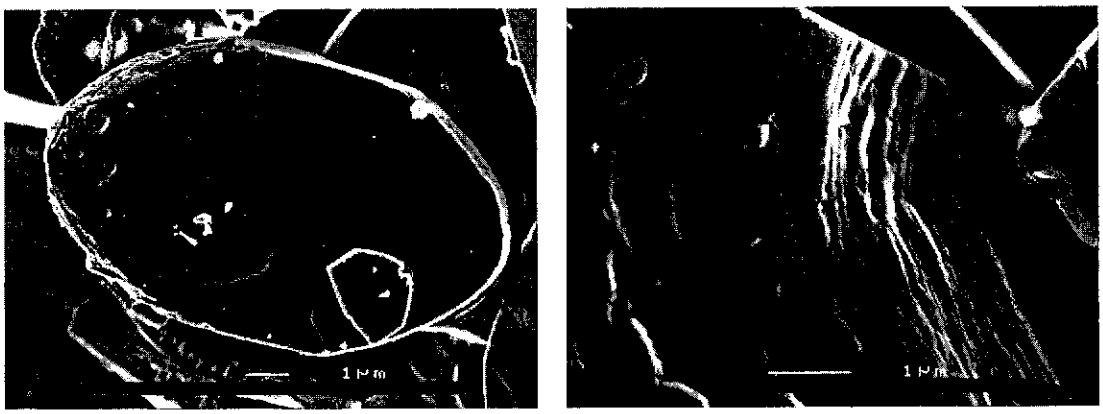

a b

Figure 10.5 Electron micrographs of whole (a) and fractured (b) COM crystals precipitated from UF urine, after four hours incubation in fresh urine in the absence of added protease inhibitors

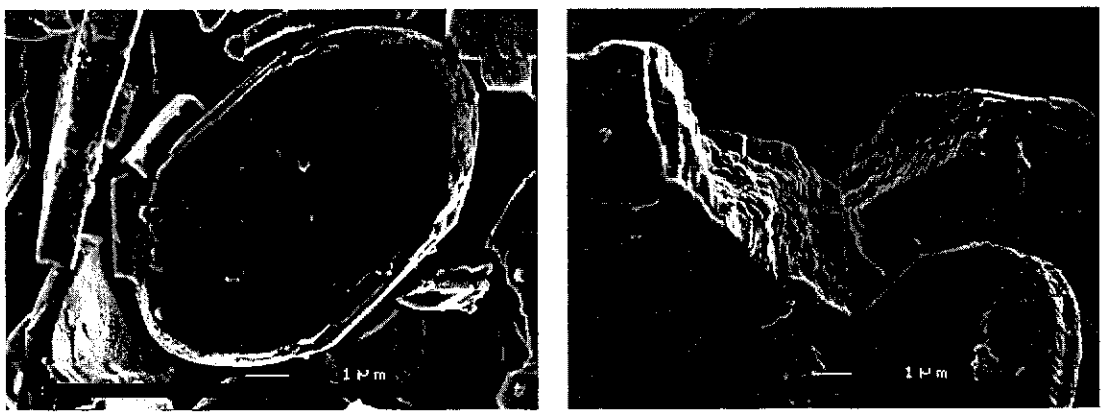

a b

Figure 10.6 Electron micrographs of whole (a) and fractured (b) COM crystals obtained from CF urine, after four hours incubation in fresh urine in the presence of added protease inhibitors

a b

Figure 10.7 Electron micrographs of whole (a) and fractured (b) COM crystals derived from UF urine, after four hours incubation in fresh urine in the presence of added protease inhibitors

10.3 COM produced *in vivo* in human urine

In order to determine the effects of urinary enzymes on COM crystals formed naturally in urine, a healthy male's fresh urine was immediately filtered, and the filtrate examined by FESEM (Section 3.2.26). COM crystals formed *in vivo*, like those precipitated *in vitro* from CF urine, were considerably eroded (Figure 10.8). This demonstrates the capacity of endogenous urinary enzymes to degrade COM crystals formed *in vivo* in the renal system.

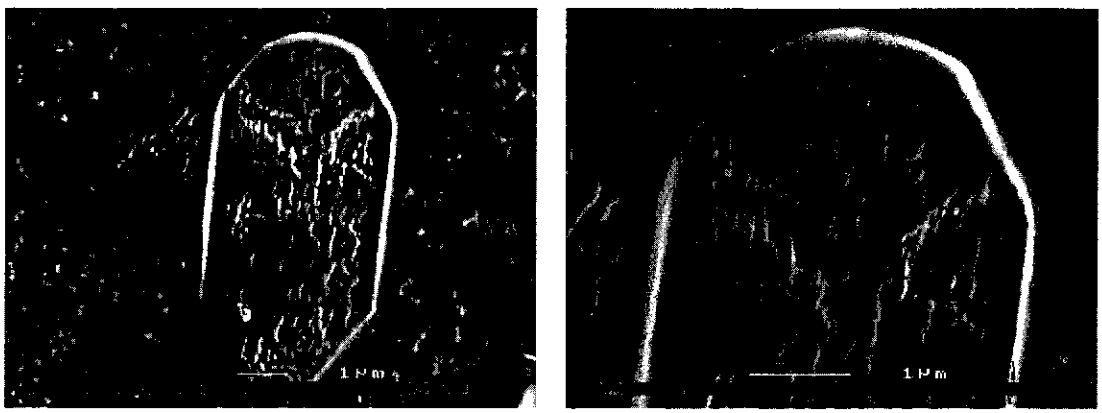

a b

Figure 10.8 Electron micrograph of COM crystals formed naturally in fresh human urine. Micrograph (b) is a higher magnification of (a).

10.4 DISCUSSION

The averaged dissolution curve profile of COM (distilled water) showed the dissolution to be a single step, whereas COM (UF) and COM (CF) were three steps. The Shrinking Core model was shown to be applicable to all stages of the dissolution of COM (distilled water), COM (UF) and COM (CF), demonstrating that the dissolution process is surface area-dependent. Deviation from the model for the final 5% of COM (distilled water) dissolution is likely to be due only to experimental error. The slow initial rates observed for the first 10% of the COM (UF) and COM (CF) dissolution curves may be attributable to the coating of non-intracrystalline organic material often seen in crystals derived from human urine such as shown in Figure 10.3. The coating is thus likely to initially screen the crystal surfaces from EDTA. This view is supported by the fact that the next and faster stage is the dissolution of the outer shell, which is presumably mostly COM with little organic material, as demonstrated in Section 9.3.

The slower rates for the dissolution of the last 20% or more of COM (UF) and COM (CF) could be the result of molecules occluded within their structures. As the crystals grow (non-steady state conditions), the solution concentration of the organic species will decrease as they are occluded into the mineral bulk. The crystals would thus have a decreasing concentration gradient of occluded molecules from their centres outward. If these molecules shield the crystalline material from the solution then they would reduce the dissolution rate, that is, outer shells with few occluded species would dissolve more rapidly than cores with greater concentration of amino acids, peptides and proteins. There is also the possibility that the macromolecules would have bound to the ions and retard their release into solution. This was supported by the comparatively slow rates found for the final UF and CF dissolution (both $k^* = 0.0010\ min^{-1}m^{-2}$).

The sequence of the dissolution rates ($0.1 < \alpha < 0.6$) observed was COM (distilled water) >> COM (UF) > COM (CF) (Table 10.1). Thus, the sequence of the rates of dissolution is inversely related to the amount of protein associated with the crystals. Researchers using SDS-PAGE analysis of the demineralised extracts of crystals from UF urine, have unambiguously shown no detectable protein >10 kDa to be present (Doyle et al., 1991). Hence, the presence of endogenous urinary molecules in the

crystals, decreases the rate of mineral dissolution, with macromolecules >10 kDa, possibly having a greater effect.

In the experiments involving the incubation of urinary COM crystals in fresh human urine, COM (CF) crystals exhibited the greatest degree of internal and superficial erosion and this is borne out in the literature (Fleming, 2000b). Such erosion did not occur in the presence of proteinase inhibitors, demonstrating that there are enzymes present in fresh urine that are capable of attacking proteins occluded in COM crystals. This was supported by the degraded appearance of COM crystals produced *in vivo*. Since COM (UF) crystals were not affected by incubation in fresh urine, it can be concluded that the erosion seen in COM (CF) crystals incubated in fresh urine for four hours resulted from destruction of proteins with Mr >10 kDa. This would suggest that COM crystals containing large quantities of such species are more susceptible to proteolytic degradation in the urinary system than COM crystals containing only low quantities of protein.

In conclusion, the dissolution and proteinase experiments reported in this chapter have shown that although COM (CF) crystals are more difficult to dissolve than COM (UF) in aqueous solutions, they are far more susceptible to endogenous proteolytic degradation in urine. These effects on crystal stability, studied separately, indicate a complexity in the *in vivo* renal environment that would be difficult to mimic, and for a better understanding, it is vital that proteolysis and mineral dissolution studies be conducted simultaneously. *In vivo*, both dissolution and proteolysis can occur simultaneously because the pH in the phagolysosome is acidic, favouring CaOx dissolution, and the proteases in the phagolysosome operate maximally at low pH (Bohley and Seglen, 1992, Lieske et al., 1996b). Thus, an experimental model is required that will combine and satisfy both these aspects simultaneously.

Despite the stated limitations, the observations from the studies presented in this chapter have important ramifications for the formation of CaOx kidney stones in urine. As retention of CaOx crystals in the urinary tract, either as a result of aggregation or by attachment to the epithelium, is recognised as a critical step in urolithiasis (Ryall, 1993), it follows that any process that facilitates the removal of crystalline waste from the renal system is advantageous in preventing kidney stone

formation. Once retained in the urinary tract, the fate of CaOx crystals would be primarily dependent on their vulnerability to dissolution and degradation, either in the urine or intracellularly following phagocytosis. Proteinases could open channels throughout the interior mineral architecture, increasing the surface area available for dissolution and further degradation processes. Thus any crystals nucleated from urine in the absence proteins capable of being occluded into the mineral structure, or even at low concentrations of those proteins, would contain only small quantities of intracrystalline proteins. Such crystals would be less susceptible to the action of proteinases in urine, as well as to those present in the phagolysosome following phagocytosis.

11 SUMMARY AND CONCLUSIONS

It is well recognised that CaOx urinary stones have both a mineral and macromolecular component. While the mineral component is rarely the subject of debate, the role of the macromolecules in the formation of calculi still remains unclear. Traditionally, the primary role of urinary proteins in CaOx urolithiasis was generally assumed to be associated with the inhibition of crystal nucleation, growth and particularly, aggregation (Ryall, 1997). As aggregation inhibitors, proteins were assumed to play a major role in healthy urine by preventing the formation of large crystal clusters likely to be retained within the renal collecting system. Their occurrence in stones may therefore be a consequence of an inadequate or defective protective function (Ryall, 1997). However, crystals may also attach directly to the epithelial surface (Khan and Hackett, 1991), which has particular implications for stone pathogenesis or prevention.

Lieske et al., (1996b, 1997) showed that exogenous COD and COM crystals were internalized by cultured monkey renal BSC-1 cells. These crystals dissolved over a period of several weeks within lysosomal inclusion bodies (Lieske et al., 1999), whose acidic interiors are rich in proteinases (Bohley and Seglen, 1992). They hypothesized that crystal attachment and subsequent dissolution may represent a series of events occurring continually in the kidney as a routine means of evading stone formation (Lieske et al., 1996b). They also postulated that the surfaces of epithelial cells could serve as templates for the nucleation of crystals from supersaturated tubular fluid (Lieske et al., 1999). Their subsequent attachment would be facilitated by stereospecific interactions between structures on the apical surface of renal tubular cells and the assemblage of molecules on the (100) face of COD crystal (Lieske et al., 1996b) and similar arrays on the COM crystal surface (Lieske et al., 1998). These interactions would depend, in turn, upon the concentration and structure of specific anionic molecules, either on the surface of renal cells or within the luminal fluid, both influencing and impacting on attachment, endocytosis and dissolution of crystals (Lieske et al., 1996, 1998). This hypothesis is extended by proposing that the ultimate fate of attached crystals, and, therefore the likelihood of stone formation also depend upon the nature and concentration of

urinary proteins incorporated within the precipitated crystals since they could facilitate crystal degradation and removal following attachment and phagocytosis. Erosion of any mineral shell surrounding a protein-laden interior of a crystal would be assisted by an acidic lysosomal environment, while protein filled pores would be susceptible to proteinases that would open channels throughout the interior architecture. This would facilitate degradation and dissolution of crystals, as well as the removal of the resulting particles and ions by exocytosis.

The strong relationship between proteins and crystal attachment consequently raises an important question in urolithiasis, one of biological control. Are stones examples of uncontrolled biomineralization, as they are generally accepted to be, or are they products that have some features in common with controlled biomineralization? In controlled biomineralization, intracrystalline proteins are vitally important to the construction of marine shells, sea urchin spines, teeth and bone (Weiner and Addadi, 1997), but it is more difficult to envisage a role for intracrystalline proteins in urolithiasis. To define a role for proteins in kidney stone formation, it is necessary to know what proteins are present in stones. The invariable presence of proteins in stones suggests that they are actively involved in their formation. However, the presence of proteins inside renal calculi could also be the result of inflammatory products of the disease process and play no decisive part at all (Stapleton and Ryall, 1994). Owing to the association of stones with haematuria, studies in the late 80's and early 90's were directed to crystals generated from urine (Ryall and Stapleton, 1995). The results suggested that proteins were not just bound to crystal surfaces, but also apparently *inside* urinary crystals (Morse and Resnick, 1988b, Doyle et al., 1991). This finding, if correct, could have major ramifications for stone formation, because crystals with proteins inside them could be more easily degraded and stone formation averted. Therefore the study of the relationship between crystals and proteins is important.

The overall goal of the work described in this thesis was to obtain detailed information about the physical relationship between the intracrystalline proteins and mineral phase of CaOx urinary crystals. In view of the importance of the type and structure of amino acids in determining whether a protein will interact with a calcium mineral, a study of the adsorption affinity of amino acids with calcium salts comprising human kidney stones was considered to be the first step. Although the

available literature indicated that free amino acids are unlikely to fulfil a prominent inhibitory role in stone pathophysiology, it was reasoned that they could, nonetheless, fulfil an important function as terminal residues or as exposed components of calcium-binding domains of proteins involved in stone formation. Acidic amino acids, such as Asp, Glu and Gla, are present as end groups, or as part of calcium-binding domains in certain urinary proteins, which have been shown to have a marked effect on CaOx crystal formation, growth or aggregation. Among these proteins are UPTF1 (Ryall et al., 1995, Grover et al., 1998) and osteopontin (Asplin et al., 1998, Min et al., 1998), both of which are present in the organic matrix of CaOx stones. Initial investigations were directed towards assessing the adsorption of twenty amino acids to COM, calcium hydrogen phosphate, tricalcium phosphate and hydroxyapatite over the physiological urinary pH range (pH 5-8) in aqueous solutions. All adsorbed strongest at pH 5 and this decreased as the pH increased as a result of the increasing negative charge of both substrate and adsorbate. Binding was higher to COM than to the phosphate minerals, owing to differences in the surface charge or coordination-site availability. Asp, Glu and Gla, which each have at least two carboxyl groups, exhibited the highest binding affinities, suggesting that binding occurs by chelation. Further, binding affinity was reasoned to result from the ability of the zwitterions of Asp, Glu and Gla to adopt favourable conformations in which two carboxyl groups, and possibly the amine group, can interact with the mineral surface without further rotation. The strong binding affinity of acidic amino acids for calcium stone minerals, but particularly for COM at low pH, suggested that urinary proteins rich in these amino acids are also more likely to play a functional role in stone pathogenesis than those possessing only few such residues (Ryall et al., 1995, Grover et al., 1998). For example, UPTF1, a known intracrystalline fragment of PT, contains 10 residues of Gla located in the N-terminal units of the molecule (Stapleton and Ryall, 1994, Ryall, 1995). Gla, an amino acid found only in the vitamin K-dependent proteins possesses an extraordinary capacity for binding calcium ions (Ryall et al 2000). Hence any irreversible binding of amino acids and proteins on the surfaces of growing COM, could result in these molecules becoming incorporated within the crystal. However, because the concept of protein intercalation into calcium oxalate crystals has been disputed (Mandel, 1997) and because its implications for stone formation were major, it was necessary to clarify the issue.

The existence of intracrystalline proteins and amino acids in COM crystals was clearly demonstrated by SXRD analysis. Non-uniform strain and crystallite size were derived from SXRD whole pattern line widths. Since they are indicators of crystal disorder, it was reasoned that demonstration of an increase in non-uniform strain and a decrease in crystallite size, relative to those found in control COM grown in the absence of any additives, would confirm the occlusion of selected proteins and amino acids within COM crystals grown in their presence. Rietveld whole pattern fitting showed an increase in average non-uniform strain and decrease in average crystallite size, which was attributed to the presence of intracrystalline molecules. Occluded molecules were Glu, Gla, PT and to a lesser extent HSA, as well as CME, which consists of an undefined mixture of organic species remaining after demineralization of the mineral phase of COM crystals precipitated from human urine. A dominant factor that must influence the occlusion of these molecules in COM is their ability to bind to calcium. Of the amino acids, this is especially true for Gla, which, well known for its strong affinity for calcium, is likely to attach irreversibly to the COM surface and be enveloped by a growing crystal front. Amino acids with lower binding affinity are less likely to become interred within the mineral bulk. It follows that known proteins, such as UPTF1 and PT, which contain 10 Gla residues each (Stapleton et al., 1993, Stapleton and Ryall, 1995) would behave in a similar manner to each other. The non-uniform strain and crystallites size for COM (CME) and COM (CF urine) were similar as expected. COM grown in CF urine possessed greater non-uniform strain and smaller crystallite size than COM grown in UF urine, indicating that the majority of intracrystalline macromolecules in crystals derived from CF urine were > 10kDa. Proteinase treatment of COM crystals grown in CF urine produced a marked decrease in non-uniform strain and an increase crystallite size, suggesting that smaller crystallite material, more intimately associated with proteins than the bulk COM, was liberated during the treatment. Results also indicated that HSA was only weakly incorporated into COM. This finding may be due to the large number of hydrophobic domains located on the protein molecule (Zunszain et al., 2003), which would have comparatively less affinity for calcium atoms on COM than acidic amino acid residues. The structural composition of HSA may also help to explain the fact why the protein is a poor inhibitor of CaOx growth (Edyvane et al., 1986). However, structural information alone is insufficient to explain the binding affinity of HSA to substrates, and

conformation considerations, must also be taken into account (Sukhishvili and Granick, 1999). Thus the propensity of proteins to become incorporated into COM will not only depend on the sequence of amino acids positioned along the protein but also the folding of the macromolecule's backbone.

No notable increase in non-uniform strain and corresponding decrease in crystallite size were found in COM crystals grown in aqueous solutions of Asp, AspAsp, GluGlu and THG, indicating that these molecules were not occluded into the mineral phase. The reason for Glu and not Asp being occluded in COM, despite their similar structures and adsorption affinities for the mineral, is not understood. However, as the dimer of these two amino acids (AspAsp and GluGlu) has an amide linkage, intramolecular hydrogen bonding may be an important factor in reducing their binding affinity for COM, and thus prevent them from being occluded. The reversible binding of THG to COM crystals, consistent with its weak inhibition of CaOx crystal growth in urine (Ryall et al., 1991b) and inorganic media, is suspected to be related to its structural composition. THG is a heavily glycosylated protein and has carbohydrates accounting for approximately 30% of the total molecular mass (Pak et al., 2001), and the abundance of these groups may shield and subsequently reduce the effectiveness of any COM binding residues.

A reciprocal relationship was found between non-uniform crystal strain and crystallite size, which was dependent upon the type of molecule(s) present in the COM growth media. For a given increment in non-uniform strain, the corresponding decrease in crystallite size was found to be considerably greater for the occluded macromolecules, than for the amino acids. This disparity is attributed to the capacity of macromolecules to disrupt a larger volume of the mineral structure than amino acids, once they are incorporated in COM. In addition to altering non-uniform strain and crystallite size, intracrystalline amino acids and proteins also created and stabilised an amorphous phase in some CaOx crystals, as indicated by a very broad band at 25° (2θ) in the X-ray diffractograms. An amorphous phase in CaOx crystals has important urological implications in that the stability of CaOx crystals, once formed in the urinary system, will depend to some degree on their solubility, which in turn will be affected by the presence and quantity of such a phase. Amorphous contributions resulting from the occlusion of PT and molecules from CF urine (>10kDa) and UF urine (<10kDa) in COM were 9%, 8% and 5% respectively. These

crystals were also associated with the greatest non-uniform strain and stacking faults. The decrease of amorphous material in COM (CF urine) crystals to 4% following proteinase treatment supplied further evidence that proteins are intimately involved in the stabilization of this phase. These findings support the work of Wang et al. 1997, Addadi et al., 1999, Keller and Dollase 2000 and Aizenberg et al., 2003. The degree of control over the amorphous phase may depend on the adsorption affinity of the protein's amino acid residues for calcium. PT possesses Gla residues, which can strongly complex calcium, and can thus have a large influence on the crystal structure of COM, whereas HSA is unable to do this because it lacks these amino acid residues. This could explain why an amorphous phase was found in COM (PT) but was absent from COM (HSA). The absence of amorphous material in COM (CME) was unexpected as crystals grown in the presence of CME possessed a similar lattice strain and crystallite size as PT. The absence of an amorphous phase from COM grown in the presence of intracrystalline amino acids, Gla and Glu, probably resulted from the smaller regions of influence of those amino acids around their attachment sites in comparison with the incorporated proteins.

The SXRD data derived from the COM crystals was further analysed for anisotropy using Williamson-Hall plots and individual peak analysis (SHADOW). Williamson-Hall plots, while useful in discerning the degree of stacking faults in crystals, is only semi-quantitative at best for determining anisotropy for non-uniform strain and crystallite size. Because large uncertainties were associated with the two methods, a combination of both was used to assess the anisotropic behaviour along eleven selected crystallographic planes. Crystals of COM (distilled water) and COM (Asp, AspAsp, GluGlu, Gla, HSA, THG and PT) were isotropic with respect both to non-uniform strain and crystallite size. COM (Glu), although isotropic with respect to non-uniform strain, exhibited a smaller crystallite size along the "a" axis than the other two principal axes, which suggested that Glu preferentially adsorbed on the (100) face. COM (UF) was also isotropic with respect to non-uniform strain, but the crystallites were smaller along the "c" axis. Crystals of COM (CF urine), COM (CME) also showed anisotropy, but only of crystallite size. These crystallites were found to have short "a" and "c" axes, which suggested that CME and the molecules present in CF urine preferentially adsorbed on the (100) and (001) faces of the crystal and thus slowed the growth rate relative to the other principal face. These findings

suggest that certain proteins can act as COM modifiers and change the morphology. For example the COM crystals found in urine are hexagonal and flat with rounded edges, differing considerably in morphology from the pure mineral.

Williamson-Hall plots showed that stacking faults were a major contributor to crystal disorder. Largest stacking faults, highest non-uniform strain and lowest crystallite sizes were generally found along the $(13\bar{1})$ plane. As in single peak analysis, COM (Gla), COM (CF urine) and COM (PT) crystals were associated with the greatest disorder. From computer-generated models it was deduced that molecules as large as proteins could not effectively be incorporated along the $(13\bar{1})$ plane in COM. Rather, they transmit disorder from the principal planes (100, 010, 001) in the crystal to the $(13\bar{1})$ plane by diagonal sliding of one or more rows of oxalate ions, calcium ions and water molecules. Thus it would be expected that stacking faults caused by macromolecules adsorbed onto crystal growing faces would create the largest rises in disorder, and hence peak broadening, in zones such as the $(13\bar{1})$ plane. The increase in crystal disorder, as like the presence of an amorphous phase in COM, is likely to affect solubility, therefore have an impact on the stability of crystals formed in the urinary system.

Single peak analysis along the $(13\bar{1})$ plane and whole pattern analysis of SXRD data from CaOx crystals grown in aqueous solutions of increasing concentrations of PT, HSA, CME and Gla showed that non-uniform strain increased, crystallite size decreased, and stacking faults increased, to limiting values. This was also found for COM crystals grown in UF urine with increasing concentrations of CME and HSA. The increase in crystal disorder suggested an increase in uptake of these additives by the growing crystal from the surrounding solution. The minimum aqueous solution concentrations of PT, HSA, CME and Gla as well as urinary concentrations of CME and HSA, to achieve plateau values of non-uniform strain and crystallite size single peak analysis, were approximately 10, 60, 4, 200, 3 and 10 mg/L respectively. This supported the view that the organic molecules were occluded and there was a limit to the non-uniform strain that the lattice was able to tolerate because of their presence. If agglomeration of smaller crystals with adsorbed organic molecules had occurred, then the increase in non-uniform strain and decrease in crystallite size with concentration, and their limiting values would not have been seen.

Of the macromolecules, HSA required the highest aqueous concentration to achieve a plateau in the inverse relationship between non-uniform strain and crystallite size, followed by PT and CME. The reason for this finding may be associated with the protein's relative affinity for COM and the limit of deformation that the crystal will allow in order to maintain structural integrity. Thus relatively smaller quantities of the stronger COM binding proteins, PT and the proteins present in CME, would be expected to produce the same non-uniform strain and crystallite size as HSA. Taking into account the limiting non-uniform strain values, the above order suggested that the affinity of the macromolecules for COM is CME > PT > HSA. The plateau average non-uniform strain values for UF urine, HSA (aqueous) and HSA (UF urine) were comparable and indicated that the contribution to non-uniform strain from HSA was similar to low molecular weight (<10 kDa) species present in UF urine. The contribution of component molecules of UF urine to both plateau non-uniform strain and plateau concentration was smaller than that of CME, which indicated that CME has a much larger effect than UF urine. Crystals from UF urine are likely to contain organic molecules with Mr values <10kDa whereas COM (UF/CME) contains, in addition to these molecules, UPTF1 and other intracrystalline proteins with Mr values of >10 kDa (Stapleton, 1995). It can thus be concluded that changes in non-uniform strain and crystallite size, and stacking faults produced are dependent on the concentration and type of the molecular species present in COM.

FESEM observations showed that CaOx grown in aqueous solutions of Asp, Gla, Glu were indistinguishable from COM crystals precipitated from distilled water, indicating that these amino acids had no effect on morphology. However, the morphology of COM crystals grown in aqueous PT solutions, UF urine and CF urine were markedly different from the distilled water control, confirming the preferential adsorption for different crystal faces that had previously shown by SXRD analysis. In particular, COM grown in CF urine, had features consistent with adsorption of urinary molecules on to the (100) face, which slowed the growth of that face relative to the others and produced thinner, and more plate like crystals than COM grown in distilled water. The rounding of the (001)/(021) and (021)/(010) edges compared to distilled water COM, was caused by the slowing of growth on the (001) face. Individual peak analysis of crystallites of COM (CF) and COM (UF) showed that they possessed the same adsorption characteristics as their corresponding crystals

with CF urinary components. The "a" and "c" axes were smaller than the "b" axis of the crystallites, indicating preferential adsorption on the (100) and (001) faces. This effectively slows the growth in the "a" and "c" directions, leading to an ovoid, "plate-like" shape, similar to the morphology of fully developed crystals. Similar observations have been found natural biomineralization systems where proteins exert control over the morphology and other properties of the crystal by the preferential adsorption of proteins for selected faces of the parent mineral. The three-dimensional molecular configurations and chemical properties of intracrystalline proteins ensure that only crystals of a particular shape and composition are formed, for example, sea urchin spines, sponge spicules and mollusc shells (Addadi and Weiner, 1992, Aizenberg, et al., 1996a, Addadi et al., 1999). Weiner and Addadi (1997) showed that intracrystalline proteins intercalated along the (001) planes of calcite in sea urchins, greatly affect the morphology and mechanical properties of the parent mineral.

FESEM observations of the internal architecture of fractured CaOx crystals grown in human urine and synthetic solutions containing PT, revealed an inhomogeneous microstructure containing "low-density" zones not observed in pure calcium crystals or CaOx crystals grown in UF urine. Proteolytic treatment of the fractured crystals, created an internal honey combed structure that replaced the "low-density" zones. However the sizes of the pores were far too large to be proteins alone, and must be due to associated amorphous material, previously detected by SXRD. The external and fractured surfaces of COM grown in aqueous solutions of Asp, Glu and Gla were similar in appearance to the distilled water control. The lack of any significant affect of proteolytic etching of these crystals was expected. A timed growth study showed the internal ultrastructure of urinary COM crystals depended to a large extent, upon the ratio of crystal-binding proteins to the available quantities of solute ions during growth. This finding has important urological ramifications, since crystals formed in urinary system with high concentrations of CaOx-binding proteins, once subjected to proteolysis, will be degraded and perforated (Fleming 2000b). This is expected to result in an increase in crystal surface area and consequently dissolution rate.

Dissolution studies of CaOx crystals showed that the process obeyed the Shrinking Core model and was therefore surface area dependent. Pure CaOx dissolved more rapidly than crystals derived from UF urine, which dissolved at a faster rate than

crystals precipitated from CF urine. The slow initial rates observed for the first 10% of CaOx (UF) and CaOx (CF) dissolution were attributable to surface coating of organic material often seen in crystals precipitated from urine. The slower rates for the dissolution of the last 20% or more of both crystal types were reasoned to be the result of occluded molecules within their structure, which would have shielded newly exposed COM surface, thereby reducing the effective surface area and slowing dissolution. There is also the possibility that the macromolecules would have bound to the ions and retard their release into solution. This was verified by the slowest dissolution rate of all crystals, COM (CF urine), which had additional higher molecular mass proteins (>10 kDa) incorporated in them than in COM (UF) crystals. It was thus concluded that occluded amino acids, peptides and macromolecules in CaOx increases its resistance to dissolution, with macromolecules >10 kDa having a greater effect. Thus the capacity of CaOx crystals to resist dissolution in the renal system will be dependent on the quantity and size of macromolecules present in them.

In crystal degradation studies, COM crystals derived from CF urine and incubated in fresh CF human urine were shown by FESEM, to be far more eroded than crystals grown in the same urine after ultrafiltration. Similarly, erosion did not occur in the presence of proteinase inhibitors, demonstrating that there are enzymes present in fresh urine that are capable of attacking proteins occluded in COM crystals (Fleming et al., 2000b). This was supported by the degraded appearance of COM crystals produced *in vivo*, which also suggests that the renal system is capable of degrading COM crystals. Furthermore, COM (UF) crystals, which contain no proteins with molecular masses greater than 10 kDa, were not affected by incubation in fresh urine. Thus, crystals containing larger quantities of proteins are more susceptible to proteolytic degradation, and that it is reasonable to conclude that the ratio of intracrystalline protein to mineral would be important *in vivo*. This supposition seems to contradict the results of the dissolution experiments which showed that COM (CF) crystals were more difficult to dissolve than COM (UF) crystals in aqueous solutions. However, these effects on crystal stability were studied separately, and did not take into account the complex behaviour of the renal environment, that would be difficult to mimic. For a better understanding, it is vital that proteolysis and mineral dissolution studies be conducted simultaneously. *In*

vivo, both dissolution and proteolysis can occur simultaneously because the pH in the phagolysosome is acidic, favouring CaOx dissolution, and the proteases in the phagolysosome operate maximally at low pH (Bohley and Seglen, 1992, Lieske et al., 1996b). Thus, an experimental model is required that will combine and satisfy both these aspects simultaneously.

The work reported in this thesis has, for the first time, provided both physicochemical and visual evidence that selected proteins and amino acids can become incorporated within the mineral fabric of COM crystals, whether precipitated from inorganic solutions or deposited from human urine. Moreover, it has shown unequivocally that the occlusion of such molecules was accompanied by changes to the physical texture and properties of the crystal, which altered the rate of dissolution of the mineral phase, as well as the susceptibility of the entire structure to erosion by endogenous and exogenous proteolysis. These findings have formed the basis of a novel hypothesis, which proposes that the type and concentration of urinary proteins incorporated inside CaOx crystals are fundamental to process of disposing CaOx crystals precipitated from within the renal system. As retention of CaOx crystals in the urinary tract, either as a result of aggregation or by attachment to the epithelium, is recognised as a critical step in urolithiasis (Ryall, 1993), it follows that any process that facilitates the removal of crystalline waste from the renal system is advantageous in preventing kidney stone formation. Once retained in the urinary tract, the fate of CaOx crystals would be primarily dependent on their vulnerability to dissolution and degradation, either in the urine or intracellularly following phagocytosis. Proteinases could open channels throughout the interior mineral architecture, increasing the surface area available for dissolution and further degradation processes. Thus any crystals nucleated from urine in the absence proteins capable of being occluded into the mineral structure, or even at low concentrations of those proteins, would contain only small quantities of intracrystalline proteins. Such crystals would be less susceptible to the action of proteases in urine, as well as to those present in the phagolysosome following phagocytosis.

In conclusion, the findings presented in this thesis have not only impacted on the way we view the relationship between CaOx crystals and proteins, but perhaps more importantly, suggest that a dynamic and potentially reversible process exists in the renal system in which proteins and renal proteases perform a definitive role: one of

CaOx crystal regulation. To extend the work of this thesis, future studies could be directed towards determining the position and shape of intracrystalline macromolecules throughout the structure of COM. Initial experimental work carried out at ISIS (Rutherford Appleton Laboratory) using Small Angle Neutron Scattering (SANS), showed promise towards achieving these objectives. More detailed work in this area should further help to elucidate the relationship between the organic molecules and mineral phase, and may provide therapeutic opportunities by facilitating stone degradation *in situ*. Heenan, (1997) gives an excellent introduction to the SANS technique.

REFERENCES

Addadi, L., Aizenberg, J., Beniash, E. and Weiner, S. (1999) 'On the concept of a single crystal in biomineralization' In: *Molecules and Crystals to Materials.*, pp. 1-22. Ed. D. e. a. Braga. Kluwer Academic Publishers, The Netherlands.

Addadi, L., Berkovitch-Yellin, Z., Weissbuch, I., van Mil, J., Shimon, L., Lahav, M. and Leiserowitz, L. (1985) 'Growth and dissolution of organic crystals with "tailor-made" inhibitors - implications in stereochemistry and materials science', *Angew Chem Int Ed Eng,* **24,** 466-485.

Addadi, L. and Weiner, S. (1986) 'Interactions between acidic macromolecules and structured crystal surfaces. Stereochemistry and biomineralization', *Mol Cryst Liq Cryst,* **134,** 305-322.

Addadi, L. and Weiner, S. (1992) 'Control and design principles in biological mineralization', *Angew Chem Int Ed Engl,* **31,** 153-169.

Addadi, L., Weiner, S. and Geva, M. (2001) 'On how proteins interact with crystals and their effect on crystal formation', *Zeitschrift fur Karldiologie,* **90,** 92-98.

Ahlstrand, C. and Tiselius, H. (1981) 'Renal stone disease in a Swedish district during one year', *Scand J Urol Nephrol,* **15,** 143-146.

Aizenberg, J., Hanson, J., Koetzle, T., Weiner, S. and Addadi, L. (1997) 'Control of macromolecule distribution within synthetic and biogenic single calcite crystals', *J Am Chem Soc,* **119,** 881-886.

Aizenberg, J., Ilan, M., Weiner, S. and Addadi, L. (1996a) 'Intracrystalline macromolecules are involved in morphogenesis of calcitic sponge spicules', *Connective Tissue Research,* **34,** 255-261.

Aizenberg, J., Lambert, G., Addadi, L. and Weiner, S. (1996b) 'Stabilization of amorphous calcium carbonate by specialized macromolecules in biological and synthetic precipitates', *Advanced Materials,* **8,** 222-226.

Aizenberg, J G., Weiner, S. and Addadi, L. (2003) 'Coexistence of amorphous and crystalline calcium carbonate in skeletal tissues', *Connective Tissue Research,* **44** (Suppl 1), 20-25.

Albeck, S., Addadi, L. and Weiner, S. (1996) 'Regulation of calcite crystal morphology by intracrystalline acidic proteins and glycoproteins', *Connective Tissue Research,* **35,** 365-370.

Andersen, H. (1983) 'Calcific diseases', *Arch Pathol Lab Med,* **107,** 341-48.

Asplin, J., Arsenault, D., Parks, J., Coe, F. and Hoyer, J. (1998) 'Contribution of uropontin to inhibition of calcium oxalate crystallization', *Kidney Int,* **53,** 194-199.

Asplin, J., Parks, J. and Coe, F. (1997) 'Dependence of upper limit of metastability on supersaturation in nephrolithiasis', *Kidney Int,* **52,** 1602-1608.

Atanassova, S., Neykov, K. and Gutzow, I. (1996) 'Solubility, inhibited growth and dissolution of calcium oxalate crystals in solutions, containing a-ketoglutaric acid', *J Crystal Growth,* **160,** 148-153.

Atmani, F. and Khan, S. (2002) 'Quantification of proteins extracted from calcium oxalate and calcium phosphate crystals induced in vitro in the urine of healthy controls and stone-forming patients', *Urologia Internationalis,* **68,** 54-59.

Atmani, F., Lacour, B., Drueke, T. and Daudon, M. (1993a) 'Isolation and purification of a new glycoprotein from human urine inhibiting calcium oxalate crystallization', *Urol Res,* **21,** 61-66.

Atmani, F., Lacour, B., Jungers, P., Drueke, T. and Daudon, M. (1994) 'Reduced inhibitory activity of uronic-acid-rich protein (UAP) in the urine of stone formers', *Urol Res,* **22,** 257-260.

Atmani, F., Lacour, B., Strecker, G., Parvy, P., Drueke, T. and Daudon, M. (1993b) 'Molecular characteristics of uronic-acid-rich protein, a strong inhibitor of calcium oxalate crystallization in vitro', *Biochem Biophys Res Commun,* **91,** 1158-1165.

Atmani, F., Opalko, F. and Khan, S. (1996) 'Association of urinary macromolecules with calcium oxalate crystals induced in vitro in normal human and rat urine', *Urol Res,* **24,** 45-50.

Azoury, R., Garti, N. and Sarig, S. (1986) 'The amino acid factor in stone former's and normal urines', *Urol Res,* **14,** 295-298.

Bautista, DS., Densteldt, J., Chambers, AF. and Harris, JF. (1996) 'Low weight variants of osteopontin generated by serine proteases in urine of patients with kidney stones', *Journal of Cellular Biochemistry*, **61**, 402-409.

Bennema, P. (1967) 'Analysis of crystal growth models for slightly supersaturated solutions', *Journal of Crystal Growth,* **1,** 225-32.

Bennema, P. (1969) 'The influence of surface diffusion for crystal growth from solution', *Journal of Crystal Growth,* **5,** 29-43.

Binette, J. and Binette, M. (1993) 'A cationic protein from a urate-calcium oxalate stone: Isolation and purification of a shared protein', *Scan Microsc,* **7,** 1107-10.

Binette, J. and Binette, M. (1994) 'Sequencing of proteins extracted from stones', *Scan Microsc,* **8,** 233-39.

Binette, J., Binette, M., Gawinowicz, M. and Kendrick, N. (1996) 'Urinary stone proteins: An update', *Scanning Microscopy,* **10,** 509-18.

Blackburn, S. (1968) 'Automatic amino acid analysers' In: *Amino acid determination*, pp. 81-101, Arnold, E: London.

Blomen, L. and Bijvoet, O. (1983) 'Physicochemical considerations in relation to urinary stone formation', *World J Urol,* **1,** 119-25.

Bohley, P. and Seglen, P. (1992) 'Proteases and proteolysis in the lysosome', *Experientia*, **48**, 151-157.

Boskey, A. (1981) 'Current concepts of physiology and biochemistry of calcification', *Clin Orthop,* **1527,** 225-57.

Boskey, A. (1992) 'Mineral-Matrix Interactions in Bone and Cartilage', In: *Clinical Orthopaedics and Related Research.*, pp. 244-74, Cornell University Medical College: New York.

Boskey, A. (1996) 'Matrix proteins and mineralization: An overview', *Connective Tissue Research,* **35,** 357-63.

Boskey, A., LS, B. and Mandel, I. (1983) 'Phospholipids associated with human parotid gland sialoliths', *Archs oral Biol,* **28,** 655-57.

Bouropoulos, K., Bouropoulos, N., Melekos, M., Koutsoukos, P., Chitanu, G., Anghelescu-Dogaru, A. and Carpov, A. (1998) 'The inhibition of calcium oxalate monohydrate crystal growth by maleic acid copolymers', *J Urol,* **159,** 1755-1761.

Bowyer, R., Brockis, J. and McCulloch, R. (1979) 'Glycosaminogycans as inhibitors of calcium oxalate crystal growth and aggregation', *Clin Chim Acta,* **95,** 23-8.

Boyan, B., Schartz, Z., Swain, I. and Khare, A. (1989) 'Role of lipids in calcification of cartilage', *Anat Rec,* **22,** 211-19.

Boyce, W. (1968) 'Organic matrix of human urinary concretions', *Am J Med,* **45,** 673-83.

Boyce, W. and Garvey, F. (1956) 'The amount and nature of the organic matrix in urinary calculi: a review', *J Urol,* **76,** 213-27.

Boyce, W., Garvey, F. and Norfleet, C. (1954a) 'Ion-binding properties of electrophoretically homogeneous mucoproteins of urine in normal subjects and in patients with renal calculus disease', *J Urol,* **72,** 1019-31.

Boyce, W., Garvey, F. and Norfleet, C. (1954b) 'Proteins and other biocolloids of urine in health and in calculous disease', *J Clin Invest,* **33,** 1287-97.

Boyce, W. and King, J. (1959) 'Crystal-matrix interelations in calculi', *J Urol,* **81,** 351-65.

Boyce, W. and King, J. (1963) 'Present concepts concerning the origin of matrix and stones', *Ann N Y Acad Sci,* **104,** 563-78.

Boyce, W., King, J. and Fielden, M. (1962) 'Total non-dialyzable solids (TNDS) in human urine XIII. Immunological detection of a component peculiar to renal calculous matrix and to urine of calculous patients', *J Clin Invest,* **41,** 1180.

Boyce, W. and King, J. J. (1968) 'Present concepts concerning the origin of matrix and stones', *Am J Med,* **45,** 563-78.

Brown, L., Berse, B., Van De Water, L., Papadopoulos-Sergiou, A., Perruzzi, C., Manseau, E., Dvorak, H. and Senger, D. (1992) 'Expression and distribution of osteopontin in human tissues: widespread association with luminal epithelial surfaces', *Mol Biol Cell,* **3,** 1169.

Buchholz, N., Kim, D., Grover, P., Dawson, C. and Ryall, R. (1999) 'The effect of warfarin therapy on the charge properties of urinary prothrombin fragment 1 and crystallization of calcium oxalate in undiluted urine', *Journal of Bone and Mineral Research,* **14,** 1003-12.

Burnier, J., Borowski, M., Furie, B. and Furie, B. (1981) 'Gamma-carboxyglutamic acid', *Mol Cellular Biochem,* **39,** 191-99.

Burns, J. and Finlayson, B. (1980) 'The effect of seed crystals on calcium oxalate nucleation', *Invest Urol,* **81,** 133.

Butz, M. (1986) 'Metabolic disorders in patients with calcium urolithiasis', *Int Urol Neph,* **18,** 131-9.

Cagliotti, G., Paoletti, A. and Ricci, F. (1958) 'Choice of collimators for a crystal spectrometer for neutron diffraction', *Nucl Instrum,* **3,** 223-28.

Callejas Fernandez, J., De Las Nieves, F., Salcedo, J., Salcedo, R. and Hidalgo-Alvarez, R. (1990) 'The microelectrophoretic mobility and colloid stability of calcium oxalate monohydrate dispersions in aqueous media', *J Colloid Interface Sci,* **135,** 154-64.

Campbell, A., Ebrahimpour, A., Perez, L., Smeska, S. and Nancollas, G. (1989) 'The dual role of polyelectrolytes and proteins as mineralization promoters and inhibitors of calcium oxalate monohydrate', *Calcif Tissue Int,* **45,** 122-28.

Campbell, A., Gardella, J. and Richardson, C. (1990) 'Urinary stone analysis by small spot electron spectroscopy for chemical analysis (ESCA)', *Appl Spectroscopy,* **44,** 1015-19.

Canduri, F., Teodoro, LVGL., Lorenzi, CCB. and Gomes, RAS. (1998) 'Crystallization, preliminary X-ray analysis and Patterson research of a new aspartic protease isolated from human urine' *Biochem Mol Biol Int*, **46**, 355-363.

Cao, L., Boeve, E., de Bruijn, W., Robertson, W. and Schroder, F. (1993) 'A review of new concepts in renal stone research', *Scan Microsc,* **7,** 1049-65.

Cao, L., Deng, G., Boeve, E., Bruijn, W., de Water, R., Verkoelen, J., Romijn, J. and Schroder, F. (1996) 'Zeta potential measurement and particle size analysis for a better understanding of urinary inhibitors of calcium oxalate crystallization', *Scanning Microscopy,* **10,** 401-14.

Cerini, C., Geider, S., Dussol, B., Hennequin, C., Daudon, M., Veesler, S., Nitsche, S., Boistelle, R., Berthezene, P., Dupuy, P., Vazi, A., Berland, Y., Dagorn, J. and Verdier, J. (1999) 'Nucleation of calcium oxalate crystals by albumin: Involvement in the prevention of stone formation', *Kidney Int,* **55,** 1776-86.

Certificate of Analysis, S. R. M. (1974) 'Silicon Powder Lattice Parameter Standard for X-ray Powder Diffraction', National Institute of Standards: Gaithersburg, MD.

Certificate of Analysis, S. R. M. (1989) 'Instrument Line Position and Profile Shape Standard for X-ray Powder Diffraction', National Institute of Standards and Technology: Gaithersburg, MD.

Chabra, H. and Manocha, K. (1991) 'Idiopathic kidney stone formation', *Br J Urol,* **70,** 336-37.

Chauvet, M., Grover, P. and Ryall, R. (2001) 'Tamm-Horsfall glycoprotein is not an intracrystalline component of urinary calcium oxalate crystals', In: *Eurolithiasis, 9th European Symposium on Urolithiasis on Urolithiasis*, pp. 58. Eds. D. Kok, H. Romijn, P. Verhagen and C. Verkoelen: Rotterdam, the Netherlands.

Chen, W., Lin, H., Tsai, F. and Li, C. (2001) 'Effects of Tamm-Horsfall protein and albumin on the inhibition of free radicals', *Urologia Internationalis,* **67,** 305-9.

Chernov, A. (1989) 'Formation of crystals in solution', *Contemporary Physics,* **30,** 251-76.

Cifuentes-Delatte, L. (1982) 'Crystalluria', In: *Stones, clinical management of urolithiasis.*, pp. 21-52. Eds. R. Roth and B. Finlayson. Williams and Wilkins: Baltimore-London.

Coe, F. (1973) 'Uric acid and calcium oxalate nephrolithiasis', *Am J Clin Nutr,* **26,** 758.

Coe, F., Margolis, H., Deutsch, L. and Strauss, A. (1980) 'Urinary macromolecular crystal growth inhibitors in calcium nephrolithiasis', *Miner Electrolyte Metab,* **3,** 268-75.

Collette, C., Benmbarek, A., Boniface, H., Astre, C., Pares-Herute, N., Monnier, L. and Guitter, J. (1991) 'Determination of protein-bound urinary gammacarboxyglutamic acid in calcium nephrolithiasis', *Clin Chim Acta,* **204,** 43.

Crassweller, P., Oreopoulos, D., Toguri, A., Husdan, H., Wilson, D. and Rapoport, A. (1978) 'Studies in inhibitors of calcification and levels of urine saturation with calcium salts in recurrent stone patients', *J Urol,* **120,** 6-10.

Cullity, B. (1956) *Elements of x-ray diffraction,* Addison-Wesley Publishing Company, Reading: University of Notre Dame.

Curhan, G. and Curhan, S. (1994) 'Dietary factors and kidney stone formation', *Comprehensive therapy,* **20,** 485-89.

Curhan, G., Willett, W., Rimm, E. and Stampfer, M. (1993) 'A prospective study of dietary calcium and other nutrients and the risk of symptomatic kidney stones', *N Engl J Med,* **328,** 833-38.

Curtain, C. (1953) 'The action of urea on the urinary inhibitor of influenza virus hemagglutination', *Aust J Exp Biol,* **31,** 615-22.

Daudon, M., Bader, C. and Jungers, P. (1993) 'Urinary calculi: review of classification methods and correlations with etiology', *Scanning Microscopy,* **7,** 1081-106.

Davis, N. and Walker, T. (1972) 'The role of carboxyl groups in collagen calcification', *Biochem Biophys Res Commun,* **48,** 1656-62.

Dawson, C., Grover, P., Kanellos, J., Pham, H., Kupczyk, G., Oates, A. and Ryall, R. (1998a) 'Inter-a-inhibitor in calcium stones', *Clin Sci,* **95,** 187-93.

Dawson, C., Grover, P. and Ryall, R. (1998b) 'Inter-a-inhibitor in urine and calcium oxalate urinary crystals', *Br J Urol,* **81,** 20-6.

de Water, R., Nordermeer, C., van der Kwast, T., Nizze, T., Boeve, E., Kok, D. and Schroder, F. (2000) 'Calcium oxalate nephrolithiasis: Effect of renal crystal deposition on the cellular composition of the renal interstitium', *Am J Kidney Dis,* **33,** 761-71.

Dean, C., Kanellos, J., Pham, J., Gomes, M., Oates, A., Grover, P. and Ryall, R. (2000) 'The effect of inter-a-inhibitor and several of its derivatives on calcium oxalate crystallization in vitro', *Clin Sci,* **98,** 471-80.

Deganello, S. (1993) 'The interaction between Nephrocalcin and Tamm-Horsfall proteins with calcium oxalate dihydrate' *Scanning Microsc,* **7,** 1111-18.

Denhardt, DT. and Guo, X. (1993) 'Osteopontin: a protein with diverse functions', *FASEB Journal,* **7,** 1475-1482.

Dent, C. and Sutor, D. (1971) 'Presence or absence of inhibitor of calcium oxalate crystal growth in urine of normals and stone formers', *Lancet,* **2,** 775-8.

Doremus, R., Teich, S. and Silis, P. (1978) 'Crystallization of calcium oxalate from synthetic urine', *Invest Urol,* **15,** 469-72.

Doyle, I., Marshall, V., Dawson, C. and Ryall, R. (1995) 'Calcium oxalate crystal matrix extract: the most potent macromolecular inhibitor of crystal growth and aggregation yet tested in undiluted human urine in vitro', *Urol Res,* **23,** 53-62.

Doyle, I., Ryall, R. and Marshall, V. (1991) 'Inclusion of proteins into calcium oxalate crystals precipitated from human urine: a highly selective phenomenon', *Clin Chem,* **37,** 1589-94.

Drach, G., Kraljevich, Z. and Randolph, A. (1982) 'Effects of high molecular weight urinary macromolecules on crystallization of calcium oxalate dihydrate', *J Urol,* **127,** 805-10.

Durrbaum, D., Rodgers, A. and Sturrock, E. (2001) 'A study of crystal matrix extract and urinary prothrombin fragment 1 from a stone-prone and stone-free population', *Urol Res,* **29,** 83-88.

Dussol, B., Geider, S., Lilova, A., Leonetti, F., Dupuy, P., Daudon, M., Berland, Y., Dagorn, J. and Verdier, J. (1995) 'Analysis of the soluble matrix of five morphologically different kidney stones', *Urol Res,* **23,** 45-51.

Ebisuno, S., Umehara, M., Kohjimoto, Y. and Ohkawa, T. (1999) 'The effects of human urine on the adhesion of calcium oxalate crystals to Madin-Darby canine kidney cells', *Br J Urol,* **84,** 118-22.

Ebrahimpour, A., Perez, L. and Nancollas, G. (1991) 'Induced crystal growth of calcium oxalate monohydrate at hydroxyapatite surfaces. The influence of human serum albumin, citrate and magnesium', *Langmuir,* **7,** 577-83.

Edyvane, K., Hibberd, C., Harnett, R., Marshall, V. and Ryall, R. (1987) 'Macromolecules inhibit calcium oxalate crystal growth and aggregation in whole urine', *Clinica Chimica Acta,* **167,** 329-338.

Edyvane, K., Ryall, R. and Marshall, V. (1986) 'The influence of serum and serum proteins on calcium oxalate crystal growth and aggregation', *Clinica Chimica Acta,* **157,** 81-8.

Felix, R., Monod, A., Broge, L., Hansen, N. and Fleisch, H. (1977) 'Aggregation of calcium oxalate crystals: effects of urine and various inhibitors', *Urol Res,* **5,** 21-8.

Fellstrom, B., Danielson, B., Ljunghall, S. and Wikstrom, B. (1986) 'Crystal inhibition: the effects of polyanions on calcium oxalate crystal growth' *Clin Chim Acta,* **158,** 229-35.

Fellstrom, B., Lindsjo, M., Danielson, B., Karlsson, F. and Ljunghall, S. (1989) 'Binding of glycosaminoglycans inhibitors to calcium oxalate crystal in relation to ionic strength', *Clin Chim Acta,* **180,** 213-20.

Fievet, F., Germi, P., de Bergevin, F. and Figlarz, M. (1979) 'Lattice parameter, microstrains and non-stoichiometry in NiO. Comparison between mosaic microcrystals and quasi-perfect single microcrystals', *J Appl Crystallogr,* **12,** 387-94.

Finlayson, B. (1972) 'The concept of the continuous crystallizer: its theory and application to *in vivo* and *in vitro* urinary tract models', *Invest Urol,* **9,** 258-64.

Finlayson, B. (1977a) 'Calcium metabolism in renal failure and nephrolithiasis', In: *Calcium stones: some physical and clinic aspects*, pp. 337-82. Ed. D. David. J Wiley and Sons: New York.

Finlayson, B. (1977b) 'Where and how does urinary stone disease start? An essay on the expectation of free and fixed particle urinary stone disease', In: *Idiopathic urinary bladder stone disease*, pp. 7-31. Fogarty Int Centre Proc No 37 US Printing Office: Washington DC.

Finlayson, B. (1978) 'Physicochemical aspects of urolithiasis', *Kidney Int,* **13,** 344-60.

Finlayson, B., Khan, S. and Hackett, R. (1984a) 'Mechanisms of stone formation', *Scanning Electron Microscopy,* **111,** 1419-25.

Finlayson, B., Khan, S. and Hackett, R. (1984b) 'Mechanisms of stone formation: an overview', *Scanning Microscopy,* **3,** 1419.

Finlayson, B. and Reid, F. (1978) 'The expectation of free and fixed particles in urinary stone disease', *Invest Urol,* **15,** 442-8.

Finlayson, B., Vermeulen, C. and Stewart, E. (1961) 'Stone matrix and mucoprotein from urine', *J Urol,* **86,** 355-63.

Fleisch, H. (1978) 'Inhibitors and promoters of stone formation', *Kidney Int,* **13,** 361-71.

Fleming, D., Dean, C., Chauvet, M., Parkinson, G., Marshall, V. and Ryall, R. (2000a) 'A timed study of the relationship between mineral and protein during calcium oxalate crystal growth in human urine', In: *Urolithiasis 2000*, pp. 174-77. Eds. A. Rodgers, B. Hibbert, B. Hess, S. Khan and G. Preminger. University of Cape Town: University of Cape Town, Rondebosch, South Africa.

Fleming, D., Doyle, I., Evans, N., Marshall, V., Parkinson, G. and Ryall, R. (1999) 'Proteins associated with calcium oxalate crystals formed in human urine are

intracrystalline', In: *8th European Symposium on Urolithiasis*. Eds. L. Borghi, T. Meschi, A. Briganti, T. Schianchi and A. Novarini. Editoriale Bios, Cosenza: Parma, Italy.

Fleming, D., Grover, P., Chauvet, M., Marshall, V. and Ryall, R. (2000b) 'An unexpected role for urinary proteins in the prevention of calcium oxalate urolithiasis?', In: *Urolithiasis 2000 Vol. 1*, pp. 169-71. Eds. A. Rodgers, B. Hibbert, B. Hess, S. Khan and G. Preminger. University of Cape Town: Cape Town, South Africa.

Fleming, D., van Bronswijk, W. and Ryall, R. (2001) 'A comparative study of the adsorption of amino acids on to calcium minerals found in renal calculi', *Clin Sci,* **101,** 159-168.

Fraij, B. (1989) 'Separation and identification of urinary proteins and stone-matrix proteins by mini-slab sodium dodecyl sulphate-polyacrylamide gel electrophoresis', *Clin Sci,* **35,** 652-62.

Franceschi, V. and Loewus, F. (1995) 'Oxalate biosynthesis and function in plants and fungi', In: *Calcium oxalate in biological systems*, pp. 113-30. Ed. S. Khan. CRC Press: Boca Raton.

Frank, F. (1958) Kinematic theory of crystal growth and dissolution processes, Roberts and Turnbull: Doremus, pp 411-420.

Franzen, A. and Heinegard, D. (1985) 'Isolation and characterization of two sialoproteins present only in stone calcified matrix', *Biochem J,* **232,** 715-24.

Gardner, G. and Doremus, R. (1978) 'Crystal growth inhibitors in human urine', *Invest Urol,* **15,** 478-85.

Giachelli, CM. and Steitz, S. (2000) 'Osteopontin: a versatile regulator of inflammation and biomineralization', *Matrix Biol*, **19**, 615-622.

Gibbs, J. W. (1948) Thermodynamics, Yale University Press: New Haven, pp 11-12.

Gill, W., Karesh, J., Garsin, L. and Roma, J. (1977) 'Inhibitory effects of urinary macromolecules on the crystallization of calcium oxalate', *Invest Urol,* **15,** 95-9.

Gohel, M., Shum, D. and Li, M. (1992) 'The dual effect of urinary macromolecules on the crystallization of calcium oxalate endogenous in urine', *Urol Res,* **20,** 13-7.

Grases, F., Conte, A. and Gil, J. (1988) 'Simple method for the study of heterogeneous nucleation in calcium oxalate urolithiasis', *Br J Urol,* **61,** 468-73.

Gray, A., Spector, A. and Prien, E. (1976) 'Kidney stone matrix - Differences in acidic protein composition', *Invest Urol,* **13,** 387-89.

Grover, P., Kim, D. and Ryall, R. (2002) 'The effect of seed crystals of hydroxyapatite and brushite on the crystallisation of calcium oxalate in undiluted human urine in vitro: Implications for urinary stone pathogenesis', *Mol Med,* **8,** 200-09.

Grover, P., Moritz, R., Simpson, R. and Ryall, R. (1998) 'Inhibition of calcium oxalate crystal growth and aggregation in vitro. A comparison of four human proteins', *Eur J Biochem,* **253,** 637-44.

Grover, P. and Resnick, M. (1995) 'Evidence for the presence of abnormal proteins in the urine of recurrent stone formers', *J Urol,* **153,** 1716-21.

Grover, P. and Ryall, R. (1994) 'Urate and calcium oxalate stones: from repute to rhetoric to reality', *Miner Electrolyte Metab,* **20,** 361-70.

Grover, P. and Ryall, R. (1999) 'Inhibition of calcium oxalate crystal growth and aggregation by prothrombin and its fragment *in vitro*. Relationship between protein structure and inhibitory activity', *Eur J Biochem,* **263,** 50-6.

Grover, P. and Ryall, R. (2002) 'Inhibition of calcium oxalate crystal growth and aggregation by prothrombin and its activation fragments in undiluted human urine *in vitro*: Relationship between protein structure and inhibitory activity', *Clin Sci,* **102,** 425-34.

Grover, P., Ryall, R. and Marshall, V. (1990a) 'Does Tamm-Horsfall mucoprotein inhibit or promote calcium oxalate crystallization in human urine?', *J Urol,* **190,** 223-38.

Grover, P., Ryall, R. and Marshall, V. (1990b) 'Effect of urate on calcium oxalate crystallization in human urine: evidence for a promotory role of hyperuricosuria in urolithiasis', *Clinical Science,* **79,** 9-15.

Grover, P., Ryall, R. and Marshall, V. (1993) 'Dissolved urate promotes calcium oxalate crystallization: epitaxy is not the cause', *Clin Sci,* **85,** 303-07.

Grover, P., Ryall, R. and Marshall, V. (1994) 'Tamm-Horsfall mucoprotein reduces promotion of calcium oxalate crystal aggregation induced by urate in human urine *in vitro*', *Clin Sci,* **87,** 137- 42.

Guo, S., Ward, M. and Wesson, J. (2002) 'Direct visualization of calcium oxalate monohydrate crystallization and dissolution with atomic force microscopy and the role of polymeric additives', *Langmuir,* **18,** 4284-91.

Hallson, P. and Rose, G. (1976) 'Crystalluria in normal subjects and in stone formers urine, with and without thiazide and cellulose phosphate treatment', *Br J Urol,* **48,** 515-24.

Hallson, P. and Rose, G. (1978) 'A new urinary test for stone "activity"', *Br J Urol,* **50,** 442-8.

Hallson, P. and Rose, G. (1979) 'Uromucoids and urinary stone formation', *Lancet,* **1,** 1000-02.

Hallson, P., Rose, G. and Sulaiman, S. (1982) 'Magnesium reduces calcium oxalate crystal formation in human whole urine', *Clin Sci,* **62,** 17-19.

Hallson, P., Rose, G. and Sulaiman, S. (1983) 'Raising urinary citrate lowers calcium oxalate and calcium phosphate crystal formation in whole urine', *Urol Int,* **38,** 179-81.

Heijnen, W. (1982) 'The growth morphology of calcium oxalate trihydate. A contribution to urinary stone research', *J Crystal Growth,* **57,** 216-32.

Heenan, R., Penfold, J. and King, S (1997) 'SANS at pulsed neutron sources: Present and future prospects', *Journal of Applied Crystallography*, **30**, 1140-1147.

Henisch, H. (1970) *Crystal growth in gels*, The Pennsylvania State University Press: University Park and London, pp 21-26.

Hess, B. (1991) 'The role of Tamm-Horsfall glycoprotein and nephrocalcin in calcium oxalate monohydrate crystallization processes', *Scan Microsc,* **5,** 689-96.

Hess, B., Nakagawa, Y. and Coe, F. (1989) 'Inhibition of calcium oxalate monohydrate crystal aggregation by urine proteins', *Am J Physiol,* **257,** 99-106.

Hess, B., Nakagawa, Y., Parks, J. and Coe, F. (1991) 'Molecular abnormality of Tamm-Horsfall glycoprotein in calcium oxalate nephrolithiasis', *Am J Physiol,* **260,** F569-F578.

Hesse, A., Wuzel, H. and Vahlensieck, W. (1991) 'Significance of glycosaminoglycans in the formation of calcium oxalate stones', *Am L Kidney Dis,* **17,** 414-19.

Heuer, A., Fink, D. and Laraia, V. (1992) 'Innovative materials processing strategies: A biomimetic approach', *Science,* **255,** 1098-1105.

Heywood, B. and Mann, S. (1994) 'Template-directed nucleation and growth of inorganic materials', *Advanced Materials,* **6,** 9-20.

Hill, R., Howard, C. and Hunter, B. (1995) 'A computer program for Rietveld analysis of fixed wavelength x-ray and neutron powder diffraction patterns', Australian Atomic Energy Commission (now ANSTO). Rept. No. M112: Lucas Heights Research Laboratories, New South Wales, Australia.

Hodgkinson, A. (1962) 'Citric acid excretion in normal adults and in patients with renal calculus', *Clin Sci,* **23,** 203-12.

Honda, M., Yoshioka, T., Yamaguchi, S., Yoshimura, K., Miyake, O., Utsunomiya, M., Koide, T. and Okuyama, A. (1997) 'Characterization of protein components of human urinary crystal surface binding substance', *Urological Research,* **25,** 355-60.

Horner, H. and Wagner, B. (1995) 'Calcium oxalate formation in higher plants', In: *Calcium oxalate in biological systems*, pp. 53-72. Ed. S. Khan. CRC Press: Boca Raton.

Howard, J. and Thomas, W. (1958) 'Some observations on rachitic rat cartilage of probable significance in the etiology of renal calculi', *Trans Am Clin Climatol Assoc,* **70,** 94-102.

Hoyer, J. (1995) 'Uropontin in urinary calcium stone formation', *Miner Electrolyte Metab,* **29,** 385-92.

Hoyer, J. and Seiler, M. (1979) 'Pathophysiology of Tamm-Horsfall protein', *Kidney Int,* **16,** 179-289.

Hunt, J., McGiven, A., Grouvsky, A., Lynn, K. and Taylor, M. (1994) 'Affinity-purified antibodies of defined specificity for use in a solid-phase microplate radioimmunoassay of human Tamm-Horsfall glycoprotein in urine', *Biochem J,* **227,** 957.

Hunter, B. (1998) 'Rietica - a visual Rietveld program'. *International Union of Crystallography, Commission on Powder Diffraction, Newsletter* 20 and 21.

Hunter, GK., Hauschka, PV., Poole, AR., Rosenberg, LC. and Goldberg, HA. (1996) 'Nucleation and inhibition of hydroxyapatite formation by mineralized tissue proteins', *Biochem J,* **317**, 59-64.

Inorganic Crystal Structure Database, C. C. (1999) 'The crystal structures of whewellite and weddellite: re-examination and comparison', The National Institute of Standards and Technology: Gaithersburg, MD 20899.

Ito, H. and Coe, F. (1977) 'Acidic peptide and polyribonucleotide crystal growth inhibitors in human urine', *Am J Physiol,* **233,** F455-F463.

Ivaska, K., Hellman, J., Likojärvi, J., Käkönen, S-M., Gerdhem, P., Åkesson, K., Obrant, K., Petterson, K. and Väänänen, H. (2003) 'Identification of novel proteolytic forms of osteocalcin in human urine', *Biochem Biophys Res Comm*, **306**, 973-980.

Iwata, H., Nishio, S., Wakatsuki, A., Ochi, K. and Takeuchi, M. (1985) 'Architecture of calcium oxalate monohydrate urinary calculi', *J Urol,* **133,** 334-38.

Kaiser, E. and Bock, S. (1989) 'Protein inhibitors of crystal growth', *J Urol,* **141,** 750-2.

Kajander, E. and Ciftcioglu, N. (1998) 'Nanobacteria an alternative mechanism for pathogenic intra and extracellular calcification and stone formation', *Proc Natl Acad Sci USA,* **95,** 8274-79.

Kavanagh, J. (2000) 'Supersaturation: What role doe it play in calcific stone formation?', In: *Urolithiasis 2000. 9th International Symposium on Urolithiasis.*, pp. 41-6. Eds. A. Rodgers, B. Hibbert, B. Hess, S. Khan and G. Preminger. University of Cape Town: Rondebosch, Cape Town.

Keller, L. and Dollase, WA. (2000) 'X-ray determination of crystalline hydroxyapatite to amorphous calcium-phosphate ratio in plasma sprayed coatings', *Journal of Biomedical Materials Research*, **49**(2), 244-249.

Khan, S. (1995a) 'Calcium oxalate crystal interaction with renal tubular epithelium, mechanism of crystal adhesion and its impact on stone development', *Urol Res,* **23,** 71-9.

Khan, S. (1995b) 'Heterogeneous nucleation of calcium oxalate crystals in mammalian urine', *Scanning Microscopy,* **9,** 597-616.

Khan, S. (1997a) 'Calcium phosphate/calcium oxalate crystal association in urinary stones: Implications for heterogeneous nucleation of calcium oxalate', *J Urol,* **157,** 376-83.

Khan, S. (1997b) 'Tubular cell events during nephrolithiasis', *Current Opinion in Urology,* **7,** 240-47.

Khan, S., Finlayson, B. and Hackett, R. (1979) 'Histologic study of the early events in oxalate induced intranephronic calculosis', *Invest Urol,* **17,** 199-202.

Khan, S., Finlayson, B. and Hackett, R. (1982) 'Experimental calcium oxalate nephrollithiasis in the rat - role of the renal papilla', *Am J Pathol,* **107,** 59-69.

Khan, S., Finlayson, B. and Hackett, R. (1983) 'A technique useful for studying microscopic architecture', *J Urol,* **130,** 992-95.

Khan, S. and Hackett, R. (1984) 'Microstructure of decalcified human calcium oxalate urinary stones', *Scan Electron Microsc,* **11,** 935-41.

Khan, S. and Hackett, R. (1987) 'Crystal-matrix relationships in experimentally induced calcium oxalate monohydrate crystals: An ultrastructural study', *Calcif Tissue Int,* **41,** 157-63.

Khan, S. and Hackett, R. (1991) 'Retention of calcium oxalate crystals in renal tubules', *Scan Microsc,* **5,** 707-12.

Khan, S. and Hackett, R. (1993) 'Role of organic matrix in urinary stone formation: an ultrastructural study of crystal matrix interface of calcium oxalate monohydrate stones', *J Urol,* **150,** 239-45.

Khan, S., Hackett, R. and Finlayson, B. (1986) 'Morphology of urinary stone particles resulting from ESWL treatment', *J Urol*,**136,** 1367-72.

Khan, S., Shevock, P. and Hackett, R. (1988a) '*In vitro* precipitation of calcium oxalate in the presence of whole matrix or lipid components of the urinary stones', *J Urol,* **139,** 418-22.

Khan, S., Shevock, P. and Hackett, R. (1988b) 'Presence of lipids in urinary in urinary stones: results of preliminary studies', *Calcif Tissue Int,* **42,** 91.

Khan, S., Shevock, P. and Hackett, R. (1989) 'Urinary enzymes and calcium oxalate urolithiasis', *J Urol,* **142,** 846.

Khan, S., Shevock, P. and Hackett, R. (1990) 'Membrane-associated crystallization of calcium oxalate *in vitro', Calcif Tissue Int,* **46,** 116-120.

Kiefer, M., Bauer, D. and Barr, P. (1989) 'The cDNA and derived amino acid sequence for human osteopontin', *Nucl Acids Res,* **17,** 3306.

Kim, K. (1976) 'Calcification of matrix vesicles in human aortic valve and aortic media', *Fed Proc,* **35,** 156-62.

Kim, K. (1983) 'Mulberry particles formed by red blood cells in human weddelite stones', *J Urol* **129,** 855.

Kim, K. (1996) 'Determinants of weddellite formation: chondroitin sulphates and citrate determine weddellite formation in vitro', *Scanning Microsc,* **10,** 445-457.

Kim, K., Chang, S., Trump, B. and H, S. (1986) 'Calcification in aging canine aortic valve', *Scanning Electron Microscopy,* **3,** 1151-56.

Kim, K. and Huang, S. (1971) 'Ultrastructural study of dystrophic calcification of human aortic valve', *Lab Invest,* **25,** 357-66.

King, J. and Boyce, W. (1959) 'Analysis of renal Calculous matrix compared with other matrix materials and with uromucoid', *Arch Biochem Biophys,* **82,** 455-61.

Kitamura, T. and Pak, C. (1982) 'Tamm and Horsfall glycoprotein does not promote spontaneous precipitation and crystal growth of calcium oxalate *in vitro*', *J Urol*, **127**, 1024.

Kitamura, T., Zerwekh, J. and Pak, C. (1982) 'Partial biochemical and physicochemical characterization of organic macromolecules in urine from patients with renal stones and control subjects', *Kidney Int*, **21**, 379-86.

Klug, H. and Alexander, L. (1974) *X-ray Diffraction Procedures for Polycrystalline and Amorphous Materials*, John Wiley and Sons inc.: New York.

Kobayashi, H., Shibata, K., Fujie, M., Sugino, D. and Terao, T. (1998) 'Identification of structural domains in inter-a-trypsin inhibitor involved in calcium oxalate crystallization', *Kidney Int*, **53**, 1727-35.

Kohri, K., Garside, J. and Blacklock, N. (1989a) 'The effect of glycosaminoglycans on the crystallization of calcium oxalate', *Br J Urol*, **63**, 584-90.

Kohri, K., Suzuki, K., Yoshida, K., Yamamoto, K., Amasaki, N., Yamate, T., Umekawa, T., Iguchi, M., Sinohara, H. and Kurita, T. (1992) 'Molecular cloning and sequencing of cDNA encoding urinary stone protein, which is identical to osteopontin', *Biochem Biophys Res Commun*, **184**, 859-64.

Kohri, K., Takada, M., Katoh, Y., Kataoka, K., Iguchi, M. and Kurita, T. (1989b) 'Amino acids in urine and plasma of urolithiasis patients', *Int Urol Neph*, **21**, 9-16.

Kohri, K., Umekawa, T., Kodama, M., Katayama, Y., Ishikawa, Y., Takada, M., Katoh, Y., Kataoka, K., Iguchi, M. and Kurita, T. (1990) 'Inhibitory effect of glutamic acid and aspartic acid on calcium oxalate crystal formation', *Eur Urol*, **17**, 173-7.

Koide, T., Takemoto, M., Itatani, H., Takaha, M. and Sonoda, T. (1981) 'Urinary macromolecular substances as natural inhibitors of calcium oxalate crystal aggregation', *Invest Urol*, **18**, 382-86.

Kok, D. (1996) 'Crystallization and stone formation inside the nephron', *Scanning Microscopy,* **10,** 471-86.

Kok, D. and Khan, S. (1994) 'Calcium oxalate nephrolithiasis, a free or fixed particle disease', *Kidney Int,* **46,** 847-54.

Kok, D., Papapoulos, S. and Bijvoet, O. (1990) 'Crystal agglomeration is a major element in calcium oxalate urinary stone formation', *Kidney Int,* **37,** 51-6.

Koul, H., Koul, S. and Menon, M. (2000) 'Role of renal tubular damage / dysfunction in urolithiasis', In: *Urolithiasis 2000 - 9th International Symposium on Urolithiasis. Vol. 1,* pp. 235-237. Eds. A. Rodgers, B. Hibbert, B. Hess, S. Khan and G. Preminger. University of Cape Town: Rondebosch, Cape Town.

Koutsoukos, P., Sheehan, M. and Nancollas, G. (1981) 'Epitaxial considerations in stone formations', *Invest Urol,* **18,** 358-61.

Kumar, S., Sigmon, D., Miller, T., Carpenter, B., Khan, S., Malhotra, R., Scheid, C. and Menon, M. (1991) 'A new model of nephrolithiasis involving tubular dysfunction/injury', *J Urol,* **146,** 1384-89.

Langford, J. (1978) 'A rapid method for analysing the breadths of diffraction and spectral lines using the Voigt function', *J Appl Crystallogr,* **11,** 10-14.

Langford, J., Cernik, R. and Louer, D. (1991) 'The breadth and shape of instrumental line profiles in high resolution powder diffraction', *J Appl Crystallogr,* **24,** 913-19.

Langford, J. (1999) 'Use of pattern decomposition or simulation to study microstructure: theoretical considerations' In: *Defect and Microstructure Analysis by Diffraction,* pp. 59-81. Ed. Snyder, RL., Fiala, J. and Bunge, HJ. Oxford University Press.

Lanzalaco, A., Singh, R., Smesko, S., Nancollas, G., Sufrin, G., Binette, M. and Binette, J. (1988) The influence of urinary macromolecules on calcium oxalate monohydrate crystal growth. *J Urol* **139,** 190-95.

Leal, J. and Finlayson, B. (1977) 'Adsorption of naturally occurring polymers onto calcium oxalate crystal surfaces', *Invest Urol,* **14,** 278-83.

Li, M., Blacklock, N. and Garside, J. (1985) 'Effects of magnesium on calcium oxalate crystallization', *J Urol,* **133,** 123-25.

Lian, J., Glimcher, M. and Gallop, P. (1977a) 'Identification of carboxylic acid', In: *Urinary proteins in calcium binding proteins and calcium function*, pp. 479-581. Eds. R. Wasserman, R. Corradino, E. Carfoli, R. Kretsinger, D. MacLennan and F. Siege. North Holland: New York.

Lian, J., Prien, E., Glimcher, M. and Gallop, P. (1977b) 'The presence of protein-bound G-carboxyglutamic acid in calcium-containing renal calculi', *J Clin Invest,* **59,** 1151-7.

Lide, D. (1999) *CRC Handbook of Chemistry and Physics*, CRC Press: New York, pp. 7-12.

Liebmann, M. and Chai, W. (1997) 'Effect of dietary calcium on urinary oxalate excretion after oxalate loads', *Am J Clin Nutr,* **65,** 1453-59.

Lieske, J. and Deganello, S. (1999) 'Nucleation, adhesion and internalization of calcium-containing urinary crystals by renal cells', *J Am Nephrol Soc,* **10,** S422-S429.

Lieske, J., Deganello, S. and Toback, G. (1999) 'Cell-crystal interactions and kidney stone formation', *Nephron,* **81,** 8-17.

Lieske, J., Hammes, M., Hoyer, J. and Toback, G. (1997) 'Renal cell osteopontin production is stimulated by calcium oxalate monohydrate crystals', *Kidney Int,* **51,** 679-86.

Lieske, J., Hammes, M. and Toback, G. (1996) 'Role of calcium oxalate monohydrate crystal interactions with renal epithelial cells in the pathogenesis of nephrolithiasis: A review', *Scanning Microscopy,* **10,** 519-34.

Lieske, J., Leonard, R., Swift, H. and Toback, G. (1996) 'Adhesion of calcium oxalate monohydrate crystals to anionic sites on the surface of renal epithelial cells', *Am J Physiol,* **270,** F192-F199.

Lieske, J., Toback, F. and Deganello, S. (1996b) ' Face-selective adhesion of calcium oxalate dihydrate crystals to renal epithelial cells', *Calcif. Tissue Int*, **54**, 195-200.

Lieske, J., Leonard, R. and Toback, G. (1995) 'Adhesion of calcium oxalate monohydrate crystals to renal epithelial cells is inhibited by specific anions', *Am J Physiol,* **268,** F604-F612.

Lieske, J., Norris, R., Swift, H. and Toback, G. (1997) 'Adhesion, internalisation and metabolism of calcium oxalate monohydrate crystals by renal epithelial cells', *Kidney Int,* **52,** 1291-1301.

Lieske, J. and Toback, G. (1996) 'Interaction of urinary crystals with renal epithelial cells in the pathogenesis of nephrolithiasis', *Seminars in Nephrology,* **16,** 458-73.

Lieske, J., Toback, G. and Deganello, S. (1998) 'Direct nucleation of calcium oxalate dihydrate crystals onto the surface of living renal epithelial cells in culture', *Kidney Int,* **54,** 796-803.

Lonsdale, K. (1968) 'Human stones', *Science,* **159,** 1199-208.

Lowenstam, H. (1981) 'Minerals formed by organisms', *Science,* **211,** 1126-1131.

Lowenstam, H. and Weiner, S. (1985) 'Transformation of amorphous calcium phosphate to crystalline dahllite in the radular teeth of chitons', *Science,* **227,** 51-3.

Lowenstam, H. and Weiner, S. (1989) *On Biomineralisation,* Oxford University Press: New York, Oxford, pp.324.

Madore, F., Stanpfer, M., Rimm, E. and Curhan, G. (1998) 'Nephrolithiasis and risk of hypertension', *American Journal of Hypertension,* **11,** 46-53.

Mandel, G. and Mandel, N. (1996) 'Crystal-crystal interactions', In: *Kidney stones: Medical and surgical management.* Eds. F. Coe, M. Favus, C. Pak and G. Preminger. Raven press: Boston, pp 32.

Mandel, N. (1994) 'Crystal-membrane interaction in kidney stone disease' *J Am Soc Nephrol,* **5,** S37-S45.

Mandel, N. (1997) 'Commentary on the growth of renal calculi', *J Urol,* **157,** 2.

Mandel, N. and Mandel, G. (1989) 'Urinary tract stone disease in the United States veteran population. II. Geographical analysis of variations in composition', *J Urol,* **142,** 1516-21.

Mandel, N. and Riese, R. (1991) 'Crystal-cell interactions: Crystals binding to rat renal papillary tip collecting duct cells in culture', *Am J Kidney Dis,* **17.**

Mann, S. (1993) 'Molecular tectonics in biomineralization and biomimetic materials chemistry', *Nature,* **365,** 499-505.

Mann, s., Heywood, B., Rajam, S. and Wade, V. (1991) 'Molecular Recognition in Biomineralization', In: *Proceedings of the sixth international conferfence on biomineralization,* pp. 47-54. Ed. S. Suga. Springer Verlag, Berlin.

Marangella, M., Daniele, P., Ronzani, M., Sonego, S. and Linari, F. (1985) 'Urine saturation with calcium salts in normal subjects and idiopathic calcium stone-formers estimated by an improved computer model system', *Urol Res,* **13,** 189-93.

Marengo, S., Resnick, M., Yang, L. and Chung, J. (1998) 'Differential expression of urinary inter-a-trypsin inhibitor trimers and dimers in normal compared to active calcium oxalate stone forming men', *J Urol,* **159,** 1444-50.

Masao, T., Osamu, M., Kazuhiro, Y., Ken-Ichi, K., Shiro, T. and Akihiko, O. (2000) 'Fibronectin as a potent inhibitor of calcium oxalate urolithiasis', *J Urol,* **164,** 1718-23.

Masterton, W. (1977) 'Physical properties as related to structure', In: *Chemical Principles*, pp. 215-7. W.B. Saunders Company: Philadelphia / London / Toronto.

McCartney, E. and Alexander, A. (1958) 'The effects of additives upon the process of crystallization. Crystallinity of calcium sulphate', *J Colloid Interface Sci,* **13,** 383.

McGeown, M. (1957) 'The urinary excretion of amino acids in relation to calculus diseases', *J Urol,* **78,** 318-22.

McKee, M., Nanci, A. and Khan, S. (1995) 'Ultrastructural immunodetection of osteopontin and osteocalcin as major matrix components of renal calculi', *J Bone Min Res,* **10,** 1913-29.

Melick, R., Quelch, K. and Rhodes, M. (1980) 'The demonstration of sialic acid in kidney stone matrix', *Clin Sci,* **59,** 401-04.

Menon, M. and Mahle, C. (1983) 'Urinary citrate excretion in patients with renal calculi', *J Urol,* **129,** 1158-60.

Meyer, A., Finlayson, B. and DuBois, L. (1971) 'Direct observation of urinary stone ultrastructure', *Br J Urol,* **43,** 154-63.

Meyer, J. (1981) 'Nucleation kinetics in the calcium oxalate-sodium urate monohydrate system', *Invest Urol,* **19,** 197-201.

Meyer, J., Bergert, J. and Smith, L. (1975) 'Epitaxial relationships in urolithiasis: the calcium oxalate monohydrate-hydroxyapatite system', *Clin Sci Mol Med,* **49,** 369-74.

Meyer, J., Bergert, J. and Smith, L. (1976) 'The epitaxial induced crystal growth of calcium oxalate by crystalline uric acid', *Invest Urol,* **14,** 115-21.

Meyer, J., Bergert, J. and Smith, L. (1977) 'Epitaxial relationships in urolithiasis: the brushite-whewellite system', *Clin Sci Mol Med,* **52,** 143-8.

Meyer, J. and Smith, L. (1975a) 'Growth of calcium oxalate crystals: A model for urinary stone growth', *Invest Urol,* **13,** 31-5.

Meyer, J. and Smith, L. (1975b) 'Growth of calcium oxalate crystals: II. Inhibition by natural urinary crystal growth inhibitors', *Invest Urol,* **13,** 36-9.

Michalski, C., Piva, F., Balduyck, M., Mizon, C., Burnouf, T., Huart, J. and Mizon, J. (1994) 'Preparation and properties of a therapeutic inter-alpha-trypsin inhibitor concentrate from human plasma', *Vox Sang,* **67,** 329.

Miller, J., Randolph, A. and Drach, G. (1977) 'Observations upon calcium oxalate crystallization kinetics in simulated urine', *J Urol,* **117,** 342-5.

Min, W., Shiraga, H., Chalko, C., Goldfarb, S., Krishna, G. and Hoyer, J. (1998) 'Quantitative studies of human urinary excretion of uropontin', *Kidney Int,* **53,** 189-93.

Modlin, M. (1967) 'The aetiology of renal stones: a new concept arising from studies on a stone-free population', *Ann R Coll Eng,* **40,** 155-78.

Morse, R. and Resnick, M. (1988a) 'Current trends in urologic research: Urinary stone matrix', *J Urol,* **139,** 602-6.

Morse, R. and Resnick, M. (1988b) 'A new approach to the study of urinary macromolecules as participant in calcium oxalate crystallization', *J Urol,* **139,** 869-73.

Morse, R. and Resnick, M. (1989) 'A study of the incorporation of urinary macromolecules onto crystals of different mineral compositions', *J Urol,* **141,** 641-44.

Muchmore, A. and Decker, J. (1985) 'Uromodulin: a unique 85-kilodalton immunosuppressive glycoprotein isolated from urine of pregnant women', *Science,* **229,** 479-81.

Mullin, J. (1993a) 'Crystal Growth', In: *Crystallization*, Butterworth-Heinemann Ltd: Oxford, London, Boston pp., 202-263.

Mullin, J. (1993b) 'Nucleaction', In: *Crystallization*, Butterworth-Heinemann: Oxford, London, Boston pp., 173-201.

Muthukumar, A. and Selvam, R. (1997) 'Renal injury mediated calcium oxalate nephrolithiasis: role of lipid peroxidation', *Ren Fail,* **19,** 401-8.

Nagy, I. and Noszal, B. (2000) 'Theoretical study of the tautomeric / conformational equilibrium of aspartic acid zwitterions in aqueous solution', *J Phy Chem,* **104,** 6834-43.

Nakagawa, Y., Abram, V. and Coe, F. (1984) 'Isolation of calcium oxalate crystal growth inhibitor from rat kidney and urine', *Am J Physiol,* **247,** F765-772.

Nakagawa, Y., Abram, V., Kezdy, F., Kaiser, E. and Coe, F. (1983) 'Purification and characterisation of the principal inhibitor of calcium oxalate monohydrate crystal growth in human urine', *J Biol Chem,* **258,** 1259.

Nakagawa, Y., Abram, V., Parks, J., Lau, H., Kawooya, H., Kawooya, J. and Coe, F. (1985) 'Urine glycoprotein crystal growth inhibitors. Evidence for a molecular abnormality in calcium oxalate nephrolithiasis', *J Clin Invest,* **76,** 1455-62.

Nakagawa, Y., Ahmed, M., Hall, S., Deganello, S. and Coe, F. (1987) 'Isolation from human calcium oxalate renal stones of nephrocalcin, a glycoprotein inhibitor of calcium oxalate crystal growth. Evidence that nephrocalcin from patients with calcium oxalate nephrolithiasis is deficient in g-carboxyglutamic acid', *J Clin Invest,* **79,** 1782-87.

Nakagawa, Y., Kaiser, E. and Coe, F. (1978) 'Isolation and characterisation of calcium oxalate crystal growth inhibitors from human urine', *Biochem Biophys Res Commun,* **84,** 1038-44.

Nakagawa, Y., Margolis, H., Yokoyama, S., Kezdy, F., Kaiser, E. and Coe, F. (1981) 'Purification and characterization of a calcium oxalate monohydrate crystal growth inhibitor from human kidney tissue culture medium', *J Biol Chem,* **256,** 3936-44.

Nakagawa, Y., Netzer, M. and Coe, F. (1994) 'Immunohistochemical localisation of nephrocalcin (NC) to proximal tubule and thick ascending limb of Henle's loop (TALH) of human and mouse kidney', *Kidney Int,* **37,** 474.

Nakagawa, Y., Parks, J., Kezdy, F. and Coe, F. (1995) 'Molecular abnormality of urinary glycoprotein crystal growth inhibitor in calcium nephrolithiasis', *Assos Am Phys Trans,* **98,** 281-89.

Nakai, H., Yanagawa, M., Kameda, K., Ogura, Y. and Kawamura, J. (1996) 'Transformation of calcium oxalate dihydrate crystals in solution: Why is not calcium oxalate dihydrate detected in urinary calculi?', In: *Urolithiasis 1996 International Symposium on Urolithiasis*, pp. 323-5. Eds. C. Pak, M. Resnick and G. Preminger: Dallas, Texas.

Nancollas, G. (1979) 'The growth of crystals in solution', *Advances in Colloid and Interface Science,* **10,** 215-252.

Nancollas, G. (1981) 'Biological Mineralization and Demineralization', In: *Proceedings of the Dahlem Conference*, pp. 1-415. Ed. G. Nancollas. Springer-Verlag, Berlin: Berlin.

Nancollas, G. (1983) 'Crystallization theory relating to urinary stone formation', *World J Urol,* **1,** 131-7.

Nancollas, G. (1984) 'The nucleation, growth and dissolution of stones', In: *Urolithiasis and related clinical research*, pp. 749-56. Eds. P. Schwille, L. Smith, W. Robertson and W. Vahlensieck. Plenum Press: New York-London.

Nancollas, G. (1990) 'Physical chemistry of crystal nucleation, growth and dissolution of stones', In: *Renal tract stone. Metabolic basis and clincal practice.*,

pp. 71-85. Eds. J. Wickham and A. Buck. Churchill Livingstone: Edinburgh-London-Melbourne-New York.

Nancollas, G. and Gardner, G. (1974) 'Kinetics of growth of calcium oxalate monohydrate', *J Crystal Growth,* **21,** 267-76.

Nancollas, G. and Gaur, S. (1984) 'Crystallization in urine', *Scanning Electron Microscopy,* **4,** 1759-64.

Nancollas, G., Smeso, S., Campbell, A., Richardson, C., Johnsson, M., Iadiccico, R., Binette, J. and Binette, M. (1991) 'Physical chemical studies of calcium oxalate crystallization', *Am J Kidney Dis,* **17,** 392-5.

Nancollas, G. and Tomson, M. (1975) 'The precipitation of biological materials', *Faraday Discuss Chem Soc,* **61,** 175-83.

Nancollas, G. and Wu, W. (2000) 'Biomineralization mechanisms: a kinetics and interfacial energy approach', *J Crystal Growth,* **211,** 137-42.

Napper, D. (1983) *Polymeric stabilisation of colloidal dispersions,* Academic Press: London-Orlando-Nan Diego-New York-Sydney, pp., 12-32.

Navazio, L., Baldan, B. and Dainese, P. (1995) 'Evidence that spinach leaves express calreticulin but not calsequestrin', *Plant Physiol,* **109,** 983-90.

Netzer, M., Nakagawa, Y. and Coe, F. (1990) 'Characterization of a new antibody to nephrocalcin (NC), a major urinary inhibitor of calcium oxalate monohydrate (COM) crystal growth', *Kidney Int,* **37,** 474.

Nicar, M., Holt, K. and Pak, C. (1980) 'Ion binding by small molecular weight substances (1,000-10,000 daltons) in urine', *Invest Urol,* **18,** 162-4.

Nicar, M., Skula, C., Sakhaee, K. and Pak, C. (1983) 'Low citrate excretion in nephrolithiasis', *Urology,* **21,** 8-14.

Nielson, A. E. (1984) 'Electrolyte crystal growth mechanisms', *Journal of Crystal Growth,* **67,** 289-310.

Nishio, S., Abe, Y., Wakatsuki, A., Iwata, H., Ochi, K., Takeuchi, M. and Matsumoto, A. (1985) 'Matrix glycosaminoglycan in urinary stones', *J Urol,* **134,** 503-5.

Norde, W., Arai, T. and Shirahama, H. (1991) 'Protein adsorption in model systems', *Biofouling,* **4,** 37-41.

Noszal, B. and Sandor, P. (1989) 'Rota-microspeciation of aspartic acid and asparagine', *Anal Chem,* **61,** 2631-37.

Pak, C. (1978) 'Calcium urolithiasis: is it analogous to bone formation?', *Calcif Tissue Res,* **26,** 195-7.

Pak, C. and Arnold, L. (1975) 'Heterogeneous nucleation of calcium oxalate by seeds of monosodium urate', *Proc Soc Exp Bio Med,* **149,** 930.

Pak, C., Hayashi, Y., Finlayson, B. and Chu, S. (1977) 'Estimation of the state of supersaturation of brushite and calcium oxalate in urine', *J Lab Clin Med,* **89,** 891-901.

Pak, C., Holt, K. and Zerwekh, J. (1979) 'Attenuation by monosodium urate of the inhibitory effect of glycosaminoglycans on calcium oxalate nucleation', *Invest Urol,* **17,** 138-40.

Pak, C., Skurla, C. and Harvey, J. (1985) 'Graphic display of urinary risk factors for renal stone formation', *J Urol,* **19,** 867-70.

Pak, J., Pu, Y., Zhang, Z-T., Hasty, D. and Wu, X-R. (2001) 'Tamm-Horsfall protein binds to type 1 Fimbriated *Escherichia coli* and prevents *E. coli* from binding to Uroplakin Ia and Ib receptors', *The Journal of Biological Chemistry,* **276** (13), 9924-9930.

Patriquin, H. and Robitaille, P. (1986) 'Renal calcium deposition in children: sonographic demonstration of the Anderson-Carr progression', *Am J Roentgenol,* **146,** 1253-56.

Peach, R., Day, W., Ellingson, P. and McGiven, A. (1988) 'Ultrastructural localisation of Tamm-Horsfall protein in human kidney using immunogold electron microscopy', *Histochem J,* **20,** 156-64.

Perl-Treves, D. and Addadi, L. (1988) 'A structural approach to pathological crystallizations. Gout: the possible role of albumin in sodium urate crystallization', *Proc R Soc Lond (Biol),* **235,** 145-59.

Pesce, A., Kant, K., Clyne, D. and Pollak, V. (1977) 'A model of urinary cast formation', *Clin Chem,* **23,** 1146.

Petersen, T., Thogersen, I. and Petersen, S. (1989) 'Identification of hemaglobin and two serine proteases in acid extracts of calcium containing kidney stones', *J Urol,* **142,** 176-80.

Phillips, F. (1971) *An introduction to crystallography,* Oliver and Boyd, Edinburgh: Edinburgh, pp. 10-65.

Pillay, S., Asplin, J. and Coe, F. (1998) 'Evidence that calgranulin is produced by kidney cells and is an inhibitor of calcium oxalate crystallization' *Am J Physiol,* **275,** F255-F261.

Power, C., Blacklock, N. and Barker, D. (1984) 'Incidence of renal stones in Britain', In: *Urinary stone*, pp. 86-9. Eds. R. Ryall, J. Brockis, V. Marshall and B. Finlayson. Churchill Livingstone: Melbourne, Edinburgh, London, New York.

Prien, E. (1963) 'Crystallographic analysis of urinary calculi: a 23 year survey study', *J Urol,* **89,** 917-24.

Prien, E. and Prien, E. J. (1968) 'Composition and structure of urinary stones' *Am J Med,* **45,** 654-72.

Prince, C., Oosawa, T., Butler, W., Tomann, M., Bhown, A., Bhown, M. and Schrohenloher, R. (1987) 'Isolation, characterization and biosynthesis of a phosphorylated glycoprotein from rat bone', *J Biol Chem,* **262,** 2900-07.

Randall, A. (1936) 'An hypothesis for the origin of renal calculus', *N Engl J Med,* **214,** 234-42.

Randall, A. (1937) 'The origin and growth of renal calculi', *Ann Surg,* **105,** 1009-27.

Randall, S. (1992) 'Characterisation of vacuolar calcium binding proteins' *Plant Physiol,* **100,** 859-67.

Randolph, A. and Drach, G. (1981) 'Some measurements of calcium oxalate nucleation and growth rates in urine-like liquors', *J Crystal Growth,* **53,** 195-99.

Read, W. (1953) *Dislocations in crystals.* McGraw-Hill: New York, pp. 7-34.

Reimann, B. (1964) 'Deposition of silica inside a diatom cell', *Exper cell Res,* **34,** 605-08.

Resnick, M., Gammon, C., Sorrell, M. and Boyce, W. (1980) 'Calcium-binding proteins and renal lithiasis', *Surgery,* **88,** 239-43.

Riese, R., Riese, J., Kleinman, J., Wiessner, J., Mandel, G. and Mandel, N. (1988) 'Specificity in calcium oxalate adherence to papillary epithelial cells in culture', *Am J Physiol,* **255,** F1025-F1032.

Roberts, S. and Resnick, M. (1986) 'Glycosaminoglycans content of stone matrix', *J Urol,* **135,** 1078-83.

Robertson, W. (2001) 'The changing pattern of urolithiasis in the UK and its causes', In: *Ninth European Urolithiasis Symposium,* pp. 9-11. Eds. D. Kok, H. Romijn, P. Verhagen and C. Verkoelen. Shaker Publishing, Maastricht, the Netherlands: Rotterdam, the Netherlands.

Robertson, W. and Hughes, H. (1993) 'Importance of mild hyperoxaluria in the pathogenesis of urolithiasis - New evidence from studies in the Arabian peninsula', *Scanning Microscopy,* **7,** 391-402.

Robertson, W., Knowles, F. and Peacock, M. (1976a) 'Urinary acid mucopolysaccharide inhibitors of calcium oxalate crystallization', In: *Urolithiasis Research*, pp. 331-34. Eds. H. Fleisch, W. Robertson, L. Smith and W. Vahlensieck. Plenum Press: New York.

Robertson, W., Latif, A., Scurr, D., Casewell, A., Drach, G. and Randolph, A. (1984) 'Inhibitors of calcium oxalate crystallization in urine from stone formers and normals', In: *Urinary stone*, pp. 167-72. Eds. R. Ryall, J. Brockis, V. Marshall and B. Finlayson. Churchill Livingstone: London.

Robertson, W. and Peacock, M. (1972) 'Calcium oxalate crystalluria and inhibitors of crystallization in recurrent renal stone formers', *Clin Sci,* **43**, 499-503.

Robertson, W. and Peacock, M. (1985) 'Pathogenesis of urolithiasis', In: *Urolithiasis, etiology, diagnosis*, pp. 185-334. Eds. M. Peacock, W. Robertson, W. Schneider and W. Vahlensieck. Springer-Verlag: Berlin.

Robertson, W., Peacock, M., Marshall, R., Marshall, D. and Nordin, B. (1976b) 'Saturation-inhibition index as a measure of the risk of calcium oxalate stone formation in the urinary tract', *N Engl J Med,* **294,** 249-52.

Robertson, W., Peacock, M. and Nordin, B. (1968) 'Activity products in stone-forming and non-stone forming urine', *Clin Sci,* **34,** 579-94.

Robertson, W., Peacock, M. and Nordin, B. (1969) 'Calcium oxalate crystalluria in recurrent renal stone formers', *Lancet,* **2,** 21-4.

Robertson, W., Peacock, M. and Nordin, B. (1973) 'Inhibitors of the growth and aggregation of calcium oxalate crystals *in vitro*', *Clin Chim Acta*, **43,** 31-7.

Robertson, W., Peacock, M. and Nordin, B. (1979) 'Inhibitors of growth and aggregation of calcium oxalate crystals *in vitro*', *Clin Chim Acta*, **43,** 31-7.

Robertson, W. and Scurr, D. (1986) 'Modifiers of calcium oxalate crystallization found in urine. I. Studies with a continuous crystallizer using an artificial urine', *J Urol*, **135,** 1322-26.

Robertson, W., Scurr, D. and Bridge, C. (1981) 'Factors influencing the crystallization of calcium oxalate in urine – critique', *J Crystal Growth,* **53,** 182-94.

Robinson, W. (1990) 'Epidemiology of urinary stone disease', *Urol Res,* **18,** S3-S8.

Rodgers, A., Ball, D. and Harper, W. (1994) 'Effect of urinary macromolecules and chondroitin sulphate on calcium oxalate crystallization in urine', *Scanning Microscopy,* **8,** 71-7.

Rodgers, A. and Jappie, D. (1996) 'Studies on the role of urinary macromolecules in urolithiasis:review of methodologies and a proposal for a standard reference crystallization system', *Scanning Microscopy,* **10,** 535-46.

Rose, G. and Sulaiman, S. (1982) 'Tamm-Horsfall mucoprotein promotes calcium oxalate crystal formation in urine', *J Urol*, **127,** 177-79.

Rosenberg, H. (1988) 'Dislocation in crystals', In: *The solid state*, pp. 69. Oxford university press.

Rudman, D., Kutner, M., Redd, S., Waters, W., Gerron, G. and Bleier, J. (1982) 'Hypocitraturia in calcium nephrolithiasis', *J Endocrinol Metab*, **55,** 1052-57.

Ryall, R. (1989) 'The formation and investigation of urinary calculi', *Clin Biochem Revs*, **10,** 149-57.

Ryall, R. (1993) 'The scientific basis of calcium oxalate urolithiasis', *World J Urol*, **11,** 59-65.

Ryall, R. (1996) 'Glycosaminoglycans, proteins, and stone formation: adult themes and child's play', *Pediatr Nephrol*, **10,** 656-66.

Ryall, R. (1997) 'Urinary inhibitors of calcium oxalate crystallization and their potential role in stone formation', *World J Urol*, **15,** 155-64.

Ryall, R. (2000) 'The mystery of macromolecules: modulators, matrix and mineralization', In: *Urolithiasis 2000*, pp. 99-105. Eds. B. Hibbert, B. Hess, S. Khan and G. Preminger: Rondebosch: University of Cape Town.

Ryall, R. (2003) 'Macromolecules and kidney stone formation: Waste of space or space for waste?', In: *Stone Disease Vol. 21*, pp. 69-79. Eds. J. Segura, P. Conort, K. S, C. Pak and G. Preminger. Health Publications 2003: Paris.

Ryall, R., Bagley, C. and Marshall, V. (1981a) 'Independent assessment of the growth and aggregation of calcium oxalate crystals using the Coulter Counter', *Invest Urol*, 401-5.

Ryall, R., Chauvet, M. and Grover, P. (2001a) 'A space oddity', In: *Urolithiasis, 9th European Symposium on Urolithiasis*, pp. 273-74. Eds. D. Kok, H. Romijn, P. Verhagen and C. Verkoelen: Rotterdam, the Netherlands.

Ryall, R., Fleming, D., Doyle, I., Evans, N., Dean, C. and Marshall, V. (2001b) 'Intracrystalline proteins and the hidden ultrastructure of calcium oxalate urinary crystals: Implications for kidney stone formation', *J Structural Biology*, **134,** 5-14.

Ryall, R., Fleming, D., Grover, P., Chauvet, M., Dean, C. and Marshall, V. (2000) 'The hole truth: Intracrystalline proteins and calcium oxalate kidney stones', *Molecular Urology*, **4,** 391-402.

Ryall, R., Grover, P., Doyle, I., Harnett, R., Hibberd, C., Edyvane, K. and Marshall, V. (1988) 'The effect of macromolecules on the crystallization of calcium oxalate in human urine', In: *Inhibitors of crystallization in renal lithiasis and their clinical application*, pp. 51-6. Eds. A. Martelli, B. Buli and B. Marchesini. Acta Medica: Rome.

Ryall, R., Grover, P., Harnett, R., Hibberd, C. and Marshall, V. (1989) 'Small molecular weight inhibitors', In: *Urolithiasis*, pp. 91-6. Eds. V. Walker, R. Sutton, E. Cameron, C. Pak and W. Robertson. Plenum Press: New York-London.

Ryall, R., Grover, P. and Marshall, V. (1991a) 'Urate and calcium oxalate stones - picking up a drop of mercury with one's fingers?', *Am J Kidney Dis*, **17,** 416-20.

Ryall, R., Grover, P., Stapleton, A., Barrell, D., Tang, Y., Moritz, R. and Simpson, R. (1995) 'The urinary F1 activation peptide of human prothrombin is a potent inhibitor of calcium oxalate crystallization in undiluted human urine *in vitro*', *Clin Sci*, **89,** 533-541.

Ryall, R., Harnett, R., Hibberd, C., Edyvane, K. and Marshall, V. (1991b) 'Effects of chondroitin sulphate, human serum albumin and Tamm-Horsfall mucoprotein on calcium oxalate crystallization in undiluted human urine', *Urol Res*, **19,** 181-188.

Ryall, R., Harnett, R. and Marshall, V. (1981b) 'The effect of urine, pyrophosphate, citrate, magnesium and glycosaminoglycans on the growth and aggregation of calcium oxalate crystals in *vitro*', *Clin Chim Acta*, **112,** 349-356.

Ryall, R., Hibberd, C. and Marshall, V. (1985) 'A method for studying inhibitory activity in whole urine', *Urol Res*, **13,** 285-289.

Ryall, R., Hibberd, C., Mazzachi, B. and Marshall, V. (1986) 'Inhibitory activity of whole urine: a comparison of urines from stone formers and healthy subjects', *Clinica Chimica Acta*, **154,** 59-68.

Ryall, R. and Marshall, V. (1983) 'The value of the 24-hour urine analysis in the assessment of stone formers attending a general hospital outpatient clinic', *Br J Urol*, **55,** 1-5.

Ryall, R. and Marshall, V. (1984) 'The relationship between urinary inhibitory activity and endogenous concentrations of glycosaminoglycans and uric acid: comparison of urines from stone-forming and normal subjects', *Clin Chim Acta,* **141,** 197-204.

Ryall, R., Ryall, R. and Marshall, V. (1981c) 'Interpretation of particle growth and aggregation patterns obtained from the Coulter Counter: A simple theoretical model', *Invest Urol*, **18,** 396-400.

Ryall, R. and Stapleton, A. (1995) 'Urinary macromolecules in calcium oxalate stone and crystal matrix: good, bad, or indifferent?', In: *Calcium Oxalate in Biological Systems*, pp. 265-290. Ed. S. Khan. CRC Press Inc: Boca Raton, Florida.

Salier, J. (1990) 'Inter-a-inhibitor: emergence of a family within the Kunitz-type protease inhibitor superfamily', *T I B S*, **15,** 435.

Sallis, J. (1987) 'Glycosaminoglycans as inhibitors of stone formation', *Miner Electrolyte Metab*, **13,** 273-77.

Scheid, C., Koule, H., Hill, W., Luber-Narod, J., Kennington, L., Honeyman, T., Jonassen, J. and Menon, M. (1996) 'Oxalate toxicity in LLC-PK1 cells: role of free radicals', *Kidney Int*, **49,** 413-19.

Scurr, D. and Robertson, W. (1986) 'Modifiers of calcium oxalate crystallization found in urine. II. Studies on their mode of action in an articial urine', *J Urol*, **136,** 128-31.

SHADOW (1998) 'A system for x-ray powder diffraction pattern analysis', pp. 1-177. Materials Data Inc.: Livermore, CA 94550.

Sharma, S., Khullar, M., Vaishnav, P., Sharma, M., Singh, S. and Nath (2000) 'Isolation and detection of nanobacteria in human renal calculi', In: *Urolithiasis 2000 Vol. 1*, pp. 206-07. Eds. A. Rodgers, B. Hibbert, B. Hess, S. Khan and G. Preminger. University of Cape Town, Cape Town, South Africa: Cape Town, South Africa.

Shaw, D. (1980) 'Colloid Stability', In: *Introduction to Colloid and Surface Chemistry*, pp. 183-212. Butterworths: London - Boston - Singapore - Sydney - Toronto - Wellington.

Sheehan, M. and Nancollas, G. (1984) 'The kinetics of crystallization of calcium oxalate trihydrate', *J Urol*, **132,** 158-63.

Shiraga, H., Min, W., VanDusen, W., Clayman, M., Miner, D., Terrell, C., Sherbotie, J., Foreman, J., Przysiecki, C., Neilson, E. and Hoyer, J. (1992) 'Inhibition of calcium oxalate crystal growth in vitro by uropontin: another member of the aspartic acid-rich protein superfamily', *Proc Natl Acad Sci USA*, **89,** 426-30.

Sidhu, H., Schmidt, M., Cornelius, J., Thamilselvan, S., Khan, S., Hesse, A. and Peck, A. (1999) 'Direct correlation between hyperoxaluria/oxalate stone disease and the absence of the gastrointestinal tract-dwelling bacterium Oxalobacter formigenes: possible prevention by gut recolonisation or enzyme replacement therapy', *J Am Soc Nephrol*, **10,** 334-40.

Sierakowski, R., Finlayson, B., Landes, R., Finlayson, C. and Sierakowski, N. (1978) 'The frequency of urolithiasis in hospital discharge diagnoses in the United States', *Invest Urol*, **15,** 143-41.

Sikri, K., Foster, C., MacHugh, N. and Marshall, R. (1981) 'Localization of Tamm-Horsfall glycoprotein in the human kidney using immuno-fluorescence and immuno-electron microscopical techniques', *J Anatomy*, **132,** 597-605.

Slavin, R., Wen, J., Kumar, D. and Evans, E. (1993) 'Familial tumoral calcinosis, a clinical, histopathologic and ultrastructural study with an analysis of its calcifying process and pathogenesis', *Am J Surg Path*, **17,** 788-802.

Snyder, R., Fiala, J. and Bunge, H. (1999a) 'Use of pattern decomposition or simulation to study microstructure: theoretical considerations', In: *Defect and microstructure analysis by diffraction*, pp. 59-81. Oxford University Press: New York.

Snyder, R., Fiala, J. and Bunge, H. (1999b) 'Use of pattern decomposition or simulation to study microstructure: theoretical considerations', In: *Defect and microstructure analysis by diffraction*, pp. 69-70. Oxford university press: New York.

Sobczak, E. (1990) 'A simple method of determination of mass transfer constants for crystal growth', *Chemical Engineering Science*, **45,** 561-64.

Sophasan, S., Chatasingh, S., Thanphaichitr, P. and Dhanamitta, S. (1980) 'Tamm Horsfall mucoprotein in urine of potential bladder stone formers', *J Urol*, **124,** 522-24.

Sorensen, D., Hansen, K., Bak, S. and Justesen, S. (1990) 'An unidentified macromolecular inhibitory constituent of calcium oxalate growth in human urine', *Urol Res*, **18,** 373-79.

Soriano-Garcia, M., Padmanabhan, K., De-Vos, A. and Tulinsky, A. (1992) 'The Ca^{2+} ion and membrane binding structure of the Gla domain of Ca-prothrombin fragment 1', *Biochemistry*, **31,** 2554.

Spackman, D., Stein, W. and Moore, S. (1958) 'Automatic recording apparatus for use in the chromatography of amino acids', *Anal Chem*, **30,** 1191-1206.

Stapleton, A., Dawson, C., Grover, P., Hohmann, A., Comacchio, R., Boswarva, V., Tang, Y. and Ryall, R. (1996) 'Further evidence linking urolithiasis and blood coagulation: Urinary prothrombin fragment 1 is present in stone matrix', *Kidney Int*, **49,** 880-88.

Stapleton, A. and Ryall, R. (1994) 'Crystal matrix protein-getting blood out of a stone', *Miner Electrolyte Metab*, **20,** 399-409.

Stapleton, A. and Ryall, R. (1995) 'Blood coagulation proteins and urolithiasis are linked: crystal matrix protein is the F1 activation peptide of human prothrombin', *B J Urol*, **75,** 712-19.

Stapleton, A., Seymour, A., Brennan, J., Doyle, I., Marshall, V. and Ryall, R. (1993a) 'Immunohistochemical distribution and quantification of crystal matrix protein', *Kidney Int*, **44,** 817-24.

Stapleton, A., Simpson, R. and Ryall, R. (1993b) 'Crystal matrix protein is related to human prothrombin', *Biochem Biophys Res Commun*, **195,** 1199-1203.

Stapleton, A., Timme, T. and Ryall, R. (1998) 'Gene expression of prothrombin in the human kidney and its potential relevance to kidney stone disease', *Br J Urol*, **81,** 666-72.

Stevenson, F., Cleave, A. and Kent, P. (1971) 'The effect of ions on the viscometric and ultracentrifugal behaviour of Tamm-Horsfall glycoprotein', *Biochim Biophys Acta*, **236,** 59-66.

Stokes, A. and Wilson, A. (1944a) 'The diffraction of x-rays by distorted crystal aggregates', *Proceedings of the Physical Society, London*, **56,** 174-81.

Stokes, A. and Wilson, A. (1944b) 'A method of calculating the integral breadths of Debye-Scherrer lines. Generalisation to noncubic crystals', *Proc. Cambridge Phil. Soc*, **40,** 197-198.

Stumm, W. (1990) 'Colloid Stability: Qualitative Considerations', In: *Chemistry of the Solid-Water Interface*, pp. 252. John Wiley & Sons, Inc: New / York / Chichester / Brisbane / Toronto / Singapore.

Sutor, D. (1969) 'Growth studies of calcium oxalate in the presence of various ions and compounds', *Br J Urol*, **41,** 171-78.

Suzuki, K., Mayne, K., Doyle, I. and Ryall, R. (1994a) 'Urinary glycosaminogycans are selectively included into calcium oxalate crystals precipitated from whole urine', *Scan Electron Microsc*, **8,** 523-30.

Suzuki, K., Moriyama, M., Nakajima, C., Kawamura, K., Miyazawa, K., Tsugawa, R., Kikuchi, N. and Nagata, K. (1994b) 'Isolation and partial characterization of crystal matrix protein as a potent inhibitor of calcium oxalate crystal aggregation: Evidence of activation peptide of human prothrombin', *Urol Res*, **22,** 45-50.

Suzuki, K., Nakajima, C., Moriyama, M., Miyazawa, K. and Tsugawa, R. (1995) 'Backscattered electron imaging of crystal matrix protein on the surface of calcium oxalate crystals using colloidal gold', *Int J Urol*, **2,** 87-91.

Suzuki, K., Tanaka, T., Miyazawa, K., Nakajima, C., Moriyama, M., Suga, K., Murai, M. and Yano, J. (1999) 'Gene expression of prothrombin in human and rat kidneys: Basic and clinical approach', *J Am Nephrol Soc*, **10,** S408-S411.

Sukhishvili, S. and Granick, S. (1999) 'Adsorption of human serum albumin: Dependence on molecular architecture of the oppositely charged surface', *Journal of Chemical Physics*, **110**(20), 10153-10161.

Tamm, I. and Horsfall, F. (1950) 'Characterisation and separation of an inhibitor of viral hemagglutination present in urine', *Proc Soc Exp Bio Med*, **74,** 108.

Tang, Y., Grover, P., Moritz, R., Simpson, R. and Ryall, R. (1995) 'Is nephrocalcin related to the urinary derivative (bikunin) of inter-a-tripsin inhibitor?', *Br J Urol*, **75,** 425-30.

Tawada, T., Fujita, K., Sakakura, T., Shibutani, T., Nagata, T., Iguchi, M. and Kohri, K. (1999) 'Distribution of uropontin and calprotectin as matrix protein in calcium-containing stone', *Urol Res*, **27,** 238-42.

Tazzoli, V. and Domeneghetti, C. (1980) 'The crystal structures of whewellite and weddellite: re-examination and comparison', *American Mineralogist*, **65,** 327-334.

Thamilselvan, S., Hackett, R. and Khan, S. (1997) 'Lipid peroxidation in ethylene glycol induced hyperoxaluria and calcium oxalate nephrolithiasis', *J Urol*, **157,** 1059-63.

Thomas, W. (1994) 'Urinary silicate in calculous patients', In: *Seventh International Symposium on Urolithiasis.*, pp. 373-74. Eds. R. Ryall, R. Bais, V. Marshall, A. Rofe, L. Smith and V. Walker. Plenum Press, New York: Cairns, Australia.

Thorne, I. and Resnick, M. (1983) 'Urinary macromolecules and renal lithiasis', *World J Urol*, **1,** 138-45.

Tomažič, B. and Nancollas, G. (1979a) 'The kinetics of dissolution of calcium oxalate hydrates', *J Crystal Growth*, **46,** 355-61.

Tomažič, B. and Nancollas, G. (1979b) 'A study of the phase transformation of calcium oxalate trihydrate-monohydrate', *Invest Urol*, **16,** 329-35.

Tomažič, B. and Nancollas, G. (1982) 'The dissolution of calcium oxalate kidney stones. A kinetic study', *J Urol*, **128**, 205-208.

Trewick, A. and Rumsby, G. (2000) 'Isoelectric focusing of native urinary uromodulin (Tamm-Horsfall protein) shows no physicochemical differences between stone formers and non stone formers', *Urol Res*, **27,** 250-54.

Umekawa, T., Kohri, K., Amasaki, N., Yamate, T., Yoshida, K., Yamamoto, K., Suzuki, Y., Sinohara, H. and Kurita, T. (1993) 'Sequencing of a urinary stone protein identical to a 1-antitrypsin', *Biochem Biophys Res Commun*, **193,** 1049-53.

Umekawa, T. and Kurita, T. (1994) 'Calprotectin-like protein is related to soluble organic matrix in calcium oxalate urinary stone', *Biochem Mol Biol Int*, **34,** 309-13.

Ungar, T., Ott, S., Sanders, P., Borbely, A. and Weertman, J. (1988) 'Dislocations, grain size and planar faults in nanostructured copper determined by high resolution x-ray diffraction and a new procedure of peak profile analysis', *Acta Materials*, **46,** 3693-3699.

Utsunomiya, M., Koide, T., Yoshioka, T., Yamaguchi, S. and Okuyama, A. (1993) 'Influence of ionic strength on crystal adsorption and inhibitory activity of macromolecules', *Brit J Urol*, **71**, 516-522.

van de Loo, P., Soute, B., Johan, L., van Haarlem, M. and Vermeer, C. (1987) 'The effect of Gla-containing proteins on the precipitation of insoluble salts', *Biochem Biophys Res Commun*, **142,** 113-19.

Van der Eerden, J., Bennema, P. and Cherepanova, T. (1978) 'Survey of Monte Carlo simulations of crystal surfaces and crystal growth', *Progress in Crystal Growth and Characterisation*, **1,** 219-64.

van Leeuwen, C. (1979) 'On the driving force for crystallization: the growth affinity', *J Crystal Growth*, **46,** 91-5.

van Leeuwen, C. and Blomen, L. (1979) 'On the presentation of growth curves for growth from solution', *J Crystal Growth*, **46,** 96-104.

Verkoelen, C., Romijn, J., DeBruijn, C., Boeve, E., Cao, L. and Schroder, F. (1995) 'Association of calcium oxalate monohydrate crystals with MDCK cells', *Kidney Int*, **48,** 129-38.

Verma, A. (1953) *Crystal growth and dislocations,* Butterworths: London, pp.7-28.

Vermeulen, C. and Lyon, E. (1968) 'Mechanisms of genesis and growth of calculi', *Am J Med*, **45,** 684-92.

Verwey, E. and Overbeek, J. (1948) *Theory of the stability of lyophobic colloids,* Elsevier: New York.

Vogel, A. (1961a) *A Text-book of quantitative inorganic analysis*. Longmans: London, pp. 1166.

Vogel, A. (1961b) *A Text-book of quantitative inorganic analysis*. Longmans: London, pp 418.

Wadsworth, M. (1979) 'Hydrometallurgical processes', In: *Rate processes of extractive metallurgy*, pp. 135, 141-3, 146-148. Eds. H. Sohn and M. Wadsworth. Plenum Press: New York.

Wang, RZ., Addadi, L. and Weiner, S. (1997) 'Design strategies of sea urchin teeth: structure, composition and micromechanical relations to function', *Philosphical Transactions of the Royal Society of London*, **352** (1352), 469-80.

Walker, PD., Kaushal, GP. and Shah, SV. (1994) 'Presence of a distinct extracellular matrix-degrading metalloproteinase activity in renal tubules', *J Am Soc Nephrol*, **5**, 55-61.

Warpehoski, M., Buscemi, P., Osborn, D., Finlayson, B. and Goldberg, E. (1981) 'Distribution of organic matrix in calcium oxalate renal calculi', *Calcif Tissue Int*, **33,** 211-22.

Weiner, S. and Addadi, L. (1997) 'Design strategies in mineralized biological materials', *J Mater Chem*, **7,** 689-702.

Welshman, S. and McGeown, M. (1972) 'A quantitative investigation of the effects on the growth of calcium oxalate crystals of potential inhibitors' *Br J Urol*, **44,** 677-80.

Wesson, J., Weissner, J., Mandel, N. and Kleinman, J. (2000) 'Polymer chemical structures that control calcium oxalate polymorphism', In: *Urolithiasis 2000*, pp. 109-12. Eds. A. Rodgers, B. Hibbert, B. Hess, S. Khan and G. Preminger: Rondebosch: University of Cape Town.

Wesson, J., Worcester, E., Wiessner, J., Mandel, N. and Kleinman, J. (1998) 'Control of calcium oxalate crystal structure and cell adherence by urinary macromolecules', *Kidney Int*, **53,** 952-57.

Whalley, N., Moraes, M., Shar, T., Pretorius, S. and Meyer, A. (1998) 'Lithogenic risk factors in the urine of black and white subjects', *B J Urol*, **82,** 783-90.

Wickham, J. (1976) 'The matrix of renal calculi', In: *Scientific Foundations of Urology Vol. 1*, pp. 323-29. Eds. D. Williams and G. Chrisholm. Heinemann: London.

Wilbur, K. and Saleuddin, A. (1983) *Shell formation in the Mollusca,* Academic press: New York, pp. 1-235.

Williams, H. and Wandzilak, T. (1989) 'Oxalate synthesis, transport and the hyperoxaluric syndromes', *J Urol*, **141,** 742-47.

Williamson, G. and Hall, W. (1953) 'X-ray line broadening from filed aluminium and wolfram', *Acta Metallurgica*, **1,** 22-31.

Wisniewski, Z., Armstrong, B. and Brockis, J. (1981) 'The pattern of urinary calculus diseases in Western Australia', In: *Urinary calculus*, pp. 47-51. Eds. J. Brockis and B. Finlayson. PSB Publishing: Littleton.

Wolsey, W., Yu, G. and Heytens, T. (2000) 'Calcium oxalate complexation studies - a progress report', In: *Urolithiasis 2000 Vol. 1*, pp. 63. Eds. A. Rodgers, B. Hibbert, B. Hess, S. Khan and G. Preminger. University of Cape Town, Rondebosch, Cape Town: Cape Town, South Africa.

Worcester, E., Blumenthal, S. and Beshensky, A. (1992) 'The calcium oxalate crystal growth inhibitor protein produced by mouse kidney cortical cells in culture is osteopontin', *J Bone Min Res*, **7,** 1029-36.

Worchester, E., Sebastian, J., Hiatt, J., Beshensky, A. and Sadowski, J. (1993) 'The effect of Warfarin on urine calcium oxalate crystal growth inhibition and urinary excretion of calcium and nephrocalcin', *Calcif Tissue Int*, **53,** 242-48.

Xu, YC., Zacharias, U., Peraldi, MN., Lu, CY., Sraer, JD., Brass, LF. and Rondeau, E. (1995) 'Constitutive expression and modulation of the functional thrombin receptor in the human kidney' *Am J Pathol*, **146**, 101-110.

Yamaguchi, S., Yoshioka, T., Utsunomiya, M., Koide, T., Osafune, M., Okuyama, A. and Sonoda, T. (1993) 'Heparin sulphate in the stone matrix and its inhibitory effect on calcium oxalate crystallization', *Urol Res*, **21,** 187-92.

Yamate, T., Kohri, K., Konya, E., Ishikawa, Y., Iguchi, M. and Kurita, T. (1999) 'Interaction between osteopontin on Madin-Darby Canine Kidney cell membrane and oxalate crystal', *Urol Int*, **62,** 81-6.

Yamate, T., Kohri, K. and Umekawa, T. (1996) 'The effect of osteopontin on the adhesion of calcium oxalate crystals to Madin-Darby Canine Kidney cells', *Eur Urol*, **30,** 388-93.

Yoshida, O. and Okada, Y. (1990) 'Epidemiology of urolithiasis in Japan: a chronological and geographic study', *Urol Int*, **45,** 104-11.

Yoshioka, T., Koide, T., Utsunomiya, M., Itatani, H., Oka, T. and Sonoda, T. (1989) 'Possible role of Tamm-Horsfall glycoprotein in calcium oxalate crystallization', *Br J Urol*, **64,** 463-67.

Zaremba, C., Belcher, A., Fritz, M., Li, Y., Mann, S., Hansma, P., Morse, D., Speck, J. and Stucky, G. (1996) 'Critical transitions in biofabrication of abalone shells and flat pearls', *Chem Mater*, **8,** 679-690.

Zieba, A., Sethuraman, G., Perez, F., Nancollas, G. and Cameron, D. (1996) 'Influence of organic phosphonates on hydroxyapatite crystal growth kinetics', *Langmuir*, **12,** 2853-2858.

Zunszain, P., Ghuman, J., Komatsu, T., Tsuchida, E. and Curry,S. (2003) 'Crystal structural analysis of human serum albumin complexed with hemin and fatty acid', *BMC Structural Biology*, **3** (6), 1-9.

APPENDIX I

DATA USED IN THIS THESIS

I.1. Average adsorption of amino acids on calcium minerals in the presence of 1000 mg/L calcium chloride at different pH values. (chapter 4)

Amino acid pH 5	CaOx monohydrate ($\mu mol\ m^{-2}$)	$Ca_3(PO_4)_2$ ($\mu mol\ m^{-2}$)	$CaHPO_4.2H_2O$ ($\mu mol\ m^{-2}$)	$Ca_5(PO_4)_3OH$ ($\mu mol\ m^{-2}$)
Aspartic	0.1310	0.0086	0.0025	0.0013
γ-Carboxyglutamic	0.2025	0.0629	0.1311	0.0627
Glutamic	0.1112	0.0089	0.0028	0.0015
Alanine	0.0468	nd	0.0009	0.0001
Cystine	0.0082	0.0008	0.0041	0.0015
Glycine	0.0241	0.0011	0.0067	0.0036
Histidine	0.0412	nd	0.0046	0.0007
Leucine	0.0143	nd	0.0069	0.0002
iso Leucine	0.0172	nd	0.0049	0.0001
nor Leucine	0.0067	nd	0.0001	0.0001
Methionine	0.0196	0.0010	0.0131	0.0005
Methionine sulfate	0.0040	0.0015	0.0098	0.0012
Phenylalanine	0.0310	nd	0.0001	0.0001
Proline	0.0360	0.0041	0.0001	0.0008
Serine	0.0401	0.0023	0.0108	0.0027
Threonine	0.0138	0.0029	0.0120	0.0022
Tyrosine	0.0348	nd	0.0017	0.0001
Valine	0.0110	nd	0.0039	0.0003
Arginine	0.0204	0.0031	0.0073	0.0007
Lysine	0.0160	nd	0.0078	0.0004

Amino acid pH 6	CaOx monohydrate ($\mu mol\ m^{-2}$)	$Ca_3(PO_4)_2$ ($\mu mol\ m^{-2}$)	$CaHPO_4.2H_2O$ ($\mu mol\ m^{-2}$)	$Ca_5(PO_4)_3OH$ ($\mu mol\ m^{-2}$)
Aspartic	0.0718	0.0052	0.0026	0.0010
γ-Carboxyglutamic	0.1500	0.0512	0.1110	0.0580
Glutamic	0.0674	0.0068	0.0023	0.0009
Alanine	0.0366	nd	0.0006	0.0001
Cystine	0.0047	0.0009	0.0041	0.0011
Glycine	0.0226	0.0011	0.0064	0.0028
Histidine	0.0332	nd	0.0036	0.0004
Leucine	0.0102	nd	0.0068	0.0002
iso Leucine	0.0158	nd	0.0049	0.0001
nor Leucine	0.0068	nd	0.0001	nd
Methionine	0.0118	0.0007	0.0129	0.0005
Methionine sulfate	0.0031	0.0011	0.0087	0.0005
Phenylalanine	0.0226	nd	nd	nd
Proline	0.0309	0.0038	0.0001	0.0001
Serine	0.0310	0.0032	0.0107	0.0021
Threonine	0.0088	0.0027	0.0110	0.0015
Tyrosine	0.0291	nd	0.0014	0.0001
Valine	0.0058	nd	0.0039	0.0002
Arginine	0.0169	0.0038	0.0066	0.0005
Lysine	0.0141	nd	0.0073	0.0002

I.1 (continued)

Amino acid pH 7	CaOx monohydrate ($\mu mol\ m^{-2}$)	$Ca_3(PO_4)_2$ ($\mu mol\ m^{-2}$)	$CaHPO_4.2H_2O$ ($\mu mol\ m^{-2}$)	$Ca_5(PO_4)_3OH$ ($\mu mol\ m^{-2}$)
Aspartic	0.0464	0.0018	0.0013	0.0005
γ-Carboxyglutamic	0.1498	0.0514	0.0984	0.0524
Glutamic	0.0442	0.0056	0.0012	0.0004
Alanine	0.0221	0.0001	0.0001	nd
Cystine	0.0018	0.0004	0.0024	0.0005
Glycine	0.0088	0.0008	0.0055	0.0010
Histidine	0.0326	0.0001	0.0019	0.0003
Leucine	0.0092	0.0001	0.0044	nd
iso Leucine	0.0082	nd	0.0033	nd
nor Leucine	0.0062	nd	nd	nd
Methionine	0.0081	0.0006	0.0115	nd
Methionine sulfate	0.0029	0.0010	0.0089	0.0001
Phenylalanine	0.0203	nd	nd	nd
Proline	0.0187	0.0031	0.0001	nd
Serine	0.0275	0.0015	0.0088	0.0007
Threonine	0.0080	0.0014	0.0105	0.0009
Tyrosine	0.0221	0.0001	0.0007	nd
Valine	0.0015	nd	0.0024	nd
Arginine	0.0166	0.0026	0.0037	0.0003
Lysine	0.0147	nd	0.0057	nd

Amino acid pH 8	CaOx monohydrate ($\mu mol\ m^{-2}$)	$Ca_3(PO_4)_2$ ($\mu mol\ m^{-2}$)	$CaHPO_4.2H_2O$ ($\mu mol\ m^{-2}$)	$Ca_5(PO_4)_3OH$ ($\mu mol\ m^{-2}$)
Aspartic	0.0066	0.0011	0.0001	0.0003
γ-Carboxyglutamic	0.1473	0.0519	0.0724	0.0514
Glutamic	0.0060	0.0008	0.0001	0.0002
Alanine	nd	nd	nd	nd
Cystine	nd	nd	0.0002	0.0001
Glycine	nd	nd	0.0013	0.0002
Histidine	0.0064	nd	nd	nd
Leucine	0.0001	nd	0.0008	nd
iso Leucine	0.0026	nd	0.0007	nd
nor Leucine	nd	nd	nd	nd
Methionine	0.0051	nd	0.0052	nd
Methionine sulfate	0.0001	0.0004	0.0024	nd
Phenylalanine	0.0055	nd	nd	nd
Proline	nd	0.0011	nd	nd
Serine	nd	0.0006	0.0008	0.0005
Threonine	nd	nd	0.0033	0.0004
Tyrosine	0.0049	nd	nd	nd
Valine	nd	nd	0.0004	nd
Arginine	0.0103	0.0008	nd	nd
Lysine	0.0049	nd	0.0003	nd

nd, not detected

I.2 Adsorption densities of amino acids on calcium minerals at different pH values.

Amino acid	CaOx monohydrate	$Ca_3(PO_4)_2$	$CaHPO_4.2H_2O$	$Ca_5(PO_4)_3OH$
pH 5	($\mu mol\ m^{-2}$)	($\mu mol\ m^{-2}$)	($\mu mol\ m^{-2}$)	($\mu mol\ m^{-2}$)
Aspartic	0.1385	0.0076	0.0028	0.0016
	0.1259	0.0086	0.0030	0.0012
	0.1280	0.0081	0.0026	0.0014
γ-Carboxyglutamic	0.2137	0.0648	0.1428	0.0664
	0.1930	0.0634	0.1358	0.0642
	0.1963	0.0608	0.1234	0.0584
Glutamic	0.1140	0.0082	0.0028	0.0015
	0.1150	0.0089	0.0023	0.0011
	0.1058	0.0084	0.0027	0.0013
Alanine	0.0493	nd	0.0009	0.0002
	0.0459	nd	0.0011	nd
	0.0428	nd	0.0013	0.0001
Cystine	0.0080	0.0006	0.0045	0.0018
	0.0077	0.0010	0.0041	0.0014
	0.0071	0.0008	0.0043	0.0016
Glycine	0.0255	0.0015	0.0074	0.0036
	0.0235	0.0013	0.0067	0.0034
	0.0221	0.0011	o.0066	0.0032
Histidine	0.0425	nd	0.0046	0.0003
	0.0427	nd	0.0040	0.0008
	0.0414	nd	0.0043	0.0007
Leucine	0.0151	0.0006	0.0076	0.0002
	0.0161	0.0004	0.0072	0.0001
	0.0138	0.0005	0.0068	0.0003
iso Leucine	0.0187	0.0002	0.0053	0.0001
	0.0170	0.0001	0.0051	0.0002
	0.0177	0.0002	0.0049	0.0001
nor Leucine	0.0073	nd	0.0001	nd
	0.0071	nd	nd	nd
	0.0066	nd	0.0002	nd
Methionine	0.0219	0.0009	0.0142	0.0006
	0.0215	0.0013	0.0134	0.0002
	0.0196	0.0011	0.0123	0.0004
Methionine sulfate	0.0043	0.0015	0.0105	0.0009
	0.0041	0.0013	0.0092	0.0014
	0.0039	0.0011	0.0097	0.0010
Phenylalanine	0.0324	nd	0.0001	nd
	0.0301	nd	0.0003	nd
	0.0278	nd	0.0002	nd
Proline	0.0371	0.0049	0.0004	0.0007
	0.0380	0.0040	nd	0.0006
	0.0344	0.0046	0.0002	0.0011
Serine	0.0428	0.0029	0.0114	0.0030
	0.0411	0.0026	0.0108	0.0028
	0.0388	0.0023	0.0111	0.0026
Threonine	0.0142	0.0030	0.0128	0.0019
	0.0146	0.0036	0.0120	0.0026
	0.0135	0.0033	0.0118	0.0024
Tyrosine	0.0327	nd	0.0013	0.0001
	0.0368	nd	0.0019	nd
	0.0364	nd	0.0016	0.0002
Valine	0.0105	nd	0.0041	0.0005
	0.0116	nd	0.0044	0.0001
	0.0118	nd	0.0038	0.0003
Arginine	0.0204	0.0025	0.0075	0.0004
	0.0190	0.0031	0.0073	0.0010
	0.0206	0.0028	0.0068	0.0010
Lysine	0.0151	0.0003	0.0084	0.0004
	0.0155	0.0001	0.0078	0.0002
	0.0165	0.0002	0.0075	0.0003

I.2 (continued)

Amino acid	CaOx monohydrate	$Ca_3(PO_4)_2$	$CaHPO_4.2H_2O$	$Ca_5(PO_4)_3OH$
pH 6	($\mu mol\ m^{-2}$)	($\mu mol\ m^{-2}$)	($\mu mol\ m^{-2}$)	($\mu mol\ m^{-2}$)
Aspartic	0.0747	0.0058	0.0020	0.0005
	0.0710	0.0052	0.0026	0.0011
	0.0685	0.0055	0.0023	0.0008
γ-Carboxyglutamic	0.1522	0.0569	0.1228	0.0548
	0.1506	0.0494	0.1105	0.0540
	0.1502	0.0527	0.1147	0.0502
Glutamic	0.0625	0.0074	0.0019	0.0009
	0.0668	0.0073	0.0023	0.0005
	0.0714	0.0066	0.0021	0.0007
Alanine	0.0342	nd	0.0005	0.0001
	0.0373	nd	0.0007	0.0001
	0.0395	nd	0.0009	nd
Cystine	0.0052	0.0011	0.0043	0.0009
	0.0048	0.0009	0.0040	0.0014
	0.0050	0.0007	0.0034	0.0016
Glycine	0.0243	0.0015	0.0062	0.0026
	0.0240	0.0011	0.0062	0.0022
	0.0216	0.0013	0.0056	0.0024
Histidine	0.0339	nd	0.0044	0.0002
	0.0318	nd	0.0033	0.0008
	0.0324	nd	0.0040	0.0005
Leucine	0.0114	nd	0.0060	0.0002
	0.0103	nd	0.0064	0.0003
	0.0104	nd	0.0059	0.0001
iso Leucine	0.0161	nd	0.0046	nd
	0.0171	nd	0.0049	0.0002
	0.0148	nd	0.0043	0.0001
nor Leucine	0.0065	nd	0.0002	nd
	0.0069	nd	0.0001	nd
	0.0061	nd	nd	nd
Methionine	0.0127	0.0007	0.0129	0.0005
	0.0118	0.0011	0.0133	0.0003
	0.0118	0.0009	0.0119	0.0004
Methionine sulfate	0.0027	0.0014	0.0099	0.0005
	0.0031	0.0010	0.0086	0.0009
	0.0029	0.0012	0.0091	0.0007
Phenylalanine	0.0248	nd	nd	nd
	0.0224	nd	nd	nd
	0.0218	nd	nd	nd
Proline	0.0310	0.0039	nd	0.0001
	0.0322	0.0037	0.0002	nd
	0.0307	0.0032	0.0001	0.0001
Serine	0.0326	0.0021	0.0116	0.0021
	0.0285	0.0018	0.0110	0.0018
	0.0301	0.0024	0.0101	0.0015
Threonine	0.0084	0.0027	0.0125	0.0018
	0.0089	0.0021	0.0115	0.0016
	0.0079	0.0024	0.0114	0.0017
Tyrosine	0.0306	nd	0.0013	0.0001
	0.0297	nd	0.0015	0.0002
	0.0291	nd	0.0011	nd
Valine	0.0057	nd	0.0040	0.0001
	0.0052	nd	0.0034	0.0002
	0.0050	nd	0.0037	0.0002
Arginine	0.0181	0.0038	0.0069	0.0009
	0.0168	0.0034	0.0060	0.0005
	0.0161	0.0036	0.0066	0.0007
Lysine	0.0151	nd	0.0070	0.0001
	0.0148	nd	0.0065	0.0005
	0.0133	nd	0.0075	0.0003

I.2 (continued)

Amino acid	CaOx monohydrate	$Ca_3(PO_4)_2$	$CaHPO_4.2H_2O$	$Ca_5(PO_4)_3OH$
pH 7	($\mu mol\ m^{-2}$)	($\mu mol\ m^{-2}$)	($\mu mol\ m^{-2}$)	($\mu mol\ m^{-2}$)
Aspartic	0.0490	0.0019	0.0012	0.0003
	0.0449	0.0015	0.0015	0.0005
	0.0459	0.0017	0.0009	0.0007
γ-Carboxyglutamic	0.1496	0.0536	0.1036	0.0537
	0.1549	0.0506	0.0972	0.0516
	0.1425	0.0518	0.0962	0.0507
Glutamic	0.0411	0.0059	0.0008	0.0001
	0.0469	0.0051	0.0012	0.0005
	0.0455	0.0055	0.0010	0.0003
Alanine	0.0236	nd	0.0002	nd
	0.0223	nd	nd	nd
	0.0213	nd	0.0001	nd
Cystine	0.0017	0.0006	0.0029	0.0005
	0.0018	0.0002	0.0023	0.0005
	0.0016	0.0004	0.0026	0.0008
Glycine	0.0090	0.0011	0.0050	0.0009
	0.0093	0.0009	0.0056	0.0013
	0.0084	0.0007	0.0053	0.0011
Histidine	0.0332	nd	0.0023	0.0003
	0.0321	nd	0.0022	0.0001
	0.0313	nd	0.0021	0.0002
Leucine	0.0095	nd	0.0049	nd
	0.0100	nd	0.0043	nd
	0.0096	nd	0.0046	nd
iso Leucine	0.0086	nd	0.0033	nd
	0.0087	nd	0.0031	nd
	0.0082	nd	0.0029	nd
nor Leucine	0.0058	nd	nd	nd
	0.0064	nd	nd	nd
	0.0061	nd	nd	nd
Methionine	0.0088	0.0009	0.0112	nd
	0.0087	0.0007	0.0118	nd
	0.0080	0.0005	0.0106	nd
Methionine sulfate	0.0029	0.0011	0.0090	0.0002
	0.0025	0.0009	0.0080	0.0001
	0.0027	0.0007	0.0085	nd
Phenylalanine	0.0210	nd	nd	nd
	0.0220	nd	nd	nd
	0.0197	nd	nd	nd
Proline	0.0203	0.0034	nd	nd
	0.0179	0.0031	nd	nd
	0.0191	0.0025	nd	nd
Serine	0.0252	0.0014	0.0095	0.0011
	0.0282	0.0020	0.0084	0.0005
	0.0285	0.0017	0.0085	0.0008
Threonine	0.0076	0.0012	0.0108	0.0006
	0.0071	0.0010	0.0096	0.0012
	0.0081	0.0014	0.0099	0.0009
Tyrosine	0.0234	nd	0.0005	nd
	0.0224	nd	0.0010	nd
	0.0220	nd	0.0009	nd
Valine	0.0019	nd	0.0025	nd
	0.0017	nd	0.0027	nd
	0.0018	nd	0.0023	nd
Arginine	0.0140	0.0027	0.0042	0.0004
	0.0138	0.0024	0.0036	0.0002
	0.0130	0.0021	0.0039	0.0003
Lysine	0.0134	nd	0.0060	nd
	0.0137	nd	0.0055	nd
	0.0125	nd	0.0050	nd

I.2 (continued)

Amino acid	CaOx monohydrate	$Ca_3(PO_4)_2$	$CaHPO_4.2H_2O$	$Ca_5(PO_4)_3OH$
pH 8	($\mu mol\ m^{-2}$)	($\mu mol\ m^{-2}$)	($\mu mol\ m^{-2}$)	($\mu mol\ m^{-2}$)
Aspartic	0.0063	0.0013	0.0002	0.0002
	0.0071	0.0016	0.0001	0.0005
	0.0067	0.0010	nd	0.0002
γ-Carboxyglutamic	0.1560	0.0546	0.0782	0.0534
	0.1390	0.0510	0.0714	0.0499
	0.1460	0.0474	0.0694	0.0497
Glutamic	0.0065	0.0005	0.0001	0.0001
	0.0062	0.0009	0.0002	0.0003
	0.0059	0.0007	nd	0.0002
Alanine	nd	nd	nd	nd
	nd	nd	nd	nd
	nd	nd	nd	nd
Cystine	nd	nd	0.0005	0.0002
	nd	nd	0.0002	0.0001
	nd	nd	0.0002	0.0002
Glycine	nd	nd	0.0009	0.0003
	nd	nd	0.0011	0.0001
	nd	nd	0.0013	0.0002
Histidine	0.0073	nd	nd	nd
	0.0064	nd	nd	nd
	0.0067	nd	nd	nd
Leucine	nd	nd	0.0010	nd
	nd	nd	0.0008	nd
	nd	nd	0.0006	nd
iso Leucine	0.0021	nd	0.0006	nd
	0.0025	nd	0.0011	nd
	0.0023	nd	0.0010	nd
nor Leucine	nd	nd	nd	nd
	nd	nd	nd	nd
	nd	nd	nd	nd
Methionine	0.0058	nd	0.0057	nd
	0.0056	nd	0.0053	nd
	0.0052	nd	0.0055	nd
Methionine sulfate	nd	0.0002	0.0018	nd
	nd	0.0006	0.0023	nd
	nd	0.0004	0.0025	nd
Phenylalanine	0.0056	nd	nd	nd
	0.0052	nd	nd	nd
	0.0051	nd	nd	nd
Proline	nd	0.0008	nd	nd
	nd	0.0012	nd	nd
	nd	0.0010	nd	nd
Serine	nd	0.0006	0.0005	0.0002
	nd	0.0010	0.0012	0.0006
	nd	0.0008	0.0010	0.0004
Threonine	nd	nd	0.0034	0.0005
	nd	nd	0.0030	0.0003
	nd	nd	0.0029	0.0004
Tyrosine	0.0050	nd	nd	nd
	0.0055	nd	nd	nd
	0.0048	nd	nd	nd
Valine	nd	nd	0.0005	nd
	nd	nd	0.0004	nd
	nd	nd	0.0003	nd
Arginine	0.0112	0.0011	nd	nd
	0.0108	0.0009	nd	nd
	0.0104	0.0007	nd	nd
Lysine	0.0052	nd	0.0005	nd
	0.0056	nd	0.0002	nd
	0.0048	nd	0.0005	nd

I.3 Data from Rietveld refinement (Chapters 5-7)

$\lambda = 0.149576$ nm

REFERENCE STANDARDS	Lanthanum hexaboride	esd	Silicon	esd
Space group	P M 3 M		F D 3 M	
Phase scale	9.04876E-9	0.08573E-9	2.32535E-7	0.03256E-7
Overall thermal	Not refined		Not refined	
Thermal (La)	-1.59862	0.01312	-	-
Thermal (B)	-2.18725	0.01433	-	-
Thermal (Si)	-	-	-0.57941	0.05079
a	4.15690	0.00001	5.43124	0.00001
U	0.00040	0.00002	0.000030	0.0000009
V	-0.00140	0.00010	-0.00140	
W	0.00330	0.00007	0.00330	
U anisotropy	Not refined		0.00066	0.00007
Asymmetry	Not refined		Not refined	
Lorentzian value	0.0172	0.0036	0.01625	0.00017
P.Orientation	1.02228	0.00434	1.01208	0.00471
Rp (total R)	2.85		6.82	
Rwp (total R)	4.11		10.96	
Background				
Histogram 1 20.0000 - 37.0000				
B_0	28.837	0.039	11.073	0.037
B_1	-4.7535	0.0614	2.6762	0.0668
B_2	-5.0969	0.0631	-4.7998	0.0598
B_3	2.0233	0.0516	-0.1829	0.0582
Histogram 2 45.0000 - 81.5000				
B_0	22.753	0.019	15.374	0.039
B_1	1.2697	0.0337	2.6866	0.0581
B_2	-1.2305	0.0280	-0.3633	0.0219
B_3	-0.2095	0.0278	-0.9752	0.0585
Histogram 3 83.0000 - 120.0000				
B_0	21.768	0.019	16.825	0.040
B_1	0.7725	0.0344	0.5304	0.0747
B_2	0.1959	0.0281	0.2465	0.0594
B_3	-0.0686	0.0279	-0.3616	0.0596
Histogram 4 122.4195 - 161.000				
B_0	25.955	0.027	18.693	0.042
B_1	2.5193	0.0427	3.9092	0.0712
B_2	-0.3945	0.0436	-1.2776	0.0606
B_3	0.1084	0.0345	1.7819	0.0584

I.3 (continued)

$\lambda = 0.149576$ nm

CALCIUM OXALATE	Distilled water	esd	Asp	esd
Space group	P 1 21/C 1		P 1 21/C 1	
Phase scale	8.91739E-6	3.78632E-9	8.83322E-6	0.07119E-6
Overall thermal	-3.26330	0.00175	-2.74527	0.12562
a	6.29460	0.000004	6.29910	0.00017
b	14.59570	0.00001	14.60040	0.00042
c	10.12490	0.00002	10.12700	0.00038
β	109.4522	0.0006	109.4575	0.00201
U	0.01700	0.00049	0.01990	0.00051
V	-0.00140	not refined	-0.00140	Not refined
W	0.00330	not refined	0.00330	Not refined
U anisotropy	0.00230	0.00002	0.00220	0.00128
Asymmetry	Not refined		Not refined	
Crystallite size (μm)	2.59	0.19	2.54	0.23
P.Orientation	1.00390	0.01577	0.98760	0.00337
Rp (total R)	4.63		6.3	
Rwp (total R)	6.28		8.48	
Background				
Histogram 1				
B_0	18.088	0.037	15.591	0.042
B_1	2.4511	0.0666	2.9790	0.0659
B_2	-5.2627	0.0572	-4.0149	0.0659
B_3	1.9408	0.0589	2.0691	0.0564
Histogram 2				
B_0	42.1783	5.5458	16.733	0.038
B_1	-1.3763	0.2736	0.3263	0.0623
B_2	0.0260	0.0044	-0.1579	0.0500
B_3	-0.00015	0.00002	-0.1583	0.0488
Histogram 3				
B_0	29.3154	0.2119	15.689	0.047
B_1	-0.1855	0.0433	-0.3263	0.0669
B_2	0.00082	0.00002	0.1824	0.0507

I.3 (continued)

$\lambda = 0.149576$ nm

CALCIUM OXALATE	AspAsp	esd	Gla	esd
Phase scale	1.04818E-5	0.00826E-5	2.77457E-5	0.02167E-5
Overall thermal	-1.23223	0.06076	0.43289	0.01242
a	6.29640	0.00011	6.30030	0.00017
b	14.59370	0.00022	14.58480	0.00031
c	10.12140	0.00017	10.12340	0.00031
β	109.4538	0.0010	109.4106	0.0019
U	0.02250	0.00088	0.09590	0.00208
V	-0.00140	not refined	-0.00140	not refined
W	0.00330	not refined	0.00330	not refined
U anisotropy	0.00240	0.00199	0.01344	0.00815
Asymmetry	Not refined		Not refined	
Crystallite size (μm)	2.54	0.23	1.19	0.09
P.Orientation	0.99390	0.00349	0.96120	0.00369
Rp (total R)	5.13		4.85	
Rwp (total R)	6.96		6.62	
Background				
Histogram 1				
B_0	22.307	0.049	26.492	0.058
B_1	4.3941	0.0768	6.0252	0.0905
B_2	-6.5253	0.0761	-7.8536	0.0873
B_3	2.2389	0.0649	2.9507	0.0733
Histogram 2				
B_0	22.452	0.0418	28.898	0.058
B_1	0.2185	0.0690	2.0208	0.0684
B_2	0.2138	0.0548	-0.4976	0.0674
B_3	-0.2539	0.05365		
Histogram 3				
B_0	20.051	0.048	27.679	0.069
B_1	-0.2648	0.0732	0.1844	0.0713
B_2	0.3029	0.0562	0.1530	0.0680

I.3 (continued)

$\lambda = 0.149576$ nm

CALCIUM OXALATE	Glu	esd	GluGlu	esd
Phase scale	2.49856E-5	0.02123E-5	3.55037E-6	0.03263E-6
Overall thermal	-1.76410	0.19449	-1.47177	0.15639
a	6.29700	0.00020	6.29690	0.00012
b	14.59820	0.00039	14.59660	0.00023
c	10.11980	0.00032	10.12190	0.00018
β	109.4435	0.0019	109.4665	0.0011
U	0.03500	0.00154	0.01310	0.00064
V	-0.00140	Not refined	-0.00140	Not refined
W	0.00330	Not refined	0.00330	Not refined
U anisotropy	0.01100	0.00493	0.00450	0.00065
Asymmetry	Not refined		Not refined	
Crystallite size (μm)	2.01	0.26	2.54	0.23
P.Orientation	0.99011	0.00281	1.00580	0.00460
Rp (total R)	8.39		3.60	
Rwp (total R)	11.60		4.82	
Background				
Histogram 1				
B_0	17.594	0.073	25.027	0.031
B_1	3.5769	0.1333	3.3085	0.0478
B_2	-4.8426	0.1146	-8.7766	0.0481
B_3	2.1298	0.1155	3.1649	0.0420
Histogram 2				
B_0	20.401	0.067	21.944	0.025
B_1	1.2097	0.1045	-0.6657	0.0404
B_2	0.2647	0.0844	-0.8341	0.0329
B_3	-0.2076	0.0818	-0.2939	0.0323
Histogram 3				
B_0	19.645	0.079	18.312	0.026
B_1	0.8902	0.1088	-0.3973	0.0401
B_2	0.2714	0.0855	0.3062	0.0312

I.3 (continued)

$\lambda = 0.149576$ nm

CALCIUM OXALATE	Prothrombin	esd	THG	esd
Phase scale	1.32641E-5	0.00834E-5	8.90271E-6	0.08981E-6
Overall thermal	-1.41779	0.09781	-1.60820	0.16250
a	6.29530	0.00017	6.29780	0.00014
b	14.58910	0.00032	14.59460	0.00027
c	10.12320	0.00033	10.12390	0.00027
β	109.4283	0.00204	109.4532	0.0016
U	0.12450	0.00263	0.01730	0.00082
V	-0.00140	Not refined	-0.00140	Not refined
W	0.00330	Not refined	0.00330	Not refined
U anisotropy	0.01468	0.00110	0.00824	0.00128
Asymmetry	Not refined		Not refined	
Crystallite size (μm)	0.31	0.03	2.45	0.17
P.Orientation	0.96830	0.00327	0.97520	0.00510
Rp (total R)	3.65		5.45	
Rwp (total R)	4.73		7.83	
Background				
Histogram 1				
B_0	28.957	0.049	24.035	0.058
B_1	6.3296	0.0745	4.5492	0.0914
B_2	-8.4847	0.0732	-6.9659	0.0901
B_3	3.9516	0.0595	2.2902	0.0764
Histogram 2				
B_0	28.077	0.047	24.010	0.051
B_1	0.2393	0.0674	-0.2846	0.0794
B_2	-0.8094	0.0512	-0.2421	0.0643
B_3	-0.4105	0.0488	-0.3323	0.0622
Histogram 3				
B_0	24.792	0.062	20.833	0.061
B_1	-0.8144	0.0806	-0.5470	0.0801
B_2	0.2742	0.0535	0.2154	0.0623
B_3	0.1554	0.0569	0.2055	0.0632

I.3 (continued)

$\lambda = 0.149576$ nm

CALCIUM OXALATE	UF Urine	esd	CF Urine	esd
Phase scale	1.75403E-5	0.012207E-5	1.51206E-5	0.01293E-5
Overall thermal	-1.06179	0.11884	-1.15967	0.13587
a	6.29410	0.00016	6.29880	0.00020
b	14.58820	10.11980	14.58710	0.00036
c	10.11980	0.00030	10.12430	0.00033
β	109.4435	0.0018	109.4678	0.0028
U	0.06130	0.00184	0.12370	0.00238
V	-0.00140	Not refined	-0.00140	Not refined
W	0.00330	Not refined	0.00330	Not refined
U anisotropy	0.01653	0.00297	0.02268	0.00569
Asymmetry	Not refined		Not refined	
Crystallite size (μm)	0.50	0.04	0.31	0.03
P.Orientation	0.94390	0.00375	1.01430	0.00430
Rp (total R)	4.02		4.88	
Rwp (total R)	5.55		6.78	
Background				
Histogram 1				
B_0	39.444	0.076	32.945	0.079
B_1	7.3885	0.1385	6.5822	0.1217
B_2	-12.0931	0.1174	-8.4076	0.1207
B_3	2.7218	0.1197	3.5498	0.0990
Histogram 2				
B_0	39.822	0.066	32.842	0.070
B_1	1.1039	0.1014	0.5529	0.1143
B_2	-1.4964	0.0799	0.2737	0.0863
B_3	-0.7107	0.0772	-0.2011	0.02551
Histogram 3				
B_0	36.511	0.084	28.986	0.088
B_1	-0.5315	0.1199	-0.6305	0.0839
B_2	0.9279	0.0840	0.3207	0.0774
B_3	-0.49705	0.0877	-0.01229	0.0019

I.3 (continued)

$\lambda = 0.149576$ nm

CALCIUM OXALATE	CF Urine with protease	esd	Gelatin	esd
Phase scale	3.00275E-6	0.19477E-6	5.26304E-6	0.05194E-6
Overall thermal	-1.41187	0.11033	-6.09875	0.15628
a	6.29920	0.00018	6.29510	0.000072
b	14.59660	0.00074	14.59460	0.00014
c	10.10990	0.00080	10.12330	0.00010
β	109.5182	0.0013	109.4860	0.00058
U	0.06620	0.00512	0.00520	0.00018
V	-0.00140	Not refined	-0.00140	Not refined
W	0.00330	Not refined	0.00330	Not refined
U anisotropy	0.01121	0.00623	0.00320	0.00013
Asymmetry	Not refined		Not refined	
Crystallite size (μm)	0.51	0.13	>2.6	
P.Orientation	0.98480	0.00344	0.95130	0.00133
Rp (total R)	6.56		6.46	
Rwp (total R)	9.89		9.46	
Background				
Histogram 1				
B_0	25.501	0.175	12.585	0.040
B_1	4.6421	0.2715	2.9357	0.0628
B_2	-6.2845	0.2704	-3.5888	0.0628
B_3	2.3762	0.1261	0.9747	0.0528
Histogram 2				
B_0	24.593	0.1424	15.214	0.040
B_1	0.7485	0.0232	0.6732	0.0591
B_2	-0.2905	0.0182	-0.5220	0.0494
B_3	-0.2693	0.0178	-0.3487	0.0473
Histogram 3				
B_0	21.735	0.174	16.163	0.042
B_1	-0.1879	0.0126	-0.1436	0.0649
B_2	0.1143	0.0146	0.0768	0.0505
B_3	0.3666	0.0186	-0.0644	0.0506

I.3 (continued)

$\lambda = 0.153979$ nm

CALCIUM OXALATE	HSA	esd	CME	Esd
Phase scale	0.89652 E-3	0.00678 E-3	2.21871 E-3	0.01815 E-3
Overall thermal	1.75178	0.12553	2.80702	0.13859
a	6.29728	0.00033	6.29849	0.000174
b	14.58649	0.00081	14.58772	0.00037
c	10.12080	0.00051	10.11962	0.00027
β	109.4413	0.0011	109.4355	0.0014
Ca_1 (x)	0.97329	0.00079	0.97936	0.00113
Ca_1 (y)	0.13101	0.00061	0.13213	0.00056
Ca_1 (z)	0.05854	0.00062	0.05860	0.00084
Ca_2 (x)	0.99310	0.00083	1.00022	0.00115
Ca_2 (y)	0.12703	0.00070	0.12569	0.00068
Ca_2 (z)	0.43552	0.00062	0.43776	0.00083
C_1 (x)	1.00002	0.00400	1.00091	0.00625
C_1 (y)	0.32960	0.00184	0.33260	0.00187
C_1 (z)	0.20700	0.00211	0.22446	0.00287
C_2 (x)	1.00302	0.00611	0.99623	0.00767
C_2 (y)	0.43182	0.00167	0.433260	0.00176
C_2 (z)	0.25703	0.00436	0.25311	0.00438
U	0.04820	0.00101	0.08290	0.00161
V	-0.00240	Not refined	-0.00240	Not refined
W	0.00190	Not refined	0.00190	Not refined
U anisotropy	0.02302	0.00252	0.01730	0.00382
Crystallite size (μm)	0.63	0.02	0.64	0.02
P.Orientation	0.99310	0.00336	0.98430	0.00364
Rp (total R)	5.02		6.24	
Rwp (total R)	6.69		8.72	

I.4 Discrete peak profiles – FWHM (chapter 6)

Angle 2θ	14.49	14.85	18.04	19.04	22.82	23.67	29.19	30.52	34.88
Crystal Plane	(100)	$(02\bar{1})$	(002)	$(10\bar{2})$	$(13\bar{1})$	(040)	(200)	$(14\bar{2})$	$(22\bar{3})$
Medium	FWHM 2θ °								
Gelatine	0.0411 ±0.0007	0.0412 ±0.0004	0.0414 ±0.0021	0.0396 ±0.0008	0.0554 ±0.0005	0.0417 ±0.0004	0.0423 ±0.0005	0.0478 ±0.0009	0.0534 ±0.0006
Distilled water	0.0490 ±0.0007	0.0528 ±0.0007	0.0440 ±0.0028	0.0519 ±0.0019	0.0693 ±0.0019	0.0530 ±0.0004	0.0560 ±0.0007	0.0661 ±0.0012	0.0684 ±0.0013
Asp	0.0456 ±0.0002	0.0500 ±0.0006	0.0470 ±0.0027	0.0436 ±0.0013	0.0750 ±0.0025	0.048 ±0.0004	0.051 ±0.0005	0.049 ±0.0012	0.047 ±0.0031
AspAsp	0.0506 ±0.0009	0.0561 ±0.0022	0.0463 ±0.0029	0.0473 ±0.0021	0.0828 ±0.0043	0.0506 ±0.0005	0.0657 ±0.0013	0.0748 ±0.0016	0.0565 ±0.0077
GluGlu	0.0411 ±0.0006	0.0451 ±0.0019	0.0431 ±0.0018	0.0464 ±0.0005	0.0684 ±0.0055	0.0485 ±0.0013	0.0581 ±0.0010	0.0650 ±0.0030	0.0700 ±0.0014
THG	0.0435 ±0.0005	0.0477 ±0.0024	0.0429 ±0.0022	0.0445 ±0.0016	0.0693 ±0.0072	0.0484 ±0.0004	0.0562 ±0.0004	0.0684 ±0.0030	0.0717 ±0.0048
Gla	0.0714 ±0.0007	0.0831 ±0.0012	0.0674 ±0.0035	0.0667 ±0.0025	0.1652 ±0.0049	0.0761 ±0.0006	0.08640 ±0.0032	0.1232 ±0.0028	0.1408 ±0.0035
Glu	0.0534 ±0.0002	0.0665 ±0.0012	0.0468 ±0.0029	0.0503 ±0.0022	0.1037 ±0.0060	0.0522 ±0.0003	0.0752 ±0.0006	0.0922 ±0.0023	0.1026 ±0.0051
HSA-	0.0551 ±0.0029	0.0682 ±0.0015	0.0531 ±0.0021	0.0534 ±0.0016	0.1112 ±0.0042	0.0581 ±0.0022	0.0771 ±0.0034	0.0963 ±0.0041	0.1099 ±0.0045
PT	0.0920 ±0.0004	0.1100 ±0.0013	0.1058 ±0.0068	0.1058 ±0.0053	0.2007 ±0.0060	0.1021 ±0.0006	0.1183 ±0.0012	0.1576 ±0.0026	0.1813 ±0.0038
CME	0.0653 ±0.0026	0.0822 ±0.0023	0.1128 ±0.0035	0.0563 ±0.0021	0.1612 ±0.0042	0.0872 ±0.0028	0.08123 ±0.0024	0.1305 ±0.0037	0.1210 ±0.0031
UF urine	0.0555 ±0.0007	0.0823 ±0.0024	0.0883 ±0.0048	0.0530 ±0.0036	0.1076 ±0.0065	0.0620 ±0.0006	0.0723 ±0.0007	0.0979 ±0.0025	0.0923 ±0.0046
CF urine	0.0662 ±0.0004	0.0846 ±0.0015	0.1137 ±0.0031	0.0571 ±0.0019	0.1681 ±0.0006	0.0982 ±0.0024	0.0858 ±0.0006	0.1382 ±0.0021	0.1231 ±0.0014
CF + PK	0.0582 ±0.0008	0.0803 ±0.0029	0.0532 ±0.0046	0.0522 ±0.0031	0.0891 ±0.0012	0.0659 ±0.0006	0.0682 ±0.0016	0.0721 ±0.0025	0.1078 ±0.0045

I.4 (continued)

Angle 2θ	36.56	48.77							
Crystal Plane	(004)	(080)							
Medium	FWHM 2θ °								
Gelatine	0.0447 ±0.0008	0.0508 0.0032							
Distilled water	0.0524 ±0.0019	0.0604 ±0.0102							
Asp	0.0528 ±0.0023	0.0583 ±0.0132							
AspAsp	0.0570 ±0.0025	0.0771 ±0.0181							
GluGlu	0.0526 ±0.0021	0.0696 ±0.0188							
THG	0.0547 ±0.0022	0.0733 ±0.0124							
Gla	0.0872 ±0.0031	0.0934 ±0.0209							
Glu	0.0741 ±0.0027	0.0821 ±0.0215							
HSA	0.0801 ±0.0028	0.0921 ±0.019							
PT	0.1409 ±0.0042	0.1221 ±0.0305							
CME	0.1324 ±0.0042	0.1256 ±0.0261							
UF urine	0.1010 ±0.0028	0.0901 ±0.0238							
CF urine	0.1360 ±0.0033	0.1213 ±0.0277							
CF + PK	Missing	Missing							

I.5 Gaussian and Lorentzian contributions to peak profiles (chapter 6)

Calcium oxalate grown in gelatin

Crystal plane	Gaussian	esd	Lorentzian	esd
(100)	0.04184	0.00121	0.01282	0.00185
$(02\bar{1})$	0.04350	0.00174	0.01010	0.00325
(002)	0.04193	0.00221	0.02142	0.00255
$(10\bar{2})$	0.03256	0.00387	0.02000	0.00254
$(13\bar{1})$	0.04945	0.00121	0.04690	0.00189
(040)	0.04096	0.00067	0.02623	0.00117
(200)	0.04192	0.00121	0.02517	0.00163
$(14\bar{2})$	0.04683	0.00183	0.02904	0.00369
$(22\bar{3})$	0.04756	0.00186	0.04010	0.00185
(004)	0.04901	0.00276	0.04031	0.00223
(080)	0.05011	0.00255	0.04012	0.01242

Calcium oxalate grown in distilled water

Crystal plane	Gaussian	esd	Lorentzian	esd
(100)	0.04485	0.00049	0.01882	0.00053
$(02\bar{1})$	0.04353	0.00143	0.01538	0.00105
(002)	0.04904	0.00049	0.02902	0.00222
$(10\bar{2})$	0.03911	0.00502	0.02554	0.00551
$(13\bar{1})$	0.06587	0.00442	0.05430	0.00758
(040)	0.04980	0.00072	0.03222	0.00095
(200)	0.05523	0.00119	0.03170	0.00245
$(14\bar{2})$	0.06387	0.00266	0.03801	0.00504
$(22\bar{3})$	0.06325	0.00251	0.04601	0.00338
(004)	0.06086	0.02442	0.04692	0.00241
(080)	0.05721	0.01265	0.04601	0.01215

I.5 (continued)

Calcium oxalate grown with THG

Crystal plane	Gaussian	esd	Lorentzian	esd
(100)	0.04299	0.00078	0.01750	0.00141
$(02\bar{1})$	0.047206	0.00317	0.01577	0.00125
(002)	0.04922	0.00383	0.02801	0.00434
$(10\bar{2})$	0.03737	0.00366	0.02547	0.00282
$(13\bar{1})$	0.06569	0.00294	0.05632	0.00345
(040)	0.05091	0.00063	0.03324	0.00050
(200)	0.05949	0.00072	0.03310	0.00106
$(14\bar{2})$	0.05102	0.00341	0.03696	0.00438
$(22\bar{3})$	0.06201	0.00878	0.04690	0.00466
(004)	0.06008	0.00465	0.04680	0.004235
(080)	0.05641	0.01027	0.04671	0.01423

Calcium oxalate grown with GluGlu

Crystal plane	Gaussian	esd	Lorentzian	esd
(100)	0.04485	0.00118	0.01851	0.00092
$(02\bar{1})$	0.04459	0.00385	0.01545	0.00251
(002)	0.04966	0.00118	0.02933	0.00251
$(10\bar{2})$	0.03990	0.00264	0.02549	0.00251
$(13\bar{1})$	0.06631	0.00418	0.05411	0.00438
(040)	0.04951	0.00271	0.03244	0.00373
(200)	0.05542	0.00208	0.03181	0.00074
$(14\bar{2})$	0.06361	0.00816	0.03720	0.00468
$(22\bar{3})$	0.06250	0.00315	0.04612	0.00124
(004)	0.05314	0.00306	0.04651	0.00347
(080)	0.06803	0.01862	0.04630	0.01884

I.5 (continued)

Calcium oxalate grown with Asp

Crystal plane	Gaussian	esd	Lorentzian	esd
(100)	0.04391	0.00033	0.01865	0.00144
$(02\bar{1})$	0.04460	0.00110	0.01602	0.00284
(002)	0.05110	0.00345	0.02883	0.00558
$(10\bar{2})$	0.03771	0.00301	0.02597	0.00666
$(13\bar{1})$	0.06032	0.00596	0.05371	0.00565
(040)	0.04908	0.00074	0.03242	0.00188
(200)	0.05501	0.00096	0.03499	0.00136
$(14\bar{2})$	0.05898	0.00254	0.03791	0.00309
$(22\bar{3})$	0.06216	0.00684	0.04705	0.00247
(004)	0.05134	0.00228	0.04661	0.00328
(080)	0.05360	0.01736	0.04662	0.01327

Calcium oxalate grown with AspAsp

Crystal plane	Gaussian	esd	Lorentzian	esd
(100)	0.04471	0.00150	0.01890	0.00115
$(02\bar{1})$	0.04885	0.00238	0.04760	0.00135
(002)	0.05158	0.00153	0.02922	0.00253
$(10\bar{2})$	0.03926	0.00220	0.02560	0.00287
$(13\bar{1})$	0.0.0653	0.00326	0.05461	0.00318
(040)	0.04931	0.00087	0.03251	0.00095
(200)	0.05432	0.00257	0.03201	0.00109
$(14\bar{2})$	0.06301	0.00312	0.03769	0.00123
$(22\bar{3})$	0.06202	0.00395	0.04616	0.00345
(004)	0.06541	0.00105	0.04671	0.00433
(080)	0.07011	0.01158	0.04652	0.01476

I.5 (continued)

Calcium oxalate grown with Glu

Crystal plane	Gaussian	esd	Lorentzian	esd
(100)	0.05412	0.00039	0.02881	0.00089
$(02\bar{1})$	0.04565	0.00044	0.06917	0.00091
(002)	0.05112	0.00235	0.03113	0.00094
$(10\bar{2})$	0.04095	0.00266	0.02652	0.00229
$(13\bar{1})$	0.06761	0.00312	0.06917	0.00521
(040)	0.04889	0.00103	0.03531	0.00122
(200)	0.07504	0.00119	0.04410	0.00277
$(14\bar{2})$	0.05661	0.00364	0.03499	0.00297
$(22\bar{3})$	0.06103	0.00039	0.04621	0.00318
(004)	0.06661	0.00283	0.04812	0.00362
(080)	0.08362	0.01522	0.04834	0.01659

Calcium oxalate grown in UF urine

Crystal plane	Gaussian	esd	Lorentzian	esd
(100)	0.04681	0.00120	0.02112	0.00120
$(02\bar{1})$	0.05820	0.00485	0.03050	0.00404
(002)	0.05808	0.00423	0.03702	0.00373
$(10\bar{2})$	0.05311	0.00348	0.04022	0.00390
$(13\bar{1})$	0.06587	0.00516	0.05880	0.00206
(040)	0.04980	0.00102	0.03321	0.00077
(200)	0.05960	0.00168	0.03602	0.00143
$(14\bar{2})$	0.06387	0.00246	0.03930	0.00218
$(22\bar{3})$	0.08061	0.00332	0.05280	0.00169
(004)	0.08624	0.00265	0.05632	0.00434
(080)	0.08766	0.01372	0.04912	0.01533

I.5 (continued)

Calcium oxalate grown with CF urine after treatment with protease

Crystal plane	Gaussian	esd	Lorentzian	esd
(100)	0.04728	0.00157	0.02231	0.00089
$(02\bar{1})$	0.04447	0.00365	0.01565	0.00123
(002)	0.04728	0.00157	0.03222	0.00243
$(10\bar{2})$	0.05211	0.00322	0.04111	0.00113
$(13\bar{1})$	0.06822	0.00221	0.05733	0.00442
(040)	0.05692	0.00269	0.03591	0.00239
(200)	0.06249	0.00381	0.03821	0.00271
$(14\bar{2})$	0.06387	0.00268	0.04010	0.00138
$(22\bar{3})$	0.08890	0.00119	0.05889	0.00203
(004)	No peak	-	No peak	-
(080)	No peak	-	No peak	-

Calcium oxalate grown with Gla

Crystal plane	Gaussian	esd	Lorentzian	esd
(100)	0.07326	0.00056	0.03084	0.00148
$(02\bar{1})$	0.06651	0.00260	0.07957	0.00157
(002)	0.05139	0.00164	0.03413	0.00167
$(10\bar{2})$	0.06158	0.00316	0.04956	0.00384
$(13\bar{1})$	0.14838	0.00118	0.13753	0.00149
(040)	0.07392	0.00112	0.04927	0.00194
(200)	0.0.0837	0.00236	0.03987	0.00546
$(14\bar{2})$	0.11006	0.00450	0.10468	0.00438
$(22\bar{3})$	0.13396	0.00349	0.09980	0.00225
(004)	0.09743	0.00355	0.05521	0.00313
(080)	0.08356	0.01332	0.04842	0.01277

I.5 (continued)

Calcium oxalate grown with CF urine

Crystal plane	Gaussian	esd	Lorentzian	esd
(100)	0.06029	0.00069	0.03112	0.00125
$(02\bar{1})$	0.08520	0.00322	0.07340	0.00125
(002)	0.07802	0.00069	0.06207	0.00184
$(10\bar{2})$	0.05345	0.00315	0.03934	0.00525
$(13\bar{1})$	0.15948	0.00429	0.12076	0.00166
(040)	0.09931	0.00119	0.04950	0.00466
(200)	0.08036	0.00103	0.04760	0.00138
$(14\bar{2})$	0.13150	0.00421	0.09733	0.00381
$(22\bar{3})$	0.11172	0.00283	0.12814	0.00326
(004)	0.09633	0.00227	0.05541	0.00354
(080)	0.11861	0.01268	0.05432	0.01435

Calcium oxalate grown with PT

Crystal plane	Gaussian	esd	Lorentzian	esd
(100)	0.08829	0.00079	0.06271	0.00119
$(02\bar{1})$	0.09216	0.00308	0.10213	0.00245
(002)	0.07581	0.00079	0.05932	0.02119
$(10\bar{2})$	0.07642	0.00147	0.10711	0.00574
$(13\bar{1})$	0.18673	0.00157	0.15658	0.00233
(040)	0.10274	0.00123	0.05266	0.00326
(200)	0.11689	0.00246	0.07154	0.00544
$(14\bar{2})$	0.14949	0.00428	0.11091	0.00173
$(22\bar{3})$	0.18056	0.00577	0.12822	0.00227
(004)	0.14617	0.00548	0.07305	0.00335
(080)	0.1033	0.02132	0.05213	0.01189

I.6 Non-uniform strain (%) along eleven planes for COM grown in various media (chapter 6)

Angle 2θ	14.49	14.85	18.04	19.04	22.82	23.67	29.19	30.52	34.88
Crystal Plane	(100)	$(02\bar{1})$	(002)	$(10\bar{2})$	$(13\bar{1})$	(040)	(200)	$(14\bar{2})$	$(22\bar{3})$
Medium	Non-uniform strain %								
Distilled water	0.047 ±0.003	0.027 ±0.005	0.059 ±0.009	0.048 ±0.007	0.080 ±0.010	0.050 ±0.003	0.051 ±0.003	0.059 ±0.003	0.049 ±0.002
THG	0.029 ±0.002	0.052 ±0.008	0.060 ±0.010	0.041 ±0.003	0.079 ±0.009	0.054 ±0.003	0.060 ±0.004	0.027 ±0.006	0.047 ±0.004
GluGlu	0.047 ±0.005	0.028 ±0.004	0.062 ±0.008	0.051 ±0.006	0.081 ±0.003	0.049 ±0.004	0.052 ±0.006	0.058 ±0.005	0.048 ±0.005
Asp	0.039 ±0.003	0.028 ±0.008	0.068 ±0.013	0.042 ±0.003	0.063 ±0.012	0.048 ±0.004	0.051 ±0.005	0.049 ±0.006	0.047 ±0.010
AspAsp	0.046 ±0.003	0.063 ±0.005	0.070 ±0.007	0.048 ±0.004	0.078 ±0.008	0.048 ±0.005	0.049 ±0.005	0.057 ±0.006	0.047 ±0.006
Glu	0.100 ±0.008	0.039 ±0.009	0.068 ±0.009	0.055 ±0.004	0.085 ±0.009	0.047 ±0.003	0.088 ±0.004	0.043 ±0.011	0.045 ±0.003
UF urine	0.061 ±0.008	0.110 ±0.004	0.094 ±0.011	0.093 ±0.007	0.080 ±0.010	0.050 ±0.004	0.060 ±0.012	0.059 ±0.004	0.077 ±0.004
CF + PK	0.064 ±0.007	0.026 ±0.009	0.051 ±0.012	0.090 ±0.006	0.086 ±0.008	0.070 ±0.004	0.066 ±0.006	0.059 ±0.004	0.089 ±0.006
Gla	0.175 ±0.009	0.143 ±0.006	0.069 ±0.008	0.116 ±0.008	0.257 ±0.022	0.109 ±0.020	0.106 ±0.006	0.135 ±0.009	0.148 ±0.009
CF urine	0.126 ±0.011	0.208 ±0.008	0.154 ±0.012	0.094 ±0.004	0.278 ±0.017	0.160 ±0.005	0.098 ±0.004	0.167 ±0.005	0.119 ±0.004
PT	0.227 ±0.007	0.231 ±0.011	0.147 ±0.010	0.153 ±0.032	0.331 ±0.028	0.167 ±0.004	0.155 ±0.006	0.193 ±0.008	0.206 ±0.010

I.6 (continued)

Angle 2θ	36.56	48.77							
Crystal Plane	(004)	(080)							
Medium	**Non-uniform strain %**								
Distilled water	0.040 ±0.009	0.022 ±0.016							
THG	0.039 ±0.007	0.021 ±0.013							
GluGlu	0.023 ±0.008	0.037 ±0.030							
Asp	0.017 ±0.008	0.016 ±0.032							
AspAsp	0.049 ±0.009	0.040 ±0.022							
Glu	0.051 ±0.008	0.055 ±0.024							
UF urine	0.079 ±0.009	0.059 ±0.018							
CF + PK	no peak	no peak							
Gla	0.094 ±0.006	±0.055 ±0.045							
CF urine	0.093 ±0.008	±0.088 ±0.017							
PT	0.155 ±0.012	0.074 ±0.029							

I.7 Crystallite size (μm) along eleven planes for COM grown in various media (chapter 6)

Angle 2θ	14.49	14.85	18.04	19.04	22.82	23.67	29.19	30.52	34.88
Crystal Plane	(100)	$(02\bar{1})$	(002)	$(10\bar{2})$	$(13\bar{1})$	(040)	(200)	$(14\bar{2})$	$(22\bar{3})$
Medium	Crystallite size μm								
Distilled water	1.44 ±0.07	1.64 ±0.06	1.14 ±0.09	1.57 ±0.11	1.18 ±0.08	1.46 ±0.06	1.36 ±0.05	0.99 ±0.05	1.52 ±0.06
THG	1.84 ±0.08	1.52 ±0.06	1.31 ±0.11	1.59 ±0.06	0.93 ±0.05	1.25 ±0.04	1.12 ±0.04	1.12 ±0.05	1.32 ±0.12
GluGlu	1.52 ±0.08	1.61 ±0.09	1.09 ±0.09	1.58 ±0.09	1.21 ±0.08	1.41 ±0.07	1.33 ±0.10	1.09 ±0.03	1.49 ±0.04
Asp	1.48 ±0.10	1.46 ±0.12	1.17 ±0.11	1.46 ±0.05	1.28 ±0.06	1.42 ±0.06	0.90 ±0.04	1.00 ±0.08	1.29 ±0.13
AspAsp	1.42 ±0.05	1.62 ±0.08	1.11 ±0.08	1.55 ±0.10	1.13 ±0.06	1.39 ±0.07	1.29 ±0.06	1.03 ±0.05	1.48 ±0.07
Glu	0.54 ±0.08	1.47 ±0.08	0.89 ±0.11	1.33 ±0.09	0.39 ±0.06	0.96 ±0.05	0.47 ±0.03	1.49 ±0.10	1.47 ±0.13
UF urine	1.04 ±0.05	0.42 ±0.04	0.56 ±0.13	0.43 ±0.03	0.73 ±0.10	1.25 ±0.04	0.82 ±0.03	0.86 ±0.04	0.71 ±0.07
CF +PK	0.91 ±0.04	1.56 ±0.06	0.80 ±0.11	0.41 ±0.04	0.84 ±0.08	0.90 ±0.09	0.68 ±0.04	0.80 ±0.09	0.48 ±0.05
Gla	0.48 ±0.03	0.12 ±0.03	0.69 ±0.08	0.29 ±0.03	0.10 ±0.02	0.38 ±0.02	0.60 ±0.02	0.12 ±0.03	0.15 ±0.02
CF urine	0.47 ±0.03	0.14 ±0.02	0.21 ±0.11	0.45 ±0.03	0.12 ±0.02	0.38 ±0.03	0.40 ±0.04	0.13 ±0.02	0.10 ±0.03
PT	0.17 ±0.03	0.09 ±0.02	0.23 ±0.07	0.10 ±0.02	0.08 ±0.02	0.33 ±0.03	0.19 ±0.03	0.11 ±0.03	0.10 ±0.02

I.7 (continued)

Angle 2θ	36.56	48.77							
Crystal Plane	(004)	(080)							
Medium	**Crystallite size µm**								
Distilled water	1.37 ±0.08	1.59 ±0.29							
THG	1.39 ±0.11	1.42 ±0.31							
GluGlu	1.46 ±0.07	1.52 ±0.28							
Asp	1.43 ±0.12	1.45 ±0.32							
AspAsp	1.41 ±0.14	1.47 ±0.28							
Glu	1.16 ±0.09	1.15 ±0.25							
UF urine	0.56 ±0.07	1.06 ±0.27							
CF +PK	no peak ±	no peak ±							
Gla	0.61 ±0.03	1.15 ±0.31							
CF urine	0.60 ±0.06	0.66 ±0.19							
PT	0.28 ±0.03	0.78 ±0.32							

I.8 Data from Rietveld refinement (Chapter 8)

$\lambda = 0.153979$ nm

REFERENCE STANDARDS	Lanthanum hexaboride	esd	Silicon	esd
Space group	P M 3 M		F D 3 M	
Phase scale	4.81059 E-7	0.34707E-7	3.30651 E-6	0.02355 E-6
Overall thermal	Not refined		Not refined	
Thermal (La)	-1.6384	0.0614		
Thermal (B)	-1.2925	0.1389		
Thermal (Si)			0.31076	0.04933
La (x)	0.0000	Not refined		
La (y)	0.0000	Not refined		
La (z)	0.0000	Not refined		
B (x)	0.19728	0.00175		
B (y)	0.50000	Not refined		
B (z)	0.50000	Not refined		
Si (x)			0.125	Not refined
Si (y)			0.125	Not refined
Si (z)			0.125	Not refined
U	0.00149	0.00025	0.00087	0.00008
V	-0.00240	Not refined	-0.00240	Not refined
W	0.00190	Not refined	0.00190	Not refined
U anisotropy	-0.00062	0.00016	0.00013	0.00001
Lorentzian value	0.01915	0.00025	0.01738	0.00014
P.Orientation	1.01391	0.00611	0.94928	0.00529
Rp (total R)	4.36		7.17	
Rwp (total R)	6.06		9.79	

I.8 (continued)

CALCIUM OXALATE	Distilled water	esd	Gla (2.5 mg/L)	esd
Space group	P 1 21/C 1		P 1 21/C 1	
Phase scale	1.30256 E-3	0.00753 E-3	0.93157 E-3	0.00893 E-3
Overall thermal	0.39903	0.09061	1.64830	0.15398
a	6.29290	0.00012	6.30045	0.00037
b	14.59300	0.00026	14.59208	0.00093
c	10.12170	0.00017	10.12320	0.00058
β	109.4543	0.0005	109.4433	0.0014
Ca_1 (x)	0.96601	0.00045	0.97948	0.00119
Ca_1 (y)	0.12424	0.00055	0.12441	0.00096
Ca_1 (z)	0.05376	0.00032	0.05850	0.00092
Ca_2 (x)	9.99187	0.00048	0.99777	0.00124
Ca_2 (y)	0.12415	0.00055	0.11854	0.00081
Ca_2 (z)	0.43373	0.00033	0.43625	0.00092
C_1 (x)	0.97999	0.00293	1.01233	0.00647
C_1 (y)	0.31576	0.00137	0.32057	0.00321
C_1 (z)	0.23660	0.00216	0.21817	0.00310
C_2 (x)	1.01402	0.00208	1.00608	0.00910
C_2 (y)	0.42014	0.00134	0.42319	0.00308
C_2 (z)	0.25994	0.00217	0.25033	0.00616
U	0.02806	0.00042	0.03943	0.00127
V	-0.00240	Not refined	-0.00240	Not refined
W	0.00190	Not refined	0.00190	Not refined
U anisotropy	0.00163	0.00016	0.01208	0.00180
Crystallite size (μm)	1.52	0.02	1.00	0.04
P.Orientation	0.93960	0.00240	0.96393	0.00420
Rp (total R)	3.95		5.42	
Rwp (total R)	5.37		7.38	

I.8 (continued)

CALCIUM OXALATE	Gla (10.0 mg/L)	esd	Gla (50.6 mg/L)	esd
Phase scale	1.07233 E-3	0.00895 E-3	1.01053 E-3	0.00941 E-3
Overall thermal	1.39403	0.13434	1.92340	0.15044
a	6.29773	0.00035	6.29930	0.00034
b	14.58870	0.00086	14.58860	0.00097
c	10.12010	0.00055	10.12220	0.00061
β	109.4431	0.00131	109.1363	0.00157
Ca_1 (x)	0.97425	0.00097	0.97893	0.00118
Ca_1 (y)	0.13071	0.00072	0.13193	0.00072
Ca_1 (z)	0.05848	0.00075	0.05912	0.00092
Ca_2 (x)	0.99596	0.00100	0.99837	0.00120
Ca_2 (y)	0.12758	0.00082	0.12688	0.00086
Ca_2 (z)	0.43708	0.00075	0.43754	0.00091
C_1 (x)	1.00224	0.00563	1.01189	0.00552
C_1 (y)	0.33391	0.00193	0.33938	0.00216
C_1 (z)	0.21734	0.00293	0.21112	0.00302
C_2 (x)	1.01037	0.00692	1.01252	0.00720
C_2 (y)	0.43420	0.00179	0.43169	0.00186
C_2 (z)	0.26015	0.00516	0.26451	0.00510
U	0.05480	0.00121	0.05262	0.00129
V	-0.00240	Not refined	-0.00240	Not refined
W	0.00190	Not refined	0.00190	Not refined
U anisotropy	0.01419	0.00171	0.01251	0.00498
Crystallite size (μm)	0.86	0.02	0.87	0.03
P.Orientation	0.97762	0.00374	0.96630	0.00415
Rp (total R)	4.80		5.14	
Rwp (total R)	6.55		7.04	

I.8 (continued)

CALCIUM OXALATE	Gla (71.8 mg/L)	esd	Gla (98.0 mg/L)	esd
Phase scale	0.93119 E-3	0.00903E –3	1.06050 E-3	0.00833 E-3
Overall thermal	1.77415	0.15594	1.90198	0.12831
a	6.30050	0.00038	6.29894	0.00033
b	14.59210	0.00093	14.59240	0.00083
c	10.12320	0.00059	10.12270	0.00052
β	109.4433	0.00141	109.4326	0.00122
Ca_1 (x)	0.97682	0.00122	0.97459	0.00091
Ca_1 (y)	0.12474	0.00093	0.12966	0.00072
Ca_1 (z)	0.05834	0.00095	0.05878	0.00071
Ca_2 (x)	0.99545	0.00126	0.99580	0.00095
Ca_2 (y)	0.11832	0.00083	0.12656	0.00082
Ca_2 (z)	0.43635	0.00096	0.43584	0.00071
C_1 (x)	1.00948	0.00796	1.00829	0.00507
C_1 (y)	0.31689	0.00306	0.33413	0.00197
C_1 (z)	0.22679	0.00396	0.21503	0.00261
C_2 (x)	1.00588	0.00951	1.00812	0.00649
C_2 (y)	0.42079	0.00305	0.43376	0.00180
C_2 (z)	0.24618	0.00631	0.25882	0.00484
U	0.05533	0.00129	0.055354	0.00114
V	-0.00240	Not refined	-0.00240	Not refined
W	0.00190	Not refined	0.00190	Not refined
U anisotropy	0.01743	0.00177	0.01309	0.00228
Crystallite size (μm)	0.85	0.04	0.78	0.01
P.Orientation	0.96606	0.00431	1.00160	0.00364
Rp (total R)	5.42		4.74	
Rwp (total R)	7.39		6.45	

I.8 (continued)

CALCIUM OXALATE	Gla (162 mg/L)	esd	Gla (250 mg/L)	esd
Phase scale	1.04162 E-3	0.01039 E-3	1.22675 E-3	0.01164 E-3
Overall thermal	1.50693	0.16198	1.65549	0.14810
a	6.29811	0.00048	6.30096	0.00024
b	14.58607	0.00120	14.58674	0.00053
c	10.12111	0.00075	10.12322	0.00039
β	109.4328	0.00225	109.4186	0.0019
Ca_1 (x)	0.98143	0.00128	0.97801	0.00127
Ca_1 (y)	0.13263	0.00077	0.13126	0.00082
Ca_1 (z)	0.05922	0.00111	0.05778	0.00102
Ca_2 (x)	0.99923	0.00131	0.99788	0.00128
Ca_2 (y)	0.12660	0.00095	0.12589	0.00096
Ca_2 (z)	0.43668	0.00111	0.43724	0.00100
C_1 (x)	1.02419	0.00495	1.02056	0.00816
C_1 (y)	0.35027	0.00261	0.33341	0.00282
C_1 (z)	0.20991	0.00302	0.22664	0.00426
C_2 (x)	1.00376	0.00761	1.00934	0.00951
C_2 (y)	0.43024	0.00179	0.43059	0.00262
C_2 (z)	0.26589	0.00546	0.24942	0.00672
U	0.06318	0.00154	0.09961	0.00211
V	-0.00240	Not refined	-0.00240	Not refined
W	0.00190	Not refined	0.00190	Not refined
U anisotropy	0.01666	0.00364	0.01516	0.00356
Crystallite size (μm)	0.80	0.03	0.61	0.03
P.Orientation	0.94775	0.00447	0.97754	0.00450
Rp (total R)	5.22		4.72	
Rwp (total R)	7.32		6.55	

I.8 (continued)

CALCIUM OXALATE	Prothrombin (0.66 mg/L)	esd	Prothrombin (4.34 mg/L)	esd
Phase scale	1.00052 E-3	0.00875 E-3	2.91783 E-3	0.09264 E-3
Overall thermal	1.33394	0.14191	1.32941	0.09264
a	6.29880	0.00035	6.29640	0.00013
b	14.59080	0.00086	14.58950	0.00030
c	10.12150	0.00054	10.11980	0.00020
β	109.4428	0.00133	109.4447	0.00067
Ca_1 (x)	0.97191	0.00095	0.96970	0.00051
Ca_1 (y)	0.13011	0.00077	0.12623	0.00066
Ca_1 (z)	0.05776	0.00076	0.05455	0.00039
Ca_2 (x)	0.99370	0.00100	0.99547	0.00053
Ca_2 (y)	0.12785	0.00088	0.12537	0.00068
Ca_2 (z)	0.43514	0.00076	0.43461	0.00039
C_1 (x)	0.99132	0.00470	0.98059	0.00328
C_1 (y)	0.33854	0.00206	0.32153	0.00294
C_1 (z)	0.20365	0.00281	0.23210	0.00203
C_2 (x)	1.01276	0.00667	1.00776	0.00394
C_2 (y)	0.43168	0.00182	0.42821	0.00288
C_2 (z)	0.26780	0.00469	0.25380	0.00267
U	0.04130	0.00112	0.04870	0.00066
V	-0.00240	Not refined	-0.00240	Not refined
W	0.00190	Not refined	0.00190	Not refined
U anisotropy	0.01870	0.00388	0.01031	0.00134
Crystallite size (μm)	0.92	0.04	0.75	0.02
P.Orientation	0.96490	0.00388	0.97780	0.00227
Rp (total R)	4.80		4.73	
Rwp (total R)	6.51		6.43	

I.8 (continued)

CALCIUM OXALATE	Prothrombin (10.3 mg/L)	esd	Prothrombin (21.4 mg/L)	esd
Phase scale	2.25142 E-3	0.01768 E-3	1.17117 E-3	0.01256 E-3
Overall thermal	1.13537	0.11717	2.32547	0.18898
a	6.29820	0.00019	6.30110	0.00028
b	14.58840	0.00046	14.59190	0.00070
c	10.12040	0.00031	10.12320	0.00043
β	109.4434	0.0012	109.4431	0.0009
Ca_1 (x)	0.97498	0.00084	0.97130	0.00125
Ca_1 (y)	0.12529	0.00090	0.13012	0.00100
Ca_1 (z)	0.05703	0.00066	0.05795	0.00089
Ca_2 (x)	0.99817	0.00087	0.99286	0.00130
Ca_2 (y)	0.12147	0.00083	0.12487	0.00115
Ca_2 (z)	0.43605	0.00067	0.43193	0.00089
C_1 (x)	0.99987	0.00565	0.98485	0.00522
C_1 (y)	0.31564	0.00217	0.33560	0.00264
C_1 (z)	0.22692	0.00286	0.17277	0.00290
C_2 (x)	1.00026	0.00685	1.00182	0.00890
C_2 (y)	0.41959	0.00212	0.43714	0.00217
C_2 (z)	0.24527	0.00461	0.25714	0.00551
U	0.07425	0.00126	0.09754	0.00061
V	-0.00240	Not refined	-0.00240	Not refined
W	0.00190	Not refined	0.00190	Not refined
U anisotropy	0.01103	0.00308	0.01246	0.00079
Crystallite size (μm)	0.64	0.03	0.42	0.01
P.Orientation	0.98160	0.00333	1.16180	0.00559
Rp (total R)	5.97		6.25	
Rwp (total R)	8.18		8.91	

I.8 (continued)

CALCIUM OXALATE	CME (0.72 mg/L)	esd	CME (2.3 mg/L)	Esd
Phase scale	2.24009 E-3	0.01729 E-3	2.21871 E-3	0.01815 E-3
Overall thermal	1.33828	0.12665	2.80702	0.13859
a	6.29629	0.00021	6.29849	0.000174
b	14.58719	0.00050	14.58772	0.00037
c	10.11900	0.00034	10.11962	0.00027
β	109.4364	0.00132	109.4355	0.0014
Ca_1 (x)	0.97368	0.00079	0.97936	0.00113
Ca_1 (y)	0.13174	0.00052	0.13213	0.00056
Ca_1 (z)	0.05747	0.00060	0.05860	0.00084
Ca_2 (x)	0.99463	0.00082	1.00022	0.00115
Ca_2 (y)	0.12555	0.00063	0.12569	0.00068
Ca_2 (z)	0.43590	0.00059	0.43776	0.00083
C_1 (x)	1.00456	0.00463	1.00091	0.00625
C_1 (y)	0.33361	0.00177	0.33260	0.00187
C_1 (z)	0.21797	0.00223	0.22446	0.00287
C_2 (x)	0.99971	0.00604	0.99623	0.00767
C_2 (y)	0.43285	0.00164	0.433260	0.00176
C_2 (z)	0.25387	0.00409	0.25311	0.00438
U	0.07132	0.00139	0.08290	0.00161
V	-0.00240	Not refined	-0.00240	Not refined
W	0.00190	Not refined	0.00190	Not refined
U anisotropy	0.01908	0.004020	0.01730	0.00382
Crystallite size (μm)	0.65	0.02	0.64	0.02
P.Orientation	0.96733	0.00329	0.98430	0.00364
Rp (total R)	5.74		6.24	
Rwp (total R)	7.89		8.72	

I.8 (continued)

CALCIUM OXALATE	CME (3.1 mg/L)	esd	CME (4.2 mg/L)	Esd
Phase scale	2.42305 E-3	0.01976 E-3	2.02787 E-3	0.01460 E-3
Overall thermal	2.12390	0.13498	1.10668	0.11639
a	6.29919	0.00019	6.29441	0.00028
b	14.58788	0.00043	14.58419	0.00068
c	10.12091	0.00032	10.11756	0.00044
β	109.4307	0.0017	109.4370	0.0012
Ca_1 (x)	0.97741	0.00101	0.97213	0.00071
Ca_1 (y)	0.13240	0.00055	0.13051	0.00054
Ca_1 (z)	0.05918	0.00077	0.05667	0.00055
Ca_2 (x)	0.99646	0.00105	0.99410	0.00074
Ca_2 (y)	0.12598	0.00066	0.12638	0.00063
Ca_2 (z)	0.43632	0.00076	0.43529	0.00054
C_1 (x)	1.00203	0.00506	0.99854	0.00459
C_1 (y)	0.33643	0.00186	0.32826	0.00192
C_1 (z)	0.21467	0.00240	0.22225	0.00219
C_2 (x)	1.00002	0.00706	1.00682	0.00556
C_2 (y)	0.43045	0.00165	0.43210	0.00184
C_2 (z)	0.25279	0.00405	0.25125	0.00391
U	0.09992	0.00198	0.09831	0.00139
V	-0.00240	Not refined	-0.00240	Not refined
W	0.00190	Not refined	0.00190	Not refined
U anisotropy	0.03205	0.00244	0.03102	0.00244
Crystallite size (μm)	0.50	0.02	0.46	0.01
P.Orientation	0.96045	0.00370	0.97185	0.00308
Rp (total R)	6.15		5.33	
Rwp (total R)	8.44		7.26	

I.8 (continued)

CALCIUM OXALATE	CME (10.9 mg/L)	esd	CME / UF (0.05 mg/L)	esd
Phase scale	2.18585 E-3	0.01873 E-3	2.14902 E-3	0.01611 E-3
Overall thermal	2.60015	0.14339	3.05968	0.11839
a	6.29878	0.00027	6.30186	0.00017
b	14.58652	0.00063	14.60063	0.00393
c	10.12071	0.00041	10.12779	0.00027
β	109.4453	0.0015	109.4616	0.0012
Ca_1 (x)	0.97737	0.00119	0.98442	0.00122
Ca_1 (y)	0.13122	0.00071	0.12786	0.00061
Ca_1 (z)	0.05874	0.00087	0.05812	0.00104
Ca_2 (x)	0.99974	0.00123	1.00850	0.00128
Ca_2 (y)	0.12524	0.00090	0.13072	0.00058
Ca_2 (z)	0.43727	0.00086	0.43908	0.00105
C_1 (x)	0.99949	0.00550	1.00093	0.00770
C_1 (y)	0.33779	0.00219	0.33109	0.00154
C_1 (z)	0.21472	0.00260	0.24384	0.00521
C_2 (x)	0.99513	0.00844	0.99391	0.00654
C_2 (y)	0.43344	0.00194	0.43519	0.00152
C_2 (z)	0.25273	0.00464	0.26053	0.00410
U	0.10573	0.00172	0.06100	0.00109
V	-0.00240	Not refined	-0.00240	Not refined
W	0.00190	Not refined	0.00190	Not refined
U anisotropy	0.02803	0.00324	0.01844	0.00293
Crystallite size (μm)	0.36	0.01	0.86	0.03
P.Orientation	0.97795	0.00393	1.01193	0.00333
Rp (total R)	5.53		5.88	
Rwp (total R)	7.80		8.39	

I.8 (continued)

CALCIUM OXALATE	CME / UF (0.50 mg/L)	esd	CME / UF (1.0 mg/L)	esd
Phase scale	2.09091 E-3	0.01386 E-3	2.26330 E-3	0.01559 E-3
Overall thermal	2.61581	0.11168	3.11308	0.11827
a	6.29864	0.00014	6.29706	0.00017
b	14.59393	0.00032	14.59072	0.00038
c	10.12498	0.00023	10.12463	0.00028
β	109.4661	0.0009	109.4706	0.0013
Ca_1 (x)	0.98427	0.00117	0.98659	0.00125
Ca_1 (y)	0.12982	0.00060	0.12210	0.00065
Ca_1 (z)	0.05858	0.00087	0.05935	0.00093
Ca_2 (x)	1.00705	0.00121	1.00942	0.00130
Ca_2 (y)	0.12952	0.00063	0.11816	0.00057
Ca_2 (z)	0.43827	0.00086	0.44046	0.00094
C_1 (x)	0.99863	0.00604	1.00286	0.00675
C_1 (y)	0.32741	0.00149	0.31582	0.00184
C_1 (z)	0.23151	0.00293	0.23226	0.00362
C_2 (x)	0.99345	0.00723	0.99414	0.00728
C_2 (y)	0.43404	0.00146	0.42262	0.00185
C_2 (z)	0.25270	0.00498	0.23954	0.00432
U	0.06311	0.00100	0.07409	0.00149
V	-0.00240	Not refined	-0.00240	Not refined
W	0.00190	Not refined	0.00190	Not refined
U anisotropy	0.01726	0.00243	0.01035	0.00348
Crystallite size (μm)	0.52	0.01	0.34	0.01
P.Orientation	1.00054	0.00292	1.01454	0.00323
Rp (total R)	4.73		5.02	
Rwp (total R)	6.65		6.91	

I.8 (continued)

CALCIUM OXALATE	CME / UF (5.0 mg/L)	esd	HSA (12.2 mg/L)	esd
Phase scale	1.96020 E-3	0.01889 E-3	0.61791 E-3	0.00496 E-3
Overall thermal	3.36009	0.15935	2.96549	0.13441
a	6.29334	0.00074	6.29584	0.00032
b	14.58510	0.00181	14.58526	0.00078
c	10.12673	0.00112	10.11866	0.00049
β	109.4823	0.0028	109.4345	0.0011
Ca_1 (x)	0.98248	0.00196	0.96669	0.00084
Ca_1 (y)	0.12341	0.00101	0.13028	0.00077
Ca_1 (z)	0.05788	0.00131	0.05730	0.00069
Ca_2 (x)	1.00613	0.00207	0.98696	0.00089
Ca_2 (y)	0.11706	0.00082	0.12727	0.00089
Ca_2 (z)	0.43977	0.00134	0.43586	0.00069
C_1 (x)	1.01450	0.01208	1.00399	0.00450
C_1 (y)	0.31015	0.00231	0.33402	0.00217
C_1 (z)	0.24585	0.00630	0.20594	0.00288
C_2 (x)	0.99913	0.00946	1.00779	0.00627
C_2 (y)	0.41280	0.00256	0.43370	0.00196
C_2 (z)	0.23174	0.00458	0.26570	0.00480
U	0.06828	0.00499	0.03811	0.00086
V	-0.00240	Not refined	-0.00240	Not refined
W	0.00190	Not refined	0.00190	Not refined
U anisotropy	0.02374	0.00149	0.01249	0.00125
Crystallite size (μm)	0.10	0.01	0.86	0.01
P.Orientation	0.94899	0.00467	1.02390	0.00393
Rp (total R)	5.42		3.69	
Rwp (total R)	7.77		4.92	

I.8 (continued)

CALCIUM OXALATE	HSA (31.6 mg/L)	esd	HSA (61.4 mg/L)	esd
Phase scale	0.89652 E-3	0.00678 E-3	0.94529 E-3	0.00655 E-3
Overall thermal	1.75178	0.12553	2.19369	0.11786
a	6.29728	0.00033	6.29813	0.00013
b	14.58649	0.00081	14.58996	0.00030
c	10.12080	0.00051	10.12286	0.00020
β	109.4413	0.0011	109.4515	0.0008
Ca_1 (x)	0.97329	0.00079	0.97109	0.00073
Ca_1 (y)	0.13101	0.00061	0.12991	0.00060
Ca_1 (z)	0.05854	0.00062	0.05682	0.00055
Ca_2 (x)	0.99310	0.00083	0.99390	0.00077
Ca_2 (y)	0.12703	0.00070	0.12668	0.00069
Ca_2 (z)	0.43552	0.00062	0.43702	0.00058
C_1 (x)	1.00002	0.00400	0.98605	0.00429
C_1 (y)	0.32960	0.00184	0.32564	0.00208
C_1 (z)	0.20700	0.00211	0.22322	0.00239
C_2 (x)	1.00302	0.00611	1.00117	0.00571
C_2 (y)	0.43182	0.00167	0.42982	0.00200
C_2 (z)	0.25703	0.00436	0.25674	0.00416
U	0.04820	0.00101	0.05153	0.00091
V	-0.00240	Not refined	-0.00240	Not refined
W	0.00190	Not refined	0.00190	Not refined
U anisotropy	0.02302	0.00252	0.01446	0.00172
Crystallite size (μm)	0.63	0.02	0.68	0.02
P.Orientation	0.99310	0.00336	1.00235	0.00297
Rp (total R)	5.02		4.36	
Rwp (total R)	6.69		6.01	

I.8 (continued)

CALCIUM OXALATE	HSA (123.9 mg/L)	esd	HSA (160.4 mg/L)	esd
Phase scale	0.78953 E-3	0.00736 E-3	0.70749 E-3	0.00657 E-3
Overall thermal	2.30501	0.15553	2.89521	0.15522
a	6.29798	0.00034	6.29804	0.00036
b	14.58417	0.00083	14.58310	0.00088
c	10.11957	0.00054	10.12005	0.00057
β	109.4444	0.0017	109.4327	0.0018
Ca_1 (x)	0.97760	0.00124	0.97996	0.00144
Ca_1 (y)	0.13400	0.00067	0.13481	0.00066
Ca_1 (z)	0.05977	0.00097	0.06103	0.00111
Ca_2 (x)	0.99631	0.00128	0.99876	0.00147
Ca_2 (y)	0.12639	0.00084	0.12595	0.00083
Ca_2 (z)	0.43726	0.00096	0.43804	0.00110
C_1 (x)	1.00107	0.00536	1.00459	0.00581
C_1 (y)	0.33899	0.00209	0.33967	0.00223
C_1 (z)	0.20323	0.00301	0.20638	0.00316
C_2 (x)	0.99952	0.00831	0.99861	0.00881
C_2 (y)	0.43542	0.00180	0.43057	0.00188
C_2 (z)	0.26453	0.00567	0.26222	0.00616
U	0.05352	0.00137	0.05542	0.00148
V	-0.00240	Not refined	-0.00240	Not refined
W	0.00190	Not refined	0.00190	Not refined
U anisotropy	0.01141	0.00536	0.01449	0.00147
Crystallite size (μm)	0.66	0.04	0.73	0.03
P.Orientation	0.99066	0.00450	0.99241	0.00466
Rp (total R)	5.27		4.88	
Rwp (total R)	7.26		6.80	

I.8 (continued)

CALCIUM OXALATE	HSA (312.5 mg/L)	esd	HSA / UF (0.0 mg/L)	esd
Phase scale	0.91488 E-3	0.00692 E-3	0.53138 E-3	0.01118 E-3
Overall thermal	1.44652	0.12627	3.83968	0.35586
a	6.29851	0.00032	6.29469	0.00039
b	14.58737	0.00079	14.57970	0.00084
c	10.12226	0.00050	10.11555	0.00070
β	109.4405	0.0010	109.45030	0.00372
Ca_1 (x)	0.97216	0.00078	0.98701	0.00443
Ca_1 (y)	0.13078	0.00061	0.12864	0.00216
Ca_1 (z)	0.05794	0.00061	0.05826	0.00360
Ca_2 (x)	0.99350	0.00082	1.01022	0.00459
Ca_2 (y)	0.12683	0.00070	0.13104	0.00208
Ca_2 (z)	0.43671	0.00061	0.44071	0.00362
C_1 (x)	0.99729	0.00418	1.00842	0.02384
C_1 (y)	0.32891	0.00190	0.33471	0.00495
C_1 (z)	0.21331	0.00226	0.23939	0.01567
C_2 (x)	1.00135	0.00610	0.99406	0.01767
C_2 (y)	0.43151	0.00177	0.43856	0.00487
C_2 (z)	0.25777	0.00439	0.27482	0.01054
U	0.05590	0.00105	0.04824	0.00277
V	-0.00240	Not refined	-0.00240	Not refined
W	0.00190	Not refined	0.00190	Not refined
U anisotropy	0.01089	0.00234	0.01222	0.00193
Crystallite size (μm)	0.64	0.02	1.02	0.05
P.Orientation	1.00744	0.00336	0.96616	0.00998
Rp (total R)	4.75		6.59	
Rwp (total R)	6.46		8.38	

I.8 (continued)

CALCIUM OXALATE	HSA / UF (10 mg/L)	esd	HSA / UF (30 mg/L)	esd
Phase scale	0.78743 E-3	0.01160 E-3	0.48571 E-3	0.01542 E-3
Overall thermal	1.72087	0.242104	1.55556	0.35416
a	6.29411	0.00029	6.29421	0.00834
b	14.57923	0.00065	14.57893	0.00206
c	10.11390	0.00046	10.11441	0.00131
β	109.4412	0.0021	109.4380	0.0036
Ca_1 (x)	0.98012	0.00253	0.98253	0.00441
Ca_1 (y)	0.12487	0.00177	0.12166	0.00232
Ca_1 (z)	0.05773	0.00176	0.05660	0.00306
Ca_2 (x)	1.00618	0.00264	1.00962	0.00455
Ca_2 (y)	0.12557	0.00174	0.12531	0.00234
Ca_2 (z)	0.43876	0.00177	0.44091	0.00309
C_1 (x)	0.99577	0.00972	1.01508	0.01478
C_1 (y)	0.30934	0.00334	0.29997	0.00360
C_1 (z)	0.21095	0.00469	0.21045	0.00814
C_2 (x)	0.99404	0.01739	0.99750	0.02790
C_2 (y)	0.41678	0.00309	0.40533	0.00384
C_2 (z)	0.24670	0.01056	0.24296	0.01742
U	0.05712	0.00206	0.05249	0.00294
V	-0.00240	Not refined	-0.00240	Not refined
W	0.00190	Not refined	0.00190	Not refined
U anisotropy	0.02280	0.00545	0.02204	0.00116
Crystallite size (μm)	0.89	0.09	0.89	0.08
P.Orientation	0.97924	0.00649	0.95450	0.01003
Rp (total R)	5.85		5.99	
Rwp (total R)	9.98		10.75	

I.8 (continued)

CALCIUM OXALATE	HSA / UF (60 mg/L)	esd	THG (7.6 mg/L)	esd
Phase scale	0.79495 E-3	0.01519 E-3	0.97185 E-3	0.00862 E-3
Overall thermal	2.15751	0.11273	2.15705	0.14384
a	6.29556	0.00040	6.30121	0.00049
b	14.58213	0.00089	14.59193	0.00122
c	10.11605	0.00068	10.12689	0.00075
β	109.4471	0.0034	109.4188	0.0023
Ca_1 (x)	0.98182	0.00368	0.98106	0.00143
Ca_1 (y)	0.12392	0.00231	0.13406	0.00064
Ca_1 (z)	0.05819	0.00287	0.05874	0.00108
Ca_2 (x)	1.00733	0.00390	0.99801	0.00150
Ca_2 (y)	0.12566	0.00223	0.12607	0.00081
Ca_2 (z)	0.44008	0.00284	0.43597	0.00106
C_1 (x)	1.01714	0.01419	1.01446	0.00518
C_1 (y)	0.30889	0.00362	0.34741	0.00227
C_1 (z)	0.22096	0.00739	0.20798	0.00269
C_2 (x)	1.00134	0.02419	0.99761	0.00856
C_2 (y)	0.40762	0.00382	0.43273	0.00169
C_2 (z)	0.25449	0.01558	0.25854	0.00474
U	0.06462	0.00301	0.02869	0.00108
V	-0.00240	Not refined	-0.00240	Not refined
W	0.00190	Not refined	0.00190	Not refined
U anisotropy	0.02298	0.00114	0.01371	0.00108
Crystallite size (μm)	0.75	0.07	1.47	0.09
P.Orientation	0.95352	0.00852	0.94240	0.00420
Rp (total R)	6.38		4.40	
Rwp (total R)	10.19		6.10	

I.8 (continued)

CALCIUM OXALATE	THG (22.3 mg/L)	esd	THG (34.0 mg/L)	esd
Phase scale	1.05781 E-3	0.00889 E-3	1.18532 E-3	0.01093 E-3
Overall thermal	2.64076	0.13947	2.39863	0.15029
a	6.30251	0.00046	6.29996	0.00039
b	14.59606	0.00114	14.58763	0.00094
c	10.12768	0.00071	10.12399	0.00062
β	109.4340	0.0016	109.4224	0.00232
Ca_1 (x)	0.97469	0.00104	0.98155	0.00159
Ca_1 (y)	0.13109	0.00070	0.13432	0.00064
Ca_1 (z)	0.05893	0.00084	0.05829	0.00121
Ca_2 (x)	0.99541	0.00107	1.00117	0.00163
Ca_2 (y)	0.12613	0.00086	0.12655	0.00079
Ca_2 (z)	0.43734	0.00083	0.43719	0.00119
C_1 (x)	1.00572	0.00579	1.01256	0.00568
C_1 (y)	0.33614	0.00221	0.34825	0.00226
C_1 (z)	0.21973	0.00303	0.21272	0.00296
C_2 (x)	1.00064	0.00764	0.99890	0.00905
C_2 (y)	0.43051	0.00200	0.42867	0.00167
C_2 (z)	0.25925	0.00494	0.25865	0.00518
U	0.02834	0.00109	0.02849	0.00178
V	-0.00240	Not refined	-0.00240	Not refined
W	0.00190	Not refined	0.00190	Not refined
U anisotropy	0.02348	0.00132	0.01899	0.00178
Crystallite size (μm)	1.51	0.06	1.49	0.09
P.Orientation	0.96491	0.00126	0.94597	0.00449
Rp (total R)	4.98		4.91	
Rwp (total R)	6.87		6.77	

I.9 Discrete peak analysis using the $(13\bar{1})$ plane (chapter 8)

Aqueous solutions

COM growing medium and concentration (mg/L)	Strain (%)	esd	Crystallite Size (μm)	esd
Gla (aqueous)				
0.00	0.053	0.016	1.01	0.01
2.5	0.064	0.022	0.65	0.01
10.0	0.086	0.018	0.34	0.01
50.6	0.144	0.008	0.20	0.01
71.8	0.173	0.011	0.18	0.01
98.0	0.213	0.016	0.13	0.01
162.0	0.246	0.016	0.10	0.01
250.1	0.256	0.020	0.10	0.01
PT (aqueous)				
0.00	0.053	0.016	1.01	0.01
0.7	0.166	0.016	0.12	0.01
4.3	0.204	0.020	0.10	0.01
10.3	0.238	0.012	0.09	0.01
21.4	0.249	0.022	0.08	0.01
HSA (aqueous)				
0.00	0.053	0.016	1.01	0.01
12.2	0.075	0.006	0.22	0.01
31.6	0.135	0.020	0.14	0.01
61.4	0.143	0.021	0.13	0.01
123.9	0.137	0.030	0.17	0.01
160.4	0.152	0.020	0.17	0.01
312.5	0.152	0.028	0.14	0.01
CME (aqueous)				
0.00	0.053	0.016	1.01	0.01
0.7	0.141	0.010	0.15	0.01
2.3	0.202	0.014	0.11	0.01
3.1	0.208	0.013	0.10	0.01
4.2	0.220	0.018	0.09	0.01
11.0	0.235	0.011	0.09	0.01

I.9 (continued)

Ultrafiltered urine

COM growing medium and concentration (mg/L)	Strain (%)	esd	Crystallite Size (μm)	esd
HSA (UF)				
0.0	0.086	0.009	0.51	0.01
10.0	0.148	0.023	0.20	0.01
30.0	0.152	0.036	0.13	0.01
60.0	0.150	0.020	0.14	0.01
CME (UF)				
0.0	0.086	0.009	0.51	0.01
0.05	0.103	0.020	0.23	0.01
0.5	0.144	0.009	0.14	0.01
1.0	0.179	0.016	0.11	0.01
5.0	0.221	0.017	0.08	0.01

I.10 Statistics - Rietveld (chapter 8)

Null hypothesis tests for Rietveld derived non-uniform strain versus reciprocal crystallite size relationships for COM

Growing medium 1	Growing medium 2	z	p
Gla	PT	6.58	~0
Gla	HSA	7.28	~0
Gla	CME	8.97	~0
Gla	HSA (UF)	3.56	~0
Gla	CME (UF)	9.22	~0
PT	HSA	0.77	0.22
PT	CME	1.23	0.11
PT	HSA (UF)	0.98	0.16
HSA	CME	0.40	0.34
HSA	HSA (UF)	1.59	0.06
CME	HSA (UF)	2.01	0.02
CME (UF)	PT	7.32	~0
CME (UF)	HSA	7.03	~0
CME (UF)	CME	6.85	~0
CME (UF)	HSA (UF)	7.52	~0

I.11 Statistics- Shadow (chapter 8)

Null hypothesis tests for Shadow derived non-uniform strain versus reciprocal crystallite size relationships for COM

Growing medium 1	Growing medium 2	z	p
Gla	PT	9.23	~0
Gla	HSA	1.51	0.07
Gla	CME	13	~0
Gla	HSA (UF)	2.60	<0.01
Gla	CME (UF)	12	~0
PT	HSA	1.37	0.08
PT	CME	0.00	0.50
PT	HSA (UF)	1.38	0.08
HSA	CME	0.40	0.34
HSA	HSA (UF)	1.84	0.03
CME	HSA (UF)	1.39	0.08
CME (UF)	PT	5.39	~0
CME (UF)	HSA	3.89	~0
CME (UF)	CME	5.89	~0
CME (UF)	HSA (UF)	0.17	0.43

I.12 Gaussian, Lorentzian and FWHM on four crystal planes (Chapter 8)

Aqueous

Crystal Plane	Gaussian	Lorentzian	FWHM
Gla 2.50 mg/L			
(100)	0.05282 ± 0.00086	0.03255 ± 0.00143	0.0536 ± 0.0006
$(02\bar{1})$	0.04714 ± 0.00401	0.06371 ± 0.00164	0.0633 ± 0.0024
$(13\bar{1})$	0.06093 ± 0.00158	0.06071 ± 0.00830	0.0677 ± 0.0095
(040)	0.04872 ± 0.00074	0.04196 ± 0.00081	0.0532 ± 0.0004
Gla 10.00 mg/L			
(100)	0.05982 ± 0.00075	0.03219 ± 0.00150	0.0596 ± 0.0005
$(02\bar{1})$	0.06207 ± 0.00496	0.04764 ± 0.00184	0.0664 ± 0.0024
$(13\bar{1})$	0.06881 ± 0.00769	0.07311 ± 0.00401	0.0801 ± 0.0098
(040)	0.05787 ± 0.00054	0.04733 ± 0.00065	0.0622 ± 0.0003
Gla 50.60 mg/L			
(100)	0.05676 ± 0.00078	0.03253 ± 0.00148	0.0571 ± 0.0005
$(02\bar{1})$	0.05597 ± 0.00372	0.05113 ± 0.00169	0.0622 ± 0.0019
$(13\bar{1})$	0.09431 ± 0.00453	0.09192 ± 0.00619	0.0966 ± 0.0064
(040)	0.05309 ± 0.00059	0.04751 ± 0.00060	0.0582 ± 0.0003
Gla 71.80 mg/L			
(100)	0.05475 ± 0.00124	0.05997 ± 0.00080	0.0652 ± 0.0007
$(02\bar{1})$	0.05945 ± 0.00396	0.06677 ± 0.00270	0.0719 ± 0.0020
$(13\bar{1})$	0.10862 ± 0.00582	0.09784 ± 0.00122	0.1108 ± 0.0067
(040)	0.05223 ± 0.00083	0.06377 ± 0.00042	0.0655 ± 0.0005
Gla 98.00 mg/L			
(100)	0.05754 ± 0.00077	0.03392 ± 0.00217	0.0581 ± 0.0005
$(02\bar{1})$	0.06419 ± 0.00387	0.06546 ± 0.00328	0.0750 ± 0.0020
$(13\bar{1})$	0.12921 ± 0.01883	0.11503 ± 0.02223	0.1299 ± 0.0074
(040)	0.05181 ± 0.00059	0.04433 ± 0.00065	0.0531 ± 0.0003
Gla 162.00 mg/L			
(100)	0.06030 ± 0.00078	0.02646 ± 0.00205	0.0591 ± 0.0005
$(02\bar{1})$	0.06137 ± 0.00350	0.06573 ± 0.00255	0.0665 ± 0.0018
$(13\bar{1})$	0.14631 ± 0.00879	0.13502 ± 0.02513	0.1490 ± 0.0066
(040)	0.05521 ± 0.00057	0.05044 ± 0.00055	0.0613 ± 0.0004
Gla 250.00 mg/L			
(100)	0.06989 ± 0.00152	0.03336 ± 0.00363	0.0687 ± 0.0009
$(02\bar{1})$	0.07849 ± 0.00627	0.04179 ± 0.01083	0.0801 ± 0.0030
$(13\bar{1})$	0.15172 ± 0.00902	0.13820 ± 0.03112	0.1568 ± 0.0199
(040)	0.06963 ± 0.00144	0.05214 ± 0.00201	0.0733 ± 0.0008

I.12 (continued)

Aqueous

Crystal Plane	Gaussian	Lorentzian	FWHM
PT 0.66 mg/L			
(100)	0.06711 ± 0.00112	0.05376 ± 0.00375	0.0647 ± 0.0007
$(02\bar{1})$	0.07023 ± 0.00533	0.05670 ± 0.01088	0.0737 ± 0.0027
$(13\bar{1})$	0.10504 ± 0.00840	0.12213 ± 0.00553	0.1124 ± 0.0087
(040)	0.06516 ± 0.00081	0.05290 ± 0.00139	0.0671 ± 0.0005
PT 4.34 mg/L			
(100)	0.07146 ± 0.00097	0.06672 ± 0.00211	0.0712 ± 0.0006
$(02\bar{1})$	0.07032 ± 0.00393	0.06599 ± 0.00593	0.0745 ± 0.0020
$(13\bar{1})$	0.12462 ± 0.02179	0.13977 ± 0.02033	0.1301 ± 0.0090
(040)	0.07161 ± 0.00082	0.04658 ± 0.00050	0.0716 ± 0.0005
PT 10.34 mg/L			
(100)	0.08686 ± 0.00115	0.06810 ± 0.00292	0.0886 ± 0.0007
$(02\bar{1})$	0.08251 ± 0.00453	0.07820 ± 0.00193	0.0881 ± 0.0023
$(13\bar{1})$	0.14203 ± 0.00698	0.14964 ± 0.00236	0.1498 ± 0.0038
(040)	0.08039 ± 0.00046	0.06883 ± 0.00066	0.0828 ± 0.0003
PT 21.40 mg/L			
(100)	0.08576 ± 0.0006	0.08744 ± 0.00087	0.0894 ± 0.0004
$(02\bar{1})$	0.08603 ± 0.00167	0.08647 ± 0.00205	0.0889 ± 0.0009
$(13\bar{1})$	0.14804 ± 0.01235	0.15123 ± 0.07125	0.1576 ± 0.0047
(040)	0.08013 ± 0.00115	0.07322 ± 0.00230	0.0805 ± 0.0007

I.12 (continued)

Aqueous

Crystal Plane	Gaussian	Lorentzian	FWHM
HSA 12.21 mg/L			
(100)	0.06268 ± 0.00076	0.03902 ± 0.00185	0.0636 ± 0.0005
$(02\bar{1})$	0.05935 ± 0.00258	0.04985 ± 0.00315	0.0645 ± 0.0014
$(13\bar{1})$	0.06533 ± 0.00925	0.08862 ± 0.00308	0.0847 ± 0.0052
(040)	0.05917 ± 0.00109	0.03979 ± 0.00179	0.0609 ± 0.0004
HSA 31.62 mg/L			
(100)	0.05461 ± 0.00092	0.03204 ± 0.00165	0.0550 ± 0.0006
$(02\bar{1})$	0.06216 ± 0.00468	0.06776 ± 0.00335	0.0748 ± 0.0024
$(13\bar{1})$	0.09023 ± 0.01764	0.11122 ± 0.01004	0.0986 ± 0.0096
(040)	0.05958 ± 0.00094	0.04715 ± 0.00085	0.0608 ± 0.0005
HSA 61.41 mg/L			
(100)	0.05677 ± 0.00088	0.03290 ± 0.00164	0.0572 ± 0.0005
$(02\bar{1})$	0.05185 ± 0.00528	0.07578 ± 0.00195	0.0737 ± 0.0026
$(13\bar{1})$	0.09412 ± 0.02720	0.11618 ± 0.01069	0.1196 ± 0.0115
(040)	0.05285 ± 0.00084	0.05221 ± 0.00070	0.0603 ± 0.0005
HSA 123.93 mg/L			
(100)	0.05350 ± 0.00126	0.04962 ± 0.00074	0.0549 ± 0.0007
$(02\bar{1})$	0.05388 ± 0.00355	0.04994 ± 0.00236	0.0543 ± 0.0018
$(13\bar{1})$	0.09133 ± 0.01985	0.09805 ± 0.01475	0.1181 ± 0.0093
(040)	0.05157 ± 0.00106	0.04452 ± 0.00071	0.0535 ± 0.0006
HSA 160.42 mg/L			
(100)	0.05015 ± 0.00071	0.03425 ± 0.00105	0.0519 ± 0.0005
$(02\bar{1})$	0.05459 ± 0.00265	0.05593 ± 0.00167	0.0599 ± 0.0015
$(13\bar{1})$	0.09831 ± 0.01869	0.09817 ± 0.01020	0.1133 ± 0.0103
(040)	0.05092 ± 0.00140	0.04868 ± 0.00123	0.0576 ± 0.0008
HSA 312.52 mg/L			
(100)	0.05223 ± 0.00149	0.03636 ± 0.00185	0.0537 ± 0.0007
$(02\bar{1})$	0.07209 ± 0.00480	0.05010 ± 0.00190	0.0725 ± 0.0024
$(13\bar{1})$	0.09844 ± 0.01286	0.11045 ± 0.01427	0.1168 ± 0.0058
(040)	0.05797 ± 0.00075	0.04790 ± 0.00088	0.0624 ± 0.0004

I.12 (continued)

Aqueous

Crystal Plane	Gaussian	Lorentzian	FWHM
CME 0.72 mg/L			
(100)	0.06679 ± 0.00078	0.02866 ± 0.00206	0.0682 ± 0.0005
$(02\bar{1})$	0.06544 ± 0.00351	0.07691 ± 0.00196	0.0808 ± 0.0018
$(13\bar{1})$	0.09332 ± 0.00550	0.10726 ± 0.01357	0.1082 ± 0.0075
(040)	0.06528 ± 0.00064	0.04769 ± 0.00089	0.0680 ± 0.0004
CME 2.32 mg/L			
(100)	0.05726 ± 0.00118	0.02382 ± 0.00453	0.0580 ± 0.0007
$(02\bar{1})$	0.05840 ± 0.00582	0.08103 ± 0.00227	0.0682 ± 0.0029
$(13\bar{1})$	0.12330 ± 0.00750	0.12982 ± 0.00846	0.1294 ± 0.0058
(040)	0.06641 ± 0.00066	0.04886 ± 0.00091	0.0695± 0.0004
CME 3.13 mg/L			
(100)	0.06873 ± 0.00087	0.03062 ± 0.00261	0.0763 ± 0.0005
$(02\bar{1})$	0.06698 ± 0.00379	0.06916 ± 0.00402	0.0767 ± 0.0019
$(13\bar{1})$	0.12643 ± 0.0072	0.13420 ± 0.01519	0.1337 ± 0.0076
(040)	0.07011 ± 0.00061	0.05146 ± 0.00090	0.0719 ± 0.0004
CME 4.21 mg/L			
(100)	0.06951 ± 0.00075	0.03472 ± 0.00171	0.0701 ± 0.0005
$(02\bar{1})$	0.06753 ± 0.00260	0.06676 ± 0.00225	0.0771 ± 0.0014
$(13\bar{1})$	0.13254 ± 0.01002	0.14322 ± 0.01860	0.1455 ± 0.0046
(040)	0.06558 ± 0.00060	0.05604 ± 0.00058	0.0689 ± 0.0004
CME 10.96 mg/L			
(100)	0.07083 ± 0.00081	0.04297 ± 0.00147	0.0717 ± 0.0005
$(02\bar{1})$	0.06763 ± 0.00295	0.06848 ± 0.00257	0.0783 ± 0.0016
$(13\bar{1})$	0.14044 ± 0.00598	0.15122 ± 0.00597	0.1517 ± 0.0060
(040)	0.06910 ± 0.00066	0.05578 ± 0.00062	0.0720 ± 0.0004

I.12 (continued)

UF urine

Crystal Plane	Gaussian	Lorentzian	FWHM
HSA/UF 0.00 mg/L			
(100)	0.06460 ± 0.00184	0.04694 ± 0.00553	0.0660 ± 0.0010
$(02\bar{1})$	0.05807 ± 0.00682	0.04754 ± 0.00511	0.0684 ± 0.0037
$(13\bar{1})$	0.06901 ± 0.00415	0.06447 ± 0.00402	0.0721 ± 0.0115
(040)	0.05988 ± 0.00112	0.04212 ± 0.00138	0.0639 ± 0.0006
HSA/UF 10.00 mg/L			
(100)	0.06017 ± 0.00131	0.03193 ± 0.00279	0.0599 ± 0.0008
$(02\bar{1})$	0.06174 ± 0.00391	0.03332 ± 0.00959	0.0618 ± 0.0020
$(13\bar{1})$	0.09654 ± 0.01189	0.09178 ± 0.01351	0.1089 ± 0.0050
(040)	0.05817 ± 0.00083	0.04575 ± 0.00089	0.0591 ± 0.0004
HSA/UF 30.00 mg/L			
(100)	0.06901 ± 0.00129	0.03440 ± 0.00379	0.06911 ± 0.0007
$(02\bar{1})$	0.05813 ± 0.00476	0.04450 ± 0.00726	0.0615 ± 0.0023
$(13\bar{1})$	0.09843 ± 0.01777	0.11671 ± 0.00577	0.1195 ± 0.0068
(040)	0.05936 ± 0.00078	0.04227 ± 0.00093	0.0596 ± 0.0004
HSA/UF 60.00 mg/L			
(100)	0.05700 ± 0.00137	0.03706 ± 0.00350	0.0581 ± 0.0008
$(02\bar{1})$	0.05954 ± 0.00546	0.05643 ± 0.00351	0.0609 ± 0.0027
$(13\bar{1})$	0.09742 ± 0.01042	0.10999 ± 0.00805	0.1177 ± 0.0045
(040)	0.05754 ± 0.00061	0.04321 ± 0.00089	0.0604 ± 0.0003

I.12 (continued)

UF urine

Crystal Plane	Gaussian	Lorentzian	FWHM
CME/UF 0.05 mg/L			
(100)	0.06574 ± 0.00134	0.03374 ± 0.00425	0.0684 ± 0.0430
$(02\bar{1})$	0.06766 ± 0.00474	0.03621 ± 0.01136	0.0675 ± 0.0025
$(13\bar{1})$	0.07604 ± 0.00945	0.08544 ± 0.00511	0.0970 ± 0.0041
(040)	0.05624 ± 0.00049	0.04427 ± 0.00059	0.0599 ± 0.0003
CME/UF 0.50 mg/L			
(100)	0.06899 ± 0.00145	0.03530 ± 0.00321	0.0683 ± 0.0009
$(02\bar{1})$	0.06751 ± 0.00476	0.04608 ± 0.00841	0.0698 ± 0.0024
$(13\bar{1})$	0.09440 ± 0.00517	0.11306 ± 0.00291	0.1165 ± 0.0041
(040)	0.05940 ± 0.00065	0.05128 ± 0.00071	0.0648 ± 0.0004
CME/UF 1.00 mg/L			
(100)	0.08143 ± 0.00141	0.04279 ± 0.00308	0.0809 ± 0.0008
$(02\bar{1})$	0.07528 ± 0.00536	0.07069 ± 0.00549	0.0841 ± 0.0027
$(13\bar{1})$	0.11193 ± 0.00853	0.12910 ± 0.00608	0.1350 ± 0.0044
(040)	0.07576 ± 0.00078	0.06397 ± 0.00090	0.0815 ± 0.0004
CME/UF 5.00 mg/L			
(100)	0.08502 ± 0.00829	0.06117 ± 0.00422	0.0921 ± 0.0042
$(02\bar{1})$	0.08819 ± 0.00548	0.06010 ± 0.00982	0.0926 ± 0.0059
$(13\bar{1})$	0.13304 ± 0.00940	0.15442 ± 0.00562	0.1591 ± 0.0126
(040)	0.09228 ± 0.00198	0.09948 ± 0.00144	0.1094 ± 0.0010

I.13 Dissolution of calcium oxalate crystals (chapter 10)

Calcium oxalate grown in distilled water

Time	1	2	3	4	Average
minutes	Ca mg/L				
0.0	0.0	0.0	0.0	0.0	0.0
0.3	5.3	5.0	5.2	4.8	5.1
1.0	21.2	24.8	19.7	22.0	21.9
2.0	37.7	40.6	35.2	38.6	38.0
3.0	51.0	54.7	57.5	49.0	53.1
4.0	60.2	62.6	71.3	65.9	65.0
5.0	78.0	69.2	73.8	70.9	73.0
7.0	80.5	84.7	81.5	86.4	83.3
10.0	84.7	87.8	89.9	89.9	88.1
15.0	94.4	84.4	89.6	91.7	90.0
30.0	90.3	86.6	93.6	93.3	90.9
60.0	93.3	89.6	92.4	88.6	91.0

Calcium oxalate grown in UF urine

Time	1	2	3	4	Average
minutes	Ca mg/L				
0.0	0.0	0.0	0.0	0.0	0.0
0.3	4.4	4.6	4.4	3.8	4.3
1.0	5.5	5.8	5.8	4.9	5.5
2.0	7.9	9.0	9.8	8.1	8.7
3.0	10.4	13.0	16.2	13.1	13.2
4.0	16.1	17.4	23.1	17.7	18.6
5.0	18.1	21.7	28.8	23.1	22.9
7.0	24.8	31.4	39.3	31.8	31.8
10.0	34.3	42.1	50.4	39.8	41.6
15.0	44.9	55.0	59.5	50.4	52.5
30.0	54.8	70.7	66.9	63.3	63.9
60.0	64.3	76.0	73.1	71.9	71.3

Calcium oxalate grown in CF urine

Time	1	2	3	4	Average
minutes	Ca mg/L				
0.0	0.0	0.0	0.0	0.0	0.0
0.3	4.2	4.2	5.1	3.6	4.3
1.0	7.8	8.4	7.8	7.6	7.9
2.0	13.3	16.1	13.9	16.1	14.9
3.0	25.7	25.3	22.5	26.6	25.0
4.0	36.0	36.9	28.7	35.3	34.2
5.0	42.2	49.3	36.0	42.8	42.6
7.0	52.0	62.0	48.9	54.1	54.2
10.0	59.3	74.9	64.0	62.5	65.2
15.0	68.2	79.0	73.3	70.6	72.8
30.0	81.6	80.1	78.5	78.6	79.7
60.0	88.0	85.2	83.6	86.6	85.8

APPENDIX II

PAPERS PUBLISHED BASED ON WORK PRESENTED IN THIS THESIS

APPENDIX II

PAPERS PUBLISHED BASED ON WORK PRESENTED IN THIS THESIS

MOLECULAR UROLOGY
Volume 4, Number 4, 2000
Mary Ann Liebert, Inc.

The Hole Truth: Intracrystalline Proteins and Calcium Oxalate Kidney Stones

ROSEMARY LYONS RYALL, D.Sc.,[1] DAVID E. FLEMING, M.Sc.,[2] PHULWINDER K. GROVER, Ph.D.[1] MAGALI CHAUVET, B.Sc.,[1] CAROLINE J. DEAN, Ph.D.,[1] and VILLIS R. MARSHALL, M.D.[1]

ABSTRACT

The ultimate aim of our research is to understand the role of macromolecules in the formation of human kidney stones, particularly their interactions with calcium oxalate (CaOx) crystals. The invariable association of stones with proteins raises the possibility that proteins play a role in their formation, similar to the role of proteins in healthy biomineralization. Do these proteins induce mineralization? Are they merely a response to the disease process? Or are they protective molecules that were overwhelmed by mineral supersaturation? A protein of particular interest is fragment 1 (F1) of prothrombin. We have shown that mRNA for prothrombin is present in the kidney. Because the F1 fragment of prothrombin present in urine is slightly different from that found in the blood, we refer to this protein as "urinary prothrombin fragment 1" (UPTF1). Available evidence suggests that the kidney manufactures the protein for protection against stone disease and that the protein has a directive role in stone formation. We now have evidence that proteins are interred within CaOx crystals precipitated from human urine, where it is distributed in continuous channels. These proteins could facilitate crystal deconstruction and removal after attachment to the renal epithelium and endocytosis. We suspect that the formation of CaOx crystals in the urine is a normal process designed to permit harmless disposal of an excess of calcium, oxalate, or both. The incorporation of proteins provides a second line of defense against stone formation by enabling the destruction and removal of retained crystals. Understanding the basic molecular strategies by which plants produce protein-containing CaOx crystals may provide insight into human CaOx stone formation.

UROLITHIASIS AND MOLECULAR BIOLOGY: WHAT'S IN A NAME?

MOLECULAR BIOLOGY is a scientific chimera whose scope encompasses a broad range of disciplines, ranging from cell biology and genetics to organic chemistry and biophysics. The term has been ascribed to William Astbury, who in 1945 used it to define the study of the chemical and physical structure of macromolecules.[1] However, in recent years, the term has come to describe a substantive field whose multidisciplinary origins make it difficult to categorize any particular area of biologic research as belonging specifically to "molecular biology" rather than to one of the many scientific areas from which the discipline emerged. However, when faced with the need to decide whether the work described here could be classified as molecular biology, we returned to William Astbury for guidance. The ultimate aim of our research is to understand what role, if any, macromolecules play in the formation of human kidney stones, particularly in their molecular interaction with the unit blocks of which they are constructed—calcium oxalate (CaOx) crystals. The work outlined in this review represents a chronological transition from biochemistry to biophysical chemistry and, because our research has led us further into the world of proteins, inexorably, to the world of molecular biology.

MACROMOLECULES AND KIDNEY STONES: PARADOX LOST

Were it not for their pathological ramifications, study of the formation of kidney stones might forever have languished as

[1]Department of Surgery, Flinders University School of Medicine, Flinders Medical Centre, Bedford Park, South Australia.
[2]School of Applied Chemistry, Curtin University of Technology, and Chemistry Centre, Perth, Western Australia.

academic fodder for inquisitive physical and inorganic chemists. Indeed, for many years, it was assumed that the occurrence of stones could be explained simply in terms of ionic equilibria and urinary saturation—despite the fact that the association of their mineral component with organic matter, principally proteins, had long been recognized.[2] In this respect, stones are no different from a huge range of minerals manufactured by living organisms, including ourselves, throughout the natural world. Biomineralization occurs throughout the entire phylogenetic tree and typically musters the forces of a diversity of proteins that provide a framework for the deposition of crystals, induce their nucleation, dictate their morphology, determine the rate of their growth, and prescribe its limits.[3] Although kidney stones can be regarded as examples of uncontrolled rather than controlled mineralization, their invariable association with proteins raises the possibility that proteins play roles in their formation similar to those in healthy biomineralization. However, such an analogy is inadequate to explain the occurrence and role of proteins in urinary calculus formation. Unlike predetermined biomineralization, which occurs in compartments (syncytia) specifically designed for the nucleation and ordered storage of crystalline material, stones form in urine, a complex medium consisting of an enormous array of low and high molecular weight *waste* products, all of which have at least the potential to influence the crystallization of insoluble salts in the urinary tract. It comes as no surprise, then, to learn that although an increasing number of urinary proteins have been identified in human stones,[4] at the present time, their specific functions, if any, have still not been defined.

The study, diagnosis, and treatment of any disease depend in no small measure on the investigator's being able first to recognize what is abnormal, which in turn depends absolutely on the ability to define the limits of normality. Traditionally, investigation into the causes of stone disease has entailed comparing the excretion or concentration of certain urinary components (principally calcium and oxalate) of stone formers with those of people who have never formed a stone. It should be possible, at least theoretically, to adopt the same approach with urinary macromolecules: for instance, we could compare the urinary concentration or net excretion of particular proteins in patients and normal persons or examine the protein structures in detail to ascertain whether there are molecular disparities between them that might account for differences in function. We could isolate proteins from kidney stones and identify them in order to find out which ones are actually present in stones—an exercise that has been carried out repeatedly and yielded a veritable cocktail of stone proteins.[4] But having found them, how do we know why they are there? It would be fair to say that the organic matrix of stones remains the most niggling paradox of stone disease, as its presence can just as easily be explained by its component proteins having acted in completely contradictory ways. Did they actively induce mineral precipitation? Are they merely irritative or inflammatory products of the disease process, chance inclusions that got in the way, or protective molecules that succumbed to overpowering levels of mineral supersaturation? Of course, answering these questions would be considerably easier if we could determine which urinary proteins might possibly be actively involved in forming *pathological* stones if we could compare them with those in a "normal" stone. Oxymoronic? Of course! Ridiculous? Not really. We owe much of what we know about the potential roles of urinary proteins in stone formation to observations made of their involvement in an ordinary event that occurs to varying extents in all of us—the formation of CaOx crystals in urine. And as we shall later see, there is at least one other less obvious avenue simply begging to be explored.

THE PROTEINS OF CRYSTAL MATRIX: OUT OF SIGHT, INTO MIND

Perhaps the most remarkable aspect of the relation between urinary proteins and CaOx crystals is the fact that the external appearance of the crystals provides no clues to suggest the presence of resident protein guests. It was probably because of this that it was not until 1988 that the first attempts were made to determine whether crystals of stone minerals are associated with organic material—despite the long-known occurrence of organic material in kidney stones themselves. In that year, Morse and Resnick[5] demonstrated that CaOx crystals experimentally induced to form in urine were associated with urinary proteins. Using two-dimensional sodium dodecylsulfate gel electrophoresis analysis, they observed that relatively few of the large number of proteins excreted in human urine were to be found in the organic matrix remaining after dissolution of the crystal mineral phase. This approach was revolutionary insofar as it allowed for the first time the identification in association with a stone mineral *only* of the proteins routinely excreted in healthy human urine and so provided an opportunity to assess their possible role in the initial, crucial stage of stone formation—crystal nucleation. We later confirmed that only a selective few proteins were associated with CaOx urinary crystals and demonstrated the presence of a predominant protein band with an apparent M_r of 31 kD, which could not be detected in urine samples from which the crystals had been derived.[6] The sheer abundance of the protein in CaOx crystals, as well as its predominance over more plentiful urinary proteins such as serum albumin and Tamm-Horsfall glycoprotein, suggested that it might play a significant role in the formation and fate of CaOx crystals in urine and was therefore worthy of more careful scrutiny. Mistakenly believing the band to represent a previously undescribed protein, we initially named it "crystal matrix protein" until later work proved it to be closely related to the fragment 1 (F1) activation product of the blood clotting protein prothrombin.[7-9]

WAITING IN VEIN: PROTHROMBIN AND ITS FRAGMENTS

The structure of the complete prothrombin molecule is presented diagrammatically in Figure 1, which also delineates the boundaries of the portions of the molecule released as individual proteins during blood clotting, including F1. Although prothrombin mRNA is known to be expressed in other tissues,[12] the protein is synthesized principally in the liver[13] whence it is released into the plasma. The protein has a relative molecular mass of approximately 72 kD and so does not normally occur

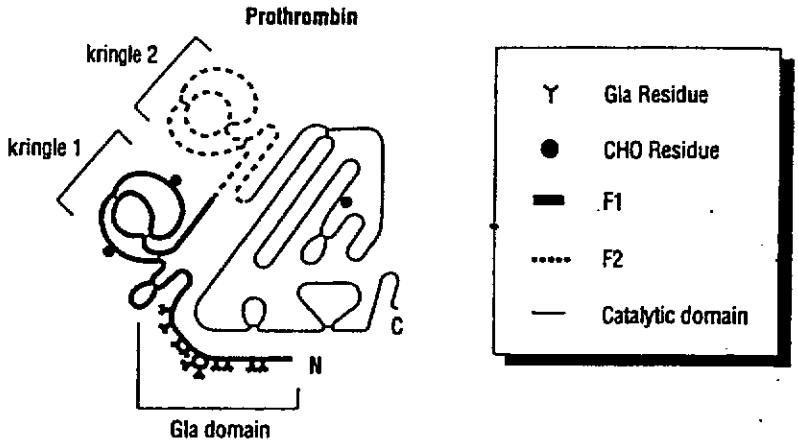

FIG. 1. Schematic prothrombin molecule, indicating its various domains and component fragments, F1 and F2, which are released during blood coagulation. Catalytic domain encompasses the full amino acid sequence of thrombin. (Adapted from references 10 and 11).

in human urine in significant quantities. On the other hand, with a much lower molecular mass, any F1 arising from routine prothrombin turnover could be released as a component of the glomerular filtrate into the urine, where it could undergo modifications producing the subtle chromatographic differences that distinguish it from its sibling in serum.[9] We certainly cannot discount this possibility, and it probably occurs under physiologic conditions. Equally, however, perhaps the F1 present in CaOx crystals is manufactured directly in the kidney, or is derived from prothrombin synthesized there? Although seemingly unlikely, this possibility has since proved to be correct. Using reverse transcriptase-polymerase chain reaction (RT-PCR), we have shown that mRNA for prothrombin is present in the human[14] and rat[15] kidney. In recognition of the renal synthesis of prothrombin and the slight differences between F1 from blood and urine, we now refer to the form of the protein associated with CaOx crystals as "urinary prothrombin fragment 1" (UPTF1).

Of course, the simple demonstration of prothrombin mRNA in the kidney, along with the abundance of UPTF1 in CaOx crystals precipitated from human urine, are insufficient justification for supposing that UPTF1 might be important in stone formation. But, combined with other features of the protein, available evidence suggests that the kidney manufactures UPTF1 or prothrombin as a form of protection against stone disease.

The UPTF1 protein is present in calcium stones but not in struvite stones, confirming that its association with calculi cannot simply be the result of bleeding caused by the stone itself.[16] The protein has been shown in immunohistochemical studies of the human kidney to be located specifically in the most lithogenic regions of the nephron, namely, the thick ascending limb of the loops of Henlé and the distal convoluted tubules, where it is present in greater quantities in stone formers than in healthy subjects.[7] Although these facts would at least support the notion that UPTF1 is an important player in CaOx stone formation, even more compelling is the fact that it is a potent inhibitor of both CaOx crystal growth and aggregation in an inorganic medium[17] and in undiluted, ultrafiltered human urine.[18] The protein's inhibitory potency, as well as its disproportionate quantity in CaOx crystals deposited from urine,[6] can almost certainly be attributed to its Gla domain,[19] which is located in the N-terminal region of the molecule and contains 10 residues of γ-carboxyglutamic acid (Gla), an amino acid found only in the vitamin K-dependent proteins, upon which it confers an extraordinary capacity for binding calcium ions. The evidence suggests, therefore, that UPTF1 fulfils some directive role in stone formation, but further results are required before it will be possible to state with certainty that variations in the amount of the protein excreted in the urine, or alterations in its molecular structure, predispose some individuals to urolithiasis. Thus, UPTF1 has many properties expected of a protein fulfilling a directive role in CaOx crystal formation in human urine; but does its pattern of excretion in stone formers differ from that in healthy individuals?

RENAL UPTF1 EXCRETION: ODIOUS COMPARISONS

Unfortunately, the very features of the UPTF1 molecule that confer its inhibitory properties and make it such an excellent candidate for controlling CaOx crystal formation *in vivo* also confound its accurate measurement in urine. We now have a functioning enzyme-linked immunosorbent assay (ELISA) that has enabled us to make quantitative and reproducible measurements of urinary UPTF1 excretion—but only, of course, if the protein is actually in solution. And not all of it is. The Gla domain of UPTF1 (see Fig. 1) causes the protein to bind like a limpet to the CaOx crystal surface. Any CaOx crystals in the urine sample, whether formed endogenously or after excretion, will bind any UPTF1 and thereby cause an underestimation of the amount of the protein excreted by the kidney.[20] Furthermore, because chelating agents and protein denaturation interfere with the ELISA, it is not possible to measure accurately the UPTF1 released from CaOx crystals by acid or EDTA dissolution. As if these were not sufficient reasons for questioning the validity or utility of measuring UPTF1 as a potential marker of stone disease, CaOx crystalluria is more common and more extensive in recurrent stone formers than in normal subjects.[21] Thus, the potential for serious error is greatest in the very group in which the measurement of UPTF1 might impart the most benefit. And the problem is certainly not confined to UPTF1: doubts must now be raised about published excretion

data for bikunin,[22] osteopontin,[23] and, indeed, *any* protein implicated in urolithiasis that binds irreversibly to crystals of CaOx.

We have confirmed that the concentration of UPTF1 declines significantly in direct proportion to the amount of synthetic CaOx crystals added to urine, as well as in response to increasing quantities of sodium oxalate solution added to induce CaOx precipitation.[20] Immediate dilution of freshly voided urine to avoid crystal formation *in vitro* is only partly successful. Although 5- and 10-fold dilution increases the measured concentration of UPTF1, the increment is variable, probably reflecting uncontrollable changes in the ambient concentration of calcium ions, which are known to influence the protein's steric conformation and will affect its binding to the antibody used in the ELISA.[20] In any event, even if postvoiding crystal formation could be avoided by dilution, this would not address the question of CaOx nucleation within the urinary tract, which is a much more difficult problem to solve. We are currently considering different strategies for preventing the formation of urinary crystals in an attempt to enable accurate measurements of urinary protein concentrations for urolithiasis research or diagnostic purposes. In the meantime, we have also adopted an alternative approach, although it, too, is associated with unavoidable difficulties, which are of a different nature but just as frustrating to solve.

If our proposal that UPTF1 plays a controlling role in urinary CaOx crystal formation is correct, then it should be possible to demonstrate that renal synthesis of the protein in stone patients differs from that in healthy subjects. The problem now is not a tedious technical one but an ethical one. In order to test the hypothesis directly, it would be necessary to induce the formation of CaOx crystals in vivo under controlled experimental conditions, remove the kidneys, and compare quantitatively any changes in mRNA corresponding to the F1 region of prothrombin with the level in healthy controls. This is clearly impossible to do in humans; but it *is* possible in rats, although this depends, of course, on the availability of an appropriate quantitative assay system. We have recently developed a rapid, sensitive, competitive PCR method for the quantification of prothrombin mRNA in kidney and other tissues. The technique does not involve heteroduplex formation, and competitor synthesis does not entail cloning.[24] Unlike methods used by others[25,26] to quantify prothrombin RNA in kidney specimens, our technique incorporates a second competitive PCR to measure mRNA for the housekeeping protein β-actin. This step enables normalization of the amount of prothrombin mRNA to that of β-actin and enables correction for any intersample variations in RNA extraction efficiency and downstream processing. Using the technique, studies are currently being undertaken to compare the amount of renal prothrombin message in healthy and stone-forming rats in order to throw further light on the potential role of UPTF1 in CaOx stone formation. Nonetheless, even if data confirm that the amount of prothrombin message is different in stone-forming rats, we are still none the wiser about what the protein actually does. However, we have not yet exhausted the possibilities. One property of the relation between UPTF1 and CaOx crystals, which has implications for crystal and stone formation extending well beyond traditional imagination, is so obvious that it has tended to be overlooked. UPTF1 is *intracrystalline*.

THE INSIDE STORY: THE INTRACRYSTALLINE DISTRIBUTION OF ORGANIC MATRIX

Although it is now 9 years since we first suggested that UPTF1 occurs within the structure of CaOx crystals generated from urine,[6] as recently as 1997, doubts were still being openly expressed about the scientific credibility of our proposal.[27] Our assumption that the organic matrix of the crystals is internally distributed was based on indirect evidence and strong inference: we had shown that specific proteins were released by EDTA dissolution from crystals that had been scrupulously washed with sodium hydroxide solution to remove any superficially bound macromolecules.[6,9,29,30] However, we now have direct evidence that proteins are indeed interred *within* the mineral bulk of CaOx crystals precipitated from human urine, where it is distributed in continuous channels throughout the mineral phase. Figure 2 shows data we have obtained by field emission scanning electron microscopic (FESEM) examination of fractured CaOx monohydrate (COM) crystals precipitated from human urine. Clearly, although crystals precipitated in ultrafiltered urine (lacking all macromolecules >10 kD) are solid, those generated in the presence of urinary macromolecules are not the homogeneous, solid mineral structures they are generally assumed to be. Figure 2C shows a side view of a CaOx monohydrate crystal whose internal cribriform structure is rather reminiscent of a cookie that has been snapped in half. The internal detail and intracrystalline lacunae become even more evident following treatment with protease (Fig. 2D), demonstrating conclusively that the material trapped inside the internal cavities of the crystal structure is protein.

We have therefore obtained the first direct, visual proof that large organic molecules, in this case proteins, can become incarcerated inside the mineral component of what appear externally to be normal, solid crystals. Rietveld refinement with synchrotron X-ray diffraction data from pure and urinary CaOx crystals has substantiated our scanning electron microscopy findings (unpublished observations from our laboratory). But do the presence of intracrystalline proteins and their effects on the fabric and properties of the crystals in which they reside have significant implications for stone formation? Indeed they do, and not just for urolithiasis—they are also of vital importance for biomineralization generally.

INTERIOR DESIGNERS: INTRACRYSTALLINE PROTEINS AND BIOMINERALIZATION

One of the features of controlled, healthy biomineralization that distinguishes it clearly from its chaotic counterpart is that crystals are typically laid down in membrane-bound containers specifically designed for their accommodation and storage. Not surprisingly, until relatively recently, it was generally assumed that the size and shape of the crystals were dictated principally by the cytoplasmic membranes defining the physical limits of the compartments[31,32]—rather like creating specific shapes by pouring unset plaster of Paris into a rubber mould. However, it is now acknowledged that the morphology and dimensions of crystals comprising the calcified structures of some marine organisms are determined, not by the general shape of their cel-

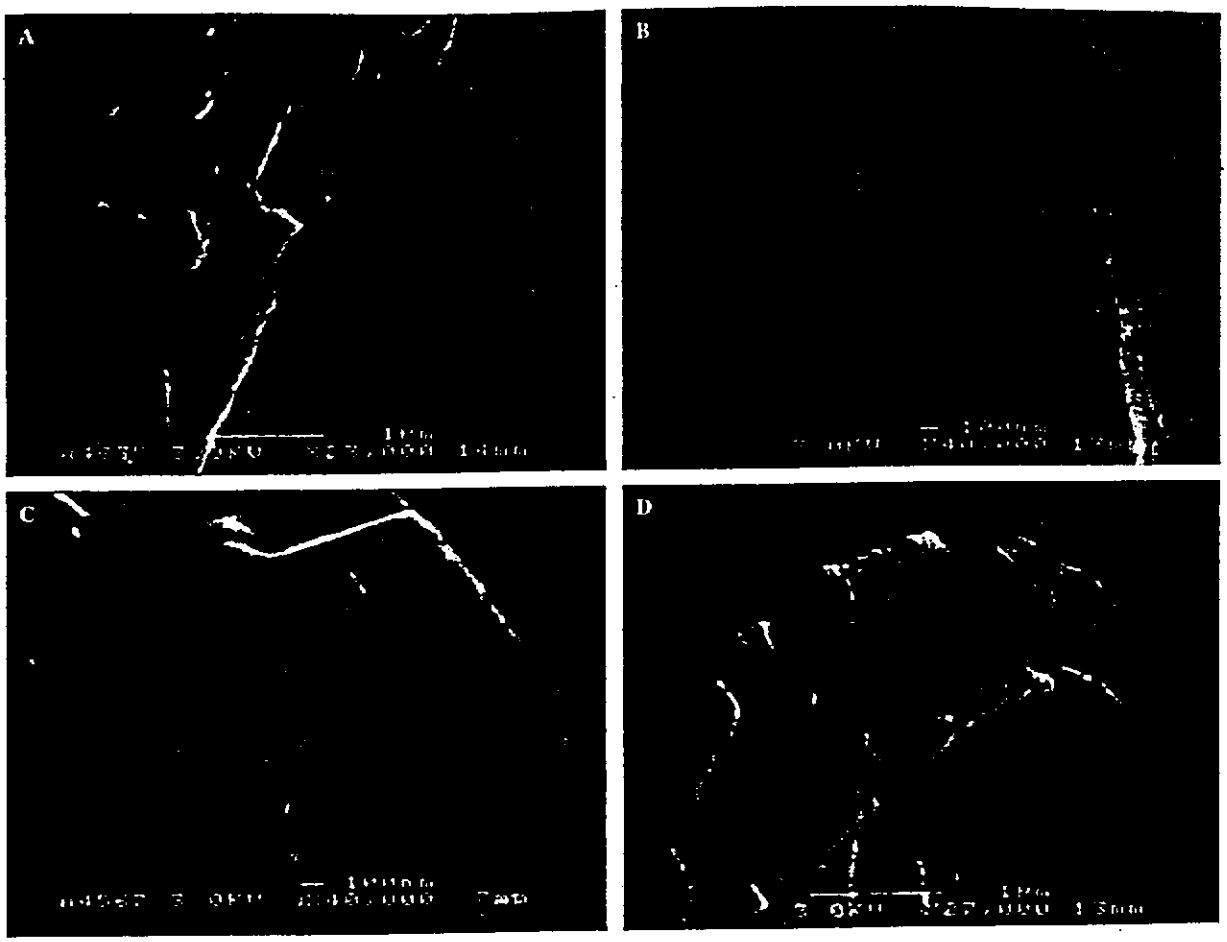

FIG. 2. Field emission scanning electron micrographs of fractured CaOx crystals precipitated from ultrafiltered (10–kD) human urine by addition of fixed load of sodium oxalate above an experimentally determined metastable limit. Images obtained before (A) and after (B) digestion with Protease K (Sigma Chemical, St. Louis, MO). Note that crystals are completely solid. (C, D) Crystals deposited from same urine specimen after centrifugation and filtration before (C) and after (D) protease treatment. Note porous nature of crystal in panel C, which is even more pronounced after removal of the intracrystalline material by protease treatment. Crystals were fractured using a diamond cell. (Reprinted by permission from reference 28.)

lular containers, but rather by proteins occurring within the crystals themselves.[31,32] These intracrystalline protein "guests" act in a fashion similar to the steel rods in reinforced concrete: they create and stabilize lattice discontinuities and alter crystal texture and tensile properties.[33] Their low density and distribution throughout the mineral phase allow the formation of lighter, porous structures without compromising mechanical strength, a principle which the sea urchin has exploited spectacularly to achieve the seemingly impossible task of creating a spine up to 25 cm in length from a single crystal of calcite.[34] However, the production of a structure with a low mass and high physical strength is hardly likely to be the prime function of proteins buried within urinary CaOx crystals: they are more probably responsible for other properties that have far greater implications for the formation of stones. As occurs with healthy biominerals, the three-dimensional molecular configuration and chemical properties of intracrystalline proteins ensure that only crystals of a particular composition are formed, guarantee that their various faces will grow only in certain directions to produce a structure of a strictly defined shape, and determine the physicochemical features (and thus the binding properties and aggregability) of the resulting structures.[35] The distinction between internal and superficial proteins involved in the development of healthy biominerals is therefore crucial; but how important is it for urolithiasis?

SUNKEN TREASURE: ROLE OF INTRACRYSTALLINE PROTEINS IN STONE FORMATION

Our demonstration of intracrystalline proteins in CaOx urinary crystals provides clear evidence that ordered incorporation of proteins into crystals does not require orchestration by an array of complex cellular processes. This fact has enormous ramifications for urolithiasis. To the present time, it has generally been assumed that the primary role of urinary proteins is to inhibit the nucleation of crystals or, should that occur, their subsequent growth or aggregation.[36] Certainly, several urinary proteins are efficient inhibitors of CaOx crystal aggregation, and

it has been assumed that their function in healthy urine is to prevent the formation of large crystal clusters likely to be retained within the renal collecting system.[36] However, in addition to these putative functions, it is now widely recognized that stone formation often also involves attachment of crystals to the epithelial surface, a process that is affected by their binding properties, which will in turn be influenced by their resident proteins. This process, too, is inhibited by certain proteins.[37] However, the fact is that the same inhibitory proteins, particularly UPTF1, are also found in stones, which would suggest that no matter how potent their assumed protective properties, they are not always equal to the task: if they were, stones would never form. It is difficult to imagine, therefore, that inhibiting crystallization is their only, or even primary, function.

INTERNAL COMPOSTURE ENGINES: AN UNSUSPECTED ROLE FOR PROTEASES IN UROLITHIASIS

It has recently been demonstrated that exogenous CaOx monohydrate (COM) crystals internalized by cultured monkey renal BSC-1 cells subsequently dissolve over a period of several weeks.[38] Similar results have been reported for exogenous CaOx dihydrate (COD) crystals,[39] as well as COD crystals nucleated directly on to the cell surface.[40] The same authors have hypothesized that crystal attachment and subsequent dissolution represent a means of evading stone formation, postulating that the surfaces of epithelial cells could serve as templates for the nucleation of crystals from supersaturated tubular fluid.[41] The subsequent adherence of crystals would be facilitated by stereospecific interactions between structures on the apical surface of renal tubular cells and the assemblage of molecules on COD[39] and COM crystal surfaces.[41] These interactions would depend, in turn, on specific anionic molecules, either on the surface of renal cells or within the luminal fluid.[40,41] Although these findings highlight one possible role of proteins in the attachment of CaOx crystals in the development of kidney stones, they provide no clues about another less obvious, but potentially crucial, one.

If the principal function of proteins were to prevent retention of crystals within the urinary tract, their inhibitory effects would presumably be greatest if they were concentrated on the crystal surface—the part of the structure that actually comes into contact with other crystals or with epithelial membranes. It is difficult to imagine why there would be any advantage in their being interred within the mineral. However, their presence on the crystal *surface* would be only temporary in the face of extreme levels of supersaturation, because, no matter how inhibitory, they would be incapable of preventing the deposition of further mineral and become buried within the structure. Wasted effort, perhaps? Not at all! We propose that the ultimate fate of attached crystals, and thereby the likelihood of stone formation, also depends on the nature and concentration of urinary proteins incorporated *inside* the crystals, where they could facilitate crystal deconstruction and removal after attachment and endocytosis. Crystals with protein-filled, labyrinthine interiors would be much more susceptible to degradation by intracellular proteases than would solid minerals. Proteolytic digestion of protein-riddled CaOx mineral would facilitate excavation into channels deep within the crystal structure, allowing protease access to the crystalline core and vastly increasing the surface area available for further degradative processes. This concept is entirely in keeping with the proposal that matrix proteins of CaOx crystals are chemotactic for cells such as macrophages whose release is provoked by inflammation induced by crystal attachment.[42] Secretion of neutral proteases by such cells would digest the intracrystalline proteins, as suggested above, and disrupt the mineral phase into nanometer-sized particles for removal by opsonins[42] or dissolution and disposal of the released ions by calcium-binding and transporting proteins. This proposal is corroborated by our demonstration that proteolytic digestion of intracrystalline proteins can occur in urine, even before attachment,[43] as well as other observations from our laboratory showing that small discrete intracrystalline particles and mineral channels are visible inside CaOx crystals treated with protease (Fig. 3). The credibility of the proposal is further supported by other data confirming the occurrence of phagocytosis, induction of protease activity, and subsequent dissolution of calcium phosphate (CaP) crystals implanted in bone.[44,45] It is also noteworthy that the rate of intracellular dissolution of CaP cylinders and phagocytosis of small mineral particles by mononuclear macrophages depend on the size and continuity of pores within the implanted material.[46] In addition, protease activity is present in mouse,[47] rat,[48] and human[49] kidneys. The human kidney also contains a receptor for thrombin,[50] a protease which degrades prothrombin and another CaOx intracrystalline protein, osteopontin.[51]

Collectively, these data emphasize the potential importance of intracrystalline proteins in the urinary genesis of CaOx crystals. More importantly, they strongly suggest that crystalluria is a dynamic and potentially reversible process in which proteins and proteases may perform separate, but complementary, roles, which interdict the progression from crystalluria to stone formation. We therefore hypothesize that in direct parallel with controlled biomineralization throughout Nature, the formation of CaOx crystals in urine is a *healthy, normal process* designed to permit harmless disposal of excessive amounts of calcium, oxalate, or both. Although this is a radical departure from current thinking, the concept is supported by the recent demonstration that the human kidney synthesizes significant quantities of oxalate.[52] Considering the toxicity of oxalate to the nephron, it is difficult to conceive of any reason for this—other than to act as a counter-ion to excess Ca^{2+}. Furthermore, crystal nucleation, growth, and assembly are controlled by specific, intracrystalline proteins, in particular, UPTF1 and osteopontin, excreted into the urine for the express purpose of inducing nucleation of crystals, inhibiting their enlargement, and preventing their attachment to, and endocytosis by, renal epithelial cells, particularly during periods of excessive CaOx supersaturation. And finally, should that supersaturation overwhelm the availability of such proteins and attachment and endocytosis of crystals occur, their distribution throughout the crystalline bulk creates a second line of defense against urolithiasis by providing a mechanism for enabling the erosion, disintegration, dissolution, and removal of retained crystals.

These hypotheses, which are illustrated in Figure 4, are well supported by empirical experimental evidence, as detailed

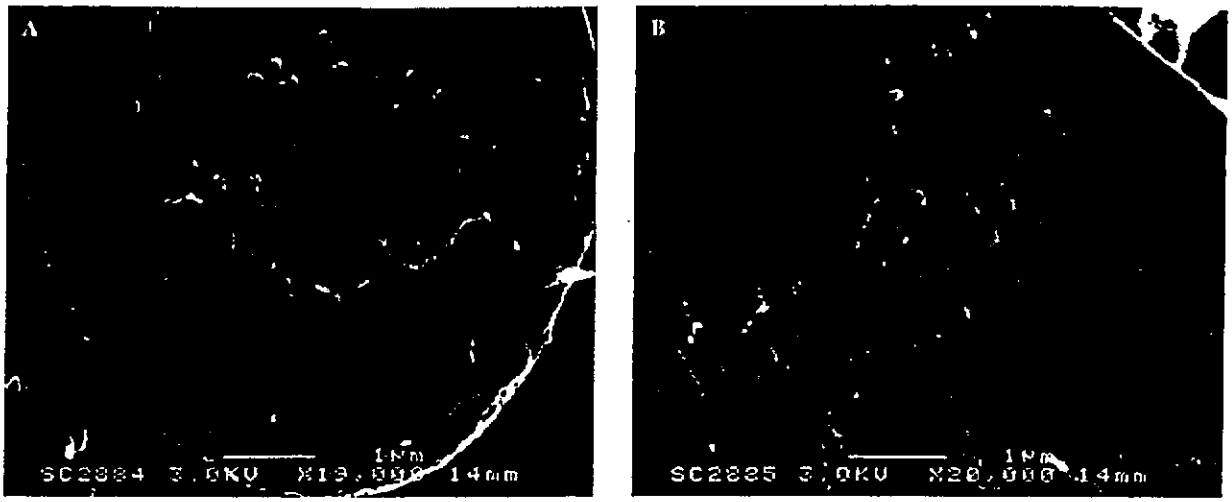

FIG. 3. Crystals of COM precipitated from centrifuged and filtered urine and treated with protease, showing discrete, closely packed subcrystalline particles. (A) Particles appear to be mixed with composite projections of mineral and organic matter, which may represent stacks or sheets of particles linked in linear fashion. (B) Exposed crystal surface seems to consist entirely of highly ordered particles interspersed with organic material.

above. Nonetheless, until relatively recently, we and our stone colleagues would have regarded them as heretical, even though, as will be seen, in comparison with other work being undertaken in our laboratory, they are very conservative indeed!

SHEDDING BLINKERS AND DISCOVERING COMMON ROOTS

Although we have edged closer, and with increasing justification, to the conclusion that proteins must play some role in

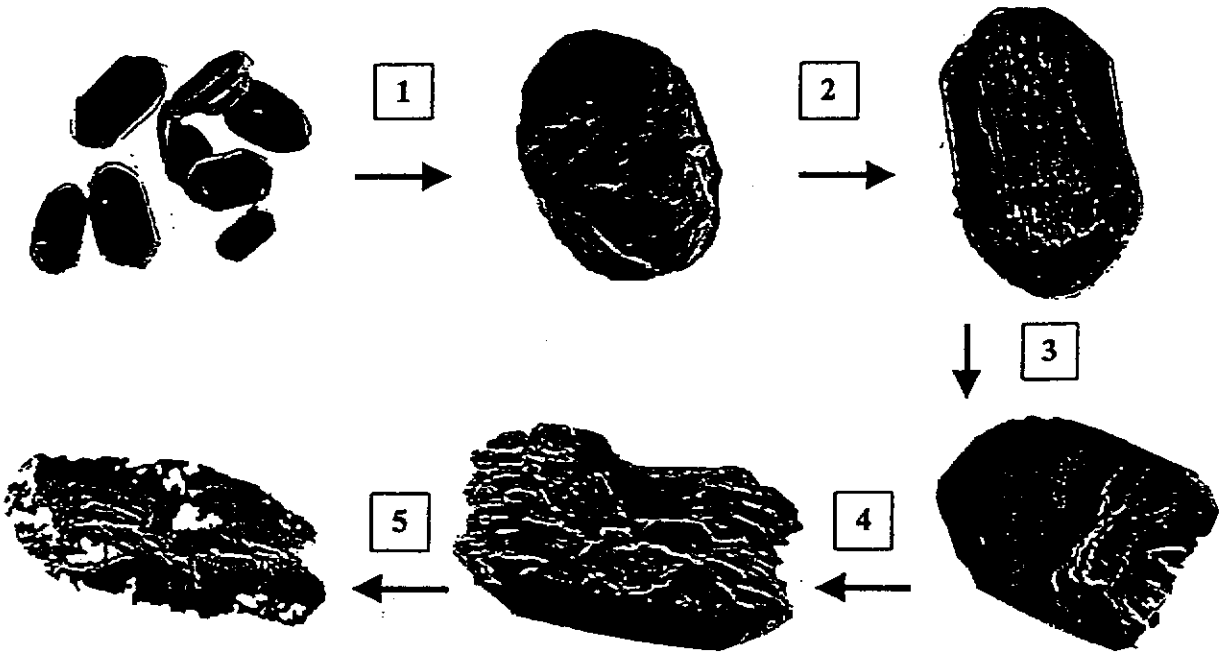

FIG. 4. Schema of proposed hypotheses. Supersaturation of urine with CaOx causes formation of small COM nuclei. Adsorption of specific urinary proteins inhibits crystal aggregation and attachment to the epithelium (1). Further solute deposition traps proteins inside crystal structure, forming protein-mineral particles and interconnecting channels (2). If this fails, crystal attaches to epithelium, and urinary proteases initiate preparatory digestion of intracrystalline proteins (3). Crystal is endocytosed and is exposed to intracellular protease digestion (4). Crystal erodes and disintegrates, phagocytosis occurs, and subcrystalline particles are dissolved by Ca^{2+}-binding proteins or localized acidification of cellular pH (5). Ions are then excreted via the plasma and excreted in gut or urine.[46]

urolithiasis, we still know virtually nothing about the mechanisms by which they exercise control over their mineral hosts or the effects that they evince in the mineral's internal structure, texture, or mechanical and biophysical properties. More particularly, we have no natural precedent with which to validate any assumptions we do make, however reasonable they may be.

Or do we? Earlier in this article, we introduced the notion of a "normal" stone, being cautious to use quotation marks in order to reassure the reader that we have not entirely taken leave of our senses! We do not, of course, have normal stones to provide us with information about how proteins might control the formation and fate of CaOx crystals under healthy conditions. However, Nature is full of surprises, and perhaps the time has come to abandon our all-too-human tunnel vision and look elsewhere for clues. We have for too long been almost completely preoccupied with a process that is unwanted and uncontrolled and have overlooked the fact that we might learn far more about how to restore control by studying its healthy counterpart, which occurs abundantly in a myriad of perfect forms throughout Nature. The time has come to put aside our studious absorption with a process that has obviously gone wrong and instead devote our energies to one that has clearly succeeded in getting it right.

THE HIGHEST FORM OF NATURAL FLATTERY: BIOMIMETICS

The new principles of biology which create whole movements of consequent research and discovery almost always come from studies done on laboratory animals or smaller life forms. Sir GJV Nossal

Much of what we know about ourselves and our biosphere has come from the study of basic processes occurring in what have traditionally been called "lower" forms of life. Fortunately, this approach to learning about humans and solving their problems has in recent times undergone a renaissance of sorts, leading to the emergence of a distinct discipline: biomimetics. Biomimetics can be simply defined as the mimicry of processes and principles in one healthy biologic system to understand those of another or to harness and adapt them to solve a particular problem or achieve a specific goal. One has only to skim the pages of *New Scientist* to find wonderful descriptions of applied biomimetic research, although not all are clearly labeled as such. Examples include the use of molluscan adhesive proteins for repair of bones or soft tissues in humans,[53] notch and jagged proteins in insect bristles for understanding and overcoming human deafness,[54] control of cell size by S6 kinase in flies for preventing the growth of cancer cells,[55] use of heat shock proteins from yeast for understanding Alzheimer's and other human diseases,[56] and—one of the most impressive achievements of all—mimicry of the oxygen-evolving complex of photosynthetic plants to release oxygen from water.[57]

Materials chemistry is one discipline that obviously has much to gain from imitating control and design principles in biomineralization, where it has been used for crystal engineering and synthesis of nanoscale particles required for industrial purposes.[58] It can even be used to produce mineral structures such as synthetic hollow porous aragonite shells that bear an uncanny resemblance to the natural coccospheres of marine algae.[59] However, biomimetics also has enormous potential for solving human medical problems, where it promises the fabrication of durable synthetic materials for prostheses or implants with unique physical, mechanical, and electrical properties and the ability to treat or correct pathological biomineralization, such as urolithiasis, or to replace lost or injured bone. Exploitation of the principles involved in the molecular control of crystal nucleation and growth, coupled with the use of genetic engineering, could enable production of proteins specifically tailored to control crystal morphology, growth, and assembly for a range of medical applications, from construction of reaction cages for drug delivery to the regeneration of healthy tissue.[58]

Perhaps the most exciting aspect of adopting a biomimetic approach to the study of human pathology is that crucial information can be obtained from simple, phylogenetically unrelated, organisms—plants, for example—which can be manipulated experimentally in ways that could never be physically or ethically contemplated in humans. Although *prima facie*, this idea might seem outrageously far-fetched to the committed clinical experimenter, it is wise to recall the status of a tiny plant from the mustard family. Throughout the last 10 years or so, the quest to map the complete gene sequence of *Arabidopsis thaliana* has virtually rivalled that of the Human Genome Project. Why? Because this plant has come to be recognized as an excellent model for addressing fundamental questions posed, not only by plant biology, but also others common to all eukaryotes, including those affecting human health and disease.[60] Perhaps, then, the prospect of imitating some of the principles of biomineralization operating in simpler organisms to throw light on human stone formation is not so preposterous after all, especially as biomineralization is based on a range of common elements operating throughout a disparate range of organisms in phyla with widely diverse ancestry.

Of course, if we wish to apply a biomimetic approach to the study of human stone disease, we must have access to a suitable system in which the formation and accumulation of CaOx crystals are desirable, strictly regulated processes. Fortunately for us, such a system occurs frequently in Nature, although in organisms that, like *Arabidopsis*, might at first seem far removed from human pathology—plants.

"NORMAL" CaOx STONES AND THE ECONOMY OF NATURE

Any urologist engaged in treating stone patients will have issued the oft-repeated caution to eschew consumption of foods rich in oxalate; spinach (for some unaccountable reason) is likely to have been the most maligned and patients are instructed to avoid it. What the majority of urologists probably do not know, however, is exactly what physical guise oxalate takes in such gustatory pleasures as tomatoes, strawberries, pineapple, and spinach. Most urologists probably would be quite surprised to learn that oxalate in plants occurs principally in a crystalline form—and CaOx at that! Plants in many senses are no different from humans, and calcium homeostasis is as vitally important to their healthy functioning as it is to our own: high cellular concentrations can cause severe physiological derangements.[61] However, whereas we dispose of excess quanti-

ties of calcium ions by excreting them in our urine, plants are not equipped with such convenient luxuries as kidneys and bladders and are forced to deal with surplus quantities of the element in a less handy, but nonetheless most ingenious, fashion. Most higher plants package up calcium in the form of crystalline CaOx, which in some instances can account for as much as 80% of the plant's dry weight,[62] by mechanisms which, again, illustrate the evolutionary parsimony of Nature. Using metabolic pathways shared with humans, our distant, photosynthetic, relatives specifically synthesize oxalate to achieve a charge balance for Ca^{2+} or for regulating its activity.[61] In so doing, they achieve conversion of soluble, potentially toxic, calcium to an inert insoluble product, which is formed inside vacuoles of idioblast cells, which differentiate from mesophyll cells in response to a developmental Ca^{2+} signal.[63] These vacuoles are specially designed for secure crystal storage[61] and thus act as high-capacity Ca^{2+} sinks, which spare surrounding cells from the toxic effects of high concentrations of the ion and allow them to proceed with their normal functions, such as photosynthesis. In addition to being inventive waste managers, higher plants are also accomplished artists capable of fashioning CaOx crystals into unique shapes, the likes of which can only be imagined by mere human chemists. Reflecting an extraordinary degree of exquisite control over growth, their morphologies generally fall into five basic groups: raphides (needles; usually arranged in faggots of several hundred), styloids (large single needles), crystal sand (packets of angular microcrystals), druses (stellate conglomerates), and prisms (rhombohedrons).[62]

The evolutionary economy of Nature is well illustrated by the sharing of numerous genetic and metabolic processes by a broad spectrum of apparently unrelated organisms, and calcium regulation is no exception. Cytoplasmic Ca^{2+} homeostasis follows the same rules in the animal and plant kingdoms,[64] so it comes as no surprise to learn that Ca-binding proteins occurring in higher organisms, including humans, are also found in plants. Plants contain a sequestrin-like Ca-binding protein,[65] calreticulin,[66,67] annexins, calmodulins, and S-100 proteins,[65] as well as other, unidentified Ca-binding proteins.[69] It would seem, then, at least as far as calcium regulation is concerned, that we are not so very different from our green neighbors as we might think; even to the point of precipitating CaOx crystals! However, there is one notable, *apparent* difference.

To date, the occurrence of CaOx crystals in human urine has generally been regarded as undesirable, in marked contrast to their formation in plants, which reflects an extraordinary degree of developmental and metabolic *control*. However, whereas kidney stones have justly earned their unsavory reputation, we should not be too eager to describe urinary crystals in such unflattering terms. It is difficult to imagine that the exquisite regulation of CaOx crystal formation exercised by plants has been completely denied to us; that after millennia of evolution, CaOx crystal formation in humans been left entirely to chance. If indeed it has not, then we must return, inevitably, to our earlier conclusion: that CaOx crystalluria is a salubrious physiologic event designed to permit harmless disposal of excessive amounts of calcium, oxalate, or both. Moreover, we must conclude that, as in higher plants, the formation of CaOx crystals in urine is strictly controlled by urinary proteins, which induce nucleation of crystals, regulate their enlargement, and assist in their endocytosis and disposal.

Urine certainly contains a number of proteins that modulate CaOx crystallization *in vitro*,[4] but we do not know whether they are involved under physiologic conditions and, consequently, whether they are of any relevance whatsoever to stone formation. For the sake of argument, though, let us assume that reduced excretion of intracrystalline proteins, or derangements in their molecular structures, allow nucleation of solid CaOx crystals that cannot be easily dismantled and dispatched and which therefore predispose to stone formation. What can be done to correct the problem? Nothing really. Recurrent stone formers can certainly be urged to keep their urine watery or to avoid foods rich in oxalate, but there is currently no means of enabling them to increase their urinary excretion of proteins such as UPTF1. Further, even if it were possible to do so, there is always the possibility of causing other, potentially severe, metabolic problems.

Back to the plant. . . .

THE GREEN REVOLUTION: FOOD FOR THE PHOTOSYNTHETIC GOOSE IS FOOD FOR THE ANTHROPOID GANDER

Assuming our proposal is correct, understanding the basic molecular strategies by which intracrystalline plant proteins induce formation of crystals and direct their development will enable us to acquire better insight into protein-crystal interactions at the molecular level and has the potential to increase our knowledge of the role(s) of similar proteins in urolithiasis—for a number of reasons. First, it will allow us to study the molecular features, biophysical properties, and synthetic regulation of proteins whose specific function is to regulate mineral deposition, rather than those of proteins that are primarily involved in seemingly unrelated processes. For instance, UPTF1 is a byproduct of blood coagulation, and osteopontin is a major player in bone development. Although they both inhibit CaOx crystallization, it is difficult to imagine that that is their principal physiologic role. Second, it will neatly circumvent the difficulties associated with altering urinary protein excretion *in vivo* as one approach to preventing stone recurrences, as it offers the prospect of designing synthetic structural analogs of natural peptides that are unlikely to interfere in other human processes.

Of course, this is all very well but may be of little practical value unless there are significant similarities between features of CaOx crystal formation or metabolic processes in plants and humans or other major advantages to justify adopting what appears to be an outrageously unconventional approach. Fortunately, there are.

Plants offer obvious benefits to stone research, including their controlled manufacture of CaOx crystals by design ("normal" stones), their ready availability in large quantities, and the fact that their metabolic products still constitute one of the major sources of treatments for countless human diseases, including kidney stones.[70] Their metabolism and genetics can be readily and rapidly manipulated in ways that are ethically and practically impossible in humans or animals *in vivo*, regulation of oxalate synthesis is similar in plants and humans,[61] and, as detailed previously, they possess many calcium-binding pro-

teins found in humans. However, there is one further similarity that further vindicates our proposal of using plants as models of "normal" stone formation: CaOx crystals from plants contain proteins. Preliminary, unpublished work from our laboratory has shown that CaOx crystals isolated from plants, like those from their urinary counterparts, also have an intricate interior ultrastructure characterized by the presence of numerous protein-filled meanders. This suggests perhaps that intracrystalline proteins in plants may fulfil a role similar to that which we have proposed for human crystals. Resorption of CaOx crystals in plants occurs during periods of Ca^{2+} limitation,[61] a process which must depend on the ability of plant cells to dismantle and dissolve them and which would be facilitated by cooperation between intracrystalline proteins and intracellular proteases. Similar complementarity might also expedite disposal of mineral at the end of the growing season and assist in release of essential Ca^{2+} ions into the soil for reclamation by the plant's progeny. Such ionic husbandry may also extend beyond plants to other biomineralizing organisms throughout the natural world. Formation of CaOx crystals in human urine and higher plants may therefore represent simply another metabolic process derived from a common evolutionary pedigree.

TURNING OVER A NEW LEAF

In this review, we have presented urolithiasis as an abnormal manifestation of a process which, in many other organisms, is a normal, healthy event—crystal formation—and described aspects of our work that demonstrate some of the molecular bases of its study. In particular, our research has confirmed the existence of urinary "stereoms"—fenestrated CaOx crystals wrought by interactions between certain urinary proteins and the CaOx mineral—the formation of which may hold the key to explaining why some CaOx crystals precipitated within the urinary tract are passed harmlessly in the urine, others are disposed of intracellularly, and the remainder progress to stone pathogenesis. Although our findings and proposals have specific implications for the formation of stones, they also have ramifications for other biomineralization systems, where cooperation between cellular proteases and intracrystalline proteins may also fulfil an indispensable function in the fabrication, dismantling, and regeneration of mineral architecture throughout an organism's cycle of life, reproduction, and death.

Our proposal that honeycombed CaOx crystals in urine represent a normal, healthy means of disposing of excess quantities of calcium or oxalate in humans may well be regarded with suspicion or skepticism by conventional scholars of urolithiasis research. Time will prove whether we are correct. In the meantime, we will continue to pursue the more controversial avenue of our research. Biomimetics is currently one of the fastest-growing disciplines in the scientific world, and we have nothing to lose, and everything to gain, by throwing convention to the wind. Studying the controlled formation of CaOx crystals in our distant green cousins is certainly unconventional, but is it any more outlandish than studying viruses, bacteria, yeasts, and algae to discover basic molecular knowledge about human beings—from the tricarboxylic acid cycle to the genetic code? The time has come to trade our human chauvinism for some photosynthetic insight. After all, in many respects, plants are just like us![71]

ACKNOWLEDGMENTS

This work was supported by grants from the Flinders Medical Centre Foundation, the Australasian Urological Foundation, the Australian Kidney Foundation, and Grant Number 980366 from the National and Medical Research Council of Australia. DEF is the recipient of a Curtin University of Technology Postgraduate Scholarship.

REFERENCES

1. Freifelder D. Molecular Biology: A Comprehensive Introduction to Prokaryotes and Eukaryotes. Boston: Johns and Bartlett Publishers, 1983.
2. King JS, Boyce WH. Analysis of renal calculous matrix compared with some other matrix materials and with uromucoid. Arch Biochem Biophys 1959;82:455–461.
3. Addadi L, Weiner S. Control and design principles in biological mineralization. Angew Chem Int Ed Engl 1992;31:153–169.
4. Ryall RL. Glycosaminoglycans, proteins and stone formation: Adult themes and child's play. Pediatr Nephrol 1996;10:656–666.
5. Morse RM, Resnick MI. A new approach to the study of urinary macromolecules as participant in calcium oxalate crystallization. J Urol 1988;139:869–873.
6. Doyle IR, Ryall RL, Marshall VR. Inclusion of proteins into calcium oxalate crystals precipitated from human urine: A highly selective phenomenon. Clin Chem 1991;37:1589–1594.
7. Stapleton AMF, Simpson RJ, Ryall RL. Crystal matrix protein is related to human prothrombin. Biochem Biophys Res Commun 1993;195:1199–1203.
8. Suzuki K, Moriyama M, Nakajima C, et al. Isolation and partial characterization of crystal matrix protein as a potent inhibitor of calcium oxalate crystal aggregation: Evidence of activation peptide of human prothrombin. Urol Res 1994;22:45–50.
9. Stapleton AMF, Ryall RL. Blood coagulation proteins and urolithiasis are linked: Crystal matrix protein is the F1 activation peptide of human prothrombin. Br J Urol 1995;75:712–719.
10. Davie EW, Fujikawa K, Kisiel W. The coagulation cascade: Initiation, maintenance, and regulation. Biochemistry 1991;30: 10363–10370.
11. Friezner Degen SJ, Davie EW. Nucleotide sequence of the gene for human prothrombin. Biochemistry 1987;26:6165–6177.
12. Dihanich M, Kaser M, Reinhard E, Cunningham D, Monard D. Prothrombin mRNA is expressed by cells of the nervous system Neuron 1991;6:575–581.
13. Friezner Degen SJ. The prothrombin gene and its liver-specific expression. Semin Thromb Hemostas 1992;18:230–241.
14. Stapleton AMF, Timme TL, Ryall RL. Gene expression of prothrombin in the human kidney and its potential relevance to kidney stone disease. Br J Urol 1998;81:666–672.
15. Grover PK, Dogra SC, Davidson BP, Stapleton AMF, Ryall RL. The prothrombin gene is expressed in the rat kidney: Implications for urolithiasis research. Eur J Biochem 2000;267:61–67.
16. Stapleton AMF, Dawson CJ, Grover PK, et al. Further evidence linking urolithiasis and blood coagulation: Urinary prothrombin fragment 1 is present in stone matrix. Kidney Int 1996;49:880–888.
17. Grover PK, Moritz RL, Simpson RJ, Ryall RL. Inhibition of calcium oxalate crystal growth and aggregation *in vitro*: A com-

parison of four human proteins. Eur J Biochem 1998;253: 637–644.
18. Ryall RL, Grover PK, Stapleton AMF, et al. The urinary F1 activation peptide of human prothrombin is a potent inhibitor of calcium oxalate crystallization in undiluted human urine *in vitro*. Clin Sci 1995;89:533–534.
19. Grover PK, Ryall RL. Inhibition of calcium oxalate crystal growth and aggregation by prothrombin and its fragments *in vitro*: Relationship between protein structure and inhibitory activity. Eur J Biochem 1999;263:50–56.
20. Dean CJ, Macardle PJ, Ryall RL. The effect of the presence of calcium oxalate crystals on the measurement of prothrombin fragment 1 in urine. In: Rodgers AL, Hibbert BE, Hess B, Khan SR, Preminger GM (eds): Urolithiasis 2000. Rondebosch: University of Cape Town, 2000, pp 150–152.
21. Robertson WG, Peacock M. Calcium oxalate crystalluria and inhibitors of crystallisation in recurrent renal stone formers. Clin Sci 1972;43:499–506.
22. Médétognon-Benissan J, Tardivel S, Hennequin C, Daudon M, Drüeke T, Lacour B. Inhibitory effect of bikunin on calcium oxalate crystallization in vitro and urinary bikunin decrease in renal stone formers. Urol Res 1999;27:69–75.
23. Yasui T, Fujita K, Hayashi Y, et al. Quantification of osteopontin in the urine of healthy and stone-forming men. Urol Res 1999;27:225–230.
24. Grover PK, Sallis JD, Miyazawa K, Stapleton AMF, Ryall RL. Quantification of prothrombin mRNA using competitive polymerase chain reaction. In: Rodgers AL, Hibbert BE, Hess B, Khan SR, Preminger GM (eds): Urolithiasis 2000. Rondebosch: University of Cape Town, 2000, pp 158–159.
25. Johnson-Tardieu J, Glenton PA, Moriyama MT, Peck AB, Khan SR. Osteopontin expression in kidneys and urine of rats with hyperoxaluria and nephrolithiasis . In: Rodgers AL, Hibbert BE, Hess B, Khan SR, Preminger GM (eds): Urolithiasis 2000. Rondebosch: University of Cape Town, 2000, pp 142–143.
26. Moriyama MT, Aihara K, Suga K, et al. Analysis of prothrombin mRNA expression level in the normal and stone forming rat kidneys by competitive, real time quantitative PCR In: Rodgers AL, Hibbert BE, Hess B, Khan SR, Preminger GM (eds): Urolithiasis 2000. Rondebosch: University of Cape Town, 2000, pp 156–157.
27. Mandel N. Commentary on the growth of renal calculi. J Urol 1997;157:2.
28. Fleming DE, Doyle IR, Evans N, Marshall VR VR, Parkinson GM, Ryall RL. Proteins associated with calcium oxalate crystals formed in human urine are intracrystalline. In: Borghi L, Meschi T, Briganti A, Schianchi T, Novarini A (eds): Kidney Stones. Cosenza: Editoriale Bios, 1999, pp 359–362.
29. Dawson CJ, Grover PK, Ryall RL. Inter-α-trypsin inhibitor in urine and calcium oxalate urinary crystals. Br J Urol 1997;81:20–26.
30. Buchholz N-P, Kim DS, Grover PK, Dawson CJ, Ryall RL. The effect of warfarin therapy on the charge properties of urinary prothrombin fragment 1 and crystallization of calcium oxalate in undiluted human urine. J Bone Miner Res 1999;14:1003–1012.
31. Aizenberg J, Hanson J, Koetzle TF, Weiner S, Addadi L. Control of macromolecule distribution within synthetic and biogenic single calcite crystals. J Am Chem Soc 1997;119:881–886.
32. Aizenberg J, Ilan M, Weiner S, Addadi L. Intracrystalline macromolecules are involved in the morphogenesis of calcitic sponge spicules. Connect Tiss Res 1996;34:255–261.
33. Weiner S, Addadi L. Design strategies in mineralized biological materials. J Mater Chem 1997;7:689–702.
34. Aizenberg J, Hanson J, Ilan M, et al. Morphogenesis of calcitic sponge spicules: A role for specialized proteins interacting with growing crystals. FASEB J 1995;9:262–268.
35. Heuer AH, Fink DJ, Laraia VJ, et al. Innovative materials processing strategies: A biomimetic approach. Science 1993;255: 1098–1105.
36. Ryall RL. Urinary inhibitors of calcium oxalate crystallization and their potential role in stone formation. World J Urol 1997;15: 155–164.
37. Lieske JC, Leonard R, Toback FG. Adhesion of calcium oxalate monohydrate crystals to renal epithelial cells is inhibited by specific anions. Am J Physiol 1995;268:F604–F612.
38. Lieske JC, Norris R, Swift H, Toback FG. Adhesion, internalization and metabolism of calcium oxalate monohydrate crystals by renal epithelial cells. Kidney Int 1997;52:1291–1301.
39. Lieske JC, Toback FG, Deganello S. Face-selective adhesion of calcium oxalate dihydrate crystals to renal epithelial cells. Calcif Tiss Int 1996;58:195–200.
40. Lieske JC, Toback FG, Deganello S. Direct nucleation of calcium oxalate dihydrate crystals onto the surface of living renal epithelial cells in culture. Kidney Int 1998;54:796–803.
41. Lieske JC, Deganello S, Toback FG. Cell-crystal interactions and kidney stone formation. Nephron 1999;81:8–17.
42. de Water R, Nordermeer C, van der Kwast TH. Calcium oxalate nephrolithiasis: Effect of renal crystal deposition on the cellular composition of the renal interstitium. Am J Kidney Dis 1999;33:761–771.
43. Fleming DE, Grover PK, Chauvet MC, Marshall VR, Ryall RL. An unexpected role of urinary proteins in the prevention of calcium oxalate urolithiasis. In: Rodgers AL, Hibbert B, Hess B, Khan SR, Preminger GM (eds): Urolithiasis 2000. Rondebosch: University of Cape Town, 2000, pp 169–171.
44. Heymann D, Pradal G, Benahmed M. Cellular mechanisms of calcium phosphate ceramic degradation. Histol Histopathol 1999;14:871–877.
45. McCarthy GM, Mitchell PG, Struve JA, Cheung HS. Basic calcium phosphate crystals cause coordinate induction and secretion of collagenase and stromelysin. J Cell Physiol 1992;153:140–146.
46. Eggli PS, Müller W, Schenk RK. Porous hydroxyapatite and tricalcium phosphate cylinders with two different pore size ranges implanted in cancellous bone of rabbits. Clin Orthop Rel Res 1987;232:127–138.
47. Mori KM, Ogawa Y, Tamura N, et al. Molecular cloning of a novel mouse aspartic protease-like protein that is expressed abundantly in the kidney. FEBS Lett 1997;401:218–222.
48. Walker PD, Kaushal GP, Shah SV. Presence of a distinct extracellular matrix-degrading metalloproteinase activity in renal tubules. J Am Soc Nephrol 1994;5:55–61.
49. Kaushal GP, Walker PD, Shah SV. An old enzyme with a new function: Purification and characterization of a distinct matrix-degrading metalloproteinase in rat kidney cortex and its identification as meprin. J Cell Biol 1994;126:1319–1327.
50. Ravid A, Koren R, Rotem C, et al. 1,25–Dihydroxyvitamin D3 increases the cellular content of the calcium-activated neutral protease μ-calpain in renal cell carcinoma. Endocrinology 1994;136 :2822–2825.
51. Bautista DS, Densteldt J, Chambers AF, Harris JF. Low molecular weight variants of osteopontin generated by serine proteases in urine of patients with kidney stones. J Cell Biochem 1996;61:402–409.
52. Applewhite JC, Kennedy M, Assimos DG, Holmes RP. Renal oxalate synthesis. J Urol 2000;163(suppl):229–230.
53. Marks P. Mussel power. New Scientist Oct 23, 1999, p 12.
54. Knight J. Now hear this. New Scientist March 13, 1999, p 10.
55. Cohen P. Minuscule but perfectly formed. New Scientist July 18, 1998, p 23.
56. Knight J. An unfolding story: Meet the proteins that could uncook an egg. New Scientist July 18, 1998, p 23.
57. Burke M. Green miracle. New Scientist August 14, 1999, pp 27–30.

58. Mann S. Molecular tectonics in biomineralization and biomimetic materials chemistry. Nature 1993;365:499–505.
59. Walsh D, Mann S. Fabrication of hollow porous shells of calcium oxalate from self-organizing media. Nature 1995;377:320–323.
60. Meinke DW, Cherry JM, Dean C, et al. *Arabidopsis thaliana*: A model plant for genome analysis. Science 1998;282:662–682.
61. Franceschi VR, Loewus FA. Oxalate biosynthesis and function in plants and fungi. In: Khan SR (ed): Calcium Oxalate in Biological Systems. Boca Raton: CRC Press, 1995, pp 113–130.
62. Horner HT, Wagner BL. Calcium oxalate formation in higher plants. In: Khan SR (ed): Calcium Oxalate in Biological Systems. Boca Raton: CRC Press, 1995, pp 53–72.
63. Borchert R. Ca^{2+} as developmental signal in the formation of Ca-oxalate crystal spacing patterns during leaf development in *Carya ovata*. Planta 1990;182:339–347.
64. Gilroy S, Bethke PC, Jones RL. Calcium homeostasis in plants. J Cell Sci 1993;106:453–462.
65. Franceschi VR, Li X, Zhang D, Okita TW. Calsequestrin-like calcium-binding protein is expressed in calcium-accumulating cells of *Pistia stratiotes*. Proc Natl Acad Sci USA 1993;90:6986–6990.
66. Navazio L, Baldan B, Dainese P. Evidence that spinach leaves express calreticulin but not calsequestrin. Plant Physiol 1995; 109:983–990.
67. Hassan A-M, Wesson C, Trumble WR. Calreticulin is the major Ca^{2+} storage protein in the endoplasmic reticulum of the pea plant (Pisum sativum). Biochem Biophys Res Comm 1995;211:54–59.
68. Williams RJP. Calcium in health and disease. Cell Calcium 1998;24:233–237.
69. Randall SK. Characterization of vacuolar calcium-binding proteins. Plant Physiol 1992;100:859–867.
70. Koide T, Yamaguchi S, Utsunomiya M, Yoshioka T, Suguyama K. The inhibitory effect of Kampou extracts on *in vitro* calcium oxalate crystallization and *in vivo* stone formation in an animal model. Int J Urol 1995;2:81–86.
71. Coghlan A. Sensitive flower. New Scientist Sept 26, 1998, pp 24–28.

Address reprint requests to:
Rosemary Lyons Ryall, D.Sc.
Department of Surgery
Flinders Medical Centre
Bedford Park
South Australia 5042
Australia

E-mail: rose.ryall@flinders.edu.au

Journal of Structural Biology 134, 5–14 (2001)
doi:10.1006/jsbi.2001.4363, available online at http://www.idealibrary.com on IDEAL®

Intracrystalline Proteins and the Hidden Ultrastructure of Calcium Oxalate Urinary Crystals: Implications for Kidney Stone Formation

Rosemary Lyons Ryall,[1] David E. Fleming,*† Ian R. Doyle, Natalie A. Evans, Caroline J. Dean, and Villis R. Marshall

*Department of Surgery, Flinders University School of Medicine, Flinders Medical Centre, Bedford Park, South Australia 5042, Australia; *School of Applied Chemistry, and Curtin University of Technology, Perth, Western Australia, Australia; and †Chemistry Centre, Perth, Western Australia, Australia*

Received December 4, 2000; accepted April 30, 2001; published online June 28, 2001

The external appearance of urinary calcium oxalate (CaOx) crystals suggests that they are solid, homogeneous structures, despite their known association with proteins. Our aim was to determine whether proteins comprising the organic matrix of CaOx crystals are superficial or intracrystalline in order to clarify the role of urinary proteins in the formation of kidney stones. CaOx crystals were precipitated from centrifuged and filtered, or ultrafiltered, healthy human urine. They were then treated with dilute NaOH to remove bound proteins, partially demineralized with EDTA, or fractured and subjected to limited proteolysis before examination by low-resolution scanning electron microscopy or field emission scanning electron microscopy. Crystals precipitated from centrifuged and filtered urine had a complex interior network of protein distributed throughout the mineral phase, which appeared to comprise closely packed subcrystalline particles stacked in an orderly array among an amorphous organic matrix. This ultrastructure was not evident in crystals deposited in the absence of macromolecules, which were completely solid. This is the first direct evidence that crystals generated from cell-free systems contain significant amounts of protein distributed throughout a complex internal cribriform ultrastructure. Combined with mineral erosion in the acidic lysosomal environment, proteins inside CaOx crystals would render them susceptible to attack by urinary and intracellular renal proteases and facilitate their further dissolution or disruption into small particles and ions for removal by exocytosis. The findings also have broader ramifications for industry and the materials sciences, as well as the development and resorption of crystals in biomineralization systems throughout nature. © 2001 Academic Press

Key Words: **biomineralization; calcium oxalate; crystal ultrastructure; intracrystalline proteins; urolithiasis.**

INTRODUCTION

Biomineralization is used by living organisms to convert soluble ions into insoluble minerals, which are used to construct a spectacular array of intricate structures. The phenomenon occurs in all five kingdoms and involves the deposition of more than 60 minerals in organisms as evolutionarily diverse as bacteria and *Homo sapiens* (Addadi and Weiner, 1992). Biomineralizers manufacture unique, often exquisitely beautiful bioceramics with disparate functions and structures, such as pearls, shells, spines, teeth, and bones, whose component crystals are typically deposited in confined spaces specifically designed for their accommodation (Heuer *et al.*, 1992). Consequently, until relatively recently it was generally assumed that the size and shape of biogenic crystals are largely determined by the physical structure of the membranous cellular compartments in which they are deposited (Aizenberg *et al.*, 1995, 1996). However, Addadi, Weiner, and their colleagues have demonstrated that proteins associated with the calcified structures of a variety of marine organisms are *intracrystalline* (Albeck *et al.*, 1993, 1996a, 1996b; Aizenberg *et al.*, 1995, 1996, 1997). The resulting structures, comprising a "host" crystal and a "guest" protein, resemble reinforced concrete, with the guests effectively acting as intracrystalline steel rods that create and stabilize discontinuities in the lattice and alter crystal texture and tensile properties (Weiner and Addadi, 1997).

Throughout the natural world, crystal nucleation, growth, morphology, and assembly in living organ-

[1] To whom correspondence should be addressed. Fax: 618-8374-0832. E-mail: rose.ryall@flinders.edu.au.

1047-8477/01 $35.00

isms are regulated by acidic proteins with characteristic molecular structures and biochemical properties (Addadi and Weiner, 1992; Heuer *et al.*, 1992; Mann, 1993; Weiner and Addadi, 1997). Although they are pathological products, kidney stones are, nonetheless, biominerals, and like all biogenic minerals, they are intimately associated with proteins. Approximately 20 specific proteins have been detected in the organic matrix of human kidney stones (Ryall, 1996, 1997), but at present little is known about the role, if any, that proteins play in stone pathogenesis. Nonetheless, the parallel between stones and salubrious biomineralization has been too tempting to ignore, and it is now widely acknowledged that urinary proteins could, at least in theory, fulfill roles in the construction of kidney stones similar to those of their counterparts in healthy systems (Ryall and Stapleton, 1995). However, whereas a high proportion of proteins in stone matrix will derive from those comprising the usual complement of human urine, others will be deposited in successive layers as the stone enlarges, irritates the urothelial lining, and releases structural cellular macromolecules and blood products. Much of the organic matrix is therefore a product rather than a cause of the stone, and most proteins would be principally extracrystalline, having specifically or adventitiously bound to the surfaces of preformed crystals or having been trapped inside the interstices between them as the stone enlarged (Ryall, 1997).

A large number of ultrastructural studies have previously demonstrated the existence of an intimate association between the crystalline and the organic components of calcium oxalate (CaOx) stones (e.g., Iwata *et al.*, 1985; Khan and Hackett, 1984, 1987, 1993; Khan, 1995a, b), but have not provided direct evidence that the organic matrix is intracrystalline. In a number of studies the presence of organic material within ghosts of crystalluric particles or stones was demonstrated (Khan and Hackett, 1987, 1993; Khan, 1995b; Khan *et al.*, 1996) but the crystalluric particles were polycrystalline dumbbells, not individual crystals. Organic striations observed in those studies therefore probably represented transverse sections of an organic coating delineating the surfaces of individual crystallites or associated with cracks in their boundaries. In some cases, crystal ghosts themselves were described as "mostly empty spaces" (Khan *et al.*, 1983) while others showed no evidence of intracrystalline inclusions (Khan and Hackett, 1993; Khan, 1995a, b). Moreover, the studies were performed on stones, which are unable to provide detailed information on individual crystals and, as stated above, also contain inflammatory proteins produced by cellular trauma.

It is now well known that CaOx crystals nucleated *de novo* from human urine, and which cannot, therefore, contain proteins released secondarily by cellular injury, are closely associated with proteins (Morse and Resnick, 1988; Doyle *et al.*, 1991). We have proposed that the proteins are included within the crystalline structure, that is, are *intra*crystalline (Doyle *et al.*, 1991). This suggestion is supported by theoretical considerations confirming that large immobile organic molecules can adsorb strongly to a crystal surface and become incorporated inside the crystal as growth steps move around and past them (Cabrera and Vermilyea, 1958), as well as by the demonstration of organic material in ghosts of demineralized uric acid crystals generated from human urine (Iwata *et al.*, 1988). However, the concept is still regarded with skepticism by some in the stone field (Mandel, 1997), despite wide recognition that the morphology and structural properties of some biominerals are influenced by the presence of proteins *within* the individual crystals constituting their fabric (Addadi and Weiner, 1992; Weiner and Addadi, 1997). Whether the proteins associated with CaOx crystals are superficial or intracrystalline has significant implications for the development and study of human urolithiasis. Therefore the aim of this study was to demonstrate directly that proteins occur within the crystalline architecture of CaOx crystals precipitated from human urine, in order to gain insight into their possible function in the crystallization and fate of CaOx during the formation or prevention of urinary stones.

MATERIALS AND METHODS

Chemicals and Biochemicals

All reagents were of the highest purity commercially available. Sodium oxalate and sodium dodecyl sulfate (SDS) were obtained from BDH Chemicals Australia (Kilsyth, Victoria, Australia); sodium hydroxide and ethylenediaminetetra-acetic acid (EDTA) were from Ajax Chemicals (Auburn, NSW, Australia). Calcium chloride and Tris[hydroxymethyl]-aminomethane (Tris) were purchased from Sigma Chemical Co. (St. Louis, MO) and Proteinase K1 was obtained from Boehringer Mannheim (Mannheim, Germany). Solutions were prepared using high quality water from a Hi Pure water purification system fitted with a 0.2-μm filter (Permutit Australia, NSW, Australia).

Study 1

Collection and Treatment of Urines

Urine samples were collected under refrigeration without preservative from four healthy men between 25 and 43 years of age and five healthy women between 18 and 41 years of age. The samples were pooled according to gender, confirmed to be free of blood by dipstick analysis (Miles Diagnostics, Mulgrave, Victoria, Australia), and divided into three aliquots. One of these (Si) was sieved through a 20-μm sieve. The remaining samples were centrifuged ($\times$10 000*g*) at room temperature in a Beckman J2-21M/E centrifuge and then filtered (0.22 μm; Millipore). One specimen (SF) was stored at 4°C until required, while the other (UF) was

ultrafiltered using an Amicon hollow fiber bundle (Amicon Corp., Danvers, MA), with a nominal molecular mass cutoff of 10 kDa.

Isolation and Sodium Dodecyl Sulfate–Polyacrylamide Gel Electrophoresis (SDS–PAGE) Analysis of CaOx Crystals

Following determination of the metastable limit (Ryall *et al.*, 1985), CaOx crystallization was induced by the dropwise addition of sodium oxalate solution, and the crystals were isolated and washed briefly with 0.1 M NaOH as previously described (Doyle *et al.*, 1991). A 10-mg portion of each crystal specimen was demineralized in EDTA, electrodialyzed, and analyzed by SDS–PAGE as previously detailed (Doyle *et al.*, 1991).

Effect of Alkaline Washing and EDTA Demineralization on CaOx Crystals

Washing. Crystals were isolated by filtration, washed off the filter surface with 0.1 M NaOH, and vortexed in 30 ml of the same solution. Washing was repeated for a total of eight cycles, with distilled water being substituted for NaOH in the last two cycles. Then 25-μl aliquots of the crystal suspensions were diluted in 0.5 ml of distilled water and Millipore filtered (0.22 μm).

Partial dissolution. Ten-milligram portions of crystals isolated from the Si, SF, and UF urines were suspended in 5 ml of 50 mmol/L EDTA (pH 8.0) and mixed at 4°C. At timed intervals, 200-μl aliquots were withdrawn, suspended in 1 ml of distilled water, and filtered. The filters were rinsed twice with distilled water.

Scanning Electron Microscopy

The filtered crystals were dried in air, mounted on aluminum stubs, and gold-sputtered for 210 s (SEM Autocoating Unit E5200; Polaron Equipment Ltd., Watford, England). They were then examined using an ETEC Auto Scan electron microscope (Siemans AG, Hayward, CA) at an operating voltage of 20 kV.

Study 2

Because the results of Study 1 demonstrated that CaOx crystals precipitated from male and female urines, as well as the proteins associated with them, were qualitatively similar, only healthy female urine was used for Study 2. A 24-h urine specimen was collected from a healthy woman, age 48 years. One-half of the specimen was centrifuged and filtered (SF), while the other was ultrafiltered (UF), as described above. The crystals were isolated by filtration and washed exhaustively with distilled water as outlined for Study 1 and dried.

SDS–PAGE Analysis of Urine and Crystal Proteins

The crystals were harvested and demineralized as described above, and the resulting solution was passed through a desalting column of Bio-Gel P-6 DG (Bio-Rad Laboratories, Richmond, CA), prior to lyophilization. Proteins in the crystal matrix from each sample were reconstituted in water and analyzed by SDS–PAGE (Doyle *et al.*, 1991). Protein concentrations were determined using the Bio-Rad Laboratories protein assay (Bio-Rad Laboratories).

Proteolytic Digestion of CaOx Crystals and Examination by Field Emission Electron Microscopy

Specimens of SF and UF crystals were fractured under light microscopy using a diamond cell (High Pressure Diamond Optics Inc). A 5-mg sample of each type of fractured crystal was incubated at 37°C for 12 h in 2 ml of a saturated CaOx solution containing 0.25 mg/ml Proteinase K1; 12.5 mmol/L Tris–HCl buffer, pH 7.5, and 0.125 mol/L NaCl. The crystals were then dried under nitrogen, coated with carbon (SpeediVac Model 12E6), and examined using a FESEM Jeol 6300F field emission electron microscope (Jeol, Akishima, Tokyo, Japan). Untreated samples of each crystal type were retained to enable observation of the effects of proteolytic digestion. Pure crystals of CaOx (see below) and crystals deposited from UF urine samples served as controls.

Preparation of Pure CaOx Crystals

Crystals of CaOx were generated in distilled water at 37°C by introducing 5 ml each of aqueous solutions of 0.15 mol/L $CaCl_2$ and 0.15 mol/L $(COONa)_2$ into 50 ml of distilled water at a rate of 0.4 ml/h from glass syringes using an infusion pump (Sage Instruments, Cambridge, MA). The mixture was gently mixed with an overhead stirrer fitted with a glass stirring rod and incubated for 8 h at 37°C. The precipitated crystals were separated by vacuum filtration and dried under nitrogen.

RESULTS

Protein and SDS–PAGE Analysis of Crystals

The SDS–PAGE patterns of the proteins derived from the crystals precipitated from the Si, SF, and UF urine specimens were qualitatively identical to those that we have previously reported (Doyle *et al.*, 1991), the principal protein associated with the crystals being urinary prothrombin fragment 1 (Ryall *et al.*, 1995). Because the pattern of protein bands was identical to those we have previously published (Doyle *et al.*, 1991; Ryall *et al.*, 1995), they are not presented here. As expected, no protein bands were clearly visible in the electrophoretograms of the organic extracts of the crystals from the UF urines. Protein measurements showed significant amounts of protein in the soluble organic matrix of the crystals, the ratio of intracrystalline protein mass to mineral mass being consistently in the order of 0.03%. There were no detectable proteins in crystals precipitated from the UF urine.

Effect of NaOH Washing and Partial EDTA Dissolution on Crystal Structure

Although both disc-shaped CaOx monohydrate (COM) and octahedral CaOx dihydrate (COD) crystals were precipitated from the urines, most were COM. The effects of NaOH washing and partial EDTA demineralization were identical in the crystals from the male and female urines: therefore, only results from the female urines are presented. Figure 1 shows SEM micrographs of crystals that had all been precipitated from the same original pooled urine specimen.

Untreated Crystals

The COM crystals from the Si urine (Si1) were concave and rounded and showed evidence of distinct plate-like layering along their edges, rather reminiscent of shale or mica (see Fig. 1, top row). The COD crystals, although superficially smooth, also had rounded corners. The surface of the filtra-

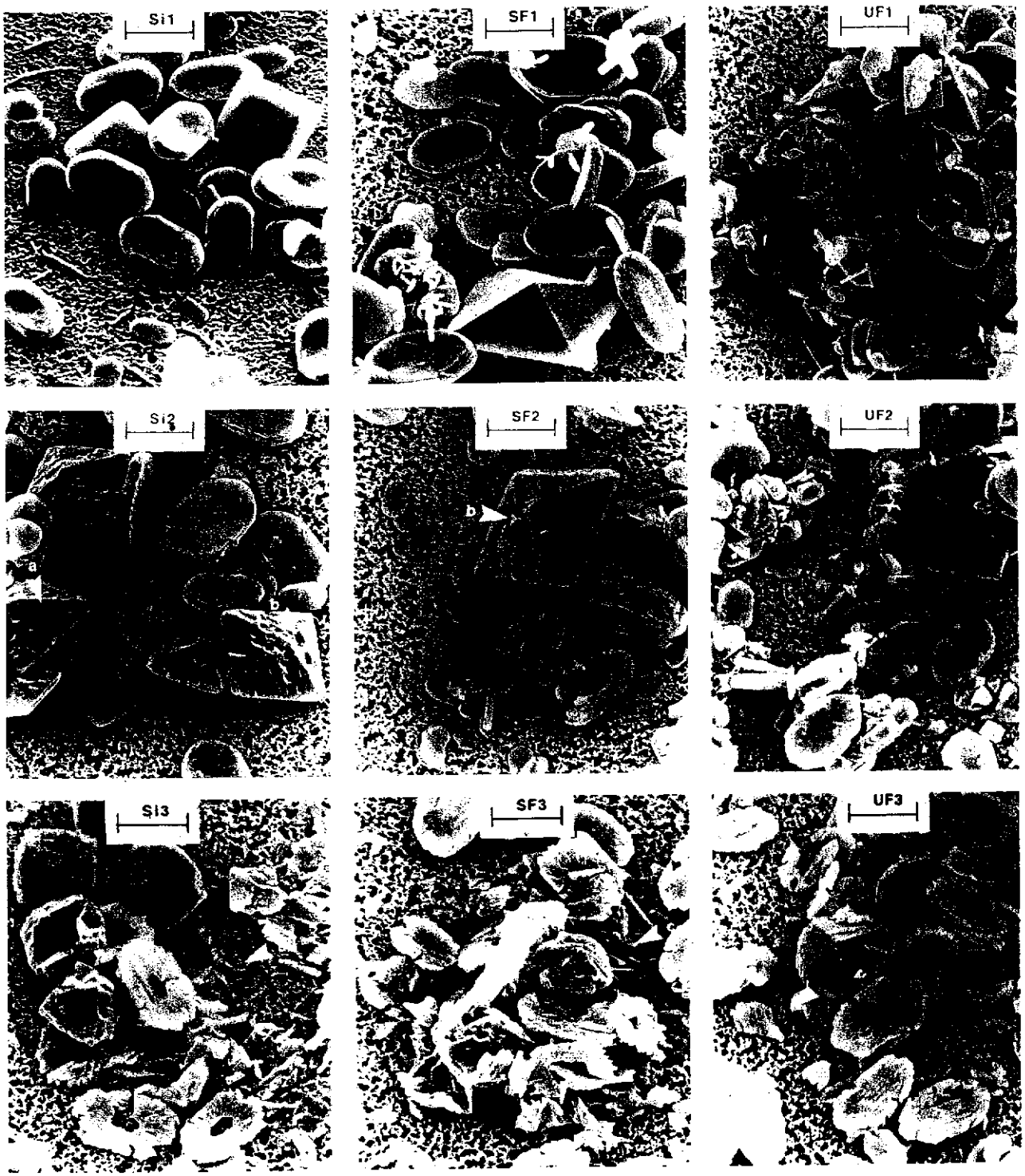

FIG. 1. CaOx crystals precipitated from sieved (Si), centrifuged and filtered (SF), and ultrafiltered (UF) urine. The top horizontal row shows untreated crystals from each treatment group, the middle row illustrates crystals that had been washed with NaOH, and the bottom row depicts those that had been partially dissolved with EDTA.

tion membrane was covered with an organic "mud." This is principally Tamm–Horsfall glycoprotein (THG), which is almost completely removed from urine by centrifugation and filtration (Doyle *et al.*, 1991) and cannot be seen in the samples derived from the SF and UF urines. COM and COD crystals

precipitated from the SF urine (SF1) exhibited crisper margins and displayed little of the layering evident in the Si crystals. A single deformed COM crystal can be seen in the lower left-hand corner of the micrograph, while the large COM lying directly above the only COD crystal shows very faint evidence of surface pitting, which is more evident in COM crystals in Si2. As we consistently observe with CaOx precipitated from SF urine (Ryall *et al.*, 1995), the crystals were principally single or clustered into small aggregates. The crystals precipitated from the UF urine (UF1) were smooth, had sharply delineated margins, and, as invariably occurs (Ryall *et al.*, 1995), were aggregated into large clumps. The presence of numerous small crystals upon the surfaces of the larger ones suggests the occurrence of secondary nucleation.

Effect of NaOH Washing

After the crystals were washed, organic material was no longer visible on either the filter surface or the crystals themselves (see Fig. 1, middle row). Its absence may be attributed to the solubility of THG in alkaline solutions of low ionic strength (McQueen and Engel, 1966). COD crystals from the sieved urine (Si2) were extensively etched with shallow teardrop-shaped pits (Fig. 1, arrow a) and deep cavities (Fig. 1, arrow b), while the COM crystals were covered with a fine network of small fissures similar to those that were barely visible in SF1. Crystals precipitated from the SF urine (SF2) still had significant pitting (Fig. 1, arrow b) but were devoid of the shallow depressions observed on the surfaces of the corresponding Si crystals. This suggests that the depressions were probably caused by the removal of aggregated proteins such as THG lying loosely upon the crystal superficies. Although deep crevices were not present in the COM crystals, the structural integrity of some of them was severely disrupted, as seen in those located on the right-hand side of the micrograph, where it appears that layers of the crystals have been sheared off. The external appearances of crystals from the UF urine (UF2) were largely unaffected by the alkaline washing, which nonetheless significantly disrupted the crystal aggregates. In some cases, this caused the exposure of regions of crystals that had abutted others; for instance, the horizontal scissure visible on one of the COM crystals immediately southeast of the center of the picture probably represents the former attachment site of the edge of another crystal.

Effect of EDTA Demineralization

While the COD crystals tended to erode from the outer edges inward, the COM crystals characteristically dissolved from the center to the periphery, creating distinct doughnut shapes with crenated edges (see Fig. 1, bottom row). Amorphous organic material can be seen lying upon the membrane surface (Si3; Fig. 1, arrow c). Because this was not visible in Si2, and increased in quantity as dissolution proceeded, it must have originated from the interior of the crystals. Crystals from the SF urine (SF3) were similar to those shown in Si3. Again, organic material can be clearly seen (Fig. 1, arrow c) associated with the dissolving crystals, usually with crystalline fragments embedded within it. Crystals precipitated from the ultrafiltered urine (UF3) were not associated with organic material. Erosion of both COD and COM crystals typically occurred from the outside edges. Deep, ordered pitting of COD crystals was not apparent; nor was the regular, pinked appearance of the margins seen in Si3 and SF3.

FIG. 2. COD crystals precipitated from a female subject's sieved urine that had been washed with NaOH. In the large central crystal note the regular, rectangular erosions that are surrounded by a more solid shell of mineral and note the crenations along the edges of fracture planes in crystal fragments.

Alkali washing studies were also carried out on crystals isolated from individual urine specimens. Qualitatively, the effects of NaOH washing were consistent, with all samples exhibiting some degree of pitting and/or surface etching. However, the extents of these phenomena varied markedly between crystals precipitated from different urines and even between crystals isolated from the same urine: some showed few depressions and relatively little chasing, while others were profoundly affected. This is evident in Fig. 2, which shows a higher magnification of NaOH-washed COD crystals from the sieved urine of a female subject and demonstrates clearly that crevices all had a characteristic square or rectangular shape and were arranged in a highly ordered

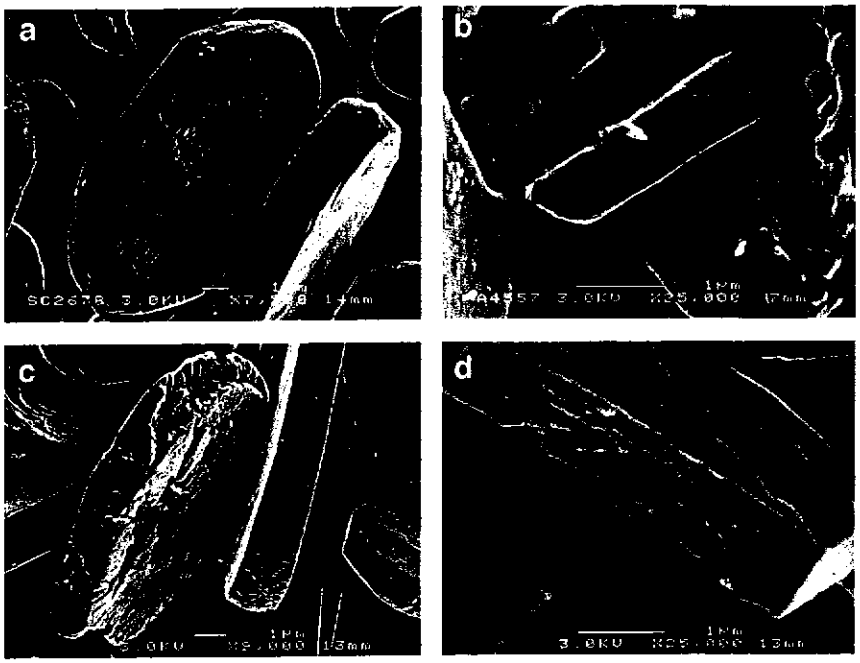

FIG. 3. COM crystals precipitated from a single female urine specimen that had been centrifuged and filtered. The top row shows intact (a) and fractured (b) crystals that had not been treated with protease, while the bottom row shows intact (c) and fractured (d) crystals from the same batch, after proteolytic digestion.

fashion. This regularity was also obvious in the internal structure of individual crystals, in the form of crenations visible along the edges of fracture planes, and on the boundaries of several smaller crystals in the lower left-hand corner of Fig. 2.

FESEM Studies: Effect of Proteolytic Digestion of Fractured Crystals

Figure 3 shows COM crystals generated from urine that had been centrifuged and filtered. As was also seen after NaOH washing (Fig. 1; SF1, Si2), the {101} surface was covered with a network of fine fissures, which are more obvious here at higher magnification. Crystals from the same batch, but which had been fractured, are shown in Fig. 3b. Most notable is a transverse view of a single COM crystal, which occupies the center of the field. This shows considerable honeycombing of the mineral. Proteolytic digestion (Fig. 3c) of intact crystals removed much of the associated organic material and enabled the capture of sharper images, which facilitated visualization of the network of numerous internal lacunae, as well as the layering seen in Fig. 1 (SF2). The crystals were significantly excavated, particularly at the end {120} faces and in the central region of the large {101} face, while the sides {010} were more refractory to protease treatment. The pattern of erosion resembled that of COM crystals subjected to EDTA treatment (Fig. 1; Si3, SF3) and indicates that the concentration of protein was greatest at the crystal center, where that of mineral was lowest. This supposition is strengthened in Fig. 3d, which shows a transverse view of a fractured COM crystal after digestion with protease. It can be seen that the central region of the crystal contained less mineral than did the periphery.

The occurrence of what appeared to be discrete, closely packed subcrystalline particles was a frequent observation, particularly in COM crystals that had been treated with protease. This phenomenon is illustrated in Fig. 4a. Here, the periphery of a COM crystal appears to comprise interconnected sheets of mineral interspersed with organic material, but the crystal center, which is almost completely eroded, contains small particles (approximately 50–80 nm in diameter) coated with organic material. These small particles were a common finding and are more obvious in Fig. 4b, which shows another crystal from the same batch at a similar magnification. Subcrystalline particles, which may be amorphous mineral (Addadi *et al.*, 1999) were also visible in COD crystals (results not shown).

Figure 5a depicts intact, pure COM crystals, while Fig. 5b shows a higher power view of the fractured surface of one of these crystals after digestion with protease. The crystals were completely solid throughout, and there was no evidence of surface or interior erosion, even at a magnification of ×40 000. This was also true of crystals precipitated from the

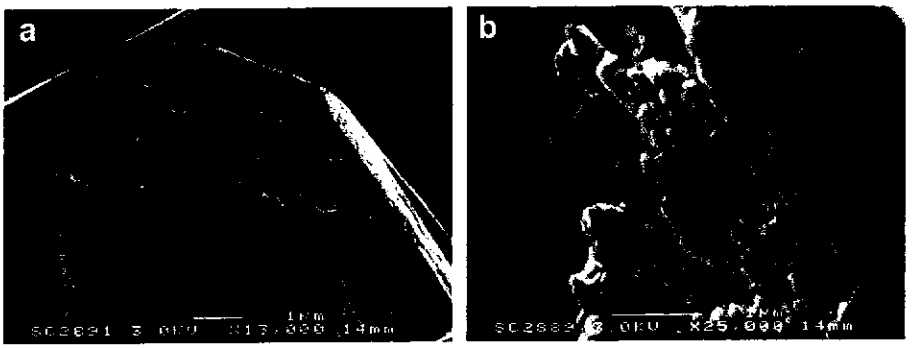

FIG. 4. COM crystals precipitated from centrifuged and filtered urine, after treatment with protease, showing discrete, closely packed subcrystalline particles. In (a) the particles appear to be mixed with composite projections of mineral and organic matter, which may represent stacks or sheets of particles linked in a linear fashion. The exposed crystal surface in (b) seems to consist entirely of highly ordered particles interspersed with organic material.

ultrafiltered urine. Again, the fractured crystals were solid (Fig. 5c), even after treatment with protease (Fig. 5d).

DISCUSSION

Although the occurrence and critical function of intracrystalline proteins in biogenic crystals are now widely recognized (Weiner and Addadi, 1997), to date, evidence that the phenomenon occurs in CaOx crystals from human urine has been indirect (Morse and Resnick, 1988; Doyle *et al.*, 1991). Numerous ultrastructural studies of kidney stones (Iwata *et al.*, 1985; Khan and Hackett, 1984, 1987, 1993; Khan, 1995a) have confirmed the existence of an intimate association between macromolecules and stone mineral, but have provided no direct evidence that proteins in stones actually occur within individual crystals. In this study, rather than attempt to examine the organic material remaining after removal of the mineral component, we chose instead to examine the structure of CaOx crystals following removal of protein. Alkali washing of crystals generated from urine that had been centrifuged and filtered caused shallow etching of the crystal

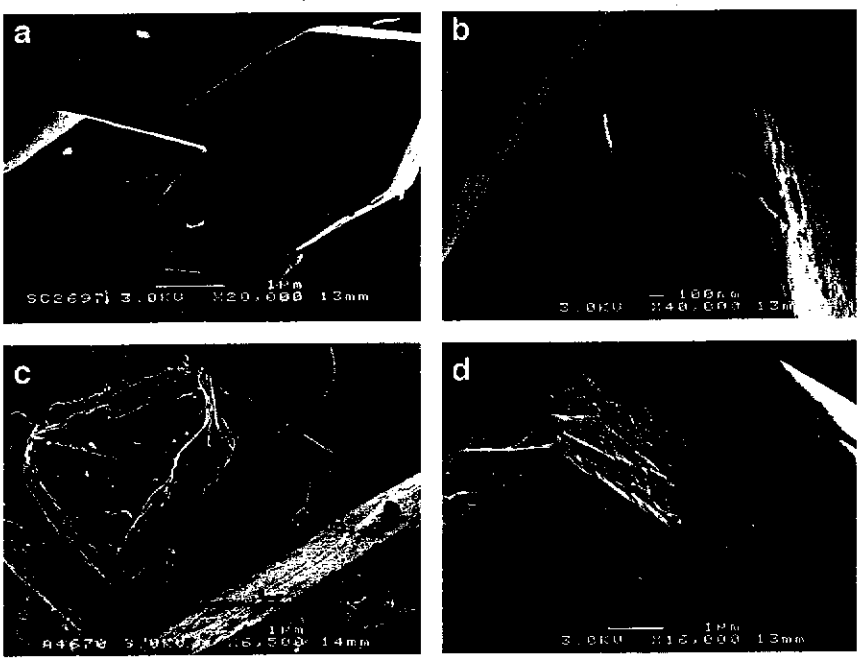

FIG. 5. COM crystals included as controls. The top row shows intact crystals (a) generated from an inorganic solution and an example of the same crystals following fracture and protease treatment (b). Crystals precipitated from ultrafiltered urine are shown in the bottom row, depicting fractured, untreated crystals (c) and the same crystals after protease digestion (d).

surface, as well as extensive erosion of both COM and COD crystals. In particular, COD crystals exhibited deep, right-angular pits that appeared to extend well into the crystal interior. That the formation of these pits must have been caused by the removal of organic material from the crystal interior was confirmed by carrying out similar studies on CaOx crystals precipitated from the same urine after removal of all macromolecules greater than 10 kDa in mass. These showed no sign of cavities.

Using FESEM examination of fractured crystals before and after protease digestion, we observed significant amounts of organic material lying upon and within COM and COD crystals. The amount of this material was significantly reduced by proteolytic digestion, confirming that the majority of it was protein, removal of which left a highly ordered array of pores. The absence of pores throughout pure inorganic CaOx crystals, as well as those precipitated from ultrafiltered urine, confirmed that the pores must have been formed by incorporation into the crystal bulk of proteins originating from the urinary tract. We have observed identical porosity in CaOx crystals precipitated spontaneously from urine specimens refrigerated during the collection period prior to processing for experiments (unpublished observations), which confirms that inclusion of proteins within the crystalline structure is not simply an artifact caused by addition of excess sodium oxalate to induce crystal formation. Perhaps the most compelling evidence that intracrystalline proteins are involved in the formation or prevention of stones is the observation of identical, regularly arranged spaces in COD crystals attached to the tubular epithelium of rats that had received intraperitoneal injections of sodium oxalate (Khan *et al.*, 1979) as well as within CaOx particles passed in urine following extracorporeal shock wave lithotripsy (ESWL) to remove renal stones (Khan *et al.*, 1986).

Another consistent feature of the COM crystals was the high concentration of organic material at the crystal core, which decreased toward the periphery. The core consisted of small discrete particles, perhaps of amorphous mineral (Addadi *et al.*, 1999), buried in organic material, while the material toward the perimeter resembled continuous sheets of mineral interwoven with organic matter. Although this suggests that urinary proteins might have been actively involved in the initial formation of small crystal nuclei, it does not exclude the possibility that they had also bound to newly formed mineral surfaces immediately after crystal nucleation. The contrasting structures of the core and perimeter indicate that as deposition of CaOx mineral proceeded, the urine was quickly depleted of strongly binding proteins. Subsequently deposited material contained less protein and formed a shell of more solid mineral around the composite interior. It was also apparent that protein adsorption was face-selective, since the {010} faces were more resistant to proteolysis than the {101} and {120} faces, which were highly susceptible to protease treatment. Adsorption and subsequent inclusion of protein within the crystal structure would therefore almost certainly have occurred by stereochemical recognition processes (Aizenberg *et al.*, 1997) at regularly spaced specific binding sites upon the crystal surface. The results presented here thus constitute the first direct evidence that proteins associated with CaOx crystals precipitated from human urine are incarcerated *within* the mineral structure. Under strict genetic and cellular control, intracrystalline proteins fulfill a critical function in healthy biomineralization (Albeck *et al.*, 1993; 1996a, 1996b; Aizenberg *et al.*, 1995, 1996, 1997). Our demonstration of their existence in CaOx urinary crystals provides clear evidence that ordered incorporation of proteins into crystals also occurs in the complete absence of any form of cellular processes. This has enormous ramifications for the development of kidney stones. Several urinary proteins are efficient inhibitors of CaOx crystal aggregation, and it has been assumed that their primary role in healthy urine is to prevent the formation of large crystal clusters likely to be retained within the renal collecting system; their occurrence in stones may therefore be a consequence of an inadequate or defective protective function (Ryall, 1997). However, crystals may also attach directly to the epithelial surface (Khan and Hackett, 1991), which has particular implications for stone pathogenesis or prevention.

Lieske and his colleagues have shown that exogenous COM (Lieske *et al.*, 1997) and COD (Lieske *et al.*, 1996) crystals are internalized by cultured monkey renal BSC-1 cells and subsequently dissolve over a period of several weeks within lysosomal inclusion bodies (Lieske *et al.*, 1999), whose acidic interiors are rich in proteases with pH maxima in the acid range (Bohley and Seglen, 1992). They hypothesized that crystal attachment and subsequent dissolution may represent a series of events occurring continually in the kidney as a routine means of evading stone formation (Lieske *et al.*, 1996), postulating that the surfaces of epithelial cells could serve as templates for the nucleation of crystals from supersaturated tubular fluid (Lieske *et al.*, 1999). Their subsequent attachment would be facilitated by stereospecific interactions between structures on the apical surface of renal tubular cells and the assemblage of molecules on the {100} face of the COD crystal (Lieske *et al.*, 1996) and similar arrays on the COM crystal surface (Lieske *et al.*, 1998).

These interactions would depend, in turn, upon specific anionic molecules either on the surface of renal cells or within the luminal fluid, the concentration and structure of which are influential in determining whether attachment, endocytosis, and dissolution of crystals occur (Lieske *et al.,* 1996; 1998).

We would like to extend this hypothesis by proposing that the ultimate fate of attached crystals and, thereby, the likelihood of stone formation also depend upon the nature and concentration of urinary proteins incorporated *within* the precipitated crystals since they could facilitate crystal deconstruction and removal following attachment and phagocytosis. Initial erosion of any mineral shell surrounding a protein-riddled interior would be assisted by the acidic lysosomal environment, while the protein-filled pores would be susceptible to proteases that would open channels throughout the interior mineral architecture, allowing infiltration into the crystalline core for further proteolytic digestion. This would expedite dismantling and dissolution of crystals, as well as removal of the resulting particles and ions by exocytosis. De Water *et al.* (1999) have also proposed that proteins comprising the organic matrix of CaOx crystals are chemotactic for cells released in response to inflammation provoked by the crystals themselves, including macrophages. By secreting neutral proteases, these could digest the organic matrix of the crystals and disrupt the mineral phase into nanometer-sized particles for removal by phagocytosis. This novel proposal is supported by other unpublished data from our laboratory that show that significant removal of organic material associated with CaOx crystals occurs upon incubation in urine, presumably as a result of digestion by urinary proteases. As discussed above, similar erosion has been observed in fragments of CaOx stones temporarily retained within the renal space following ESWL (Khan *et al.,* 1986), as well as in COD crystals undergoing internalization after cellular attachment (Lieske *et al.,* 1998).

The possibility that urinary crystals could be dismantled into small particles by proteolysis is supported by our observation of small discrete intracrystalline particles and honeycombed, continuous mineral, both intimately associated with protein, and also by the results of Dorian *et al.* (1996). Those authors reported that crystals within kidney stones comprise stacked arrays of minute crystallite particles and concluded that stone mineral consists of aggregates of crystallites that may be associated with organic material. However, our data clearly demonstrate that apparently *single* crystals possess a complex internal ultrastructure; this appears to comprise individual particles of mineral, which may be amorphous, embedded in an organic sludge. The fact that individual crystals precipitated in the presence and in the absence of organic material can have apparently identical external appearances, and yet vastly different internal architecture, brings into sharp focus the definition of what actually constitutes a single crystal (Addadi *et al.,* 1999). Nonetheless, the present study has confirmed that crystal formation and growth appear to be strictly programmed phenomena. Large urinary macromolecules can obviously be incorporated into spontaneously formed CaOx crystals in the complete absence of any cellular machinery, with no major disruption to succeeding mineral deposition, which can obviously heal the "wound" inflicted by adsorption of foreign matter and produce a structure with apparently normal external morphology. While this has obvious implications for the development of urolithiasis in humans, it also has wider ramifications for the materials sciences since it offers the possibility of tailor-made crystal–protein materials with a wide range of properties and applications. The phenomenon is also likely to be widespread throughout nature, where intracrystalline proteins may fulfill previously unsuspected functions in the disposal of unwanted mineral or its resorption for reclamation of essential ions during an organism's development and growth.

This work was supported by grants from the Flinders University of South Australia, the Flinders Medical Centre Foundation, and Grant 980366 from the National and Medical Research Council of Australia. D.E.F. is the recipient of a Curtin University of Technology Postgraduate Scholarship.

REFERENCES

Addadi, L., Aizenberg, J., Beniash, E., and Weiner, S. (1999) On the concept of a single crystal in biomineralization, *in* Braga, D., *et al.* (Ed.), Crystal Engineering: From Molecules and Crystals to Materials, pp. 1–22, Kluwer Academic, Dordrecht.

Addadi, L., and Weiner, S. (1992) Control and design principles in biological mineralization, *Angew. Chem. Int. Ed. Engl.* **31,** 153–169.

Aizenberg, J., Hanson, J., Ilan, M., Leiserowitz, L., Koetzle, T. F., Addadi L., and Weiner, S. (1995) Morphogenesis of calcitic sponge spicules: A role for specialized proteins interacting with growing crystals, *FASEB J.* **9,** 262–268.

Aizenberg, J., Hanson, J., Koetzle, T. F., Weiner, S., and Addadi, L. (1997) Control of macromolecule distribution within synthetic and biogenic single calcite crystals, *J. Am. Chem. Soc.* **119,** 881–886.

Aizenberg, J., Ilan, M., Weiner, S., and Addadi, L. (1996) Intracrystalline macromolecules are involved in the morphogenesis of calcitic sponge spicules, *Connect. Tissue Res.* **34,** 255–261.

Albeck, S., Addadi, L., and Weiner, S. (1996a) Regulation of calcite crystal morphology by intracrystalline acidic proteins and glycoproteins, *Connect. Tissue Res.* **35,** 419–424.

Albeck, S., Aizenberg, J., Addadi, L., and Weiner, S. (1993) Interactions of various skeletal intracrystalline components with calcite crystals, *J. Am. Chem. Soc.* **115,** 11691–11697.

Albeck, S., Weiner, S., and Addadi, L. (1996b) Polysaccharides of intracrystalline proteins modulate calcite crystal growth in vitro, *Chem. Eur. J.* **2,** 278–284.

Bohley, P., and Seglen, P. O. (1992) Proteases and proteolysis in the lysosome, *Experientia* **48,** 151–157.

Cabrera, N., and Vermilyea, D. A. (1958) The growth of crystals from solution, *in* Doremus, R. H., Roberts, B. W., and Turnbull, D. (Eds.), Growth and Perfection of Crystals, pp. 393–407, Wiley, New York/London.

De Water, R., Noordermeer, C., van der Kwast, T. H., Nizze, T. H., Boevé, E. R., Kok, D. J., and Schröder, F. H. (1999) Calcium oxalate nephrolithiasis: Effect of renal crystal deposition on the cellular composition of the renal interstitium, *Am. J. Kidney Dis.* **33,** 761–771.

Dorian, H. H., Rez, P., and Drach, G. W. (1996) Evidence for aggregation in oxalate stone formation: Atomic force and low voltage scanning electron microscopy, *J. Urol.* **156,** 1833–1837.

Doyle, I. R., Ryall, R. L., and Marshall, V. R. (1991) Inclusion of proteins into calcium oxalate crystals precipitated from human urine: A highly selective phenomenon, *Clin. Chem.* **37,** 1589–1594.

Heuer, A. H., Fink, D. J., Laraia, V. J., Arias, J. L., Calvert, P. D., Kendall, K., Messing, G. L., Blackwell, J., Rieke, P. C., Thompson, D. H., Wheeler, A. P., Veis, A., and Caplan, A. I. (1992) Innovative materials processing strategies: A biomimetic approach, *Science* **255,** 1098–1105.

Iwata, H., Kamel, O., Abe, Y., Nishio, S., Wakatsuki, A., Ochi, K., and Takeuchi, M. (1988) The organic matrix of urinary uric acid crystals, *J. Urol.* **139,** 607–610.

Iwata, H., Nishio, S., Wakatsuki, A., Ochi, K., and Takeuchi, M. (1985) Architecture of calcium oxalate monohydrate urinary calculi, *J. Urol.* **133,** 334–338.

Khan, S. R. (1995a) Calcium oxalate crystal interaction with renal tubular epithelium, mechanism of crystal adhesion and its impact on stone formation, *Urol. Res.* **23,** 71–79.

Khan, S. R. (1995b) Heterogeneous nucleation of calcium oxalate crystals in mammalian urine, *Scan. Microsc.* **9,** 597–616.

Khan, S. R., Atmani, F., Glenton, P., Hou, Z-C., Talham, D. R., and Khurshid, M. (1996) Lipids and membranes in the organic matrix of urinary calcific crystals and stones, *Calcif. Tissue Int.* **59,** 357–365.

Khan, S. R., Finlayson, B., and Hackett, R. L. (1983) Agar-embedded urinary stones: A technique useful for studying microscopic architecture, *J. Urol.* **130,** 992–995.

Khan, S. R., Finlayson, B., and Hackett, R. L. (1979) Scanning electron microscopy of calcium oxalate crystal formation in experimental nephrolithiasis, *Lab. Invest.* **41,** 504–510.

Khan, S. R., and Hackett, R. L. (1984) Microstructure of decalcified human calcium oxalate urinary stones, *Scan. Electron Microsc.* **II,** 935–941.

Khan, S. R., and Hackett, R. L. (1987) Crystal–matrix relationships in experimentally induced calcium oxalate monohydrate crystals: An ultrastructural study, *Calcif. Tissue Int.* **41,** 157–163.

Khan, S. R., and Hackett, R. L. (1991) Retention of calcium oxalate crystals in renal tubules, *Scan. Microsc.* **5,** 707–712.

Khan, S. R., and Hackett, R. L. (1993) Role of organic matrix in urinary stone formation: An ultrastructural study of crystal matrix interface of calcium oxalate monohydrate stones, *J. Urol.* **150,** 239–245.

Khan, S. R., Hackett, R. L., and Finlayson, B. (1986) Morphology of urinary stone particles resulting from ESWL treatment, *J. Urol.* **136,** 1367–1372.

Lieske, J. C., Deganello, S., and Toback, F. G. (1999) Cell–crystal interactions and kidney stone formation, *Nephron* **81,** 8–17.

Lieske, J. C., Norris, R., Swift, H., and Toback, F. G. (1997) Adhesion, internalization and metabolism of calcium oxalate monohydrate crystals by renal epithelial cells, *Kidney Int.* **52,** 1291–1301.

Lieske, J. C., Toback, F. G., and Deganello, S. (1996) Face-selective adhesion of calcium oxalate dihydrate crystals to renal epithelial cells, *Calcif. Tissue Int.* **58,** 195–200.

Lieske, J. C., Toback, F. G., and Deganello, S. (1998) Direct nucleation of calcium oxalate dihydrate crystals onto the surface of living renal epithelial cells in culture, *Kidney Int.* **54,** 796–803.

Mandel, N. (1997) Commentary on the growth of renal calculi, *J. Urol.* **157,** 2.

Mann, S. (1993) Molecular tectonics in biomineralization and biomimetic materials chemistry, *Nature* **365,** 499–505.

McKee, M. D., Nanci, A., and Khan, S. R. (1995) Ultrastructural immunodetection of osteopontin and osteocalcin as major matrix components of renal calculi, *J. Bone Miner. Res.* **10,** 1913–1929.

McQueen, E. G., and Engel, G. B. (1966) Factors determining the aggregation of urinary mucoprotein, *J. Clin. Pathol.* **19,** 392–396.

Morse, R., and Resnick, M. I. (1988) A new approach to the study of urinary macromolecules as a participant in calcium oxalate crystallization, *J. Urol.* **139,** 869–873.

Ryall, R. L. (1996) Glycosaminoglycans, proteins and stone formation: Adult themes and child's play, *Pediatr. Nephrol.* **10,** 656–666.

Ryall, R. L. (1997) Urinary inhibitors of calcium oxalate crystallization and their potential role in stone formation, *World J. Urol.* **15,** 155–164.

Ryall, R. L., Grover, P. K., Stapleton, A. M. F., Barrell, D. K., Tang, Y., Moritz, R. L., and Simpson, R. J. (1995) The urinary F1 activation peptide of human prothrombin is a potent inhibitor of calcium oxalate crystallization in undiluted human urine *in vitro*, *Clin. Sci.* **89,** 533–541.

Ryall, R. L., Hibberd, C. M., and Marshall, V. R. (1985) A method for studying inhibitory activity in whole urine, *Urol. Res.* **13,** 285–289.

Ryall, R. L., and Stapleton, A. M. F. (1995) Urinary macromolecules in calcium oxalate stones and crystal matrix: Good, bad, or indifferent? *in* Khan, S. R. (Ed.), Calcium Oxalate in Biological Systems, pp. 265-290, CRC Press, Boca Raton, FL.

Weiner, S., and Addadi, L. (1997) Design strategies in mineralized biological materials, *J. Mater. Chem.* **7,** 689–702.

Clinical Science (2001) 101, 159–168 (Printed in Great Britain)

A comparative study of the adsorption of amino acids on to calcium minerals found in renal calculi

David E. FLEMING*†, Wilhelm VAN BRONSWIJK* and Rosemary Lyons RYALL‡
*School of Applied Chemistry, Curtin University of Technology, GPO Box U1987, Perth, WA 6845, Australia, †Chemistry Centre of Western Australia, 125 Hay Street, East Perth, WA 6004, Australia, and ‡Department of Surgery, Flinders Medical Centre, Bedford Park, SA 5042, Australia

ABSTRACT

To assess the binding of individual amino acids to the principal calcium minerals found in human kidney stones, the adsorption of 20 amino acids on to calcium oxalate monohydrate, $CaHPO_4.2H_2O$, $Ca_3(PO_4)_2$ and $Ca_5(PO_4)_3OH$ crystals was determined over the physiological urinary pH range (pH 5–8) in aqueous solutions. All amino acids adsorbed most strongly at pH 5, and this decreased in all cases as the pH was increased. The amino acids which adsorbed most strongly were aspartic acid, glutamic acid and γ-carboxyglutamic acid, with the last displaying the strongest affinity. All amino acids bound more avidly to calcium oxalate monohydrate than to any of the phosphate minerals. Adsorption on to $CaHPO_4.2H_2O$ was generally higher than for $Ca_3(PO_4)_2$ and $Ca_5(PO_4)_3OH$, for which all amino acids, with the exception of γ-carboxyglutamic acid, had only a weak affinity. The binding affinity of these acids is thought to be due to their zwitterions being able to adopt conformations in which two carboxyl groups, and possibly the amino group, can interact with the mineral surface without further rotation. The strong binding affinity of di-and tri-carboxylic acids for calcium stone minerals indicates that proteins rich in these amino acids are more likely to play a functional role in stone pathogenesis than those possessing only a few such residues. These findings, as well as the preferential adsorption of the amino acids for calcium oxalate monohydrate rather than calcium phosphate minerals, have ramifications for research aimed at discovering the true role of proteins in stone formation and for potential application in the design of synthetic peptides for use in stone therapy.

INTRODUCTION

Urinary amino acids are recognized as one of the agents which may influence the formation of renal calculi by virtue of their effects on calcium oxalate (CaOx) crystallization [1,2]. In particular, glutamic acid and aspartic acid have been shown to inhibit significantly the nucleation and growth rates of CaOx crystals precipitated in their presence [3,4]. This inhibitory effect has been generally viewed as resulting from competition between these acidic amino acids and oxalate for calcium ions in solution, and/or their preferential adsorption on to CaOx crystal surfaces.

In addition to any effect that free amino acids may have on the crystallization of insoluble calcium salts in urine, they may also influence this process as components of urinary proteins. Acidic amino acids, such as aspartic acid and glutamic acid, are present as end groups, or as part of calcium-binding domains in certain urinary proteins, which have been shown to have a marked effect on CaOx

Key words: adsorption, amino acids, calcium oxalate, calcium phosphate, crystal morphology, urolithiasis.
Abbreviations: CaOx, calcium oxalate; CaP, calcium phosphate minerals [i.e. $CaHPO_4.2H_2O$, $Ca_3(PO_4)_2$ and $Ca_5(PO_4)_3OH$], THG, Tamm–Horsfall glycoprotein; UPTF1, urinary prothrombin fragment 1.
Correspondence: Dr W. van Bronswijk (e-mail w.vanbronswijk@info.curtin.edu.au).

Table I **Adsorption of amino acids on calcium minerals at pH 6**
nd, not detected.

Amino acid	CaOx monohydrate (μmol/m^2)	$Ca_3(PO_4)_2$ (μmol/m^2)	$CaHPO_4$ (μmol/m^2)	$Ca_5(PO_4)_3OH$ (μmol/m^2)
Acidic (pI < 5)				
Aspartic acid	0.0714	0.0055	0.0023	0.0008
γ-Carboxyglutamic acid	0.1510	0.0530	0.1160	0.0530
Glutamic acid	0.0669	0.0071	0.0021	0.0007
Neutral (5 < pI < 8)				
Alanine	0.0370	nd	0.0007	0.0001
Cystine	0.0050	0.0008	0.0039	0.0013
Glycine	0.0233	0.0013	0.0060	0.0024
Histidine	0.0327	nd	0.0039	0.0005
Leucine	0.0107	nd	0.0061	0.0002
Isoleucine	0.0160	nd	0.0046	0.0001
Norleucine	0.0065	nd	0.0001	nd
Methionine	0.0121	0.0009	0.0127	0.0004
Methionine sulphate	0.0029	0.0012	0.0092	0.0007
Phenylalanine	0.0230	nd	nd	nd
Proline	0.0313	0.0036	0.0001	0.0001
Serine	0.0304	0.0021	0.0109	0.0018
Threonine	0.0084	0.0024	0.0118	0.0017
Tyrosine	0.0298	nd	0.0013	0.0001
Valine	0.0053	nd	0.0037	0.0002
Basic (pI > 8)				
Arginine	0.0170	0.0036	0.0065	0.0007
Lysine	0.0144	nd	0.0070	0.0003

surface area of each batch of substrate was determined by nitrogen adsorption using a Quantachrome Autosorb 1 instrument (New York, NY, U.S.A.) and the Brunauer–Emmett–Teller method, with adsorption being measured at five different pressures. Their compositions were confirmed by powder X-ray diffraction analysis using a Philips PW 1830 (Almelo, The Netherlands) X-ray diffractometer. For all comparative adsorption experiments, the masses of CaOx monohydrate, $Ca_5(PO_4)_3OH$, $Ca_3(PO_4)_2$ and $CaHPO_4.2H_2O$ used were 0.500 g, 0.017 g, 0.054 g and 0.619 g respectively.

In order to determine whether the presence of free calcium ions in solution affected the ability of the amino acids to bind to CaOx monohydrate and CaP, the amino acids were dissolved in solutions of $CaCl_2$ (1000 mg/l) at a final concentration of 4 mg/l then added to each of the substrates as described in the adsorption experiments.

Molecular dimensions and surface coverage

The van der Waals dimensions of aspartic acid, glutamic acid and γ-carboxyglutamic acid in their zwitterion forms were calculated using PC Spartan Plus (Wavefunction Inc., Irvine, CA, U.S.A.) molecular modelling software. The maximum area projections of aspartic acid, glutamic acids and γ-carboxyglutamic acid were calculated to be 5.0×10^{-19} m^2, 6.0×10^{-19} m^2 and 6.5×10^{-19} m^2 respectively.

The molecular area projections were used along with measured adsorption densities and substrate surface areas to calculate the fraction of the surface area covered by the adsorbed molecules.

Calculation of adsorption and acid dissociation equilibrium constants

The equilibrium between a molecule or ion in solution and adsorbed on to a surface is described by:

$$K_{ads} = [\text{adsorbed species}]/[\text{solution species}]$$

However, as amino acids in solution are an equilibrium mixture of differently ionized species, equilibrium constants based on total solution concentrations are pseudo constants (K'). They would be expected to vary with pH, since either a dissociated or undissociated species could adsorb preferentially. Hence adsorption and dissociation were treated simultaneously, i.e.:

$$[HAA]_{ads} \leftrightarrow [HAA]_{soln} \quad K_{ads} = [HAA]_{ads}/[HAA]_{soln}$$

$$[HAA]_{soln} \leftrightarrow [H^+] + [AA^-]_{soln}$$

$$K_a = [H^+] \times [AA^-]_{soln}/[HAA]_{soln}$$

crystal formation, growth or aggregation. Among these proteins are urinary prothrombin fragment 1 (UPTF1) [5,6] and osteopontin [7,8], both of which are present in the organic matrix of CaOx stones [9]. The most likely parts of these proteins to be involved in their binding to calcium mineral surfaces are the free carboxyl groups of terminal amino acids [10].

However, the effects of individual amino acids on CaOx crystallization are difficult to study in a complex medium, such as urine, where their properties may be altered, their actions frustrated by other components in solution, or when they comprise part of the primary structure of proteins. In fact, determining whether specific amino acid residues within a protein are essential for function would require production of mutant molecules using site-directed mutagenesis. This would be an immense and unprofitable undertaking when little is currently known about the mechanisms by which urinary proteins influence CaOx crystallization in inorganic media, and when even less is understood about their true role in stone pathogenesis. An alternative approach to assessing the possible role of specific amino acids in the inhibition of CaOx crystallization is to determine their relative binding affinities for calcium stone minerals under controlled conditions free of contamination and possible interference by other agents. To date, no published study has systematically examined the binding affinity of individual amino acids for the crystal surfaces of minerals comprising human kidney stones. The broad aim of this paper was, therefore, to assess the binding of individual amino acids to the principal calcium minerals found in human kidney stones over the physiological urinary pH range. Although pure calcium phosphate stones are exceedingly rare, the salts are commonly associated with stones composed principally of CaOx [11,12]. Thus, in addition to CaOx monohydrate, three forms of calcium phosphate [$CaHPO_4.2H_2O$, $Ca_3(PO_4)_2$ and $Ca_5(PO_4)_3OH$; collectively refererred to as CaP] were included in the experiments.

MATERIALS AND METHODS

Chemicals

The amino acids studied were the L-forms of aspartic acid, threonine, serine, glutamic acid, proline, glycine, alanine, cysteine, valine, methionine, isoleucine, leucine, norleucine, tyrosine, phenylalanine, lysine, histidine, arginine and γ-carboxyglutamic acid. All were purchased from BDH (Kilsyth, Victoria, Australia), except for γ-carboxyglutamic acid, which was supplied by Sigma. CaOx monohydrate (average size 3 μm) was purchased from Ajax Chemicals (Auburn, New South Wales, Australia), $CaCl_2$ from Sigma and $(COONa)_2$ from BDH. $CaHPO_4.2H_2O$, $Ca_3(PO_4)_2$ and $Ca_5(PO_4)_3OH$ were obtained from Ajax Chemicals, Prolabo (Pelee, Paris) and Aldrich respectively. Double-distilled water was used in all experiments.

Adsorption experiments

The adsorption of amino acids was monitored over an 18 h period (e.g. glutamic acid on CaOx monohydrate and the CaP minerals) and little or no increase in adsorption density was observed after 6 h contact. To ensure that equilibrium had been reached, and for convenience, a contact time of 15 h was employed for all studies.

A saturated aqueous solution of calcium oxalate at pH 5 was prepared by stirring 2 g of CaOx monohydrate in 50 ml of distilled water at 37 °C for 1 day, adjusting the pH to 5, then leaving it to stand for a further 2 days to equilibrate. The residual crystals were separated by vacuum filtration through a 0.5 μm polyvinyl chloride membrane filter and discarded. A 10 ml aliquot of the filtrate was added to a glass vessel containing crystals of CaOx monohydrate (500 mg), and a single amino acid at a final concentration of 4 mg/l (0.02–0.04 mM), which is in the range reported for amino acids in urine [1]. The pH was checked and adjusted to the original value, and the crystal suspension incubated for 15 h at 37 °C with gentle stirring. After filtration (Acrodisc; 0.45 μm), 10 ml of each solution was mixed with 0.4 ml of 1 M HCl, and the amino acid concentration determined by HPLC (Waters Model 510) using post-column derivatization with ninhydrin. This procedure was repeated for the other amino acids and CaOx monohydrate at other pH values encompassing those occurring in healthy human urine (pH 5–8). The pH values of the aqueous solutions were adjusted with either 0.1 M HCl or 0.1 M NaOH. The difference between the concentration of amino acids before and after contact with the CaOx monohydrate was used as a measure of adsorption on the substrate. Measurements for each amino acid were performed in triplicate. To exclude the possibility of removal of amino acids by bacterial contamination, parallel experiments were carried out from which the calcium mineral salts were omitted. In every case, the concentration of amino acids at the end of the incubation period was identical to that at the beginning. Furthermore, bacteria were never evident in field emission scanning electron micrographs of crystals incubated with amino acids.

It was not possible to determine the amounts of adsorbed amino acids directly, as some desorption would occur during washing of the crystals. However, qualitative evidence for their adsorption was found by treating washed crystals with 0.1 M NaOH and amino acids were detected in the alkaline solutions.

The amino acid adsorption procedure described for CaOx monohydrate was also carried out for three CaP minerals, with the amount of substrate used in the adsorption experiments being based on masses that gave equal surface areas for the four minerals. The average

Thus

$$K' = K_{ads} - K' \times K_a/[H^+]$$

$$K' = [HAA]_{ads}/([HAA]_{soln} + [AA^-]_{soln})$$

and

$$1/K' = 1/K_{ads} + (K_a/K_{ads})/[H^+]$$

This enables both K_{ads} (the true adsorption equilibrium constant) and K_a (the amino acid dissociation constant) to be determined from the variation of K' with pH.

It should be noted that the surface charge of the substrate may also change as a function of pH, and hence the K_a values obtained may be a reflection of amino acid or surface protonation, or both.

RESULTS

Amino acid adsorption on to calcium minerals

The presence of free calcium ions in solution did not affect the ability of the amino acids to bind to the calcium minerals, since preincubation with $CaCl_2$ had no measurable effect on their equilibrium concentrations in solution following contact with the substrates.

Adsorption of the amino acids on to the minerals over the pH range 5–8 showed the degree of adsorption to be greatest at pH 5 and decreasing to pH 8, with the trend of adsorption of each amino acid being similar over the pH range. Results (expressed as μmol/m^2) obtained at pH 6 are given in Table 1, since that value is representative of the pH of normal human urine. The amino acids which adsorbed most strongly were aspartic acid, glutamic acid and γ-carboxyglutamic acid, with the last displaying a noticeably stronger affinity for all the minerals than the remaining amino acids. Adsorption on to $CaHPO_4 \cdot 2H_2O$ was generally higher than for $Ca_3(PO_4)_2$ and $Ca_5(PO_4)_3OH$, for which all amino acids, with the exception of γ-carboxyglutamic acid, had only a weak affinity. All amino acids demonstrated a stronger binding affinity for CaOx monohydrate than for any of the CaP minerals.

Amino acid adsorption on to calcium oxalate as a function of pH

Table 2 shows the adsorption of the amino acids on to CaOx monohydrate, expressed as μmol/m^2, at pH 5, 6, 7 and 8. As noted above, all amino acids adsorbed most strongly at pH 5, and this decreased in all cases as the pH

Table 2 Amino acid adsorption on CaOx monohydrate as a function of pH

nd, not detected.

Amino acid	pH 5 (μmol/m^2)	pH 6 (μmol/m^2)	pH 7 (μmol/m^2)	pH 8 (μmol/m^2)
Acidic (pI < 5)				
Aspartic acid	0.1308	0.0714	0.0466	0.0067
γ-Carboxyglutamic acid	0.2010	0.1510	0.1490	0.1470
Glutamic acid	0.1116	0.0669	0.0445	0.0062
Neutral (5 < pI < 8)				
Alanine	0.0460	0.0370	0.0224	nd
Cystine	0.0076	0.0050	0.0017	nd
Glycine	0.0237	0.0233	0.0089	nd
Histidine	0.0422	0.0327	0.0322	0.0068
Leucine	0.0150	0.0107	0.0097	nd
Isoleucine	0.0178	0.0160	0.0085	0.0023
Norleucine	0.0070	0.0065	0.0061	nd
Methionine	0.0210	0.0121	0.0085	0.0054
Methionine sulphate	0.0041	0.0029	0.0027	nd
Phenylalanine	0.0301	0.0230	0.0209	0.0053
Proline	0.0365	0.0313	0.0191	nd
Serine	0.0409	0.0304	0.0273	nd
Threonine	0.0141	0.0084	0.0076	nd
Tyrosine	0.0353	0.0298	0.0226	0.0051
Valine	0.0113	0.0053	0.0018	nd
Basic (pI > 8)				
Arginine	0.0200	0.0170	0.0136	0.0108
Lysine	0.0157	0.0144	0.0132	0.0052

Table 3 **Adsorption of aspartic acid, glutamic acid and γ-carboxyglutamic acid on calcium minerals**

*$K' = [\text{amino acid}]_{ads}/[\text{total amino acid}]_{solution}$, in units of 10^{-6}.

		Aspartic acid		Glutamic acid		γ-Carboxyglutamic acid	
Calcium salt	pH	μmol/m²	10^6 K'^* (m)	μmol/m²	10^6 K'^* (m)	μmol/m²	10^6 K'^* (m)
CaOx monohydrate	5	0.131	10.0	0.112	8.8	0.201	12.8
	6	0.071	3.43	0.067	3.60	0.151	6.81
	7	0.047	1.94	0.045	2.10	0.149	6.59
	8	0.0067	0.23	0.0062	0.23	0.147	6.56
$Ca_3(PO_4)_2$	5	0.0081	0.28	0.0085	0.32	0.063	1.81
	6	0.0055	0.19	0.0071	0.27	0.053	1.48
	7	0.0017	0.058	0.0055	0.21	0.052	1.44
	8	0.0013	0.043	0.0007	0.026	0.051	1.41
$CaHPO_4.2H_2O$	5	0.0028	0.094	0.0026	0.097	0.134	5.30
	6	0.0023	0.077	0.0021	0.078	0.116	4.23
	7	0.0012	0.040	0.0010	0.037	0.099	3.34
	8	0.0001	0.003	0.0001	0.003	0.073	2.21
$Ca_5(PO_4)_3OH$	5	0.0014	0.045	0.0013	0.048	0.063	1.93
	6	0.0008	0.027	0.0007	0.025	0.053	1.56
	7	0.0005	0.015	0.0003	0.010	0.052	1.52
	8	0.0003	0.010	0.0002	0.007	0.051	1.48

was increased. None of the amino acids, other than γ-carboxyglutamic acid, showed significant adsorption at pH 8.

γ-Carboxyglutamic acid, which has two γ-carboxyl groups, adsorbed most strongly and showed little decrease in adsorption above pH 6. Aspartic acid and glutamic acid, which have one β- or γ-carboxyl group, were slightly less adsorbed than γ-carboxyglutamic acid, and showed a similar decrease in adsorption between pH 5 and pH 6, but their adsorption continued to lessen significantly as the pH decreased from pH 6 to pH 8. The remaining amino acids, which have only α-carboxyl groups, were less adsorbed, and their adsorption decreased most rapidly over the pH 6 to pH 8 range.

Relative adsorption strengths of aspartic acid, glutamic acid and γ-carboxyglutamic acid

The difference in the adsorption behaviour of aspartic acid and glutamic acid in comparison with γ-carboxyglutamic acid is best illustrated by the pseudo equilibrium constants (K') obtained for their adsorption on to CaOx monohydrate and the three CaP minerals (Table 3). Their typical adsorption trend as a function of pH is illustrated, for CaOx monohydrate, in Figure 1. Aspartic acid and glutamic acid adsorbed identically, within experimental error, but γ-carboxyglutamic acid behaved differently above pH 6 on CaOx monohydrate and the CaP minerals

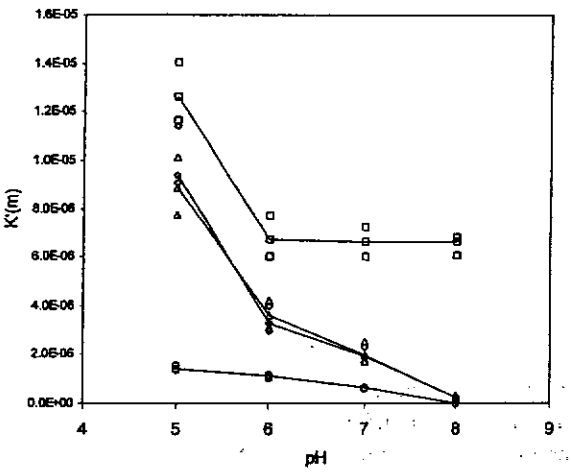

Figure 1 **Amino acid adsorption on to CaOx monohydrate as a function of pH (solid line indicates median values)**

□, γ-carboxyglutamic acid; △, glutamic acid; ◇, aspartic acid; ○, alanine.

(Figure 1). All three adsorbed differently from the monocarboxy amino acids, and alanine has been included in Figure 1 to illustrate this. The data suggest that at least two factors are involved in the adsorption process, even though the three acids are highly ionized at the β- or γ-carboxyl groups in solutions at pH 5 and above (pK_{a2} = 3.71, 4.15 and 3.20 respectively [13]).

Equilibrium constants for amino acid adsorption (K_{ads}) and dissociation (K_a) were obtained on the basis that Henry's Law (K = [adsorbed species]/[solution species])

Table 4 Adsorption and acid dissociation equilibrium constants for aspartic acid, glutamic acid and γ-carboxyglutamic acid adsorption on calcium minerals
COM, CaOx monohydrate.

	$pK_{ads}(\pm 0.2)$		$pK_a(\pm 0.2)$	
Adsorbent/substrate	$5 < pH < 6$	$6 < pH < 8$	$5 < pH < 6$	$6 < pH < 8$
Aspartic acid/COM	4.9	5.3	2.6	3.7
Glutamic acid/COM	5.0	5.2	2.7	3.6
γ-Carboxyglutamic acid/COM	4.8	5.2	3.0	6.4
γ-Carboxyglutamic acid/$Ca_3(PO_4)_2$	5.7	5.8	3.6	6.4
γ-Carboxyglutamic acid/$CaHPO_4 . 2H_2O$	5.3	5.5	3.5	5.2
γ-Carboxyglutamic acid/$Ca_5(PO_4)_3OH$	5.7	5.8	3.6	6.4

can be applied. It is reasonable to do so in this instance since the adsorption densities are low, and hence adsorbed particle–adsorbed particle interaction is minimal. Maximum surface coverage of aspartic acid, glutamic acid and γ-carboxyglutamic acid on CaOx monohydrate was 4%, 4% and 8% respectively. The pK_{ads} values show the adsorption affinity of aspartic acid, glutamic acid and γ-carboxyglutamic acid for CaOx monohydrate and the CaP minerals to have only a modest pH and substrate dependence. The major factor influencing adsorption is clearly amino acid (and/or substrate) ionization, as indicated by the significant differences in the pK_a values obtained for γ-carboxyglutamic acid and for aspartic acid and glutamic acid, and their variation with pH (Table 4).

DISCUSSION

As with all biominerals occurring throughout nature, kidney stones are intimately associated with macromolecules. These constitute the organic matrix, which is as inevitably and integrally a part of the stone as the mineral itself, meandering throughout the entire structure and occupying far more space than would be expected from its contribution of only 2.5% to the total mass [14]. The matrix consists principally of proteins [15], which have engendered particular interest, partly because of the crucial role played by proteins in directing the fabrication and assembly of natural bioceramics, but also because their very presence and abundance suggest that they may fulfil a regulatory function in stone formation.

In healthy biomineralization systems the timing of crystal nucleation, growth and organization into mineral assemblies are strictly governed by proteins [16], whose three-dimensional architecture and chemistry ensure that only crystals of a particular composition are formed, and guarantee that their various faces will grow only in certain directions to produce a structure of a strictly defined shape. Their molecules are characterized by the possession of periodic, negatively charged surfaces, which can align with the crystalline structure of the mineral and initiate crystal nucleation by acting as a template at the inorganic–organic interface [17]. In addition, some proteins can bind to exposed crystal surfaces and, by intercalating in an orderly array along specific planes inside the crystal structure [18], become included into the crystal lattice, where they create and stabilize discontinuities and alter crystal texture and tensile properties [19]. Such a phenomenon apparently also occurs during crystal formation in human urine, since evidence from our own laboratory [20–22] indicates that specific urinary proteins associated with CaOx crystals precipitated from urine are incarcerated within the crystalline architecture itself.

However, unlike the formation of healthy biominerals, stone formation is an uncontrolled, pathological process, which possibly reflects the fact that urinary proteins are known to exhibit multiple and paradoxical effects, including promotion of crystal nucleation, growth and aggregation, as well as incomplete inhibition of those processes [9]. It is hardly surprising, therefore, that relatively little is currently known about the true nature of the association between stone proteins and their mineral companions, or their functional role, if any, in urolithiasis [23]. One factor that has contributed to this lack of understanding is a general paucity of knowledge regarding the basis of the relationship between the molecular structures of urinary proteins and their binding affinities for the surfaces of stone minerals, especially CaOx and CaP. Nonetheless, it is likely that interactions between urinary proteins and calcium stone minerals are governed by conditions similar to those which operate during healthy biomineralization, where strict regulatory control by proteins is dictated by their three-dimensional structure and chemistry. These are determined by a variety of factors, including for instance, ambient conditions, disulphide bridging and post-transitional modifications such as glycosylation and phosphorylation, but especially the type and sequence of the amino acids comprising the primary backbone of the molecule.

Of the amino acids used in this study, aspartic acid, glutamic acid and γ-carboxyglutamic acid bound most strongly to all of the calcium minerals tested, especially at low pH values. These three amino acids have in common at least two carboxyl groups, and in certain proteins display a high affinity for calcium [24]. The strong correlation of adsorption with the number of carboxyl groups suggests that multiple binding (chelation) of the amino acid to the CaOx monohydrate surface is a major factor, and that entropy plays a significant role in the adsorption process. This concurs with what has been observed for citric acid, which has three carboxyl groups and is a natural component of healthy urine. It has long been known that citrate binds efficiently to CaOx crystals and inhibits deposition of further lattice ions [25]; consequently, it is now widely used as a therapeutic agent for preventing stone recurrences.

The other major factor contributing to adsorption strength is pH, as adsorption mostly decreased markedly as pH was increased. For the monocarboxy amino acids, adsorption generally decreased most rapidly between pH 6 and 8, suggesting that the zwitterion was the adsorbing species (pI ~ 6 for these acids). This decrease in adsorption as pH increases above the isoelectic point is also observed for the dicarboxy amino acids (aspartic acid pI = 2.77, glutamic acid pI = 3.22 [13]) and the tricarboxy amino acid (γ-carboxyglutamic acid, whose pI would be expected to be less than that of aspartic acid and glutamic acid), reinforcing the zwitterion hypothesis. This is intriguing, as CaOx monohydrate is considered to be positively charged owing to Ca^{2+} adsorption, under the conditions used in this study [26], and adsorption decreases as the charge on the adsorbing species become more negative (with increasing pH).

Aspartic acid and glutamic acid adsorption was significantly affected by pH and fitted to $pK_a \sim 3.7$ in the pH range 6–8, suggesting that protonation of the β- or γ-carboxyl group ($pK_a = 3.71$ for aspartic acid and 4.15 for glutamic acid [13]) increased adsorption. Below pH 6, the adsorption fitted to $pK_a \sim 2.7$, suggesting that protonation of the α-carboxyl group ($pK_1 = 1.95$ for aspartic acid and 2.16 for glutamic acid [13]) also contributed to increased adsorption. Not unexpectedly, the observed pK_a values lie between those of the α- and β- or γ-carboxyl groups, since both will be increasingly protonated in going from pH 6 to 5. In contrast, the adsorption of γ-carboxyglutamic acid at pH 6–8 fitted to $pK_a \sim 6.4$, indicating that virtually no change occurred in its protonation (relevant to adsorption) over this range. Below pH 6, adsorption increased markedly and protonation did occur, presumably at one of the two γ-carboxyl groups as $pK_a \sim 3.4$ ($pK_{3,4} = 4.75$, 3.2 [13]). Thus the results indicate that the carboxyl groups are not fully ionized over the entire pH 5–8 range, and that the adsorbing species is significantly protonated.

This is in agreement with Noszál and Sándor [27] who showed that at pH 7.2 both carboxyl groups of aspartic acid were deprotonated and that, when the pH was decreased to the isoelectric point, protonation of the β-carboxyl was not exclusive, with up to 5% of the protonation occurring at the α-carboxyl group. Furthermore, protonation was found to alter the distribution of the aspartic acid rotation isomers (rotamers), and the gauche-$\beta COO^-/\alpha COO^-$:gauche-$\beta COO^-/\alpha NH_3^+$ (g2) rotamer populations increased as pH decreased. This rotamer has all three functional groups positioned for adsorption to a surface without further rotation (Figure 2). Theoretical studies of the aspartic acid zwitterion support this view and show that the gauche-βCOOH/αCOO⁻:gauche-βCOOH/αNH_3^+ (g2) rotamer is the second most abundant species [28]. The most abundant species, *trans*-$\beta COO^-/\alpha$COOH:gauche-$\beta COO^-/\alpha NH_3^+$ (g1), would need to rotate about the CH–CH_2 bond to bring all three functional groups into contact with a surface. The different rates of change of adsorption observed for aspartic acid and glutamic acid at pH 5–6 and pH 6–8 could thus be due to relative changes in the protonation of the α- and β-carboxyl groups and consequent rotamer distributions.

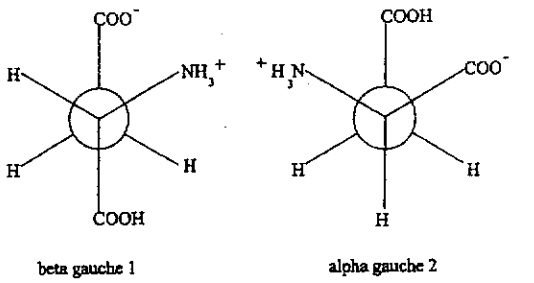

Figure 2 The two most stable of six aspartic acid zwitterion rotamers

The greater adsorption observed for γ-carboxyglutamic acid at pH 6–8 can be attributed to two of its three rotameric conformations having the required gauche–gauche arrangement, as opposed to one of three for aspartic acid. The almost negligible change in adsorption at pH 6–8 is, therefore, likely to be due to the greater capacity of the two γ-carboxyl groups to accept protons, and protonation effects on the rotamer distribution do not become apparent until pH < 6. This is conceivable as the gauche-βCOOH/αCOO⁻:gauche-βCOOH/αNH_3^+ rotamer is stabilized by βCOOH/αNH_3^+ hydrogen bonding [28].

The data are thus consistent with the adsorbing species being a protonated gauche-$\beta COO^-/\alpha COO^-$:gauche-$\beta COO^-/\alpha NH_3^+$ (g2) rotamer, with protonation most probably occurring at the β-carboxyl. The initial interaction could thus be an approach of the zero-charged amino acid to the positively charged CaOx monohydrate surface. Subsequently, this could lead to the more exposed αCOO^- binding to Ca^{2+}, followed by the loss of

a proton from the βCOOH and its binding to another Ca^{2+}, and possibly a further loss of a proton from the αNH_3^+ group to allow it to bind. This tridentate binding is similar to the hexadentate binding of EDTA to calcium ions, and would account for the greater adsorption of the di- and tri-carboxy amino acids, since the monoacids would bind as bidentates at best.

The difference in affinity of the four calcium minerals for amino acids may be a result of differences in surface charge, ion adsorption or coordination-site availability at the crystal surfaces. The pK_{ads} (5.8) obtained for both $Ca_3(PO_4)_2$ and $Ca_5(PO_4)_3OH$ suggests that these two phosphates behave similarly and with little change as a function of pH. The hydrogen phosphate ($CaHPO_4.2H_2O$, pK_{ads} 5.4) is a slightly stronger adsorbent for amino acids and the oxalate (CaOx monohydrate, pK_{ads} 4.8–5.3) is the strongest adsorbent. This sequence may be a reflection of the acid/base properties of the anions, and consequent surface charge and cation adsorption. The differences in pK_a values for aspartic acid, glutamic acid and γ-carboxyglutamic acid on CaOx monohydrate at pH 5–6 compared with pH 6–8 are just sufficient to suggest that surface changes may have occurred, e.g. displacement of calcium ions by protons.

A particularly noteworthy finding of the present study is that, of the naturally occurring amino acids, only those possessing two or more carboxyl groups bind with significant avidity to calcium minerals found in stones, and therefore have the potential to inhibit CaOx crystallization directly. However, although there have been innumerable reports attesting to the inhibitory effects of a large range of natural and synthetic agents, only a few have addressed the effects of free amino acids. Kohri et al. [4], using a mixed suspension, mixed-product-removal crystallization system, showed that glutamic acid and aspartic acid inhibited CaOx nucleation, growth and suspension density in an inorganic medium, but it is doubtful whether this is of any physiological significance because concentrations of both these amino acids in the urine of stone-formers and healthy controls are indistinguishable [1,3]. This lack of difference has also been observed for γ-carboxyglutamic acid. Collette et al. [29] measured both free and protein-bound γ-carboxyglutamic acid in urine samples from stone-formers and healthy controls and could detect no significant differences between the two groups. These data indicate that free amino acids are unlikely to fulfil prominent inhibitory roles in urine and therefore to contribute directly to stone pathophysiology. Furthermore, the continuing emergence of evidence [9,23] which reinforces the view that proteins are largely responsible for the inhibitory effects of urine on CaOx crystal aggregation, strongly suggests that any functions which aspartic acid, glutamic acid or γ-carboxyglutamic acid may have in stone formation or prevention are more likely to be related to their contribution to the inhibitory properties of proteins which contain them, rather than to those of the amino acids themselves.

The chelation, amino acid protonation and stereochemical factors of aspartic acid, glutamic acid and γ-carboxyglutamic acid, identified in the present study, must be significant in the adsorption behaviour of urinary proteins on the same mineral surfaces. For example, the principal protein associated with CaOx crystals precipitated from human urine is UPTF1 [6], an acidic peptide of prothrombin whose N-terminal region contains 10 γ-carboxyglutamic acid residues, and which almost certainly determines the extraordinary affinity of UPTF1 for CaOx crystals. Osteopontin, another urinary protein known to be present in CaOx crystals and stones, and which, like UPTF1, possesses properties consistent with a role in stone formation, is rich in aspartic acid residues [30]. In contrast, Tamm–Horsfall glycoprotein (THG) strongly inhibits CaOx crystal aggregation in urine [31], but does not bind irreversibly to CaOx, and in consequence, is not present in alkali-washed urinary CaOx crystals [20]. An important difference between these proteins, which may explain their relative affinities for the various crystal types, is the presence of acidic amino acid groups in UPTF1 and osteopontin, but their absence from THG. By removing the γ-carboxyglutamic acid residues from osteocalcin and urinary γ-carboxyglutamic acid protein by thermal decarboxylation, van de Loo et al. [32] showed that the inhibitory activity of these proteins on CaP and CaOx precipitation was lost.

There is now compelling evidence that UPTF1, osteopontin and THG can inhibit the formation, growth and/or aggregation of CaOx crystals [9,23], which would facilitate harmless expulsion of CaOx crystals in the urine. Nonetheless, stone formation could also be caused by direct attachment of urinary crystals to the renal epithelium [33], a process which must be affected by their binding properties, which will in turn be influenced by proteins bound to them [34]. Once attached, crystals have two possible fates: they can restrict urine flow and encourage the retention of other crystals, or they can be internalized by cells and destroyed. Proteins, therefore, have two potentially conflicting roles in mediating cell attachment, since they could act as inhibitors by covering the crystal and interfering with electrical attractive forces, or encourage cell adherence by functioning as a form of opsonin [35]; they may do both. However, in either case, their properties will be largely determined by the sequence and type of amino acids comprising their primary structure.

Although most human kidney stones consist principally of CaOx, most also contain one or more CaP salts as minor components [11,12]. This has led to the proposal that the formation of CaP salts in the nephron induces the subsequent nucleation of CaOx [36]. However, the predominance of CaOx over CaP in concentric mineral–organic matrix growth patterns observed in the outer

regions of many CaOx renal stones [37], could also be explained by the stronger affinity of urinary proteins possessing end-groups abundant in acidic amino acids for CaOx than for CaP. As suggested by Addadi and Weiner [38], immobilized proteins can act as excellent nucleation sites for calcium salts by exposing an array of carboxylate groups locked in an ordered, rigid conformation. If surface proteins are capable of causing the nucleation of insoluble calcium salts in urine, the preferential binding of acidic amino acids to CaOx would favour precipitation of CaOx, rather than CaP, and perhaps explain the preponderance of CaOx in human kidney stones. Once deposition of CaOx has occurred around a nucleating point, or nidus, during the initial stage of stone formation, specific proteins could be laid down to form a layer of matrix on the surface of the newly formed crystals. Thus during periods of high CaOx supersaturation, a new layer of CaOx crystals could then form on the matrix band, thereby increasing the likelihood of further deposition of proteins with an affinity for CaOx. It is noteworthy that the concentration of the organic matrix of CaOx stones, which is abundant in aspartic acid, glutamic acid and/or γ-carboxyglutamic acid [39], increases towards the outer periphery [40], probably reflecting increasing deposition of selected normal urinary proteins as described above, or others released from the urothelium in response to irritation caused by the stone as it enlarges.

In summary, this study represents the first systematic examination of the adsorption affinity of amino acids on to calcium stone minerals, and provides direct, comparative data to explain the common occurrence of acidic proteins in association with calcium stone minerals. The strong binding affinity of di- and tri-carboxylic acids for calcium stone minerals, particularly CaOx, would indicate that proteins rich in these amino acids are more likely to play a functional role in stone pathogenesis than those possessing only few such residues. The binding affinity of these acids is thought to be due to the ability of their zwitterions to adopt favourable conformations in which two carboxyl groups and the amine group can interact with the mineral surface, without further rotation. These results have ramifications for research aimed at discovering the true role of proteins in stone formation and potential application in the design of synthetic peptides for use in stone therapy.

ACKNOWLEDGMENTS

We thank Mr Bruce Youngberg of the Chemistry Centre of Western Australia, who provided technical support for the amino acid determinations. D.E.F. is the recipient of a Curtin University of Technology Postgraduate Scholarship.

REFERENCES

1 Kohri, K., Takada, M., Katoh, Y., Kataoka, K., Iguchi, M. and Kurita, T. (1989) Amino acids in urine and plasma of urolithiasis patients. Int. Urol. Nephrol. 21, 9–16
2 McGeown, M. G. (1957) The urinary excretion of amino acids in relation to calculus diseases. J. Urol. 78, 318–322
3 Azoury, R., Garti, N. and Sarig, S. (1986) The amino acid factor in stone formers' and normal urines. Urol. Res. 14, 295–298
4 Kohri, K., Umekawa, T., Kodama, M. et al. (1990) Inhibitory effect of glutamic acid and aspartic acid on calcium oxalate crystal formation. Eur. Urol. 17, 173–177
5 Grover, P. K., Moritz, R. L., Simpson, R. J. and Ryall, R. L. (1998) Inhibition of calcium oxalate crystal growth and aggregation *in vitro*. A comparison of four human proteins. Eur. J. Biochem. 253, 637–644
6 Ryall, R. L., Grover, P. K., Stapleton, A. M. F., Barrell, D. K., Tang, Y., Moritz, R. L. and Simpson, R. J. (1995) The urinary F1 activation peptide of human prothrombin is a potent inhibitor of calcium oxalate crystallization in undiluted human urine *in vitro*. Clin. Sci. 89, 533–541
7 Min, W., Shiraga, H., Chalko, C., Goldfarb, S., Krishna, G. G. and Hoyer, J. R. (1998) Quantitative studies of human urinary excretion of uropontin. Kidney Int. 53, 189–193
8 Asplin, J. R., Arsenault, D., Parks, J. H., Coe, F. L. and Hoyer, J. R. (1998) Contribution of human uropontin to inhibition of calcium oxalate crystallization. Kidney Int. 53, 194–199
9 Ryall, R. L. (1996) Glycosaminoglycans, proteins and stone formation: Adult themes and child's play. Pediatr. Nephrol. 10, 656–666
10 Addadi, L. and Weiner, S. (1986) Interactions between acidic macromolecules and structured crystal surfaces. Stereochemistry and biomineralisation. Mol. Cryst. Liq. Cryst. 134, 305–322
11 Prien, E. L. (1968) Composition and structure of urinary stone. Am. J. Med. 45, 654–672
12 Yoshida, O. and Okada, Y. (1990) Epidemiology of urolithiasis in Japan: a chronological and geographical study. Urol. Int. 45, 104–111
13 Lide, D. R. (ed.) (1999–2000) CRC Handbook of Chemistry and Physics, 80th edn, pp. 7-1–7-2, CRC Press, New York
14 Boyce, W. H. (1968) Organic matrix of human urinary concretions. Am. J. Med. 45, 673–683
15 Boyce, W. H. and Garvey, F. K. (1956) The amount and nature of the organic matrix in urinary calculi: a review. J. Urol. 76, 213–227
16 Albeck, S., Addadi, L. and Weiner, S. (1996) Regulation of calcite crystal morphology by intracrystalline acidic proteins and glycoproteins. Connect. Tissue Res. 35, 365–370
17 Heuer, A. H., Fink, D. J., Laraia, V. J. et al. (1992) Innovative materials processing strategies: A biomimetic approach. Science (Washington, D.C.) 255, 1098–1105
18 Aizenberg, J., Ilan, M., Weiner, S. and Addadi, L. (1996) Intracrystalline macromolecules are involved in morphogenesis of calcitic sponge spicules. Connect. Tissue Res. 34, 255–261
19 Weiner, S. and Addadi, L. (1997) Design strategies in mineralized biological materials. J. Mater. Chem. 7, 689–702
20 Doyle, I. R., Ryall, R. L. and Marshall, V. R. (1991) Inclusion of proteins into calcium oxalate crystals precipitated from human urine: a highly selective phenomenon. Clin. Chem. 37, 1589–1594
21 Ryall, R. L., Fleming, D. E., Grover, P. K., Chauvet, M. C., Dean, C. J. and Marshall, V. R. (2000) The hole truth: Intracrystalline proteins and calcium oxalate kidney stones. Mol. Urol. 4, 391–402
22 Fleming, D. E., Doyle, I. R., Evans, N., Marshall, V. R., Parkinson, G. M. and Ryall, R. L. (1999) Proteins associated with calcium oxalate crystals formed in human urine are intracrystalline. In Kidney Stones (Borghi, L., Meschi, T., Briganti, A., Schianchi, T. and Novarini, A., eds.), pp. 359–362, Editoriale Bios, Cosenza

23 Ryall, R. L. (1997) Urinary inhibitors of calcium oxalate crystallization and their potential role in stone formation. World J. Urol. 15, 155–164
24 Binette, J. P., Binette, M. B., Gawinowicz, M. A. and Kendrick, N. (1996) Urinary stone proteins: An update. Scanning Microsc. 10, 509–518
25 Meyer, J. L and Smith, L. H. (1975) Growth of calcium oxalate crystals II. Inhibition by natural urinary crystal growth inhibitors. Invest. Urol. 13, 36–39
26 Callejas Fernandez, J., De Las Nieves, F. J., Salcedo, J. Salcedo and Hidalgo-Alvarez, R. (1990) The microelectrophorectic mobility and colloid stability of calcium oxalate monohydrate dispersions in aqueous media. J. Colloid Interface Sci. 135, 154–164
27 Noszál, B. and Sándor, P. (1989) Rota-microspeciation of aspartic acid and asparagine. Anal. Chem. 61, 2631–2637
28 Nagy, I. N. and Noszál, B. (2000) Theoretical study of the tautomeric/conformational equilibrium of aspartic acid zwitterions in aqueous solution. J. Phys. Chem. 104, 6834–6843
29 Collette C., Benmbarek A., Boniface H., Astre C., Pares-Herbute, N., Monnier, L. and Guitter, J. (1991) Determination of protein-bound urinary gamma-carboxyglutamic acid in calcium nephrolithiasis. Clin. Chim. Acta 204, 43–50
30 Shiraga, H., Min, W., VanDusen, W. J. et al. (1992) Inhibition of calcium oxalate crystal growth *in vitro* by uropontin: another member of the aspartic acid-rich protein superfamily. Proc. Natl. Acad. Sci. U.S.A. 89, 426–430
31 Grover, P. K., Ryall, R. L. and Marshall, V. R. (1990) Does Tamm–Horsfall mucoprotein inhibit or promote calcium oxalate crystallization in human urine? Clin. Chim. Acta 190, 223–238
32 van de Loo, P. G. F., Soute, B. A. M., van Haarlem, J. M. and Vermeer, C. (1987) The effect of Gla-containing proteins on the precipitation of insoluble salts. Biochem. Biophys. Res. Commun. 142, 113–119
33 Lieske, J. C., Deganello, S. and Toback, F. G. (1999) Cell–crystal interactions and kidney stone formation. Nephron 81, 8–17
34 Lieske, J. C., Leonard, R. and Toback, F. G. (1995) Adhesion of calcium oxalate monohydrate crystals to renal epithelial cells is inhibited by specific anions. Am. J. Physiol. 268, F604–F612
35 de Water, R., Noordermeer, C., van der Kwast, T. H., Nizze, H., Boevé, E. R., Kok, D. J. and Schröder, F. H. (1999) Calcium oxalate nephrolithiasis: Effect of renal crystal deposition on the cellular composition of the renal interstitium. Am. J. Kidney Dis. 33, 761–771
36 Khan, S. R. (1997) Calcium phosphate/calcium oxalate crystal association in urinary stones: implications for heterogeneous nucleation of calcium oxalate. J. Urol. 157, 376–383
37 Ebrahimpour, A., Perez, L. and Nancollas, G. H. (1991) Induced crystal growth of calcium oxalate monohydrate at hydroxyapatite surfaces. The influence of human serum albumin, citrate and magnesium. Langmuir 7, 557–583
38 Addadi, L. and Weiner, S. (1992) Control and design principles in biological mineralization. Angew. Chem. Int. Ed. Eng. 31, 153–169
39 Gray, A., Spector, A. R. and Prien, Jr, E. L. (1976) Kidney stone matrix – differences in acidic protein composition. Invest. Urol. 13, 387–389
40 Warpehoski, M. A., Buscemi, P. J., Osborn, D. C., Finlayson, B. and Goldberg, E. P. (1981) Distribution of organic matrix in calcium oxalate renal calculi. Calcif. Tissue Int. 33, 211–222

JOURNAL OF BONE AND MINERAL RESEARCH
Volume 18, Number 7, 2003

Intracrystalline Proteins and Urolithiasis: A Synchrotron X-ray Diffraction Study of Calcium Oxalate Monohydrate

DAVID E FLEMING,[1,2] ARIE VAN RIESSEN,[3] MAGALI C CHAUVET,[4] PHULWINDER K GROVER,[4] BRETT HUNTER,[5] WILHELM VAN BRONSWIJK,[1] and ROSEMARY L RYALL[4]

ABSTRACT

The existence of intracrystalline proteins and amino acids in calcium oxalate monohydrate was demonstrated by X-ray synchrotron diffraction studies. Their presence has implications for the destruction of calcium oxalate crystals formed in the urinary tract and the prevention of kidney stones.

Introduction: Although proteins are present in human kidney stones, their role in stone pathogenesis remains unknown. This investigation aimed to characterize the nature of the relationship between the organic and mineral phases in calcium oxalate monohydrate (COM) crystals grown in human urine and in aqueous solutions of proteins and amino acids to clarify the function of proteins in urolithiasis.
Methods: COM crystals were grown in human urine and in aqueous solutions containing either human prothrombin (PT), Tamm-Horsfall glycoprotein (THG), aspartic acid (Asp), aspartic acid dimer (AspAsp), glutamic acid (Glu), glutamic acid dimer (GluGlu), or γ-carboxyglutamic acid (Gla). Controls consisted of COM crystals precipitated from pure inorganic solutions or from human urine that had been ultrafiltered to remove macromolecules. Synchrotron X-ray diffraction with Rietveld whole-pattern peak fitting and profile analysis was used to determine nonuniform crystal strain and crystallite size in polycrystalline samples.
Results: Crystals precipitated from ultrafiltered urine had lower nonuniform strain than those grown in urine or in aqueous PT solution. Nonuniform strain was much lower in crystals grown in distilled water or in the presence of THG. For the amino acids, the highest nonuniform strain was exhibited by crystals grown in Gla solution, followed by Glu. Crystallite size was inversely related to nonuniform strain, with the effect being significantly less for amino acids than for macromolecules.
Conclusions: Selected proteins and amino acids associated with COM crystals are intracrystalline. Although their incorporation into the mineral bulk would be expected to affect the rate of crystal growth, they also have the potential to influence the phagocytosis and intracellular destruction of any crystals nucleated and trapped within the renal collecting system. Crystals impregnated with protein would be more susceptible to digestion by cellular proteases, which would provide access to the crystal core, thereby facilitating further proteolytic degradation and mineral dissolution. We therefore propose that intracrystalline proteins may constitute a natural form of defense against renal stone formation.
J Bone Miner Res 2003;18:1282–1291

Key words: calcium oxalate monohydrate, urinary proteins, intracrystalline proteins, synchrotron X-ray diffraction, Rietveld refinement

INTRODUCTION

NUCLEATION OF CRYSTALS and their subsequent entrapment within the renal collecting system are obligate steps in the formation of kidney stones, most of which are composed principally of calcium oxalate (CaOx). The likelihood of crystal nucleation obviously depends on the degree to which urine is supersaturated with CaOx. However, retention of crystals will be favored by any process that causes sufficient enlargement to prevent their harmless expulsion in the urinary stream or by factors that encourage their adhesion to the renal epithelium. The well-documented

The authors have no conflict of interest.

[1]Department of Applied Chemistry, Curtin University of Technology, Perth, Western Australia, Australia.
[2]Chemistry Centre of Western Australia, East Perth, Western Australia, Australia.
[3]Department of Applied Physics, Curtin University of Technology, Perth, Western Australia, Australia.
[4]Department of Surgery, Flinders Medical Centre and Flinders University of South Australia, Bedford Park, South Australia, Australia.
[5]Australian Nuclear Science & Technology Organization, Lucas Heights, New South Wales, Australia.

association of urinary proteins with CaOx kidney stones[1–3] has led to the widespread belief that they might regulate crystallization processes during urolithiasis in a manner similar to that exerted by "control" proteins in healthy biomineralization.[4] However, whether they act as promoters or inadequate retardants of crystal nucleation, growth, or aggregation; whether they are simply nonselective, ineffectual binders; or whether they are products of the stones that then become incorporated into the structure, they will still be associated with the final calculus. Therefore, mere demonstration that protein is present in stone matrices provides few clues about the mechanism by which it came to be there or what effects it may have wrought in the process.

It is now widely accepted that some urinary proteins may help to prevent stone formation by inducing the formation of small crystals or by preventing their aggregation into large clusters likely to be retained within the renal collecting system.[2,3] It is also becoming increasingly recognized that stone formation almost certainly involves direct interaction between newly formed crystals and cells of the renal epithelium, because exposure of cultured renal cells to CaOx results in attachment of the crystals,[5–7] which then are internalized.[8–11] Proteins on crystal surfaces may therefore also act as modulators of the attachment to, and phagocytosis of CaOx crystals by, renal epithelial cells, an assumption supported by at least one report that the adhesion of crystals to cultured cells is inhibited by several macromolecules.[6] However, while the potential roles of superficial proteins may seem obvious, less apparent are those of intracrystalline proteins.

It has been known for many years that CaOx crystals generated from human urine are associated with relatively few selected proteins compared with the large number known to be present in healthy urine.[12] Predominant among these are a urinary form of prothrombin fragment 1 (UPTF1)[13] and osteopontin (OPN),[14] with serum albumin and various derivatives of inter-α-inhibitor being present in lesser quantities.[15] In contrast, the most abundant urinary protein, Tamm-Horsfall glycoprotein (THG) is reportedly absent from demineralized extracts of urinary CaOx crystals.[12] We have recently demonstrated that CaOx crystals deposited from human urine that contains most of its normal protein complement possess a complex, ordered ultrastructure comprised of labyrinthine tunnels and crystalline particles intimately associated with organic material.[4,16] The quantity of organic material diminishes after crystal fracture and proteolytic digestion, showing that it consists principally of protein. In marked contrast, no organic material can be detected in crystals derived from urine that has been ultrafiltered to remove all macromolecules with molecular mass greater than 10 kDa.[4,16]

Those observations led us to postulate that urinary proteins may fulfill a hitherto unsuspected role in the prevention of stone formation. Pure inorganic CaOx crystals internalized by renal cells in culture are known to dissolve over a period of several weeks.[17–21] However, cribriform crystals riddled with macromolecules would be expected to be dismantled and dissolve more rapidly as a result of attack by intracellular and lysosomal proteases released during the phagocytic response, because they would be more vulnerable to enzymatic degradation than solid minerals. Thus, proteins distributed throughout the crystal structure should facilitate excavation into channels deep inside the crystal, enabling burrowing into the crystalline core and vastly increasing the surface area available for further digestive processes and mineral dissolution. Intracrystalline proteins may therefore fulfil an important function as mediators in the routine destruction of retained crystals, and therefore act as a natural form of defense against stone pathogenesis.[4,16]

Current evidence showing the existence of intracrystalline proteins in urinary CaOx has consisted of SDS-PAGE and Western blot analysis,[12,13,15] as well as field emission scanning electron microscopic examination of washed, fractured crystals subjected to subsequent protease treatment.[4,16] Although showing unequivocally that urinary CaOx crystals possess an internal ultrastructure containing protein, those studies provided no direct information about the physical basis of the relationship between the organic and inorganic crystal phases or the nature of the mineral itself. Consequently, the possibility could not be discounted that the CaOx structures examined were not single crystals infiltrated with protein, but rather, crystallites or amorphous mineral stabilized by organic material and assembled into what appeared, at least externally, to be individual structures. A natural equivalent occurs in triradiate calcite spicule of the sponge *Calcarea clathrina*, which consists of a crystalline nucleus at the junction of the three rays, each of which contains an amorphous core and a crystalline sheath enveloping the entire structure. Despite this complexity, Addadi et al. have shown that the spicule behaves as a single crystal under light microscopy and synchrotron X-ray diffraction (SXRD) and that 80% of scattering intensity is contributed by the amorphous material.[22] Broadening of diffraction peaks enabled the same authors to show that the spicule of the sea urchin consists of a single crystal impregnated throughout with intercalated proteins. Located at the boundaries of the crystal domains, the proteins adsorb on to preferred crystallographic faces, where they induce crystal defects that reduce crystallite size and alter morphology and cleavage fracture characteristics.[23,24]

The aim of this study was to use SXRD analysis of CaOx crystals precipitated from ultrafiltered (UF) urine, centrifuged and filtered (CF) urine, and aqueous solutions containing selected urinary proteins to clarify the nature of the relationship between the organic and mineral phases. CaOx exists as three polymorphs: calcium oxalate monohydrate (COM), dihydrate (COD), and trihydrate (COT). COM was selected for the study because it is regarded as the critical polymorph in urolithiasis,[25,26] is thermodynamically stable, and is the dominant phase found in CaOx renal calculi.[27] Furthermore, because the binding of proteins to mineral crystals will depend significantly on their primary amino acid composition and sequence, similar studies were undertaken using COM crystals grown in the presence of amino acids, which we have shown previously to bind to CaOx.[28] Polycrystalline, rather than single crystal analysis, was carried out because the amount of protein associated with individual crystals in a given preparation is variable,[4] and an average response was required to enable comparisons to be made. Whole-pattern XRD analysis techniques

have improved sufficiently to enable this to be accomplished.

MATERIALS AND METHODS

Chemicals and biochemicals

All reagents were of the highest purity commercially available. Sodium oxalate (NaOx), gelatin, Asp, AspAsp, Glu, and GluGlu were obtained from BDH Chemicals Australia (Kilsyth, Victoria, Australia). Calcium chloride, Tris (hydroxymethyl aminomethane), and Gla were supplied by the Sigma Chemical Company (St Louis, MO, USA). Proteinase K was obtained from Boehringer (Mannheim, Germany). COM was purchased from Ajax Chemicals (New South Wales, Australia). THG[29] and PT[30] were prepared as we have described previously. Double distilled water was used in all experiments.

Sample preparation

COM crystals grown from aqueous solutions: Crystals of COM were generated by mixing 5 ml each of aqueous solutions of 0.15 M $CaCl_2$ and 0.15 M NaOx into distilled water containing the dissolved protein or amino acid at 37°C. PT (10 mg/liter) was prepared in distilled water. PT was used as a substitute for its derivative, UPTF1, a major component of CaOx urinary crystals[13] and to which it is structurally closely related. PT is easier to purify than UPTF1 and is present in demineralized extracts of CaOx crystals precipitated from human urine.[31] The concentration of THG used (20 mg/liter) was within its normal range in human urine. All amino acids were used at a final concentration of 1 g/liter. $CaCl_2$ and NaOx solutions were added at a rate of 0.4 ml/h from glass syringes using an infusion pump (Sage Instruments, Cambridge, MA, USA). The mixture was gently agitated with an overhead stirrer fitted with a glass stirring rod and incubated for 13 h at 37°C. Precipitated crystals were separated by vacuum filtration, washed with a saturated solution of CaOx, and dried under nitrogen.

COM grown in gelatin: COM crystals were grown in gelatin at room temperature in accordance with the method outlined by Henisch.[32] Solutions of $CaCl_2$ (0.15 M) and NaOx (0.15 M) were introduced into each side of a glass U tube containing a plug of gelatin gel at the U bend. After a growth period of 12 weeks, COM crystals were removed from the gelatin layer with tweezers, washed with saturated CaOx solution, separated by vacuum filtration, dried under nitrogen, and stored in a dessicator. These slowly grown crystals were assumed to be relatively free of lattice strain and were used as the "strain free" reference for Gaussian and Lorentzian contribution calculations in Eqs. 2 and 3. This assumption was later confirmed by the finding of significantly narrower X-ray diffraction peaks in comparison with COM grown in distilled water.

Collection and treatment of urine samples: Urine samples were collected over a 24-h period from healthy individuals who had no history of kidney stone disease. The samples were refrigerated during the collection period and during storage before use. Absence of blood from the specimens was confirmed using Multistix test strips (Miles Laboratories Mulgrave, Victoria, Australia). The samples were pooled and centrifuged at 8000*g* for 15 minutes at 20°C in a Beckman J2–21M/E centrifuge (Beckman Instruments, Palo Alto, CA, USA). The supernatant was filtered through 0.22-μm Millipore filters (GVWP 14250; Millipore Corp., Bedford, MA, USA). A portion of the centrifuged and filtered (CF) urine was ultrafiltered (UF) using an Amicon hollow fiber bundle (Amicon Corp., Danvers, MA, USA), with a nominal molecular mass cut-off of 10 kDa.

COM crystals from human urine: COM crystals were precipitated from CF and UF urine as described elsewhere.[12] Briefly, the metastable limit of urine with respect to CaOx, that is, the minimum amount of oxalate required to elicit spontaneous detectable crystallization using a Coulter Counter, was first determined by titration with NaOx solution. A standard load of oxalate in excess of that limit was then added to induce precipitation, and the suspension was incubated for 2 h at 37°C in a shaking water bath.

Proteolytic digestion of COM crystals: A sample of calcium oxalate crystals (5 mg) grown in CF urine was fractured using a diamond cell (High Pressure Diamond Optics, Tuscon, AZ, USA) and incubated at 37°C for 12 h in 2 ml of an aqueous saturated solution of CaOx containing 0.25 mg/ml Proteinase K and 12.5 mM Tris-HCl buffer, pH 7.0. After protease digestion, the crystals were separated by vacuum filtration, washed with a saturated solution of CaOx, and dried under nitrogen. The same procedure was carried out for COM grown in ultrafiltered urine.

Scanning electron microscopy

Crystals were mounted on double-sided carbon tape fixed on aluminum stubs, coated with carbon (25 nm, Speedivac model 12E6), and examined using a JEOL 6300F field emission scanning electron microscope (JEOL, Tokyo, Japan). Imaging was performed with secondary electrons generated by a 3-keV primary electron beam.

Synchrotron X-ray diffraction

Collection of data: Synchrotron X-ray diffraction (SXRD) patterns were collected on BIGDIFF, a synchrotron diffractometer installed on Beamline 20B, Australian National Beamline Facility (ANBF) at the Photon Factory Synchrotron-Radiation Facility within the National Laboratory for High Energy Physics (KEK), Tsukuba, Japan. The radius of the camera is 573 mm, which gives a scaling factor of 1°/cm along the circumference. The monochromator was set at a wavelength close to the CuKα radiation doublet, and the incident beam dimensions were fixed at a height of 0.8 mm and width of 10 mm. Sample run times were 900 s for both COM and a lanthanum hexaboride (LaB_6) line profile standard and 300 s for the silicon wavelength standard. Four imaging plates (400 × 200 mm; Fuji Photo Film Co., Tokyo, Japan) were used to record the diffraction patterns. The diffraction pattern image on the plate was digitized to produce an 8-bit image that gave an angular resolution of 0.01° 2θ. This is less than the ultimate resolution determined by the footprint of the capillary (0.05° for a capillary diameter of 0.5 mm). BIGDIFF is fitted with eight radioactive fiducial markers that were used to determine the 2θ offset for each imaging plate by using the known 2θ values

for the markers, as determined by tests with specimens of known Bragg angle (θ) values (i.e., silicon).

Crystals were packed into glass capillaries made of low-absorption lithium borate with a 0.5 mm internal diameter and a wall thickness of 0.01 mm.

Line broadening: The strain contributing to line broadening is described as nonuniform strain, which varies from one crystal grain to another, whereas uniform strain (macrostrain) causes shifts in the Bragg peak positions.[33] Nonuniform strain information was obtained by subtracting the instrumental broadening contribution and separating crystallite size effects from strain effects. For Rietveld analysis, the instrumental contribution was determined using a LaB_6 standard (NIST SRM 660),[34] which has little broadening caused by particle size or strain.

Rietveld whole-pattern fitting of X-ray diffractograms: The X-ray data were subjected to Rietveld refinement[35] using Rietica for Windows 95/98/NT Version 1.72 (ANSTO, Lucas Heights, New South Wales, Australia).[36] Gaussian and Lorentzian contributions to X-ray peak profiles were obtained using a Voigt function.[37,38] These contributions, expressed as whole-pattern refined values, were used in Eqs. 2 and 3 to calculate lattice strain and crystallite size. Parameters refined were phase scale, overall thermal parameter, unit cell parameters (a, b, c, β), atomic coordinates for Ca_1, Ca_2, background (Cheby 1), zero offset, Gaussian peak broadening coefficient (U), crystallite size, preferred orientation, and Gaussian peak anisotropy (U_{anis}). The model was set up for COM using the initial parameters of the space group (P 1 21/c 1) and cell parameters (a, b, c, β) obtained from the Inorganic Crystal Structure Database, collection code 30782.[39] A silicon NBS powder standard (NIST SRM 640)[40] was used to determine accurately the wavelength of the X-ray radiation used and to establish the 2θ offset for each image plate according to the fiducial marker images. SXRD data obtained from the LaB_6 powder standard was used to construct a plot of full width of the peak at half maximum height (FWHM) versus 2θ to determine the instrument profile. Coefficients U, V, and W of Eq. 1[41,42] were obtained for use in the Rietveld refinements of all X-ray crystal data. The U value was used as an initial value which was open to refinement, but the V and W values were kept constant throughout each refinement, because they are functions of the instrumental conditions.

$$\mathrm{FWHM} = [U(\tan^{2\theta}) + V(\tan\theta) + W]^{1/2} \quad (1)$$

The nonuniform lattice strain (root mean square) strain, $(\epsilon^2)^{1/2}$, was calculated using Eq. 2,[41,42] where U and U_r were determined from the Gaussian contribution to the peak shape profile of the sample and a strain-free reference, respectively, by Rietica.

$$(\epsilon^2)^{1/2} = \pi(U - U_r)^{1/2}/[(720)(2\ln 2)^{1/2}] \quad (2)$$

The error in $(\epsilon^2)^{1/2}$ was calculated using the total derivative:

$$\delta(\text{total error}) = C(\delta U - \delta U_r)/2(U - U_r)^{1/2}$$

where

$$C = \pi/[(720)(2\ln 2)^{1/2}]$$

Average crystallite size (D) was computed by Rietica and was derived from the Lorentzian contribution to the peak shape profile according to Eq. 3,[36] where the $\sec\theta$-dependent term describes particle-size effects and λ is the wavelength of X-rays used (0.149576 nm).

$$\mathrm{FWHM}_L = [180\lambda \sec\theta]/[\pi D] \quad (3)$$

The errors in nonuniform strain and crystallite size are estimated from the statistical variation of the diffraction data and do not include systematic errors.

Optical crystallography

Crystals were examined under crossed polarizers using an Olympus BH-2 microscope (Olympus, Tokyo, Japan) and $\times$1000 magnification.

Statistical analysis

Assessment of the significance of differences in nonuniform strain, crystallite size, and linear relationships was based on the null hypothesis, that is, there is no difference in the two quantities being compared. Both the z value (Eq. 4) and probability (p) of the null hypothesis being true are presented.

$$Z = [(O_1 - O_2) - (E_1 - E_2)]/[\sigma_1^2/n_1 + \sigma_2^2/n_2]^{1/2} \quad (4)$$

where O_1 and O_2 are the observed values, E_1 and E_2 are the expected values (null hypothesis, $E_1 - E_2 = 0$), σ_1 and σ_2 are the root mean standard errors of the observed values, and n_1 and n_2 are the population sizes of the observations.

RESULTS

Because the general aim of this study was to clarify the relationship between the organic and mineral phases in COM, SXRD analysis with Rietveld whole-pattern fitting analysis was carried out in association with light and scanning electron microscopy examination of crystals. This combination of techniques enabled quantification of crystal disorder, expressed in terms of nonuniform crystal strain and crystallite size, to be correlated with direct visualization of the crystal morphology.

Calcium oxalate morphology

COM was the only polymorph of CaOx generated from aqueous solutions and the major polymorph precipitated from UF and CF urine. All crystals exhibited the classic COM hexagonal plate morphology, but some thinning of the plates and rounding of edges was observed for those grown in UF urine, CF urine, and in the PT solution. X-ray diffraction lines of the sole minor phase, COD (<5%), did not interfere significantly with COM diffraction lines of the urinary crystals, and both single and two phase Rietveld refinement of the crystallographic parameters produced the same results. Peak shifts in the SXRD patterns were negligible, and the crystallographic parameters of all samples fell

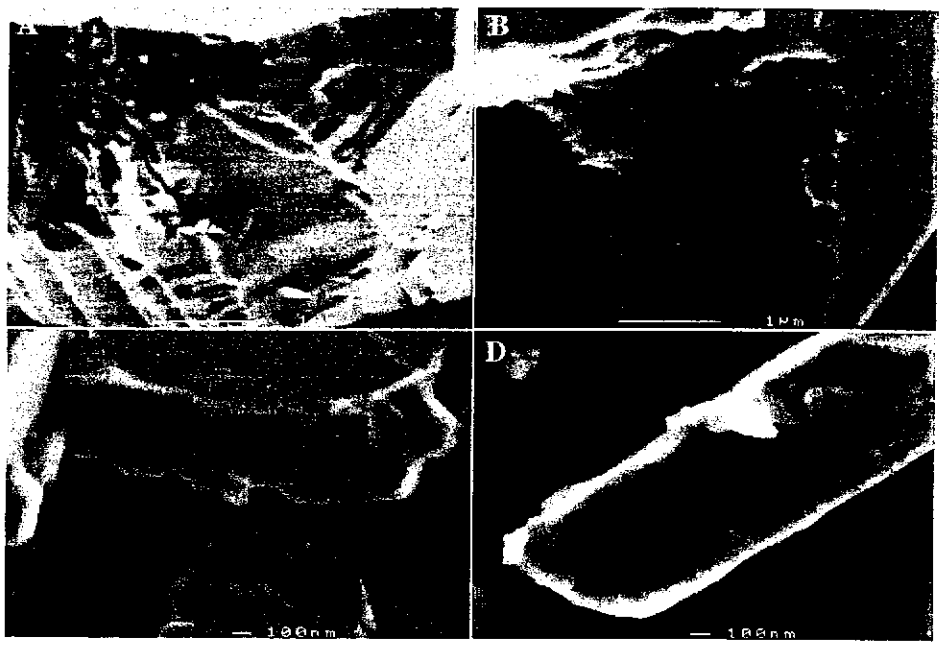

FIG. 1. Electron microscopy images of fractured COM crystals grown in (A) distilled water, (B) UF urine, (C) aqueous solution of PT, and (D) CF urine. (D) An enlargement of an image published previously.[4] Reproduced with permission from the Journal of Structural Biology.

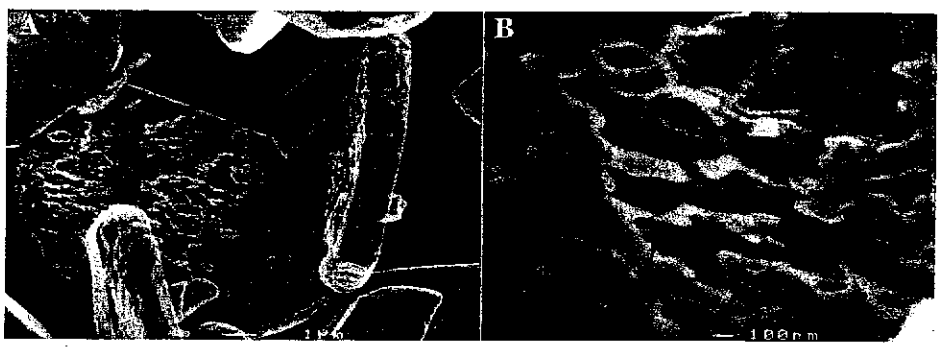

FIG. 2. Electron microscopy images of COM grown in CF urine and treated with protease, showing etching of the (100) face (B is a 5.33× magnification of the lower left area of the eroded crystal shown in image A).

in a very narrow range (0.6294 nm $< a <$ 0.6303 nm, 1.4585 nm $< b <$ 1.4600 nm, 1.0120 nm $< c <$ 1.0123 nm, 109.41° $< \beta <$ 109.49°). These are in excellent agreement with published data for COM (a = 0.6290 nm, b = 1.4583 nm, c = 1.0116 nm, and β = 109.50°).[39]

Optical crystallography

Microscopic examination under crossed polarizers of a random selection of crystals (6–50 μm) grown in each of the various aqueous and urine media showed the classic four distinct extinctions per 360° rotation of birefringent single crystals in every instance. The extinctions were uniform and demonstrated that, optically, all behaved as single crystals rather than individual structures comprised of aggregates of randomly oriented microcrystals.

Electron microscopy

Electron microscopy of fractured crystals grown in distilled water (Fig. 1A) and in UF urine (Fig. 1B) revealed solid interiors with little or no signs of pitting. Identical observations were made with fractured crystals precipitated from amino acid and THG solutions (data not shown). In contrast, Figs. 1C and 1D show a varying cross-sectional density for COM grown in the presence of PT and in CF urine, indicating a heterogeneous internal structure. Protease treatment led to significant material losses, with most erosion occurring at crystal centers (Fig. 2A). Higher magnification (Fig. 2B) shows that the boundaries of the residual material consisted mainly of columns arrayed along the (100) face.

Crystal disorder

The FWHM trends of SXRD peaks for each type of crystal, as defined by Eq. 1 and determined by Rietveld refinement, showed a marked variation in the rate of peak broadening as a function of 2θ (Fig. 3). COM grown in gelatin showed the smallest broadening rate, which confirmed it to be the least disordered. A greater rate of broadening, and hence greater disorder, was observed for COM grown in distilled water (control) and in THG solution. Solutions of GluGlu, Asp, AspAsp, and Glu produced COM with progressively greater broadening rates, whereas the

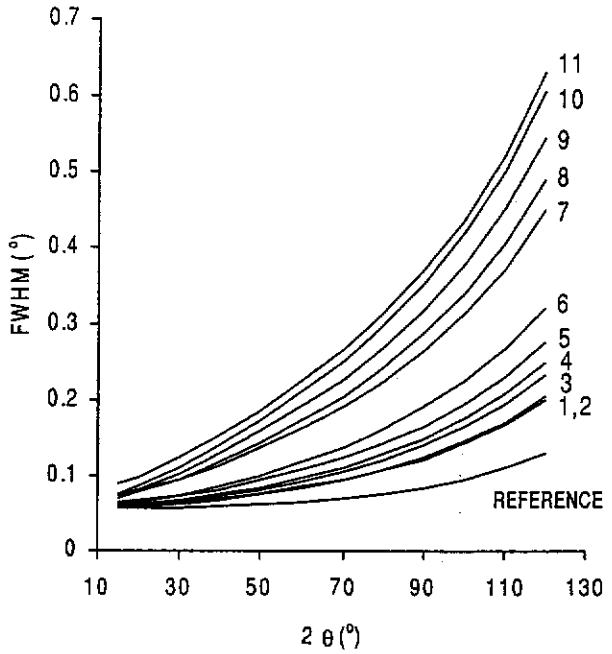

FIG. 3. FWHM trends of SXRD peaks as a function of 2θ for COM crystals grown in gelatin gel (reference), distilled water (1), UF urine (7), and CF urine (10); solutions of THG (2), GluGlu (3), Asp (4), AspAsp (5), Glu (6), Gla (9), and PT (11); and crystals grown in CF urine and subsequently treated with protease (8). Individual data points have been omitted for clarity.

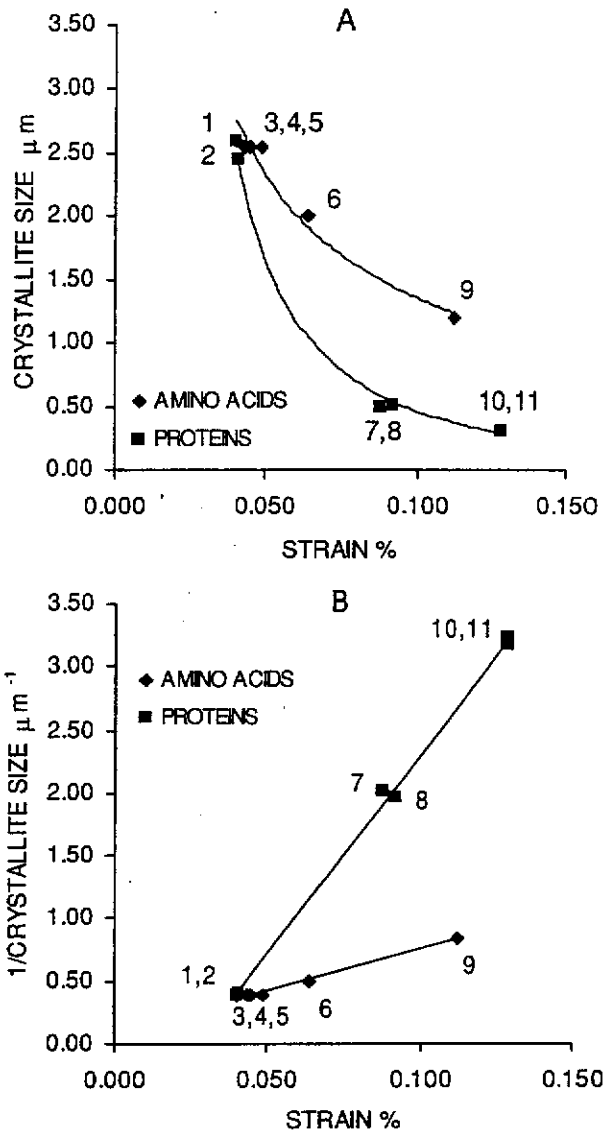

FIG. 4. (A) Crystallite size and (B) the reciprocal of crystallite size as a function of nonuniform strain for COM grown in distilled water (1), UF urine (7), CF urine (10), and CF urine followed by treatment with protease (8); solutions of THG (2), GluGlu (3), Asp (4), AspAsp (5), Glu (6), Gla (9), and PT (11). The estimated relative SD for both size and nonuniform strain is ~10%.

most marked increases in broadening rates were found for UF and CF urine, Gla, and PT. Protease treatment of COM grown in CF urine reduced its broadening rate markedly.

Nonuniform strain and crystallite sizes calculated from the fitted peak width trends using Eqs. 2 and 3 range from 0.040% to 0.128% and from 0.31 to 2.59 μm, respectively, (Fig. 4A). Rietveld refinement uses a single variable to describe peak width variation as a function of diffraction angle (U, Eq. 1) for the whole X-ray diffraction pattern. Hence, it can return only single values for crystallite size and nonuniform strain, which for a polycrystalline sample is an average over both the assemblage of crystallites in the crystal and the three crystallographic axes. The morphology of the crystallites thus cannot be deduced as they are treated as spheres, nor can anisotropy in the nonuniform strain be determined. The estimated relative SD error for both nonuniform strain and crystallite size was approximately 10%. COM grown in distilled water and in THG solution was found to have the least nonuniform strain and some of the largest crystallite sizes, relative to crystals grown in gelatin. The presence of GluGlu, Asp, or AspAsp in solution gave rise to a slight increase in nonuniform strain but had little or no effect on crystallite size, while Glu led to a more significant increase in nonuniform strain ($z = 5.6$, $p \sim 0$) and decrease in crystallite size ($z = 1.8$, $p < 0.04$). COM grown in UF urine was more strained ($z = 2.74$, $p < 0.003$) and had a significantly smaller crystallite size ($z = 5.7$, $p \sim 0$), which was approximately 20% of that of the control crystals grown in distilled water. In contrast, COM grown in Gla solution was even more strained ($z = 2.5$, $p < 0.006$) but had a much greater crystallite size ($z = 6.9$, $p \sim 0$) than that grown in UF urine, which was approximately 40% of that recorded in the control. The highest nonuniform strains and smallest crystallite sizes were found for COM grown in the PT solution (0.128 ± 0.008% and 0.31 ± 0.03 μm, respectively) and in CF urine (0.128 ± 0.009% and 0.31 ± 0.03 μm, respectively). Protease treatment of the crystals grown in CF urine reduced nonuniform strain and increased crystallite size to the levels observed for crystals grown in UF urine ($z = 3.8$, $p \sim 0$; $z = 1.5$, $p < 0.07$).

The data show that two reciprocal relationships exist between nonuniform strain and crystallite size, with proteins other than THG generating a smaller crystallite size than the amino acids for same degree of nonuniform strain

(Fig. 4A). The slopes of the transformed relationships (Fig. 4B) show that the two populations, proteins (slope = 32.3 ± 0.6) and amino acids (slope = 6.6 ± 0.3), are significantly different ($z = 95, p \sim 0$). Figure 4 thus clearly shows that the degree of crystal disorder, that is, increased nonuniform strain and decreased crystallite size, is influenced by the size and chemical composition of the guest molecules.

DISCUSSION

Although it has been known for at least 10 years that CaOx crystals precipitated from human urine are irreversibly associated with proteins,[12] there has been continuing debate as to whether they are bound only to the crystal surface or are actually located within the mineral structure. The distinction is critical, because the presence of proteins inside crystals could influence their phagocytosis by epithelial cells of the renal collecting system and facilitate their subsequent intracellular disposal,[4,16] a possibility which, if true, has implications for the design of drugs for preventing stone formation. The broad objective of this study was to obtain quantitative data to corroborate our previous qualitative findings, which indicated that selected proteins associated with CaOx crystals precipitated from human urine are intracrystalline. All crystals have imperfections caused by dislocations and/or foreign molecules that create defects and disorder and hence are an assemblage of smaller defect-free perfectly crystalline subregions (crystallites) whose alignment will exhibit some degree of disorder. An increase in the number of defects thus causes a reduction in crystallite size and increases the randomness of their orientation, the latter being manifest as an increase in nonuniform lattice strain. Consequently, a decrease in crystallite size and associated increase in nonuniform lattice strain, relative to a control, would indicate the presence of extraneous molecules inserted into the crystal bulk and thereby constitute proof that they are intracrystalline.[43]

Our specific aim was, therefore, to measure crystal strain and crystallite domain size in COM crystals precipitated from human urine and from aqueous solutions of selected proteins and amino acids to determine whether the organic additives are occluded within the mineral bulk. PT was selected for study because it has been strongly implicated in the pathogenesis of renal stones.[3] It is a potent inhibitor of both CaOx crystal growth and aggregation in an inorganic medium[44,45] and in undiluted UF urine.[46] The protein's inhibitory potency, as well as its strong affinity for CaOx crystals deposited from urine,[12] can be attributed to its Gla domain.[45] Located in the N-terminal region of the molecule, this region contains 10 Gla residues, an amino acid renowned for its extraordinary capacity for binding calcium ions[45] and which we have shown previously to adsorb strongly onto COM.[28] For those reasons, Gla was also studied. Asp and Glu were included because of their moderate adsorption affinity for COM relative to Gla,[28] as were their dimers, AspAsp and GluGlu, whose use enabled determination of the effect of doubling single amino acid chain lengths. Although lacking Gla, THG was studied because it is the most abundant urinary protein and has been reported to function in urine both as an inhibitor and promoter of CaOx crystallization[47] and also as a regulator of COM adhesion to urothelial cells.[48] A further reason for studying PT and THG is that PT is present in demineralized extracts of alkali-washed crystals precipitated from healthy male urine,[31] whereas THG is not.[12] Crystals were also grown in urine that had been centrifuged and filtered, as well as in the same urine after ultrafiltration to remove all macromolecules with molecular masses greater than 10 kDa. This enabled the generation of crystals from urine samples with an identical complement of low molecular weight components, but markedly different macromolecular compositions. COM grown in distilled water was used as the control to allow effects resulting specifically from the influence of proteins and amino acids to be identified.

COM was the only CaOx polymorph formed in distilled water and in the presence of aqueous amino acid and protein solutions, whereas two polymorphs, COM and COD, were precipitated in UF urine and in CF urine. This is in agreement with the view that the urinary matrix stabilizes the less thermodynamically stable COD phase.[49] The thinning of the hexagonal-shaped plates and rounding of edges observed for COM crystals grown in the aqueous PT solution, UF urine, and CF urine indicate a reduction in the growth rates of the (100) faces. This reduction, caused by adsorbed species, produces the familiar "coffin"-shaped COM crystals commonly found in urine. All refined Rietveld crystallographic values were close to those in published data,[39] indicating that the unit cell dimensions were not altered significantly by the presence of amino acids and proteins. Thus, the organic molecules, where present, were either surface-adsorbed or dispersed about the crystallites or both, and not intercalated in the COM crystallite lattices.

Electron microscopy of fractured crystals grown in distilled water, the amino acid solutions, and UF urine showed solid interiors, indicating that these media have little or no impact on the homogeneity of the crystal structure. However, transverse sections of fractured crystals grown in PT solution and in CF urine showed marked textural variation. Furthermore, when the crystals were treated with protease, only those grown in CF urine and PT solution showed significant erosion, particularly near their centers. As protease specifically digests proteins, it follows that the crystal cavities must have resulted, at least in part, from the removal of proteins. However, the cavities (0.3–1 μm) are undoubtedly far larger than the dimensions of individual proteins,[22] which suggests that selected, possibly aggregated proteins might induce nucleation of mineral around them. It is possible that such aggregation might be caused by the addition of the high oxalate concentration used to induce artificial nucleation of crystals in CF urine, and consequently that crystals formed in vivo would lack the intracrystalline spaces evident in those nucleate in vitro. However, similar intracrystalline spaces were present in COM crystals that were deposited from an aqueous PT solution by the slow addition of calcium and oxalate ions, and we have also observed a similar internal structure in CaOx crystals formed naturally in fresh urine on cooling (results not shown). Moreover, physiological induction of crystalluria within the renal collecting system probably oc-

curs in response to spasmodic pulses of high local oxalate and calcium concentrations resulting from dehydration or ingestion of meals rich in those ions. Alternatively, proteins with a strong affinity for CaOx could cluster into large assemblages of individual molecules competing for limited binding sites on the surfaces of nascent crystals. Concentration of organic material toward the crystal cores can be explained easily in terms of the relative quantities of protein and solute ions in solution. As solute deposition continues, protein becomes depleted, thereby allowing the deposition of CaOx relatively free of organic material and the formation of a solid mineral shell enveloping the protein-mineral composite that was once the crystal embryo. The orientation of the residual columnar material in the crystals grown in CF urine and then treated with protease (Fig. 2B) indicates that proteins prefer to dock on to the COM (100) faces. The reason for this is not known, but it is likely that preferential binding to those faces may be related to the matching of protein binding amino acid groups with the position of calcium ions on the crystal faces.

COM grown in Asp, AspAsp, GluGlu, and THG solutions exhibited nonuniform strains and crystallite sizes comparable with those of the control COM grown in distilled water. It is therefore unlikely that those molecules were occluded into the mineral. Crystals grown in solutions of Gla, Glu, and PT, as well as those generated from UF and CF urine, however, had notably higher nonuniform stains and lower crystallite sizes than the control. Because increased nonuniform strain and decreased crystallite size result from incorporated molecules or ions that increase the number of stacking faults and zones of disorder within crystals,[43] it can be concluded that Gla, Glu, PT, and endogenous urinary proteins and molecules were incorporated into COM during crystal growth. The increase in crystallite size and decrease in nonuniform strain observed after protease treatment of COM crystals grown in CF urine indicate that the smaller crystallite material, more intimately associated with proteins than with bulk COM, was liberated during the protease treatment.

A dominant factor that influences occlusion of amino acids into COM is their ability to bind calcium. Gla, which is well known for its strong affinity for calcium, is likely to attach irreversibly to the COM surface and be enveloped by a growing crystal front, whereas amino acids with lower binding affinity are less likely to become interred within the mineral bulk. This seems to be the case for Asp and Glu. Why Glu should create more crystal disorder than Asp, AspAsp, and GluGlu is not clear, but may be associated with the stereochemistry of their binding to calcium ions on the crystal face.[28] Stereochemistry may also be a determining factor in reducing the binding capacity of Asp and Glu dimers for COM, producing lower nonuniform strains and higher crystallite sizes than occurred with their corresponding monomers. The type and sequence of amino acids comprising the primary structure of proteins are of great importance in determining the nature of protein-crystal interactions.[25,50] The presence of PT within COM crystals can almost certainly be attributed to the strong calcium-binding properties of its Gla residues. However, affinity for calcium ions is insufficient to guarantee that a protein will be incarcerated within growing COM. THG has no Gla, but still has a considerable affinity for calcium,[47] and therefore might be expected to be incorporated into CaOx crystals. However, the protein is not occluded into the mineral,[12,51] probably because of its size. THG, which has a monomeric molecular mass of approximately 94 kDa, condenses in urine and at high concentrations in aqueous solutions into polymers with molecular masses in the millions. In contrast, OPN, another urinary protein thought to play a major role in stone formation and which also lacks Gla residues, is, nonetheless, an intracrystalline component of urinary CaOx crystals.[52] It has been generally assumed that the inhibitory effects of OPN on CaOx crystallization, as well as its association with CaOx crystals, can be attributed to its high content of Asp residues, which mediate its binding to the CaOx crystal surface. However, our demonstration that Asp is not an intracrystalline component of CaOx crystals suggests that OPN's properties, as well as its presence in stones and CaOx crystals, are dictated by factors other than its component Asp moieties. Collectively, these facts show that the inclusion of an individual protein into the COM mineral bulk is not solely determined by its calcium-binding ability or by the presence of Gla within its primary chain.

The reciprocal relationship between nonuniform strain and crystallite size that we found for COM powders has been noted in single crystals studies of other systems, for example, NiO,[53] where nonuniform strain and the reciprocal of crystallite size were both shown to vary linearly with uniform strain, and Addadi et al.'s qualitative observation for calcite crystals in sponges and sea urchins.[22] In those cases, it is clear that a reduction in crystallite size increased misalignment and hence nonuniform strain. However, to our knowledge, our observation that the relationship differs greatly between amino acids and proteins is the first demonstration that, for a given increment in nonuniform strain, the corresponding decrease in crystallite size is markedly greater for macromolecules than for small molecules. We attribute the difference to the large disparity between the sizes and shapes of proteins and amino acids. Because of their small size, amino acids would be expected to inhibit growth only at, or very near to, the sites at which they bind to the crystal surface and therefore to cause only small local imperfections. On the other hand, a macromolecule such as a protein has the potential to interfere with the deposition of solute ions over a much larger region of the crystal surface. Delivery and attachment of solute ions to a crystal will be prevented at any point on the surface covered by the specific binding domain of any protein. However, such domains account for only a small proportion of a protein's structure, whose remaining molecular bulk also has the potential to hinder physically the transport of solute ions to the crystal surface. Crystals formed in the presence of macromolecules would therefore be more likely to incur larger disruptions to their structures than they would from the inclusion of smaller impurities such as amino acids. Consequently, they would exhibit more pronounced non-uniform strain, because greater crystallite packing disorder would occur with decreased crystallite size. Because of their large size, proteins are unlikely to intercalate into the COM lattice, but once adsorbed onto preferred crystal faces, they could be

occluded into the structure as a consequence of engulfment by the advancing growth front.

The relationship between macromolecules and mineral that we have observed in urinary COM crystals can thus be considered analogous to that observed for calcite in some sponges and sea urchins.[24] The structures consist of morphologically identifiable single crystals containing a macromolecular core with which are associated small crystallites or amorphous material, on which is built a layer of larger and more ordered crystallites. The presence in urine of proteins with the capacity to become incorporated inside CaOx crystals is now viewed as having important implications for the development or prevention of urolithiasis.[4,16,54] Although much work has documented the possible role of various urinary macromolecules, particularly proteins,[55] which may inhibit the nucleation of CaOx crystals or interdict their subsequent growth or aggregation, the possible significance of intracrystalline proteins is only recently beginning to be appreciated. It is now widely acknowledged that attachment of newly formed crystals to the renal epithelium is a probable step in urolithiasis, but paradoxically, it could also constitute a natural, routine mechanism of avoiding stone formation. Dissolution of CaOx crystals phagocytosed by cultured renal cells[17–21] has led to the notion that intracellular destruction of crystals could act as a natural form of defense against urolithiasis,[21] a proposal that we have extended to include a specific role for intracrystalline macromolecules.[4,16] Proteins within crystals could offer a delayed, second line of defense if earlier protective mechanisms fail, because they could accelerate the dismantling and ultimate dissolution of their mineral hosts, effected by a combination of proteolytic digestion and the acidic interior of the phagolysosome. Their distribution throughout the structure would provide a series of channels through which cellular proteases could penetrate to the crystal core, thus increasing the area of exposed mineral surface to the acidic environment and increasing the rate of dissolution. This notion is supported by our observation of the presence of intracrystalline interconnecting furrows and subcrystalline particles in urinary CaOx crystals subjected to proteolytic digestion[4,16] and demonstration that protease inhibitors prevent the surface etching that occurs when urinary CaOx crystals are incubated in fresh, whole human urine.[54]

ACKNOWLEDGMENTS

This work was supported by grants from the Australian Institute of Nuclear Science and Engineering, the Australian Synchrotron Research Grant Program, the National Health and Medical Research Council of Australia (Grant No. 980336), the Urological Foundation of Australia, the Flinders Medical Research Institute, and Flinders 2000. The assistance of Drs James Hester and Garry Foran with collection of the SXRD data and the advice of Dr Kevin Ho on proteolytic digestion are gratefully acknowledged.

REFERENCES

1. Boyce WH, Garvey FK 1956 The amount and nature of the organic matrix in urinary calculi: A review. J Urol **76**:213–227.
2. Ryall RL Stapleton AMF 1995 Urinary macromolecules in calcium oxalate stone and crystal matrix: Good, bad or indifferent? In: Khan SR (ed.) Calcium Oxalate in Biological Systems. CRC Press, Boca Raton, FL, USA, pp. 265–290.
3. Ryall RL 1997 Urinary inhibitors of calcium oxalate crystallisation and their potential role in stone formation. World J Urol **15**:155–164.
4. Ryall RL, Fleming DE, Doyle IR, Evans NA, Dean CJ, Marshall VR 2001 Intracrystalline proteins and the hidden ultrastructure of calcium oxalate urinary crystals: Implications for kidney stone formation. J Struct Biol **134**:5–14.
5. Riese RJ, Riese JW, Kleinman JG, Wiessner JH, Mandel GS, Mandel NS 1988 Specificity in calcium oxalate adherence to papillary epithelial cells in culture. Am J Physiol **255**:F1025–F1032.
6. Lieske JC, Leonard R, Toback FG 1995 Adhesion of calcium oxalate monohydrate crystals to renal epithelial cells is inhibited by specific anions. Am J Physiol **268**:F604–F612.
7. Verkoelen CF, Romijn JC, de Bruijn WC, Boevé ER, Cao L, Schröder FH 1995 Association of calcium oxalate monohydrate crystals with MDCK cells. Kidney Int **48**:129–138.
8. Lieske JC, Walsh-Reitz NM, Toback FG 1992 Calcium oxalate monohydrate crystals are endocytosed by renal epithelial cells and induce proliferation. Am J Physiol **262**:F622–F630.
9. Lieske JC, Toback FG 1993 Regulation of epithelial cell endocytosis of calcium oxalate monohydrate crystals. Am J Physiol **264**: F800–F807.
10. Lieske JC, Deganello S, Toback FG 1999 Cell-crystal interactions and kidney stone formation. Nephron **81**:8–17.
11. Lieske JC, Deganello S 1999 Nucleation, adhesion and internalization of calcium-containing urinary crystals by renal cells. J Am Nephrol Soc **10**:S422–S429.
12. Doyle IR, Ryall RL, Marshall VR 1991 Inclusion of proteins into calcium oxalate crystals precipitated from human urine: A highly selective phenomenon. Clin Chem **37**:1589–1594.
13. Stapleton AMF, Ryall RL 1995 Blood coagulation proteins and urolithiasis are linked: Crystal matrix protein is the F1 activation peptide of human prothrombin. Br J Urol **75**:712–719.
14. Maslamani S, Glenton PA, Khan SR 2000 Changes in urine macromolecular composition during processing. J Urol **164**:230–236.
15. Dawson CJ, Grover PK, Ryall RL 1997 Inter-α-trypsin inhibitor in urine and calcium oxalate urinary crystals. Br J Urol **81**:20–26.
16. Ryall RL, Fleming DE, Grover PK, Chauvet M, Dean CJ, Marshall VR 2000 The hole truth: Intracrystalline proteins and calcium oxalate kidney stones. Mol Urol **4**:391–402.
17. Leiske JC, Toback FG, Deganello S 1996 Face-selective adhesion of calcium oxalate dihydrate crystals to renal epithelial cells. Calcif Tissue Int **58**:195–200.
18. Lieske JC, Hammers MS, Hoyer JR, Toback FG 1997 Renal cell osteopontin production is stimulated by calcium oxalate monohydrate crystals. Kidney Int **51**:679–686.
19. Lieske JC, Norris R, Swift H, Toback FG 1997 Adhesion, internalization and metabolism of calcium oxalate monohydrate crystals by renal epithelial cells. Kidney Int **52**:1291–1301.
20. Lieske JC, Toback FG, Deganello S 1998 Direct nucleation of calcium oxalate dihydrate crystals onto the surface of living renal epithelial cells in culture. Kidney Int **54**:796–803.
21. De Water R, Noordermeer C, van der Kwast TH, Nizze H, Boevé ER, Kok DJ Schröder FH 1999 Calcium oxalate nephrolithiasis: Effect of renal crystal deposition on the cellular composition of the renal interstitium. Am J Kidney Dis **33**:761–771.
22. Addadi L, Aizenberg J, Beniash E, Weiner S 1999 On the concept of a single crystal in biomineralization. In: Braga D (eds.) Crystal Engineering: From Molecules and Crystals to Materials. Kluwer Academic Publishers, Dordrecht, The Netherlands, pp. 1–22.
23. Aizenberg J, Hanson J, Ilan M, Leiserowitz L, Koetzle TF, Addadi L, Weiner S 1995 Morphogenesis of calcitic sponge spicules: A role for specialized proteins interacting with growing crystals. FASEB J **9**:262–268.
24. Aizenberg J, Hanson J, Koetzle TF, Weiner S, Addadi L 1997 Control of macromolecule distribution within synthetic and biogenic single calcite crystals. J Am Chem Soc **119**:881–886.
25. Wesson JA, Weissner JH, Mandel NS, Kleinman JG 2000 Polymer chemical structures that control calcium oxalate polymorphism. In: Rodgers AL, Hibbert BE, Hess B, Khan SR, Preminger GM (eds.)

Urolithiasis 2000. University of Cape Town, Rondebosch, South Africa, pp. 109–112.
26. Prien EL 1963 Crystallographic analysis of urinary calculi: A 23-year survey study. J Urol **89**:917–924.
27. Mandel NS, Mandel GS 1989 Urinary tract stone disease in the United States veteran population II. Geographical analysis of variations in composition. J Urol **142**:1516–1521.
28. Fleming DE, van Bronswijk W, Ryall RL 2001 A comparative study of the adsorption of amino acids on calcium minerals found in renal calculi. Clin Sci **101**:159–168.
29. Grover PK, Marshall VR, Ryall RL 1994 Tamm-Horsfall mucoprotein reduces promotion of calcium oxalate crystal aggregation induced by urate in human urine *in vitro*. Clin Sci **87**:137–142.
30. Grover PK, Ryall RL 2002 Inhibition of calcium oxalate crystal growth and aggregation by prothrombin and its activation fragments in undiluted human urine *in vitro:* Relationship between protein structure and inhibitory activity. Clin Sci **102**:425–434.
31. Buchholz N-P, Kim DS, Grover PK, Dawson CJ, Ryall RL 1999 The effect of warfarin therapy on the charge properties of urinary prothrombin fragment 1 and crystallization of calcium oxalate in undiluted human urine. J Bone Miner Res **14**:1003–1012.
32. Henisch HK 1970 Crystal growth in gels. The Pennsylvania State University Press, University Park and London, pp. 21.
33. Cullity BD 1956 The structure of polycrystalline aggregates. In: Cohen M (ed.) Elements of X-ray Diffraction. Addison-Wesley Publishing Company Inc., Reading, Massachusetts, USA, pp. 264.
34. Certificate of Analysis, Standard Reference Material 660. 1989 Instrument Line Position and Profile Shape Standard for X-ray Powder Diffraction. National Institute of Standards and Technology, Gaithersburg, MD, USA.
35. Hill RJ, Howard CJ, Hunter BA 1995 A computer program for Rietveld analysis of fixed wavelength x-ray and neutron powder diffraction patterns. Australian Atomic Energy Commission (now ANSTO). Report No. M112. Lucas Heights Research Laboratories, New South Wales, Australia.
36. Hunter BA 1998 Rietica – a visual Rietveld program. International Union of Crystallography, Commission on Powder Diffraction Newsletter **20**:18–24.
37. Langford JI 1978 A rapid method for analysing the breadths of diffraction and spectral lines using the Voigt function. J Appl Crystallogr **11**:10–14.
38. Langford JI, Cernik RJ, Louer D 1991 The breadth and shape of instrumental line profiles in high resolution powder diffraction. J Appl Crystallogr **24**:913–919.
39. Inorganic Crystal Structure Database, Collection Code 30782. 1999 The crystal structures of whewellite and weddellite: Re-examination and comparison. The National Institute of Standards and Technology, Gaithersburg, MD 20899.
40. Certificate of Analysis, Standard Reference Material 640. 1974 Silicon Powder Lattice Parameter Standard for X-ray Powder Diffraction. National Institute of Standards and Technology, Gaithersburg, MD.
41. Klug HP, Alexander LE 1974 X-ray Diffraction Procedures for Polycrystalline and Amorphous Materials, 2nd ed. Wiley, New York, NY, USA, pp. 660–665.
42. Caglioti G, Paoletti A, Ricci FP 1958 Choice of collimators for a crystal spectrometer for neutron diffraction. Nucl Instrum **3**:223–228.
43. Addadi L, Weiner S 1992 Control and design principles in biological mineralization. Angew Chem Int Ed **31**:153–169.
44. Grover PK, Moritz RL, Simpson RJ, Ryall RL 1998 Inhibition of calcium oxalate crystal growth and aggregation *in vitro*: A comparison of four human proteins. Eur J Biochem **253**:637–644.
45. Grover PK, Ryall RL 1999 Inhibition of calcium oxalate crystal growth and aggregation by prothrombin and its fragments *in vitro*: Relationship between protein structure and inhibitory activity. Eur J Biochem **263**:50–56.
46. Ryall RL, Grover PK, Stapleton AMF, Barrell DK, Tang Y, Moritz RL, Simpson RJ 1995 The urinary F1 activation peptide of human prothrombin is a potent inhibitor of calcium oxalate crystallization in undiluted human urine *in vitro*. Clin Sci **89**:533–541.
47. Grover PK, Ryall RL, Marshall VR 1990 Does Tamm Horsfall mucoprotein inhibit or promote calcium oxalate crystallisation in human urine? Clin Chim Acta **190**:223–238.
48. Lieske JC, Hammes MS, Toback FG 1996 Role of calcium oxalate monohydrate crystal interactions with renal epithelial cells in the pathogenesis of nephrolithiasis: A review. Scanning Microsc **10**: 519–534.
49. Wesson JA, Worcester EM, Weissner JH, Mandel NS, Kleinman JG 1998 Control of calcium oxalate crystal structure and cell adherence by urinary macromolecules. Kidney Int **53**:952–957.
50. Addadi L, Weiner S, Geva M 2001 On how proteins interact with crystals and their effect on crystal formation. Zeitschrift fur Kardiologie **90**:92–98.
51. Chauvet MC, Grover PK, Ryall RL 2001 Tamm-Horsfall glycoprotein is not an intracrystalline component of urinary calcium oxalate crystals. In: Kok DJ, Romijn HC, Verhagen PCMS, Verkoelen CF (eds.) Eurolithiasis. Shaker Publishing, Maastricht, the Netherlands, 2001, p. 58.
52. Ryall RL, Chauvet MC, Grover PK 2001 2001: A space oddity. In: Kok DJ, Romijn HC, Verhagen PCMS, Verkoelen CF (eds.) Eurolithiasis. Shaker Publishing, Maastricht, the Netherlands, pp. 273–274.
53. Fiévet F, Germi P, de Bergevin F, Figlarz M 1979 Lattice parameter, microstrains and non-stoichiometry in NiO. Comparison between mosaic microcrystals and quasi-perfect single microcrystals. J Appl Crystallogr **12**:387–394.
54. Fleming DE, Grover PK, Chauvet MC, Marshall VR, Ryall RL 2000 An unexpected role of urinary proteins in the prevention of calcium oxalate urolithiasis. In: Rodgers AL, Hibbert BE, Hess B, Khan SR, Preminger GM (eds.) Urolithiasis 2000. University of Cape Town, Rondebosch, South Africa, pp. 169–171.
55. Ryall RL 1993 The scientific basis of calcium oxalate urolithiasis: Predilection and precipitation, promotion and proscription. World J Urol **11**:59–65.

Address reprint requests to:
W van Bronswijk, BSc, PhD
School of Applied Chemistry
Curtin University of Technology
GPO Box U1987
Perth, WA 6845, Australia
E-mail: w.vanbronswijk@curtin.edu.au

Received in original form September 30, 2002; in revised form December 31, 2002; accepted February 3, 2003.

Proteins associated with calcium oxalate crystals formed in human urine are intracrystalline

*David E. Fleming, Ian R. Doyle, Natalie Evans, Villis R. Marshall,
*Gordon M. Parkinson, Rosemary Lyons Ryall

*Department of Surgery, Flinders Medical Centre, South Australia; *School of Applied Chemistry, Curtin University of Technology, Western Australia*

INTRODUCTION

The work of Boyce and Garvey more than 40 years ago (1) confirmed the occurrence of proteins in all renal calculi. Since that time, advances in protein chemistry and technology have enabled the identification of approximately 20 proteins in the organic matrix of human kidney stones (2). However, it is not known whether the presence of these proteins reflects a cause or effect of stones, or consequently, whether they play any specific role in their pathogenesis.

It is now well known that calcium oxalate (CaOx) crystals nucleated *de novo* from human urine are closely associated with proteins. We have proposed that such proteins are included within the crystalline structure, that is, are *intra*crystalline (3), a view subsequently supported by descriptive work of others (4).

However, the concept is still regarded with scepticism in the stone field (5), despite the fact that some proteins which control the nucleation, growth and assembly of inorganic salts in healthy natural biomineralization systems, are known to be intracrystalline (6). The aim of this study was to obtain direct evidence that proteins occur *within* the crystalline architecture of CaOx crystals precipitated from human urine, in order to gain insight into their possible function in the control of CaOx crystallization in the formation of urinary stones.

METHODS

Urine samples were collected without preservative from 4 healthy men between 25 and 43 years of age, and 5 healthy women aged between 18 and 41 years. Urines were pooled according to gender, and confirmed to be free of blood. CaOx crystals were precipitated from sieved (S) human urine, or after centrifugation (x 10,000 g) and 0.22 µm filtration (CF), or 10 kDa ultrafiltration (UF) (3). Portions (1 ml) of the crystal suspensions were then filtered (0.22 µm), rinsed copiously with distilled water, dried, and suspended in 0.1M NaOH or 0.05M EDTA: at timed intervals, they were removed by filtration, washed exhaustively with water, and examined by scanning electron microscopy (SEM) (7). CaOx crystals were also generated from a single 24h urine sample collected from a healthy woman, aged 48, following centrifugation and filtration, and ultrafiltration. These were fractured under light microscopy using a diamond cell (High Pressure Diamond Optics Inc). Five µg of fractured crystals were incubated at 37°C for 12 hours in 2 ml of: 0.25 mg/ml Proteinase K1 (Boehringer Mannheim); 12.5 mmol/ Tris buffer (Merck) pH 8.0; 0.125 mol/l NaCl (Sigma-Aldrich); 1.25% SDS (Sigma-Aldrich). The crystals were then dried under nitrogen and coated with carbon (SpeediVac Model 12E6) and examined using a FESEM JEOL 6300F field emission electron microscope (JEOL, Japan).

RESULTS

SEM of untreated crystals from the S, CF and UF urine samples revealed intact single crystals or aggregates, consisting principally of coffin-shaped CaOx monohydrate, but also comprising some dihydrate tetrahedral bipyramids. The S and CF crystals subjected to NaOH etching showed surface pitting and internal honeycombing, consistent with the removal of organic material, while those from the UF urine were smooth and solid. EDTA dissolution caused release of visible organic material from the S and CF, but not from the UF crystals. Results were the same for crystals from both sexes.

These findings were confirmed by FESEM using the crystals precipitated from the urine collected by the female subject. The fractured crystals deposited from the UF urine prior to protease digestion are shown in figure 1A, while figure 1B shows the same crystals after proteolysis. It is readily apparent that the crystals are completely solid, and that their gross structure is not affected by protein digestion. However, the fractured crystals from the CF urine showed evidence of extensive lacunae throughout their internal structure (figure 1C). These were more obvious following treatment with Protease K, which removed most of the associated organic material and enabled the capture of sharper images (figure 1D).

DISCUSSION

In healthy mineralization systems, acidic macromolecules can become incarcerated as "guests" within a mineral "host" (8) to produce a structure reminiscent of

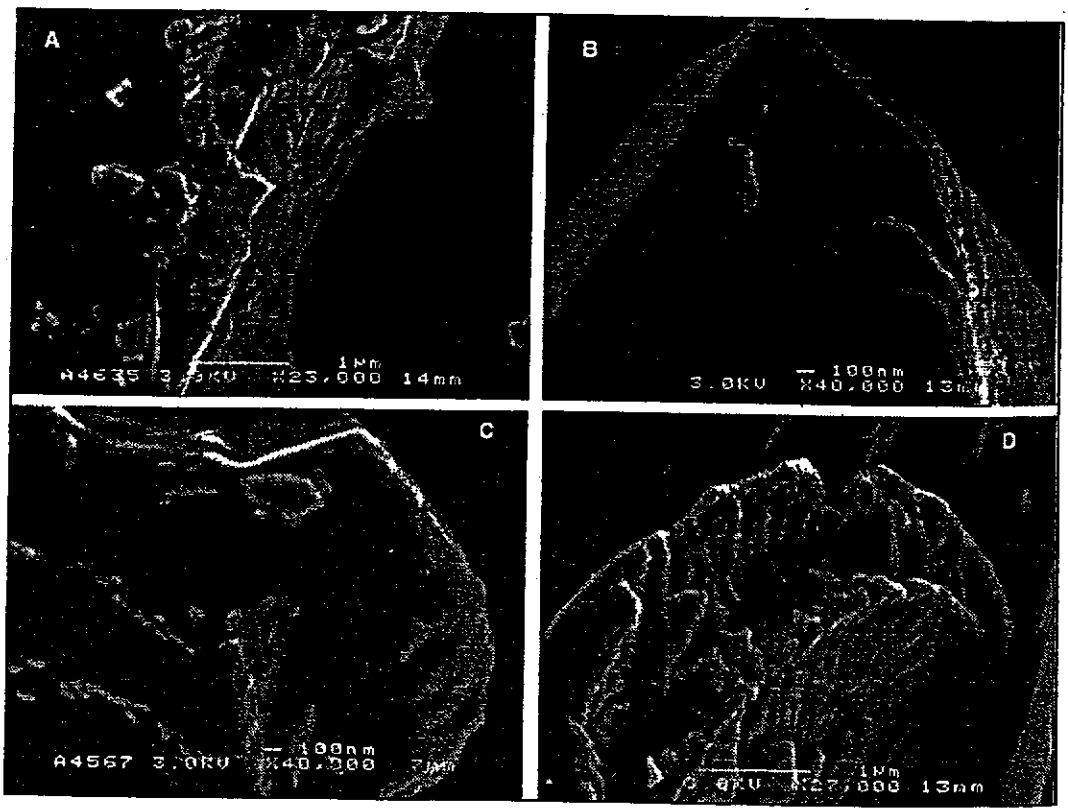

Fig. 1 - FESEM images of CaOx crystals precipitated from UF urine before (a) and after (b) digestion with protease; and from CF urine before (c) and after (d) protease treatment

reinforced cement, with the guests acting as intracrystalline steel rods which control mineral deposition and tensile properties. This is achieved by creating and stabilising discontinuities in the lattice and thereby altering crystal texture. The accommodation of proteins within crystals is now a well recognised phenomenon (6), the best characterised example being that of the sea urchin spine (9). Nonetheless, the notion that urinary proteins may play a similar role in stone formation as inclusions within individual crystals has met with some resistance (5).

Our results presented here constitute the first *direct* evidence that proteins can form part of the internal ultrastructure of CaOx crystals precipitated from human urine. We conclude that intracrystalline proteins may play directive roles in CaOx crystal formation in urine by dictating the size, morphology and texture of the mineral in a manner similar to those involved in healthy biomineralization systems.

REFERENCES

1. Boyce WH, Garvey FK: The amount and nature of the organic matrix in urinary calculi. J Urol, 1956; 76:213-227.
2. Ryall RL: Glycosaminoglycans, proteins and stone formation: Adult themes and child's play. Ped Nephrol 1996; 10: 656-666.
3. Doyle IR, Ryall RL, Marshall VR: Inclusion of proteins into calcium oxalate crystals precipitated from human urine: a highly selective phenomenon. Clin Chem 1991; 37:1589-1594.
4. Khan SR, Hackett RL: Role of organic matrix in urinary stone formation: An ultrastructural study of crystal matrix interface of calcium oxalate monohydrate stones. J Urol, 1993; 150: 239-245.
5. Mandel N: Commentary on the growth of renal calculi. J Urol 157:2.
6. Weiner S, Addadi L: Design strategies in mineralized biological materials. J Materials Chemistry, 1997; 7:689-702.
7. Grover PK, Ryall RL: Effect of seed crystals of uric acid and monosodium urate on the crystallization of calcium oxalate in undiluted human urine in vitro. Clin Sci, 1997; 92:205-213.
8. Mann S, Archibald DD, Didymus JM, Douglas T et al: Crystallization at inorganic-organic interfaces: biominerals and biomimetic synthesis. Science, 1993; 261:1286-1292.
9. Aizenberg J, Hanson J, Ilan M et al: Morphogenesis of calcitic sponge spicules: a role for specialized proteins interacting with growing crystals. FASEB J, 1995; 9:262-268.

Urolithiasis 2000;
Editors: A.L. Rodgers, B.E. Hibbert, B. Hess, S.R. Khan and G.M. Preminger

An unexpected role for urinary proteins in the prevention of calcium oxalate urolithiasis?

David E Fleming*, Phulwinder K Grover, Magali C Chauvet, Villis R Marshall, Rosemary Lyons Ryall

*Urology Unit: Flinders Medical Centre, Repatriation General Hospital and Flinders University School of Medicine, SA, and *School of Applied Chemistry, Curtin University of Technology, WA, AUSTRALIA*

INTRODUCTION

It is well recognised that calcium oxalate (CaOx) urinary stones have both a mineral and macromolecular component. While the origin of the mineral component is rarely the subject of debate, the role of the macromolecules in the formation of stones still remains unclear. Do they have a definitive role in the process? Or are they simply bystanders drawn innocently into the process - either secondary to tissue damage, or as a result of an ability to bind calcium, and as a result, adhere to crystal surfaces? Recent studies in our laboratory have shown that these proteins are not found only on the surface of CaOx crystals precipitated from human urine, but are also occluded within the crystalline structure [1].

While in previous experimental studies it has been shown that urinary proteins may retard crystal growth, aggregation [2] and urothelial attachment [3] their occlusion *within* the crystal itself opens up a new dimension requiring further investigation.

It has been shown in other systems [4-10] that intracrystalline proteins fulfil a critical controlling function in healthy biomineralization. It is possible therefore, that such proteins may play a similar pivotal role in the crystallization of CaOx within the urinary tract, since their incorporation within the crystal structure has additional, previously unsuspected ramifications for the development of calculi: enzymatic digestion of intracrystalline proteins in urine could be the starting point for the deconstruction and dissolution of CaOx crystals formed within the kidney. The present studies were undertaken to determine whether these proteins could be removed from CaOx crystals as a result of the action of natural proteases present in human urine.

MATERIALS AND METHODS

Calcium oxalate (CaOx) monohydrate crystals were precipitated from the urine of a healthy individual by the addition of oxalate. Prior to the addition of the oxalate, one half of the urine sample (CF) had undergone centrifugation at (10,000 x g) and filtration (0.22μm), and the other half (UF) had been ultrafiltered (10 KDa). Once formed, the crystals were washed continuously with distilled water [11]. They were then dried and incubated for four hours at 37°C in fresh human urine. This urine was also divided into two aliquots: one was left unaltered, while to the other was added a cocktail of protease inhibitors (all purchased from Sigma Chemical Co, St Louis, MO, USA) containing phenylmethylsulfonyl fluoride (PMSF) dissolved in 100% ethanol, N-α-p-tosyl-L-lysine chloromethyl ketone hydrochloride (TLCK) dissolved in 1mmol/L HCl, and N-tosyl-L-phenylalanine chloromethyl ketone (TPCK) dissolved in 100% ethanol. The final concentrations of PMSF, TLCK and TPCP in the incubations were 1mmol/L, 135μmol/L, and 248μmol/L, respectively.

At the end of the four hour incubation period the crystals were harvested, washed with distilled water and dried. They were then coated with carbon (speedivac model 12E6) and examined using a JEO2 6300F field emission electron microscope (JEO2, Japan).

RESULTS

Figure 1 shows the appearance of CaOx crystals incubated in urine in the absence of protease inhibitors. The presence of surface fissures and erosion of the crystal margins are easily apparent - signs which are consistent with removal of material from the crystal bulk. In contrast, **figure 2** depicts crystals derived from the same urine specimen following ultrafiltration to remove macromolecules with relative molecular masses > 10 kDa. There is no sign of dissolution or damage to the crystal surface.

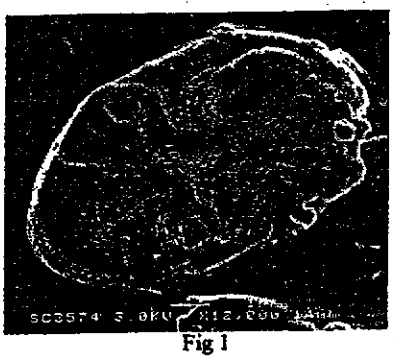
Fig 1

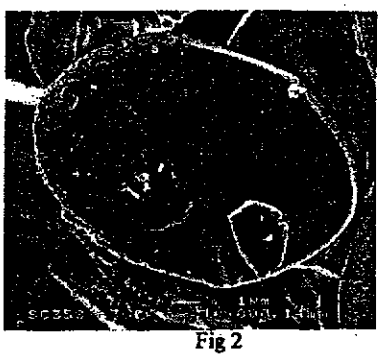
Fig 2

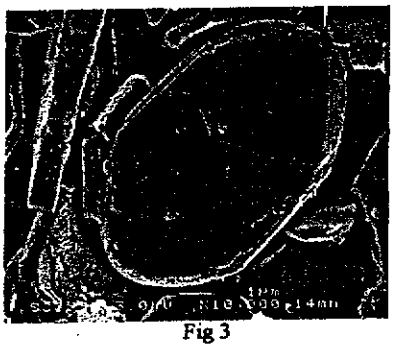
Fig 3

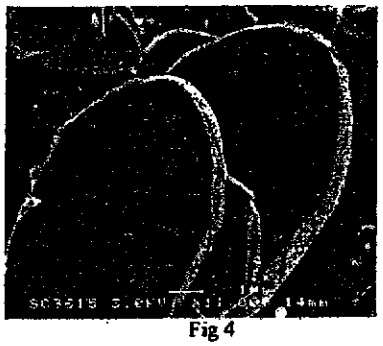
Fig 4

Figure 1: CaOx monohydrate crystal precipitated from centrifuged and filtered urine, after incubation in fresh urine in the absence of protease inhibitors.
Figure 2: Crystals deposited from the same urine which had first been ultrafiltered, following incubation in fresh urine in the absence of protease inhibitors.
Figure 3: Crystals from the same batch as depicted in figure 1, after incubation in the same fresh urine, but in the presence of protease inhibitors.
Figure 4: Crystals from the same batch as shown in figure 2, following incubation in fresh urine in the presence of protease inhibitors.

Crystals precipitated from the same centrifuged and filtered urine which were incubated in the fresh urine in the presence of the protease inhibitors (**figure 3**) exhibited a smooth surface similar to those observed in **figure 2**, indicating that the changes noted in figure 1 had been caused by proteolytic digestion of proteins within the crystal structure by endogenous proteases. As expected, crystals deposited from the ultrafiltered urine which had been incubated in fresh urine in the presence of protease inhibitors were superficially smooth and had clear, crisp margins (**figure 4**).

As the crystals shown in **figures 1** and **2** were precipitated from ultrafiltered urine, they would have been deficient in all but small proteins with molecular masses less than 10 kDa, so that the urinary proteases would not be expected to have any effect. However, crystals derived from the centrifuged and filtered urine would be expected to contain proteins, rendering them susceptible to attack by protease. Confirmation of this likelihood can be found in the changes observed in **figure 3**.

DISCUSSION

These results indicate that proteins occluded within calcium oxalate crystals are vulnerable to degradation by urinary proteases. It has often been assumed that because of the poor solubility of the compound, once CaOx crystals form in urine they are relatively inert and will remain unchanged. The findings from this study demonstrate that this is not the case, and suggest, moreover, that the presence of proteins within crystals may provide a means by which they can be dismantled and removed as a means of preventing stone formation. These observations made with proteases present in whole, healthy urine, are identical to those observed when crystals formed in the presence of urinary macromolecules are treated with protease K [1].

How then may these findings enhance our understanding of the role of proteins in calcium oxalate crystal formation? At the present time, because of the demonstrated ability of certain urinary proteins such as urinary prothrombin fragment 1 (UPTF1) [12] to act as potent inhibitors of crystal aggregation, it has been proposed that their role may be to prevent the formation of large

crystal clusters that are likely to be retained within the collecting system. The relative lack or defective function of these protein inhibitors has been proposed as a potential cause of stone formation [2].

The observations from this study open up other potential avenues by which proteins may influence stone formation. Lieske et al, in a series of papers [13-15] have shown that CaOx dihydrate crystals attach to cultured monkey renal BSC-1 cells, become internalised and then dissolve over a period of weeks. They have also postulated [16] that epithelial cells could serve as a template for crystal nucleation from supersaturated urine, then absorb the crystals, and by this means establish a mechanism for altering the saturation of CaOx in the tubule, particularly if the concentrations were excessive.

The work of Lieske and his colleagues was performed using pure crystals. However, if similar crystals, but now rich in proteins, were to be subjected to the same process, it seems highly probable that intracellular proteases could well facilitate their dissolution. This could occur by eroding the protein matrix and vastly increasing the surface area available for dissolution, and/or cause fragmentation of the crystalline structure which could then be removed by phagocytosis, as proposed by de Water et al [17].

It is also possible that crystals may not need to be trapped within the tubular cells for this process to occur. Khan et al [18] observed a similar pattern of erosion in fragments of CaOx stones that had been retained in the renal space after extracorporeal shock wave lithotripsy.

Our observations add further weight to the importance of proteins in the urinary genesis of CaOx crystals, but perhaps more importantly, highlight that this is a dynamic and potentially reversible process in which proteins and urinary proteases may perform a definitive role. Further studies to explore these mechanisms in more detail may provide therapeutic opportunities by facilitating stone dissolution *in situ*.

ACKNOWLEDGEMENTS

This study was supported by grants from the National Health and Medical Research Council of Australia (Grant No. 980366), the Flinders Medical Centre Foundation and the Flinders University of South Australia.

REFERENCES

1. FLEMING DE, DOYLE IR, EVANS N, MARSHALL VR, PARKINSON GM, RYALL RL: Proteins associated with calcium oxalate crystals formed in human urine are intracrystalline. In: *8th European Symposium on Urolithiasis, Parma, Italy*. Borgi L, Meschi T, Briganti A, Schianchi T, Novarini A (Eds). Editoriale Bios, Cosenza, Italy, pp 358-361, 1999.
2. RYALL RL: Urinary inhibitors of calcium oxalate crystallization and their potential role in stone formation. *World J. Urol.* 15, 155-164, 1997.
3. HACKETT RL, SHEVOCK PN: Crystal-cell interaction: Its role in the development of stone disease. In: *Calcium Oxalate in Biological Systems*. Khan SR (Ed).CRC Press, Boca Raton, pp 323-342.
4. AIZENBERG J, HANSON J, ILAN M, LEISEROWITZ L et al: Morphogenesis of calcitic sponge spicules: a role for specialized proteins interacting with growing crystals. *Fed Am Soc Exp Biol J* 9: 262-268, 1995.
5. AIZENBERG J, ILAN S, WEINER S, ADDADI L: Intracrystalline macromolecules are involved in the morphogenesis of calcitic sponge spicules *Conn Tiss Res* 34: 255-261, 1996.
6. AIZENBERG J, HANSON J, ILAN M, LEISEROWITZ L, KOETZLE TF, ADDADI L, WEINER S: Morphogenesis of calcitic sponge spicules: a role for specialized proteins interacting with growing crystals. *Fed Am Soc Exp Biol J* 9:262-268, 1995.
7. MORADIAN-OLAK L, FROLOW F, ADDADI L, WEINER S: Interactions between acidic matrix macromolecules and calcium phosphate ester crystals: relevance to carbonate apatite formation in biomineralization. *Proc R Soc London B* 247:47-55, 1992.
8. ALBECK S, AIZENBERG J, ADDADI L, WEINER S: Interactions of various skeletal intracrystalline components with calcite crystals. *J Am Chem Soc* 115: 11691-11697, 1993.
9. ALBECK S, ADDADI L, WEINER S: Regulation of calcite crystal morphology by intracrystalline acidic proteins and glycoproteins. *Conn Tiss Res* 35:365-370, 1996.
10. ALBECK S, WEINER S, ADDADI L: Polysaccharides of intracrystalline glycoproteins modulate calcite crystal growth *in vitro*. *Chem Euro J* 2:278-284S, 1996.
11. DOYLE IR, RYALL RL, MARSHALL VR: The inclusion of proteins into calcium oxalate crystals precipitated from human urine: A highly selective phenomenon. *Clin Chem* 37:1589-1594, 1991.
12. RYALL RL, GROVER PK, STAPLETON AMF et al: The urinary F1 activation peptide of human prothrombin is a potent inhibitor of calcium oxalate crystallization in undiluted human urine *in vitro*. *Clin Sci* 89:533-541, 1995.
13. LIESKE JC, NORRIS R, SWIFT H, TOBACK FG: Adhesion, internalization and metabolism of calcium oxalate monohydrate crystals by renal epithelial cells. *Kidney Int* 52:1291-1301, 1997.
14. LIESKE JC, TOBACK FG, DEGANELLO S: Face-selective adhesion of calcium oxalate dihydrate crystals to renal epithelial cells. *Calc Tiss Int* 58:195-200, 1996.
15. LIESKE JC, TOBACK FG, DEGANELLO S: Direct nucleation of calcium oxalate dihydrate crystals onto the surface of living renal epithelial cells in culture. *Kidney Int* 54:796-803, 1998.
16. LIESKE JC, DEGANELLO S, TOBACK FG: Cell-crystal interactions and kidney stone formation. *Nephron* 81:8-17, 1999.
17. DE WATER R, NORDERMEER C, VAN DER KWAST TH, NIZZE H, BOEVÉ ER, KOK DJ, SCHRÖDER FH: Calcium oxalate nephrolithiasis: Effect of renal crystal deposition on the cellular composition of the renal interstitium. *Am J Kidney Dis* 33:761-771, 1999.
18. KHAN SR, HACKETT RL, FINLAYSON B: Morphology of urinary stone particles resulting from ESWL treatment. *J Urol* 136:1367-1372, 1986.

Urolithiasis 2000;
Editors: A.L. Rodgers, B.E. Hibbert, B. Hess, S.R. Khan and G.M. Preminger

A timed study of the relationship between mineral and protein during calcium oxalate crystal growth in human urine

David E Fleming*ᵠ, Caroline J Dean, Magali Chauvet, Gordon M Parkinson*,
Villis R Marshall, Rosemary Lyons Ryall

Department of Surgery, Flinders Medical Centre & Flinders University School of Medicine, SA;
**Applied Chemistry, Curtin University of Technology & ᵠChemistry Centre, WA, AUSTRALIA*

INTRODUCTION

The association of proteins with urinary calculi is well documented [1-2] and has led to speculation that they may fulfil regulatory roles similar to those of proteins in healthy biomineralization systems. Proteins are normally released into the renal tubules and can be adsorbed on formed calcium oxalate (CaOx) crystal surfaces [3] or become intracrystalline [4-5]. Both pathways have significant implications for the development and study of human urolithiasis.

Proteins can affect the morphology of CaOx by binding to particular crystal faces [6] and thereby dictating the direction in which solute deposition proceeds. Adsorption can also alter the surface charge, which in turn influences the course of aggregation and growth [7], as well as crystal adherence to, and internalization by cells lining the nephron [8].

A number of studies on calcified structures of marine organisms have shown that the texture and tensile properties of the mineral phase are determined by proteins incarcerated within the crystal bulk [9-10]. Although the occurrence and critical function of intracrystalline proteins in biogenic crystals are now widely recognised, to date, evidence that the phenomenon occurs in CaOx crystals from human urine has been indirect.

Using field emission electron microscopy(FESEM) and proteolytic digestion, we have shown that proteins are distributed in an orderly fashion throughout CaOx crystals generated from human urine [11]. The aim of this study was to observe the relationship between protein and mineral during the early stages of CaOx growth in urine, and at later periods when the amount of protein available for binding would be diminishing.

MATERIALS AND METHODS

Chemicals and biochemicals

All reagents were of the highest purity commercially available. Sodium oxalate and sodium dodecyl sulphate (SDS) were obtained from BDH Chemicals Australia (Kilsyth, Victoria, Australia); sodium hydroxide and ethylenediaminetetra-acetic acid (EDTA), from Ajax Chemicals (Auburn, NSW, Australia). Calcium chloride and Tris (hydroxymethyl)-aminomethane (Tris) were purchased from Sigma Chemical Company (St Louis MO, USA) and Protease K was obtained from Boehringer Mannheim, Germany. Solutions were prepared using double distilled water filtered through a 0.2 μm membrane filter (Millipore).

Collection and treatment of urines

Approval for urine collection was obtained from the Committee on Clinical Investigation (Ethics Committee) of the Flinders Medical Centre).

Urine samples were collected under refrigeration from five healthy subjects. They were pooled, confirmed to be free of blood by dipstick analysis (Miles Diagnostics, Vic, Australia) centrifuged (10,000 x g) in a Beckman J2-21 M/E centrifuge, Millipore filtered (0.22μm) and divided into three portions.

Following determination of the metastable limit [12], CaOx crystallization was induced by the dropwise addition of sodium oxalate solution and the urines were incubated with shaking at 37°C. After one hour, crystals were isolated by filtration from flask 1, while a second oxalate load was added to the other flasks. After 2 hours, crystals were harvested from flask 2, and a further load added to flask 3, from which the crystals were removed after a further two hours incubation. They were washed with distilled water, dried and fractured using a diamond cell (High Pressure Diamond Optics).

Proteolytic digestion of crystals and examination by field emission electron microscopy

A 5 mg sample of fractured crystals was incubated at 37°C for 12 hours in 2 mL of a solution containing 0.25 mg/mL Protease K (Sigma); 12.5 mmol/L Tris-HCl buffer, pH 8.0; 0.125 mol/L NaCl; and 1.25% SDS. The crystals were then coated with carbon (SpeediVac Model) and examined using a FESEM JEOL 6300F field emission electron microscope (JEOL, Japan).

Preparation of pure CaOx crystals (Control)

Crystals of CaOx were generated by mixing 5 mL of aqueous solutions of 0.15 mol/L $CaCl_2$ and 0.15 mol/L $(COONa)_2$ at a rate of 0.4 mL per hour from glass syringes using an infusion pump (Sage Instruments, USA), into distilled water at 37°C. The mixture was gently mixed with an overhead stirrer fitted with a glass stirring rod and incubated for 13 hours at 37°C. The precipitated crystals, which were separated by vacuum filtration and dried under nitrogen, served as controls for comparison with urinary crystals in FESEM examination.

RESULTS

At one hour

Calcium oxalate monohydrate (COM) and dihydrate (COD) crystals were visible; the number of the latter far outweighed that of the former. The COM crystals consisted of tightly packed thin plates (**figure 1**) which possessed a porous texture (**figure 2**), reflecting the removal of proteinaceous material from within the structure. The shale-like layers of small hexagonal plates were assembled to form a single coffin-shaped structure (**Figure 3**). COD crystals were significantly smaller and resembled pyramidal pagodas constructed in a spiral fashion, with stepped layers being delineated by organic material. One such crystal, which had not been fractured and treated with protease, is shown in **Figure 4**.

At two hours

No CODs were visible after 2 hours, by which time the COM showed less superficial detail than those formed after one hour (**figure 5**). However, when the 2 hr COM crystals were fractured and exposed to protease, only the central sections were porous (**figure 6**), undoubtedly reflecting further deposition of CaOx in response to the additional load added after 1 hr. In contrast, pure COM crystals which had been fractured and treated with protease, remained solid and superficially smooth (**figure 7**).

At four hours

After four hours the COM crystals were thicker, larger, and exhibited little surface detail and internal porosity (Figure 8), consistent with massive deposition of CaOx caused by addition of two further loads of oxalate and early depletion of urinary proteins. Proteins incarcerated into the crystals at the induction of nucleation and in the time period shortly after are obviously buried deep within the crystal bulk.

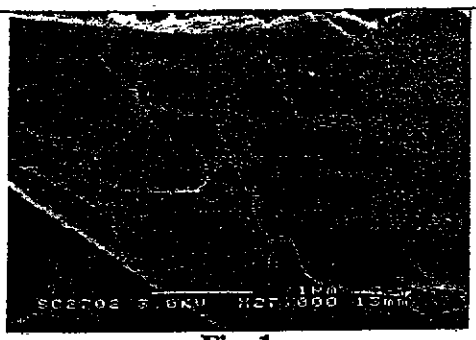

Fig. 1

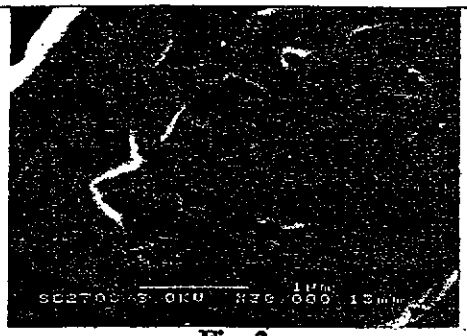

Fig. 2

Fig. 2

Fig. 3

Fig. 5

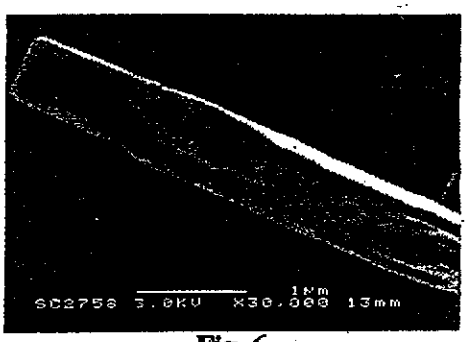

Fig. 6

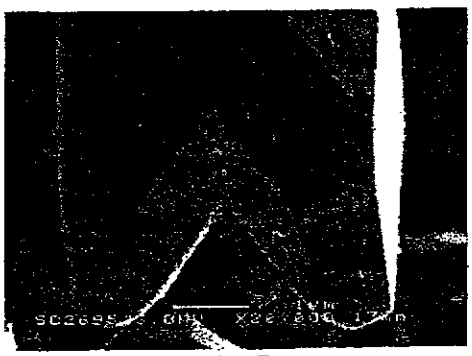

Fig. 7

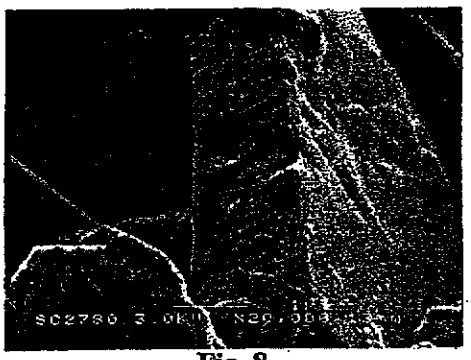

Fig. 8

Figures 1-8: FESEM images of CaOx crystals precipitated from human urine 1 hour after addition of sodium oxalate solution (figures 1-4); after 2 hours (figures 5 and 6); and after four hours (figure 8). Figure 7, which depicts pure CaOx, is included for comparison. The bars represent 1 micron.

DISCUSSION

The results of this study confirm our earlier work [11] which obtained direct evidence that urinary proteins are incorporated within CaOx crystals precipitated from human urine. They also provide insight into the mechanism by which COM and COD crystals are constructed in the

presence of macromolecules. Newly formed COM crystals consisted of layers of thin shale-like plates stacked closely one upon the other, whose margins appeared to be delineated by adsorbed proteins. Closer examination demonstrated the presence of pores within the plates, consistent with distribution of organic material throughout the mineral fabric. The plates were then assembled into inchoate coffin-shaped structures, obviously destined to become COM crystals typical of those frequently seen in human urine. As deposition of mineral proceeded in the presence of additional oxalate and decreasing availability of endogenous protein, the shale-like texture disappeared, to be replaced by a smooth coating which apparently consisted of solid mineral.

COD crystals were relatively few in number and present only in the early stages of the time course, probably transforming to the more stable COM phase during the course of the reaction. Unlike COM, the COD did not appear to develop as discrete layers in a stack, but rather in a continuous spiral structure interspersed with organic material. The lack of sufficient crystals precluded studies with protease to confirm that the organic matter was protein.

These data demonstrate, directly and for the first time, the dependence of crystal texture on the availability of urinary proteins. Obviously the internal ultrastructure of urinary CaOx crystals depends to a significant extent upon the ratio of proteins which adsorb to the CaOx crystal surface, to available quantities of solute ions. As the concentration of those proteins diminishes, crystal porosity also decreases and the structure becomes enveloped in a solid mantle of mineral.

By digesting CaOx intracrystalline proteins *in vivo*, endogenous proteases could open channels throughout the mineral architecture, allowing deeper penetration of enzyme into the crystalline core for further proteolytic digestion [13]. This would expedite dismantling and dissolution of retained crystals, as well as removal of the resulting particles and ions by opsonins and calcium-binding and transporting proteins [14]. Our observations, therefore, have important ramifications for the formation of CaOx crystals in urine *in vivo*, since crystals formed in urine containing low concentrations of CaOx-binding proteins, or in the face of overwhelming levels of supersaturation, will possess different biophysical properties which will affect their ability to aggregate and to adhere to the cells lining the urinary collecting system. Further, once endocytosed by urothelial cells, such crystals will be far more resistant to the action of cellular proteases and more likely to contribute to the formation of a stone.

ACKNOWLEDGEMENTS

This study was supported by grants from the National Health and Medical Research Council of Australia (Grant No. 980366), the Flinders Medical Centre Foundation and the Flinders University of South Australia.

REFERENCES

1. BOYCE WH, GARVEY FK: The amount and nature of the organic matrix in urinary calculi: a review. *J Urol* 76:213-227, 1956
2. RYALL RL, STAPLETON AMF: Urinary macromolecules in calcium oxalate stone and crystal matrix: good, bad or indifferent? In *Calcium Oxalate in Biological Systems*, SR KHAN (ed), CRC Press Inc, Boca Raton, Florida, pp 265-290, 1995
3. LIESKE JC, DEGANELLO S, TOBACK FG: Cell-crystal interactions and kidney stone formation. *Nephron*. 81:8-17, 1999
4. DOYLE IR, RYALL RL, MARSHALL VR: Inclusion of proteins into calcium oxalate crystals precipitated from human urine: a highly selective phenomenon. *Clin Chem*. 37:1589-1594, 1991
5. KHAN SR, HACKETT RL: Role of organic matrix in urinary stone formation: An ultra-structural study of crystal matrix interface of calcium oxalate monohydrate stones. *J Urol*. 150:239-245, 1993
6. DEGANELLO S: Interaction between nephrocalcin and calcium oxalate monohydrate: a structural study. *Calif Tissue Int*. 48:421-428, 1991
7. EDYVANE KA, HIBBERD CM, HARNETT, MARSHALL VR, RYALL RL: Macromolecules inhibit calcium oxalate crystal growth and aggregation in whole urine. *Clinica Chimica Acta*. 167:329-338, 1987
8. LIESKE JC, SWIFT H, MARTIN T, PATTERSON B, TOBACK G: Renal epithelial cells rapidly bind and internalize calcium oxalate monohydrate crystals. *Proc Natl Acad Sci*. 91:6987-6991, 1994
9. WEINER S, ADDADI L: Design strategies in mineralized biological materials. *J Mater Chem*. 7(5):689-702, 1997
10. AIZENBERG J, HANSON J, KOETZLE T F, WEINER S, ADDADI L: Control of macromolecule distribution within synthetic and biogenic single calcite crystals. J Am Chem Soc. 119(5):881-886, 1997
11. FLEMING D E, DOYLE I R, EVANS N, MARSHALL V R, PARKINSON G M, RYALL R L: Proteins associated with calcium oxalate crystals formed in human urine are intracrystalline. *8th European Symposium on Urolithiasis-Parma Italy*. pp 359-361, 1999
12. RYALL RL, HIBBERD CM, MARSHALL VR: A method for studying inhibitory activity in whole urine. *Urol Res* 13:285-289, 1985.
13. FLEMING DE, GROVER PK, CHAUVET M, MARSHALL VR, RYALL RL: An unexpected role for urinary proteins in the prevention of calcium oxalate urolithiasis? *These proceedings*, 2000.
14. DE WATER R, NOORDEMEER C, VAN DER KWAST et al: Calcium oxalate nephrolithiasis: Effect of renal crystal deposition on the cellular composition of the renal interstitium. *Am J Kidney Dis* 33: 761-771, 1999.